



Durham E-Theses

The crustal structure beneath northern England and adjacent sea areas

Green, A. S. P.

How to cite:

Green, A. S. P. (1984) *The crustal structure beneath northern England and adjacent sea areas*, Durham theses, Durham University. Available at Durham E-Theses Online: <http://etheses.dur.ac.uk/7845/>

Use policy

The full-text may be used and/or reproduced, and given to third parties in any format or medium, without prior permission or charge, for personal research or study, educational, or not-for-profit purposes provided that:

- a full bibliographic reference is made to the original source
- a [link](#) is made to the metadata record in Durham E-Theses
- the full-text is not changed in any way

The full-text must not be sold in any format or medium without the formal permission of the copyright holders.

Please consult the [full Durham E-Theses policy](#) for further details.

THE CRUSTAL STRUCTURE BENEATH NORTHERN ENGLAND
AND ADJACENT SEA AREAS

by

A. S. P. GREEN

A thesis submitted for the degree of
Doctor of Philosophy at the University of Durham

The copyright of this thesis rests with the author
No quotation from it should be published without
his prior written consent and information derived
from it should be acknowledged.

Department of Geological Sciences

October, 1984

ABSTRACT

In the summer of 1982 the Department of Geological Sciences, University of Durham carried out a seismic survey across the north Irish Sea, northern England and the Mid North Sea High. Recording stations were set up at 2 km intervals across northern England, with other stations offline. Sea-bottom sesimometers were deployed at sea. Explosions were fired at 4 km intervals in the Irish and North Seas and in two boreholes on land. Airgun shots were also fired at sea. The data has been digitised and interpreted using the plus-minus method, time-term analysis, and modelling techniques. Results from other geophysical surveys have been used to complement the interpretation.

An Upper Palaeozoic and Mesozoic sequence is underlain by Lower Palaeozoic rocks (5.5 to 5.7 km/s) at a depth of 0.5 to 3.0 km. A seismic basement (Pg) with a velocity of 6.15 km/s can be recognised at a depth of 4 km, except in the north-east where it appears to be absent, and is identified as Precambrian crystalline basement from south of the Iapetus Suture.

Beneath the whole line the crust appears to have an average crustal velocity of 6.3-6.4 km/s and a crustal thickness of about 30 km. Wide-angle reflections from a mid-crustal discontinuity are observed at a depth of 18-20 km beneath the Northumberland Trough and Mid North Sea High but appear to be absent beneath the Solway and Carlisle Basins.

Crustal phases are best developed for shots in deeper water which have energy in the 2-5 Hz band. Energy above 6 Hz from shots in shallower water is believed to be scattered by inhomogeneities within the crust.

ACKNOWLEDGEMENTS

I would like to thank Professor M.H.P. Bott and Dr. R.E. Long for their help and guidance over the last three years and Professor J.F. Dewey for allowing me the use of departmental facilities. Thanks are also due to the officers and crew of the RRS Shackleton and to Martin Sinha who acted as principal scientist during the cruise. The field work on land and at sea was a major collaborative effort by many staff and postgraduate and undergraduate students from the Department of Geological Sciences and Bob Jones and John Parker of the NERC seismic equipment pool, their unselfish hard work during the summer of 1982 is very much appreciated. The farmers and landowners of Northumberland and Cumbria are also thanked for their cooperation and helpfulness.

The loan of equipment from the NERC seismic equipment pool, Cambridge University and Reading University is gratefully acknowledged.

Dave Stephenson deserves special thanks for the effort he put into the Seismic Processing Laboratory and his advice on computing - one day I'll read the manual ! I would also like to express my gratitude to Anthony Lewis for the many useful discussions we have had over the last two years and the work he has put into the project.

Finally I would like to thank Anne for all the support and encouragement she has given me, especially over the last few months.

CONTENTS

LIST OF FIGURES

LIST OF TABLES

	PAGE
CHAPTER 1 - INTRODUCTION AND GEOLOGY	
1.1 Introduction	1
1.2 The geology	2
1.2.1 Lower Palaeozoic	3
1.2.2 Devonian	5
1.2.3 Carboniferous	7
1.2.4 Permo-Trias	10
1.2.5 Remaining Mesozoic	12
1.2.6 Tertiary	13
1.2.7 Recent	13
1.3 Solway Firth Basin	13
1.4 Carlisle Basin	15
1.5 Northumberland Trough	15
1.6 Mid North Sea High	16
1.7 Seismic structure	17
1.8 Composition of the crust	20
1.9 Gravity and magnetics	22
1.10 Aims of the CSSP	23
CHAPTER 2 - DATA ACQUISITION	
2.1 Introduction	25
2.2 Seismic stations	26
2.2.1 Geostore recorders	28
2.2.2 Durham MkII seismic recorders	30

2.2.3	Durham MkIII seismic recorders	31
2.2.4	Cassette recorders	32
2.2.5	Sea-bottom seismometers	33
2.3	Seismic sources	34
2.3.1	Land shots	35
2.3.2	Sea shots	36
2.3.3	Airgun shots	38
2.4	Quarry blasts	39
CHAPTER 3 - DATA PROCESSING		
3.1	Introduction	41
3.2	Digitising	41
3.3	Section plotting	44
3.4	Calculation of distances and travel-times	44
3.5	Quarry blasts	46
CHAPTER 4 - INTERPRETATION METHODS		
4.1	Introduction	48
4.2	Travel-time graphs	48
4.3	The time-term method	50
4.4	Frequency analysis	53
4.5	Interpretation of reflections	53
4.6	Sea-bottom refractor	54
4.7	Modelling	55
4.7.1	Ray tracing	56
4.7.2	Synthetic seismograms	57
CHAPTER 5 - PRESENTATION OF RESULTS OF UPPER CRUSTAL STRUCTURE		
5.1	Introduction	59
5.2	Presentation of Irish Sea airgun data	59

5.3	Presentation of Irish Sea explosion data	63
5.4	Presentation of the northern England data	67
5.4.1	Land shots	68
5.4.2	Sea shots	69
5.4.3	Quarry blasts	71
5.4.4	Time-term analysis	71
5.5	Presentation of the North Sea airgun data	73
5.6	Presentation of the North Sea explosion data	74
5.7	Summary	78
CHAPTER 6 - INTERPRETATION OF THE SHALLOW STRUCTURE		
6.1	Introduction	80
6.2	The shallow structure beneath the Irish Sea	80
6.3	The shallow structure beneath Northern England	86
6.4	The shallow structure beneath the North Sea	88
6.5	Discussion	90
PRELIMINARY		
CHAPTER 7 - INTERPRETATION OF THE DEEP STRUCTURE		
7.1	Introduction	94
7.2	Interpretation of the North Sea shots	94
7.3	Interpretation of the Irish Sea shots	97
7.4	Shot characteristics	100
7.5	Intereference effects	105
7.6	Anelastic losses	107
7.7	Scattering	109
7.8	Summary	111
CHAPTER 8 - SUMMARY AND CONCLUDING REMARKS		
8.1	Summary	112
8.2	Further work on the CSSP data	114

8.3	Further work	115
REFERENCES		117
APPENDIX A - STACKED RECORD SECTIONS		127
APPENDIX B - DETAILS OF SHOTS AND STATIONS		160
APPENDIX C - COMPUTER PROGRAMS		207

LIST OF FIGURES

FIGURE	FIGURE	FOLLOWING PAGE
Fig 1.1	Location of Caledonian Suture Seismic Project profile.	1
Fig 1.2	Geological map of northern England, southern Scotland and adjacent marine areas.	2
Fig 1.3	Comparative section of Lower Carboniferous strata.	8
Fig 1.4	Comparative section of Permo-Trias strata.	10
Fig 1.5	Location of seismic surveys performed in the British Isles.	17
Fig 1.6	Summary of P-wave velocity structure of the crust from the surveys shown in Fig 1.5.	17
Fig 1.7	Cross-section through the crust of northern Britain from LISPB (from Bamford 1978).	18
Fig 1.8	Bouger gravity anomaly map of northern England, southern Scotland and adjacent marine areas.	22
Fig 1.9	Profile of Bouger gravity anomaly along the CSSP line.	22
Fig 1.10	Profile of the magnetic anomaly along the CSSP line.	22
Fig 2.1	Station and shot locations for the main line.	25
Fig 2.2	Station locations and airgun profile for the Irish Sea.	25
Fig 2.3	Station locations and 2nd airgun profile for the North Sea.	25
Fig 2.4	Diagram of Geostore recording system.	29
Fig 2.5a	Airgun array used on the Irish Sea and 1st North Sea profiles.	38
Fig 2.5b	Airgun array used on the 2nd North Sea profile.	38

Fig 2.6	Location of stations used in the 1982 quarry blast survey and by Swinburn (1975).	40
Fig 3.1	Block diagram of the major steps in the processing of the CSSP data.	41
Fig 3.2	Block diagram of the seismic data processing system used at Durham.	41
Fig 3.3	Flow chart of computer program written by D. L. Stevenson to digitise the analogue tapes using Durham's Seismic Processing Laboratory.	41
Fig 3.4	Drift curves for the Geostore internal clock and MSF.	43
Fig 3.5	Travel-time curves for shots N1 and N3 showing 50 ms offset between the odd and even tracks on the Geostore recorders.	46
Fig 4.1	Sketch showing the occurrence of the sea bottom refractor.	54
Fig 4.2	Plot of the velocities determined from the sea-bottom refractor.	55
Fig 5.1	Travel-time plot for the Irish Sea airgun shots recorded by the PUSS stations.	59
Fig 5.2	Reduced section at S81 for the north-south Irish Sea airgun profile.	60
Fig 5.3	Reduced section at S91 for the north-south Irish Sea airgun profile.	60
Fig 5.4	Frequency plot of an airgun shot recorded at S81 at a range of 5.4 km.	60
Fig 5.5	Reduced travel-time plots for the north-south Irish Sea airgun profile recorded at S81 and S91.	61
Fig 5.6	Reduced travel-time plots for the north-south Irish Sea airgun profile recorded at S81 and S91.	61
Fig 5.7a	Sketch of faulting in the 5.7 km/s refractor beneath the north-south airgun profile in the Irish Sea.	62
Fig 5.7b	Theoretical travel-time plot across a fault (after Ledoux 1957).	62

Fig 5.8	Reduced section of the Irish Sea shots recorded on the hydrophone at P123.	63
Fig 5.9	Reduced section of the Irish Sea shots recorded on the hydrophone at P456.	64
Fig 5.10	Reduced travel-time plots for the Irish Sea shots recorded at P123 and P456.	64
Fig 5.11	Reduced section of the Irish Sea shots recorded at S8.	64
Fig 5.12	Reduced section of the Irish Sea shots recorded at S32.	64
Fig 5.13	Reduced travel-time plot for the Irish sea shots recorded at S1, S8 and P456.	65
Fig 5.14	Distribution of time-terms in the Irish Sea.	66
Fig 5.15	Plot of residuals against distance for the Irish Sea Pg time-term analysis.	67
Fig 5.16	Frequency plot of the Spadeadam shot at S19 at a range of 19.8 km.	68
Fig 5.17	Reduced section of the Spadeadam shot.	68
Fig 5.18	Reduced travel-time plots of the Spadeadam and Kirkwhelpington shots.	68
Fig 5.19	Plane layer interpretation of the Spadeadam and Kirkwhelpington shots.	68
Fig 5.20	Frequency plot of the Kirkwhelpington shot at S49 at range of 5.6 km.	69
Fig 5.21	Reduced section of the Kirkwhelpington shot.	69
Fig 5.22	Reduced section for shot M1.	69
Fig 5.23	Reduced section for shot M4.	69
Fig 5.24	Reduced section for shot N1.	70
Fig 5.25	Reduced section for shot N3.	70
Fig 5.26	Reduced travel-time plots of shots N1 and N3 recorded in northern England.	70
Fig 5.27	Distribution of time-terms across northern England.	72

Fig 5.28	Plot of residuals against distance for the Pg time-term analysis in England.	73
Fig 5.29	Frequency plot of an airgun shot recorded at S60 at a range of 6.3 km.	73
Fig 5.30	Frequency plot of noise at S60.	73
Fig 5.31	Reduced section of the 2nd North Sea airgun profile recorded at S60.	74
Fig 5.32	Reduced travel-time plot of the 2nd North Sea profile recorded at S60.	74
Fig 5.33	Reduced section of the North Sea shots recorded on the hydrophone at P123.	74
Fig 5.34	Reduced section of the North Sea shots recorded on the hydrophone at P456.	74
Fig 5.35	Reduced travel-time plots of the North Sea shots recorded at P123 and P456.	75
Fig 5.36	Plane layer interpretation for the North Sea PUSS stations.	75
Fig 5.37	Reduced section of the North Sea shots recorded at S30.	75
Fig 5.38	Reduced section of the North Sea shots recorded at S53.	75
Fig 5.39	Reduced travel-time plots of shots N1 to N11 recorded in northern England.	76
Fig 5.40	Plot of residuals against distance for the Pg time-term analysis in the North Sea.	78
Fig 5.41	Distribution of the time-terms in the North Sea.	78
Fig 6.1	Ray traced diagram and reduced travel-time section obtained for upper crustal model beneath the Irish Sea for station P456.	81
Fig 6.2	Ray traced diagram and reduced travel-time section obtained for upper crustal model beneath the Irish Sea for station S8.	81
Fig 6.3	Model of Solway Basin Bouger gravity anomaly with the regional trend removed.	83

Fig 6.4	Line drawing of the BIRPS deep seismic reflection section from WINCH profile (see Fig 1.5 for location).	84
Fig 6.5	Interpretation of the aeromagnetic anomaly of the Solway Firth and Southern Uplands. National grid co-ordinates of A and A' are SC 860700 and NX 223693 Respectively (from Al-Chalabi (1970)).	85
Fig 6.6	Interpretation of the upper crustal structure beneath the Irish Sea.	86
Fig 6.7	Ray traced diagram and reduced travel-time section obtained for upper crustal model beneath northern England for shot M1.	86
Fig 6.8	Ray traced diagram and reduced travel-time section obtained for upper crustal model beneath northern England for shot N1.	86
Fig 6.9	Interpretation of the upper crustal structure beneath northern England.	88
Fig 6.10	Ray traced diagram and reduced travel-time section obtained for upper crustal model beneath the North Sea for station S60.	89
Fig 6.11	Ray traced diagram and reduced travel-time section obtained for upper crustal model beneath the North Sea for station P456.	89
Fig 6.12	Interpretation of the upper crustal structure beneath the North Sea.	90
Fig 7.1	Reduced section of the North Sea shots recorded at S19.	95
Fig 7.2	Reduced section of the North Sea shots recorded at S32.	95
Fig 7.3	Reduced section of the North Sea shots recorded at S40.	95
Fig 7.4	Reduced section of the North Sea shots recorded at S54.	95
Fig 7.5	Synthetic seismogram of the North Sea shots recorded at S32.	96
Fig 7.6	Reduced section of the Irish Sea shots recorded at S15.	98

Fig 7.7	Reduced section of the Irish Sea shots recorded at S19.	98
Fig 7.8	Synthetic seismogram of the Irish Sea shots recorded at S15.	98
Fig 7.9	Frequency contour plot of Irish Sea shots recorded at S1.	102
Fig 7.10	Frequency contour plot of Irish Sea shots recorded at S8.	102
Fig 7.11	Frequency contour plot of Irish Sea shots recorded at S30.	102
Fig 7.12	Frequency contour plot of Irish Sea shots recorded at S32.	102
Fig 7.13	Frequency contour plot of North Sea shots recorded at S40.	102
Fig 7.14	Frequency contour plot of North Sea shots recorded at S53.	102
Fig 7.15	Seismic model used in the investigation of interference effects (see Fig 7.16).	107
Fig 7.16	Synthetic seismograms of crustal model with a lower crust consisting of layers 0.5 km thick used to investigate interference effects.	107
Fig 7.17	Classification of scattering problems and applicable methods (from Aki and Richards 1980).	109

LIST OF TABLES

TABLE	TITLE	FOLLOWING PAGE
Table 1.1	Compressional and shear wave velocities of rocks at different pressures (from Christensen 1982).	22
Table 2.1	Location of quarries and stations used in the quarry blast survey of 1983.	40
Table 2.2	Location of stations used by Swinburn (1975) and incorporated into the CSSP survey.	40
Table 4.1	Velocites of the sea floor determined from the sea bottom refractor.	55
Table 4.2	Velocity of the sea bottom refractor assuming a layer of low velocity sediments on the sea floor. Irish Sea hydrophone.	55
Table 5.1	Summary of velocities and intercept times for Irish Sea section.	59
Table 5.2	Summary of velocities and intercept times for northern England.	59
Table 5.3	Summary of velocities and intercept times for North Sea section.	59
Table 5.4	Velocity of the Pg refractor from the minus-times calculated between P456 and stations in northern England.	65
Table 5.5	Time-term analysis - Irish Sea.	66
Table 5.6	Velocity of the Pg refractor from the minus-times calculated between the Spadeadam shot (S28) and the North Sea shots.	70
Table 5.7	Velocities and intercept times determined from quarry blasts in Northumberland.	71
Table 5.8	Time-terms to 5.62 +/- 0.13 km/s refractor - northern England and North Sea.	72
Table 5.9	Pg time-term analysis - northern England.	72

Table 5.10	Apparent velocities and intercept times in northern England determined from shots N1 to N9.	76
Table 5.11	Velocity of the Pg refractor determined from the minus-times calculated for shots N1 to N9 between P456 and stations in northern England.	76
Table 5.12	Delay between Pg and Pg' and the thickness of the low velocity layer.	77
Table 5.13	Pg time-term analysis - North Sea.	78
Table 5.14	Summary of velocities determined for Pg.	79
Table 7.1	Analysis of mid and lower crustal reflections of the North Sea.	95
Table 7.2	Analysis of lower crustal reflections of the Irish Sea.	98
Table 7.3	Reverberation frequency and bubble pulse frequency of the Irish Sea shots.	101
Table 7.4	Reverberation frequency and bubble pulse frequency of the North Sea shots.	101

CHAPTER 1 - INTRODUCTION AND GEOLOGY

1.1 Introduction

Interest in the deep geology of Great Britain has increased rapidly over the last 15 years. This has been witnessed by the formation of the Deep Geology Unit of the British Geological Survey (B.G.S.) in 1977 and the creation of the British Institutions Reflection Profiling Syndicate (BIRPS) in 1980. Seismic refraction surveys have played a major part in helping to understand the deep structure with surveys such as LISPB (Bamford et al. 1976, 1977 and 1978), NASP (Bott et al. 1974 and 1976, Smith and Bott 1975) and HMSP (Armour 1978) making important contributions. Many of these surveys, however, have crossed major structural boundaries and had insufficiently close shots and stations to determine lateral variations and separate out the effects of the shallow and deep structure.

The Caledonian Suture Seismic Project (CSSP) set out to investigate the crustal structure across northern England avoiding some of the problems outlined above. A line along strike just south of the inferred position of the Caledonian Suture on as near uniform crustal structure as possible was chosen (Fig. 1.1). Approximately 60 seismic stations were set up across northern England at 2 km intervals with 57 shots in the Irish and North Seas at 4 km spacings. This gave a total line length of approximately 390 km. Additional data was obtained from two shots



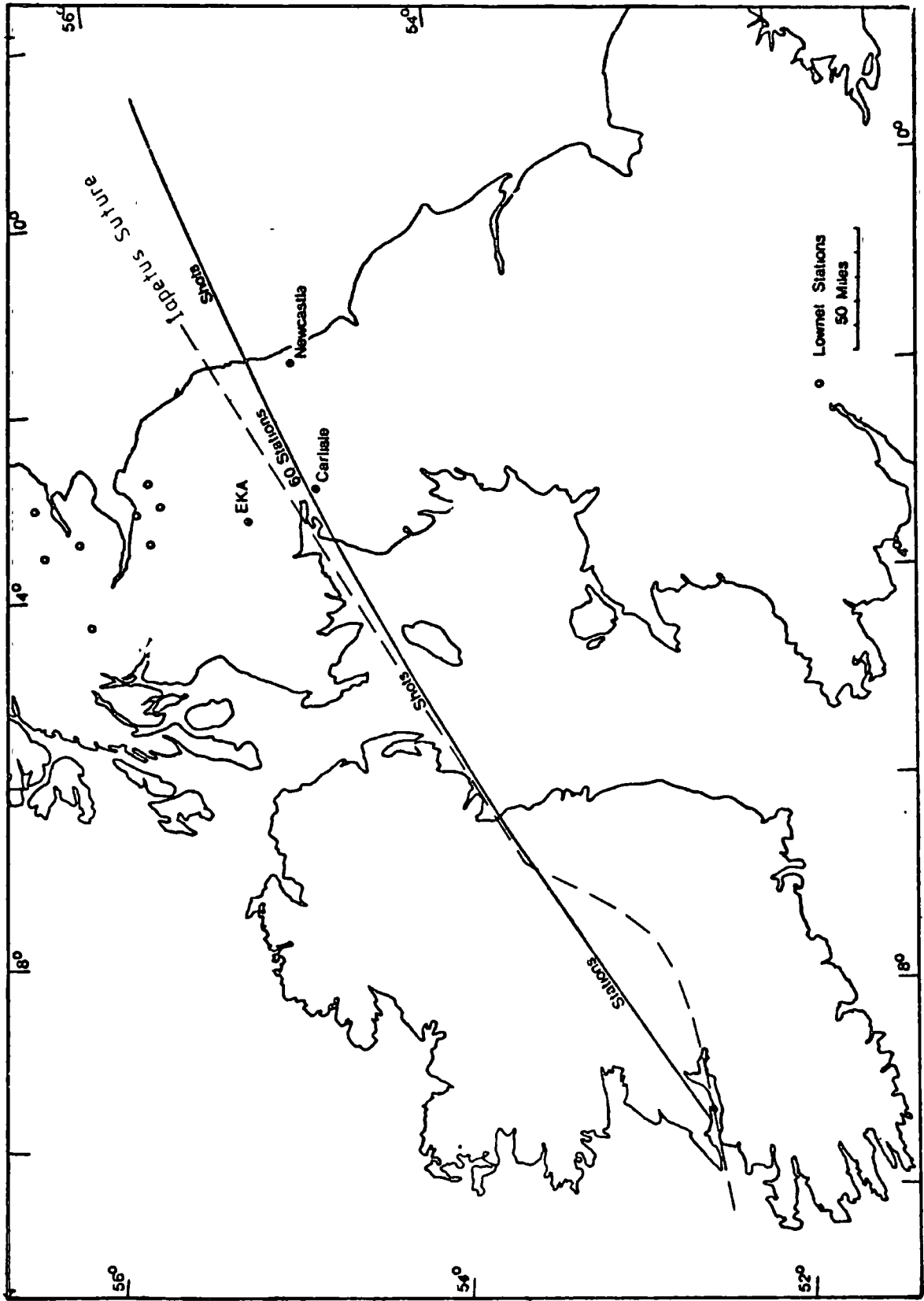


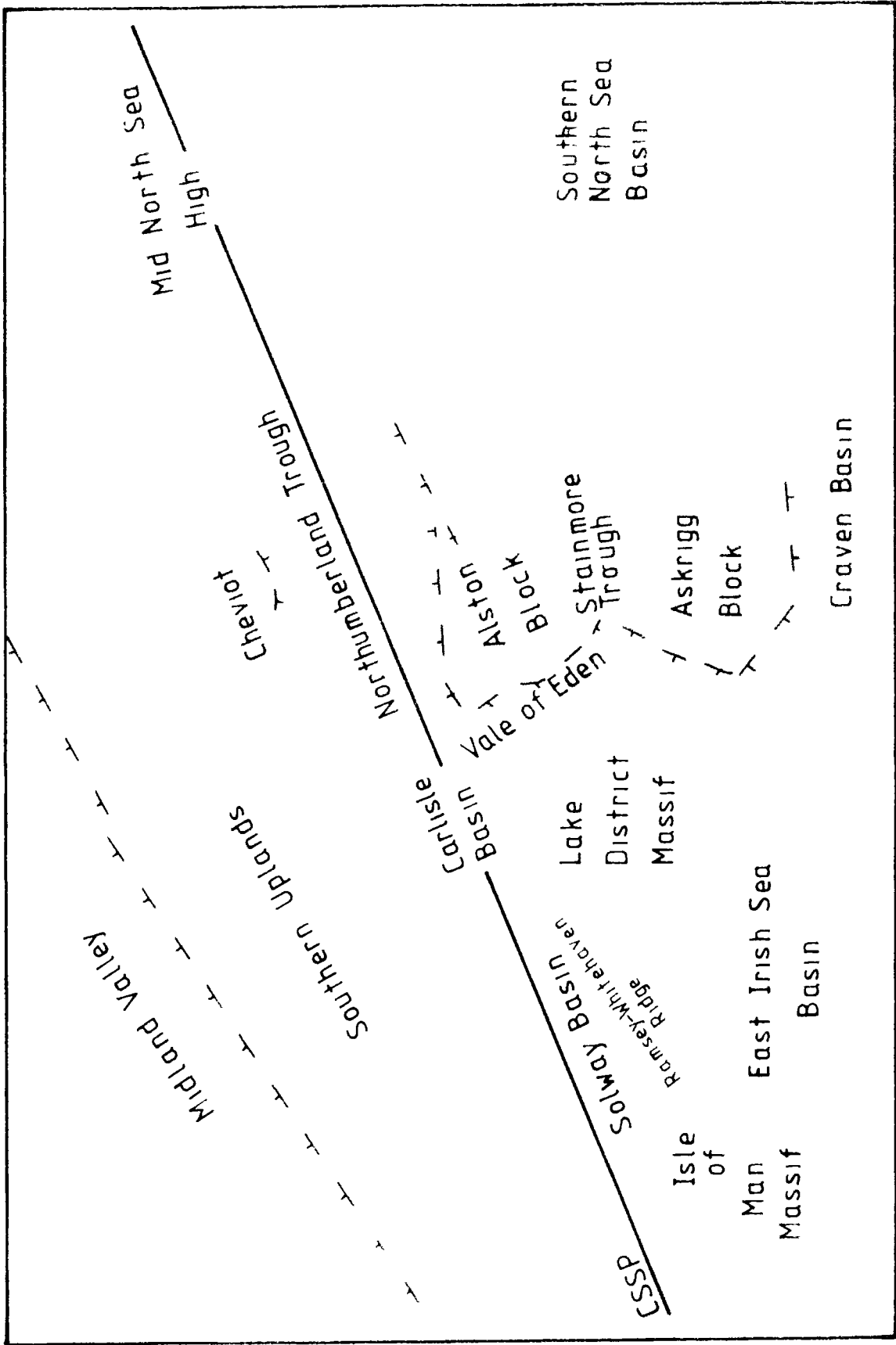
Fig 1.1 Location of Caledonian Suture Seismic Project profile

on land, the use of airguns at sea, the deployment of Cambridge University's Pull-Up Seabottom Seismometers (PUSS) and establishment of other offline seismic stations in northern England, southern Scotland, and the Isle of Man.

The profile was extended by the participation of the Dublin Institute for Advanced Studies in collaboration with Karlsruhe University with a further 51 stations across Ireland. They fired three shots in the Shannon estuary, and Durham fired another 10 shots in the Irish Sea on their behalf. The line across Ireland passed to the north of the Suture (Fig. 1.1). The total line length from the Shannon Estuary to the North Sea is 755 km.

1.2 The Geology

The present day disposition of rocks in northern England, southern Scotland and adjacent marine areas is shown in Fig. 1.2. This can best be understood by reference to the major structural units shown on the overlay of Fig. 1.2. The seismic line runs down the middle of the Solway Basin, the Carlisle Basin, the Northumberland Trough and out onto the Mid North Sea High. The basins and trough are predominantly Upper Palaeozoic and Mesozoic with more stable blocks to the north and south. To the south is the Isle of Man massif, the Lake District massif and the Alston Block, all underlain by a belt of Caledonian granites. To the north is the Southern Uplands, where the remains of an accretionary prism complex of Ordovician and Silurian age is



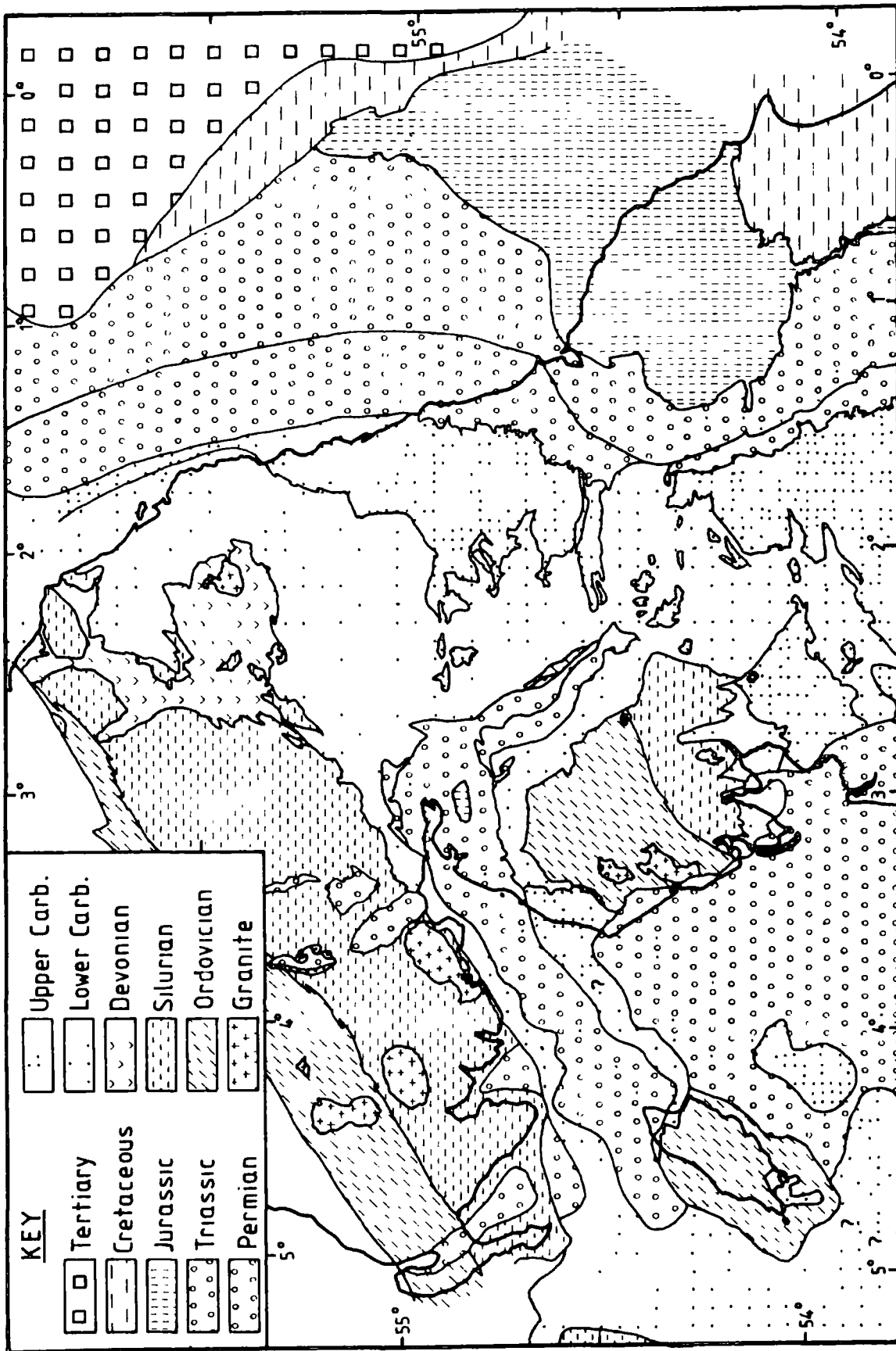


Fig 1.2 Geological map of northern England, southern Scotland and adjacent marine areas.

intruded by Caledonian granites, including the Criffel granite in the west and the Cheviot granite in the east. The Mid North Sea High is a Palaeozoic ridge separating sedimentary basins to the north and south. Much of the geological description following is taken from Taylor et al. (1971) and Greig (1971).

1.2.1 Lower Palaeozoic

Nowhere along the CSSP line are Lower Palaeozoic rocks exposed. They outcrop to the south in the Isle of Man and the Lake District and to the north in the Southern Uplands.

The oldest rocks are the Manx Group in the Isle of Man of late Tremadoc or early Arenig age. They form a sequence of alternating greywackes, siltstones and mudstones approximately 7.5 km thick.

In the Lake District the Skiddaw Group closely resembles the Manx Group in lithology and facies and was probably deposited in the same deep-water basin. They are of Arenig to Llanvirn age and composed of an alternation of flaggy and muddy formations. The strike is Caledonoid and they have been subject to several phases of compression. The total thickness is uncertain and extreme values of from 2 to 9 km have been suggested.

The Skiddaw Group is succeeded unconformably in the Lake District by about 4 km of the Borrowdale Volcanic Group. The sequence consists of a thick pile of pyroclastic rocks varying from fine-

grain tuffs to agglomerates, interbedded with many lava flows ranging in composition from rhyolites to basalts, with andesites dominant. Overlying these rocks at the end of the Ordovician are a series of shallow water calcareous sediments containing minor tuffs and lavas called the Coniston Limestone Group. Silurian rocks form the southern half of the Lake District and they are composed of approximately 4.5 km of mudstones, siltstones, grits and greywackes.

Smaller outcrops of Ordovician and Silurian rocks similar to that of the Lake District are found in the Cross Fell and Teesdale inliers on the western edge of the Alston Block. The Roddymoor borehole shows that Silurian slates are also present near Crook, Co. Durham beneath Carboniferous rocks at a depth of 869 m.

The Lower Palaeozoic rocks of the Southern Uplands are predominantly deep-water greywackes and shales. Ordovician rocks tend to dominate to the north-west and Silurian to the south-east. Practically all of these rocks are highly folded making relationships between rock formations and thicknesses difficult to estimate. The oldest rocks are those of the Ballantrae Ophiolite complex (Church and Gayer 1973) and the thickest Ordovician sequence occurs in the Caradoc and Ashgill of the Girvan region where over 5 km of greywackes are found. The Silurian rocks are similar to the Ordovician rocks comprising over 5 km of mudstones, shales and greywackes.

The Lower Palaeozoic rocks of southern Scotland and northern England were deposited on opposite sides of the Iapetus Ocean, an ocean which separated America from Europe and the Baltic. It is believed to have been between 4 km and 6 km wide in the Cambrian (Mc errow and Cocks 1976) with palaeontological evidence suggesting closure during the Ordovician and Silurian (Williams 1976, Spjeldnaes 1978 and Cocks and Fortey 1982). Closure was effected by subduction to the south-east (Fitton and Hughes 1970) and north-west (Leggett 1980, Leggett et al. 1979, 1983). The final stages of closure occurred during the Upper Ordovician (Phillips et al. 1976) bringing the Lower Palaeozoic sediments of southern Scotland and northern England together along the Iapetus Suture.

1.2.2 Devonian

In northern Britain the Devonian was a period of deposition of terrestrial, fluviatile, lacustrine and volcanic rocks which together form the Old Red Sandstone facies (O.R.S.). The O.R.S. is generally considered synonymous with the Devonian but it is a lithological grouping and may include rocks of Silurian (Thirlwall 1981) and Carboniferous ages (House et al. 1976). The post collisional environment under which these deposits were laid down makes the correlating and dating of events difficult (House et al. 1976).

The igneous activity of the Lower Devonian includes the eruption

of the predominantly andesitic lavas of the Cheviots and the intrusion of numerous granitic bodies. The granites are exposed in the Lake District, the Isle of Man and southern Scotland and buried granites underlie the Weardale and Wensleydale region. Gravity data suggests that a granite body also exists under the eastern end of the CSSP line on the Mid North Sea High (Donato et al. 1983).

O.R.S. sediments are exposed in southern Scotland. The Lower O.R.S. occupies a small area north of Berwick on the east coast where red feldspathic sandstones and conglomerates are interbedded with andesitic tuffs and flows. The Upper O.R.S. is more extensive and follows on unconformably. The rocks lie with gentle dips on the Cheviots filling in valleys in the folded Silurian. Much of the material is locally derived with thicknesses of up to 600 m. The O.R.S. in northern England is only represented by conglomerates at Mell Fell and Roman Fell. The exact age of these rocks is uncertain and although some belong to the basal Carboniferous it is likely that some are also of Upper Devonian age. Other O.R.S. rocks are believed to be absent beneath northern England.

The extent of any Devonian under the CSSP line is unknown. Suspected Devonian has been drilled under the Mid North Sea High at depths of between 1.5 and 2.0 km but the thickness is not known. It is not thought that there are any greater thicknesses under the Northumberland Trough than that seen in southern

Scotland. Palaeoslope evidence indicates that the Trough was probably not active as a depositional basin until mid-Tournaisian times (Leeder 1971).

The Devonian was brought to an end by an outpouring of basaltic lavas extending from north of the Solway Firth (Birrenswark Lavas) to Berwickshire in the borders (Kelso Lavas).

1.2.3 Carboniferous

The Carboniferous is the most widely outcropping system in the region. Stratigraphically the rocks are subdivided as follows.

Upper Carb. (Silesian)	{ Stephanian Westphalian Namurian	} Coal Measures Millstone Grit Series
Lower Carb. (Dinantian)	{ Visean Tournaisian	} Carb. Limestone Series

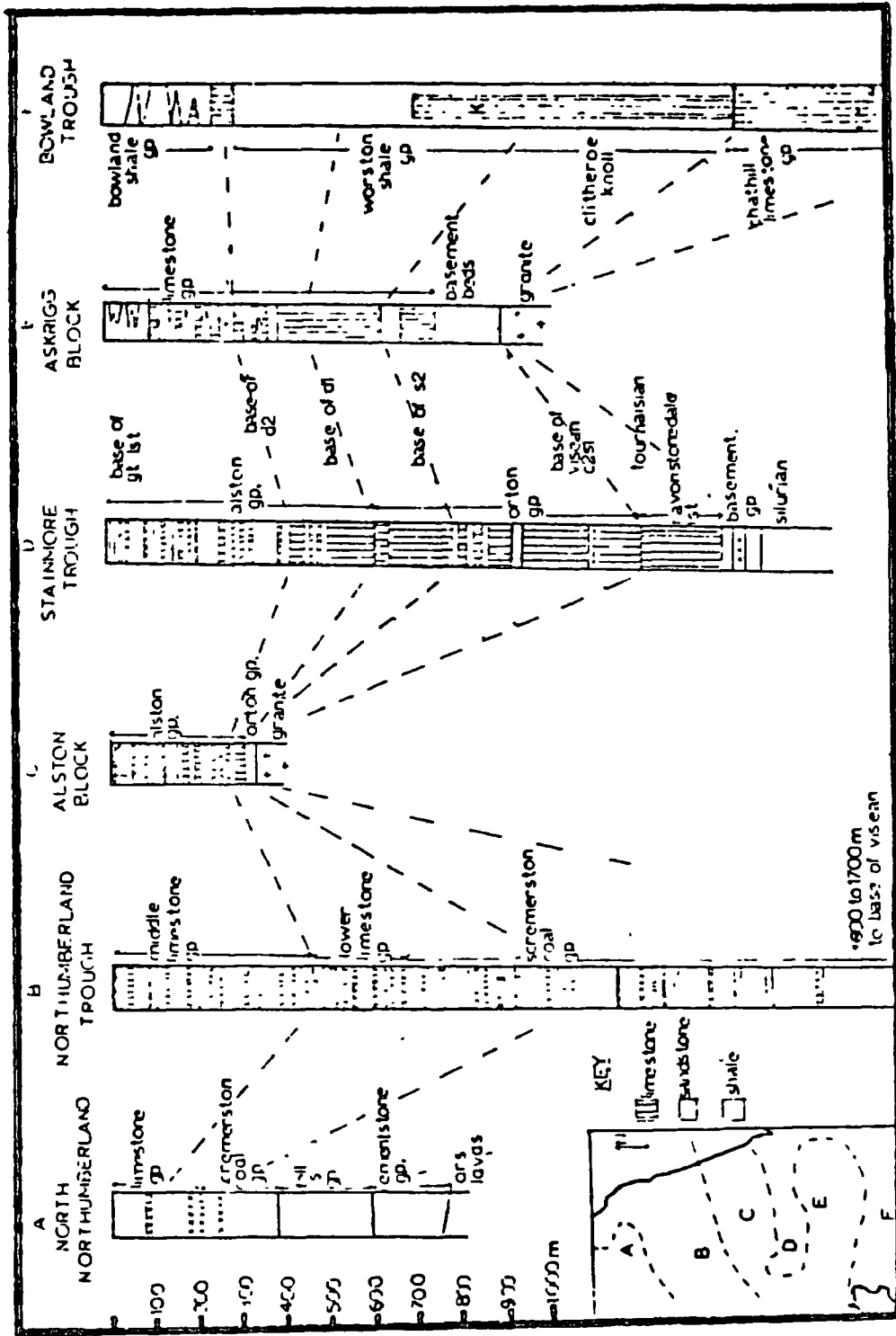
Sedimentation in the Lower Carboniferous was dominated by differential subsidence initiated in the early Tournaisian. Throughout the Tournaisian and early Visean there was continuous deposition in the Solway and Northumberland basins while the Southern Uplands, the Lake District and the Alston Block were above sea level and acted as a source of much of the sediment. The deposition was predominantly cyclic, alternating between bioclastic limestones or calcareous shales during transgression

and oolitic or calcitic mudstones in regression (Ramsbottom 1973). Subsidence rates varied, although sedimentation kept pace with it virtually everywhere and deposition throughout the Carboniferous was at or near sea level. The thickness of the Visean strata varies from 200 m on the Alston Block to over 1500 m in the Northumberland Trough (Fig. 1.3).

By the late Visean the blocks had subsided below sea level and differential subsidence ceased to be so conspicuous. A regional subsidence, however, affecting block and basin alike continued until the end of the Westphalian. Stephanian rocks are absent in northern England.

The Limestone Series was followed by the Millstone Grit Series, a period transitional from the marine estuarine conditions of the Dinantian to lagoon swamp conditions of the Westphalian Coal Measures and is also characterised by cyclic sedimentation. The Namurian in Northumberland and Durham does not have the thick development of coarse gritstone and marine shales seen in the southern Pennines. The mudstones and shales are replaced by limestones and calcareous shales and the grits are not as prominent. The Namurian is at least 500 m thick in the Northumberland Trough.

Cyclic sedimentation continued in the Westphalian Coal Measures and is mainly deltaic or estuarine in character. A complete cycle consists of a marine shale bed overlain by non-marine shale or



From British Regional Geology

Northern England
NERC/IGS 1971

4th Ed

Fig 1.3 Comparative section of Lower Carboniferous strata

mudstone, then sandstone, a rootlet bed or seatearth and a coal seam. Most cyclothe ms are incomplete and can vary from 1 to 30 m thick. The Lower and Middle Coal Measures total about 600 m in Durham and the eastern part of Northumberland (Taylor et al. 1971). The Upper Coal Measures are present in only two small areas, near Killingworth in Northumberland and just west of Sunderland. It is thought that about 150 m is preserved in these areas.

On the northern tip of the Isle of Man is a limestone group about 250 m thick which overlies 30 m of basal conglomerate. On the northern edge of the Solway Firth between Kirkcudbrightshire and Dumfries there are five small areas of the Lower Carboniferous. The thickest sequences are about 750 m each near Rerrick and Kirkbean. The thickness beneath the Solway basin is unknown but the modelling of gravity data suggests a total thickness for both the Permo-Trias and Carboniferous of between 2.5 and 4.9 km (Bott 1968).

Commercial wells on and around the Mid North Sea High indicate that the Carboniferous has been eroded during post Carboniferous uplift and as a result thins eastwards

At the end of the Carboniferous a substantial intrusion of quartz dolerite occurred as the Whin Sill complex (295 my +/- 6 my Fitch and Miller 1967). It has a maximum thickness of about 73 m but probably averages from 25 to 30 m thick. Its total area must be

at least 5000 km². There are four major groups of dykes forming a single petrographic province with the Sill. They all trend roughly east-north-east and are, from north to south, the Holy Island, Lewisburn-High Green, St Oswald's Chapel and Hett dyke echelons.

The tensional regime that gave rise to both the differential and regional subsidence is believed to have been caused by Hercynian plate processes to the south, although the relationship between the two is uncertain (Leeder 1982, Bott et al. 1984).

Uplift and erosion caused by the Hercynian orogeny brought the Carboniferous to a close.

1.2.4 Permo-Trias

The correlation of the Permian and Triassic strata of the region is complicated by rapid changes in thickness and facies, by diachronous boundaries and the lack of fossils. It is therefore usual to treat the two together. The Permo-Trias outcrops occur on the north peninsula of the Isle of Man, in the Carlisle Basin, in southern Scotland and in County Durham. Offshore exposures are also known to exist in the Solway Firth (Wright et al. 1971) and on the Mid North Sea High (Day et al. 1981). Comparative sections are shown in Fig. 1.4.

The Lower Permian was generally a time of subaerial erosion with

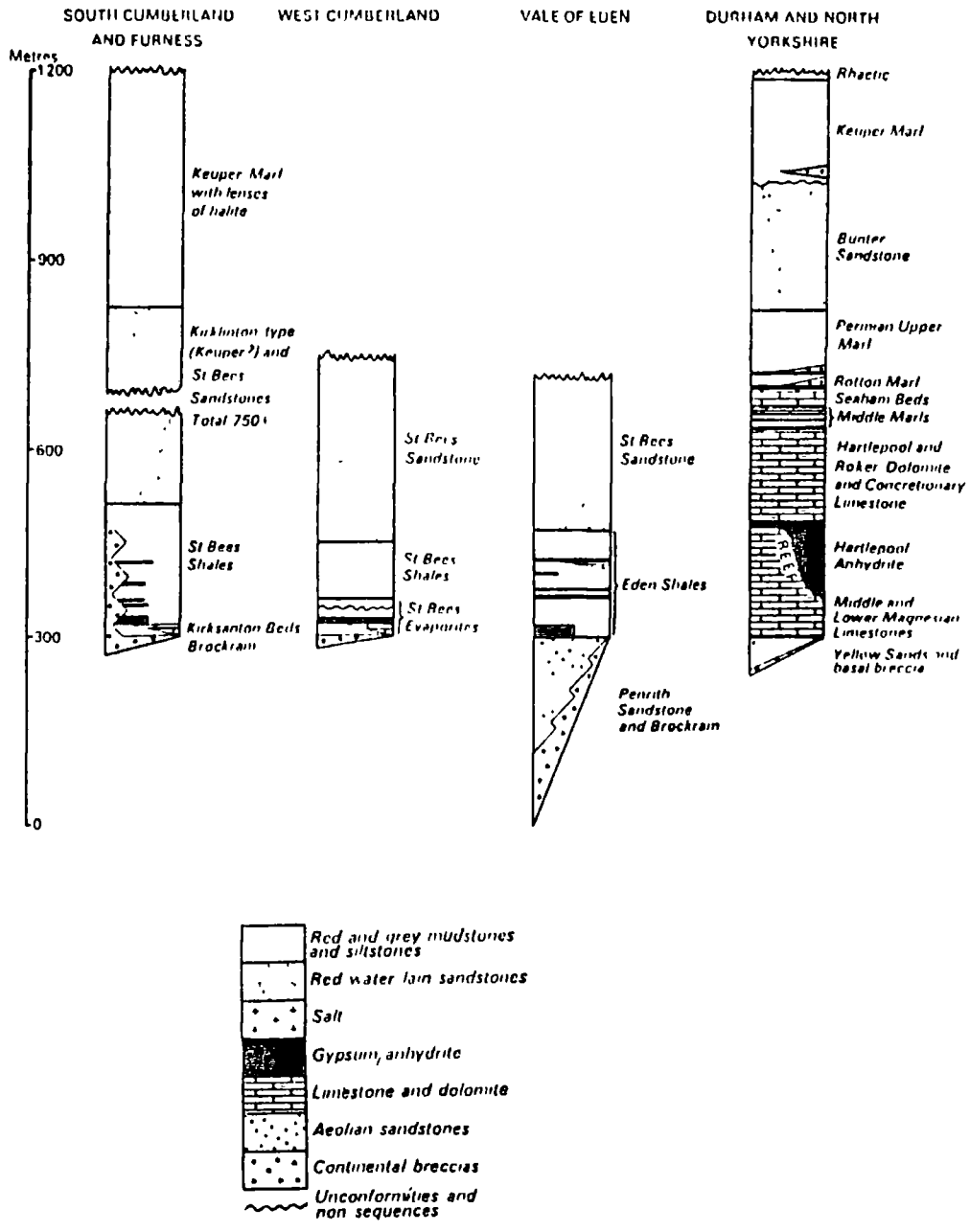


Fig 1.4 Comparative section of Permo-Trias strata

newly raised areas being deeply dissected (Smith et al. 1974). The early sediments were largely coarse water-lain breccias with the deepest parts of the largest basins including lenses of red playa-type mudstones and siltstones. In Durham it is represented by 60 m of a weakly cemented aeolian sandstone, the Yellow Sands. In the west near St Bees Head there is a thin basal breccia which contains fragments of Carboniferous Limestone.

The Upper Permian was ushered in by widespread transgression of the Bakevellia and Zechstein Seas in the Irish and North Seas respectively. These deposits included carbonates and sulphates which, in the Bakevellia Sea, were interbedded with clastic semi-continental deposits.

In Durham and just offshore Durham the Zechstein comprises up to 300 m of evaporites and magnesian limestone. Above this there is between 150 and 400 m of the Permian Upper Marl and the Triassic Bunter Sandstone and Keuper Marl. A little further north on the Mid North Sea High the Zechstein is believed to be more patchily developed probably due to a certain amount of relief during deposition.

In the Carlisle Basin the lower Permian breccia is overlain by the St Bees evaporites which in turn are overlain by the St Bees Shale. Above this is the Triassic water lain St Bees Sandstone, the Kirklington Sandstone and the Stanwix Shales, the latter being the equivalent of the Keuper Marl elsewhere. The total

thickness is unknown.

There are several Permo-Trias basins in southern Scotland to the north-west of Carlisle. They largely consist of red sandstone and breccias and are estimated by gravity survey to be at least 1 km deep (Bott and Masson-Smith 1960, Gregg et al. 1971)

The Triassic is brought to an end by the Rhaetic transgression.

1.2.5 Remaining Mesozoic

The only exposure of Mesozoic sediments on land is a small outlier of Lower Liassic dark shales just west of Carlisle.

Borehole and seismic surveys (Day et al. 1981) show that the early Jurassic is thin or non-existent on the Mid North Sea High, but that Upper Jurassic Kimmeridgian sediments were deposited in a shallow marine environment and are about 45 m thick under the eastern end of the line. This deposition was terminated in the early Cretaceous by the late Cimmerian phase of tectonic activity affecting all of the High. After this there was a widespread transgression throughout the Upper Cretaceous and Tertiary and a return to marine conditions. There are approximately 500 m to 600 m of Cretaceous sediments on the High.

1.2.6 Tertiary

The history of northern England and southern Scotland during the Tertiary era is poorly known. The only rocks remaining are the basic dykes associated with the volcanic complex of Mull. Their strike varies from south-east in Scotland to east-south-east as they are traced further south. The most southerly example is the Cleveland dyke in Yorkshire.

On the Mid North Sea High about 500 m of Tertiary sediments exist under the eastern end of the CSSP line.

1.2.7 Recent

The glacial periods in the Pleistocene were responsible for much of the topography as it is seen today. Ice sheets have on several occasions covered the area, which on retreating left clays, sands and gravels and extensive areas of boulder clay. Much of this still covers the area. Its thickness varies considerably and rapidly and is known to reach at least 60 m in the Irish Sea (Wright et al. 1971).

1.3 Solway Firth Basin

The Solway Firth Basin is an Upper Palaeozoic and Mesozoic basin. The edges can be seen in the Carboniferous deposits along the coast of southern Scotland and the Cumbrian coast, and the

Carboniferous and Permo-Trias deposits on the northern tip of the Isle of Man. Offshore the subcrop geology has been determined by a combination of shallow seismics and drilling (Wright et al. 1971). The total thickness of sediments in the basin has been determined from the gravity data to be between 2.5 and 4.9 km (Bott 1968) but how much of this is represented by the Permo-Trias is unknown. A borehole on the northern tip of the Isle of Man at Point of Ayre has proved at least 785 m of Triassic rocks (Gregory 1920). A seismic refraction line in the vicinity of the gravity minimum identified 1.3 km of rocks of velocity of 3.64 km/s underlain by a velocity of 4.38 km/s. It is difficult, however, to distinguish between the Permo-Trias and Carboniferous on the velocity alone (Blundell et al. 1964).

The northern edge of the Permo-Trias basin is mainly controlled by north-east/south-west faulting although on the north-west margin the sediments may unconformably overlap folded and faulted Upper Palaeozoic rocks (Wright et al. 1971). Evidence from several boreholes on the Isle of Man suggests the southern edge is also strongly faulted (Gregory 1920).

There is a negative magnetic anomaly associated with the gravity low but it cannot be attributed to uniformly magnetised Lower Palaeozoic rocks (Bott 1968). Al-Chalabi (1970) interpreted this anomaly in terms of Precambrian basement relief with a maximum depth of 9.4 km.

1.4 Carlisle Basin

The Carlisle Basin is a broad downwarp around the eastern end of the Solway Firth. It contains thick deposits of Upper Permian and Triassic sediments with some Lower Permian aeolian sands in the south-east and dark shales and argillaceous limestones from the Liassic to the west of Carlisle. The maximum thickness of the Permo-Trias is not known although 474 m have been proved in a borehole at St Bees Head (Fig. 1.4). The thickness of Carboniferous rocks under the Carlisle Basin is also unknown although, a borehole at Maryport on the southern edge of the Permo-Trias outcrop has proved more than 500 m of the Namurian. Another borehole near Aspatria indicates about 300 m of concealed Upper Coal Measures beneath the Permo-Trias on the southern edge of the Basin.

A seismic refraction survey by Swinburn (1975) based on the time-term method suggests that the basin might be as deep as 3 km towards the eastern end near Carlisle. Laving (1971) interpreted the Carlisle magnetic anomaly as either a plug shaped intrusion or lopolith at a depth of 4 km.

1.5 Northumberland Trough

The Northumberland Trough is a Carboniferous basin between the Cheviot volcanic pile to the north and the Alston Block to the south. The boundary with the Alston Block is marked by the

Stublick Faults and the Ninety Fathom Fault. The Stublick Faults acted as hinge lines during the Lower Carboniferous and the succession thickens across the Faults from about 450 m on the Alston Block to about 2450 m in the Northumberland Trough. Further east in the Durham coalfield a 12 mgal gravity drop across the Ninety Fathom fault also suggests a 2 km thickening of the Lower Carboniferous (Bott 1961). Seismic refraction data (Swinburn 1975) suggests the Trough contains a maximum of 3 to 4 km of Carboniferous rocks near the coast, thinning to less than 1 km to the east of Carlisle.

1.6 The Mid North Sea High

The Mid North Sea High is a broad Palaeozoic ridge which separates the Southern North Sea Basin from the Forth Approaches (Donat o et al. 1983). The oldest sediments are of Middle-Upper Devonian age and are conformably overlain by Carboniferous sediments. The thickness of these deposits is unknown. From the early Permian to the Jurassic the high was a positive feature affecting sedimentation and resulting in condensed sequences and areas of non-deposition. Seismic reflection data (Day et al. 1981) shows that the only significant deposits from this period are approximately 200 to 300 m of the Zechstein. Marine conditions returned over much of the High in the Upper Cretaceous after the Late Cimmerian phase of tectonic activity. Under the eastern end of the CSSP line there are now about 500 m of Upper Cretaceous sediments and 600 m of Tertiary and Quaternary

deposits.

1.7 Seismic structure

Seismically the crust can be divided into two types, continental and oceanic crust. The continental crust shows considerable variability in structure. The upper continental crust, however, is generally characterised by large thicknesses of rocks with velocities in the range 5.8 to 6.5 km/s. The total crustal thickness also varies considerably but has an average value of between 35 and 45 km. The oceanic crust is 5 to 7 km thick on average and has only thin layers with velocities between 5.9 and 6.4 km/s. The middle and lower oceanic crust has velocities usually in excess of 6.6 km/s.

Refraction surveys performed in Britain indicate that the crust is continental in character with a thickness in the range 25 to 30 km which is significantly thinner than average. A summary of the main crustal refraction surveys is shown in Figs. 1.5 and 1.6.

The Lithospheric Seismic Profile in Britain (LISPB) of 1974 has been the largest and most detailed refraction survey in the U.K. (Bamford et al. 1976). It extended from off Cape Wrath in Scotland to the English Channel beyond Portland Bill crossing many of the structural trends at right angles. It crosses the CSSP profile at Spadeadam on the Cumbrian/Northumberland border.

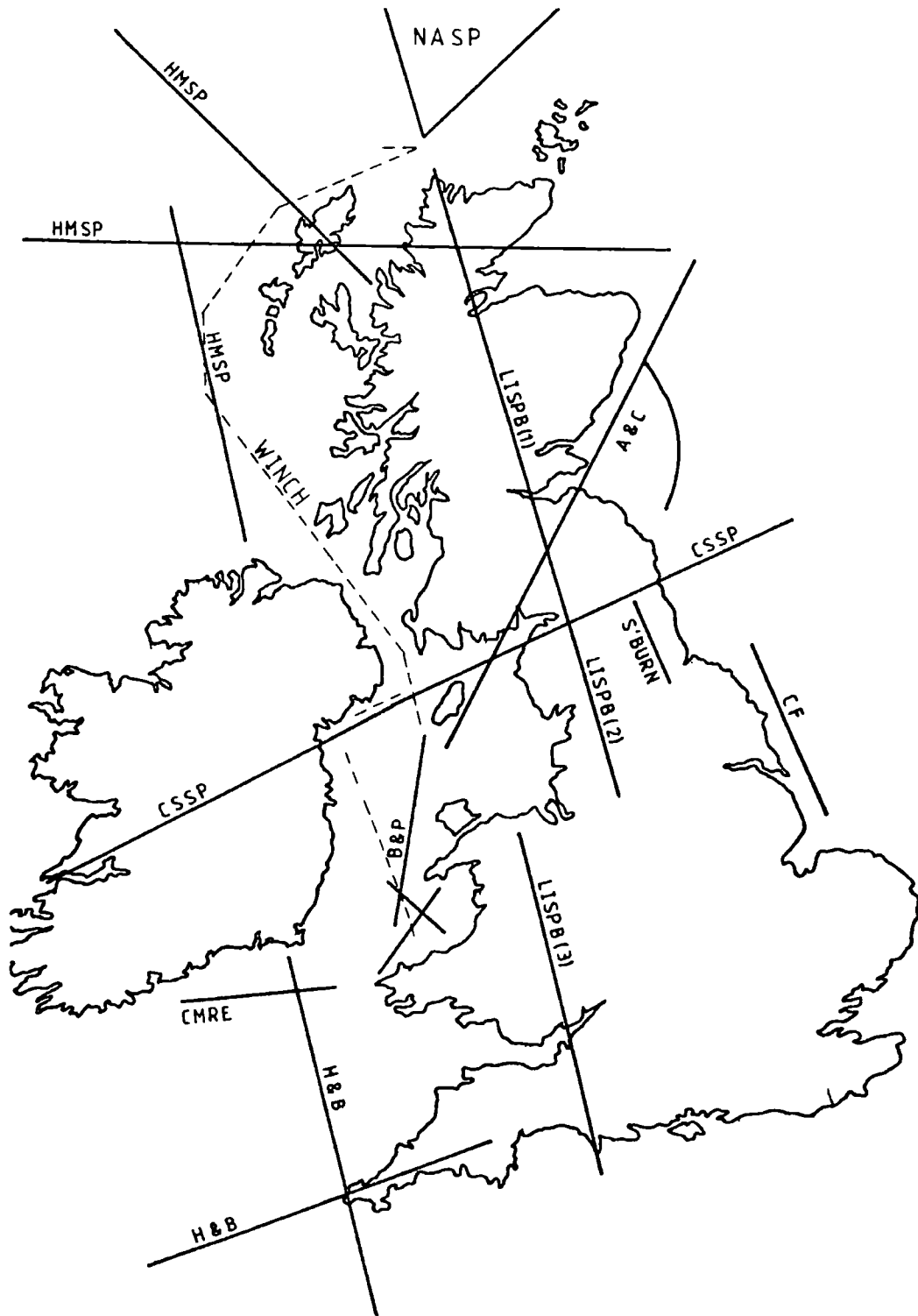


Fig 1.5 Location of seismic surveys performed in the British Isles. A & C = Agger and Carpenter (1964), CF = Collette et al. (1967,1970), LISPBI = Bamford et al. (1976, 1977 & 1978), CMRE = Bamford (1971,1972), Bamford and Blundell (1970), B & P = Blundell and Parks (1969), H & B = Holder and Bott (1971), S'BURN = Swinburn (1975), HMSP = Armour (1978), NASP = Bott et al. (1974,1976), Smith and Bott (1975)

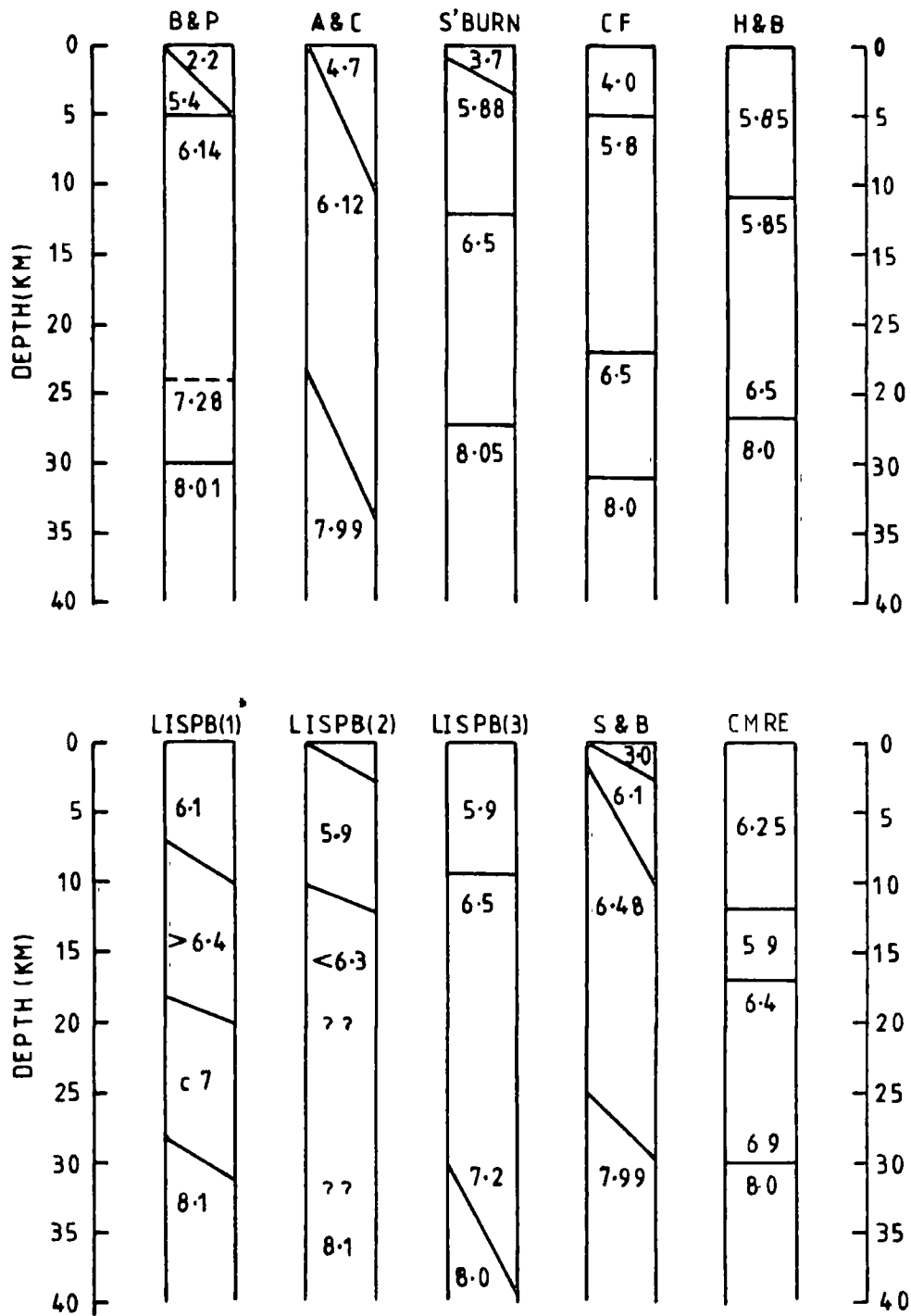


Fig 1.6 Summary of P-wave velocity structure of the crust from the surveys shown in fig 1.5

The line is divided into two halves and to date results from only the northern half covering Scotland and northern England have been published (Assumpcao and Bamford 1978, Bamford et al. 1976, 1977 and 1978).

The results of LISPB show strong differences in the crustal structure to the north and south of the Southern Uplands Fault (Fig. 1.7). To the north a three fold division of the crust is proposed. The upper crust is represented by velocities between 6.1 and 6.2 km/s which are interpreted as Caledonian belt metamorphics. Beneath this, at depths of 10 km to 20 km, the middle crust has velocities between 6.4 and 6.5 km/s, these are generally regarded as granulite facies Lewisian basement rocks (Smith and Bott 1975, Hall 1978). The velocity of the lower crust is about 7.0 km/s. The Moho is at a depth of 24 km under the northern end increasing to 34 km under the Midland Valley and the sub-Moho velocity is approximately 8.0 km/s. To the south of the Southern Upland Fault the upper crust is believed to consist of a maximum of 15 km of Lower Palaeozoic rocks of velocity 5.8 to 6.0 km/s beneath a thin veneer of Upper Palaeozoic and Mesozoic sediments. Beneath the Lower Palaeozoic a layer of velocity 6.28 km/s is present. There is uncertainty as to whether this is a significantly lower velocity than the 6.4 km/s layer to the north, nevertheless it has been suggested that it may represent a different pre-Caledonian basement south of the Iapetus Suture similar to the Pentevrian basement province of Brittany (Bamford et al 1977). Because no prominent arrivals were identified from

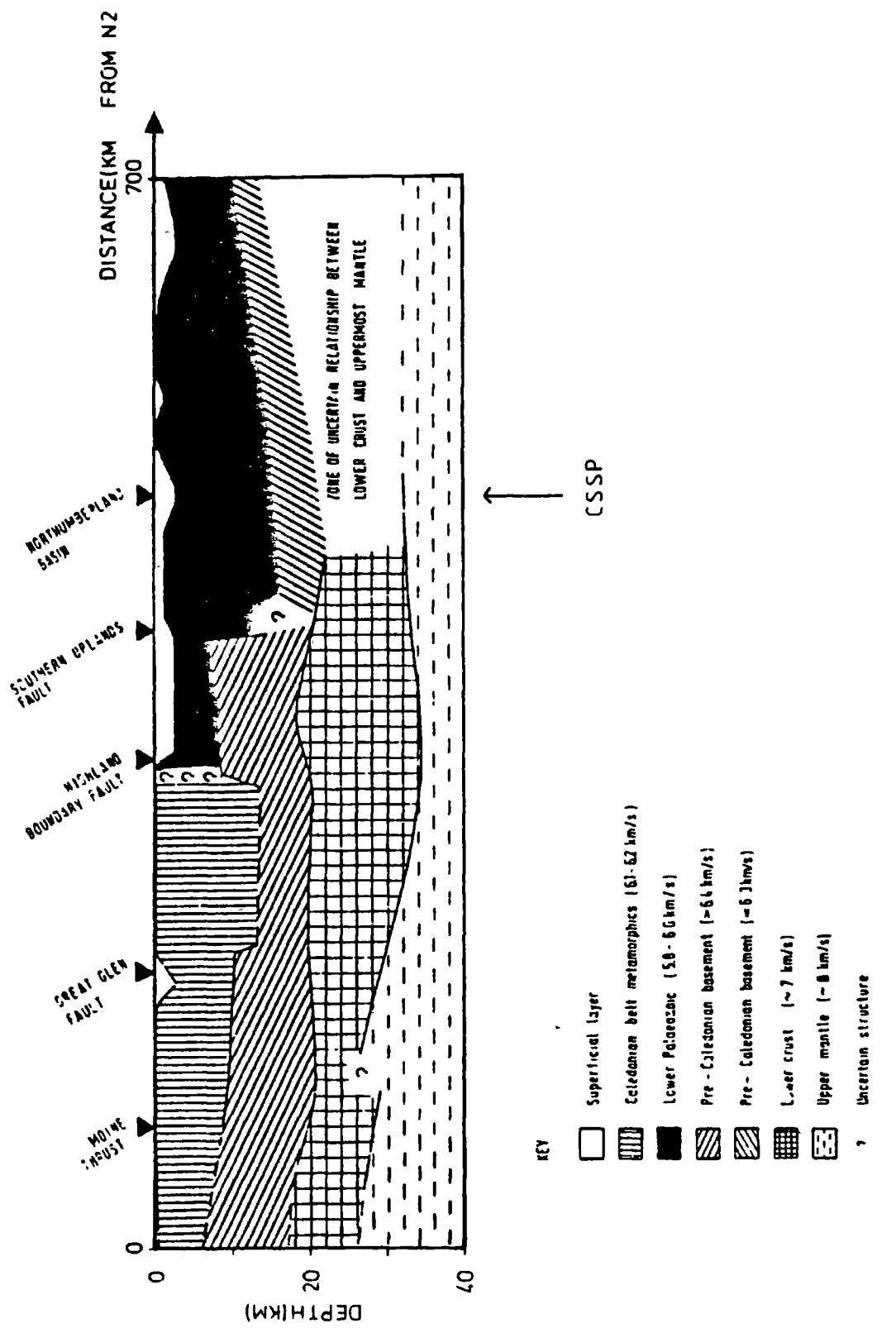


Fig 1.7 Cross-section through the crust of northern Britain from LISPB (from Bamford 1978)

the lower crust or Moho south of the Southern Uplands Fault no structure for this region has been given.

Swinburn (1975) used the LISPB shots on a north-south refraction line running parallel to but east of the LISPB line in northern England. His results contrast with the LISPB data in showing good arrivals from the Moho and a lower crustal velocity of 6.5 km/s below a discontinuity at about 12 km. His upper crustal velocity of 5.88 km/s is in agreement with LISPB. Two surveys in the Irish Sea suggest slightly higher velocities for the upper crust. Blundell and Parks (1969) found a velocity of 6.14 km/s at a depth of about 4 km in the south Irish Sea whilst Agger and Carpenter (1964) found a similar velocity of 6.12 km/s in the north Irish Sea. Neither indicate any mid-crustal layer although Blundell and Parks (1969) found a lower crustal layer of velocity 7.3 km/s at a depth of 25 km.

The existence of low velocity layers has been widely reported in continental areas (Mueller and Landisman 1966, Landisman et al. 1971, Prodehl 1970), but apart from south-west of Ireland (Bamford 1972) and near Dunany Point on the west coast of Ireland (Jacob in press) there have been few examples quoted in Britain. The nature of the refraction method makes the positive identification of such layers difficult and it is felt that the differences may have much to do with prejudice (Healy 1971).

Several cases of velocity anisotropy in the continental crust and

upper mantle have been reported but they have not raised a great deal of interest. Generally seismological observations have not been of sufficient resolution to produce good quality measurements of anisotropy. A good discussion of the topic can be found in Bamford and Crampin (1977) and Crampin et al. (1984).

Over the last few years BIRPS has produced the first good quality deep seismic reflection profiles around Britain. The WINCH sections, in general, show a seismically transparent upper crust with the lower crust shown as a zone of discontinuous reflections (Brewer et al. 1983). This is a feature of the continental crust found elsewhere (Healy 1971 Smithson and Brown 1977). The WINCH profile crosses the CSSP line east of the Isle of Man (Fig. 1.5) where the reflections from a depth of 15 km to the Moho are particularly strong. A zone of reflections in the lower crust dipping northwards from the north Irish Sea has been tentatively correlated with the Iapetus Suture (Brewer et al. 1983).

1.8 Composition of the crust

The continental crust is clearly more complicated than either refraction or reflection surveys suggest (Smithson and Decker 1974 Smithson and Brown 1977). Mueller (1977) describes the upper crust as composed of crystalline schists, banded gneisses and migmatic rocks which surround a series of lenticular or mushroom shaped metamorphic granitic bodies. With signal wavelengths of about a kilometre used in refraction surveys, however, it is not

surprising that much of the crust appears seismically homogeneous.

Rocks from the upper crust with velocities from 5.8 to 6.5 km/s are probably represented by acidic-intermediate igneous rocks, low grade metasediments and quartzo-feldspathic gneisses (Hall 1978). Rocks of velocity 6.4 to 6.5 km/s are demonstrably quartzo-feldspathic granulites in some cases (Smith and Bott 1975) and may well also represent rocks beneath the Conrad Discontinuity. Mueller (1977) suggested that the Conrad Discontinuity is a laminated high velocity layer of amphibolites only a few kilometers thick, although others have dismissed amphibolites as a major part of the crust because their velocities are too high (Smithson and Brown 1977). Smithson and Brown (1977) point out that intermediate granulites and pyroxene granulites have velocities of 6.6 to 7.0 km/s and >7.0 km/s respectively at pressures of 6 kbar (depths of 20 km); velocities commonly observed in the lower crust.

The Moho has a uniform velocity rarely falling outside of 7.8 to 8.1 km/s and is almost certainly a chemical and not a physical boundary (Upton et al. 1983). Hale and Thompson (1982) noticed that reflection profiles show zones of laminated discontinuous reflections and suggested this indicates a far more complicated transition zone of layered basic and ultramafic rocks than had been previously thought.

Knowledge of the shear wave velocity and hence Poisson's ratio would help in deciding between different rock types (Hall 1978). Measurements of shear wave velocities, however, are not common and only a few have been made. Assumpcao and Bamford (1978) examined shear waves recorded during LISPB and determined an average Poisson's ratio for the crust close to 0.25, except in the upper crust south of the Southern Uplands Fault (0.231) and in the middle crust under the Midland Valley (0.221). Laboratory measurements of shear wave and compressional wave velocities for different rock types at various pressures are listed in Table 1.1. Further laboratory measurements and field measurements of rock velocities can be found in Birch (1960) and Press (1966).

1.9 Gravity and magnetics

The Bouger gravity anomaly map for northern England southern Scotland and adjacent marine areas is shown in Fig. 1.8 and the Bouger anomaly profile along the CSSP line is shown in Fig. 1.9. The pattern on land and in the Irish Sea is dominated by negative anomalies. The prominent ones are either sedimentary basins such as in the Solway Firth, the south Irish Sea and Luce Bay or granite bodies such as the Weardale, Criffell and Cheviot granites. In the Irish Sea these lows are superimposed on a 40 mgal regional high which has been attributed to a thinning of the crust (Bott 1968). The North Sea generally shows smaller anomalies and gentler gradients. Interesting features include a north-south linear 8 mgal gradient which crosses the CSSP line

TABLE 1.1

Compressional and shear wave velocities of rocks at different pressures (from Christensen 1982).

Rock type	Wave type	Density gm/cc	Pressure (kbar)					
			0.1	0.5	1.0	2.0	4.0	6.0
Sandstone	P	2.03	3.28	3.72	3.95	4.22	4.59	4.87
	S		1.86	2.19	2.28	2.32	2.34	2.33
Sandstone	P	2.29	4.42	4.68	4.73	4.82	4.94	5.01
	S		2.72	2.87	2.92	2.95	2.99	3.01
Sandstone	P	2.40	3.84	4.58	4.75	4.85	4.94	5.01
	S		2.43	2.81	2.91	2.96	2.99	3.01
Limestone	P	2.66	5.62	-	5.68	5.72	-	-
	S		3.01	-	3.09	3.10	-	-
Greywacke	P	2.69	-	6.14	6.19	6.23	6.28	-
	S		-	3.63	3.65	3.68	3.71	-
Granulite	P	2.63	5.26	5.66	5.80	5.95	6.09	6.14
	S		3.11	3.27	3.34	3.43	3.50	3.52
Granulite	P	2.71	-	-	6.06	6.17	6.31	6.41
	S		-	-	3.31	3.39	3.51	3.58
Granite	P	2.63	5.26	5.66	5.80	5.95	6.09	6.14
	S		3.11	3.27	3.34	3.43	3.50	3.52
Andesite	P	2.64	5.08	5.17	5.27	5.48	5.57	5.58
	S		3.05	3.09	3.12	3.19	3.25	3.25
Granodiorite	P	2.67	5.91	6.24	6.34	6.41	6.47	6.51
	S		3.26	3.34	3.38	3.43	3.47	3.47
Anhydrite	P	2.93	-	-	6.00	6.06	6.15	6.19

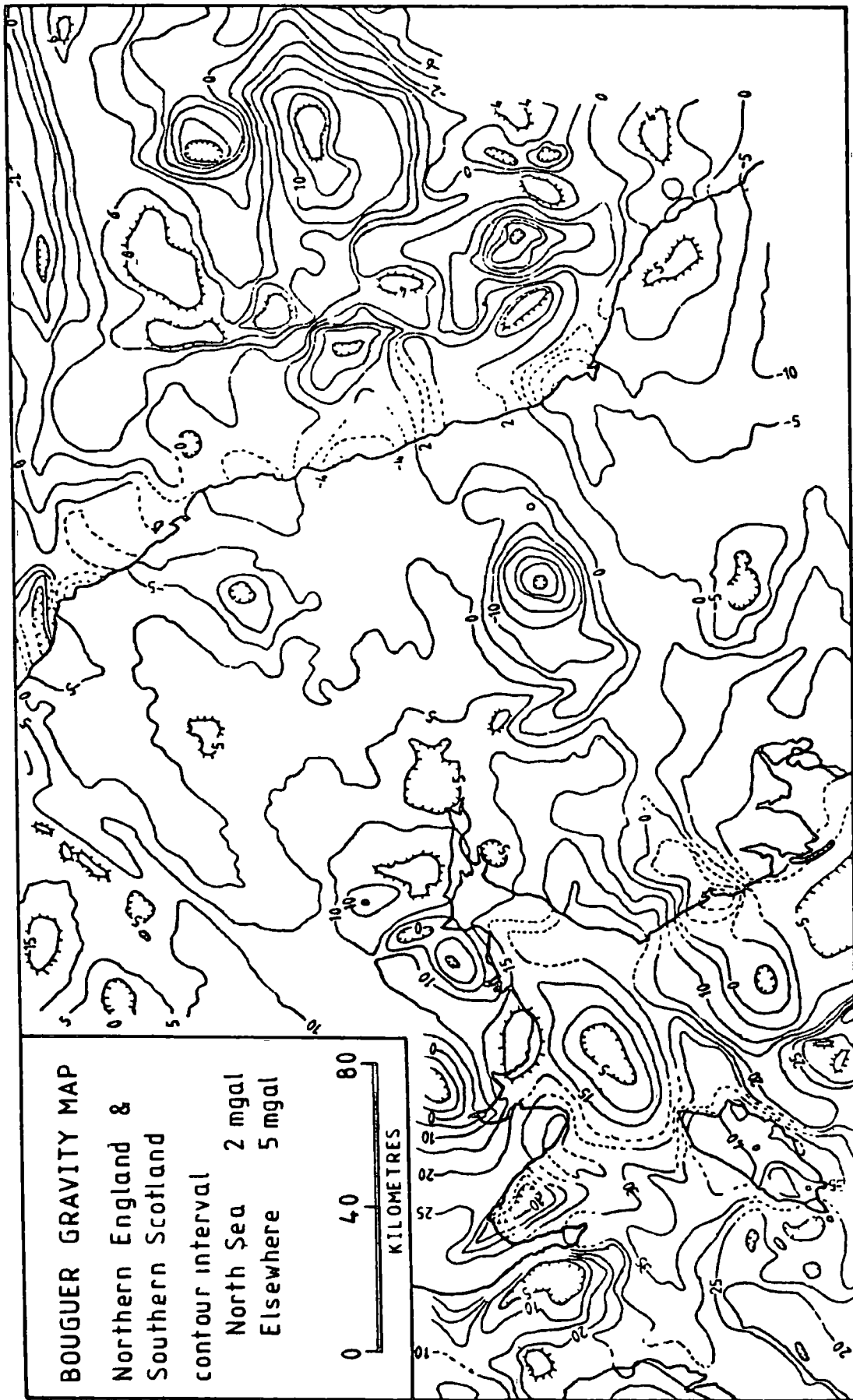


Fig 1.8 Bouguer gravity anomaly map of northern England, southern Scotland and adjacent marine areas

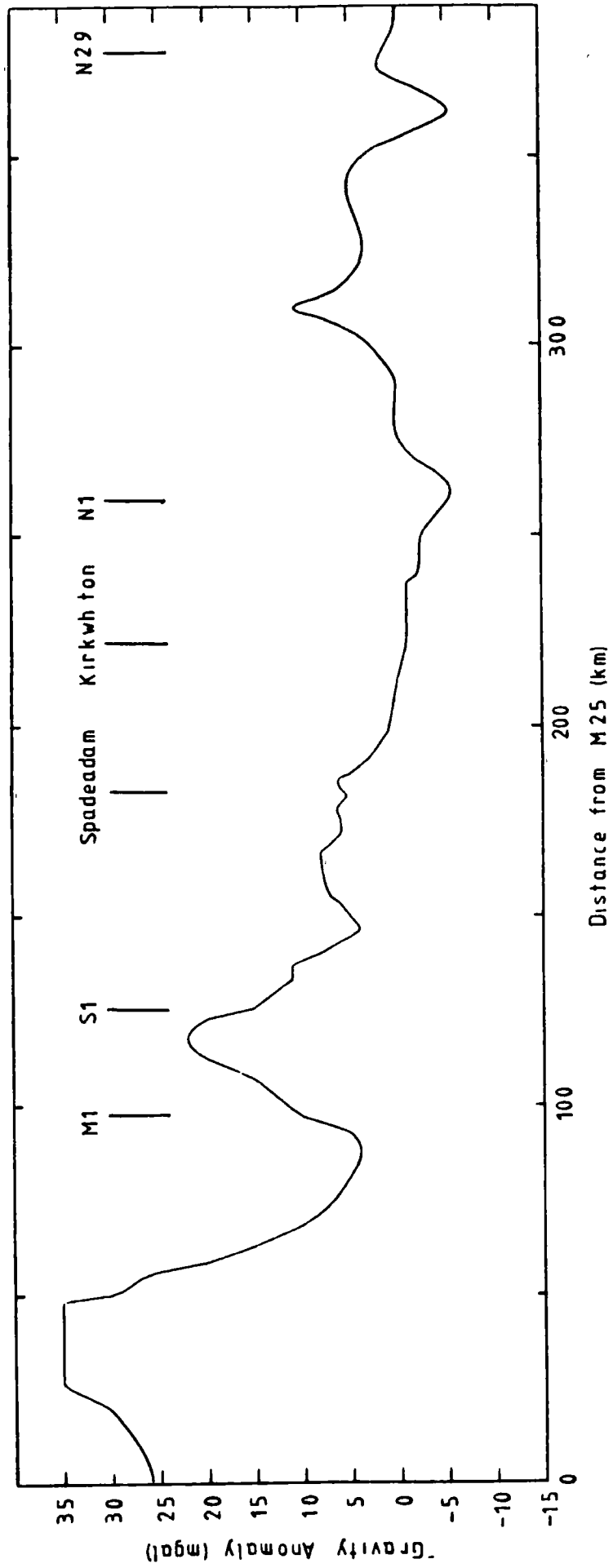


Fig 1.9 Profile of Bouguer gravity anomaly along the CSSP line

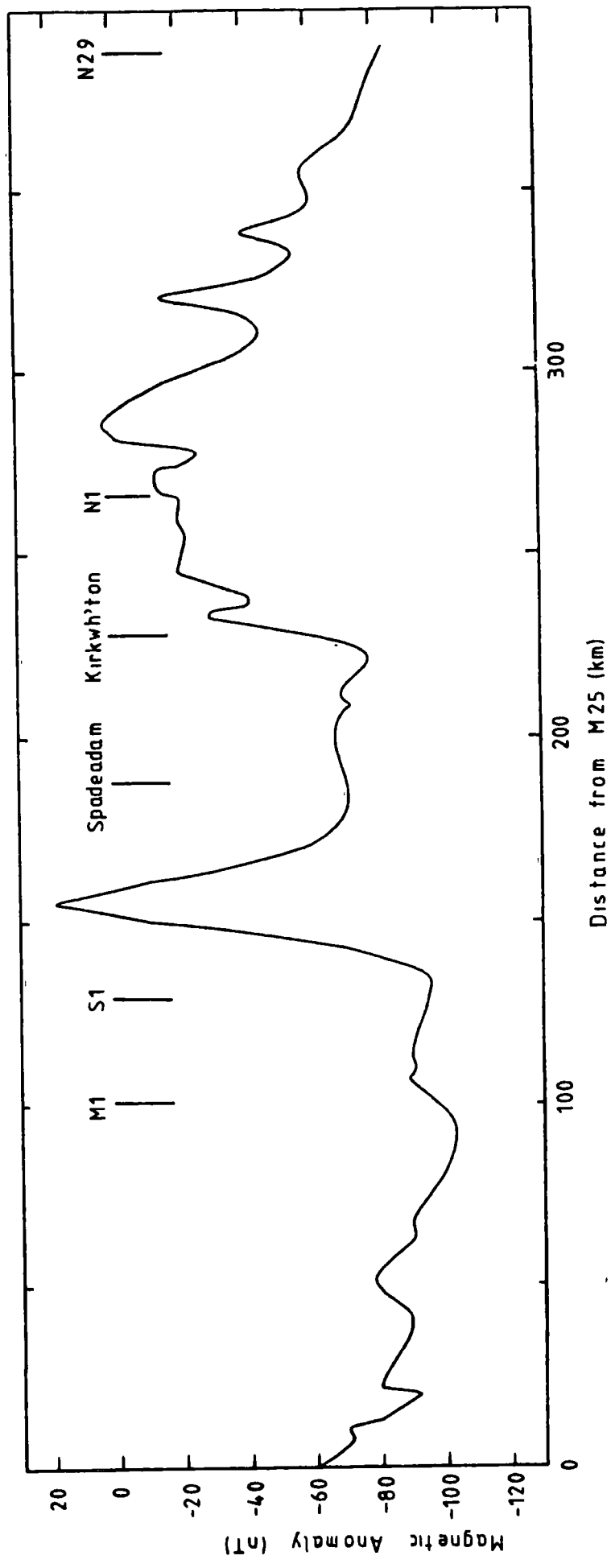


Fig 1.10 Profile of the magnetic anomaly along the CSSP line

and a negative anomaly at the end of the line thought to be a Caledonian granite (Donato et al. 1983).

The magnetic anomaly profile along the CSSP line is shown in Fig. 1.10. In the Solway Firth there is a magnetic low which has been interpreted by Al-Chalabi (1970) in terms of Precambrian basement relief at a depth of 9.4 km (see section 1.3). Further east under the Carlisle Basin a circular 100 nT positive anomaly is identified by Laving (1971) as a basic intrusion at a depth of approximately 4 km (see section 1.4). A 50 nT positive step in the magnetic anomaly near Kirkwhelpington is coincident with the outcrop of the Whin Sill. The continuation of this positive anomaly to the east is believed to be due to the existence of the Sill and associated Carboniferous dykes. Between Kirkwhelpington and the Northumberland coast the CSSP line is close to and parallel to the Causey Park Dyke, one of the St Oswalds Chapel en-echelon intrusions (Daley 1983).

1.10 Aims of the CSSP

The primary aim of the CSSP was to determine the velocity structure of the mid and lower crust in more detail than had previously been achieved. This was to be made possible with the large number of closely spaced shots and stations on a profile over as uniform an upper crustal structure as could be found. Within this broad aim and bearing in mind the preceding discussion it was hoped to answer some of the following more

specific questions.

- 1) Is there a mid-crustal discontinuity beneath northern England and is the velocity beneath it lower than that found under Scotland as suggested by LISPB (Bamford 1978) ?
- 2) Are strong moho reflections observed beneath northern England as suggested by Swinburn (1975) or are they weak or absent as suggested by LISPB ?
- 3) Do Lower Palaeozoic sediments comprise the entire upper crust or is there a shallow crystalline basement ?
- 4) Is there any evidence for the existence of oceanic crust left over from the Iapetus Ocean beneath northern England ?
- 5) What evidence is there for the existence of low velocity layers in the crust ?
- 6) What is the velocity depth distribution associated with the discovery by BIRPS of a seismically transparent upper crust and a highly reflective lower crust ?

This thesis concentrates on the shallow structure and the interpretation of the deep structure in Chapter 7 is only a preliminary interpretation. A full interpretation of the deep structure is being undertaken by A. H. J. Lewis.

CHAPTER 2 - DATA ACQUISITION

2.1 Introduction

The experiment was carried out over an eleven day period from Friday 2 July to Tuesday 13 July 1982. The shot firing was performed during the two weekends of the 3/4 July and 10/11 July using the NERC ship the RRS Shackleton (Sinha and Uruski 1982).

During the survey a total of 82 seismic stations were set up, although not all were in operation at the same time. Sixty stations occupied the main line from Dubmill Point on the Cumbrian coast to Druridge Bay in Northumberland, spaced at just over 2 km intervals (Fig. 2.1). The remainder were set up offline on the Isle of Man, southern Scotland, Weardale and along the Northumberland coast (Figs. 2.2 and 2.3). Two stations were sited on either side of the middle of the main line in order to investigate any possible side-swipe.

The equipment comprised Geostore recorders with Willmore MkIIIA seismometers loaned from NERC seismic equipment pool, Durham MkII and MkIII seismic recorders with Willmore MkII seismometers and cassette recorders from Durham and Reading Universities with HS10 seismometers.

It was intended that 60 shots of 150 kg at 4 km spacing should be fired in the Irish and North Seas. Shallow water near the

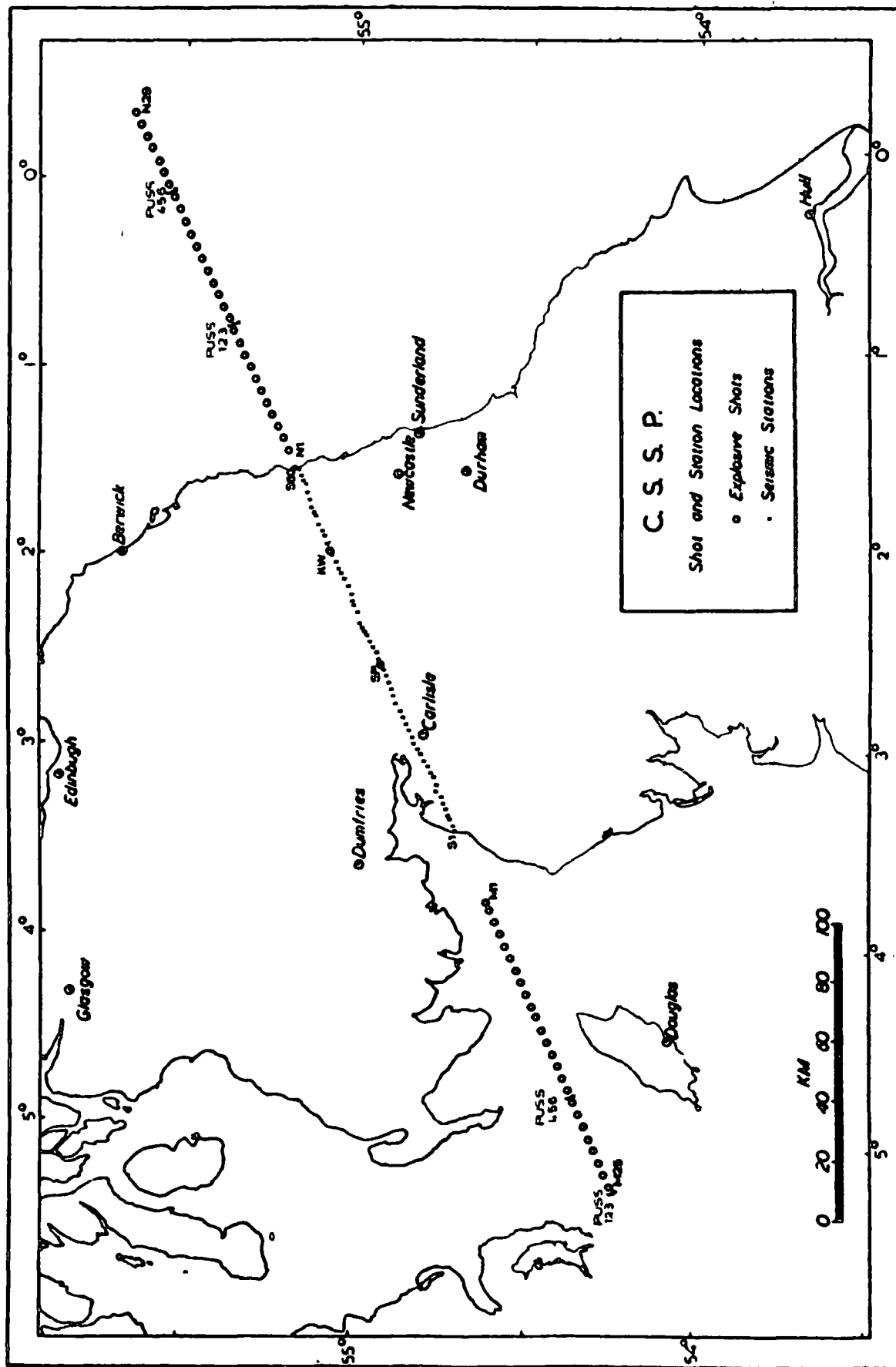


Fig 2.1 Station and shot locations for the main line

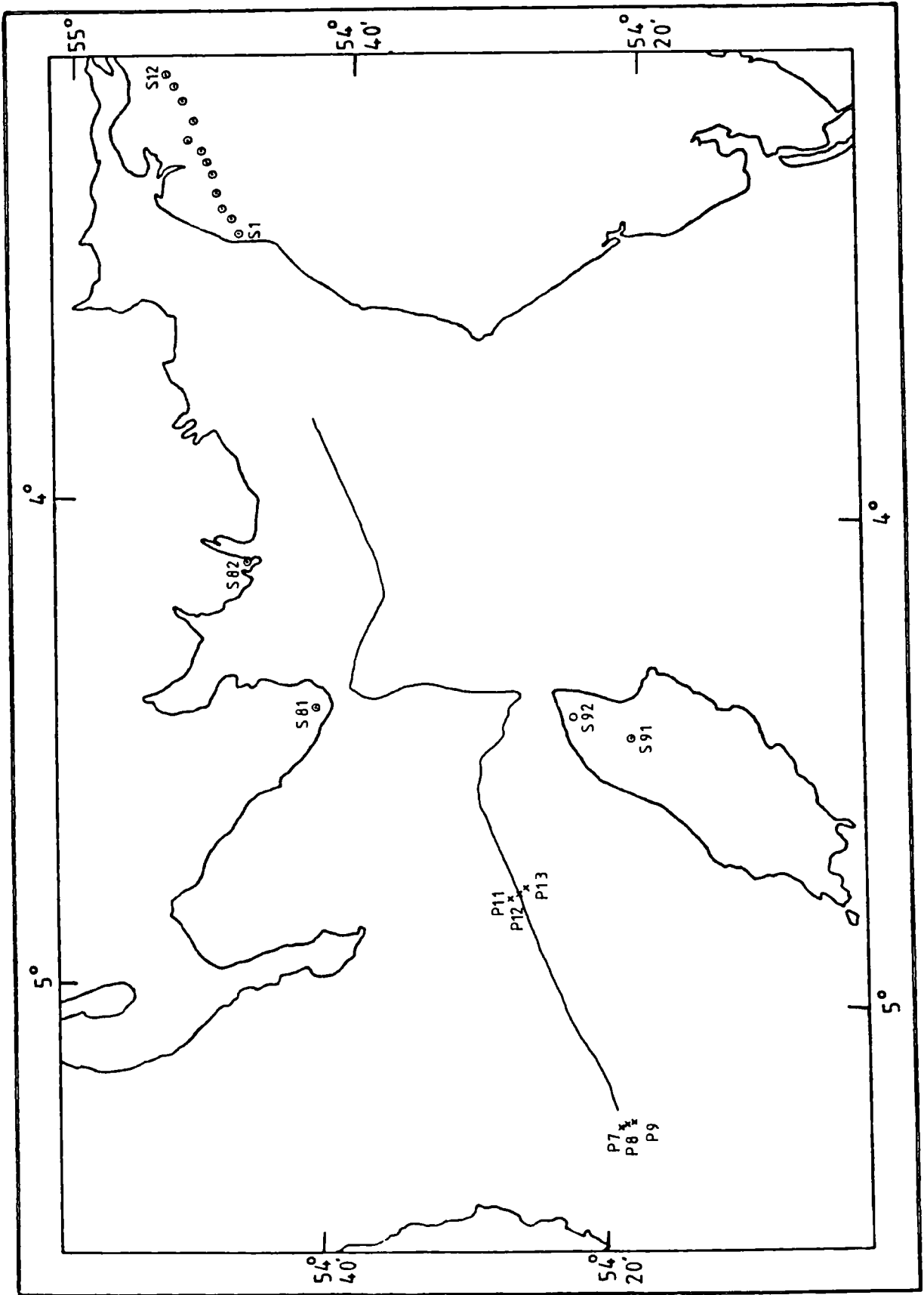


Fig 2.2 Station locations and airgun profile for the Irish Sea

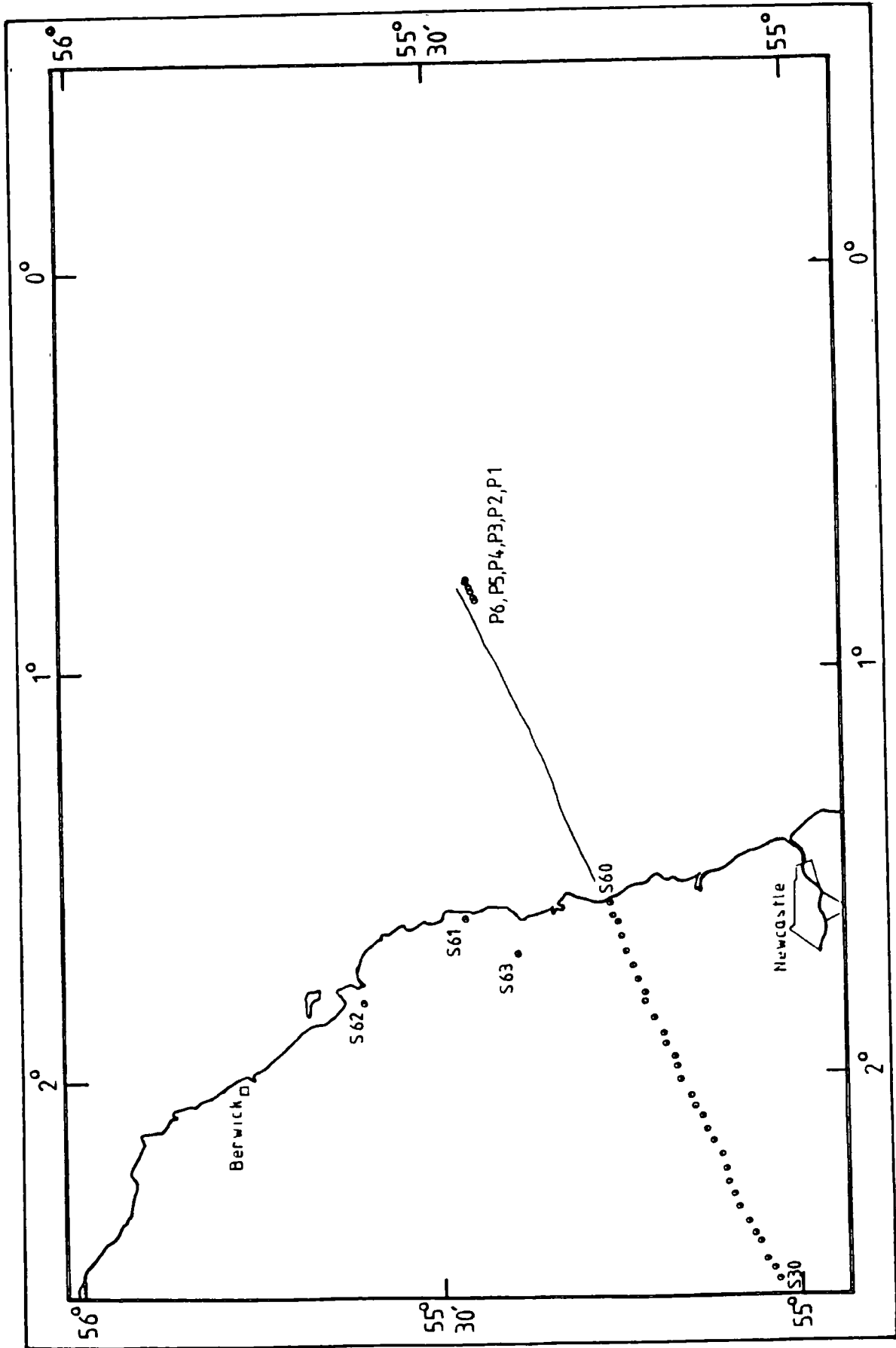


Fig 2.3 Station locations and 2nd airgun profile for the North Sea

Cumbrian coast, however, meant that five shots had to be omitted and coal mine workings under Druridge Bay caused the cancellation of another one. Shots M25 in the Irish Sea and N23 in the North Sea were repeated with 450 kg each (Fig. 2.1).

In addition to the above, two 100 kg shots were fired on land and 38 hours of airgunning were performed to provide details of the shallow structure both along and perpendicular to the profile.

Full details of the shot and station locations, the equipment used and the field tapes collected are tabulated in Appendix B. All the station and explosion shot locations are shown on a large map at the back of this thesis.

2.2 Seismic stations

The main line was selected to avoid towns, villages and industrial sites. The most problematical areas were Carlisle in the west and National Coal Board (NCB) mine workings under the east coast. Most work involved selecting and getting permission for the siting of the Geostore stations. As these were unmanned, it was important that their locations would be free from interference from man, beast or machine for two months. The six sites at which the Geostores were located also required protection for the recorders, batteries and an array of up to twelve aerials. Due to a shortage of radio links a seismometer

was located at these base stations wired directly into the recorder thus saving a radio link. Despite these limitations practically all the seismometers were sited within one kilometre of their intended positions.

The seismometers were placed in pits between 1 and 3 feet deep lined with 12 inch diameter P.V.C. piping. The top was covered with a plywood lid placed in a large plastic bag covered by turf and soil. The bottom of some of the pits was lined with concrete. The amplifier modulator unit was put in the seismometer pit but the battery was placed in a plastic bag and buried in an adjacent hole.

The sites chosen were based on three main criteria, that they be noise free, easily accessible and secure. Security proved not to be a problem despite the aerials advertising their presence. Accessibility, except in two situations, was also not a problem as the area is well covered by roads and tracks. Enviromental and cultural noise was more difficult to avoid. Sites away from roads, trees, and fields with animals or tractors in were not easy to find and close liaison with farmers was necessary to find fields that would be empty during June and July. An intimate knowledge of the farmer's year was required, especially with regards to stock movement, silage and barley.

It was hoped to place as many of the seismometers as possible on bedrock. In the central and eastern part of the line a large

number were placed on Carboniferous sandstone, with the remainder on boulder clay. It was found that both solid rock or boulder clay gave similar noise levels and that the presence of a concrete base had little effect. The western area is covered by glacial deposits and by post-glacial marine and fluviatile silts, sands and gravels. The noise levels were considerably higher than further east. Small hills tended to provide the worst locations because they were frequently capped with coarse gravels and sands but unfortunately these were difficult to avoid because the high land was needed for the radio links. It is difficult to see how such sites could have been avoided without moving the line a considerable distance to a less suitable location.

2.2.1 Geostore recorders

The Geostore equipment used was loaned from the N.E.R.C. seismic equipment pool. This totalled 10 Geostore recorders with sufficient seismometers, amplifier modulators and radio links for 57 stations. Fifty-five of the stations were deployed along the main line and the remaining two were sited a few kilometres on either side of the main line near its centre.

The Geostore recorder is a 14 channel F.M. recorder. There are two flutter channels, one channel recording the internally generated Vela-Standard time code and eleven data channels. One of the data channels can be used to record a radio transmitted time code as well as, or instead of, data. It was decided to use

this channel for the exclusive recording of the M.S.F. time code transmitted from Rugby. There are three recording speeds. The maximum speed of 15/160 in/s gives a recording time of 170 hours with a standard 2400 ft 1/2 inch tape. At this speed the recorder bandwidth is 0 - 32 Hz. It accepts F.M. data with a carrier centre frequency of 676 Hz and a maximum deviation of 40%.

Willmore MkIIIA seismometers of period 1 second were used.

The signal is modulated by an amplifier modulator (amp mod). This can amplify signals in the range of 250 mV (gain 1) to 0.25 mV (gain 10) to produce the maximum 40% deviation of the carrier. It was intended that gain settings for all stations should be the same in order to make processing of the data easier. A gain of 7 was generally found to be suitable for most sites, however, some of the noisy sites in the west often required lower gains.

The Geostore recorders occupied six sites, four of these sites had two recorders and three of these extra recorders were used as backups in case one should fail. The seismometers/amp. mods. at these six sites could be linked directly to the recorders, but the remaining 51 had to be connected through U.H.F. radio links (Fig. 2.4). Forty 25 kHz bands from 458 MHz to 459 MHz were used with some duplication to obtain the 51 links required.

These radio links were the weakest part of the operation. The transmitter and receiver units had to be strapped to the masts as

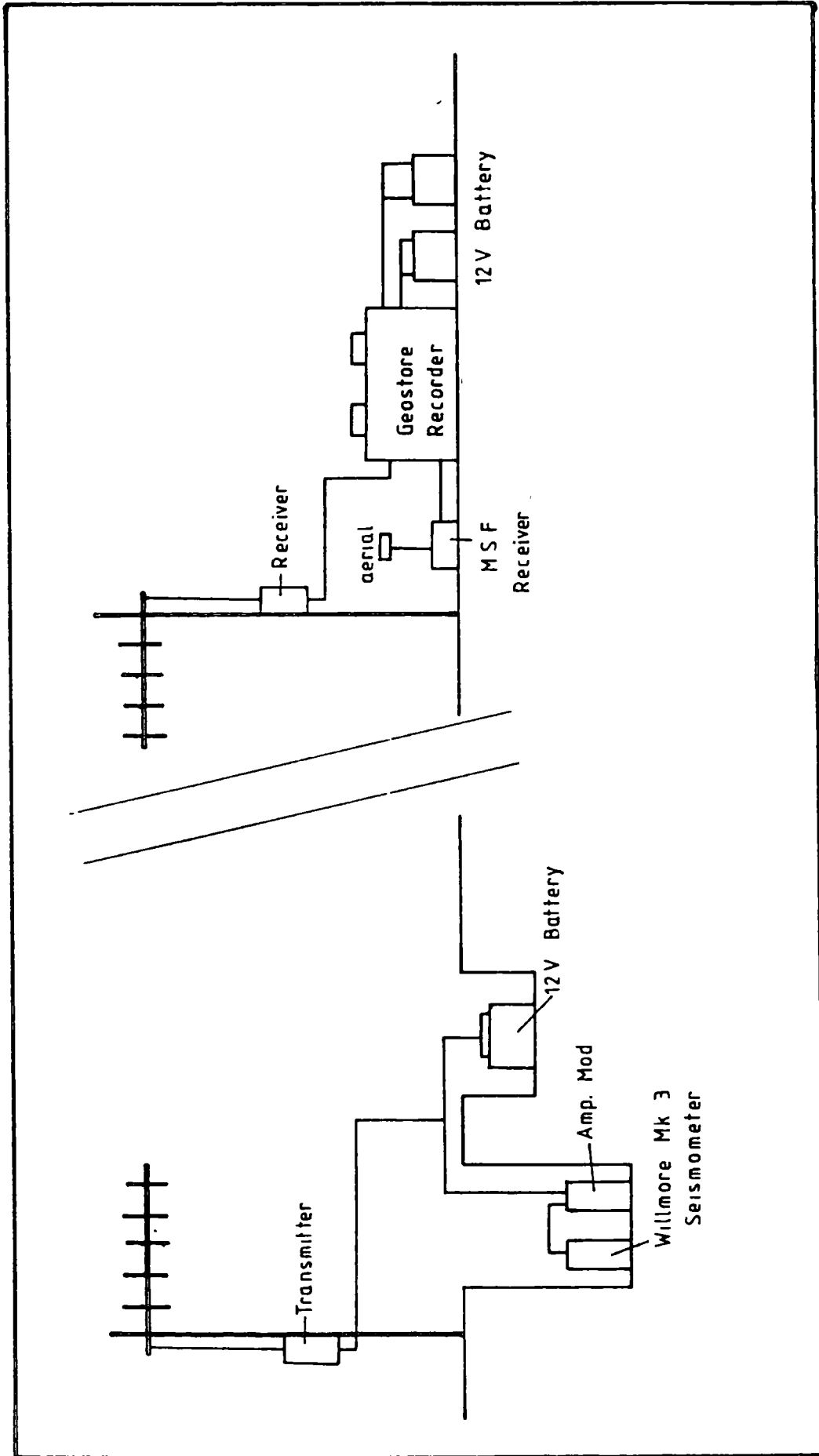


Fig 2.4 Diagram of Geostore recording system

the aerial leads were not long enough to reach the seismometer pit. The units were insufficiently robust to withstand the strong winds which were encountered and they needed repeated attention. The aerial masts were also unable to withstand strong wind unless under 2 m high. The line of sight requirement between the transmitter and receiver caused some problems. This could have been avoided, however, if sufficient radio links were available so that the Geostores could be located away from the line of the seismometer stations.

The Willmore seismometers appeared to perform well in the field but after the survey several were found to have bent spokes. This probably explains the odd response of some of the stations and has made it difficult to correct some seismograms for the effect of gain. They appear not to be as robust as is desirable for work involving frequent moves.

2.2.2 Durham MkII seismic recorders

The Durham MkII seismic recorder (Wooden Box) is a three component FM recording set (Long 1974). Wooden Boxes were deployed with Willmore MkII seismometers in the south of Scotland and the Isle of Man to record 3 component explosion and airgun data and along the Northumberland coast for vertical component data.

The recorder consists of three units; a 1/4 inch tape deck, a

digital clock and a three channel seismic amplifier and frequency modulator unit. Six channels were recorded on tape, three seismic channels, MSF, a time code and a 100 Hz reference frequency. There are 10 gain settings, increasing in powers of two, and the voltage gain is given by 100×2^n where n is the gain setting.

The original recording speed was 0.1 i.p.s. but the two recorders used in this project were adapted to record at approximately 0.44 i.p.s. giving about 18 hours recording for a 2400 foot tape. The bandwidth depends on the gain setting but for settings of 6-7 at the faster recording speed the bandwidth is about 60 Hz.

2.2.3 Durham MkIII seismic recorder

The Durham MkIII seismic recorder (Silver Box) is a development of the Wooden Box and is described in detail in the operating manual and by Savage (1979). Silver Boxes were located at stations S16, S33 and S52 to obtain recordings of three component data from vertical, radial and transverse component Willmore MkII seismometers.

The Silver Box is an F.M. 8 channel battery operated recorder which uses 1/4 inch magnetic tape. Tracks 1, 3 and 5 record seismic data in F.M. mode using a 33% deviation of a carrier at 71 Hz centre frequency. Track 6 records a 100 Hz reference frequency at saturation and is used for flutter compensation. Tracks 7 and 8 record time pulses by switching between carriers

of 50 Hz and 100 Hz and are used to record a radio time-code and an internal clock respectively. The quoted recording speed of 0.07 in/s gives a playing time of just over 4 days for 2400 feet of tape, but the actual speed of recording was found to be 0.08 in/s. Checkout facilities are available to monitor any channel before or after recording by both audio and visual means.

The three seismic channels, 1,3 and 5, were used for one vertical and two horizontal component Willmore MkII seismometers. The gain control operates by stepping up in factors of two as for the Wooden Box. The response of the system is quoted as being

gains 0 - 3	0.5 - 100 Hz
gains 4 - 7	0.5 - 15 Hz
gains 8 - 9	0.5 - 12 Hz

Summers (1982), however, found the response more complicated. He found that for gains 1 - 4 the bandwidth was 17 Hz reducing to 12 Hz at gain 6 and 8 Hz at higher gains. Because of this narrower bandwidth compared with the Geostores and Cassettes the Silver Boxes were primarily used to obtain three component data at large offsets.

2.2.4 Cassette recorders

During the project temporary mobile seismic stations using cassette recorders and HS10 seismometers were deployed. These were placed along the main line where the radio links could not

be used and in southern Scotland, the Isle of Man, Weardale and along the Northumberland coast, to record both explosions and airgun shots.

Cassette recorders from both Durham and Reading Universities were used but since data from the Reading cassettes has not been used in this thesis they will not be described here. The Durham cassettes are two channel FM recorders operating with a centre frequency of 844 Hz with a 40% maximum deviation of the carrier. This gives a bandwidth of 156 Hz. The two channels record the MSF radio time code and the amplified seismometer output. Standard C90 cassette tapes were used at a recording speed of 1 7/8 i.p.s.

The auto-reverse facility did not usually work satisfactorily and the cassettes had to be reversed manually. One recorder, however, appeared to be reversing satisfactorily but was later found to be affected by auto-erasing. This means that the first half of most cassettes recorded at station S28 (the Spadeadam shot station) are blank.

2.2.5 Sea-bottom seismometers

In order to obtain reversed coverage for the Irish and North Sea sections of the line, it was decided to deploy sea-bottom seismometers. These were located close to shots M25, M17, N11 and N25.

A set of twelve Pull-Up Seabottom Seismometers (PUSs) were loaned by Cambridge University for the project. Each PUS consisted of a 4 channel F.M. cassette recorder, one vertical and two horizontal geophones set in gimbals and a hydrophone strapped to the outer casing. The PUSs also possess their own internal clock and can, with certain restrictions, be programmed for several shot windows. The limitation on tape length required that they be deployed in groups of three, each PUS being programmed for one shot window each hour. Unfortunately this meant that only three-quarters of the shots could be recorded. Two groups of PUSs were deployed in both the Irish and North Seas. Their locations are shown in Fig. 2.1 and tabulated in Appendix B. Whenever a group of three PUSs is considered as one station it will be referred to as P123, P456 etc.

Timing was achieved by using the internal clocks which were checked for drift against MSF immediately before launching and after recovery (Davies 1983, Powell 1983).

2.3 Seismic sources

Four different seismic sources were used. The explosive shots fired at sea comprised the major part of the experiment. The explosions on land and the airguns were used to provide information on the shallow structure. The quarry blasts were used to obtain information on the structure away from the line.

2.3.1 Land shots

Two shots were fired on land, one on Forestry Commission land at Spadeadam in Cumbria and the other in a disused quarry on the Whin Sill near Kirkwhelpington in Northumberland. It was intended to fire 150 kg of explosives at the bottom of each of these two 40 m deep holes. Neither of the boreholes were charged with more than 100 kg due to difficulties in lowering the explosives into the boreholes, and at Kirkwhelpington two separate detonations were needed to completely explode the gelignite.

Two problems caused the shots to be smaller than anticipated. The first was the existence of a ledge in the boreholes where the drilling diameter was reduced from 6 in to 4 in. At Spadeadam the explosive got caught on this ledge to prevent the full 150 kg being used and energy was lost when the explosion cratered. A further problem occurred at Kirkwhelpington where, because the borehole passed through the hard Whin Sill into the weaker underlying sandstone and shales, a large amount of water appeared to flow from top to bottom in the borehole creating a cavity at its base. This flowing water probably broke up some of the explosive which, because of the cavity, was then not properly contained.

Both of the problems could have been overcome by lining the borehole with P.V.C. tubing with a sealed bottom.

The shot instant was recorded on a cassette recorder using an HS10 seismometer.

2.3.2 Sea shots

A total of 10.5 tonnes of I.C.I. Geophex was used for the shots at sea. There were 64 shots of 150 kg and two of 450 kg. 35 of the smaller shots and 1 of the large shots were exploded in the Irish Sea and the remainder in the North Sea. The shot locations are shown in Fig. 2.1 and are listed in Appendix B. The individual shots were made up from 12.5 kg sticks banded together. The shots were released from the stern with a two minute fuse attached. This was sufficient time for the shot to reach the sea bottom and for the ship to be sufficiently far away before detonation. Bottom detonation was used because it is quick and safe. In this region the depths are generally too shallow for firing at the optimum depth (Jacob 1975). All the shots detonated properly and were fired within 2 minutes of their assigned times.

The shots were received on a hydrophone towed 28 m behind the ship and on a geophone attached to the hull 33 m in front of the stern. They were recorded on a 4 track F.M. tape recorder with the M.S.F. radio time code and the ships clock. They were later played out on a jet pen recorder and the shot times picked. This time had to be corrected for the ships distance from the the shot point at the time of detonation. This correction introduced the largest error into the shot times and was a particular problem in

the Irish Sea, where large tidal streams exist and the ship speed was difficult to estimate accurately.

The time correction is given by

$$T_{\text{COR}} = ((H-28)^2 + D^2)^{1/2} / V_w$$

where V_w = Velocity of sound in water in m/s
D = Water depth at shot in metres
H = Distance travelled by the ship in metres

and 28 m represents the distance of the hydrophone behind the ship.

The shot depth (D) was obtained from the echo sounder. V_w was calculated from the temperature and salinity (Clay and Medwin 1977) which was supplied for 1° squares around Britain by the Marine Information and Advisory Service (M.I.A.S) at the Institute of Oceanographic Sciences (I.O.S.). The distance travelled (H) was obtained from the ship's flight time recorded on a stopwatch and its speed from the log. The tidal stream correction to this speed was obtained by comparing the distance and direction travelled between two Decca fixes with the same information obtained from the speed and heading on the ships log. The information from the latter is affected by the tidal stream whereas the Decca fixes are not. This calculation was made using a program called CORRNAV (see section 2.3.3 and Appendix C).

The shot position was located by taking a Decca fix as the shot was tipped off the stern. Minimal drift in the descent of the

shot was assumed.

2.3.3 Airgun shots

Three main lines were shot. The Irish Sea line (Fig. 2.2) and the first North Sea line were shot using the full array (Fig. 2.5a). Unfortunately two of the airguns failed in the North Sea so that part of this line had to be repeated (Fig. 2.3) using two 1000 cubic inch airguns (Fig. 2.5b). However, the two 1000 cubic inch airguns could be towed at a depth of 10 m instead of at 6 - 7 m for the four gun array and this probably made the two gun array as effective as the four gun array (Sinha and Uruski 1982).

The airguns were set to fire at regular intervals, usually 1, 2 or 4 minutes, on the minute. Timing was achieved by playing the output from the hydrophones attached to the airguns alongside MSF on a jet-pen recorder. It was later discovered that the pens on the recorder were misaligned so that picking the shot time from the recordings made on the ship introduced a small systematic error. In the Irish Sea every fourth shot was recorded on a four track F.M. tape recorder (Racal Store 4DS) along with MSF. This enabled the shots to be replayed in the laboratory and a correction made. Unfortunately this recording was not made in the North Sea so that the shot time error is larger.

Decca fixes were taken at 20 minute intervals throughout the shooting of the airgun lines. A computer program called CORRNAV

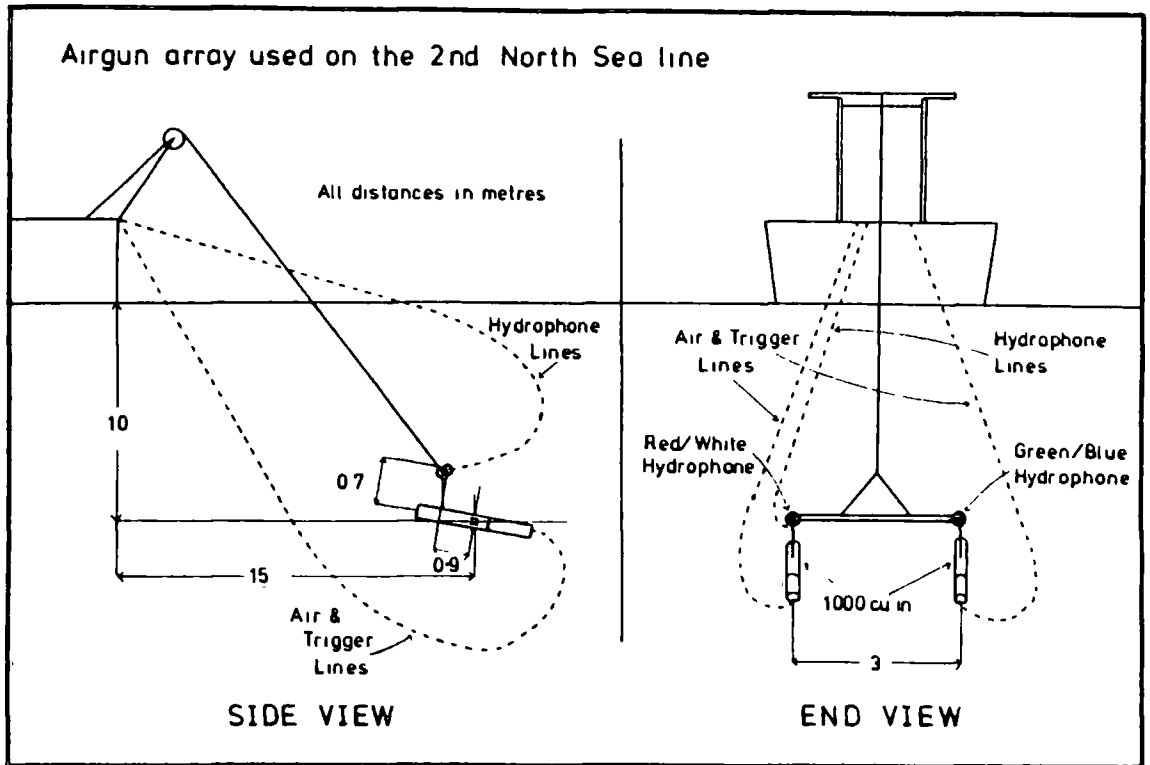


Fig 2.5b Airgun array used on the 2nd North Sea profile

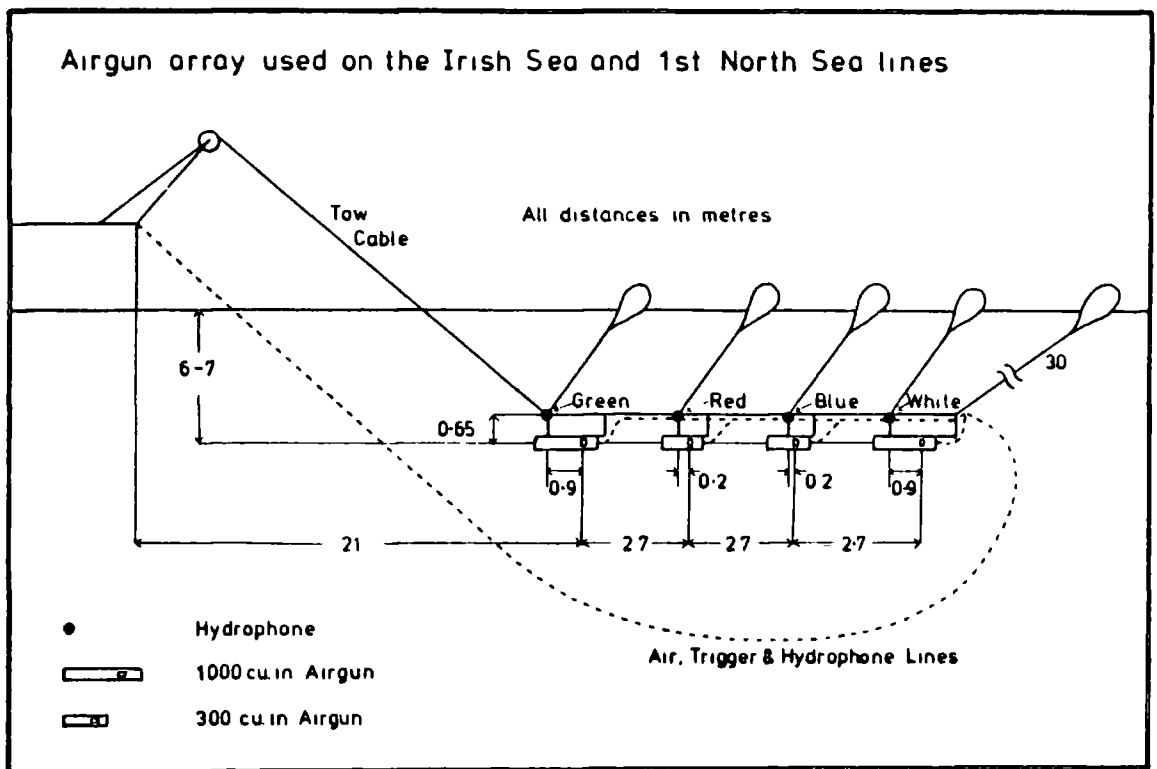


Fig 2.5a Airgun array used on the Irish Sea and 1st North Sea profiles

(Appendix C) was written to use these fixes and the ships speed and heading to calculate the location of the ship for the intervening shot times. Because of the effect of the tidal stream the shot spacing varied between 150 and 450 m.

2.4 Quarry blasts

Over the past years many Durham Msc students have studied the seismic structure of the north-east of England using quarry blasts (Archer 1971, Kidd 1972, Griffiths 1974, Lindscale 1982). Swinburn (1975) carried out further field work and added his data set to the previous workers. During the CSSP project many of the same quarries were observed although lack of time and manpower prevented the recording of the shot times. In order that this information can be used a survey using some of the same quarries and reoccupying CSSP station S49 was performed in the summer of 1983 by A.H.J. Lewis (Fig. 2.6).

The line was run north-south across the Stublick fault. During the two months of the survey 14 stations were occupied with Silver boxes and Durham cassette recorders using Willmore MkIII seismometers (Table 2.1). The shot instant of each quarry was recorded at least once by placing a geophone about 10-20 metres behind the first hole to be fired.

The locations of the stations used by Swinburn (1975) and incorporated into the CSSP data set are listed in Table 2.2 and

located on a map in Fig. 2.6.

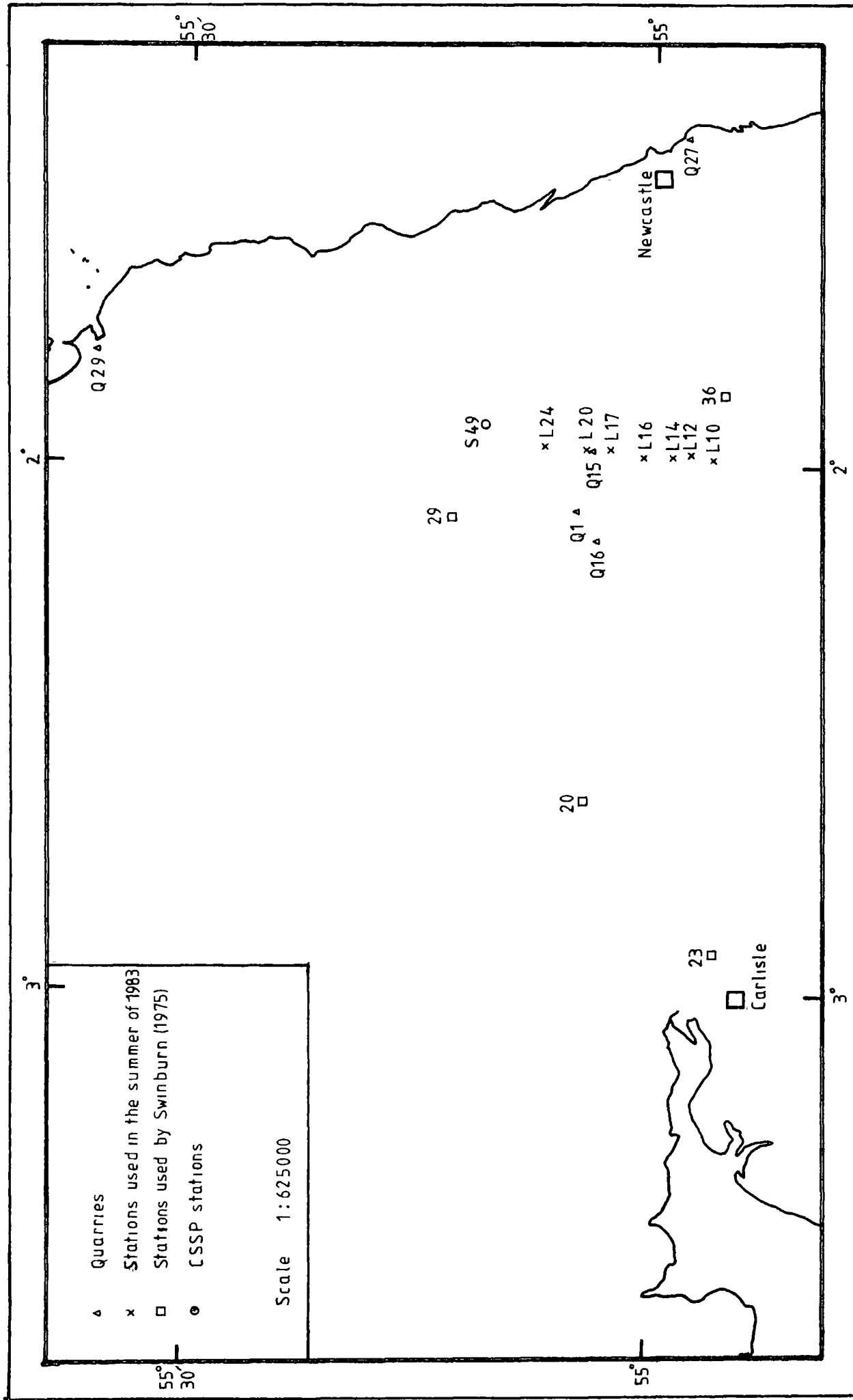


Fig 2.6 Location of stations used in the 1982 quarry blast survey and by Swinburn (1975)

TABLE 2.1

Location of quarries and stations used in the quarry blast survey of 1983.

Quarry		Location	
No.	Name	Lat.	Long.
Q1	Swinburn	55° 4.94' N	2° 4.64' W
Q15	Mootlaw	55° 4.28' N	1° 58.19' W
Q16	Barrasford	55° 3.94' N	2° 8.22' W
Q27	Marsden	54° 58.09' N	1° 22.14' W
Q29	Belford	55° 36.05' N	1° 47.28' W
Q30	Ewesly	55° 14.21' N	1° 54.64' W

Station		Location	
No.		Lat.	Long.
L10		54° 56.02' N	1° 58.98' W
L12		54° 57.78' N	1° 58.70' W
L14		54° 58.82' N	1° 58.81' W
L16		55° 0.91' N	1° 58.83' W
L17		55° 2.80' N	1° 58.11' W
L20		55° 4.51' N	1° 58.20' W
L24		55° 7.07' N	1° 57.48' W

TABLE 2.2

Location of stations used by Swinburn (1975) and incorporated into the CSSP survey.

Station		Location	
No.	Name	Lat.	Long.
20	Spadeadam	55° 4.41' N	2° 37.95' W
23	West Cliff	54° 55.81' N	2° 55.02' W
29	Elsden	55° 13.10' N	2° 5.71' W
36	Ebchester	54° 55.28' N	1° 51.62' W
Q29	Swinburne	55° 5.00' N	2° 4.81' W
Q30	Mootlaw	55° 4.15' N	1° 59.03' W
Q16	Barrasford	55° 3.72' N	2° 8.12' W
Q34	Walltown	54° 59.16' N	2° 30.94' W

CHAPTER 3 - DATA PROCESSING

3.1 Introduction

The large quantity of data collected could only be handled efficiently by computer. The traces were digitised as a first step and all subsequent processing used this digital data. A diagram indicating the major steps in the processing is shown in Fig. 3.1.

3.2 Digitising

The digitising was carried out in the Seismic Processing Laboratory (SPL) of the Durham University Geology Department (Fig. 3.2). This is based on two LSI 11/03 computers connected by a fast data link. One controls an analogue tape deck, an analogue to digital converter and a Tektronix storage tube display. The other LSI 11/03 controls two digital tape transports and two electrostatic matrix printer/plotters.

The data were digitised to 12 bit precision at a nominal 100 samples per second after using a 50 Hz anti-aliasing filter. For each shot-station record between 1 and 4 minutes of data were digitised, usually starting from close to the shot instant. A flow chart of the digitising program written by D. L. Stevenson is shown in Fig. 3.3. It operates on an events file (EVENTS.DAT) which contains the information on the shots to be digitised and

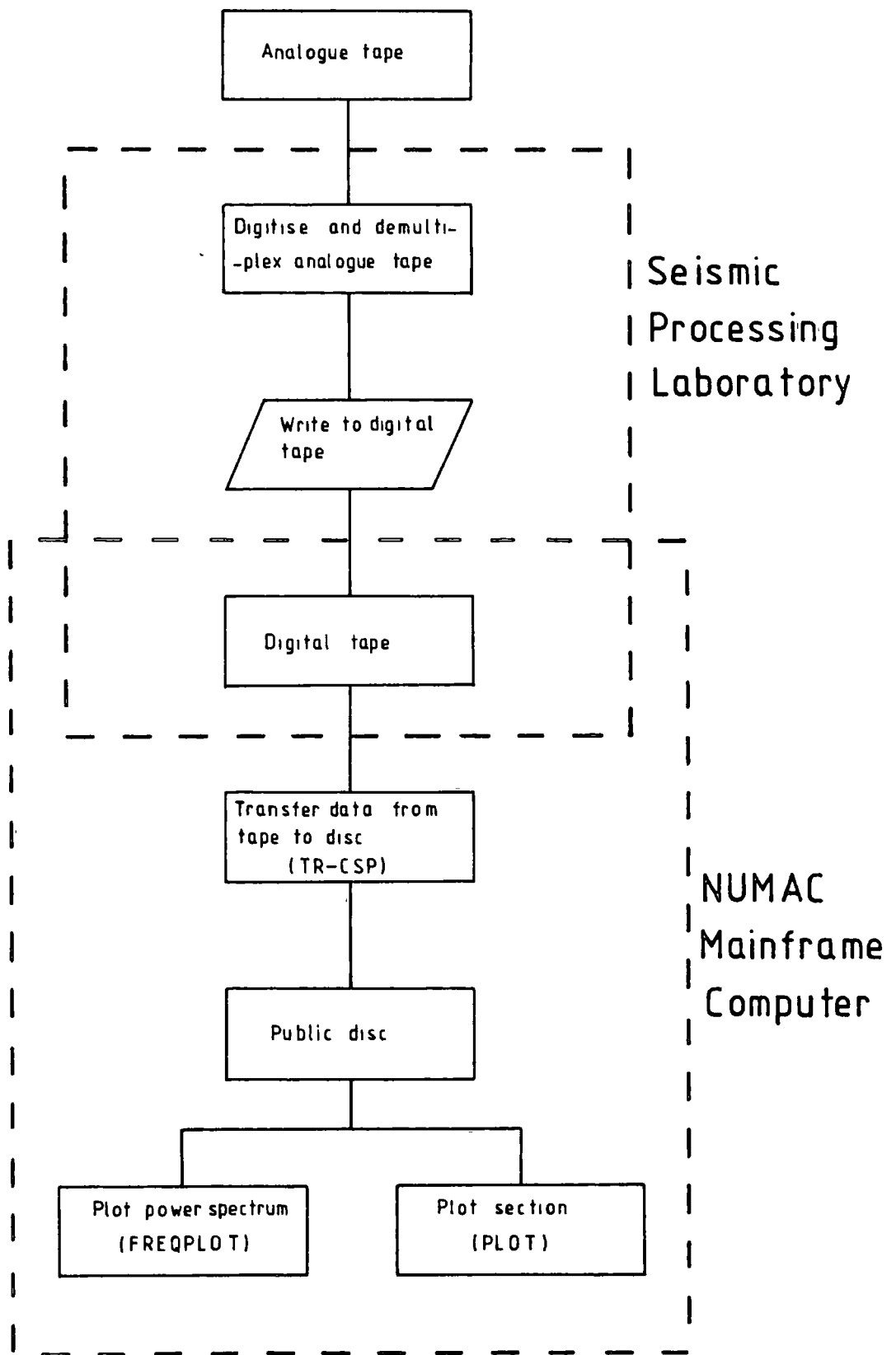


Fig 3.1 Block diagram of the major steps in the processing of the CSSP data.

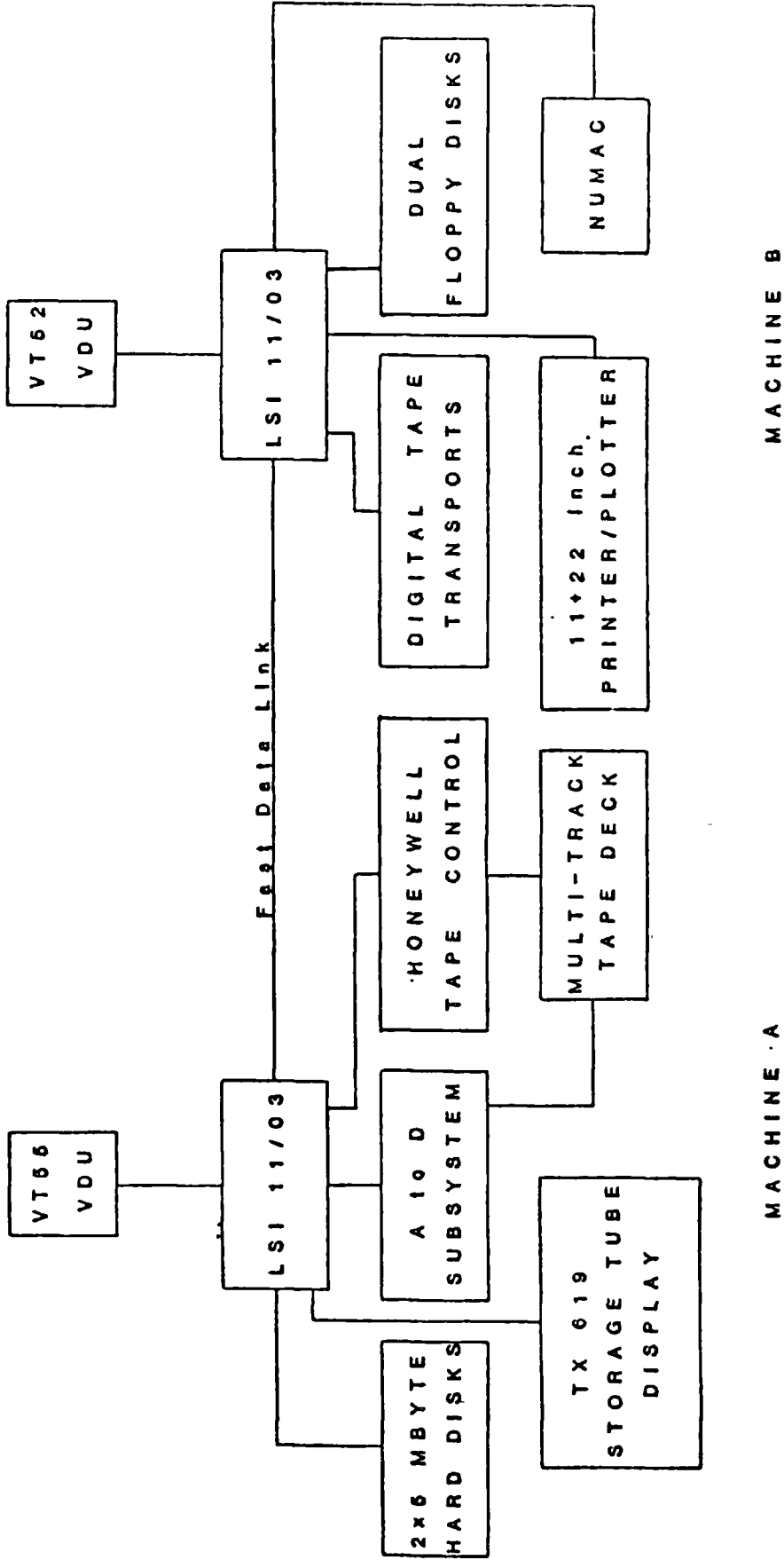


Fig 3.2 Block diagram of the seismic data processing system used at Durham

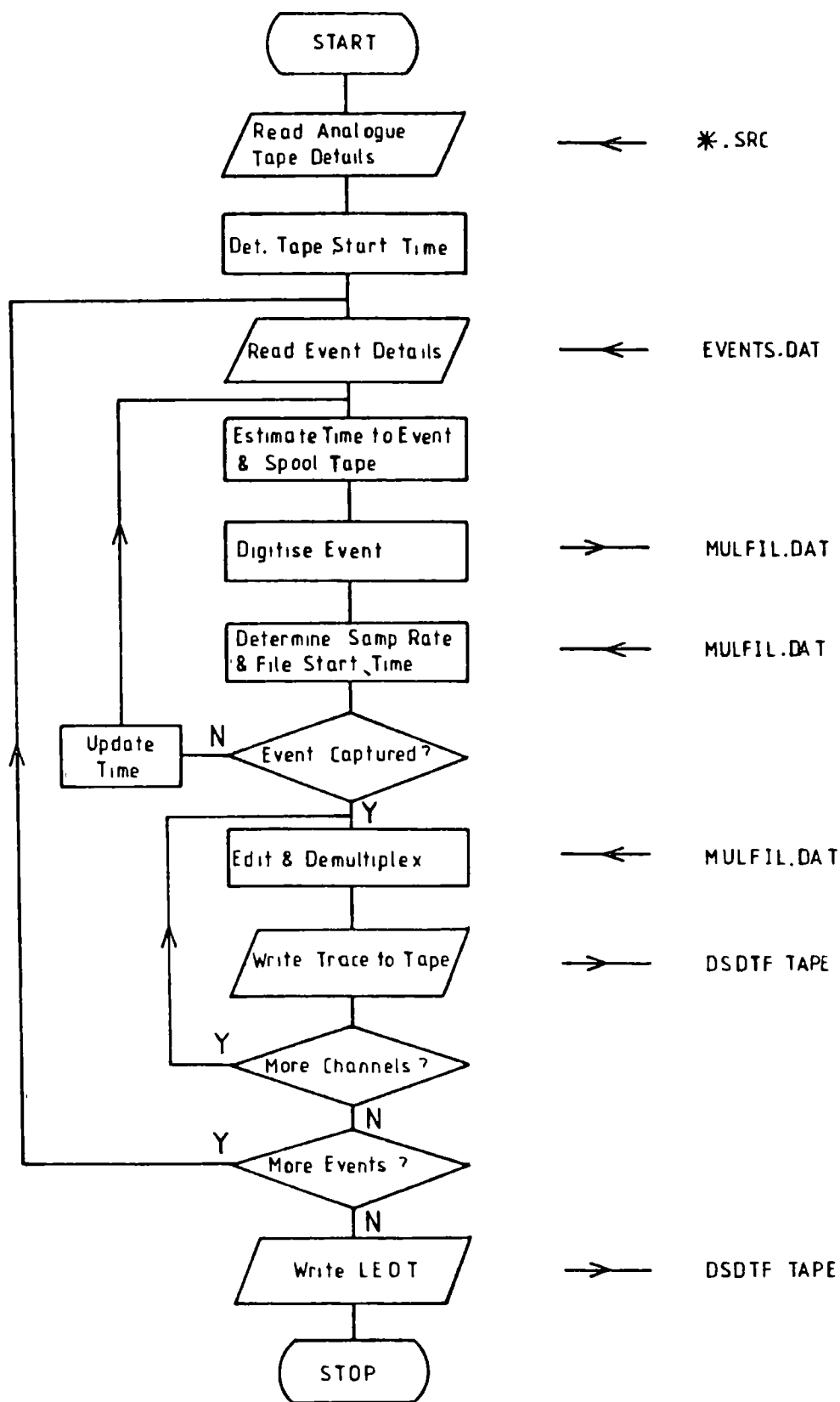


Fig 3.3 Flow chart of computer program written by D. L. Stevenson to digitise the analogue tapes using Durham's Seismic Processing Laboratory

a station file (*.SRC) containing the station information. All the events on a single Geostore tape can be digitised automatically without intervention.

A maximum of eight channels can be digitised concurrently, two of which are taken up by MSF and the internal clock. The most important part of the process is the timing of the samples. For every section of tape digitised the first process is to determine an accurate sampling rate. The number of samples in each second for 240 seconds is calculated. After spurious values greater than three standard deviations from the mean have been discarded the sampling rate is recalculated and the standard error of the final sampling rate must be less than 0.05% of the recalculated mean.

The stability of the tape speed on the Geostores and Wooden Boxes is good and timing errors are less than +/- 20 ms over 4 minutes. The tape speed on the Silver Boxes, however, is less stable and a standard error up to 0.1% of the sampling rate had to be accepted. This gives a timing error of up to +/- 20 ms over 2 minutes for the Silver Boxes.

When a well recorded section of analogue tape is located MSF is decoded and the time of the first sample of the first minute mark is determined. This is the only sample for which the time is directly calculated from the clock and is accurate to +/-0.5 of a sample interval (5 ms in this case). The time of all other samples is determined from this time using the sampling rate as

determined above.

Further inaccuracies are introduced if MSF is not decodable and the internal clock used. At the beginning of each tape run the clocks are digitised at a faster rate of 200 to 240 samples per second to calculate the offset between MSF and the internal clock. If the internal clock has to be used, it is decoded and the offset and drift correction applied. Most of the error in using the internal clock is in the internal clock drift. Fig. 3.4 shows some of the drift curves and they are clearly not all linear. However, by determining the clock offset close to patches of bad MSF it is possible to make the drift correction less than 10 ms.

The digitised data is written to tape in a format designed by D. L. Stevenson called the Durham Self-Defining Tape Format (DSDTF). The tapes are written to IBM hardware standards at 1600 bpi on 9 track tape and they are unlabelled with fixed block lengths of 2048 bytes. Each trace occupies one file written with a header block followed by the data samples written as 16 bit 2's complement integers. The header block contains all the information concerning the shot and station. The timing of the samples is defined by the time of the first sample and the sampling rate. A flag indicates whether MSF or the internal clock was used for timing. In most cases MSF and the internal clock were digitised as seismic traces so that a check on the timing accuracy could be made.

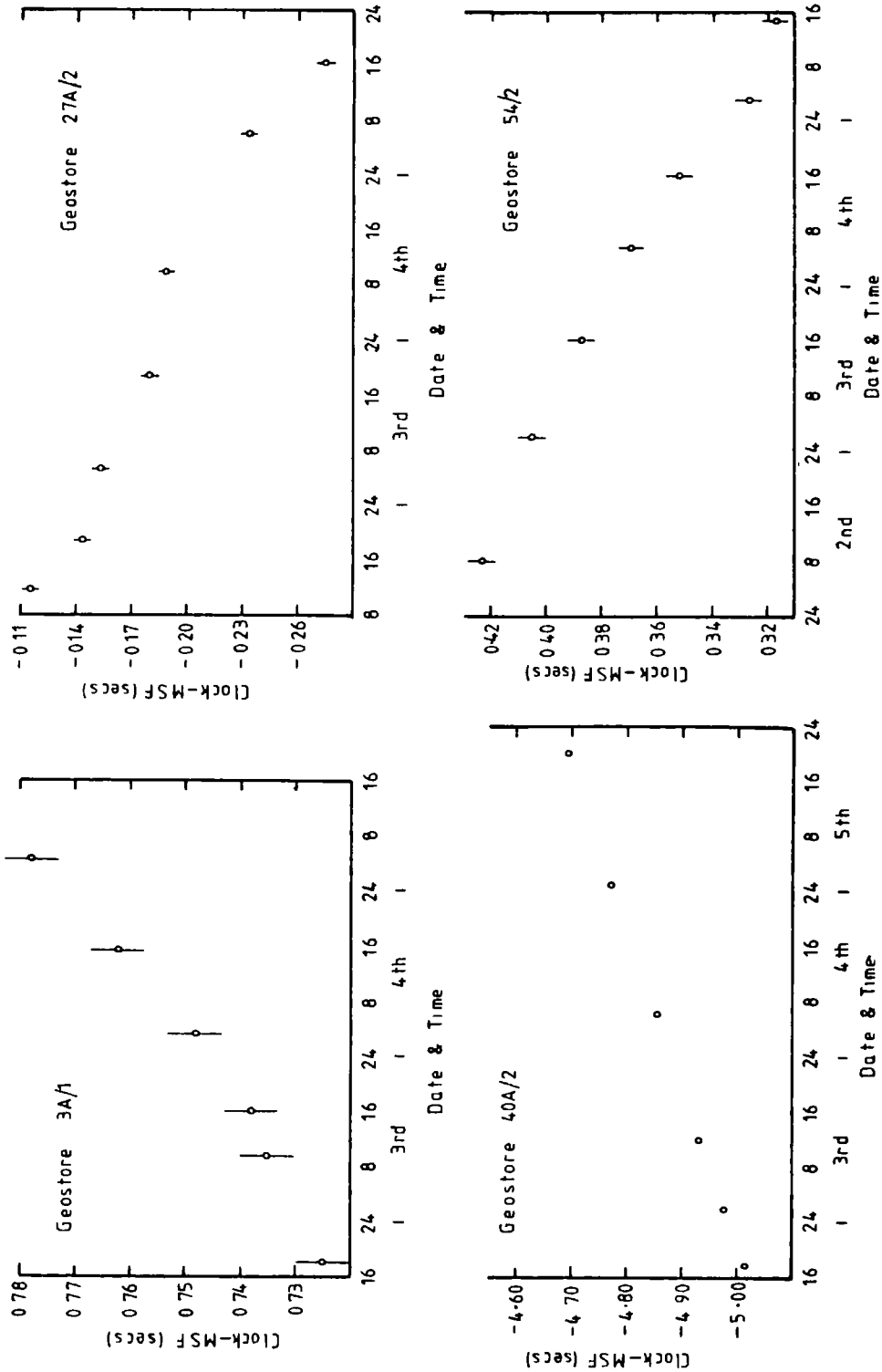


Fig 3.4 Drift curves for the Geostore internal clock and MSF

3.3 Section plotting

Because of the limited processing power available on the SPL the section plotting and further processing were performed on the University mainframe computer, an IBM 4331.

Software was written by A. H. J. Lewis to transfer a maximum of 16384 samples from any section of the DSDTF tapes to disc. Each trace on disc occupies two lines, the first containing the header information, the second the trace samples as unformatted binary data.

The plotting program (PLOT) (Appendix C) enables the plotting of up to 90 traces in either a reduced or unreduced section at any scale. The maximum number of samples permitted for each trace is given by $126000/(\text{number of traces})$, although filtering is only permitted on a maximum of 4096 samples for each trace. The program is designed to be used interactively making maximum use of the information in the header block, cutting the input required from the user to a minimum.

3.4 Calculation of distances and travel-times

Distances between shots and stations were calculated using a program called DISTAZ written by G. K. Westbrook. This uses the formula of Robbins (1962) and has an accuracy of 1 part in 10^7 at 1600 km.

The seismic stations were located on the O.S. 1:10000 and 1:10560 scale topographic maps to an accuracy of ± 20 m. The shots were located using DECCA fixes the accuracy of which depends on their position relative to the transmitters and the time of day. The accuracy, however, was probably better than ± 100 m even though the ship was moving when the fix was taken. The PUSS stations were also located by DECCA and since the ship was stationary whilst the fixes were taken they should be located at least as accurately as the shots.

The airgun shots were only fixed by DECCA every 20 minutes with intervening positions located as described in section 2.3.3. The accuracy of location of the intervening shots is not significantly worse than that of the 20 minute fixes and located to better than ± 100 m. A correction was made for the distance between the DECCA aerial on the ship and the airgun array. This was 31 m for the Irish Sea and 15 m for the second North Sea line.

The first arrivals were picked on reduced sections at a scale of 10 cm/s using both filtered and unfiltered sections at a scale of 2 cm/s. Each pick has an associated picking error of the order of 10 to 50 ms which is combined with the shot and digitising error to give a total travel-time error of 40 to 80 ms.

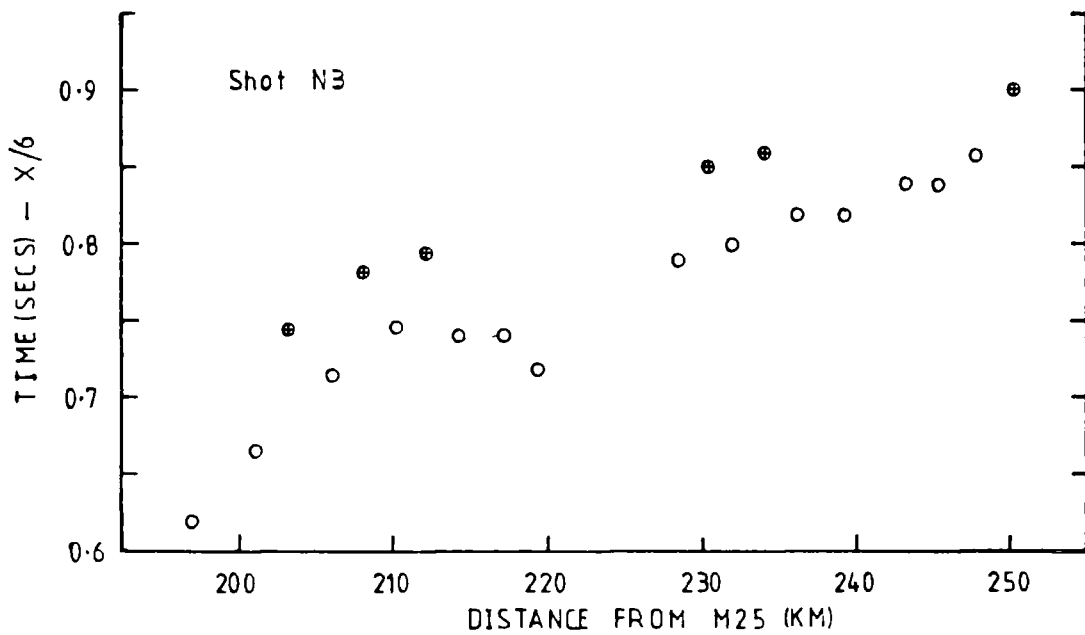
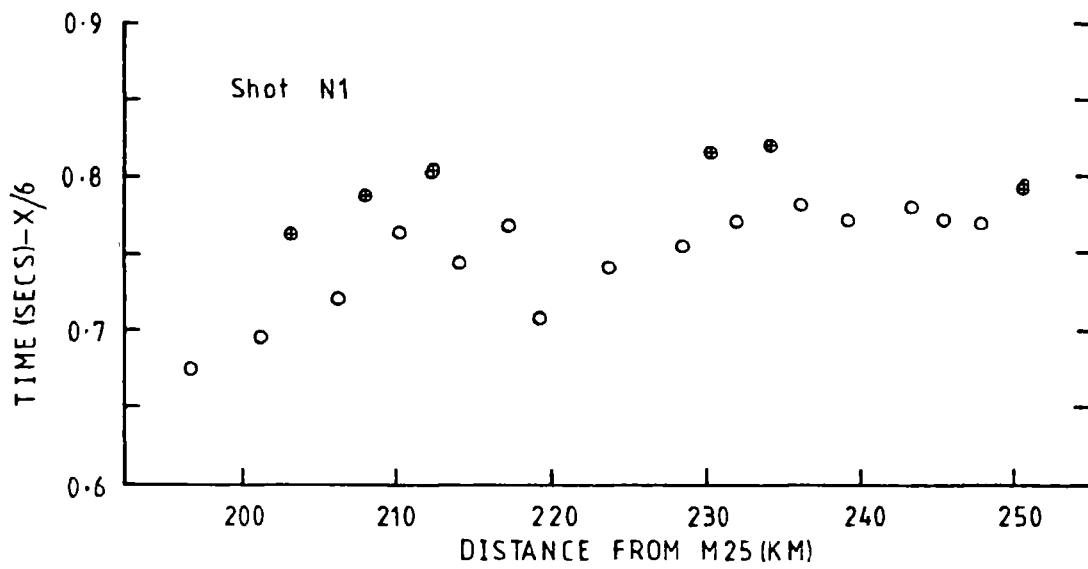
After plotting common shot travel-time curves another error came to light. The travel-times recorded by stations on odd tracks on

the Geostore recorders appeared to be different by 50 ms from those recorded on even tracks (Fig. 3.5). The odd and even tracks are on different tape heads and the error is explained by a 0.018 mm difference in the distance between the two tape heads on the record and playback systems. The error is the same on at least three Geostores and since only one playback deck was used the error was assumed to be in the playback tape head positions. Because the clocks were recorded on even channels the 50 ms correction was applied to all data recorded on odd channels. This time correction only applies for recording tape speeds of 15/160 i.p.s., for slower speeds a proportionally larger error exists.

3.5 Quarry blasts

The tapes from quarry blast recordings made during the summers of 1982 and 1983 were played out in analogue form on a jet pen recorder. The shots often involve more than ten holes with delays of up to 25 ms giving a complicated source signature. The shot instant appears as a short pulse, the initial P wave from the shot instant, followed by a larger longer signal produced by the rock hitting the quarry floor. It is important that the first pulse is picked.

The quarry managers provided the approximate shot times of the untimed blasts, although the times provided were often inaccurate by up to half an hour. These events were searched for on the stations which had already recorded a timed blast from the same



● Even track on Geostore recorder (same as clocks)

○ Odd track on Geostore recorder

Fig 3.5 Travel-time curves for shots N1 and N3 showing 50 ms offset between the odd and even tracks on the Geostore recorders

quarry. When the untimed shot was identified its shot time could then be calculated because the travel-time to the station was already known. This shot could then be used at other stations. Errors are introduced as successive shots are not at exactly the same location. Over two months the quarry face does not move far and the shot location errors are about +/- 50 m. Over a year, however, the shot location error may be as much as +/-200 m.

Occasionally shots from quarries where no shot had been timed were seen . These were usually discarded, although blasts from an open cast coal mine from near CSSP stations S59 and S60 were well recorded. Because the exact location is unknown no depth information can be obtained however they can still be used to provide information on the velocities.

CHAPTER 4 - INTERPRETATION METHODS

4.1 Introduction

The first stage in the interpretation process entails the construction of travel-time plots for the first arrivals. This enables the number of refractors and their apparent velocities to be determined. With reversed data the dip and true velocity can also be calculated. Where the data on a single refractor is more extensive the plus-minus and time-term methods can be employed to examine the variations in depth to the refractor and any changes in the refractor velocity. The time-term method is particularly useful where shots and stations are not distributed along a single profile. After the analysis of the first arrivals later arrivals are investigated. The most prominent are usually reflected phases and they can be used to determine the depth to an interface and the mean velocity of the rocks above.

The final stage entails the construction of a model making use of existing geophysical information. This model can then be tested using ray tracing and synthetic seismogram programs.

4.2 Travel-time graphs

The interpretation of travel-time graphs in terms of horizontal or dipping layers of uniform velocity is well covered by most general geophysics books (Telford et al. 1976, Dobrin 1976). The

use of this method is primarily to identify the main refractors although errors may result from the inability of the refraction method to detect low velocity zones, causing the refractor to be placed deeper, or blind zones, causing it to be placed shallower.

The travel-times were not corrected for the shot depth or station elevation because any correction depends upon the type of wave recorded and the near surface velocity structure at the shot and station.

Where the refraction line is reversed the plus-minus method can be used to establish the velocity structure and depth to a non-planar refractor. It was first described by Hagedoorn (1959) but is better explained by Hawkins (1961) and has been developed by Palmer (1980). The velocity of the refractor is obtained from the minus time, and the depth from the plus time. For the calculation of the plus time the end-to-end time needs to be known. In the CSSP profile the end-to-end time is not usually known so the plus time cannot be used for calculating the depth.

The plus-minus method assumes that the refractor is plane beneath the stations and shots and has a dip of less than 10° . It also assumes that the refractor velocity does not increase with depth. The plus-minus method is really a special case of the time-term method discussed in the next section and many of the same limitations apply.

The best fit straight lines to the travel-time and minus time graphs have been determined by the method of linear least squares. The confidence limit for the velocity is determined by multiplying the standard error by the appropriate Students t value. 95% confidence limits have been quoted throughout unless otherwise stated.

4.3 The time-term method

The time-term method was formulated by Scheidegger and Willmore (1957) and has been extensively used in interpreting refraction data (Bamford 1973, 1976, Berry and West 1966). There has also been considerable discussion on the validity of the results obtained using the method (O'Brien 1968, Reiter 1970, Whitcombe and Maguire 1979, Whitcombe and Rodgers 1981). The time-time method is only briefly described but its limitations are discussed in more detail.

The travel-time of a head wave between a shot and a receiver can be represented by

$$t_{ij} = D_{ij}/V + a_i + a_j + d_{ij}$$

where D_{ij} = Distance along the refractor between normals from the refractor to the stations. In practice the distance between stations is used (X_{ij}).

V = Velocity of the refractor.

a_i, a_j = The time-terms of the stations i and j . The delay of the refracted wave caused by the lower velocity cover.

d_{ij} = The residual time. The difference between the observed and hypothetical travel-times caused by measurement errors and the non ideal behaviour of the refractor.

With a total of n shots and stations there are a maximum $n(n-1)$ observations. If there are more observations than unknowns $(n+1)$ it is possible to solve the problem by linear regression. The computation of this is described by Swinburn (1975) and it is his program, modified by Summers (1982), that was used in this study. Swinburn (1975) also describes how he used it to cope with two different refractor velocities and a velocity gradient in the basement.

It has long been recognised that there are limitations imposed on the method where the refractor is dipping by the difference between X_{ij} and D_{ij} (Willmore and Bancroft 1960) but generally the errors have been thought to be negligible for dips of less than 10° . In theory it is possible to resolve this problem by iterating (Bamford 1973). The refractor dip obtained in the first solution is used to estimate a better value for D_{ij} than X_{ij} . This approach, however, is time consuming and the velocity structure of the overburden must be accurately known (Whitcombe and Maguire 1979). Swinburn (1975) found that on iterating the solution became unstable and that iteration was possible only

with good reversed data and if the model was simple. In this situation, however, the first solution was often adequate anyway.

The accuracy of the model is usually estimated by looking at the dispersion of the solution residuals as represented by the solution variance, but this can be misleading. If the refractor is other than uniform the effects of a complicated velocity structure will be absorbed in the time-term (Whitcombe and Maguire 1979). Similar travel-time data can be obtained from different structures with, in one extreme, the data being modelled by a constant velocity refractor with topography or in the other, by a horizontal refractor with velocity variations.

The wavelength of the topography on the refractor in relation to the profile length and station spacing also has an important effect on the meaning of the station residuals (Whitcombe and Mcguire 1979). Only when structural wavelengths are less than the station spacing will the residuals reflect the goodness of fit. With longer structural wavelengths the solution can be in error even though the solution variance shows no lack of fit.

Care has to be taken, when splitting up the data set in order to look for changes in the refractor velocity or possible anisotropy, that any differences found are not due to topography. Whitcombe and Rodgers (1981) noted that for refractor topographies which were by no means extreme, false anisotropy of about 4.4% can be induced. Anisotropy in the overburden can also

lead to the same problem, though to a lesser degree.

The error quoted for the time-terms is the Berry and West (1966) standard error. This is a statistical error and does not directly incorporate the measured errors. Swinburn (1975) quotes another error based on the travel-time and distance errors, his method is wrong and the resulting errors are meaningless.

4.4 Frequency analysis

Frequency analyses of the seismograms was obtained using a program called FREQPLOT (Appendix C). This operates on data from DSDTF tapes (see section 3.4) and plots the amplitude spectrum of up to 8192 samples using a Fast Fourier Transform routine written by Nunns (1980). The input is designed so that trace segments selected from a reduced section can be identified directly using the reduction velocity and the reduced travel-time. An option exists to smooth the amplitude spectrum using a five point quadratic smoothing routine.

4.5 Reflections

The travel-times of reflections can be interpreted using the standard technique of plotting the square of the travel-time against the square of the distance. The gradient of the resulting straight line gives the inverse square of the velocity above the reflector and the depth can be obtained from the

intercept time. In practice velocity gradients rather than sharp discontinuities are more frequent, especially in the mid and lower crust, leading to non linear X^2-T^2 plots. Reflections at small offsets often indicate a higher velocity and greater depth due to their slightly greater depth of penetration.

Holder and Bott (1971) showed that the depth and average velocity to a reflector can also be obtained from the critical distance and the head wave.

$$\text{Depth} \quad Z = 1/2(x_c t_i V_n)^{1/2}$$

$$\text{Av. Vel.} \quad V = V_n / (V_n t_i / x_c + 1)^{1/2}$$

Where V_n = Velocity of refractor

t_i = Intercept time

x_c = critical distance

To locate the critical distance it is necessary to have good amplitude information. The reflection reaches a maximum amplitude just beyond the critical distance, varying from about 8 km for a signal frequency of 15 Hz to 20 km at 3 Hz (Cerveny 1966).

4.6 Sea-bottom refractor

The hull geophone and towed hydrophone used to record the shot instant recorded a low amplitude faster phase as well as the direct water wave (Fig. 4.1). This is interpreted as a refracted

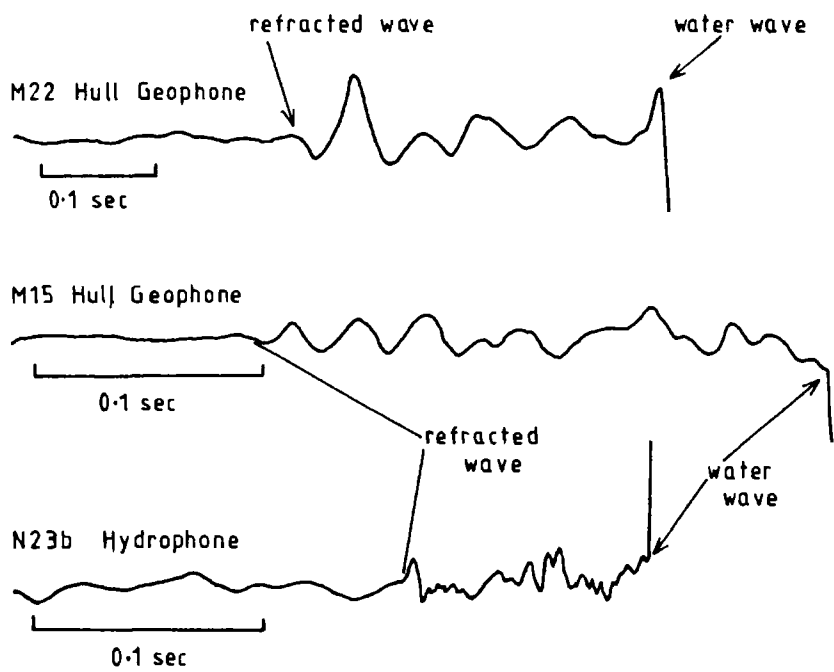
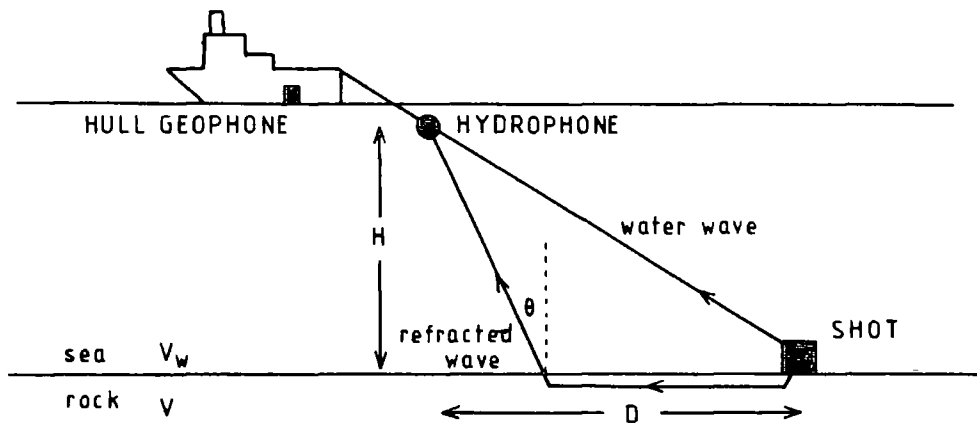


Fig 4.1 Sketch showing the occurrence of the sea bottom refractor

wave from the sea-bottom and can be used to determine the velocity of the rocks on the sea floor. The travel-time of this phase is given by

$$T = D - H \tan \theta / V + H / (V_w \cos \theta)$$

where D is the horizontal distance between the shot and hydrophone, H is the distance of the hydrophone above the sea floor, V is the velocity of the refractor, V_w the velocity of water and θ the critical angle (Fig. 4.1). This equation reduces to a quadratic in V

$$0 = (T^2 - H^2 / V_w^2) V^2 - 2TDV + (D^2 + H^2)$$

which can be solved for V.

Velocities calculated from recordings made on the hydrophone and the hull geophone are listed in Table 4.1 and shown in Fig. 4.2. The velocities obtained are probably minimum values, since it is likely the wave does not travel in the sea-bottom but in some faster refractor beneath low velocity sediments. Modelling a high velocity refractor with up to 40 m of low velocity sediments suggests the calculated velocities could be as much as 20% too low.

4.7 Modelling

Modelling can be carried out on either the travel-times or the complete seismogram. Modelling the travel-times is

TABLE 4.1

Velocities of the sea floor determined from the sea-bottom refractor.

Irish Sea			North Sea		
Shot	Velocity(km/s)		Shot	Velocity(km/s)	
	Geophone	Hydrophone		Geophone	Hydrophone
M1	2.15	-	N2	2.92	-
M2	1.83	1.85	N7	2.41	-
M4	2.27	-	N12	2.72	1.65
M5	2.84	-	N13	2.55	2.32
M8	2.25	-	N14	2.41	2.19
M9	2.59	2.48	N17	2.85	-
M10	2.79	-	N18	2.80	-
M11	2.61	-	N19	2.59	2.93
M13	3.73	-	N20	2.49	2.50
M14	3.34	-	N21	2.61	2.14
M15	3.08	-	N22	2.19	2.18
M16	2.98	-	N23A	2.12	2.10
M17	3.52	-	N24	1.92	1.85
M18	3.10	-	N25	1.70	1.65
M19	3.34	-	N26	1.76	1.75
M20	3.56	3.48	N27	1.64	1.60
M21	3.26	-	N28	1.76	1.76
M22	3.01	-	N29	1.56	1.70
M23	2.85	-	N23B	2.25	2.24
M24	2.11	-			
M25A	2.55	2.38			
M25B	3.00	2.95			

TABLE 4.2

Velocity of the sea-bottom refractor assuming a layer of low velocity sediments on the sea floor. Irish Sea hydrophone.

Shot	Velocity(km/s)		
	0	10	40
M9	2.48	2.55	2.84
M20	3.48	3.64	4.34
M25A	2.38	2.47	2.86
M25B	2.95	3.07	3.58

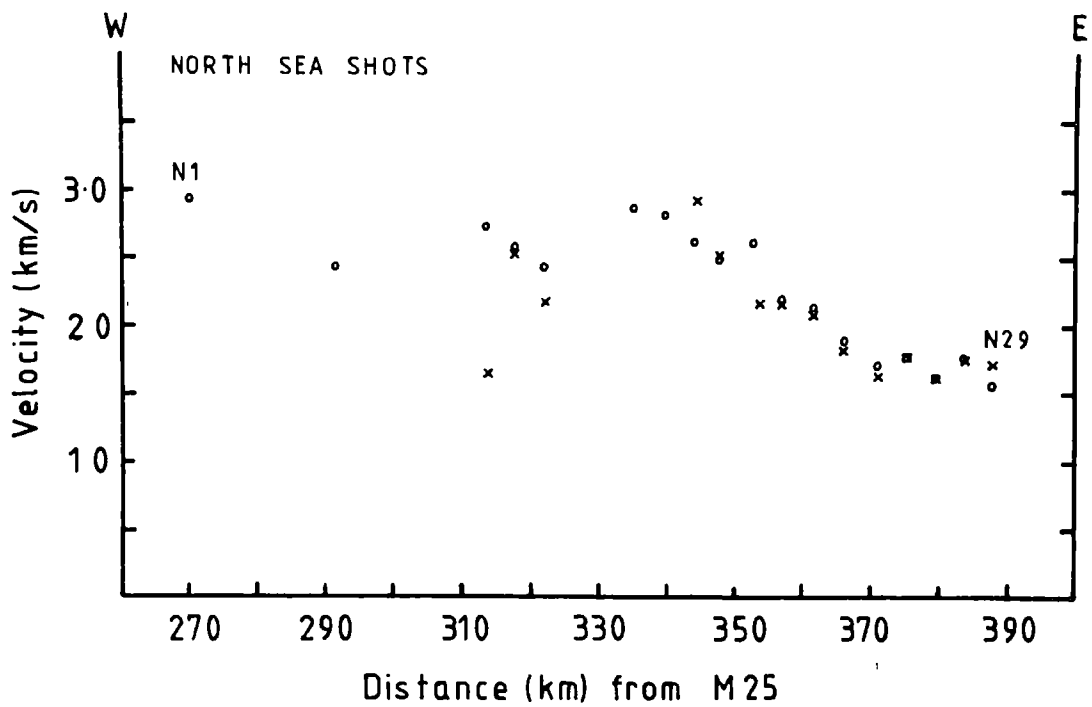
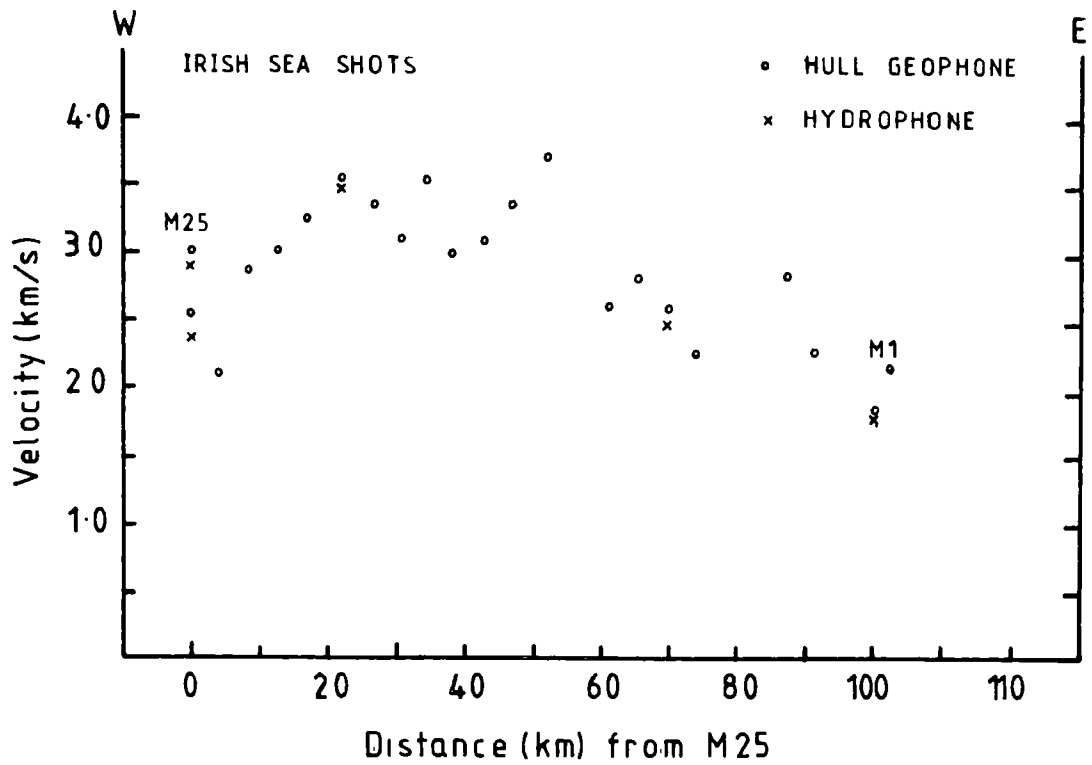


Fig 4.2 Plot of the velocities determined from the sea bottom refractor

computationally cheap but is clearly omitting much of the information within the seismogram. Modelling the whole section however is computationally very time consuming, even for simple models of homogeneous horizontal layers, but can provide information on the nature of boundaries not available from the travel-times alone.

4.7.1 Ray tracing

The modelling of travel-times was performed with a ray tracing program called RT01 written by I. Psencik. This program is designed to calculate ray paths and travel-times through laterally inhomogeneous, 2-dimensional structures containing curved interfaces.

The program uses ray tracing theory in which the path of each ray is calculated in terms of the distance and direction travelled by the ray during successive small time steps (Cerveny et al. 1977). It can cope with reflections and diving rays but not head-waves. This is not a real limitation in practice since true head-waves are seldom observed.

There are two limitations of the ray tracing program that need to be considered. The first is that velocity gradients greater than 0.1 sec^{-1} cannot be dealt with. The second concerns the way interfaces between layers are defined. They are specified by a series of co-ordinates which the program interpolates using a

smoothed polynomial function to find other points on the interface. This method of interpolation makes it difficult to model sharp changes in an interface without oscillation of the interface.

4.7.2 Synthetic seismograms

To model the amplitude characteristics of the seismograms a program called SYNSEI based on the reflectivity method of Fuchs and Mueller (1971) is employed. In this method the numerical integration of the reflectivity (or plane wave reflection coefficient) of a layered medium is carried out in the horizontal wavenumber or angle of incidence domain. Multiplication with the source spectrum and inverse Fourier transformation yield the seismograms for the displacement components.

Only horizontal layers of uniform velocity are allowed in the reflection zone. A different near surface structure is permitted under the source and receiver but only elastic transmission losses and a time shift are calculated for these layers. It has, however, the advantage over ray methods in that it can cope with multiple reflections and converted waves and provides reliable results at singularities (i.e. critical points).

The program allows the input of a source wavelet. For this study a cosine tapered, second derivative Gaussian wavelet was used (Nunns 1980) represented by

$$r(t) = 0.5(1+\cos(nf_m t))(1-2(nf_m t)^2)\exp(-(nf_m t)^2)$$

$$r(t) = 0 \text{ for } |t| > 1/f_m$$

where f_m is the frequency at which the spectral amplitude of the tapered wavelet is maximum, n is an integer and t is the time. The frequency of the explosions varied from shot to shot (see section 7.6) but larger amplitude phases were seen more often when the shot frequency was close to 4 Hz so a value of $f_m = 4$ Hz was chosen for the wavelet used in the modelling.

CHAPTER 5 - PRESENTATION OF RESULTS OF UPPER CRUSTAL STRUCTURE

5.1 Introduction

This chapter presents the data on the structure down to, and including, the Pg refractor. Approximately 5000 explosion traces and many hours of airgunning were collected during the project. It has not been possible to digitise and analyse all of this data, nevertheless a large number of sections have been used. Only a few of the stacked sections are shown in this chapter, the remainder are placed in Appendix A. Because of this abundance of data there has only been sufficient time to analyse the first arrivals in detail. Summaries of the velocities and intercept times calculated in this chapter are listed in Tables 5.1, 5.2 and 5.3. All errors refer to 95% confidence limits.

5.2 Presentation of Irish Sea airgun data

The airgun data recorded on the PUSS stations (Fig. 2.2) have not been digitised and only jet-pen recorder playouts are available. Clear first breaks are visible on only three sections, P8 window 6, P10 window 3 and P10 window 4 (see Appendix B). Four shots were recorded during each window and travel-time plots are shown in Fig. 5.1.

Two of the travel-time curves have apparent velocities of 4.65 km/s and 4.80 km/s with approximately zero intercepts. These

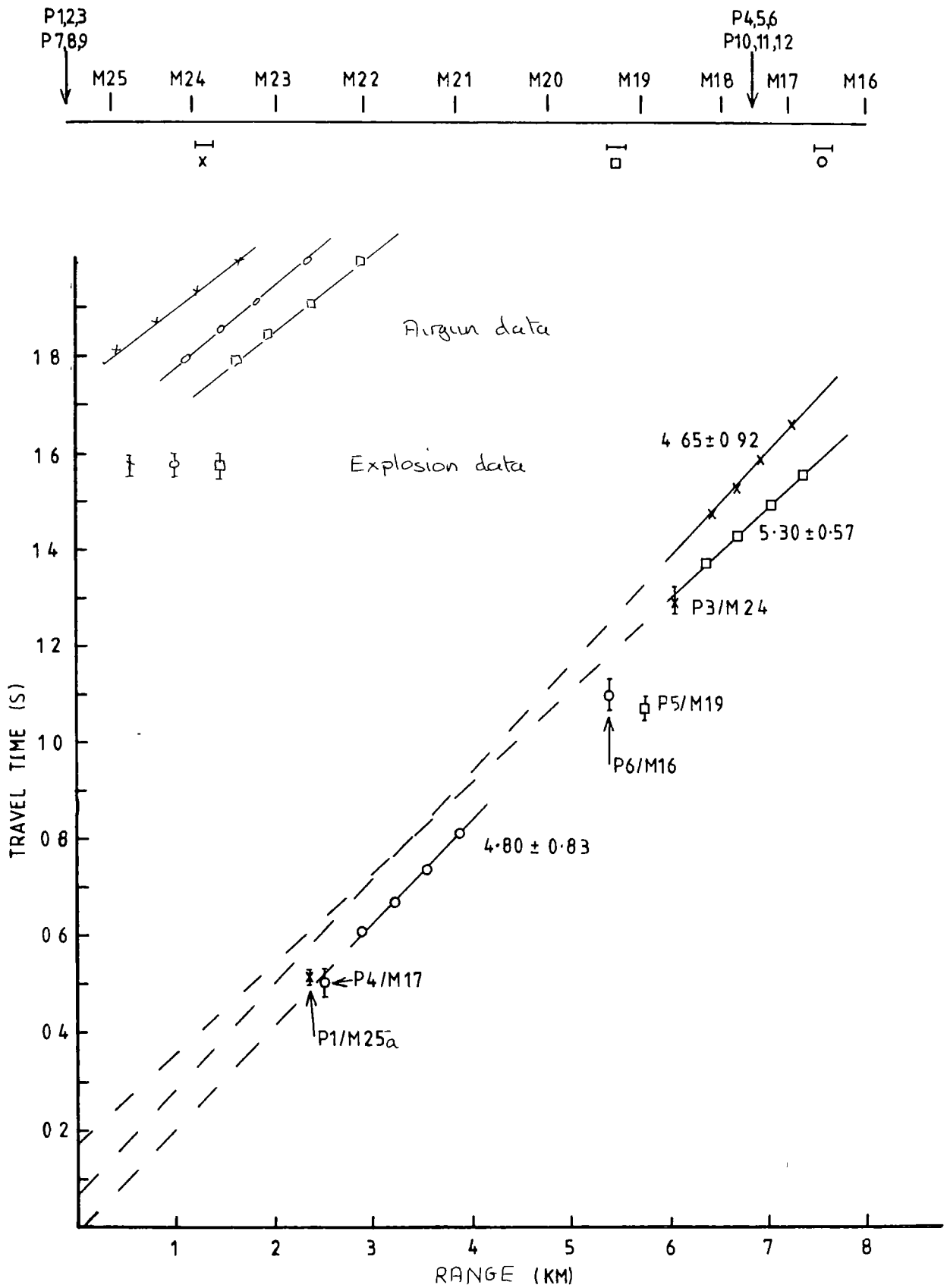


Fig 5.1 Travel-time plot for the Irish Sea airgun shots recorded by the PUSS'S

velocities must represent the near surface rocks. The third travel-time curve has an apparent velocity of 5.30 km/s with an intercept of 0.13 s. If the near surface rocks have a velocity of 4.7 km/s and an allowance is made for the water column then this layer is 0.46 km below the sea-bed. The error in the intercept, however, is large (Table 5.1)

Recordings of the airgun shots on the Wooden Boxes in southern Scotland (S81) and the Isle of Man (S91), and the Geostore recorder for stations S1 to S10 have been digitised (Fig. 2.2). The airgun shots are not visible on recordings at stations S1 to S10 and it is assumed that this is due to the 27 km offset between the nearest shots and S1. Good recordings were made on the Wooden Boxes and stacked sections reduced to 6.0 km/s for the north-south line between southern Scotland (S81) and the Isle of Man (S91) (Fig. 2.2) have been plotted (Figs. 5.2 and 5.3).

The frequency content of the airguns at a distance of 5.4 km from S81 is in two bands from 4 to 9 Hz and from 21 to 25 Hz (Fig. 5.4). The energy in the band 21 to 25 Hz, however, decays rapidly over the first few kilometres and only energy at the lower frequencies is present at greater distances. In order to enhance the signal at large offsets a 2 to 12 Hz bandpass filter has been applied to the sections (Figs. 5.2 and 5.3).

The stacked sections (Figs. 5.2 and 5.3) show clear first arrivals out to a range of 25 km and between 1 and 2 s after the

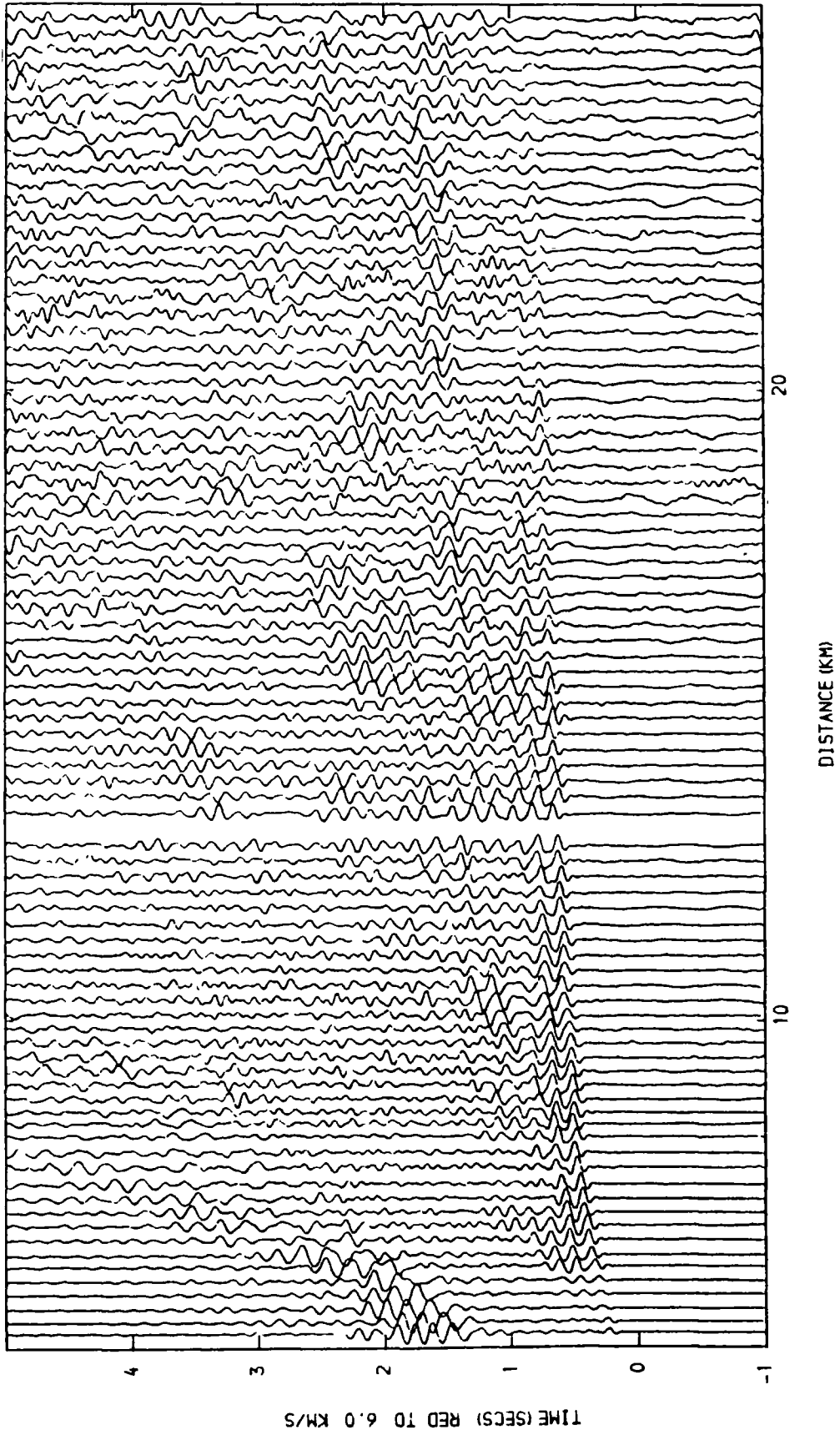


Fig 5.2 Reduced section at S81 for the north-south Irish Sea airgun profile. Filtered 2-14 Hz, amplitudes equalised

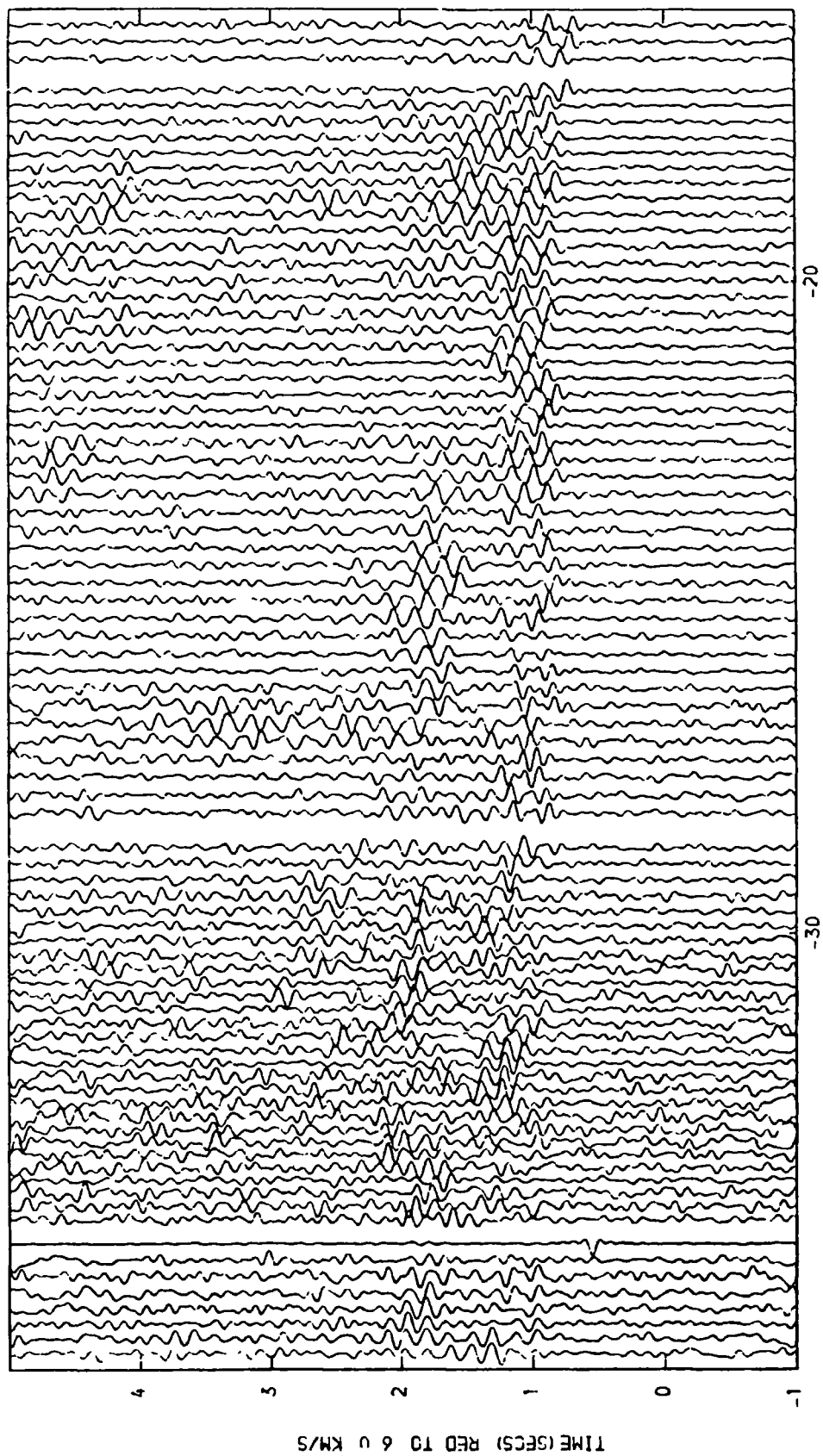
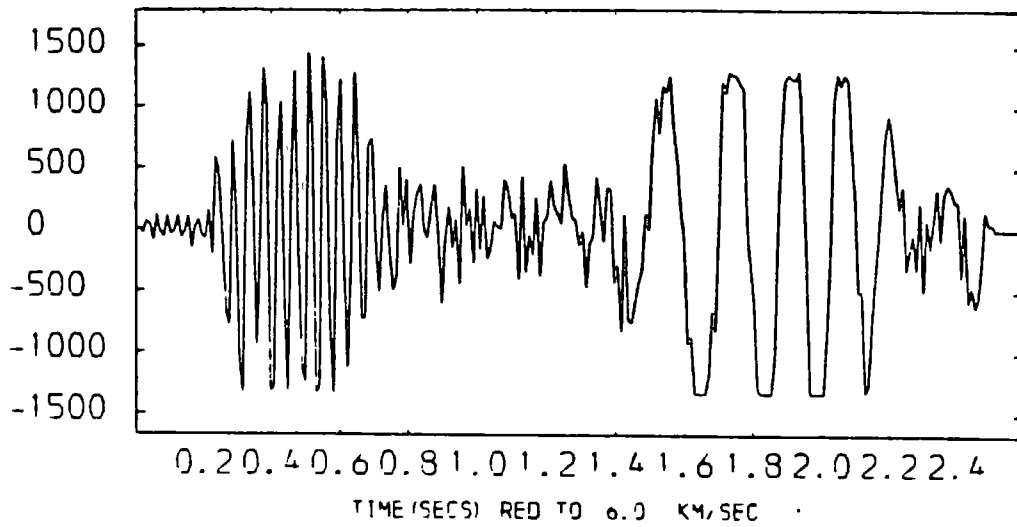


Fig 5.3 Reduced section at S91 for the north-south Irish Sea
airgun profile. Filtered 2-12 Hz, amplitudes equalised



190 5 91

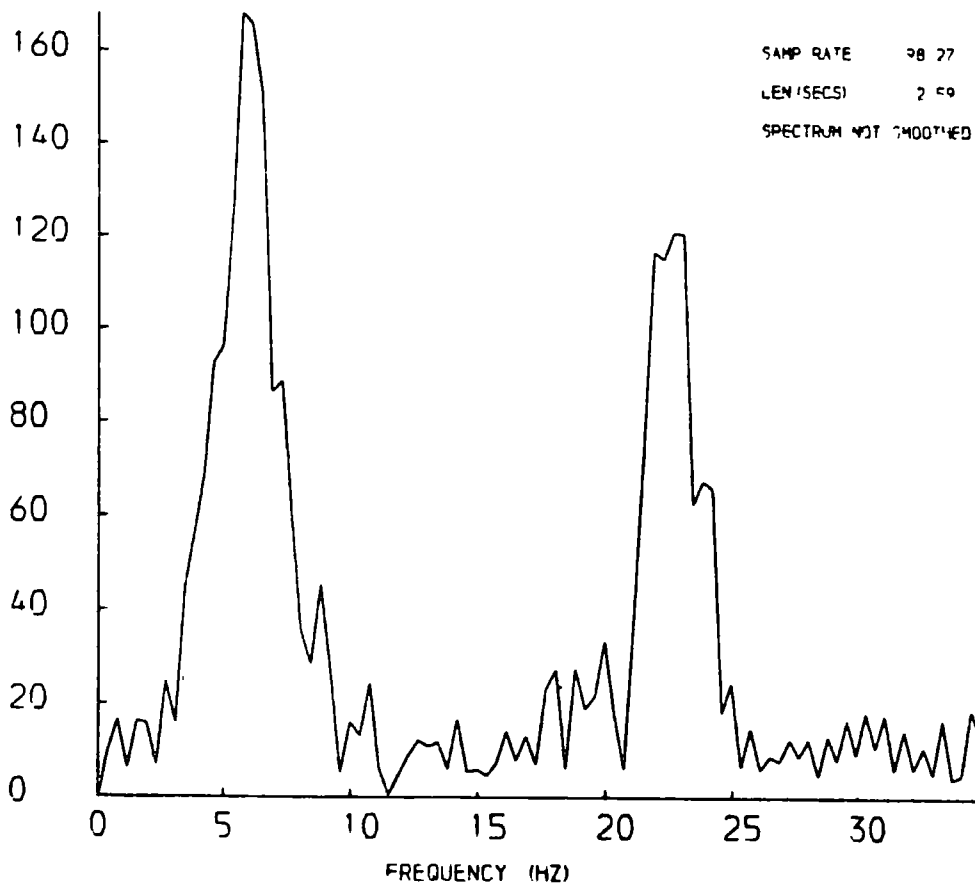


Fig 5.4 Frequency plot of an airgun shot recorded at S81 at a range of 5.4 km

first arrivals are several other phases.

The travel-time curves for S81 and S91 indicate considerable and rapid variations in the structure along the profile (Figs. 5.5 and 5.6). Between 5 and 8 km from S81 there are two branches to the travel-time curve of apparent velocity 3.67 km/s and 4.00 km/s. Both these segments have negative intercepts (Table 5.1) and this suggests that the velocity increases towards S81. These velocities probably represent Permo-Trias and Carboniferous sediments which give way laterally to Lower Palaeozoic rocks beneath S81. Beyond 8 km from S81 the average apparent velocity varies from 5.27 to 5.63 km/s (Fig. 5.5), although there are short sections between 18 and 24 km with apparent velocities as low as 3.78 km/s (Fig. 5.6).

The shots closest to S91 are at a range of 18 km and this is too great for first arrivals from the Permo-Trias and Carboniferous. Between 18 and 28 km the apparent velocity is 5.83 km/s although the curve is very broken and appears, in a similar way to S81, to be made up of a series of en-echelon segments (Fig. 5.6).

The average true velocity over the reversed section of line is 5.71 km/s with a refractor dip of between 1° and 1.5° to the south. In detail though, the arrivals at S81 between 18 and 25 km indicate considerable topography on the refractor which can be explained by a series of tilted fault blocks. The travel-time curves (Fig. 5.6) are consistent with the faults being downthrown

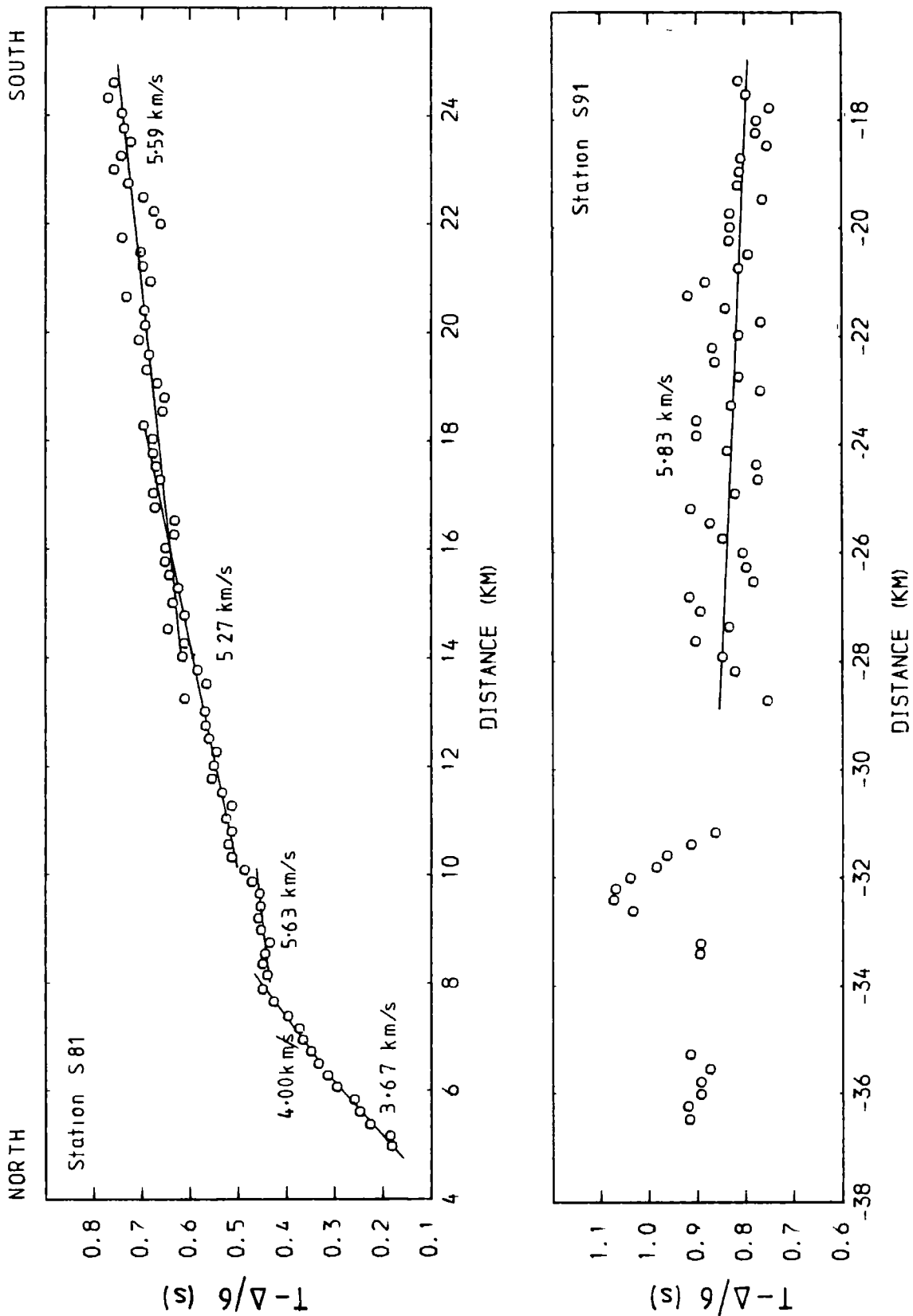


Fig 5.5 Reduced travel-time plots for the north-south Irish Sea airgun profile recorded at S81 and S91

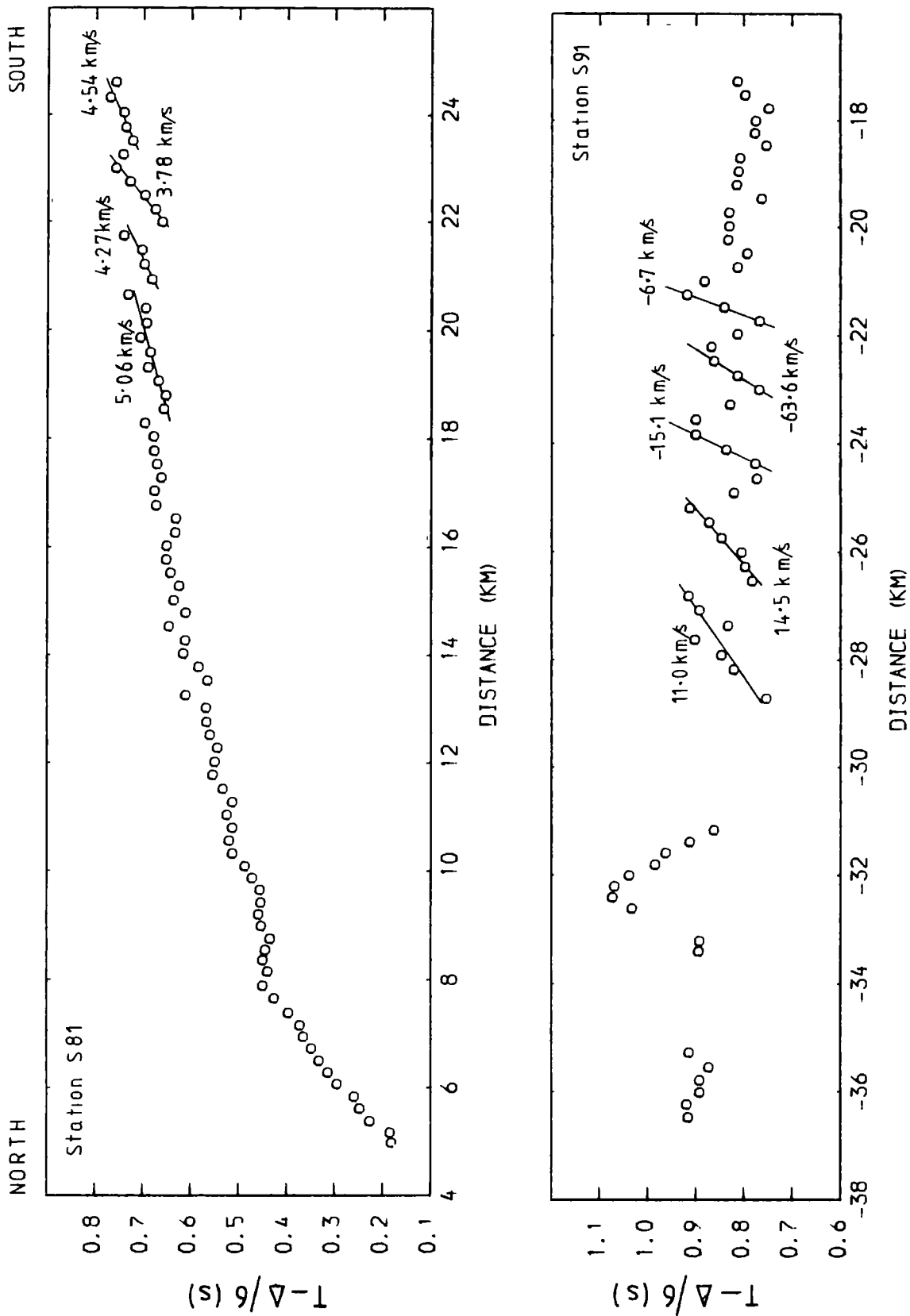


Fig 5.6 Reduced travel-time plots for the north-south Irish Sea airgun profile recorded at S81 and S91

to the north with the tops of the blocks dipping steeply to the south (Fig. 5.7a). This would preserve the gentle average southerly dip. If this model is correct one would expect to see more diffracted arrivals at S91 (Ledoux 1957) (Fig. 5.7b). It is possible that the arrivals between the short travel-time sections on S91 are diffracted arrivals. These do not exist at S81. If this is so it is not possible to apply normal methods of travel-time analysis.

It should be possible, however, to calculate the dip on the top of the blocks from the apparent velocities. The down-dip velocity (V_d) and up-dip velocity (V_u) are given by

$$V_d = V_o / \sin(i+a) \quad \text{and} \quad V_u = V_o / \sin(i-a)$$

where a is the angle of dip, i is the critical angle and V_o is the velocity above the refractor. If the velocity of the refractor is 5.7 km/s and V_o is 4.0 km/s (Fig. 5.5) then the critical angle (i) is 44.6° .

The down-dip velocities recorded at station S81 (Fig. 5.6) of 5.06 +/- 0.03 km/s, 4.27 +/- 1.38 km/s and 4.54 +/- 1.09 km/s suggest dips of 8° , 25° and 17° respectively. The apparent velocity of 3.87 +/- 0.35 km/s, also recorded at S81, is smaller than the theoretical minimum velocity of 4.0 km/s (V_o), but if it is assumed that it is equal to V_o then the refractor dip is 45.5° .

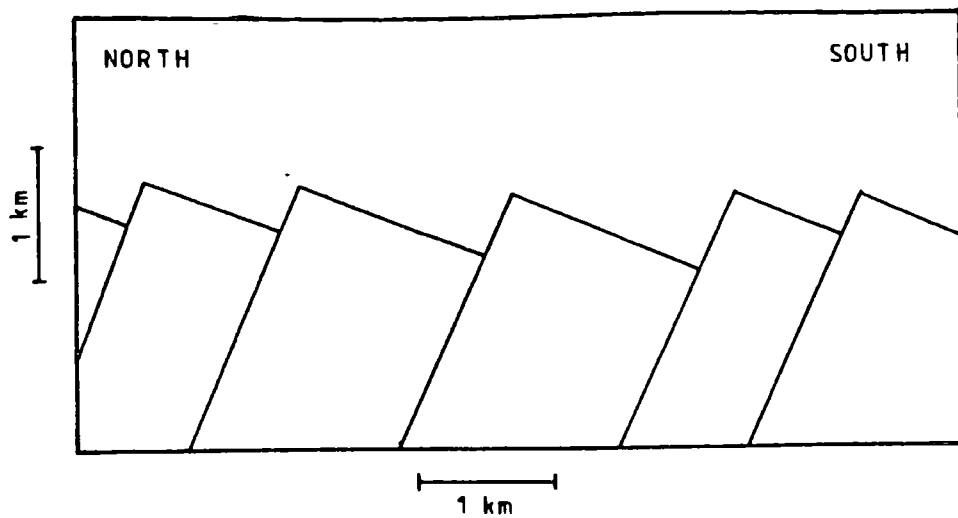


Fig 5.7a Sketch of faulting in the 5.7 km/s refractor beneath the north-south airgun profile in the Irish Sea

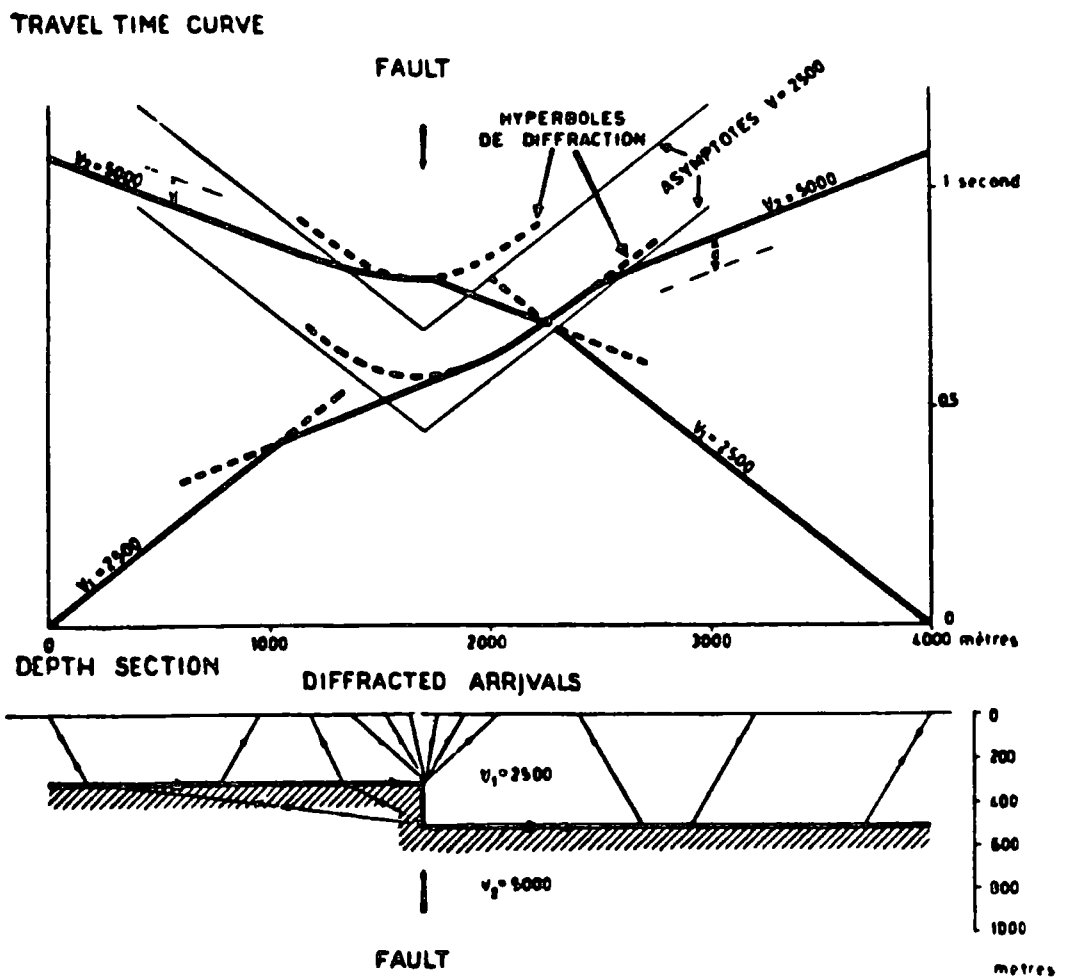


Fig 5.7b Theoretical travel-time plot across a fault (from Ledoux 1957)

The ray offset between the refractor and the surface makes it difficult to match the travel-times recorded at S81 with the travel-times recorded at S91. The up-dip velocities of 11.0 +/- 5.9 and 14.5 +/- 6.3 recorded at S91, however, suggest dips of 23° and 28° respectively, but the negative up-dip velocities indicate dips that are greater than the critical angle. The throw on these faults is difficult to estimate from the travel-time curves but would appear to be in the order of 0.3 to 0.6 km.

Some of the dips calculated appear to be large but many of the short travel-time segments in Fig. 5.6 are only defined by a few points and the errors are very large. A reflection profile, or refraction survey with shots at 50 m intervals instead of 330 m intervals, would be required to obtain a better understanding of the structure. A more detailed examination of the Irish Sea airgun profiles has been made by Thompson (1984).

5.3 Presentation of Irish Sea explosion data

Of the four components recorded by the PUSS stations the hydrophone produced the best signal to noise ratio. On P123 clear first arrivals were observed out to 70 km although the exact onset was difficult to pick beyond 50 km (Fig. 5.8). The gains were set too high on the recorders and this has caused saturation on many of the traces, making it difficult to identify first arrivals from their character. Plenty of energy is visible as second arrivals but there are few coherent identifiable phases.

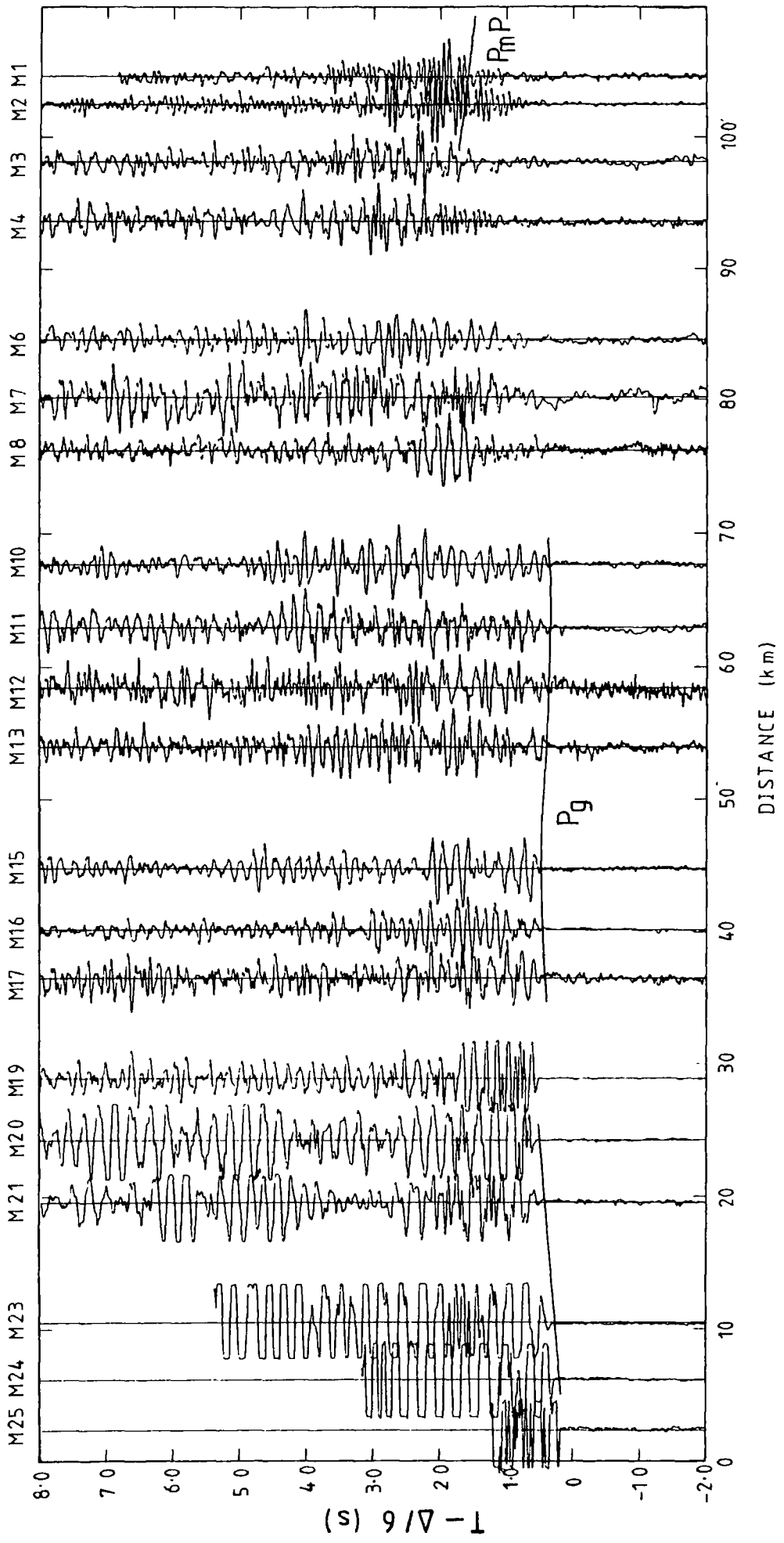


Fig 5.8 Reduced section of the Irish Sea shots recorded on the hydrophone at P123. Low pass filter - 40 Hz, amplitudes equalised

There is a burst of energy between 90 km and 110 km at a reduced time of 2 s and this is tentatively identified as a reflection or diving wave from the Moho, PmP.

P456 shows good first arrivals for all shots (Fig. 5.9). Unfortunately the gains were again set too high and little information can be obtained from the second arrivals.

The travel-time curve for P123 (Fig. 5.10) shows apparent velocities of 4.03 km/s, 5.49 km/s and 6.03 km/s with breaks of slope at 3 km and 30 km. The 6.03 km/s layer is Pg. A horizontal uniform layer interpretation indicates interfaces at depths of 0.51 km and 2.24 km.

The travel-time curve for P456 (Fig. 5.10) is more complicated. The apparent velocities of 4.87 km/s and 4.89 km/s recorded close to the station are similar to those recorded from the airgun shots nearby. The apparent velocities of 5.19 km/s and 5.89 km/s are believed to represent the same layer as the velocity of 5.49 km/s recorded at P123 and the velocity of 5.30 km/s recorded from the airguns. Pg is observed beyond 30 km.

Stacked common station sections from the stations in England show the main phases (Figs. 5.11, 5.12 and Appendix A). The sections are strongly affected by near surface delays associated with the Solway basin and differences in the shot characteristics (see section 7.4). Nevertheless there are features common to most of

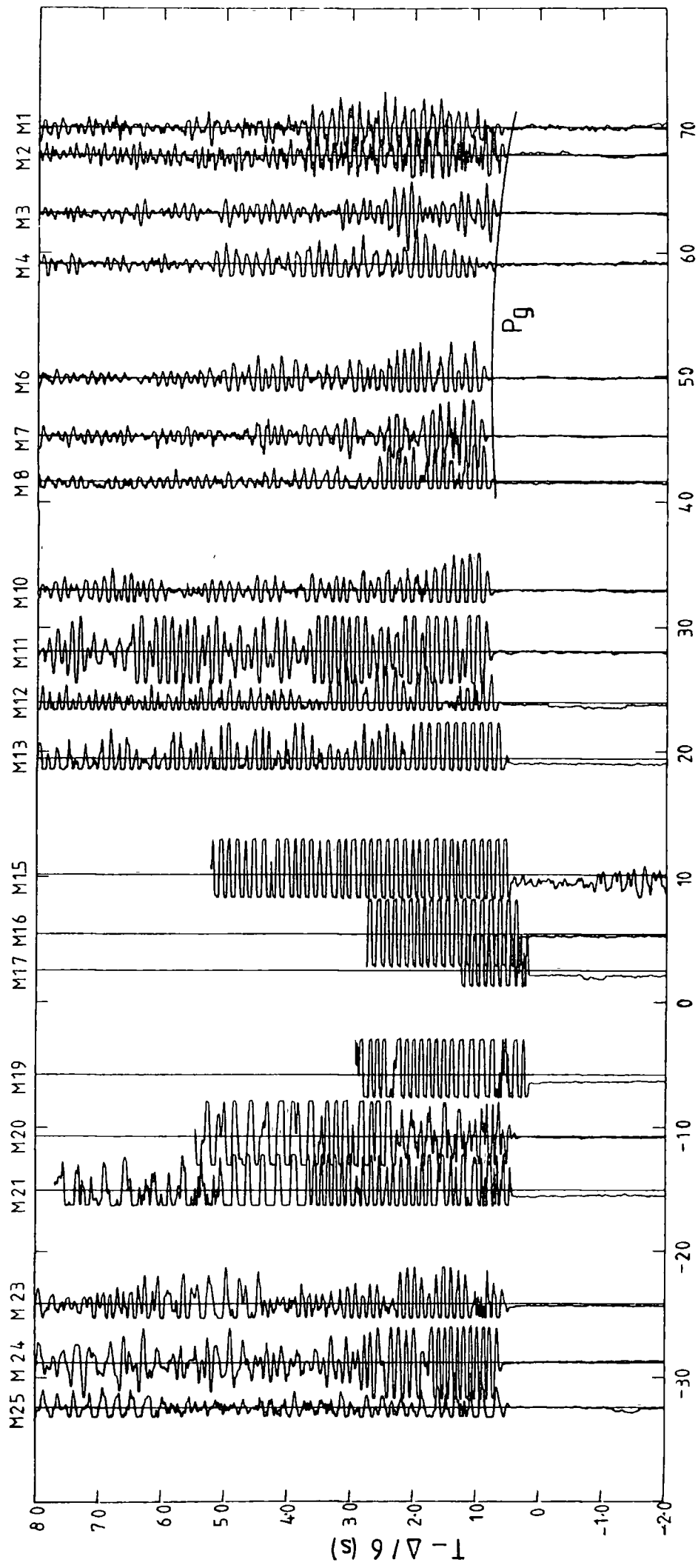


Fig 5.9 Reduced section of the Irish Sea shots recorded on the hydrophone at P456. Low pass filter - 40 Hz, amplitudes equalised

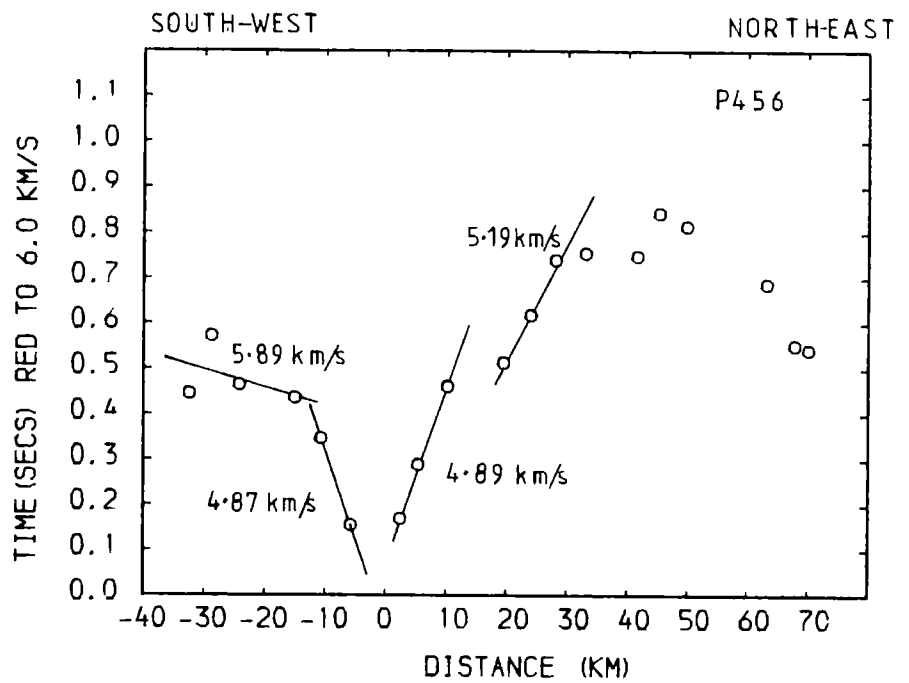
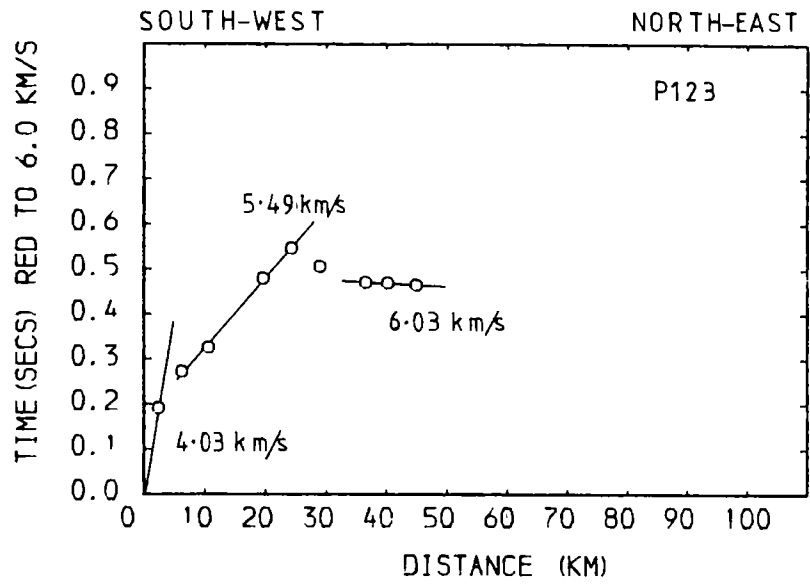


Fig 5.10 Reduced travel-time plots for the Irish Sea shots recorded at P123 and P456

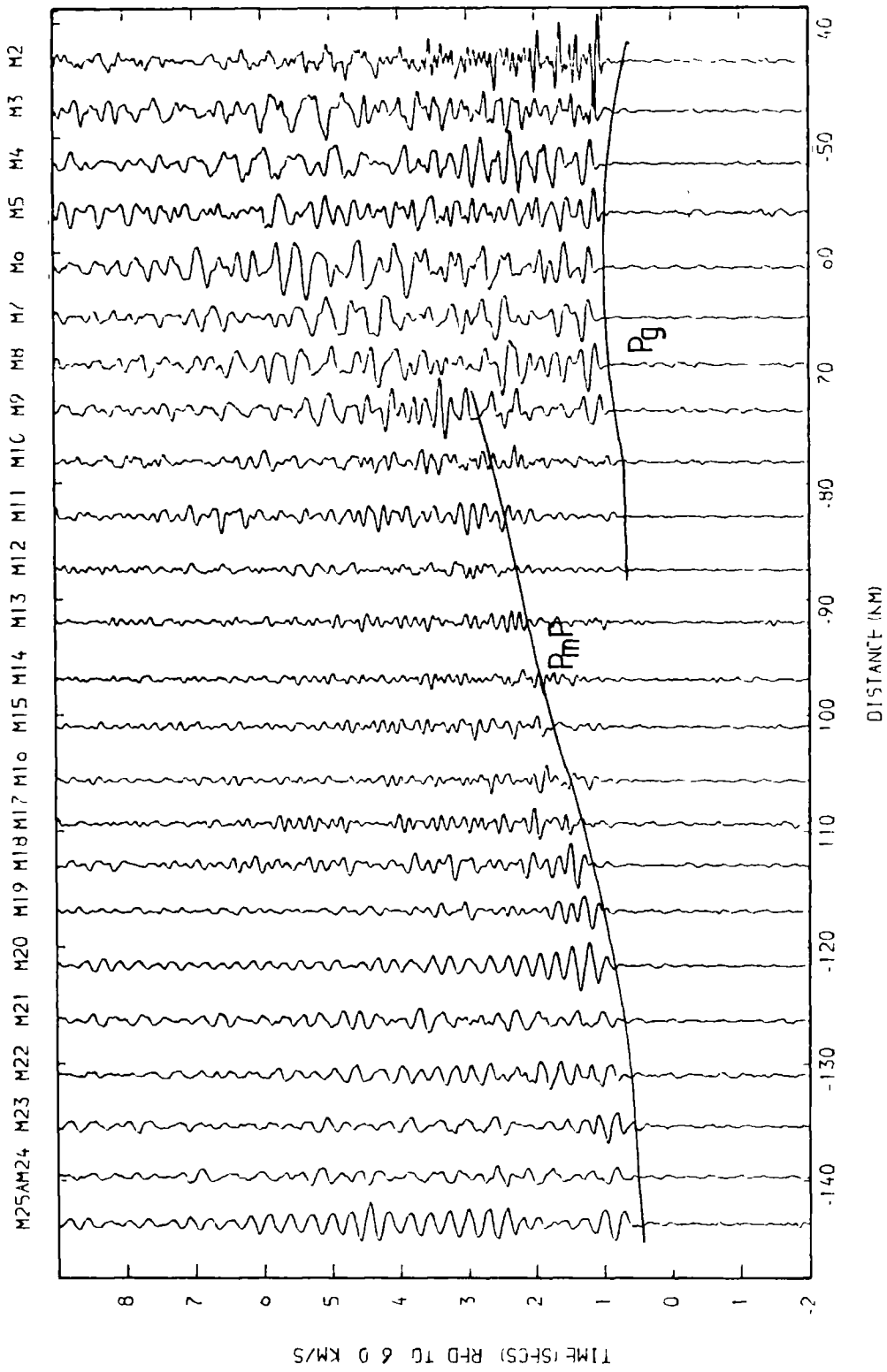


Fig 5.11 Reduced section of the Irish Sea shots recorded at S8.
 Filtered 2-12 Hz, amplitudes uncorrected

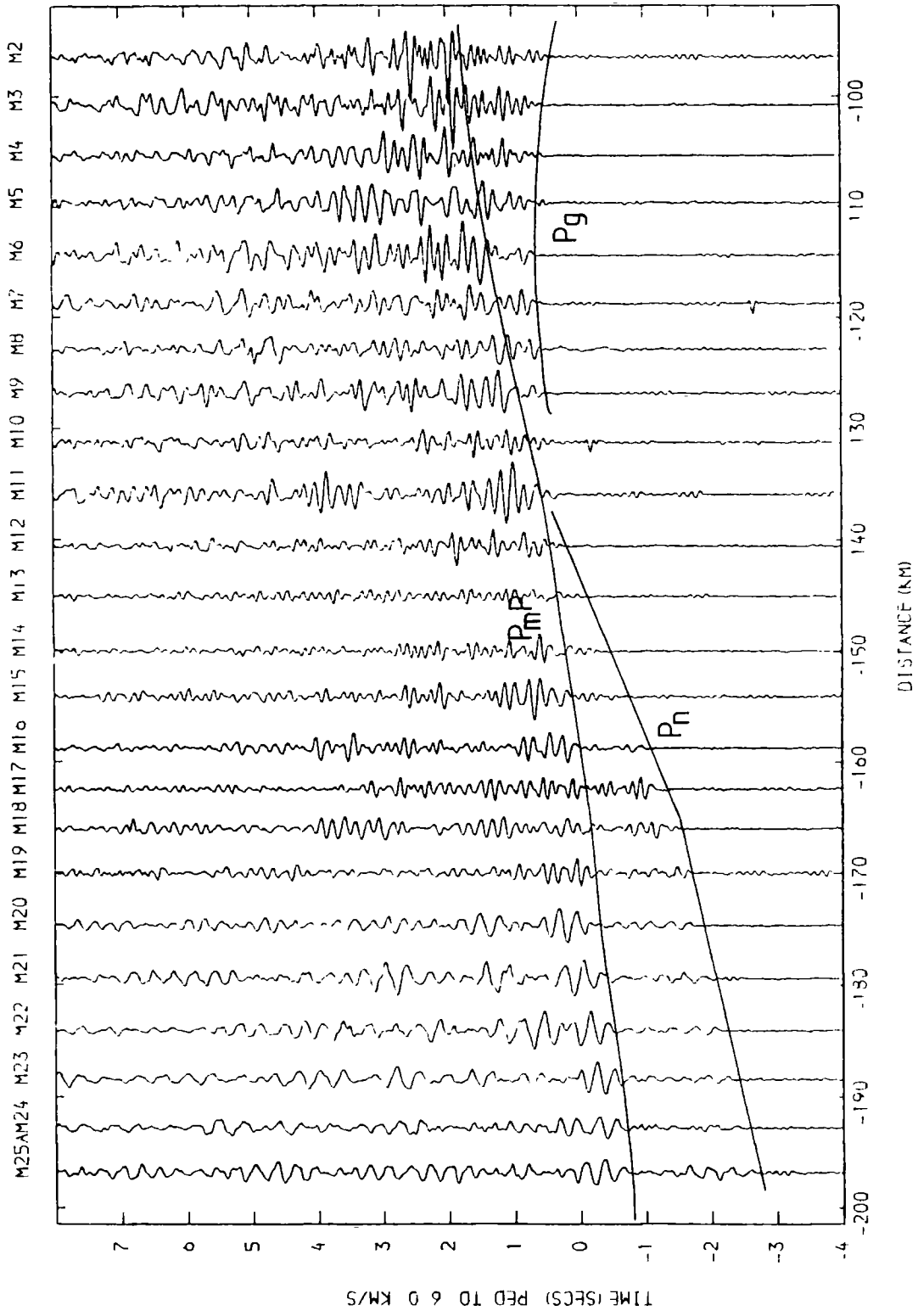


Fig 5.12 Reduced section of the Irish Sea shots recorded at S32.
 Filtered 2-12 Hz, amplitudes uncorrected

the stations receiving the Irish Sea shots. The first arrivals from 30 to 130 km represent Pg with an apparent velocity of between 6.0 and 6.2 km/s. The largest amplitude is always at shots M1 to M10 but Pg can also be observed on some sections at shots M11 and beyond at smaller amplitude. Beyond 130 km, Pn is the first arrival with an apparent velocity of 7.85 to 10.17 km/s. The high apparent velocity at many stations is due to the effects of the western flank of the Solway Basin. The only prominent second arrival is PmP, the diving wave or reflection from the Moho. It has a maximum amplitude in the range 90 to 110 km and appears to pass into a lower crustal channel wave of apparent velocity 6.8 to 7.0 km/s beyond 150 km.

There is no clear evidence for any phases from a mid-crustal discontinuity.

Travel-time curves for Pg at stations S1 and S8 show strong curvature caused by the Solway basin (Fig. 5.13). The true refractor velocity can be obtained from the minus times calculated between P456 and S1 to S8 (Table 5.4) and the average of six estimated velocities is 6.13 ± 0.06 km/s.

It is interesting to note that the maximum delay to the travel-time curves occurs at shot M7 for both P456 and the stations in England (Fig. 5.13). For a refractor of velocity 6.1 km/s with 4 km of rocks of velocity 4.5 km/s above, there is a ray offset of over 4 km between the refractor and the surface. A difference of

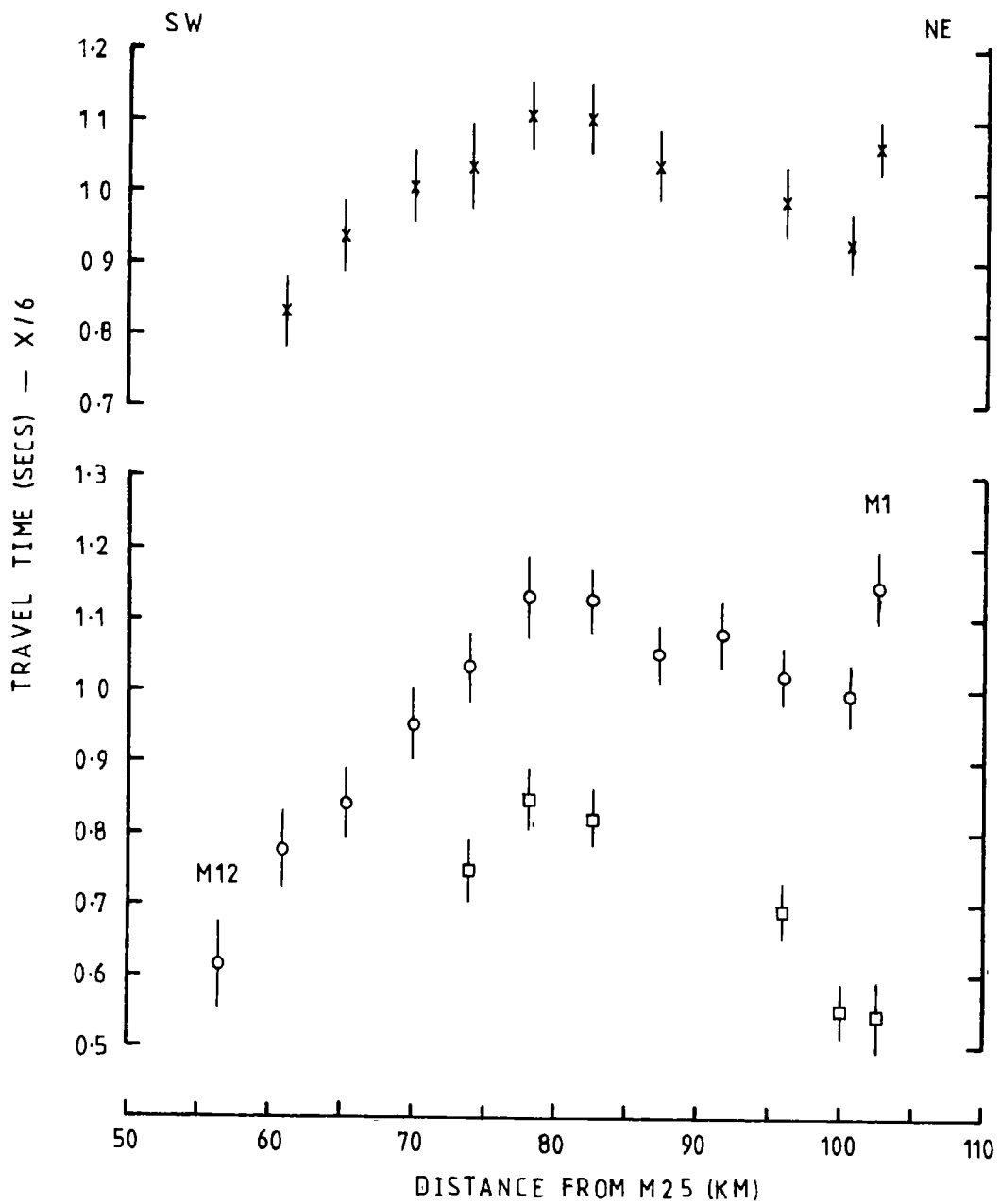


Fig 5.13 Reduced travel-time plot for the Irish sea shots recorded at S1, S8 and P456

TABLE 5.4

Velocity of the Pg refractor from the minus-times calculated between P456 and stations in northern England.

Stations	Velocity km/s	Std Err	95% Conf.
P456/S1	6.11	0.03	0.09
P456/S2	6.08	0.03	0.12
P456/S6	6.11	0.02	0.23
P456/S7	6.21	0.04	0.11
P456/S8	6.15	0.04	0.11

8 km (two shot spacings) would be expected between the position of the maximum delay on the records at receivers on opposite sides. This is not observed suggesting there is probably not a large velocity contrast across the Pg interface and that most of the delay occurs in the near surface lower velocity sediments.

The Irish Sea explosions were recorded in southern Scotland (S81) and the Isle of Man (S91) as well as in northern England. The time-term method was used to utilise all this data. From the airgun and PUSS profiles the first arrivals out to 30 km have a lower velocity than Pg and are from a shallower refractor. The data was therefore split into two groups. Shots observed between 10 and 30 km were treated separately from those beyond 30 km.

The data recorded from the shallow refractor are constrained by making shot M25 coincident with P123 and M17 coincident with P456. The shot and station in each pair are about 2 km apart. The least squares velocity is 5.50 ± 0.27 km/s. The time-terms suggest that the refractor comes close to the surface between shots M17 and M24 and at station S81 where the time-terms are close to zero (Table 5.5, Fig. 5.14). This agrees with the airgun data which gives an apparent velocity of 5.30 km/s at a shallow depth close to M19. The zero time-term at S81 indicates that this refractor represents the Lower Palaeozoic. S91, also on Lower Palaeozoic rocks, has a time-term of 0.18 s. The largest time-terms are found at M6 (0.48 s) and M8 (0.46 s) and are coincident with the gravity minimum.

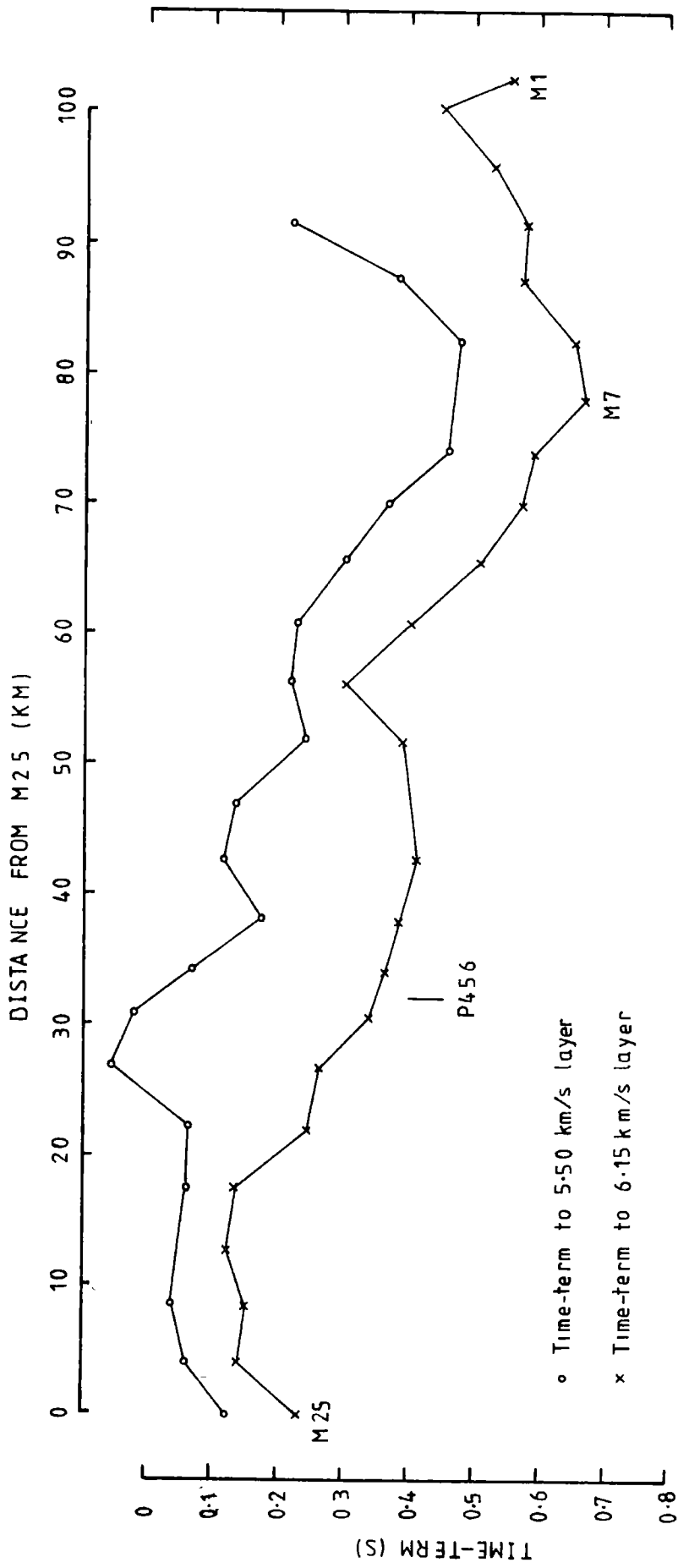


Fig 5.14 Distribution of time-terms in the Irish Sea

TABLE 5.5

Time-term analysis - Irish Sea

Shot	5.50 +/- 0.27			6.15 +/- 0.04		
	Time-term s	Error 95%	No.	Time-term s	Error 95%	No.
M1	-	-	-	0.54	0.13	4
M2	-	-	-	0.44	0.01	12
M3	-	-	-	0.52	0.04	10
M4	0.23	0.00	1	0.57	0.02	7
M5	0.38	0.00	1	0.57	0.02	9
M6	0.48	0.00	1	0.65	0.02	8
M7	-	-	-	0.67	0.02	7
M8	0.46	0.00	1	0.58	0.02	7
M9	0.37	0.00	1	0.57	0.02	6
M10	0.30	0.00	1	0.50	0.06	4
M11	0.23	0.10	2	0.40	0.04	4
M12	0.22	0.05	3	0.30	0.00	1
M13	0.24	0.06	2	0.39	0.00	1
M14	0.14	0.20	2	-	-	-
M15	0.11	0.06	2	0.41	0.00	1
M16	0.17	0.00	1	0.39	0.05	2
M17/P456	0.07	0.02	5	0.36	0.03	10
M18	-0.02	0.00	1	0.34	0.00	1
M19	-0.06	0.02	2	0.26	0.00	1
M20	0.06	0.00	1	0.25	0.07	2
M21	0.06	0.00	1	0.13	0.36	2
M22	-	-	-	0.12	0.07	2
M23	0.04	0.02	2	0.15	0.23	2
M24	0.06	0.04	2	0.13	0.00	1
M25/P123	0.12	0.01	5	0.23	0.02	6
S81	-0.01	0.01	9	0.22	0.03	8
S91	0.18	0.01	10	0.41	0.02	12

All errors represent the 95% confidence limits calculated from the Berry and West (1966) standard error.

The data used in the analysis Pg were also constrained by making the shots M17 and M25 coincident with P456 and P123. The least squares velocity is 6.15 ± 0.04 km/s and the time-terms vary between 0.12 s and 0.67 s (Table 5.5, Fig. 5.14). The smallest values are found between M21 (0.13 s) and M24 (0.13 s) and at S81 (0.22 s). The largest values are again found between M6 (0.65 s) and M8 (0.58 s). The station residuals do not show any strong correlation with range (Fig. 5.15).

In order to find whether there are any regional variations in the Pg velocity, the data were split into western and eastern data sets. The dividing line is a north south line joining stations S81 and S91 and passing between shots M11 and M12. No significant difference is noted. The velocities are 6.10 ± 1.09 km/s and 6.13 ± 0.06 km/s for the western and eastern sets respectively.

5.4 Presentation of the Northern England data

The data used in the interpretation of the line across northern England comes from the two shots on land, the Irish Sea and North Sea shots and quarry blasts. The common shot sections have not been corrected for the 50 ms difference between the odd and even channels on the Geostore recorders (see section 3.4) but the travel-time curves have been corrected. The stacked common shot sections have all been plotted with equalised amplitudes. This is because of the difficulty found in correcting for the station

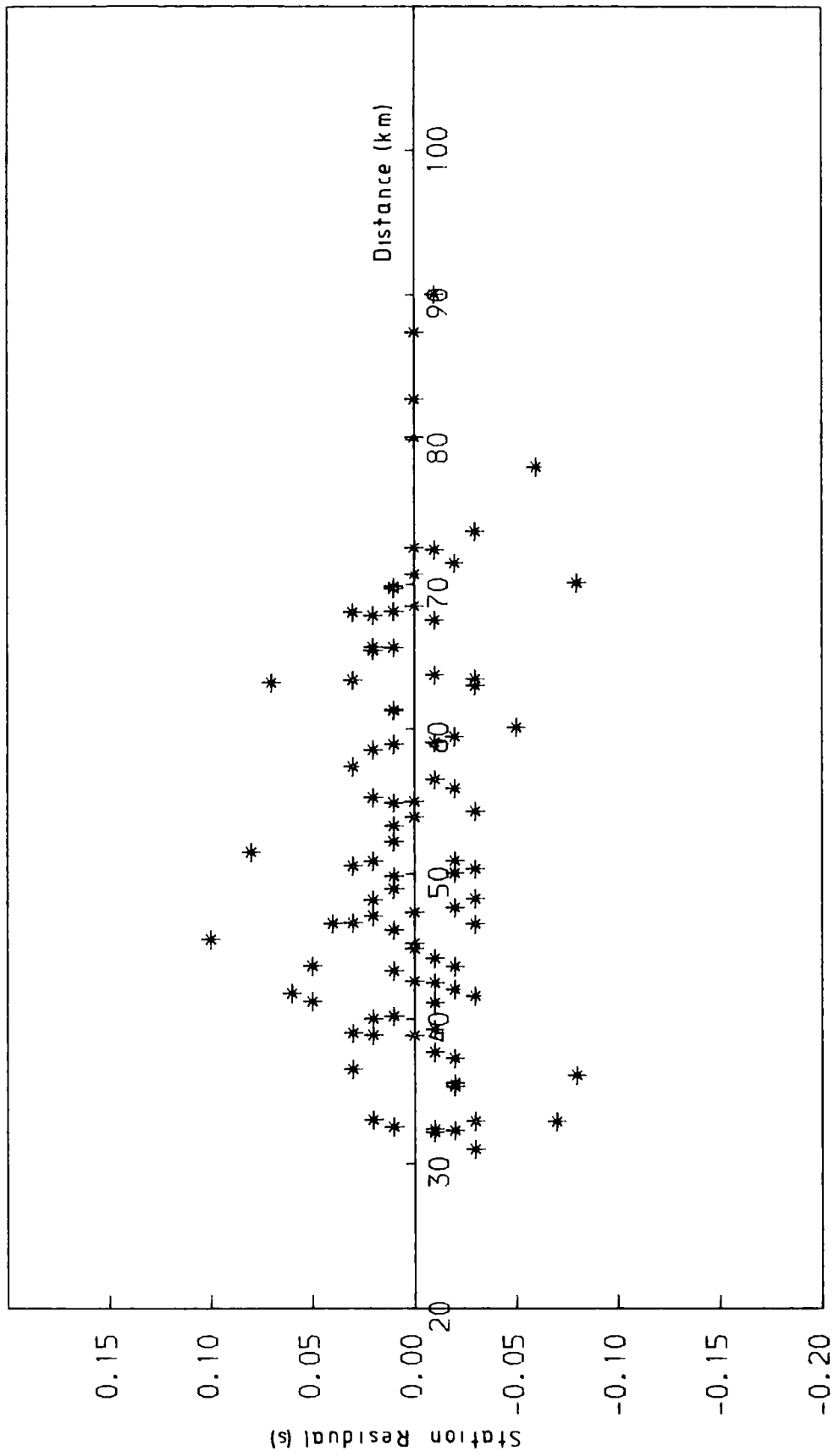


Fig 5.15 Plot of residuals against distance for the Irish Sea Pg time-term analysis

gains (see section 2.2.1).

5.4.1 Land shots

The Spadeadam shot and station S28 are coincident. The Kirkwhelpington shot and cassette station S73 are also coincident but the nearest main line station is 200 m away at S46.

The frequency content of the Spadeadam shot is largely between 11 and 18 Hz (Fig. 5.16). A 2 to 18 Hz bandpass filter was applied to the stacked section (Fig. 5.17). Prominent first arrivals are observed out to 60 km to the east but cannot be traced with confidence beyond 40 km to the west. Between stations S43 and S56 there is a considerable amount of energy arriving from 1 to 3 s after the first arrival.

The travel-time curve to the east shows breaks of slope at 2 km and at 30 km where P_g becomes the first arrival (Fig. 5.18). A homogeneous horizontal layer interpretation indicates three layers of velocities 4.01 km/s, 5.42 km/s and 6.06 km/s with boundaries at 1.2 km and 4.2 km (Fig. 5.19). The western travel-time curve does not show any clear breaks of slope, the apparent velocity shows a small increase with distance from 4.9 km/s to 5.2 km/s. These velocities are estimated from stations across the eastern flank of the Carlisle Basin and they probably underestimate the actual velocity.

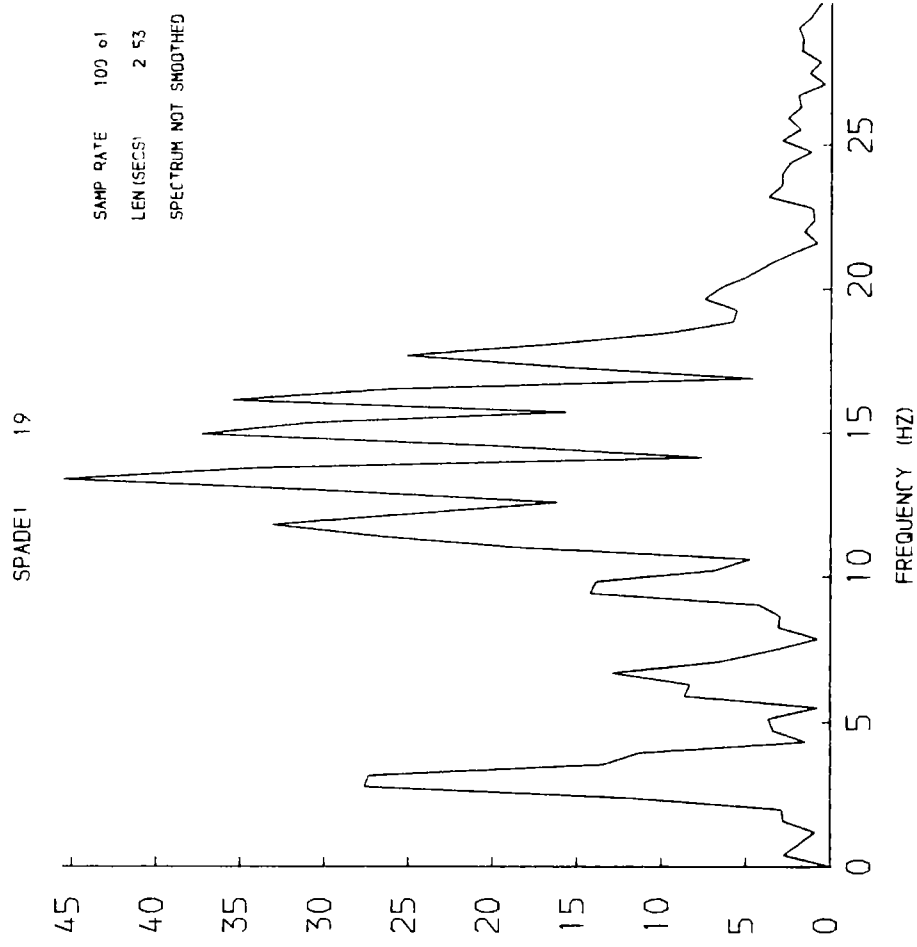
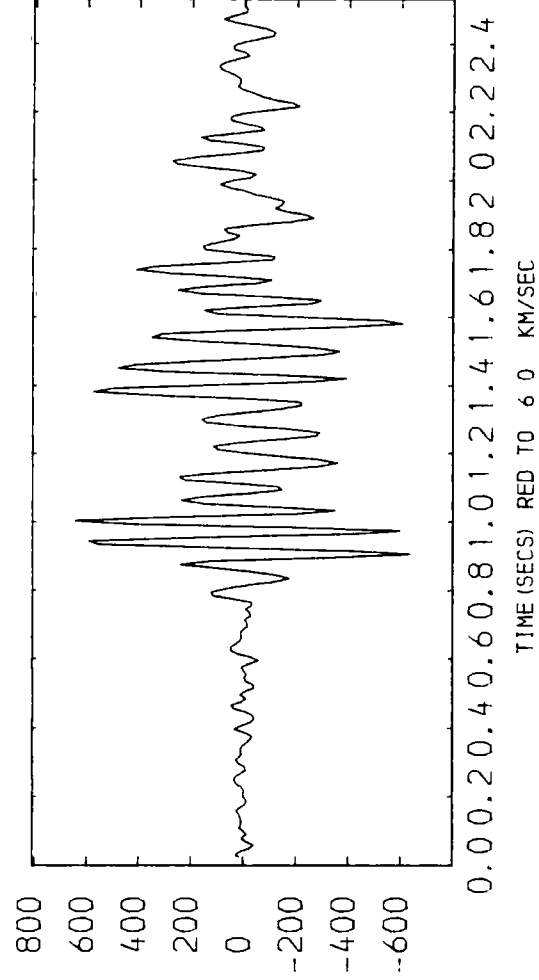


Fig 5.16 Frequency plot of the Spadeadam shot at S19 at a range of 19.8 km

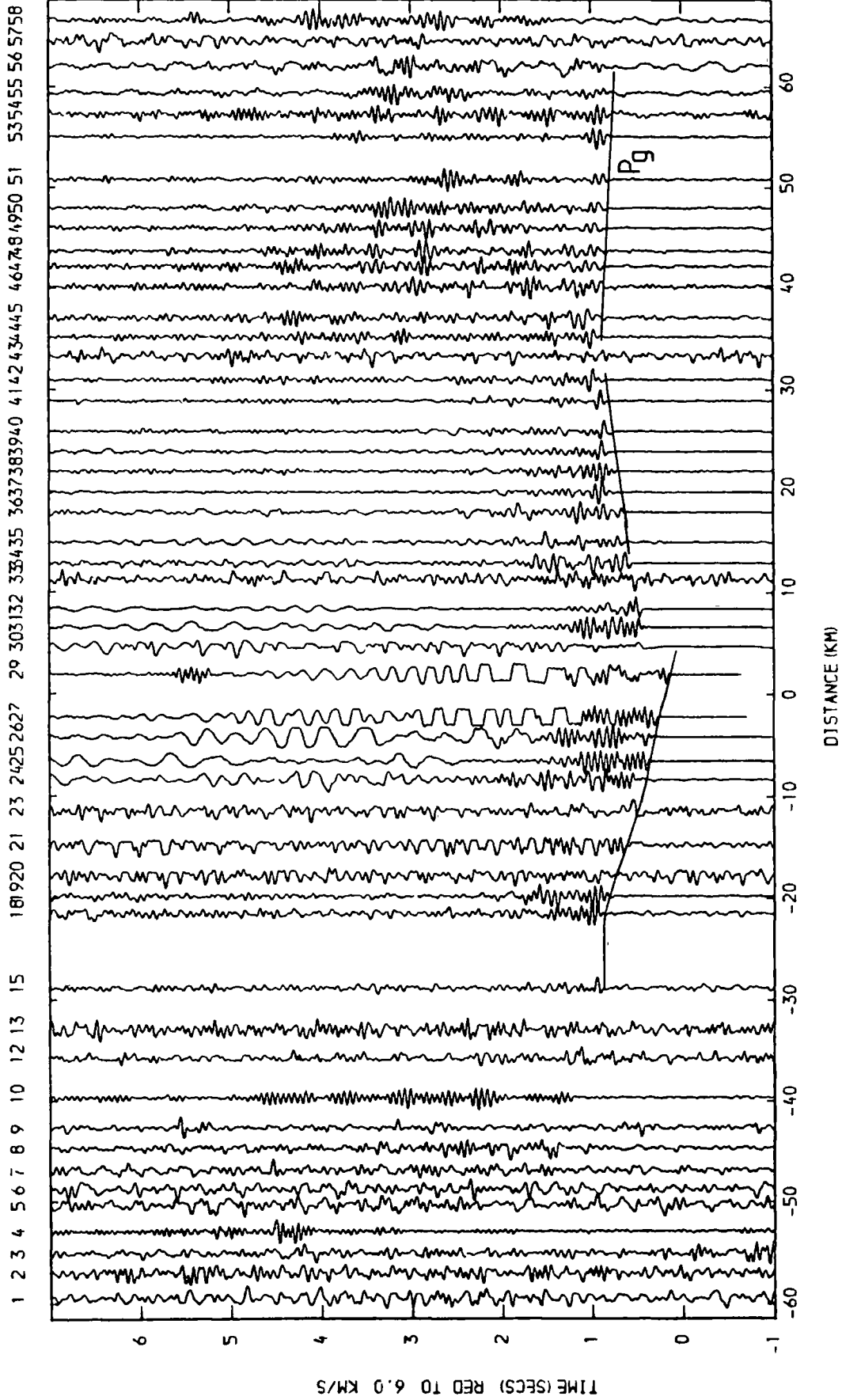


Fig 5.17 Reduced section of the Spadeadam shot. Filtered 2-18 Hz, amplitudes equalised

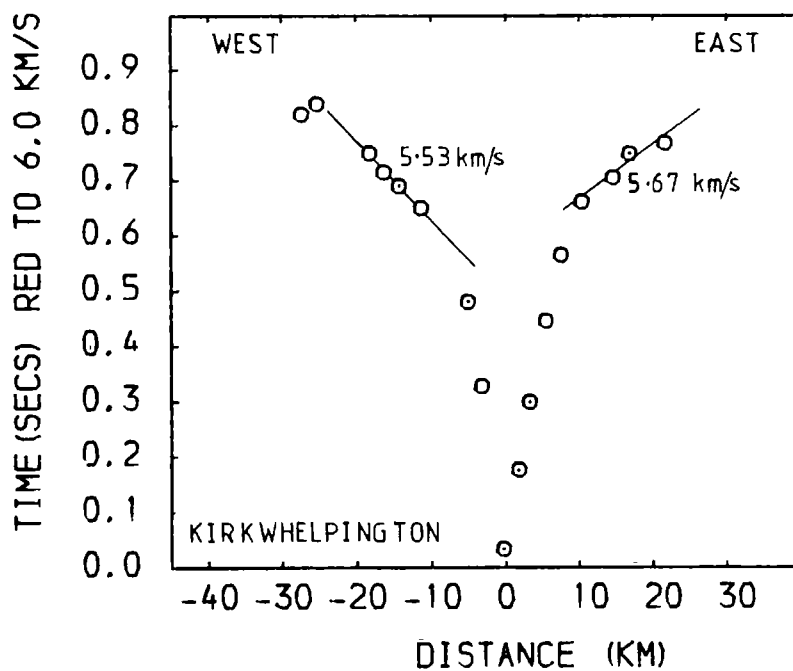
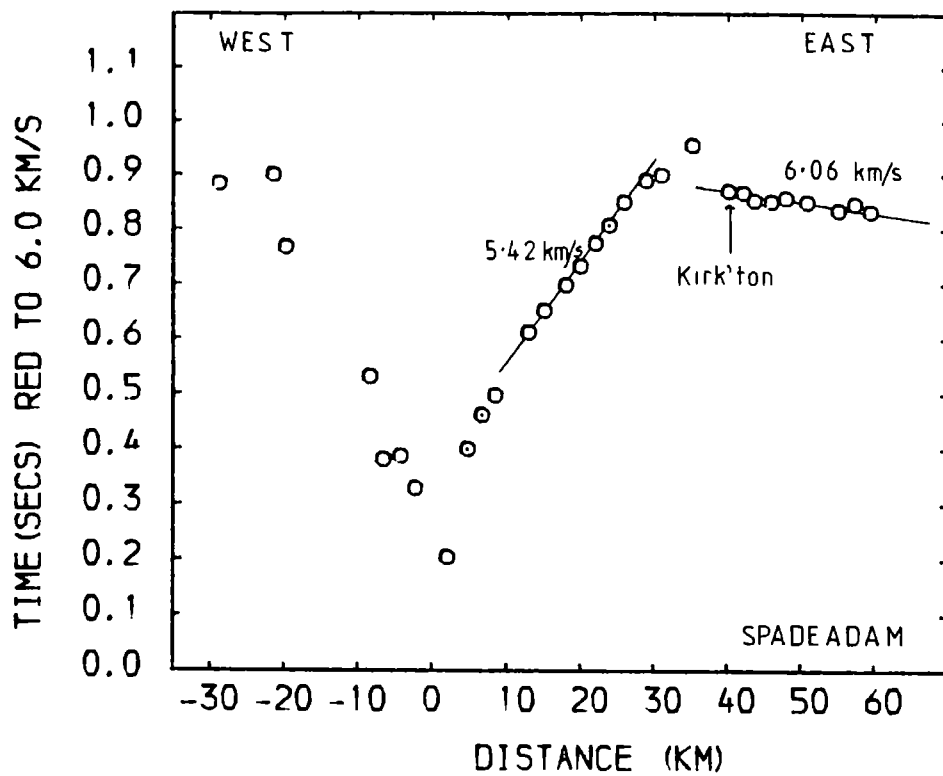
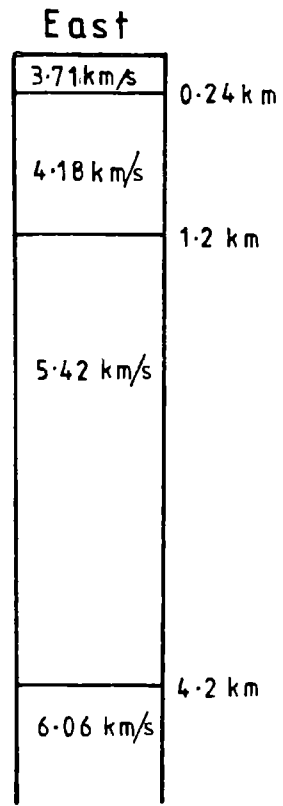


Fig 5.18 Reduced travel-time plots of the Spadeadam and Kirkwhelpington shots

Spadeadam



Kirkwhelpington

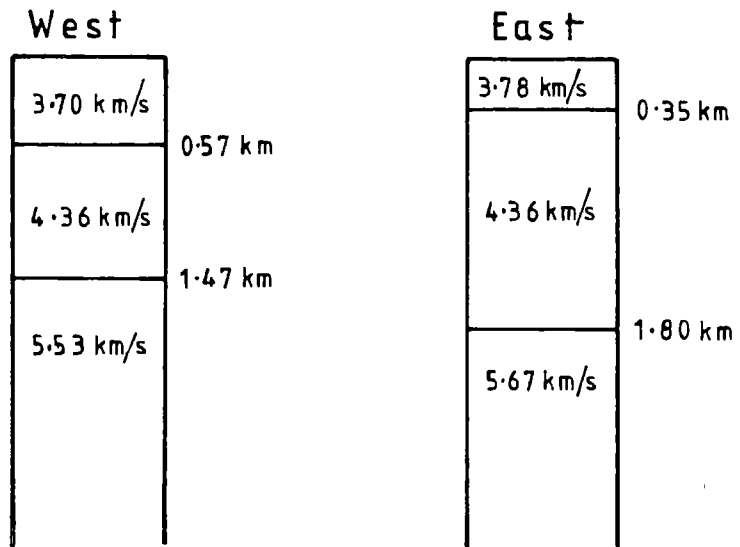


Fig 5.19 Plane layer interpretation of the Spadeadam and Kirkwhelpington shots

The frequency content of the Kirkwhelpington shot is predominantly between 7 and 16 Hz (Fig. 5.20). The shot was not as large as the Spadeadam shot and is only observed out to 30 km (Fig. 5.21). It is doubtful whether Pg is seen. The travel-time curves have been interpreted assuming homogeneous horizontal layers (Fig. 5.17). A refractor of 5.53 km/s to the west and 5.67 km/s to the east have been identified at a depth of 1.5 km and 1.8 km respectively (Fig. 5.19). If the refractor is assumed plane beneath the stations and shot the true velocity is 5.60 km/s with a refractor dip of 0.9° to the west. Stations S38 to S41 observed the same refractor from both the Spadeadam and Kirkwhelpington shots. The velocity determined for this short section from the minus times is 5.49 ± 0.08 km/s.

5.4.2 Sea shots

Common shot sections M1 and M4 show that Pg is the first arrival out to 120 km (Figs. 5.22, 5.23 and Appendix A). The first arrival beyond 130 km is Pn with an apparent velocity of 8.31 to 8.99 km/s. PmP, the reflection or diving wave from the Moho, is a recognisable second arrival from 70 to 110 km which at greater distances appears to pass into a lower crustal channel wave. Between 100 and 110 km there is a small burst of energy arriving 0.2 to 0.3 s after Pg. It is tentatively identified as PcP from a mid-crustal discontinuity or gradient.

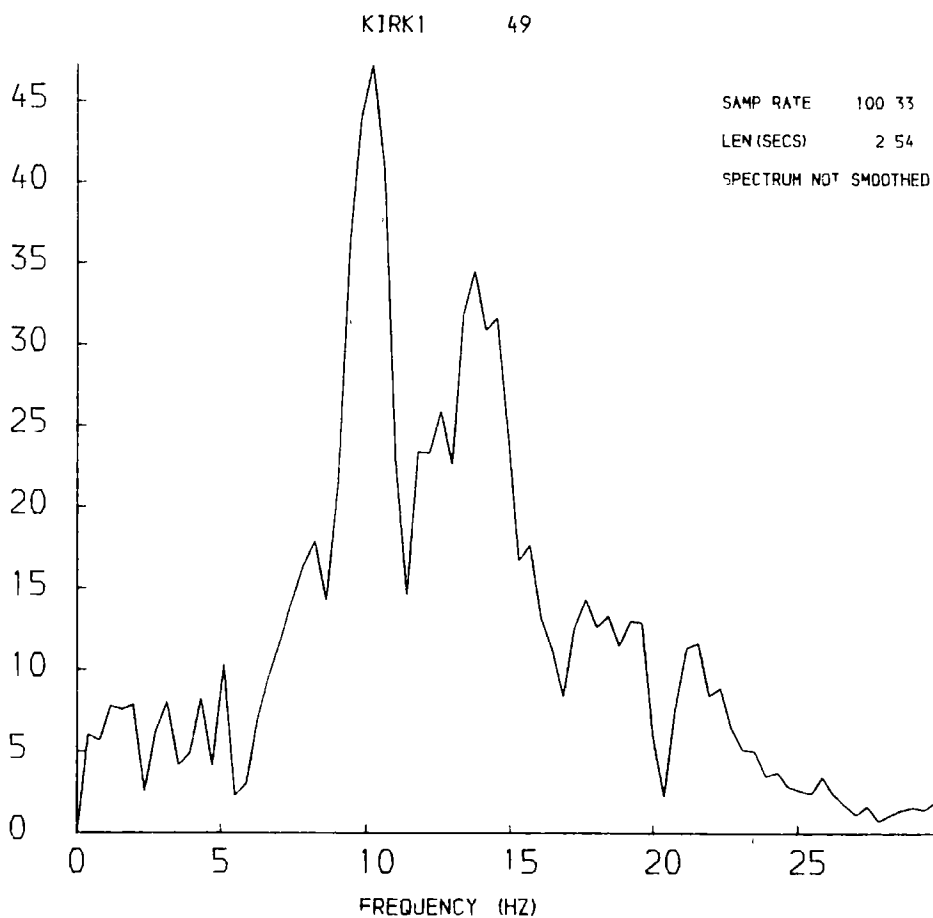
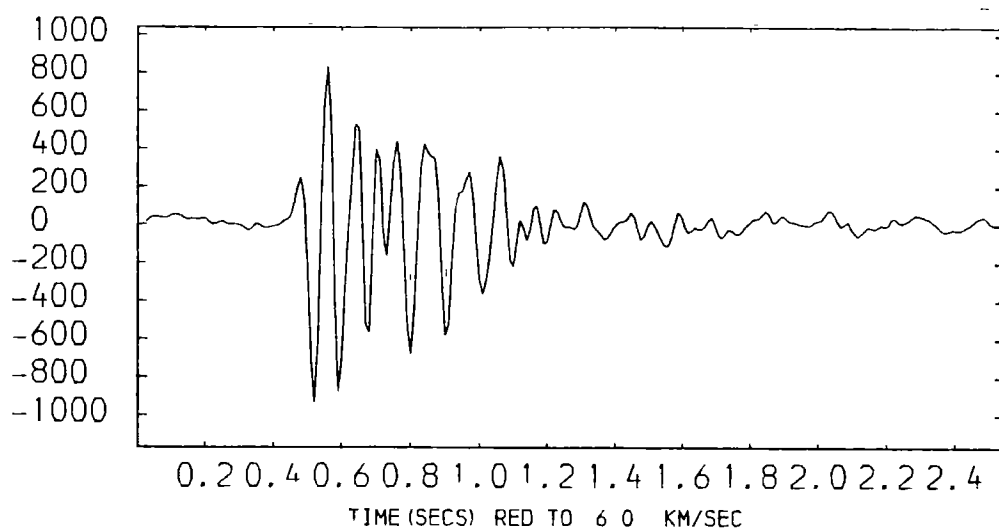


Fig 5.20 Frequency plot of the Kirkwhelpington shot at S49 at range of 5.6 km

D U R H A M U N I V E R S I T Y L I B R A R Y

LOAN OF THESES

Theses are loaned subject to the following conditions.

1. The copyright declaration form at the front of the thesis must be signed by the reader before consultation. If the thesis is not consulted please enclose a note saying so when returning it to us.
2. The thesis is for use within the library only.
IT MAY NOT BE TAKEN OUT.
3. No copy to be made without the author's written permission.
4. Please use compensation post when returning the thesis.

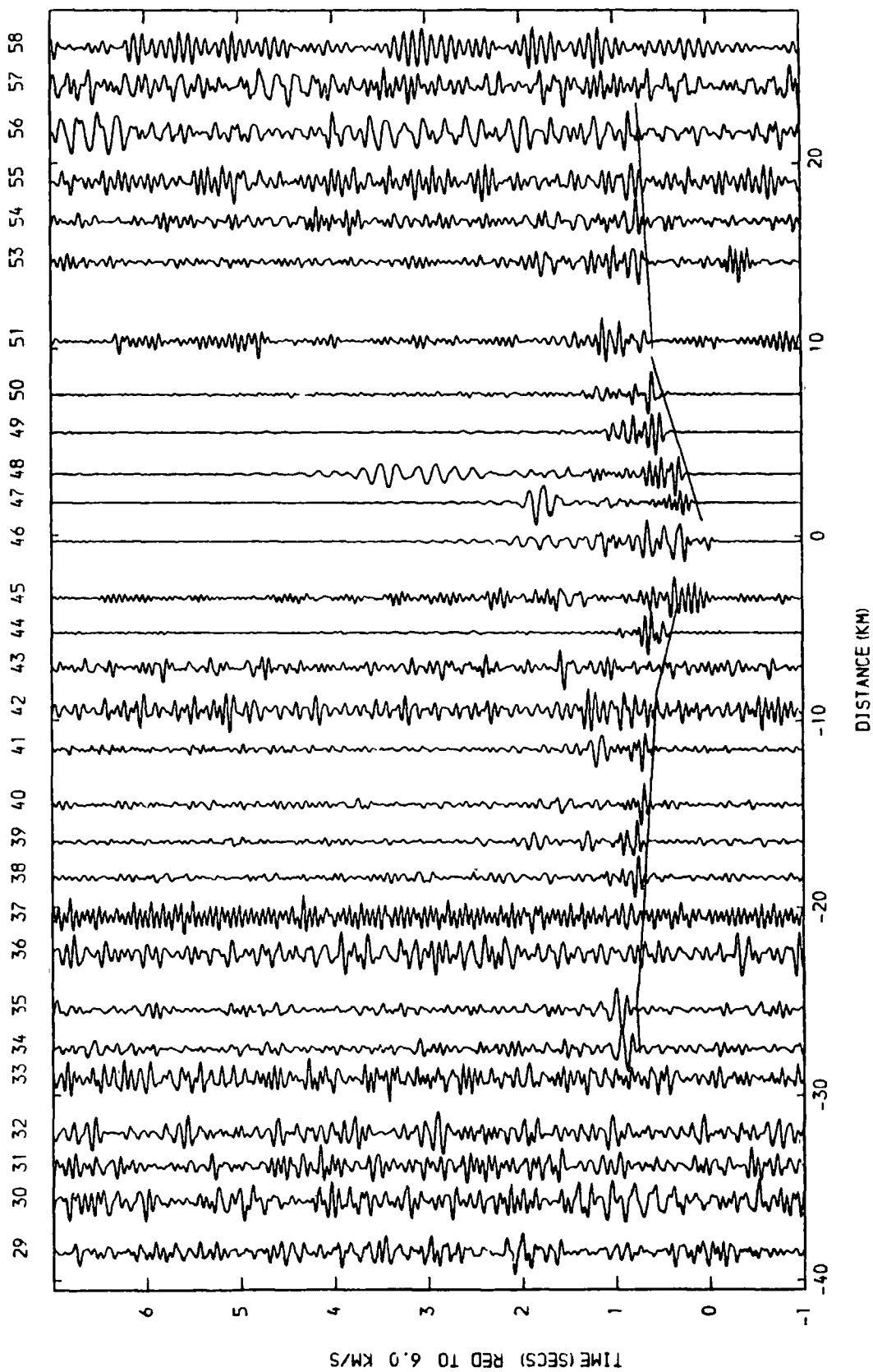


Fig 5.21 Reduced section of the Kirkwhelpington shot. Filtered 5-18 Hz, amplitude equalised

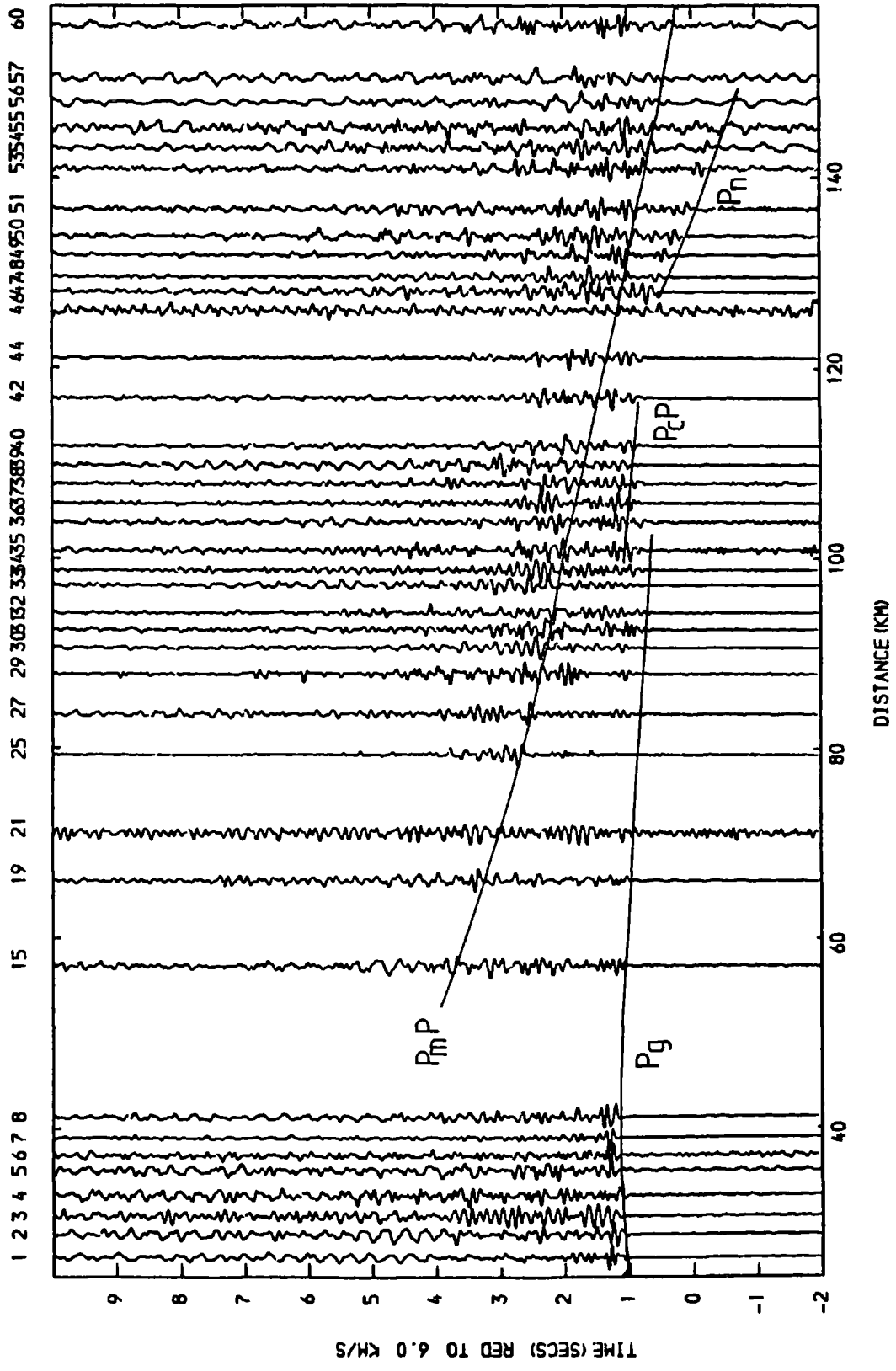


Fig 5.22 Reduced section for shot M1. Filtered 2-15 Hz, amplitudes equalised

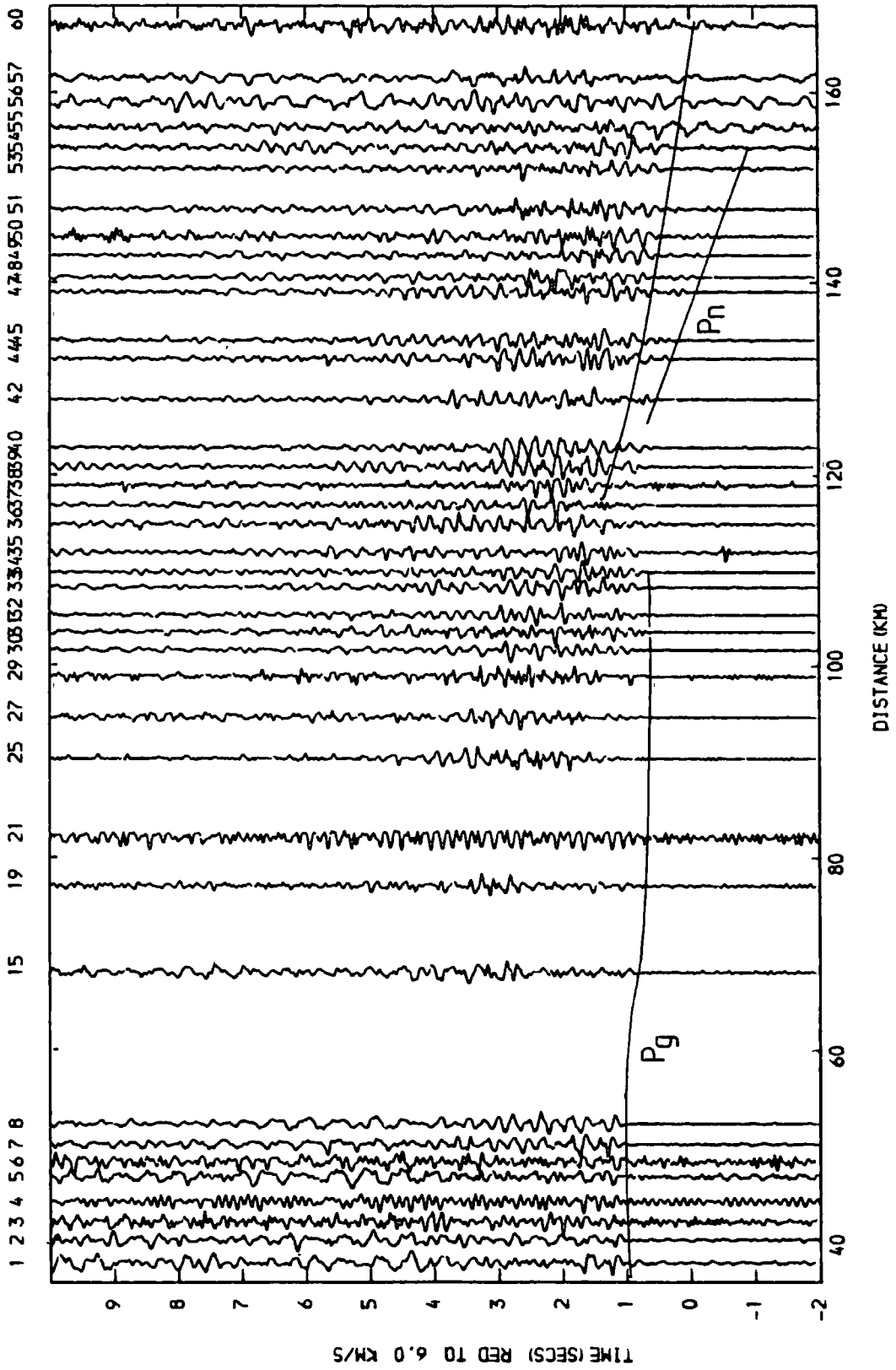


Fig 5.23 Reduced section for shot M4. Filtered 2-15 Hz, amplitudes equalised

The common shot sections for the North Sea show a much higher signal to noise ratio than those for the Irish Sea (Figs. 5.24, 5.25 and Appendix A). Pg is a prominent arrival out to at least 110 km but because of the poor quality of the data for stations S1 to S25 it is difficult to establish whether Pg is the first arrival at greater range. Pg is not observed from shots beyond N10 at any station on the main line although it is observed out to N17 at station S62. Following Pg by about 0.5 s in common shot section N1 and about 0.35 s in common shot section N3 (Fig. 5.25) is an arrival similar to Pg. This is called Pg' and is believed to result from the structure under the shots. A third arrival Pg'' is visible on recordings at some of the stations (Fig. 5.24). Beyond 130 km Pn is the first arrival with an apparent velocity of 8.52 km/s. PmP and PcP are recognisable arrivals and they are followed by similar phases called PmP' and PcP'. These arrivals tend to merge together on some traces making separate identification difficult. *

The travel-time curves for N1 and N3 show several breaks of slope (Fig. 5.26). Most of these are related to lateral changes and not layering. An increase in apparent velocity to 6.24 km/s for N1 occurs at S38 at a range of 56 km. For N3 the increase in apparent velocity also increases at S38 but at a range of 64 km.

The true velocity of Pg beneath the Northumberland Trough can be obtained from the minus times calculated between the Spadeadam and North Sea shots (Table 5.6). The estimated velocities vary

* An alternative interpretation of phases Pg', Pg'', PcP' and PmP' is that they result from bubble oscillations. All further references in the thesis to these phases should be regarded with this in mind.

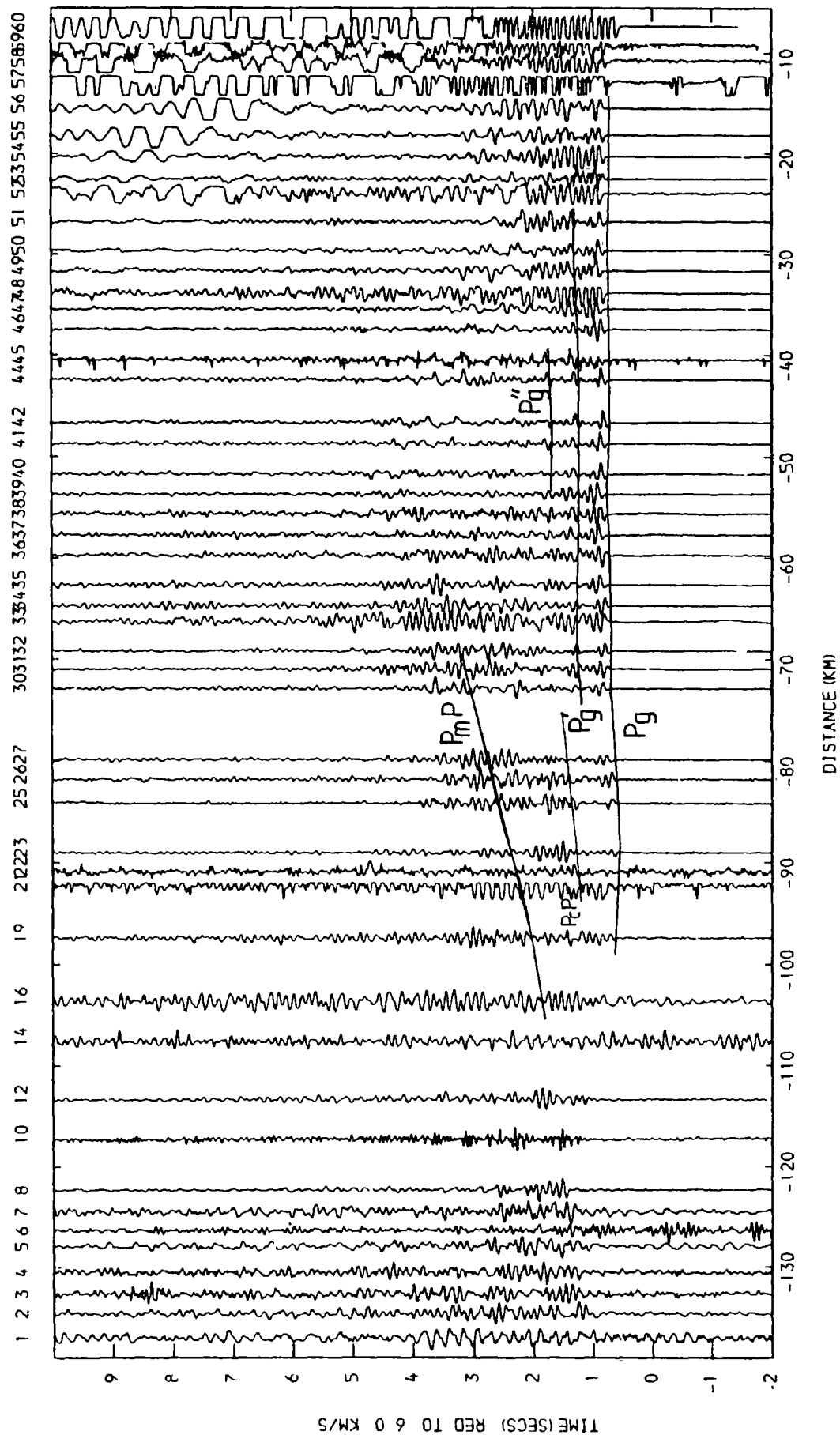


Fig 5.24 Reduced section for shot N1. Unfiltered, amplitudes equalised

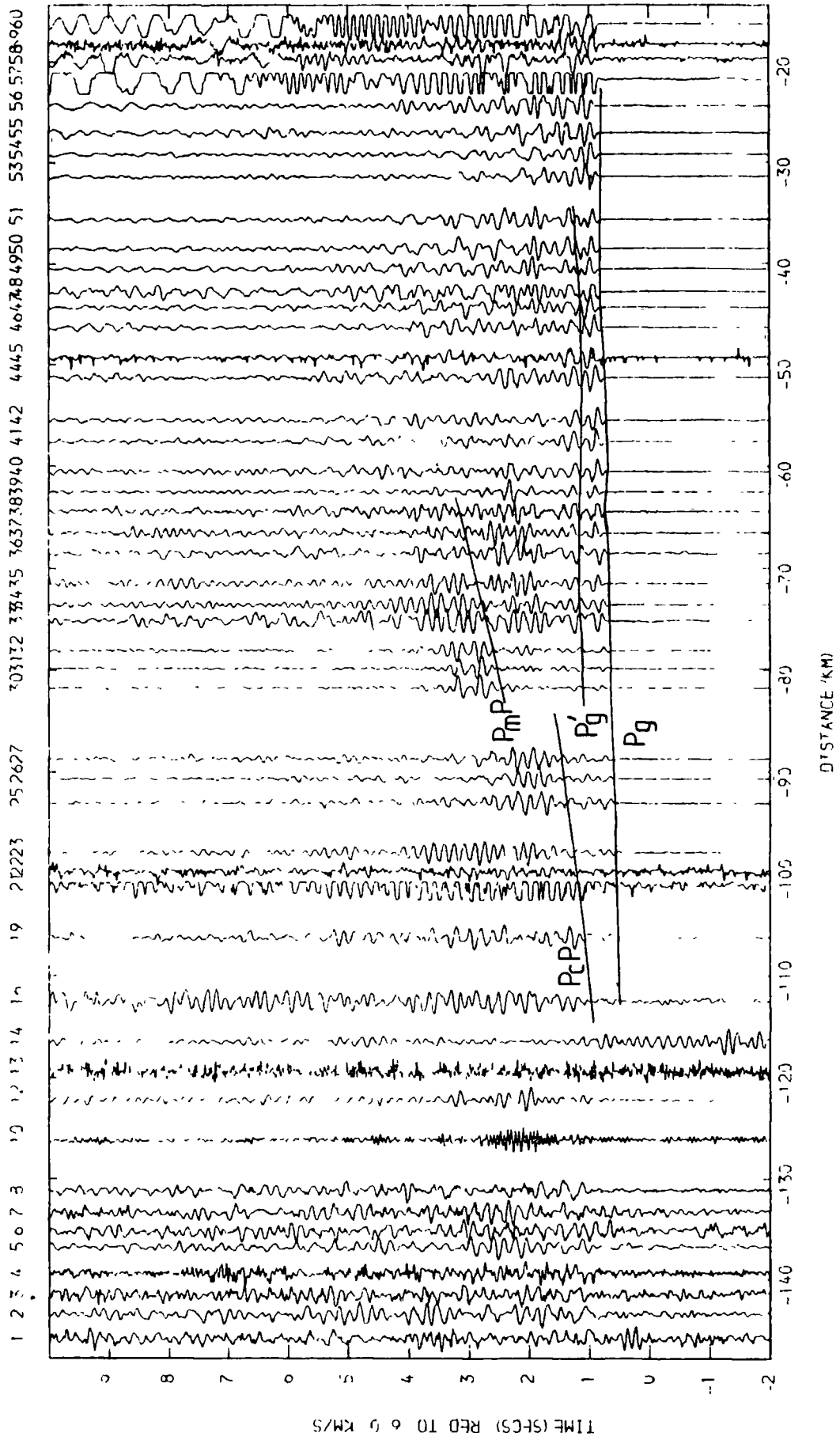


Fig 5.25 Reduced section for shot N3. Unfiltered, amplitudes equalised

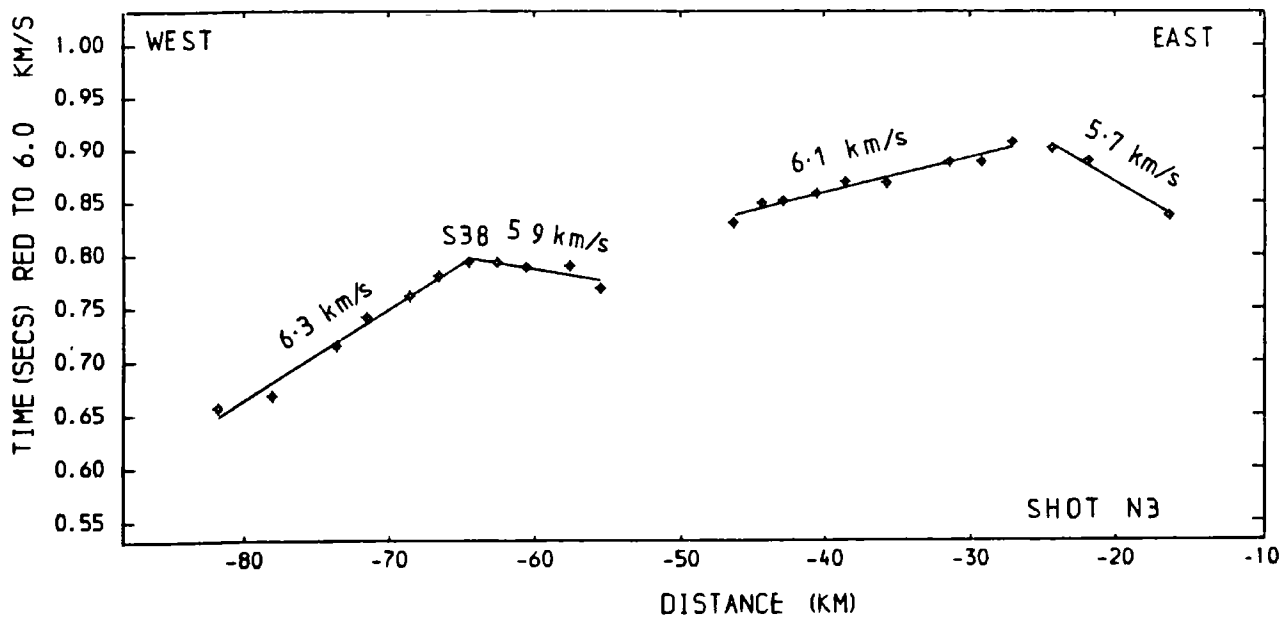
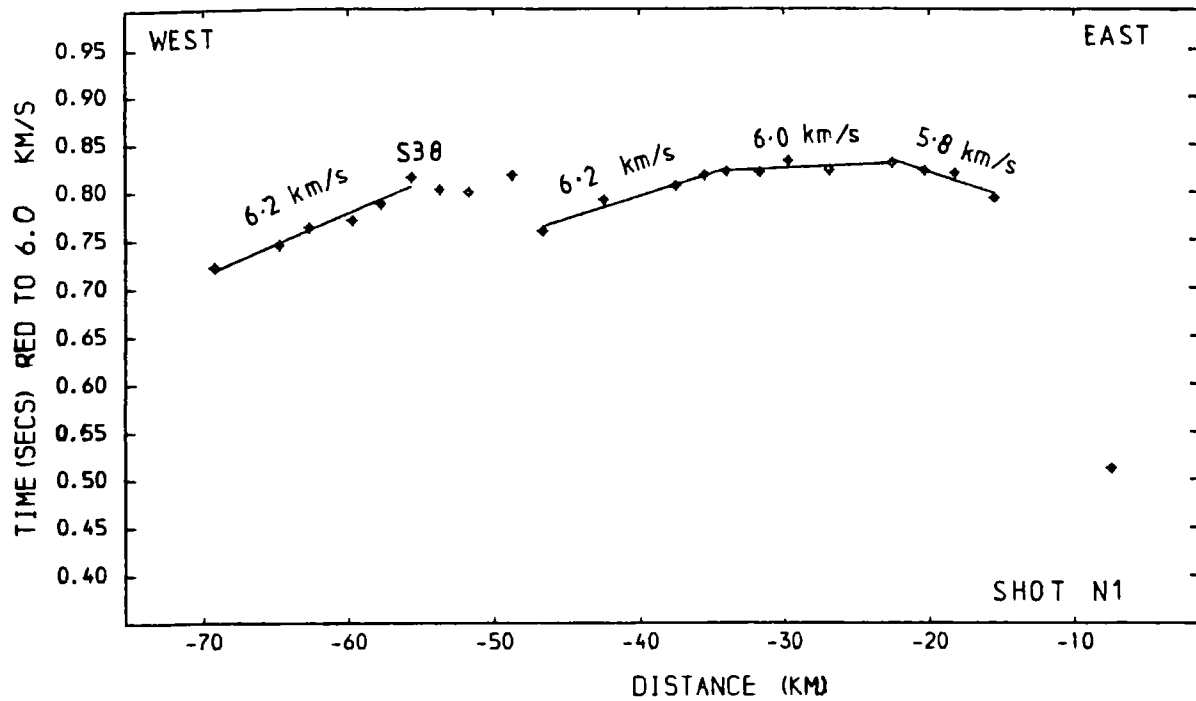


Fig 5.26 Reduced travel-time plots of shots N1 and N3 recorded in northern England

TABLE 5.6

Velocity for the Pg refractor from the minus-times calculated between the Spadadam shot (S28) and the North Sea shots

Shots	Velocity km/s	Std Err	95% Conf.
S28/N1	6.07	0.03	0.08
S28/N2	6.07	0.01	0.02
S28/N3	6.09	0.01	0.03
S28/N4	6.10	0.01	0.03
S28/N5	6.11	0.02	0.05
S28/N6	6.14	0.01	0.02
S28/N7	6.14	0.02	0.04
S28/N8	6.15	0.04	0.09
S28/N9	6.18	0.01	0.03

between 6.07 and 6.18 km/s with a mean value of 6.12 +/- 0.03 km/s.

5.4.3 Quarry blasts

The quarry blasts were usually observed at a range of less than 30 km and it was hoped that they would give information on the shallow structure in the Northumberland Trough. The recordings from the quarries at Mootlaw, Q15, and Barrasford, Q16, suggest that the velocity observed between 2 and 12 km lies in the range 4.3 to 4.6 km/s (Table 5.7). Between 12 and 30 km apparent velocities of from 5.4 to 5.6 km/s are observed.

The apparent velocity determined from an open cast coal site blast approximately 2 km offline between S59 and S60 is 6.06 +/- 0.11 km/s.

5.4.4 Time-term analysis

The time-term method was used so that the quarry blasts and offline stations could be incorporated into the analysis. On the evidence of the Spadeadam shot and the quarry blasts, the data was split between shots observed at ranges between 10 and 30 km and shots observed at ranges beyond 30 km. The former relate to a refractor with a velocity of 5.4 to 5.6 km/s and the latter relate to Pg with a velocity of 6.1 to 6.2 km/s.

TABLE 5.7

Velocities and intercept times determined from quarry blasts in Northumberland.

Quarry	Year	Range (km)	Vel. (km/s)	Err 95%	Int. (s)	Err 95%
Opencast mine	1982		6.06	0.11		
Mootlaw (Q15)	1982	10.2 - 11.1	4.58	2.00	0.03	1.02
Mootlaw (Q15)	1982	11.1 - 27.5	5.40	0.17	0.46	0.11
Mootlaw (Q15)	1983	2.8 - 12.1	4.35	1.16	0.20	0.49
Barrasford (Q16)	1983	11.0 - 18.7	5.57	1.41	0.08	0.63

The data for the shallow refractor is spread over a large area and not well reversed. It is not possible to constrain the data by making a shot and station coincident. Instead the intercept times for the shallow refractor at the Spadeadam shot and for the airgun shots recorded at S60 were used. Because of the small amount of data, the land stations and North Sea shots are treated together. The least squares velocity is 5.62 ± 0.13 km/s. The time-terms along the main line vary between 0.17 and 0.41 s (Table 5.8, Fig. 5.27). There is a 0.1 s decrease in the time-term between the stations near the coast and the shots at sea. Such a difference between shots and stations can occur if the shots and stations are not well constrained but it is necessary to be cautious, as it might reflect a real change across the coast. The results were the same whichever of the two intercept times were used to constrain the data.

The time-terms for stations numbers 20, 23, 29 and 36 operated by Swinburn (1975) are either very large or very small and do not appear to be trustworthy (Table 5.8). But they do not affect the other values as they are unconnected.

Explosions from the Irish Sea, North Sea, Spadeadam and a quarry blast at Belford (Q29) were used for the Pg analysis. The data is constrained by making Q29 and S62 coincident. Initially all shot/station travel-times between 30 and 110 km apart were used and the least squares velocity calculated is 6.16 ± 0.04 km/s (Table 5.9). A plot of the station residuals, however, shows that

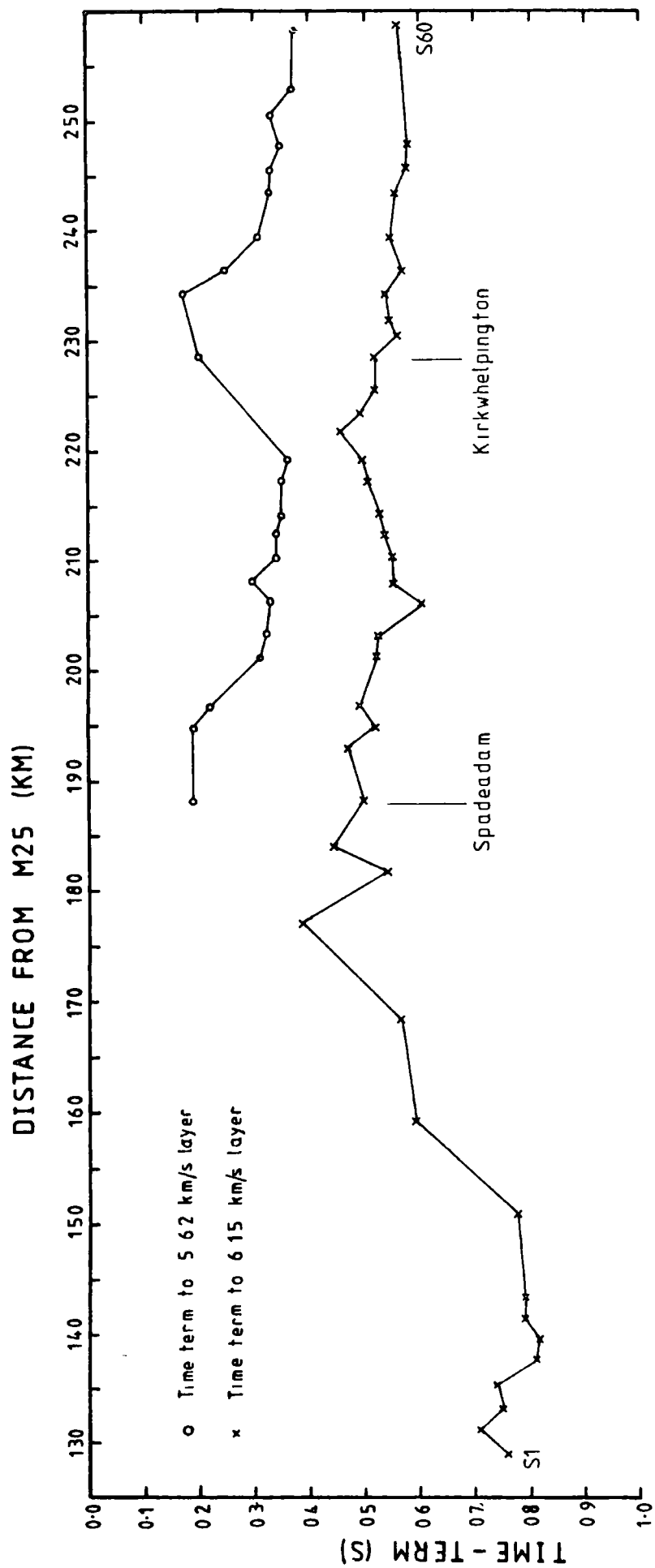


Fig 5.27 Distribution of time-terms across northern England

TABLE 5.8

Time-terms to 5.62 +/- 0.13 km/s refractor - northern England
and North Sea.

Station	Time-term (s)	Err.	No.
S28	0.19	0.01	12
S31	0.19	0.00	1
S32	0.22	0.00	1
S34	0.31	0.12	2
S35	0.32	0.04	3
S36	0.33	0.04	3
S37	0.30	0.03	3
S38	0.34	0.02	2
S39	0.34	0.06	2
S40	0.35	0.07	2
S41	0.35	0.12	2
S42	0.36	0.00	1
S46	0.20	0.02	10
S49	0.17	0.03	5
S50	0.25	0.00	1
S51	0.31	0.16	2
S53	0.33	0.03	2
S54	0.33	0.04	4
S55	0.35	0.03	2
S56	0.33	0.10	3
S57	0.37	0.00	1
S60	0.37	0.02	5
S61	0.41	0.02	5
L14	0.37	0.15	3
L16	0.14	0.12	3
L18	0.17	0.06	2
L24	0.33	0.00	1
20	0.05	0.03	3
23	-0.04	0.00	1
29	0.80	0.00	1
36	0.78	0.09	3
Q1	0.16	0.16	2
Q15	0.32	0.03	9
Q16	-0.12	0.04	10
Q34	0.06	0.00	1
N1	0.25	0.02	7
N2	0.21	0.11	2
N3	0.26	0.02	6
N4	0.25	0.09	2
N5	0.21	0.09	2
N6	0.21	0.00	1

Errors represent the 95% confidence limits

TABLE 5.9

Pg time-term analysis - northern England

Station	Range 30 km - 110 km			Range 40 km - 95 km		
	T-T (s)	Err.	No.	T-T (s)	Err.	No.
	6.16 +/- 0.04 km/s			6.15 +/- 0.04 km/s		
S1	0.74	0.03	8	0.76	0.03	7
S2	0.69	0.01	7	0.71	0.01	5
S3	0.73	0.02	5	0.75	0.01	3
S4	0.72	0.06	3	0.74	0.05	3
S5	0.81	0.03	3	0.81	0.07	2
S6	0.82	0.01	4	0.82	0.02	3
S7	0.78	0.01	8	0.79	0.01	7
S8	0.78	0.01	11	0.79	0.01	11
S11	0.78	0.03	6	0.78	0.02	6
S15	0.58	0.05	2	0.59	0.01	2
S19	0.59	0.00	1	0.57	0.00	1
S23	0.42	0.03	3	0.39	0.01	2
S25	0.57	0.03	6	0.54	0.05	3
S26	0.49	0.04	5	0.46	0.04	4
S27/S28	0.51	0.01	17	0.50	0.01	13
S30	0.51	0.04	5	0.47	0.09	2
S31	0.55	0.08	4	0.52	0.00	1
S32	0.51	0.02	10	0.49	0.02	7
S34	0.55	0.01	6	0.52	0.01	6
S35	0.56	0.02	6	0.53	0.02	6
S36	0.63	0.26	2	0.60	0.23	2
S37	0.58	0.02	2	0.55	0.05	2
S38	0.58	0.02	7	0.55	0.01	7
S39	0.56	0.01	6	0.54	0.02	6
S40	0.55	0.02	7	0.53	0.01	7
S41	0.54	0.15	2	0.51	0.12	2
S42	0.52	0.01	7	0.50	0.01	7
S43	0.50	0.00	1	0.46	0.00	1
S44	0.56	0.17	2	0.49	0.00	1
S45	0.51	0.16	2	0.52	0.00	1
S46	0.53	0.02	10	0.52	0.02	9
S47	0.56	0.02	10	0.56	0.02	8
S48	0.55	0.02	10	0.55	0.01	8
S49	0.54	0.02	12	0.54	0.01	10
S50	0.56	0.02	8	0.57	0.02	6
S51	0.54	0.02	8	0.55	0.01	5
S53	0.56	0.01	8	0.56	0.01	6
S54	0.57	0.02	7	0.58	0.02	5
S55	0.57	0.00	1	0.58	0.00	1
S60	0.55	0.01	3	0.56	0.00	1
S61	0.62	0.03	7	0.62	0.03	7
S62	0.83	0.03	8	0.81	0.02	8
L14	0.82	0.06	2	0.82	0.06	2
L24	0.48	0.00	1	0.48	0.00	1

there is an increase in velocity with range (Fig. 5.28). This will cause the time-terms for shots and station pairs close together to be underestimated and those further apart to be overestimated.

For the second calculation only shots and stations separated by 40 to 95 km were used. The velocity is 6.15 ± 0.04 km/s and has not changed significantly but the station residuals show less dependence on range (Fig. 5.28). The time-terms are larger for stations close to the coast where the average range is less and are smaller for stations near the centre of the line (Table 5.9 and Fig. 5.27).

The P_g time-terms for stations S61 and S62 along the Northumberland coast increase northwards with time-terms of 0.62 and 0.82 s respectively. The time-terms for S1 to S11 under the Carlisle basin vary from 0.7 to 0.8 s. For the rest of the line they fall between 0.5 and 0.6 s with only small variations (Table 5.9).

5.5 Presentation of the North Sea airgun data

The only airgun data processed in the North Sea is from the second profile recorded at S60 on a Geostore recorder (Fig. 2.3). The two 1000 cubic inch airguns produced energy concentrated in two bands from 5 to 7 Hz and from 12 to 15 Hz (Fig. 5.29). The noise is mainly below 3 Hz (Fig. 5.30).

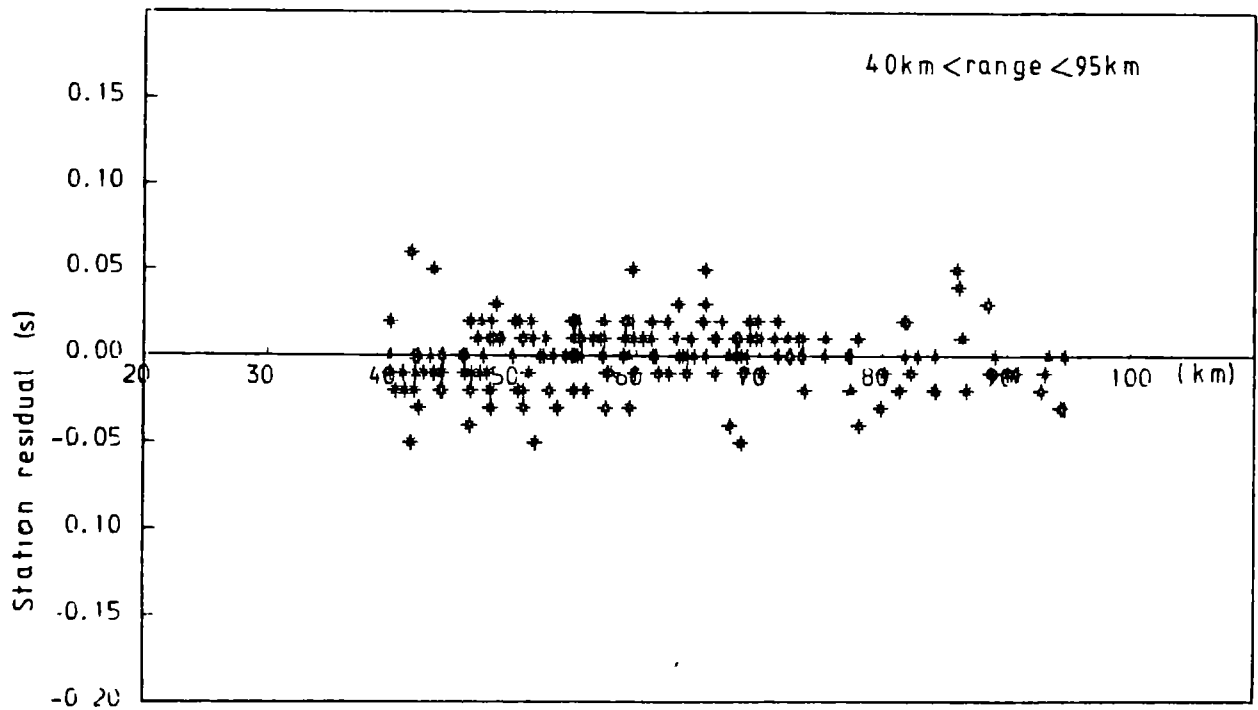
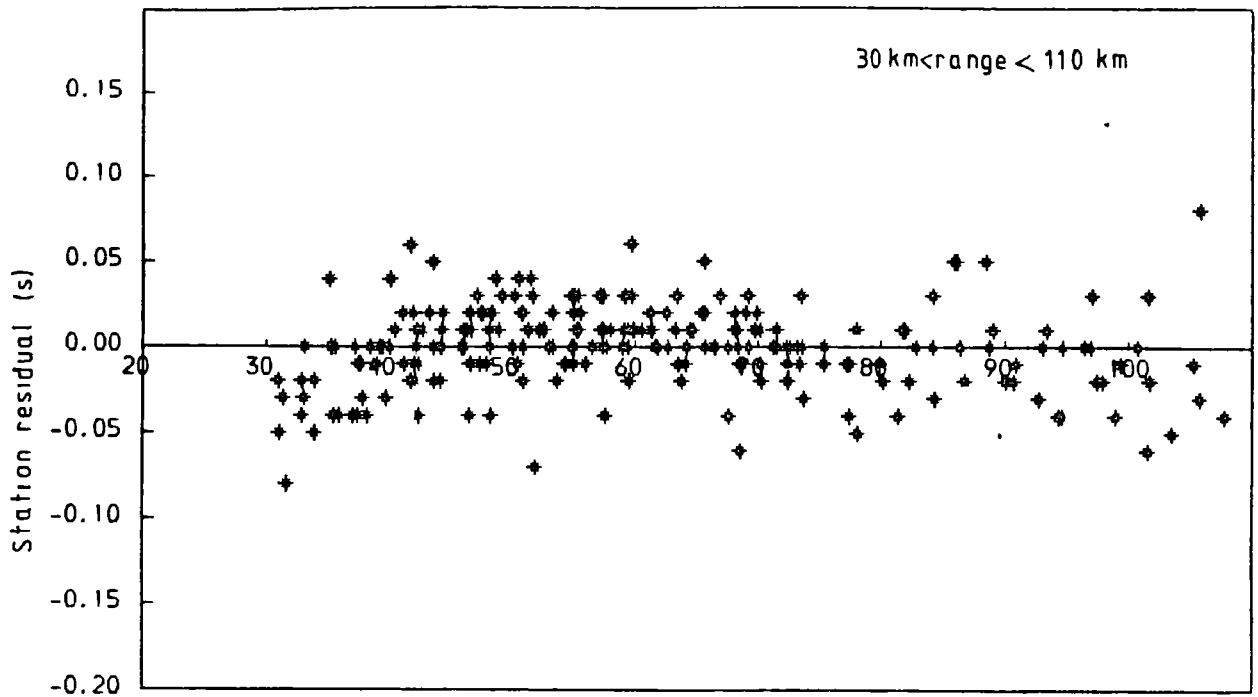


Fig 5.28 Plot of residuals against distance for the Pq time-term analysis in England

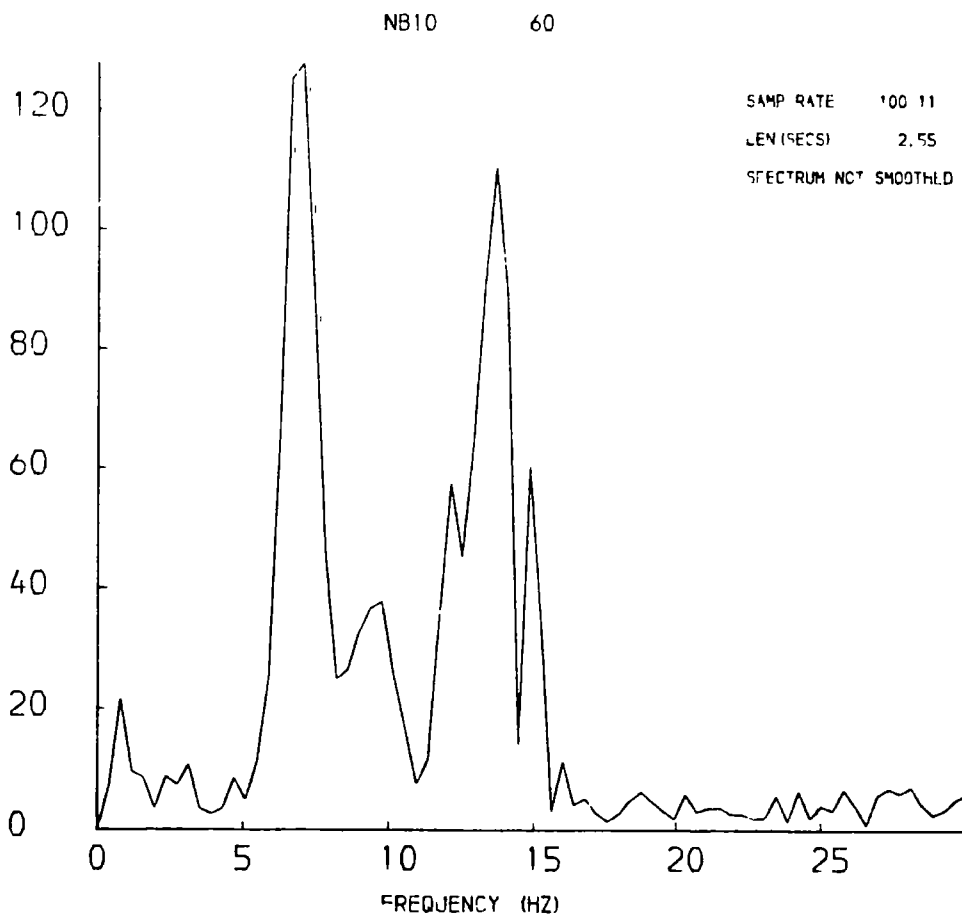
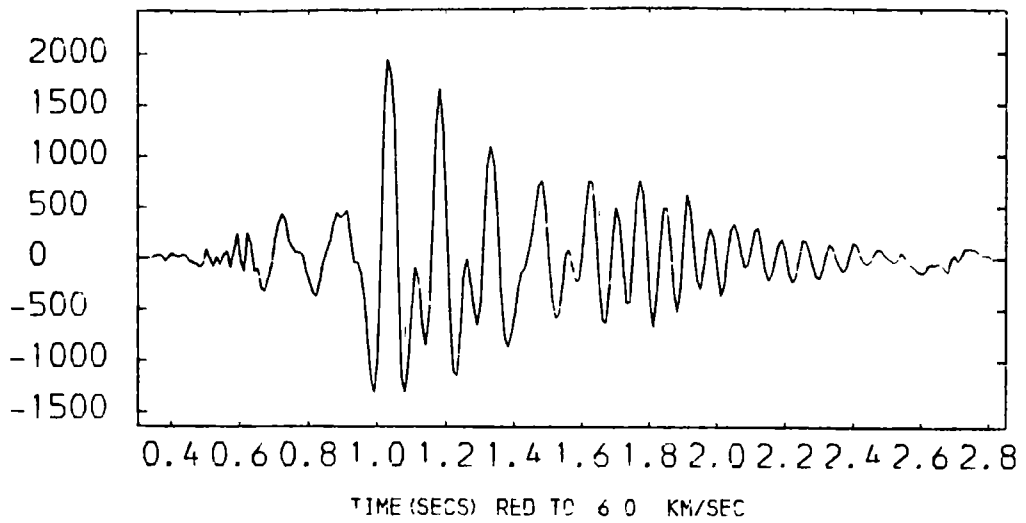


Fig 5.29 Frequency plot of an airgun shot recorded at S60 at a range of 6.3 km

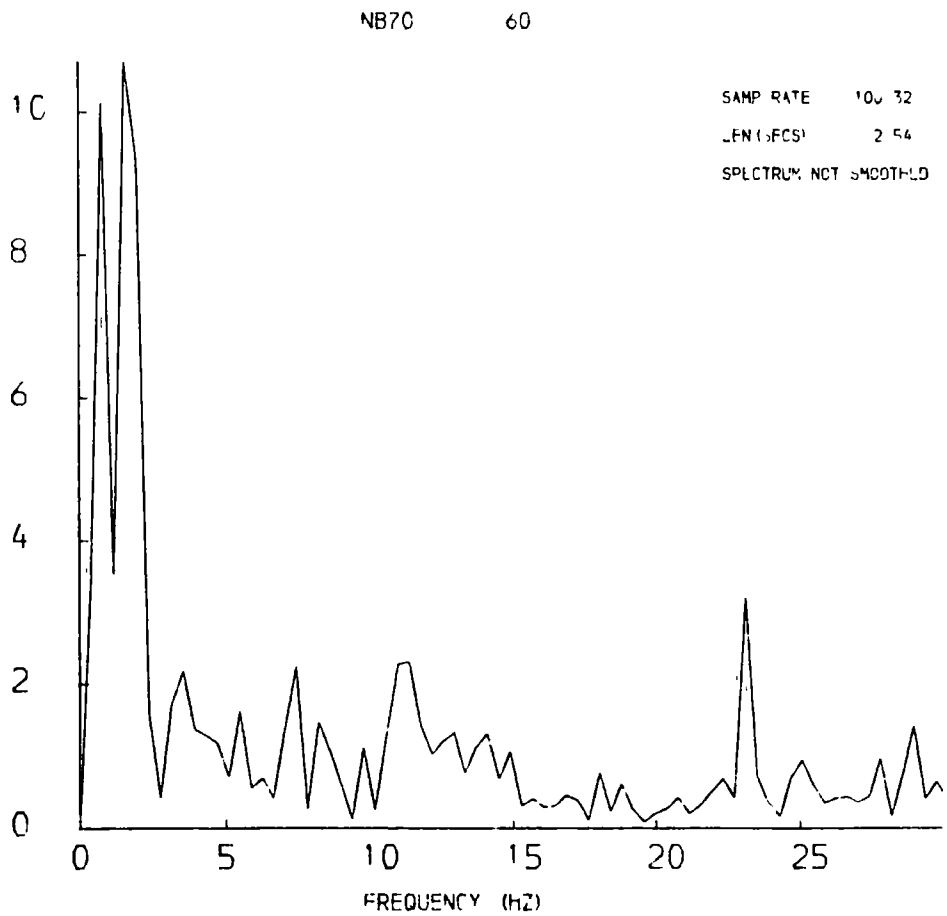
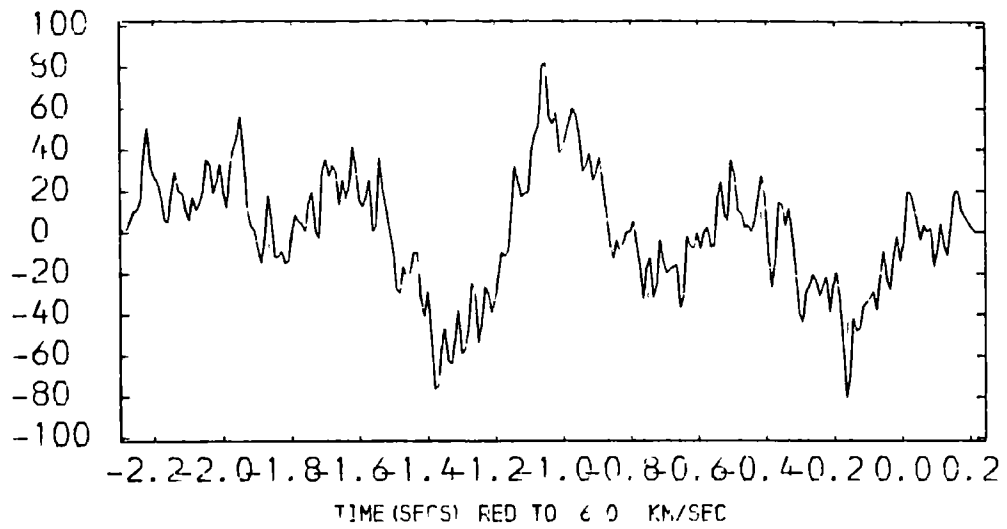
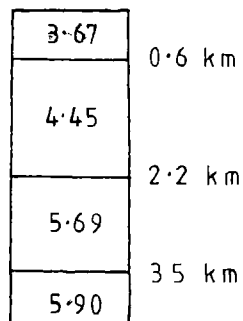


Fig 5.30 Frequency plot of noise at S60

The stacked section reduced to 6.0 km/s shows clear first arrivals out to 19 km (Fig. 5.31) but beyond this the signal to noise ratio deteriorates rapidly. The gaps in the data are caused by an unreadable time code and a tape change. The travel-time curve (Fig. 5.32) shows four branches which can be interpreted in terms of uniform horizontal layers.



There is a change in character in the first arrivals at a range 6.5 km to 8 km and it is thought that this is caused by the presence of Permian evaporites near the sea floor. Solution cavities and collapse structures are believed to be common (D Smith pers. comm.) and this has caused scattering of the shot energy at the sea-bottom.

5.6 Presentation of the North Sea explosion data

The stacked sections for the PUSS stations have been filtered with a 12 Hz low pass filter (Figs. 5.33 and 5.34). P123, close to N11, shows clear first arrivals out to 30 km, but they rapidly diminish in amplitude at a greater range where Pg is expected (Fig. 5.33). No clear coherent second arrivals are observed. An error in the timing for P2 gives a rather ragged appearance to

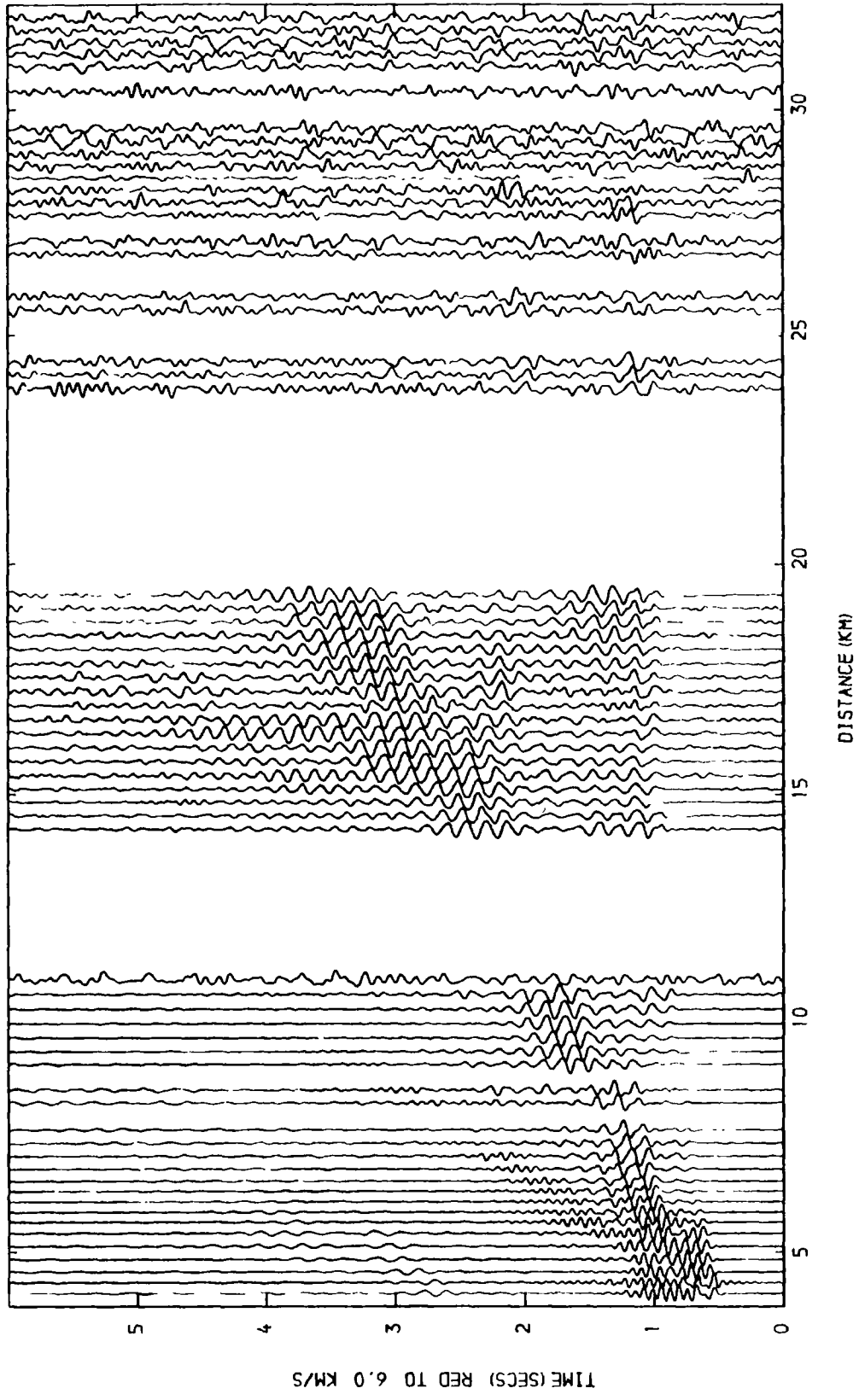


Fig 5.31 Reduced section of the 2nd North Sea airgun profile recorded at S60. Filtered 3-16 Hz, amplitudes equalised

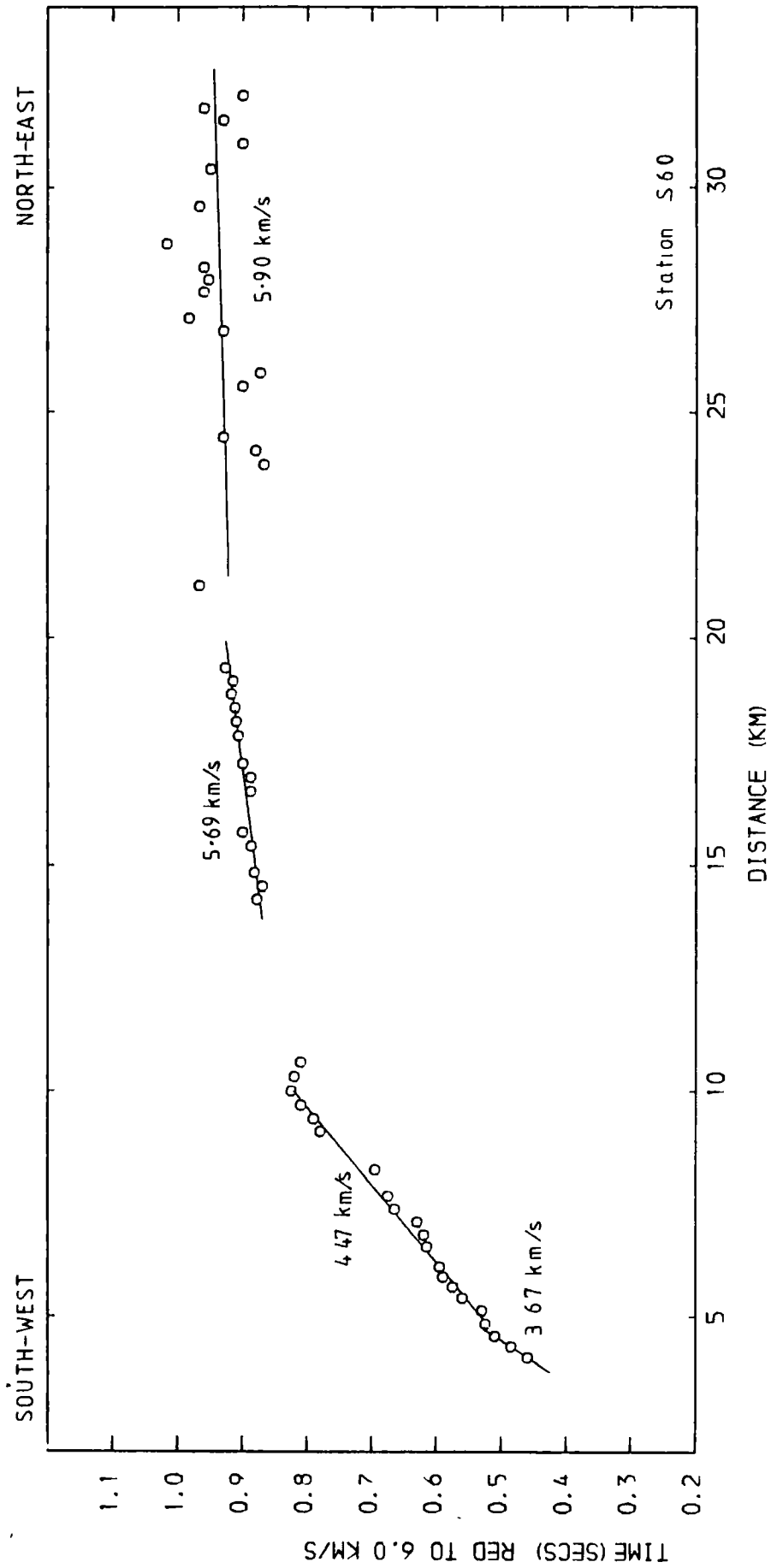


Fig 5.32 Reduced travel-time plot of the 2nd North Sea profile recorded at S60

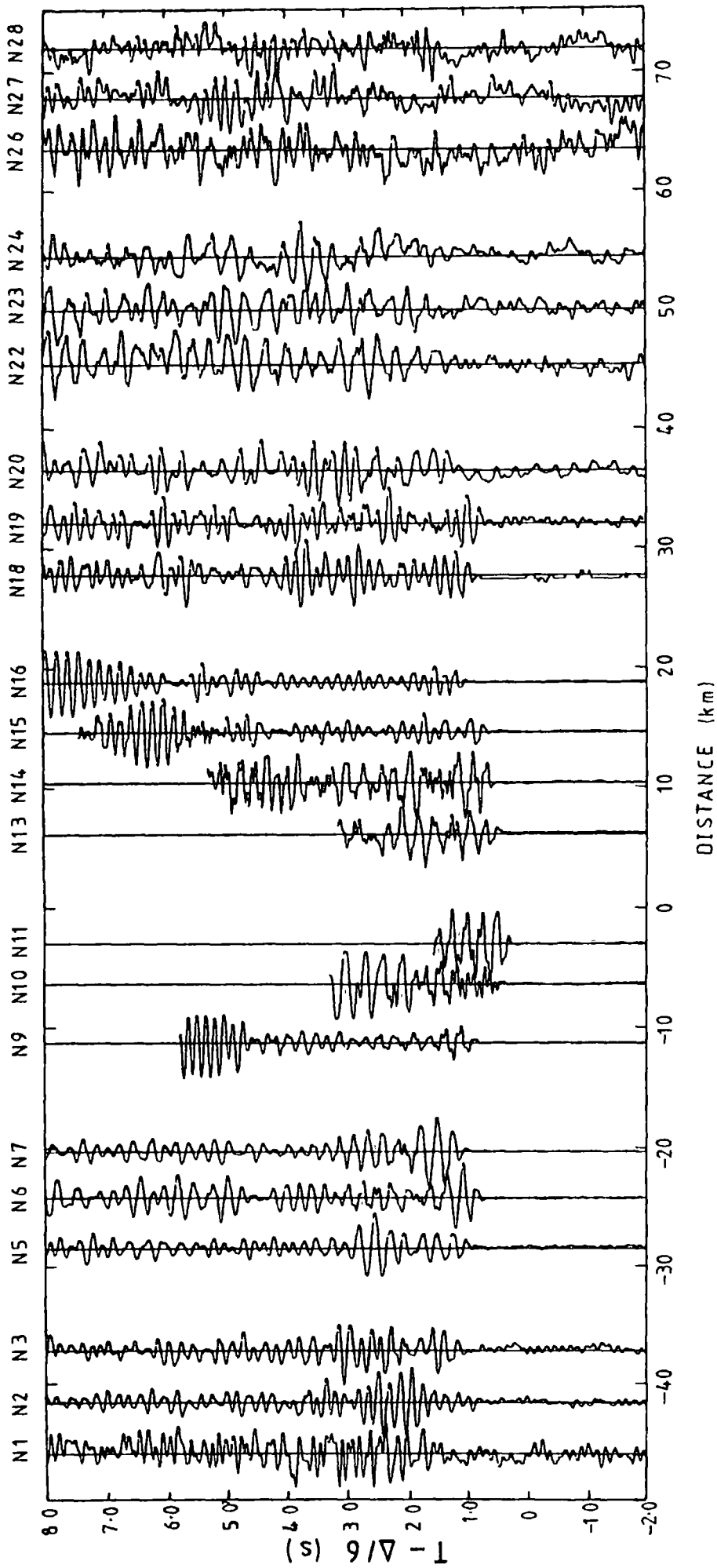


Fig 5.33 Reduced section of the North Sea shots recorded on the hydrophone at P123. Low pass filter - 12 Hz, amplitudes equalised

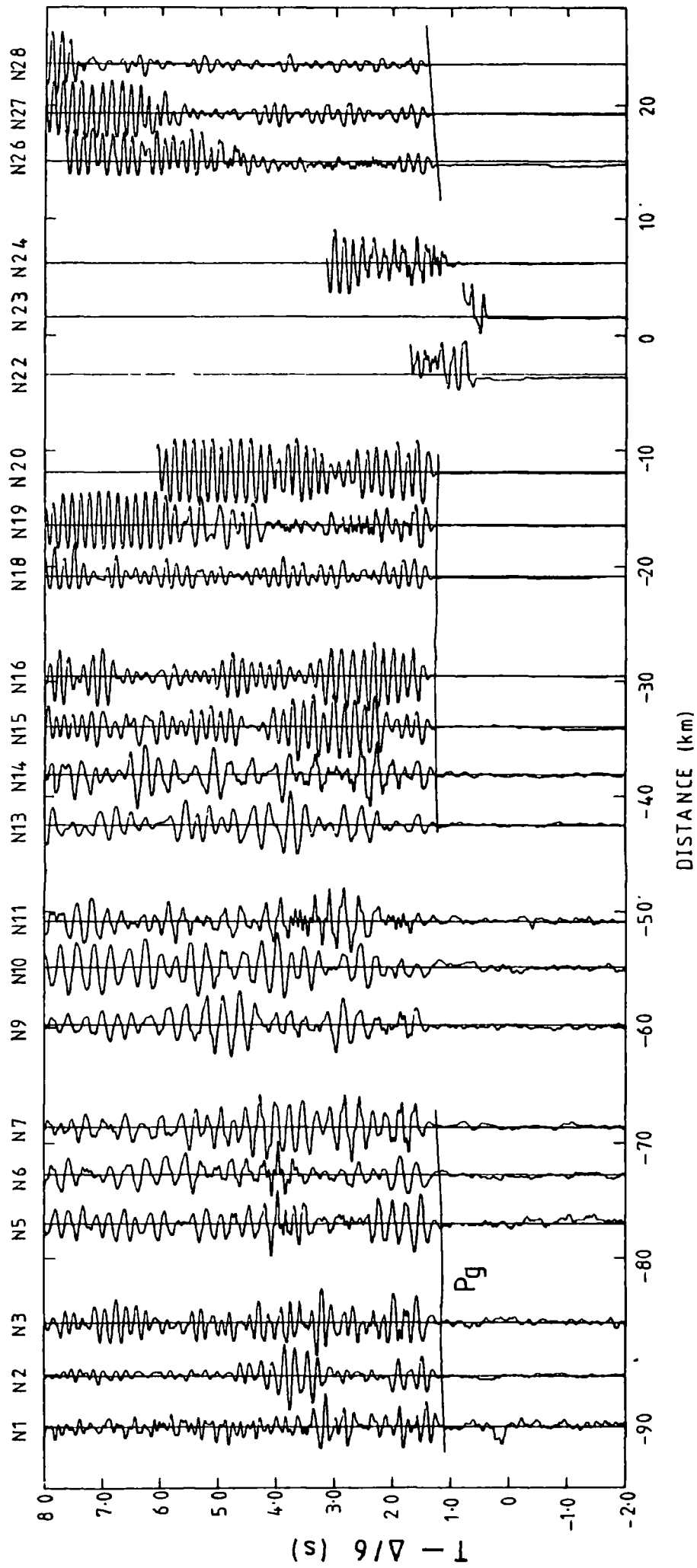


Fig 5.34 Reduced section of the North Sea shots recorded on the hydrophone at P456. Low pass filter - 12 Hz, amplitudes equalised

the stacked section. This has been corrected in the travel-time plots (Fig. 5.35).

P456 shows clear first arrivals out to 95 km except for shots in the vicinity of N11. About 2 s after Pg in the range 70 to 95 km a second arrival believed to be PmP is observed (Fig. 5.34).

The travel-times for P123 show velocities of 4.47 km/s and 4.31 km/s for the shots near the station (Fig. 5.35). At greater distances apparent velocities of 5.56 km/s and 5.90 km/s are observed. The travel-times for P456 (Fig. 5.35) indicate a much greater thickness of low velocity sediments under the station than at P123. Between 50 and 95 km the apparent velocity for Pg is 6.08 km/s. There is a 0.1 s step in the travel-time curve between N9 and N12 and it is thought that this relates to the lack of Pg at P123. A horizontal uniform layer interpretation of these travel-time curves is presented in Fig. 5.36.

Excellent recordings of the North Sea shots were made on the main line stations (Figs. 5.37 , 5.38 and Appendix A). For shots N1 to N11 the first arrivals out to more than 120 km are Pg with an apparent velocity between 6.1 and 6.3 km/s. Pg, however, is not observed at the main line stations for shots beyond N11 except at S62 where it is observed out to N17. Beyond 130 km, Pn is observed as the first arrival with an apparent velocity of 7.63 km/s to 7.81 km/s. It has a small amplitude and is almost absent from recordings of N20 to N25, which are close to the

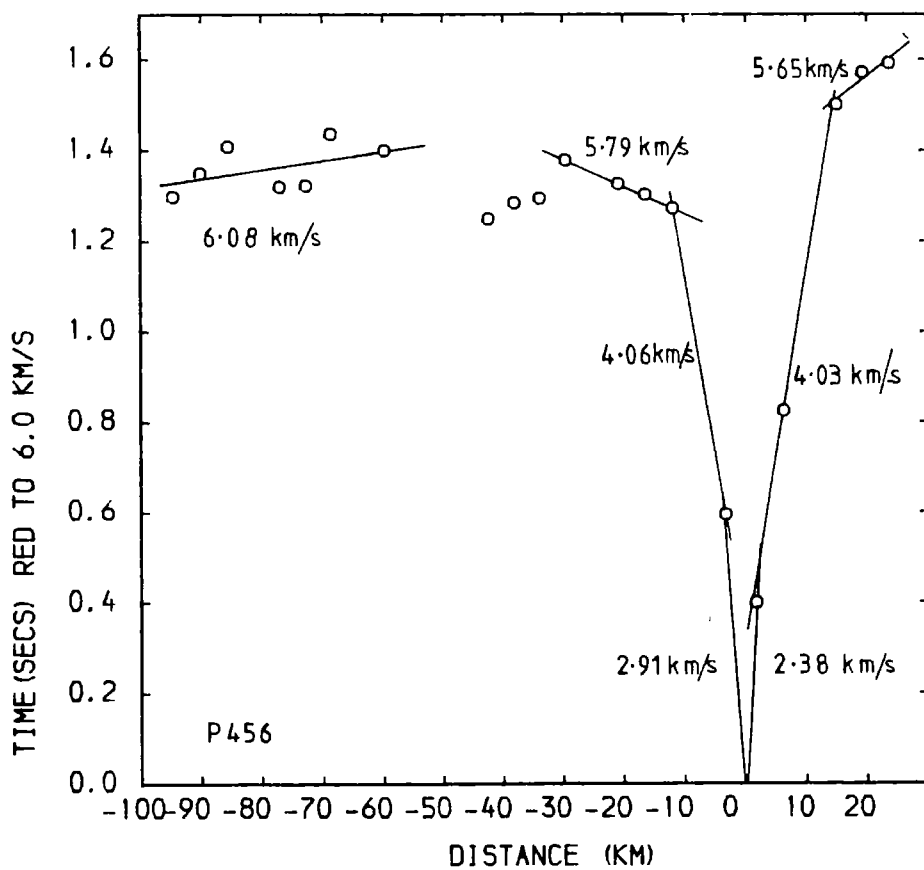
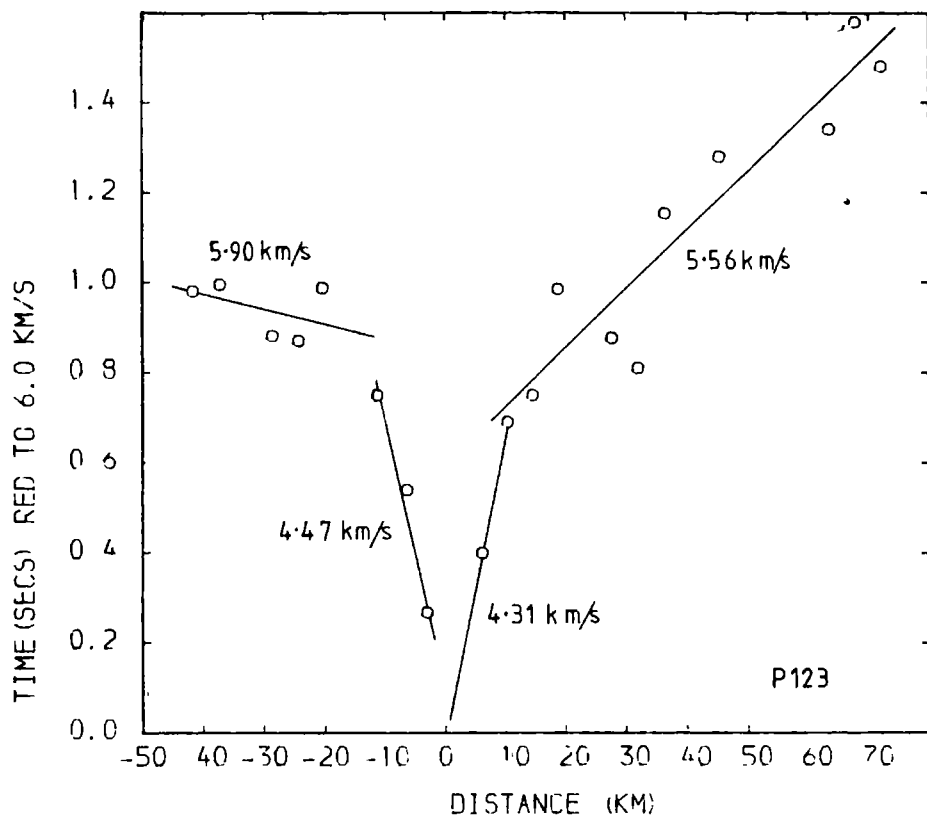
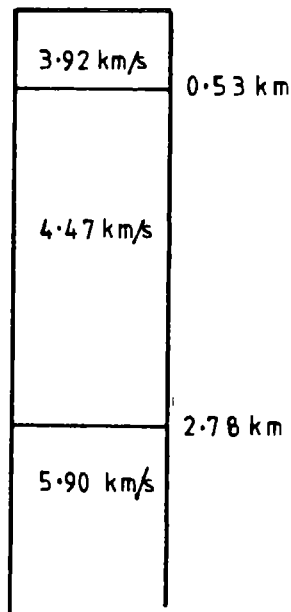
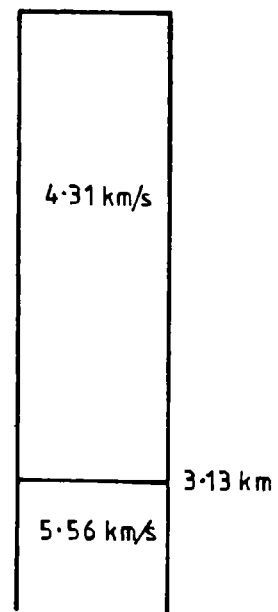


Fig 5.35 Reduced travel-time plots of the North Sea shots recorded at P123 and P456

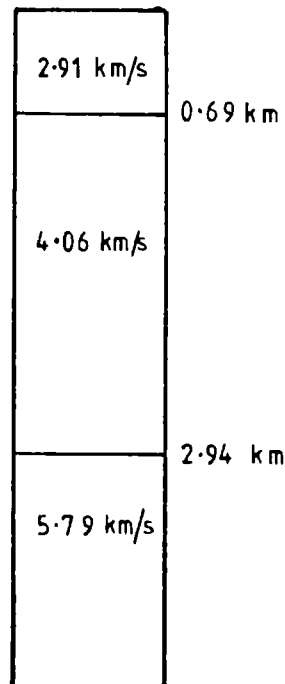
P123 West



P123 East



P456 West



P456 East

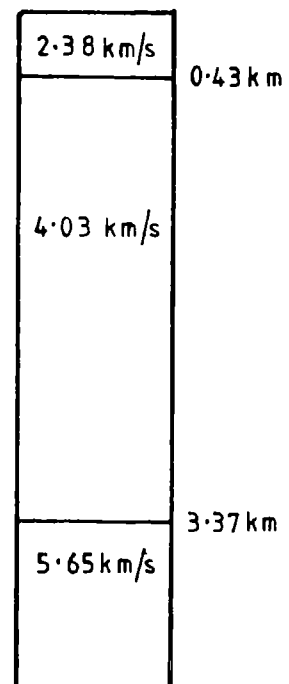


Fig 5.36 Plane layer interpretation for the North Sea PUSS stations

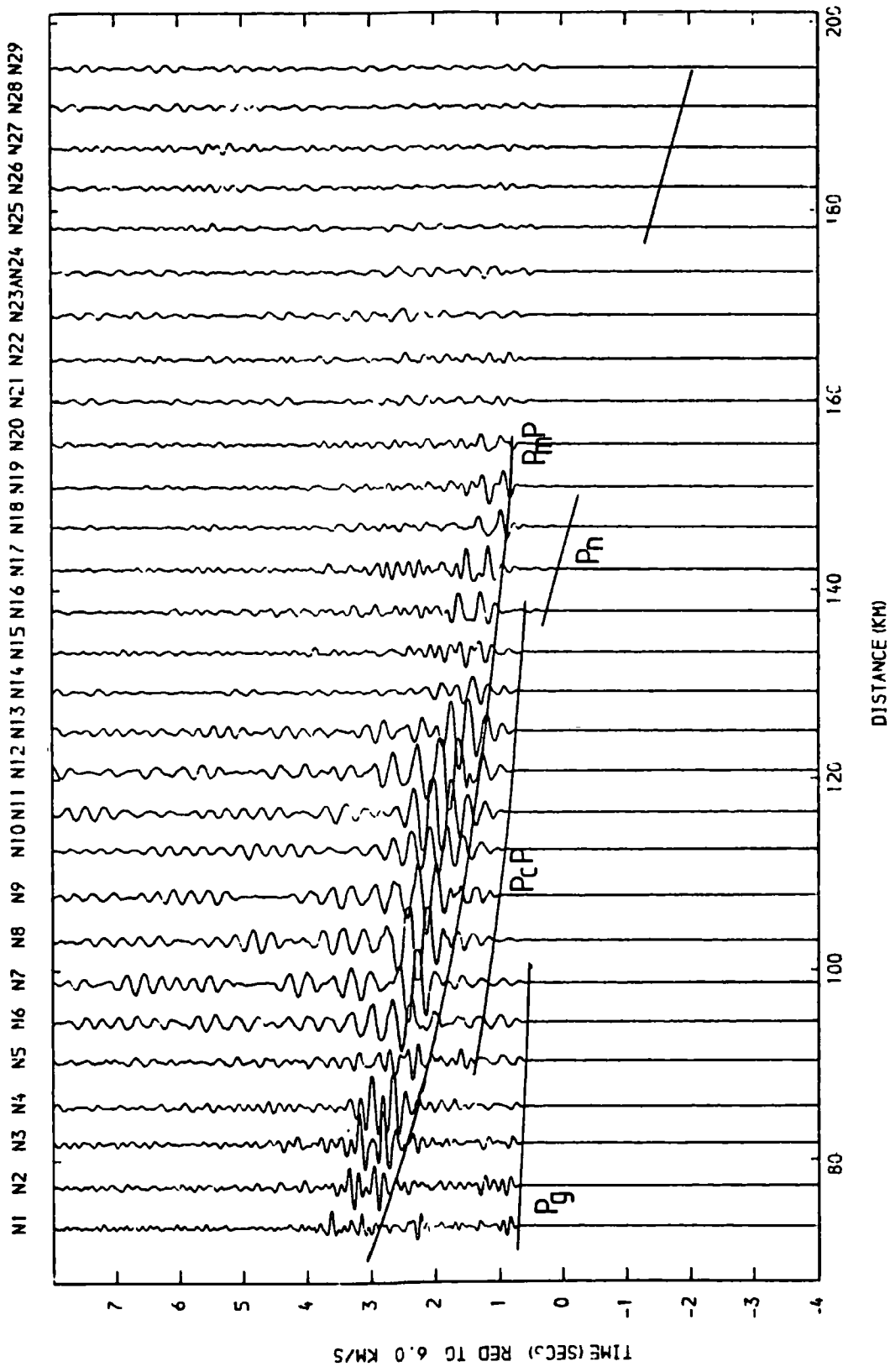


Fig 5.37 Reduced section of the North Sea shots recorded at S30.
 Unfiltered, amplitudes uncorrected

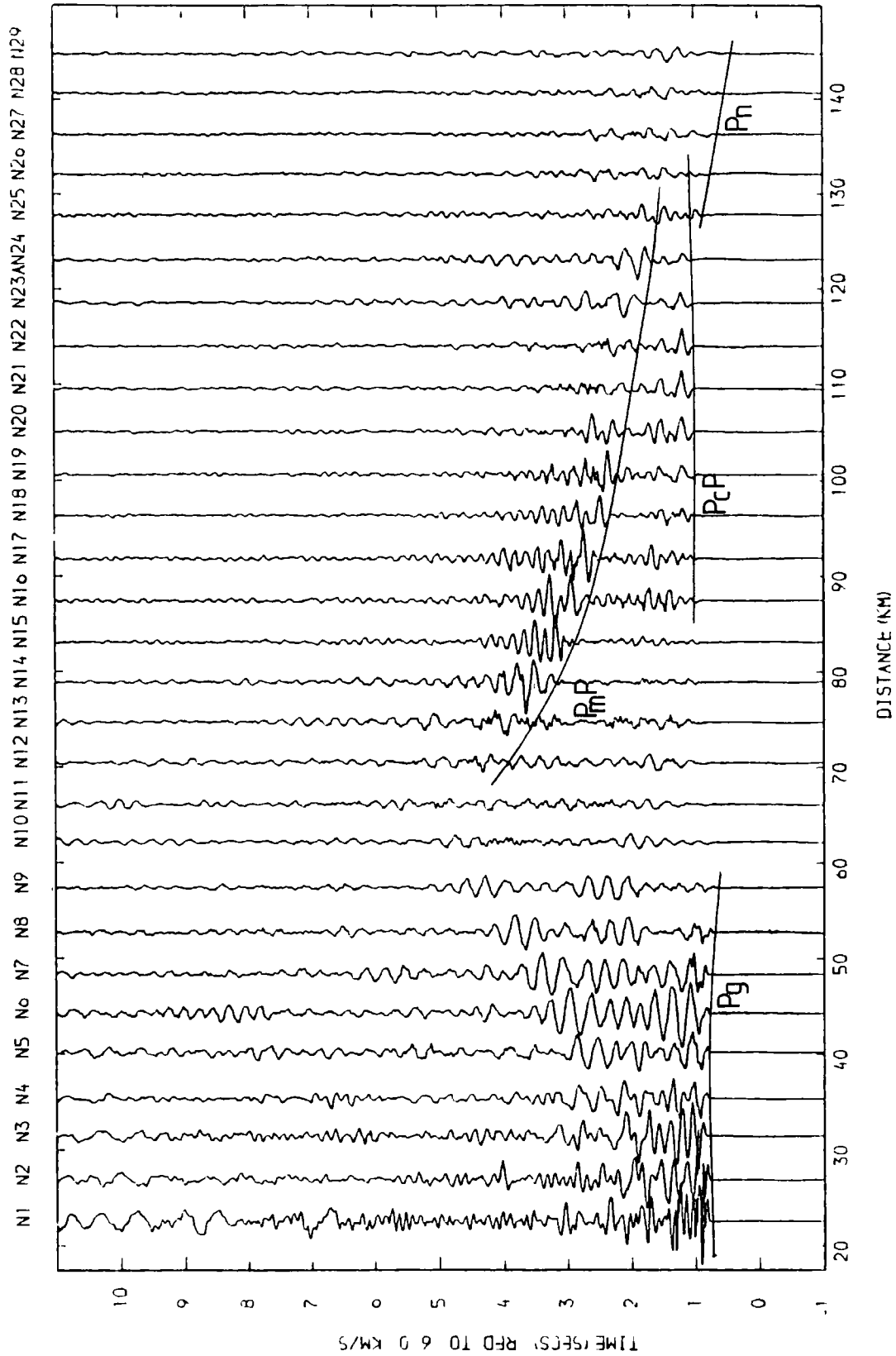


Fig 5.38 Reduced section of the North Sea shots recorded at S53. Unfiltered, amplitudes uncorrected

granite inferred from gravity data (Donato et al. 1983).

Between 80 and 120 km PcP is a prominent arrival. It initially follows Pg by about 0.8 s but where Pg dies out it becomes the first arrival. Beyond 130 km it passes into an upper crustal channel wave. PmP is the largest amplitude arrival on most of the sections. It has a maximum amplitude between 90 and 100 km and passes into a lower crustal channel wave at large ranges.

Reduced travel-time plots for Pg at different stations show that the apparent velocity varies between 6.07 and 6.37 km/s (Fig. 5.39, Table 5.10). In general the apparent velocity increases from an average of 6.12 km/s over the first 50 km to 6.26 km/s at a greater range. This suggests an increasing velocity with depth for the refractor.

The true velocity for Pg beneath shots N1 to N9 can be determined from the minus times for P456 and stations on the main line (Table 5.11). Stations S25 to S53 are used and none of the velocities differ significantly from the mean of 6.11 km/s.

Following Pg on all stations is an arrival similar to Pg called Pg'.^{*} It follows Pg on recordings of N1 by about 0.5 s but it has a faster apparent velocity such that by N7 the two pulses have begun to coalesce. In some common shot sections a third similar pulse, Pg'' is seen as well (Fig. 5.24). Where PmP is observed at shots N1 to N6 the same delayed phase, in this case

* see footnote on page 70

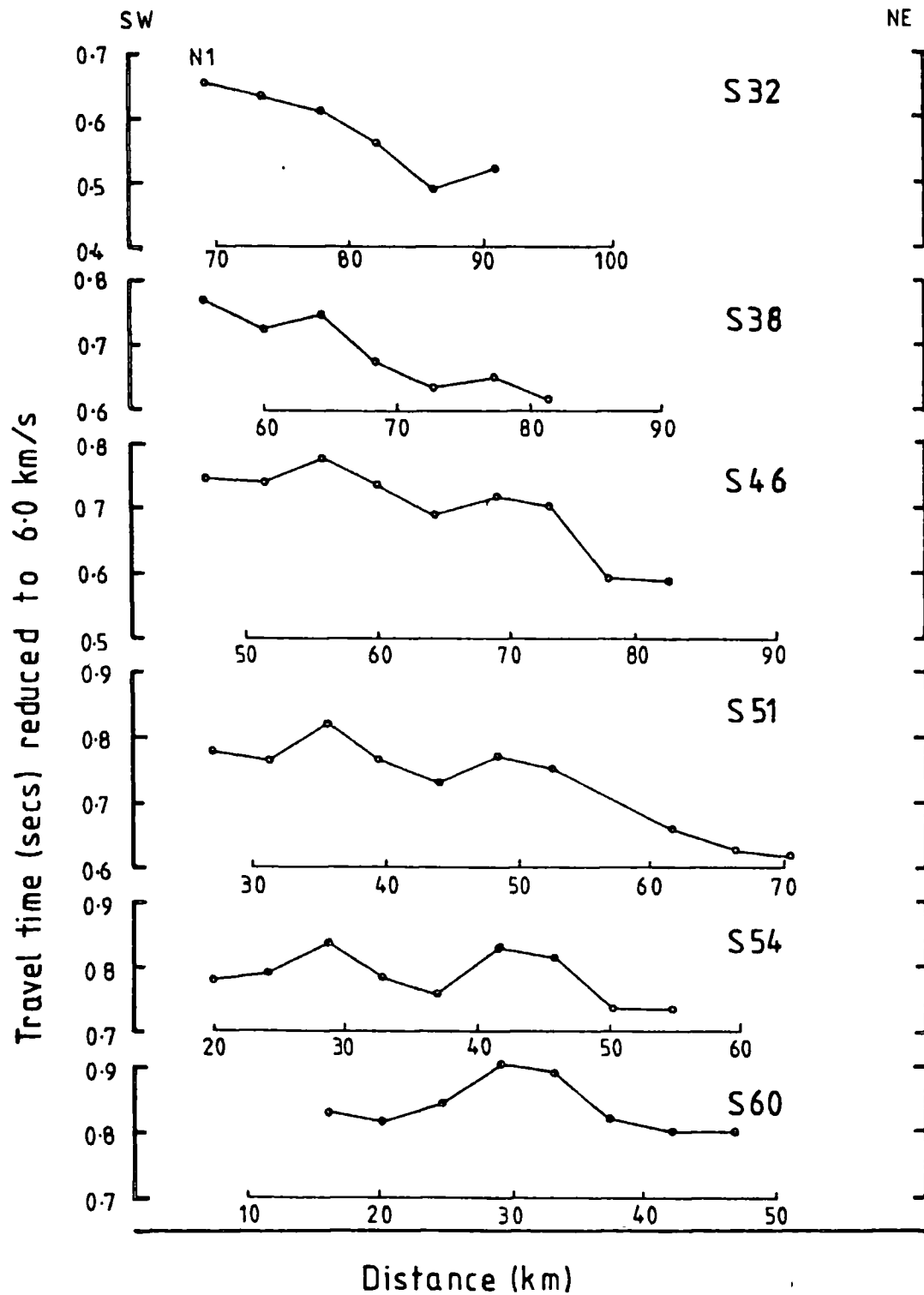


Fig 5.39 Reduced travel-time plots of shots N1 to N11 recorded in northern England

TABLE 5.10

Apparent velocities and intercept times in northern England determined from shots N1 to N9.

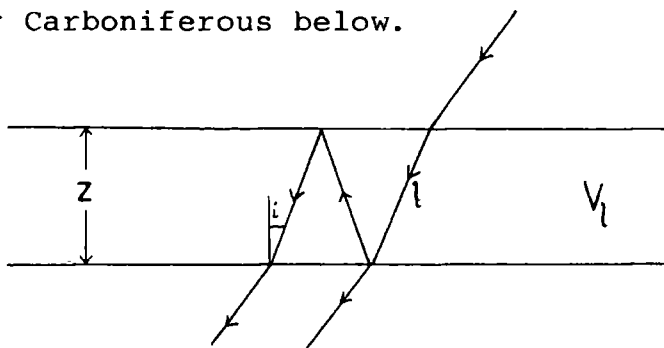
Station	Range km	Velocity km/s	Err 95%	Intercept s	Err 95%
S60	25.0 - 47.0	6.13	0.22	0.97	0.21
S55	27.1 - 57.8	6.11	0.09	0.96	0.10
S54	29.2 - 55.1	6.10	0.15	0.96	0.18
S53	26.8 - 57.3	6.11	0.12	0.95	0.14
S51	26.8 - 70.3	6.15	0.07	0.97	0.09
S50	29.7 - 59.8	6.07	0.10	0.90	0.12
S49	31.7 - 66.4	6.14	0.09	0.96	0.12
S48	34.0 - 51.3	6.15	0.09	0.99	0.13
S47	35.5 - 70.3	6.13	0.10	0.96	0.14
S46	37.5 - 72.3	6.18	0.10	1.01	0.15
S42	46.6 - 72.4	6.16	0.10	0.98	0.15
S41	48.7 - 78.9	6.24	0.09	1.13	0.15
S40	51.7 - 73.4	6.20	0.10	1.08	0.17
S39	53.7 - 75.4	6.23	0.15	1.14	0.25
S38	55.6 - 81.4	6.23	0.10	1.16	0.17
S35	62.6 - 84.3	6.27	0.06	1.23	0.32
S34	64.7 - 86.4	6.24	0.16	1.16	0.33
S32	69.2 - 90.9	6.28	0.15	1.23	0.32
S27	79.9 - 101.6	6.29	0.22	1.27	0.49
S26	81.8 - 99.4	6.37	0.27	1.44	0.60
S25	84.2 - 105.8	6.27	0.19	1.29	0.47
S23	89.0 - 97.9	6.19	0.21	0.97	0.51

TABLE 5.11

Velocity of the Pg refractor determined from minus-times calculated for shots N1 to N9 between P456 and stations in northern England.

Stations	Velocity(km/s)	Std Err	95% Conf.
P456/S53	6.09	0.04	0.11
P456/S51	6.10	0.03	0.08
P456/S50	6.04	0.03	0.07
P456/S49	6.10	0.03	0.08
P456/S48	6.11	0.03	0.08
P456/S47	6.14	0.03	0.08
P456/S46	6.11	0.03	0.08
P456/S42	6.11	0.03	0.10
P456/S41	6.12	0.04	0.12
P456/S40	6.13	0.03	0.09
P456/S39	6.10	0.03	0.10
P456/S38	6.12	0.03	0.07
P456/S35	6.06	0.05	0.17
P456/S34	6.11	0.04	0.14
P456/S32	6.13	0.05	0.14
P456/S27	6.13	0.02	0.07
P456/S25	6.12	0.04	0.14

called PmP', is also seen (Fig. 5.37). The arrivals appear to be caused by multiple reflections beneath the shots and the preservation of phase indicates that it is a multiple within a low velocity layer. The simplest explanation is that the low velocity layer is the Upper Carboniferous sandwiched between the higher velocity Permian evaporites and Magnesian Limestone above and the Lower Carboniferous below.



The thickness of this layer, z , for dips of less than a few degrees is given by $z = l \cos(i)$ where $2l = V_l T_{\text{delay}}$. Assuming a velocity of 3.67 km/s (Fig. 5.32) for the Upper Carboniferous and 6.10 km/s for Pg the thickness of this layer can be determined (Table 5.12). It thins from 0.68 km under N1 to 0.41 km under N5. If the relative dip between the top and bottom of this layer remains constant at 0.9° , it will have thinned to nothing by N11.*

For the time-term analysis in the North Sea the data has been split between a shallow refractor of velocity 5.5 to 5.7 km/s and Pg, with the limiting range at 30 km. The shallow refractor was discussed earlier (see section 5.3.4). Only the analysis of the Pg refractor is discussed here.

* see footnote on page 70

TABLE 5.12

Delay between Pg and Pg' and the thickness of the low velocity layer. *

Stations	Shots				
	N1	N2	N3	N4	N5
	Delay (s)				
	Thickness (km)				
S47	0.45 0.66				
S46	0.49 0.72	0.43 0.63		0.34 0.50	
S44	0.45 0.68				
S42	0.46 0.67	0.43 0.63	0.36 0.53	0.33 0.49	0.28 0.41
S39	0.45 0.66	0.43 0.63	0.35 0.51		0.28 0.41
S38	0.46 0.67				
S32	0.48 0.70	0.42 0.62	0.38 0.56		
Mean depth (km)	0.68	0.61	0.53	0.49	0.41

* see footnote on page 70

Stations as far west as S30 are used along with the Spadeadam shot, the North Sea shots and the quarry blast, Q29, at Belford. The data were constrained by making Q29 and S62 coincident. The first analysis was performed on all the data. The results are not included but the station residuals confirm that there is an increasing velocity with range (Fig. 5.40). The range was then restricted to less than 60 km. This gives a least squares velocity of 6.11 ± 0.05 km/s but does not enable time-terms beyond N12 to be determined. Following this the range was restricted to a minimum of 45 km. The velocity is slightly higher at 6.17 ± 0.10 km/s but the time-terms do not show any significant difference (Table 5.13, Fig. 5.41)

The last analysis was repeated with the inclusion of data from P456 and the time-term calculated for Pg is 1.22 s. It is not known, however, whether this large value is a result of a low Pg velocity beneath this part of the line, perhaps caused by the granite, or a thickening of the low velocity cover to the east.

5.7 Summary

Analysis of the first arrivals beneath the CSSP profile indicate the following structure:

- (1) First arrivals out to about 10 km reveal velocities for the near surface rocks varying between 2.4 and 4.8 km/s.

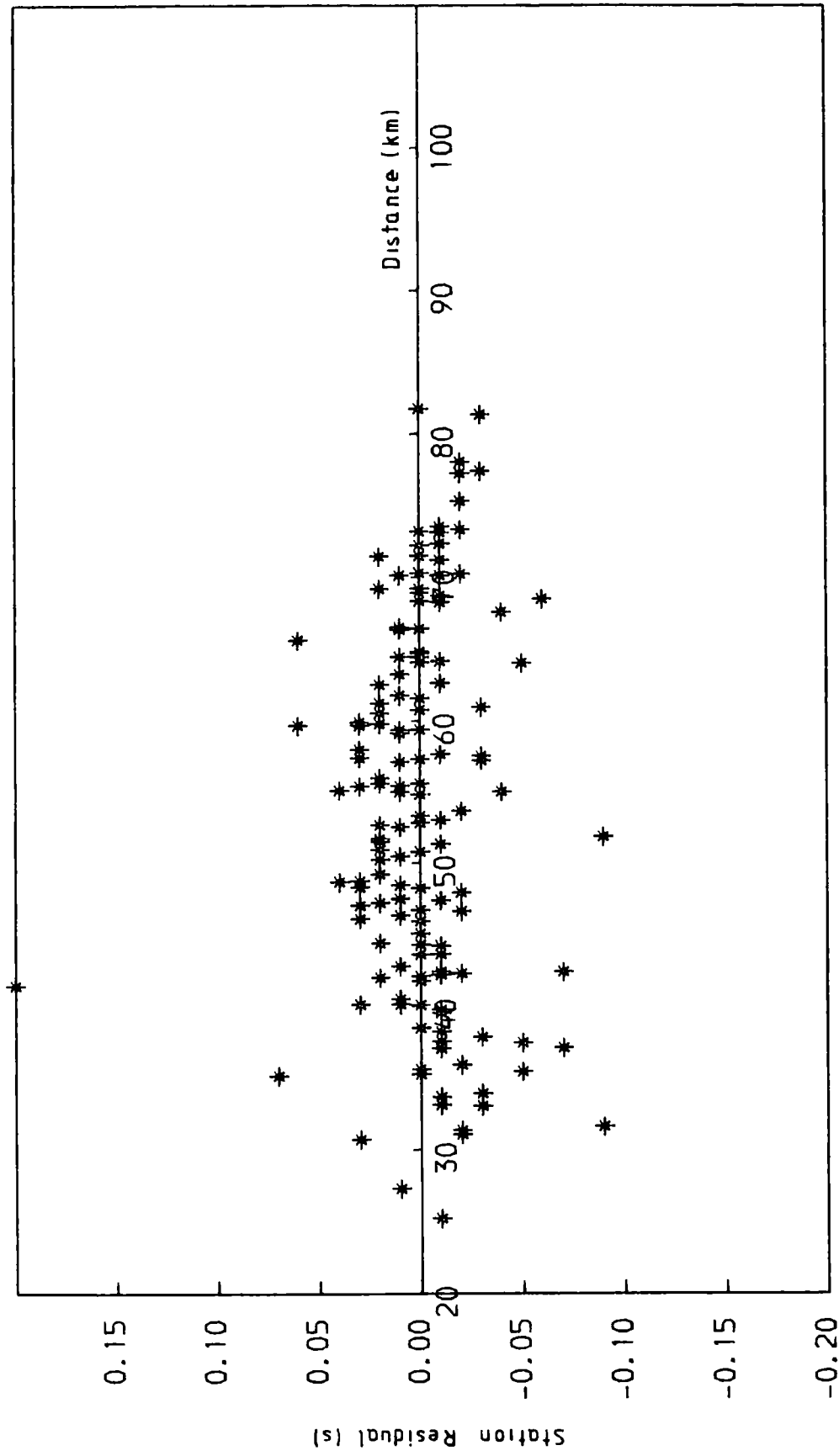


Fig 5.40 Plot of residuals against distance for the Pq time-term analysis in the North Sea

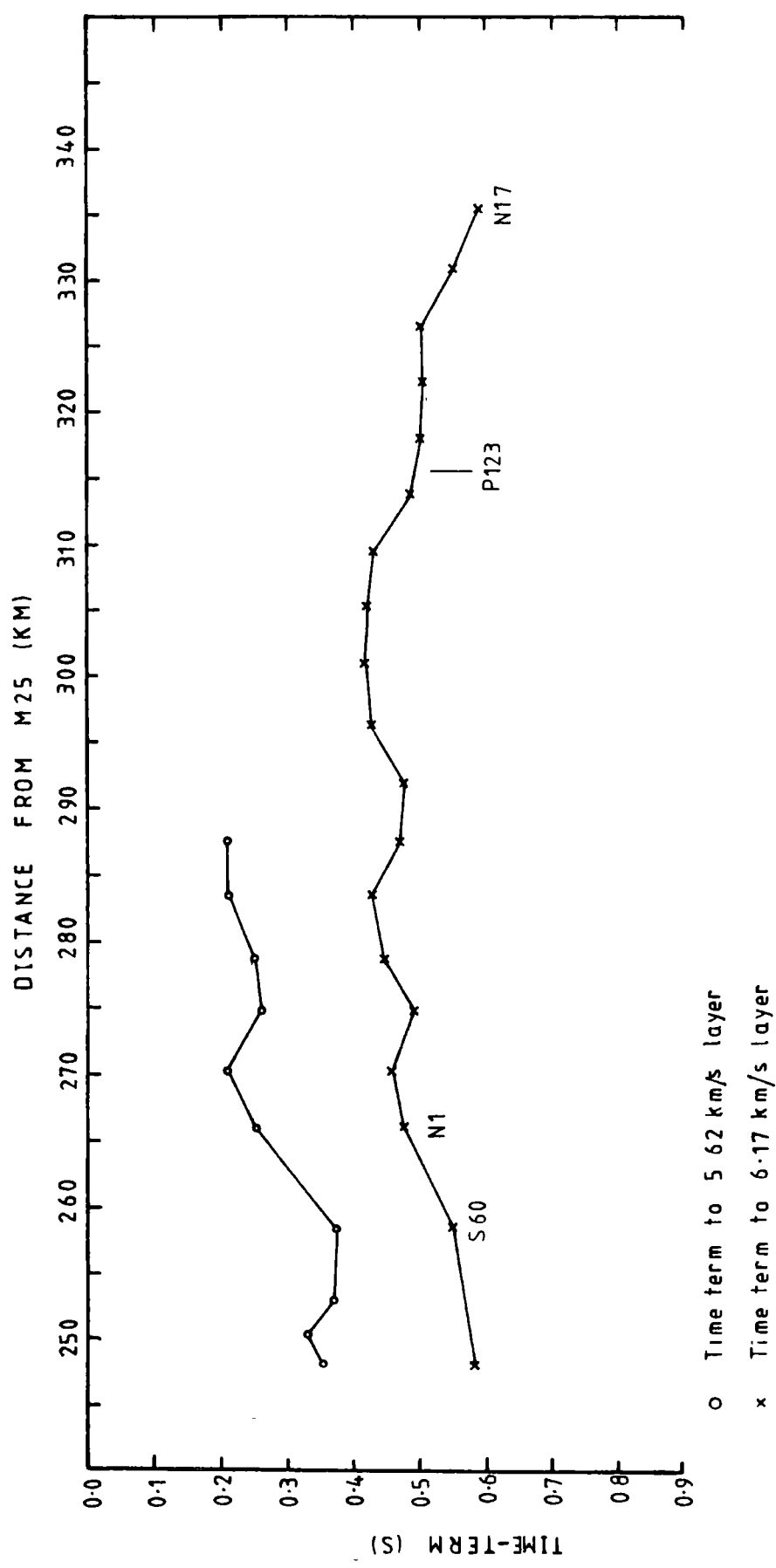


Fig 5.41 Distribution of the time-terms in the North Sea

TABLE 5.13

Pg time-term analysis - North Sea

Shot	All stations in the range 30 to 60 km			All stations greater than 45 km					
				without P456			inc. P456		
	6.11 +/- 0.05			6.17 +/- 0.10			6.14 +/- 0.04		
	No.	T-T s	Err.	No.	T-T s	Err.	No.	T-T s	Err.
N1	14	0.44	0.02	10	0.48	0.02	11	0.48	0.02
N2	11	0.43	0.01	4	0.46	0.01	5	0.47	0.02
N3	10	0.48	0.01	12	0.49	0.01	13	0.49	0.01
N4	9	0.44	0.01	7	0.45	0.01	7	0.43	0.01
N5	8	0.43	0.01	9	0.43	0.01	10	0.42	0.01
N6	9	0.48	0.02	10	0.47	0.01	11	0.45	0.01
N7	8	0.49	0.01	12	0.48	0.01	13	0.46	0.01
N8	5	0.43	0.03	7	0.43	0.03	7	0.41	0.02
N9	3	0.43	0.03	7	0.42	0.01	7	0.39	0.01
N10	2	0.43	0.04	4	0.42	0.02	4	0.39	0.03
N11	1	0.47	0.00	3	0.44	0.03	3	0.41	0.03
N12	1	0.50	0.00	1	0.49	0.00	1	0.46	0.00
N13				1	0.50	0.00	1	0.46	0.00
N14				1	0.50	0.00	1	0.45	0.00
N15				1	0.50	0.00	1	0.45	0.00
N16				1	0.55	0.00	1	0.50	0.00
N17				1	0.59	0.00	1	0.54	0.00
P456							6	1.22	0.04

Errors represent the 95% confidence limits

(2) First arrivals between a range of 10 and 30 km reveal a refractor with a velocity between 5.5 and 5.7 km/s at depths of 0.5 to 3.0 km beneath all of the profile.

(3) First arrivals beyond a range of 30 km reveal a basement refractor (Pg) with a velocity between 6.1 and 6.2 km/s beneath the whole line except the North Sea east of shot N11. Table 5.14 summarises the velocities calculated for Pg.

TABLE 5.14

Summary of velocities determined for Pg

Location	Method	Velocity km/s	Error 95%
Irish Sea (M1-M7)	Plus-minus	6.13	0.06
Irish Sea	Time-term	6.15	0.04
N. England (S46-S56)	Plus-minus	6.12	0.03
N. England	Time-term	6.15	0.04
North Sea (N1-N9)	Plus-minus	6.11	0.01
North Sea	Time-term	6.17	0.10

CHAPTER 6 - INTERPRETATION OF THE SHALLOW STRUCTURE

6.1 Introduction

The seismic models presented in this chapter have been tested using the ray tracing program described in Chapter 4. The program is not capable of modelling rapid lateral or vertical changes in the structure and faults are a particular difficulty. It must not be expected, then, that travel-time data can be matched exactly.

Due to insufficiently closely spaced shots and stations the velocity and thickness of the Permo-Trias in the Solway and Carlisle Basins and the Mesozoic and Permian in the North Sea cannot be determined from the CSSP survey. To help overcome this problem use has been made of existing geological and geophysical data. Most of this comes from published sources but Shell U.K. permitted a brief examination of seismic reflection profiles from the north Irish Sea not generally available.

The interpretation is described separately for the Irish Sea, northern England and the North Sea.

6.2 The shallow structure beneath the Irish Sea

The model constructed for testing by ray tracing consists of four layers. The top two layers are formed of Upper Palaeozoic and Mesozoic sediments, the third consists of Lower Palaeozoic rocks

and the fourth is the Pg refractor (Figs. 6.1 and 6.2).

The CSSP survey produced little information on the velocities and thickness of the Mesozoic and Permian sediments within the Solway Basin and it is necessary to rely on the results of previous surveys. Bacon and McQuillin (1972) shot a short refraction line near M7 in the centre of the Solway basin and found an interface at a depth of 1.3 km between rocks with velocities of 3.67 km/s and 4.38 km/s but it is not known if this interface represents the Permo-Trias/Carboniferous boundary. Seismic work in the south Irish Sea (Blundell et al. 1964) suggests it is not possible to distinguish between Permo-Trias and Carboniferous rocks on their velocities. The Shell U. K. seismic reflection profiles show an unconformity at a depth of 1.8 km near M7 rising close to the surface at M13. It is more likely that this represents the Permo-Trias/Carboniferous boundary than the interface located by Bacon and McQuillin (1972). Nevertheless the shallower refractor of Bacon and McQuillin (1972) is more important when determining the depths to deeper refractors and is therefore used in the ray tracing model. The velocity at the sea floor determined from the sea-bottom refractor (see section 4.3) is about 2 km/s (see section 4.3). For the ray tracing an average velocity of 3.2 km/s is used for the top layer.

The top of the second layer is the 4.38 km/s layer of Bacon and McQuillin (1972) which is assumed to be continuous with the 4.8 to 4.9 km/s layer at P456. This is probably predominantly

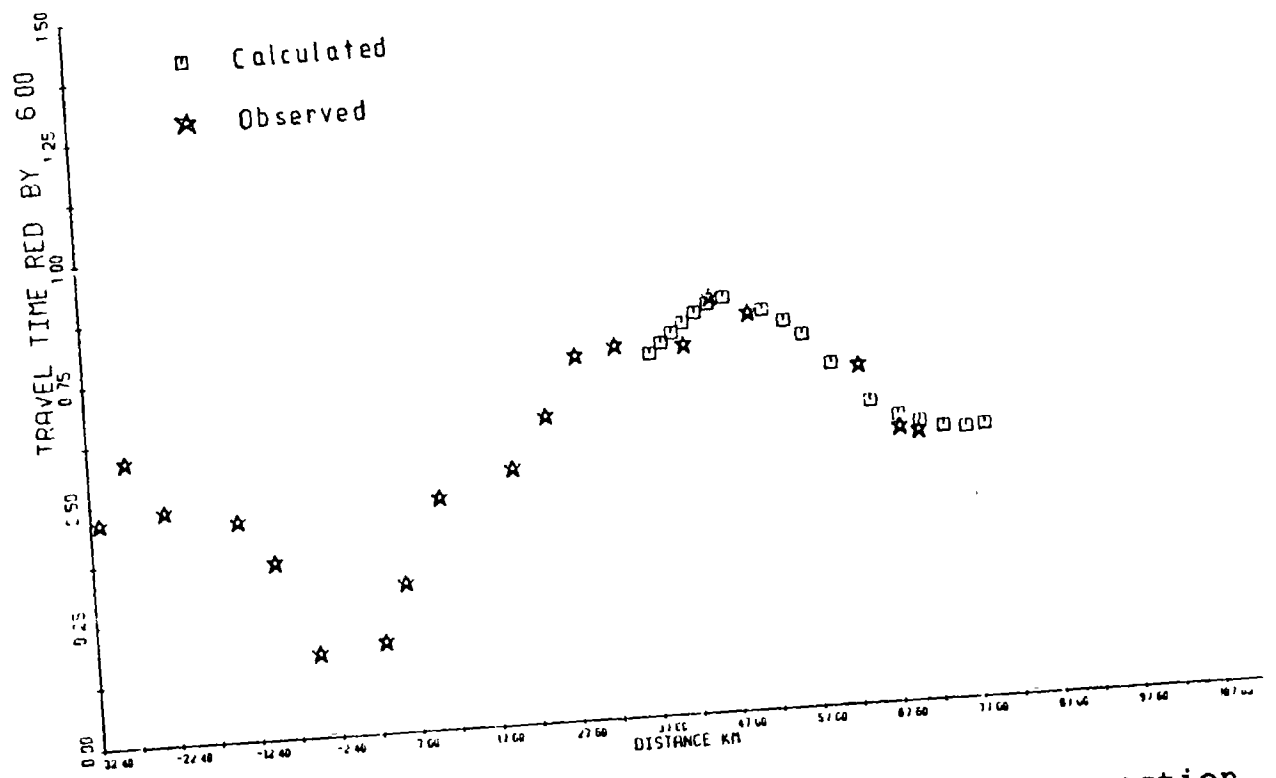
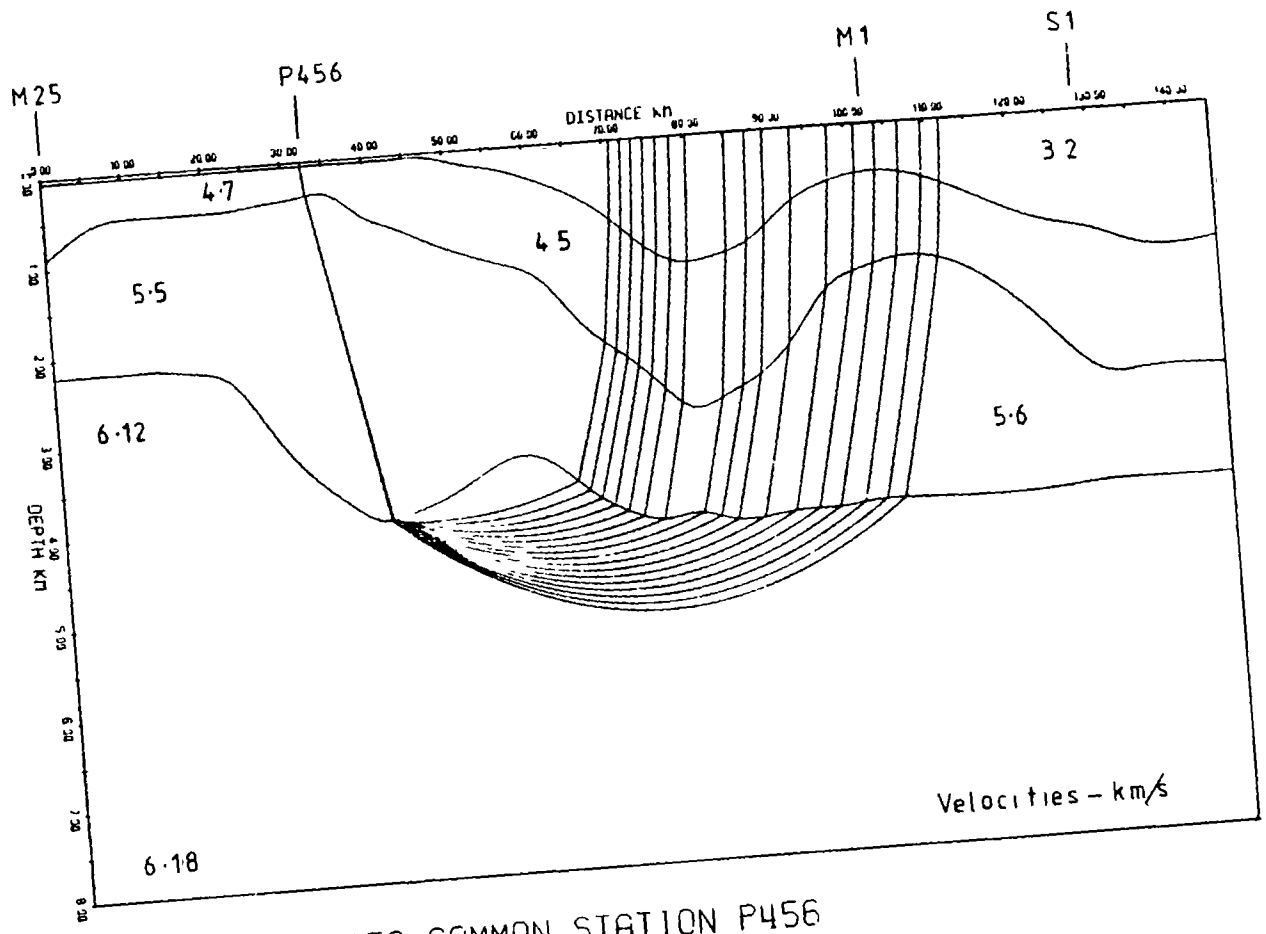
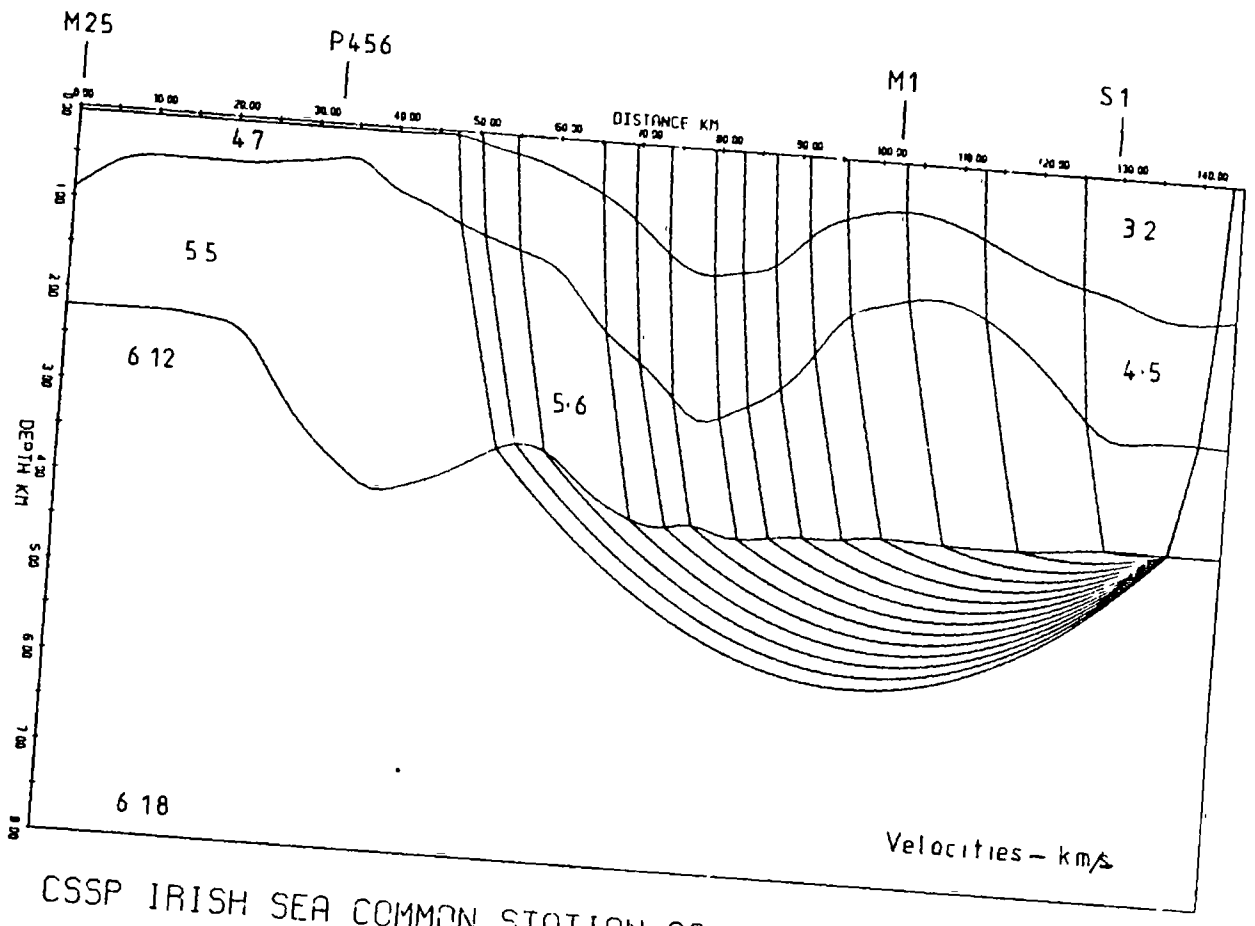


Fig 6.1 Ray traced diagram and reduced travel-time section obtained for upper crustal model beneath the Irish Sea for station P456



CSSP IRISH SEA COMMON STATION S8

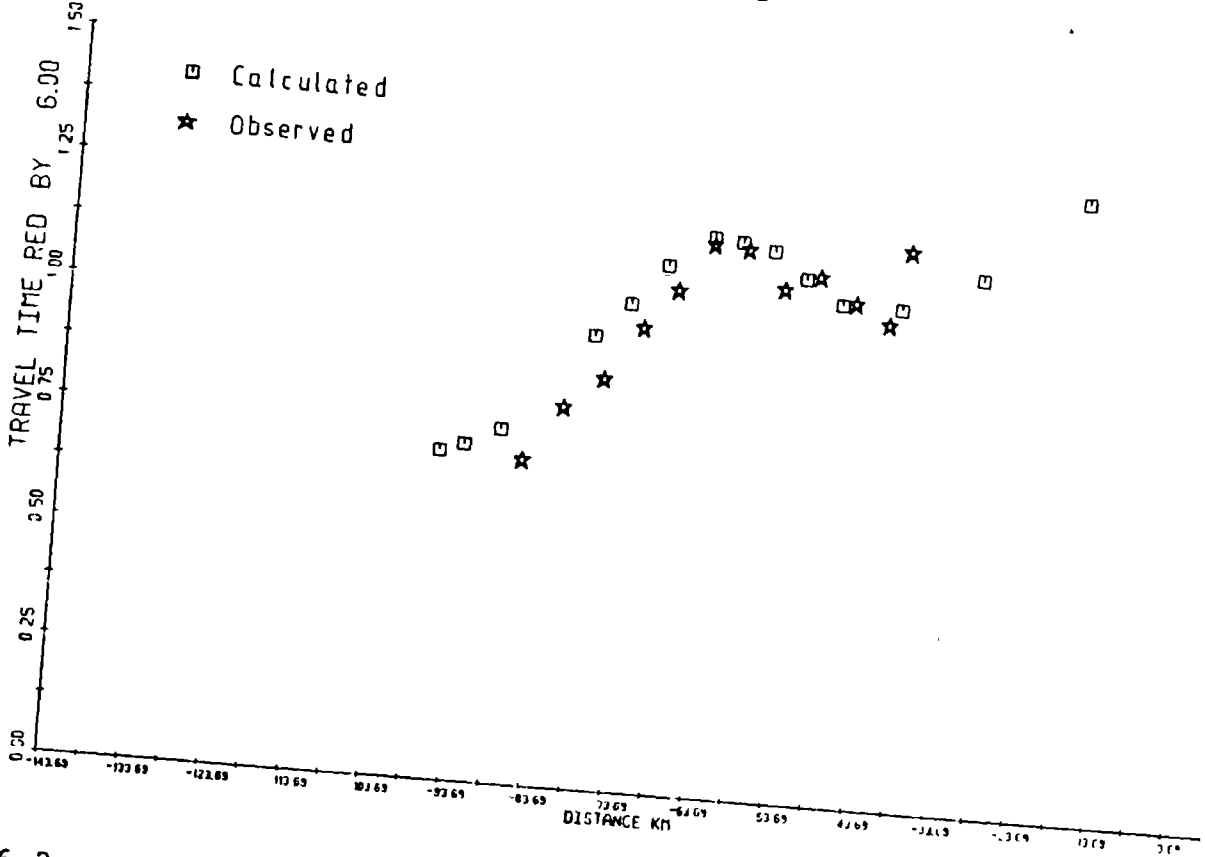


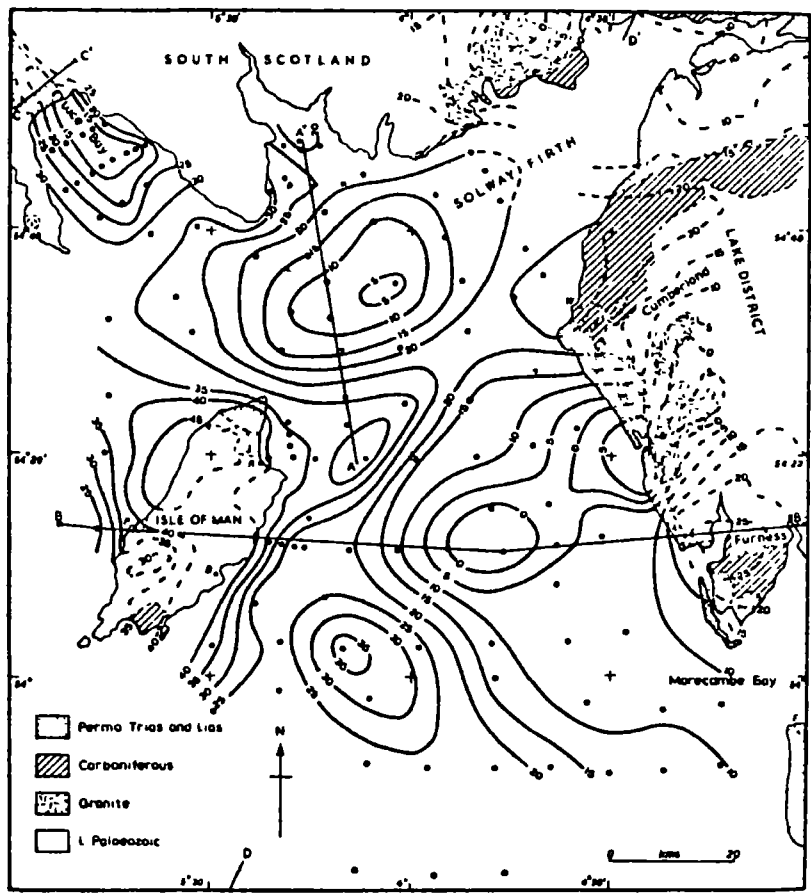
Fig 6.2 Ray traced diagram and reduced travel-time section obtained for upper crustal model beneath the Irish Sea for station S8

composed of Carboniferous and Devonian rocks although it may include some high velocity Permo-Triassic rocks. The estimated thickness for this layer of 0.5 km under the western part of the line is well controlled (Fig. 5.8) and the time-terms (Fig. 5.14) indicate the base approaches a depth of 3.0 km beneath the deepest part of the Solway Basin near M7.

The thickness of the Upper Palaeozoic and Mesozoic rocks can also be determined from the gravity data. Bacon and McQuillin (1972) suggested that the Solway gravity anomaly can be explained entirely by rocks with a velocity of less than 4.0 km/s and that rocks with velocities between 4.0 and 5.0 km/s, whether of Permo-Triassic, Carboniferous or Devonian age, make little contribution to the observed gravity anomaly. Laboratory measurements of rock densities from northern England and southern Scotland, however, indicate a significant density contrast between Lower Palaeozoic and Carboniferous rocks (Bott 1974, Bott and Masson-Smith 1957 and 1960). The densities of Ordovician and Silurian rocks in the Lake District and Southern Uplands are between 2.7 and 2.8 gm/cc whereas the densities of Carboniferous rocks in northern England vary from 2.41 gm/cc for sandstones to 2.68 gm/cc for limestones. The average density of Carboniferous rocks depends on the proportion of limestone, shale and sandstone. Bott and Masson-Smith (1957) suggested a density contrast of 0.20 gm/cc for the Lower Carboniferous and the basement in the Alston Block and Durham coalfield area but suggested a contrast of 0.15 gm/cc in the Southern Uplands near Dumfries (Bott and Masson-Smith 1960).

A density contrast of 0.40 gm/cc between the Permo-Trias and the Lower Palaeozoic was suggested by both Bacon and McQuillin (1972) and Bott and Mason-Smith (1960). Bott (1968) modelled the gravity minimum in the Solway Firth assuming a uniform density contrast between the Mesozoic/Upper Palaeozoic sediments and the basement. The same profile was remodelled (Fig. 6.3) assuming three layers with density contrasts of 0.40 gm/cc and 0.15 gm/cc. The profile passes slightly to the east of the gravity minimum close to M9 and the depth of about 2.5 km to the base of the Upper Palaeozoic is consistent with the seismic measurements (Fig. 6.3).

The third layer is defined by the 5.49 km/s refractor at P123 (Fig. 5.10) and the 5.71 km/s refractor along the S81/S91 north-south reversed airgun profile (Fig. 5.5). Similar velocities are also recorded from the Spadeadam and Kirkwhelpington shots in the Northumberland Trough (Fig. 5.18). Jacob (1969) determined a velocity of 5.5 km/s for Lower Palaeozoic rocks near the surface at Eskdalemuir and extensive laboratory measurements of the velocity of Lower Palaeozoic rocks from the Southern Uplands have been made by Adesanya (1982). Adesanya (1982) found that average velocities for greywackes from the Southern Uplands are 5.04 to 5.15 km/s at 1 bar, 5.17 to 5.27 km/s at 100 bars and 5.40 to 5.50 km/s at 750 bars, a pressure equivalent to a depth of burial of approximately 2 km. At a pressure of 1 kbar some samples of greywacke recorded velocities in excess of 5.7 km/s. Lower Palaeozoic shales from the Southern Uplands have significantly lower velocities than the greywackes with average velocities of



(from Bott 1968)

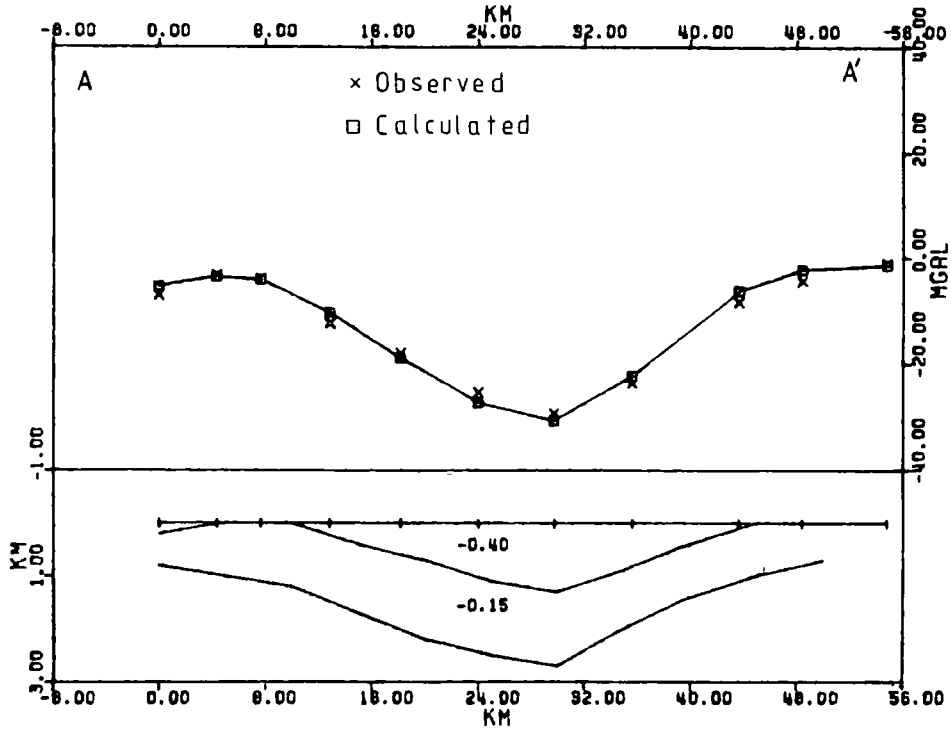
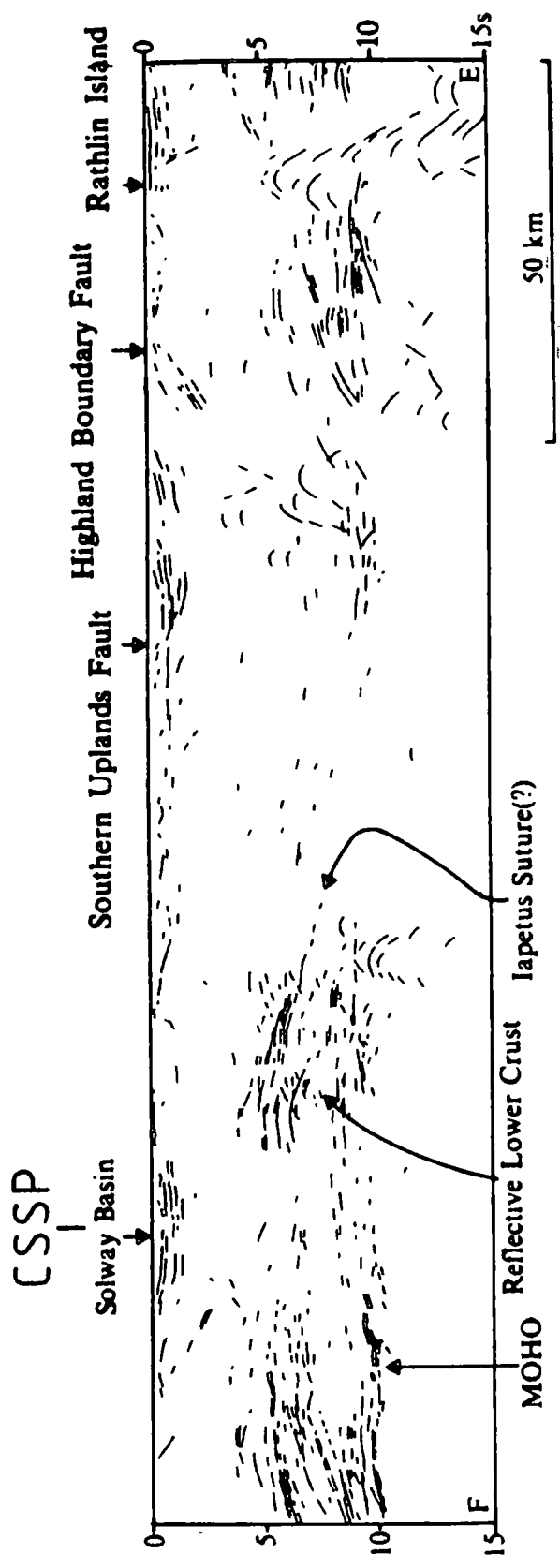


Fig 6.3 Model of Solway Basin Bouger gravity anomaly with the regional trend removed

3.63 to 4.31 km/s at 1 bar, 3.72 to 4.37 km/s at 100 bars and 4.10 to 4.63 km/s at 750 bars. These measurements suggest that the 5.5 to 5.7 km/s layer can be represented by Lower Palaeozoic greywackes similar to those found in the Southern Uplands. The zero time-term at station S81 in southern Scotland, on the Silurian, also suggests this layer represents the Lower Palaeozoic, although the time-term at station S91 in the Isle of Man, also on Lower Palaeozoic rocks, is 0.2 s. The Manx Group, however, was deposited on the other side of the Iapetus Ocean from the Lower Palaeozoic of the Southern Uplands and the two sides were brought together along the Iapetus Suture (see section 1.2.1). The BIRPS profile across the CSSP line suggests the Solway Basin lies above the hanging wall of the Suture (Fig. 6.4) with the Isle of Man as part of the footwall to the south (Brewer et al. 1983). If this is so then the refractor under the Solway Basin is not continuous under the Isle of Man and the time-terms determined for S91 are not necessarily meaningful.

The upper crustal phase (Pg) with a velocity of 6.15 km/s is well defined by both the plus-minus and time-term methods (Table 5.14) and a velocity close to this for Pg is a common occurrence in the continental crust. In situ measurements of rock velocities in the Lewisian of Scotland suggest that velocities in the upper crust of 6.0 to 6.2 km/s almost certainly represent acid gneisses (Hall and Al-Haddad 1976, Armour 1978). Velocities of 6.0 km/s at a shallow depth in the Southern Uplands are postulated as being igneous or metamorphic rocks of granodioritic to dioritic



(from Brewer et al 1983)

Fig 6.4 Line drawing of the BIRPS deep seismic reflection section from WINCH profile (see Fig 1.5 for location)

composition (Adesanya 1982, Hall et al. 1983). It is unlikely, however, that the Pg is a metamorphic facies of the Lower Palaeozoic, the velocity is rather high (Hall et al. 1984) and the transition appears to be too rapid for regional metamorphism to be the cause.

The depth to Pg determined from the time-terms is dependent on the accuracy of the shallow structure. The velocity contrast across the Pg interface is no greater than 0.4 km/s but the velocity contrasts across layers 1/2 and 2/3 are approximately 1.1 km/s and 1.0 km/s respectively. Thus relatively large variations in the depth to the Pg interface can be accommodated within the errors of the shallow structure. Consequently most of the variations in the Pg time-term have been absorbed within the shallow structure and the Pg refractor was only adjusted where necessary. The Pg refractor is 2.2 km beneath M25 to M17 deepening to approximately 4 km beneath the rest of the line. It is at a depth of about 3.3 km beneath S81 in southern Scotland.

An interpretation of the aeromagnetic anomaly in the Solway Firth and the Southern Uplands (Fig. 6.5) by Al-Chalabi (1970) suggested that a Precambrian magnetic basement underlies the Lower Palaeozoic at a depth of 9.4 km, which is 5.4 km deeper than the Pg refractor. A more detailed investigation of the Solway Firth anomaly showed that by increasing the magnetisation contrast from 0.001 to 0.002 emu/cc the magnetic basement can be placed at a depth of 5 km (Al-Chalabi 1970). This suggests that

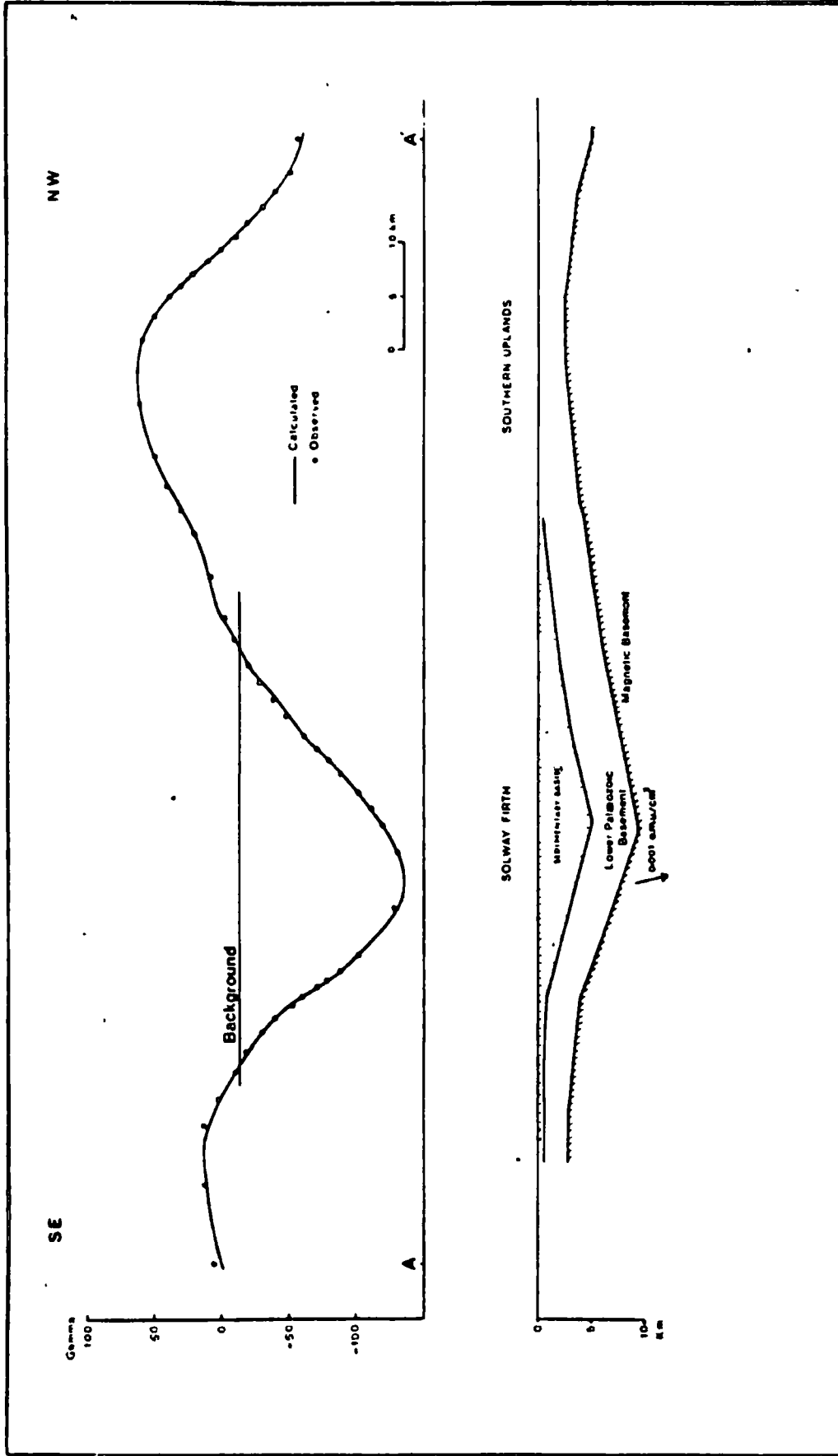


Fig 6.5 Interpretation of the aeromagnetic anomaly of the Solway Firth and Southern Uplands. National grid co-ordinates of A and A' are SC 860700 and NX 223693 Respectively (from Al-Chalabi (1970))

remodelling the magnetic anomaly with a higher magnetisation contrast between the Lower Palaeozoic and magnetic basement could bring the depth to the magnetic basement up to 4 km.

The interpretation of the profile in the Irish Sea is shown in Fig. 6.6. The important feature of the model is the 1 to 3 km thick Lower Palaeozoic sequence overlying a layer of 6.15 km/s, assumed to represent crystalline basement, at a depth of 4 km.

6.3 The shallow structure beneath northern England

The same layering is apparent beneath northern England as beneath the Irish Sea (Figs. 6.7 and 6.8). It is convenient to treat the profile to the west and east of Spadeadam separately. To the west the Carlisle Basin has broad similarities with the Solway Basin but, due to the large offset between M1 and S1 and the poor quality of many of the stations in this area, there is much less information available. The Pg time-terms are larger than in the Solway Basin suggesting a thicker Permo-Triassic sequence, although the gravity anomaly is smaller than in the Solway Basin and suggests a much thinner sequence. This contradiction may be explained by the presence of the Carlisle Basin magnetic anomaly which Laving (1971) interprets as a basic igneous intrusion. The higher density of this intrusion probably offsets the effect of the low density sediments. Using magnetisation contrasts of 0.0008 to 0.006 gm/cc Laving (1971) calculated that the depth to the highest point of the intrusion is in the range 2 to 4.5 km,

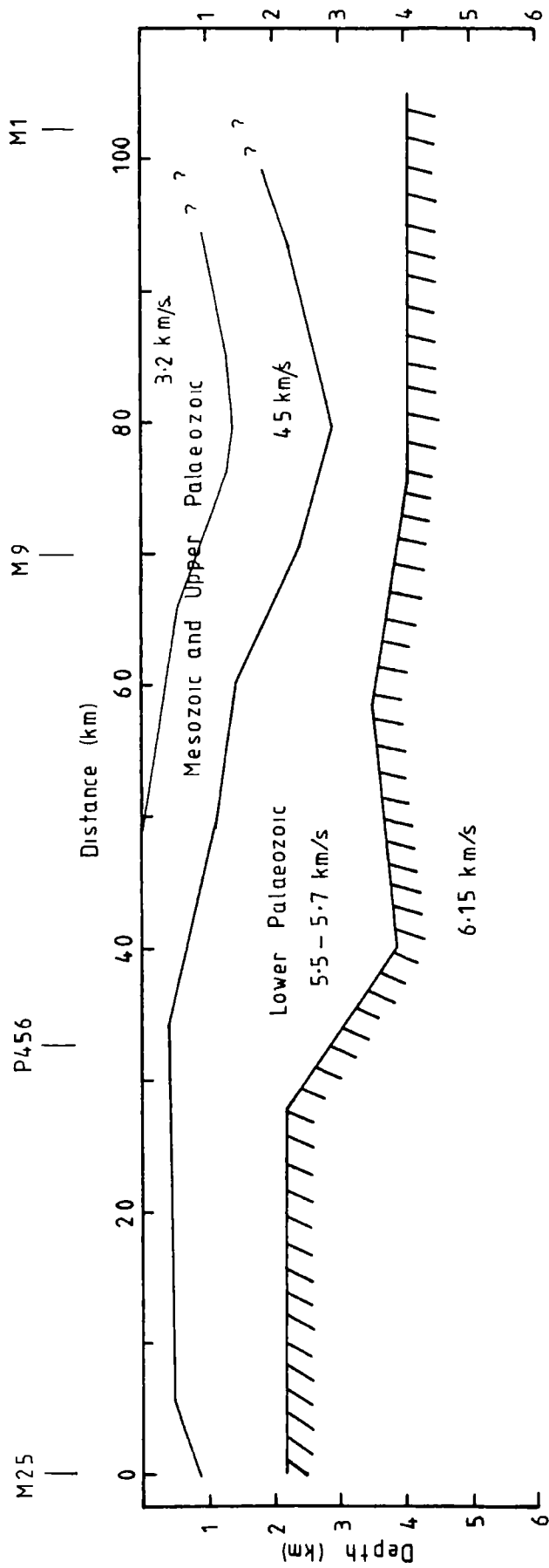
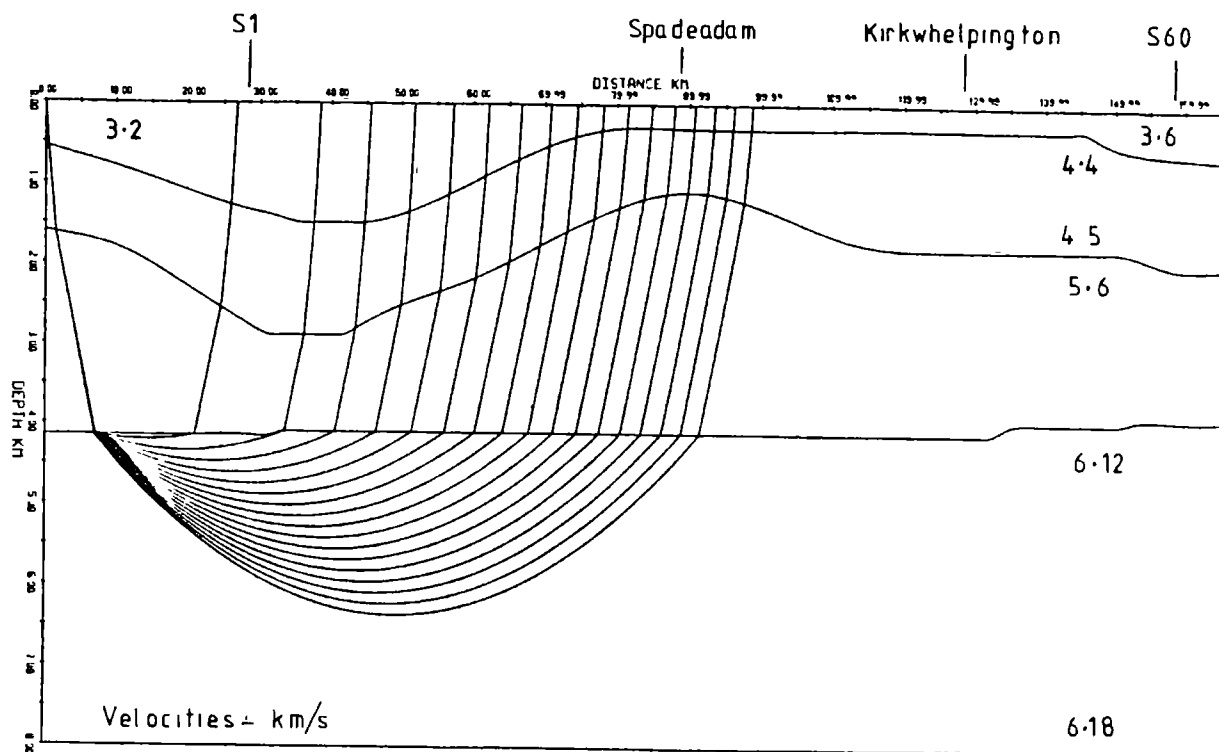


Fig 6.6 Interpretation of the upper crustal structure beneath the Irish Sea



CSSP NORTHERN ENGLAND COMMON SHOT M2

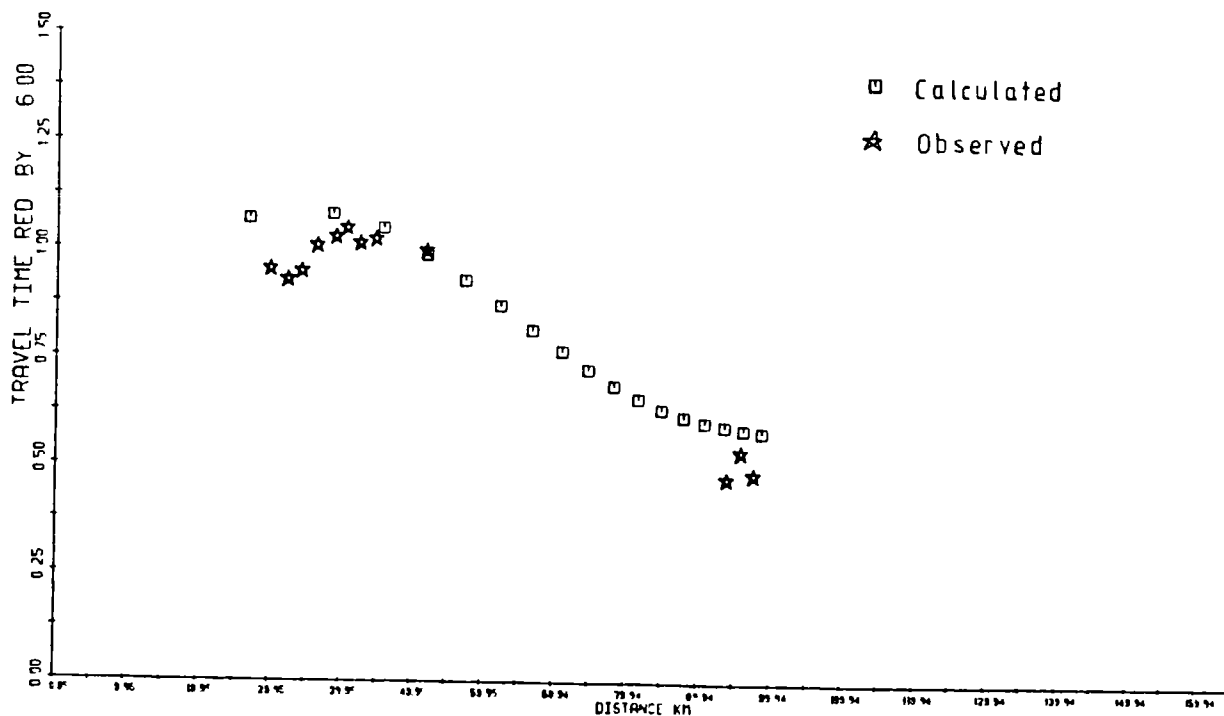


Fig 6.7 Ray traced diagram and reduced travel-time section obtained for upper crustal model beneath northern England for shot M1

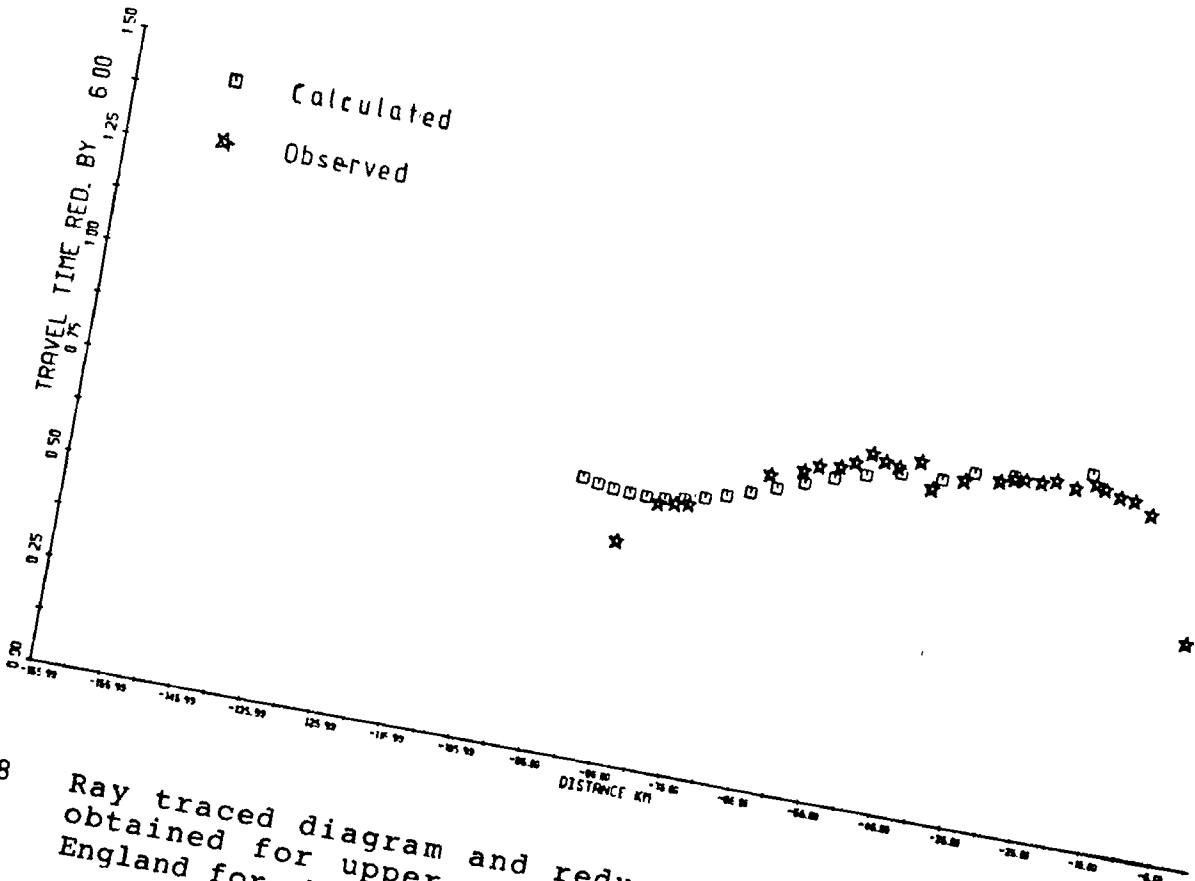
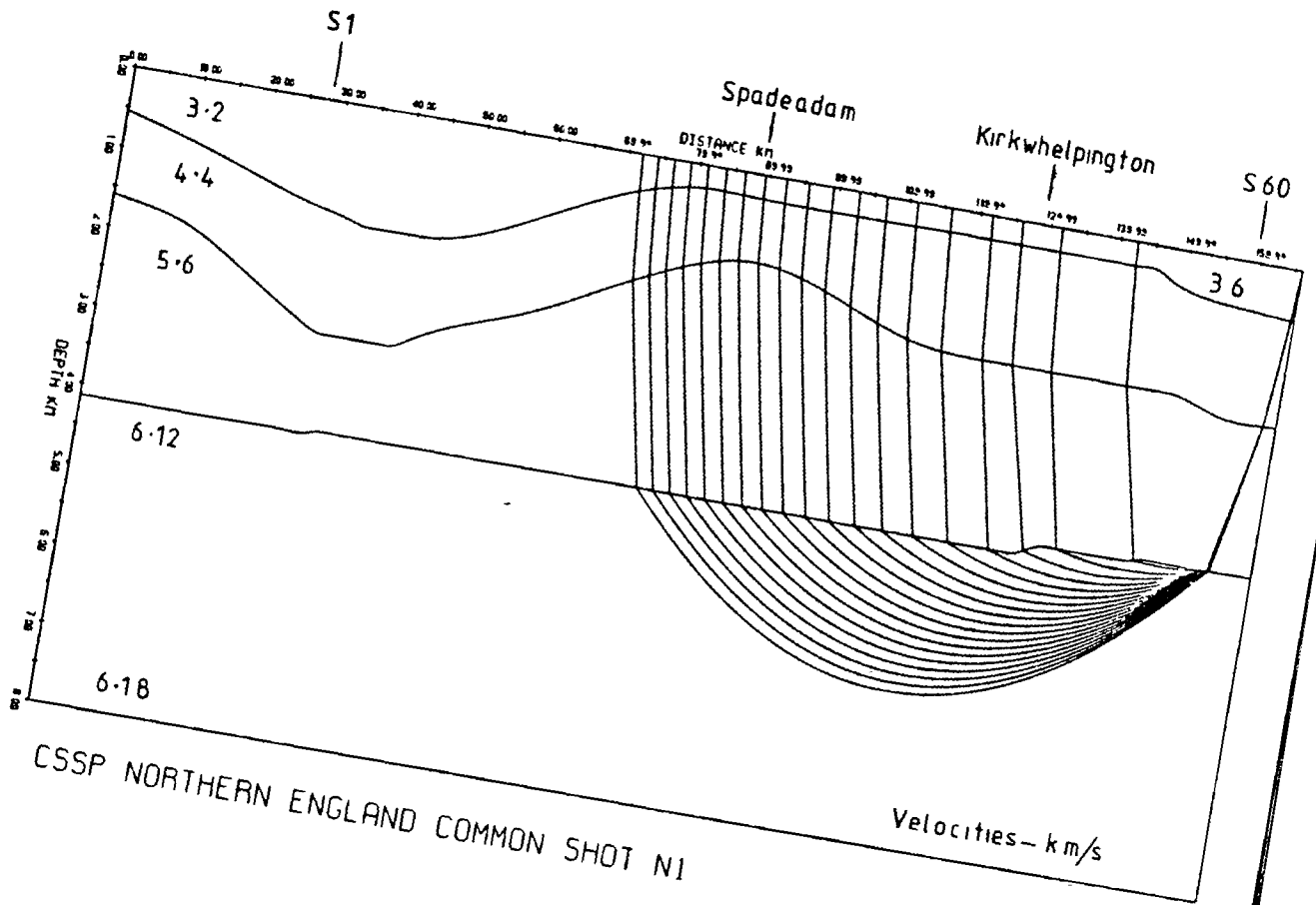


Fig 6.8 Ray traced diagram and reduced travel-time section obtained for upper crustal model beneath northern England for shot N1

with a best estimate of 4.0 km obtained using a magnetisation contrast of 0.001 gm/cc. This is the same depth as the depth for the Pg refractor under the Solway Basin. There is insufficient information on the thickness of the Mesozoic and Upper Palaeozoic layers in the Carlisle Basin to determine the depth to the Pg refractor under the Carlisle Basin but if it is assumed to be at the same depth as under the Solway Basin this suggests that the intrusion does not penetrate the Lower Palaeozoic and may be older. The relative thickness of the Mesozoic and Palaeozoic sequences is largely guesswork. The edge of the Permo-Triassic basin, however, is known from the surface geology to be close to station S24.

The Pg refractor is at a depth of about 4 km beneath Spadeadam, but the Lower Palaeozoic rises to within 1 km of the surface (Fig. 5.19). This rapid change in the depth to the Lower Palaeozoic is in line with the northern extension of the Pennine faults on the western edge of the Alston Block. The Spadeadam travel-time curve to the east clearly indicates a sharp interface between the Pg phase and arrivals from the Lower Palaeozoic (Fig. 5.18) and attempts to model the travel-times with an increasing velocity with depth fail. The depth to the top of the Lower Palaeozoic increases towards the eastern end of the line to nearly 2 km beneath S60. The small circular gravity low over Druridge bay (Fig. 1.8) is probably related to the low density Coal Measures.

The ray tracing shows a good fit to the travel-times for shot N1 (Fig. 6.8) but in the absence of good travel-time data for M1 it is difficult to create an accurate model for the Carlisle region (Fig. 6.7). The basic intrusion proposed by Laving (1971) is likely to have a higher velocity than the rest of the basement and an inability of the time-term method to account for this could cause errors in the time-terms. Assuming the intrusion has a velocity of approximately 6.7 km/s and a width of between 10 and 20 km (Laving 1971) then the time-terms could be between 0.13 s and 0.26 s too small.

The interpretation of the structure along the profile is shown in Fig. 6.9. The important features are the same as in the Irish Sea with a 1 to 3 km thick Lower Palaeozoic sequence overlying a crystalline basement of 6.15 km/s.

The depth to the Pg refractor increases northwards along the Northumberland coast with a thickness of 4.0 km, 5.0 km and 7.5 km at stations S60, S61 and S62 respectively. This gives an average northerly dip for the refractor of 8.6° .

6.4 The shallow structure beneath the North Sea

The structure down to the basal Permian has been determined largely from seismic reflection data (Day et al. 1981). The base of the Permian shows an easterly dip of between 0.5° and 1.0° with a thickness of approximately 1.3 km under N29. The thickness

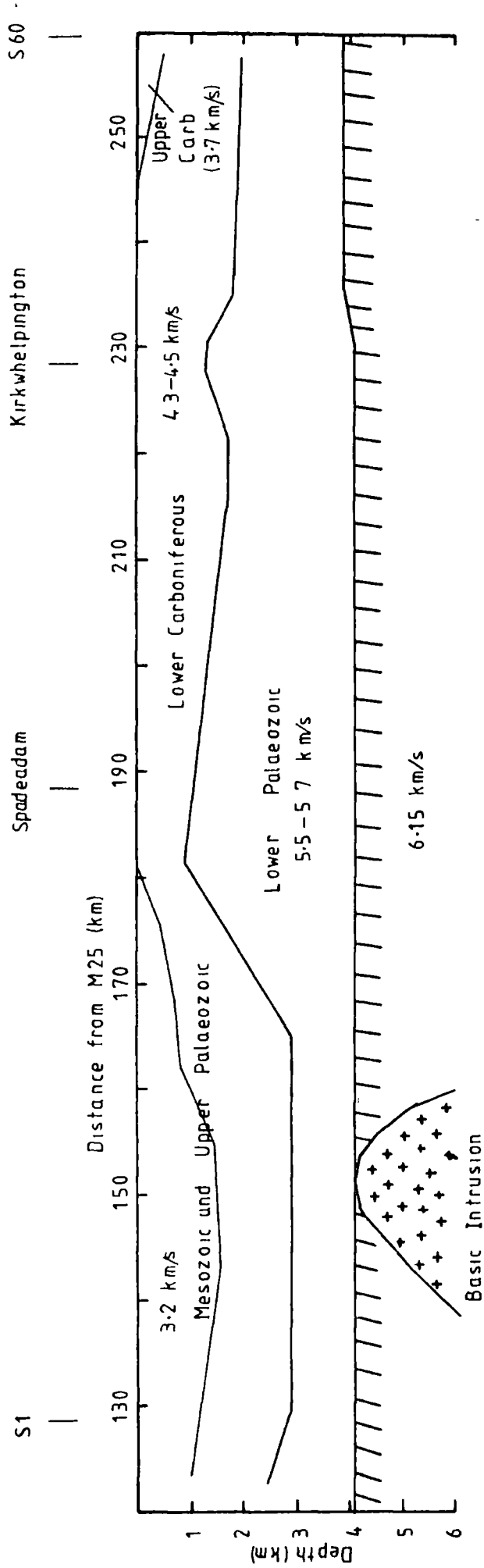


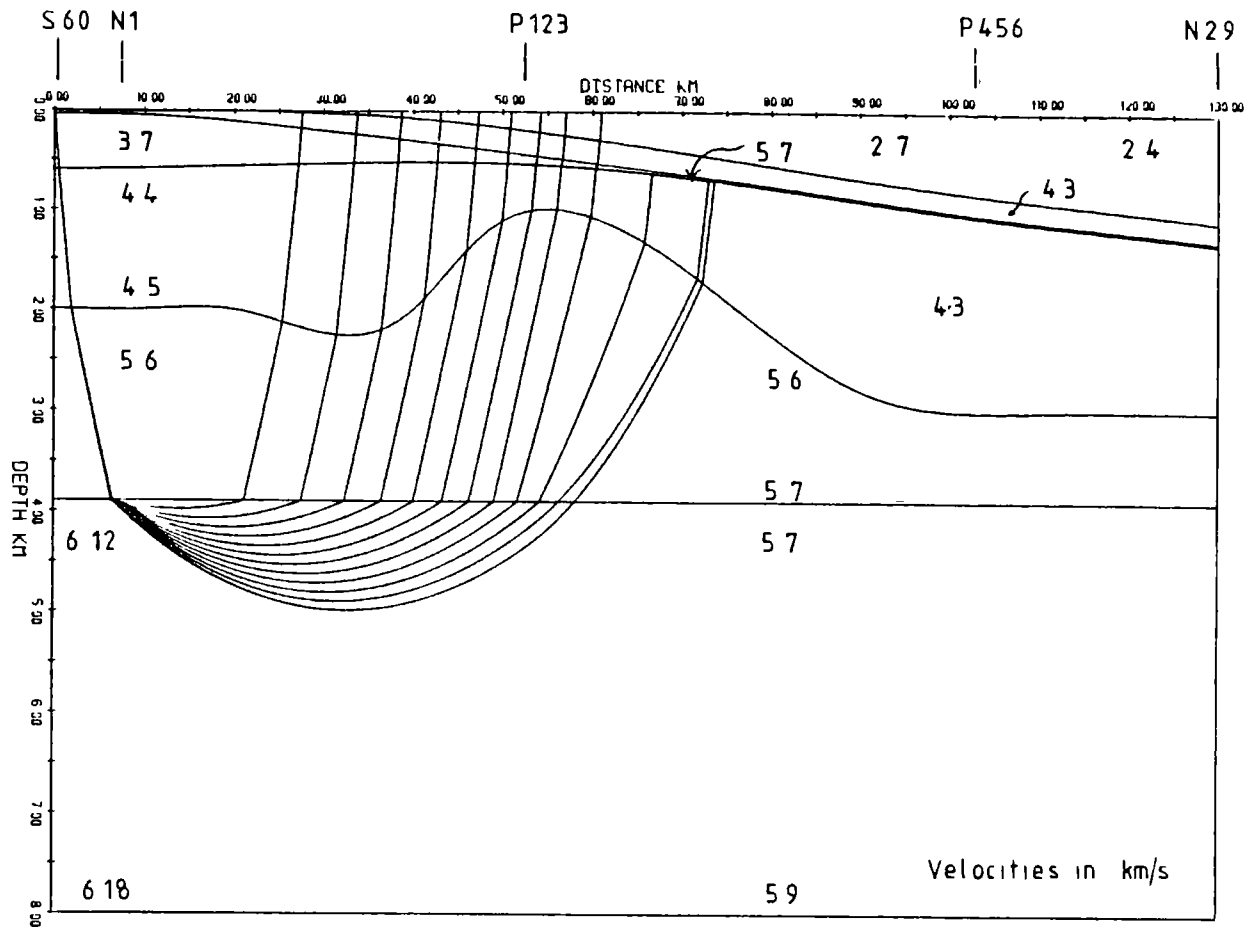
Fig 6.9 Interpretation of the upper crustal structure beneath northern England

of the Upper Carboniferous is known from the multiple reflections (section 5.3.2) and boreholes on land (Taylor et al. 1971).

The Palaeozoic basement as far east as N11 appears to be continuous with that of the Northumberland Trough, but beyond N11 the data is not so good and the structure is less clear. An 8 mgal north-south linear gravity gradient at N11 suggests a step in the 5.6 km/s refractor (Fig. 1.8). Using the infinite slab approximation (42 mgal/km/unit density contrast in gm/cc) with a density contrast of 0.2 gm/cc a step size of 1 km is determined. The depth to the 5.6 km/s refractor increases to about 3 km further east beneath under P456 (Fig. 5.36). A gravity minimum just to the south of P456 has been interpreted as a Caledonian granite at a depth of 1.8 km by Donato et al. (1983). This is shallower than the basement under the CSSP line and suggests that the top of the granite is at least 1 km higher than the surrounding basement.

There is no evidence for the continuation of the 6.17 km/s refractor east of N11. The ray tracing model can only be made to fit if the 5.6 km/s layer is extended to a depth of at least 8 km with a velocity gradient of approximately 0.05 s^{-1} (Figs. 6.10 and 6.11). It is uncertain whether this layer is a continuation of the Lower Palaeozoic west of N11 or different, lower velocity, crystalline basement from that to the west.

The absence of recordings of Pg on main line stations in northern



CSSP NORTH SEA COMMON STATION S60

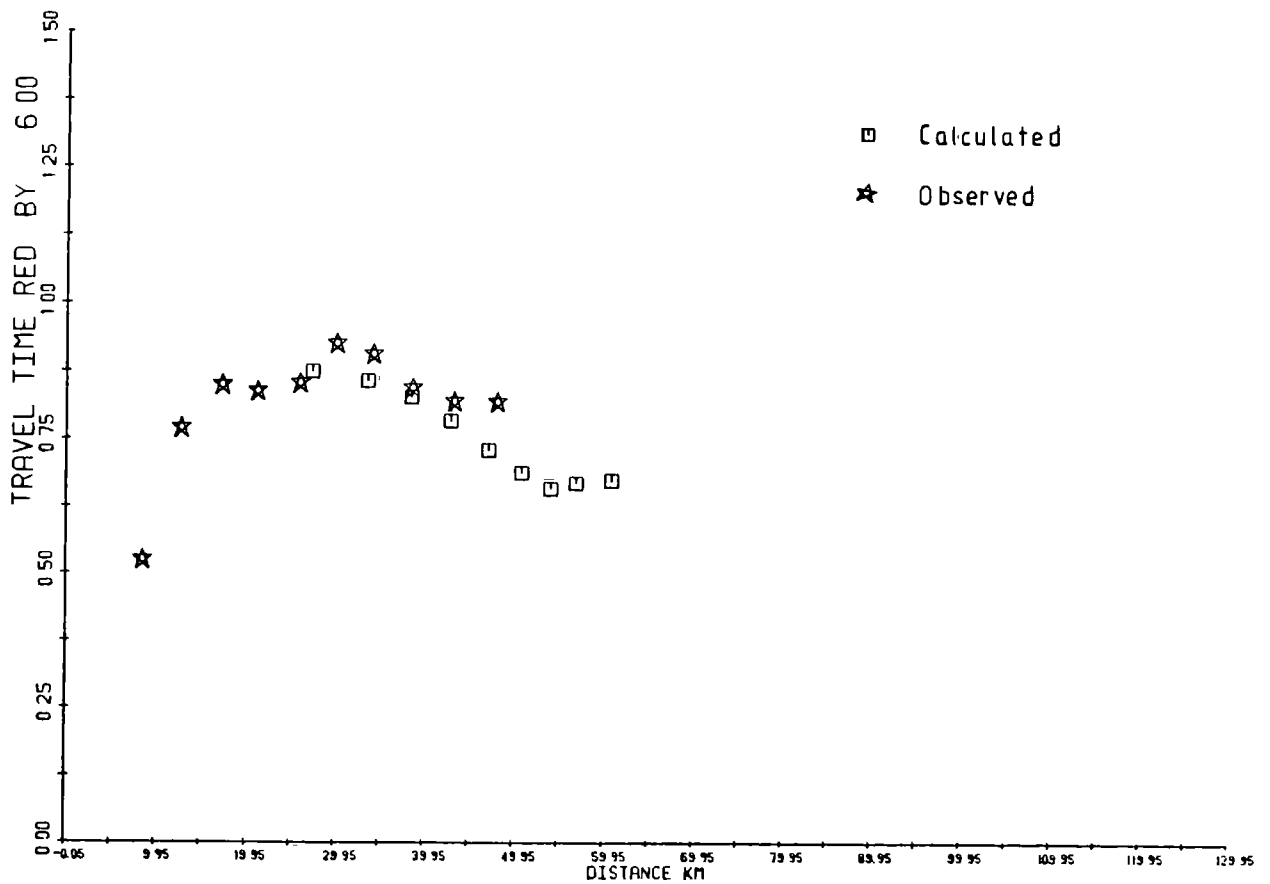
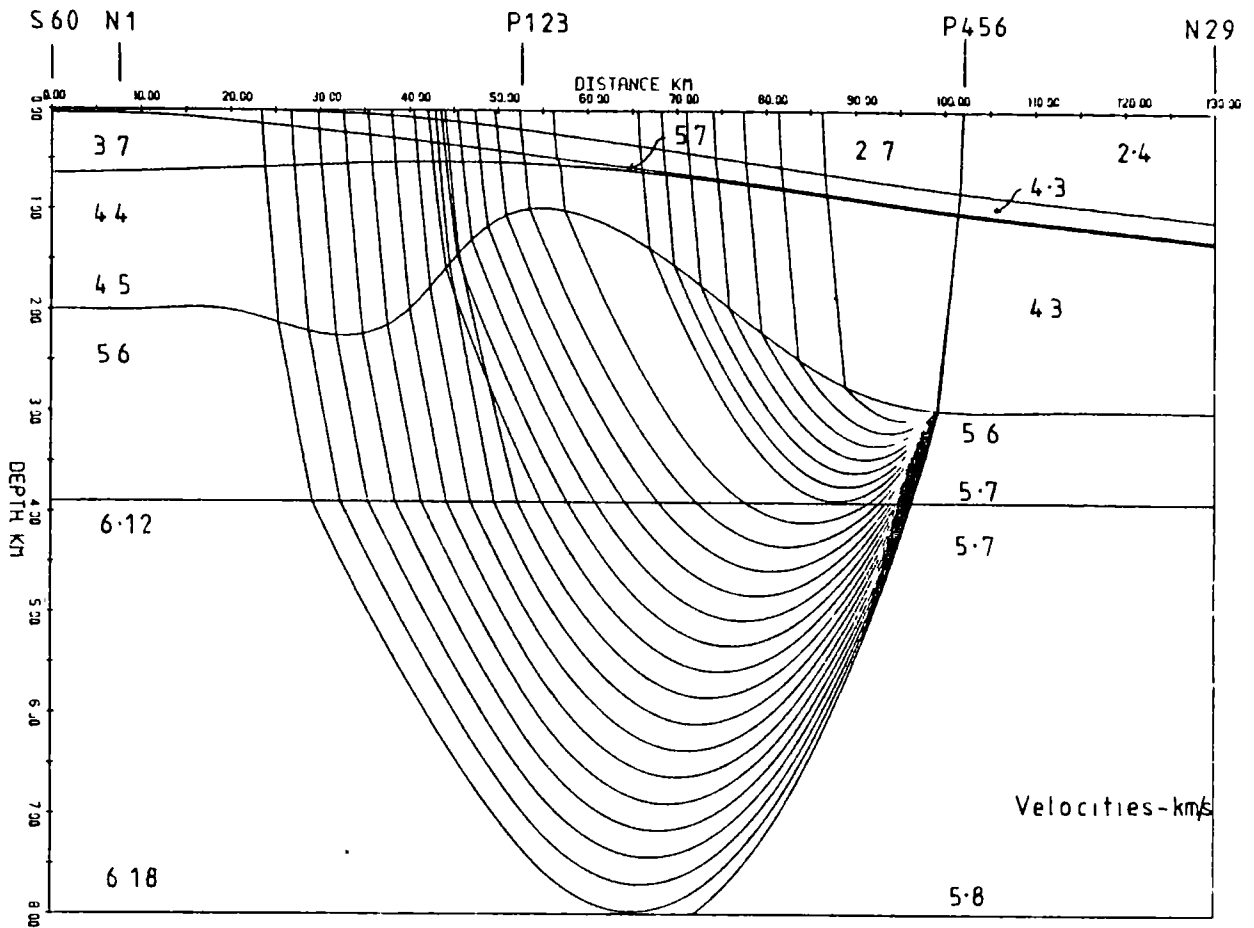


Fig 6.10 Ray traced diagram and reduced travel-time section obtained for upper crustal model beneath the North Sea for station S60



CSSP NORTH SEA COMMON STATION P456

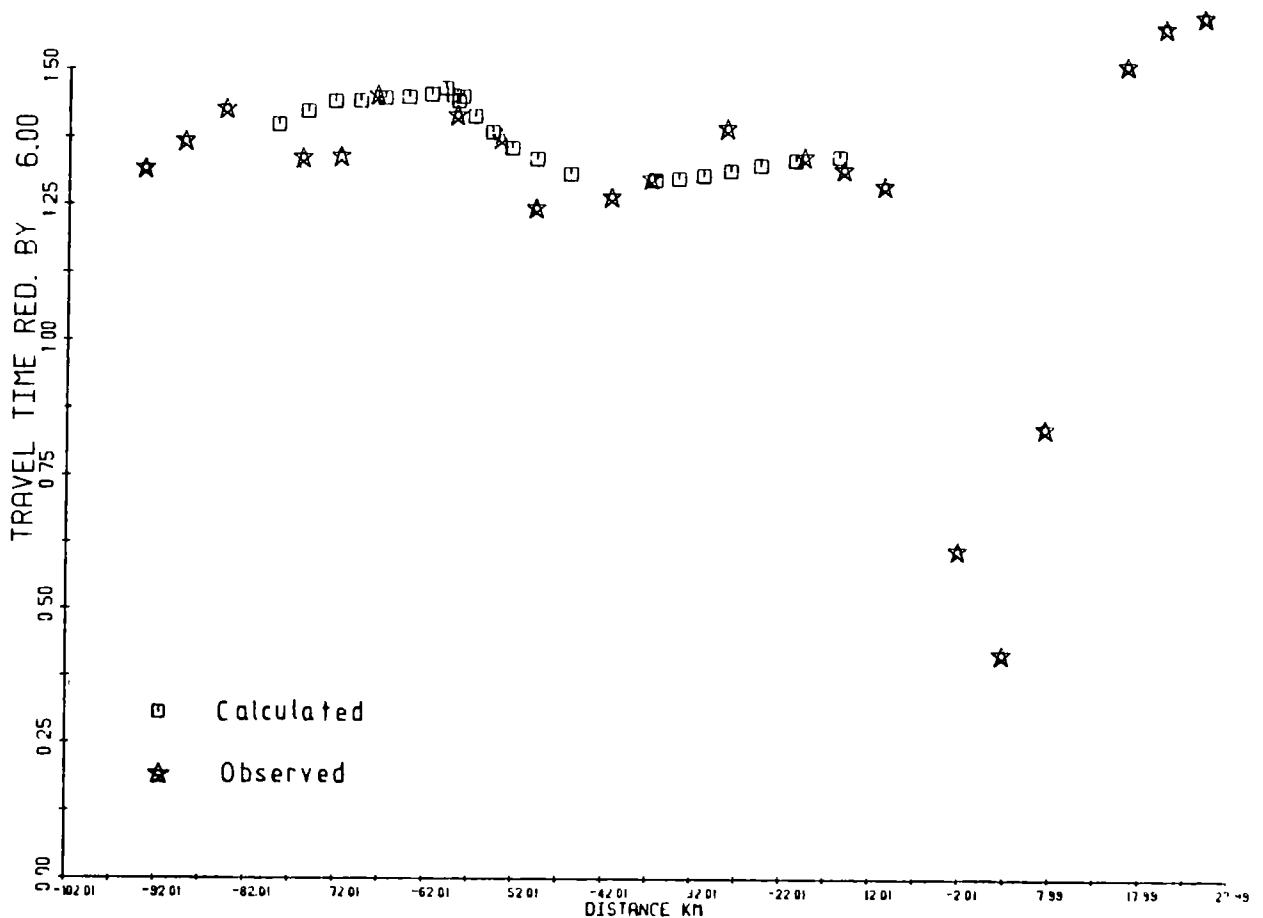


Fig 6.11 Ray traced diagram and reduced travel-time section obtained for upper crustal model beneath the North Sea for station P456

England from shots east of N11 and the observation of Pg from the same shots at P456, can be explained by the easterly dip of the basement and the presence of a 5.7 to 5.8 km/s layer above the basement (Figs. 6.10 and 6.11). The basement dip beneath the shots east of N11 gives an apparent down-dip velocity for Pg at stations on the main line of about 5.5 km/s. This is less than the overlying high velocity layer and therefore no arrivals would be observed. At P456 the apparent up-dip velocity for Pg is about 5.9-6.0 km/s and arrivals from the basement are therefore observed. The most likely composition of this high velocity layer is anhydrite. Anhydrite has a velocity in excess of 6 km/s under pressure (Table 1.1) and is a known formation of the Zechstein.

The interpretation of the North Sea data is shown in Fig. 6.12. The structure east of N11 is similar to the structure beneath the rest of the profile with the important features being a layer of velocity 5.6 km/s at a depth of 2 km, assumed to consist of Lower Palaeozoic rocks, overlying a 6.17 km/s crystalline basement. The composition of the basement east of N11 is less certain. The 6.17 km/s basement appears to be absent and it is not known whether the 5.6 km/s refractor is a continuation of the Lower Palaeozoic rocks or of a completely different origin.

6.5 Discussion

The important result of the interpretation of the shallow structure is the identification of a Lower Palaeozoic sequence

from 1 to 3 km thick of velocity 5.5 and 5.7 km/s overlying a crystalline basement of velocity 6.15 km/s.

Reconstructions of the closing stages of the Iapetus Ocean have lead many geologists to suggests that the Southern Uplands is the remains of an accretionary prism complex (see Chapter 1, Leggett et al. 1979, 1983, McKerrow et al. 1977 and Dewey 1971) with a large thickness of Lower Palaeozoic sediments overlying the remains of oceanic crust from the Iapetus Ocean. LISPB supported this by showing a maximum of 12 km of Lower Palaeozoic rocks of velocity 5.8-6.0 km/s under the Southern Uplands and northern England (Bamford et al. 1976,1977 and 1978). There has, however, been a considerable amount of evidence to the contrary. Even as early as 1964 velocities of 6.1 km/s were idenitified under southern Scotland and the Irish Sea (Agger and Carpenter 1964) and more recently other seismic surveys have identified rocks of velocity 6.0 km/s or greater under the Southern Uplands (Hall et al. 1983, Warner et al. 1982, Powell 1971). Velocities in excess of 6.0 km/s are generally thought to be too high for Lower Palaeozoic rocks even if metamorphosed to greenschist facies (Oliver and Mckerrow 1984, Hall et al. 1984). This has been supported by the study of inclusions in volcanic rocks which suggest that high-grade (granulite facies) feldspathic basement underlies the Southern Uplands (Upton et al. 1983). The interpretation of aeromagnetic data also indicates a Precambrian basement beneath the Lower Palaeozoic of southern Scotland (Powell 1970).

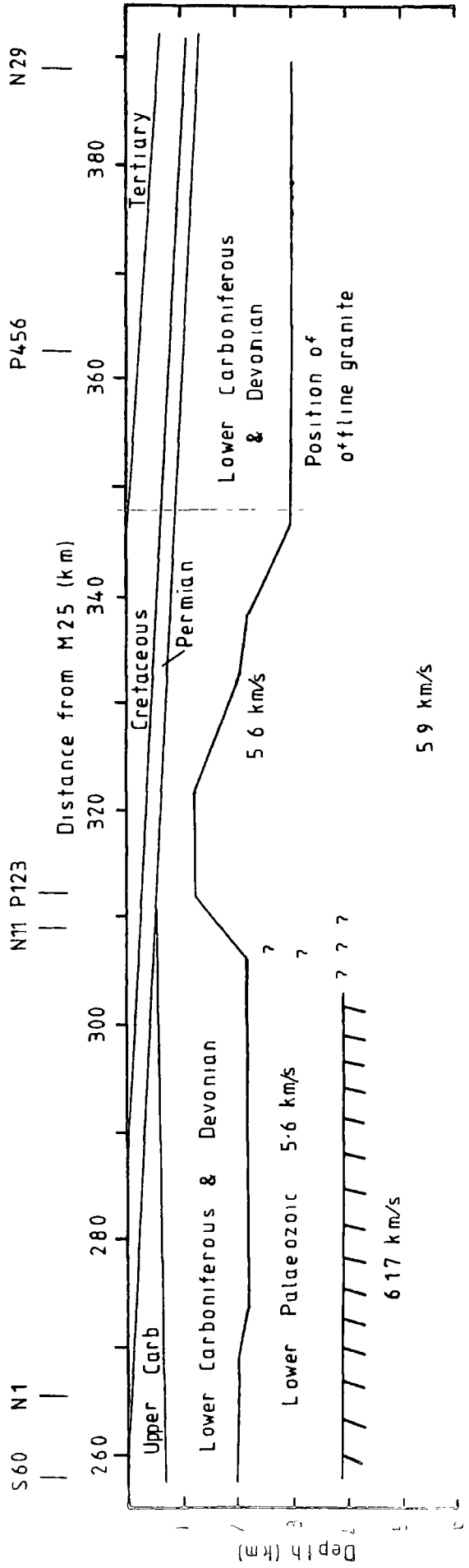


Fig 6.12 Interpretation of the upper crustal structure beneath the North Sea

There is independent evidence of Upper Carboniferous thinning to the east which is consistent with this cross-section (Donato et al. 1983).

Although the layer of 6.15 km/s velocity could represent crystalline basement north of the Suture it is suggested that a velocity of 6.15 km/s may represent Precambrian crystalline basement which was in the process of being subducted beneath the Laurentian plate during the final closure of the Iapetus Ocean. It is possible that the boundary between the Lower Palaeozoic and Pg beneath the CSSP line represents the Iapetus Suture. The Suture would be expected to dip northwards under an increasing thickness of Lower Palaeozoic sediments in the Southern Uplands. This is consistent with the 8.6° northwards dip for Pg in Northumberland beneath station S60, S63 and S61 and the BIRPS deep seismic reflection profile in the Irish Sea (see section 6.2, Fig. 6.4). The 3.3 km depth of Pg under S81 in Dumfrieshire, however, is slightly shallower than further south.

The relationship of the 6.15 km/s refractor under the CSSP line to the shallow 6.0 km/s refractor under the Southern Uplands remains unresolved. The velocities in the Southern Uplands tend to be lower and a different relationship between the Lower Palaeozoic and the high velocity refractor appears to exist. Hall et al. (1983) have suggested a block structure for the Southern Uplands whereas a clear layered structure is apparent from the the CSSP data. The investigation of the CSSP shots recorded at the Eskdalemuir array will be particularly valuable in helping to resolve this question.

The absence of a 6.15 km/s refractor in the North Sea east of N11 indicates a significant difference in the upper crustal structure

from the rest of the profile. The composition of the upper crust east of N11 is uncertain and it is not known whether the 5.6-5.9 km/s layer represents an extension of the Lower Palaeozoic rocks further west or a different, possibly Precambrian, crystalline basement similar to that suggested by Collette et al. (1967) to the south off Flamborough Head. The existence of high velocity anhydrite above the basement suggests that the seismic refraction method may not be the best means of investigating the upper crust in this region.

CHAPTER 7 - PRELIMINARY INTERPRETATION OF THE DEEP STRUCTURE

7.1 Introduction

For the discussion of the deep structure, the CSSP line is divided into two halves. The Irish Sea shots and western half of the northern England stations are treated separately from the North Sea shots and the eastern half of the northern England stations. The analysis has been largely constrained to common station sections for two reasons. (1) All the shots were detonated successfully but a number of the stations did not operate satisfactorily throughout, so that some common station sections are complete whereas there are no complete common shot sections. (2) Problems with the station gain settings makes the comparison of amplitudes on common shot sections difficult (see section 2.2.1) but because nearly all the shots were of the same size it is hoped that the trace amplitudes can be compared on the common station sections.

The average velocities and depths calculated from wide-angle reflections include the effects of the near surface sediments and assume a horizontally layered crust.

7.2 Interpretation of the North Sea shots

It has already been seen from Chapter 5 that prominent wide-angle reflections/diving waves, identified as PcP from a mid-crustal

discontinuity or velocity gradient, and PmP from the Moho are visible on common station sections for the North Sea shots (Figs. 5.38, 5.39, 7.1, 7.2, 7.3, 7.4 and Appendix A).

Using the method of Holder and Bott (1971) for interpreting reflections (see section 4.5), the depth to the Moho and average crustal velocity can be determined from PmP. For stations between S32 and S42 the average depth to the Moho is 30.2 ± 0.5 km and the average velocity 6.35 ± 0.03 km/s (Table 5.1). The x^2-T^2 (see section 4.5) method was applied to PmP for common station sections S32 and S38 giving estimated average crustal velocities of 6.27 ± 0.07 km/s and 6.38 ± 0.05 km/s and Moho depths of 29.6 ± 0.8 km and 31.5 ± 0.7 km respectively. It has already been seen from Chapter 6 (see section 6.4) that the dying out of Pg with increasing distance, often an indication of a low velocity layer, is a result of lateral variations in the upper crust. There is no other evidence for the existence of a low velocity layer in the North Sea. The apparent velocity for Pn is 7.72 ± 0.08 km/s.

PcP does not have an identifiable head wave associated with it so that it is not possible to use the method of Holder and Bott (1971). Using the x^2-T^2 method, however, average upper crustal velocities of 6.11 ± 0.08 km/s and 6.02 ± 0.05 km/s at depths of 20.8 ± 2.1 km and 17.4 ± 1.3 km were determined for stations S32 and S38 respectively (Table 7.1).

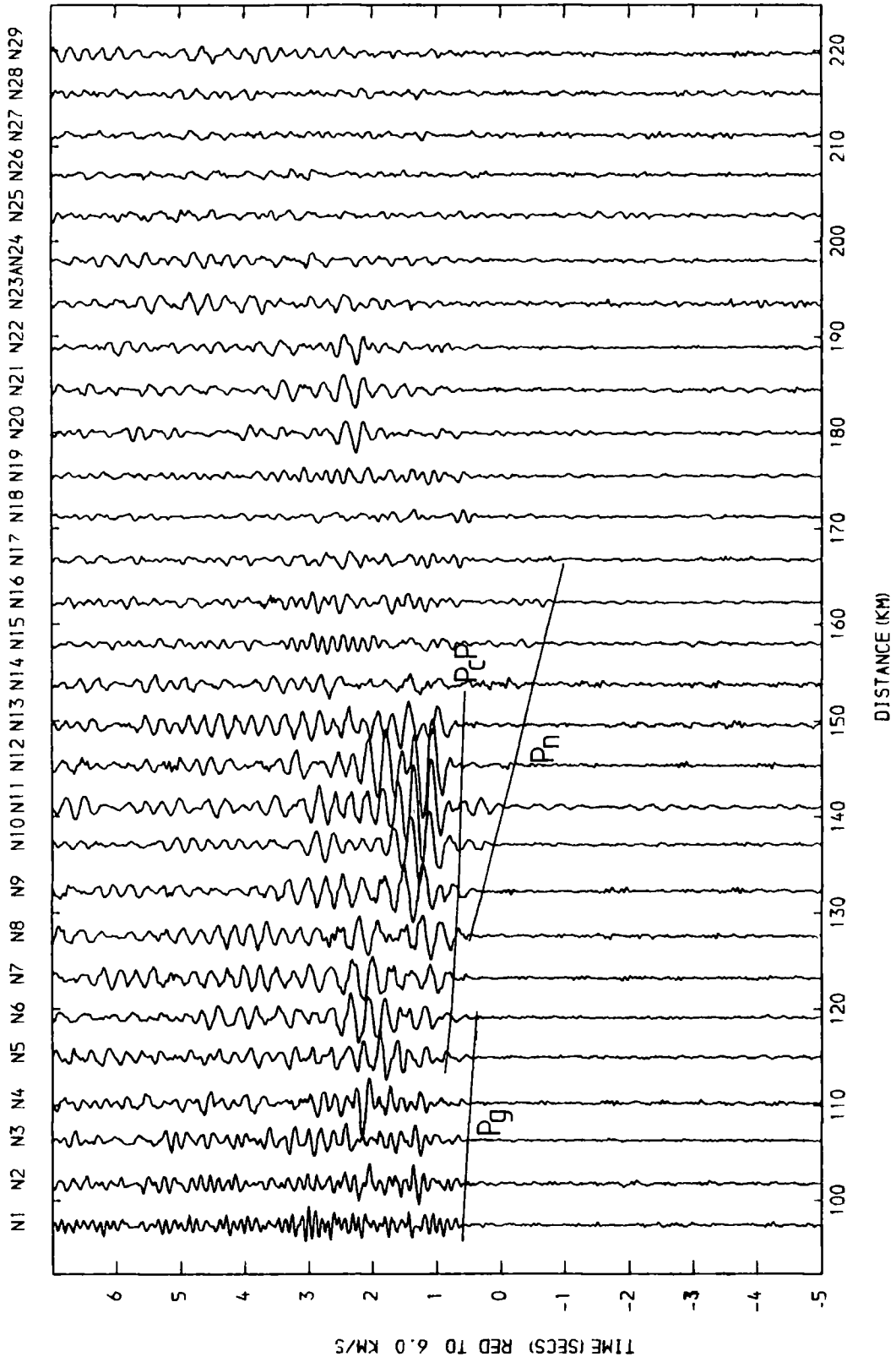


Fig 7.1 Reduced section of the North Sea shots recorded at S19. Unfiltered, amplitudes uncorrected

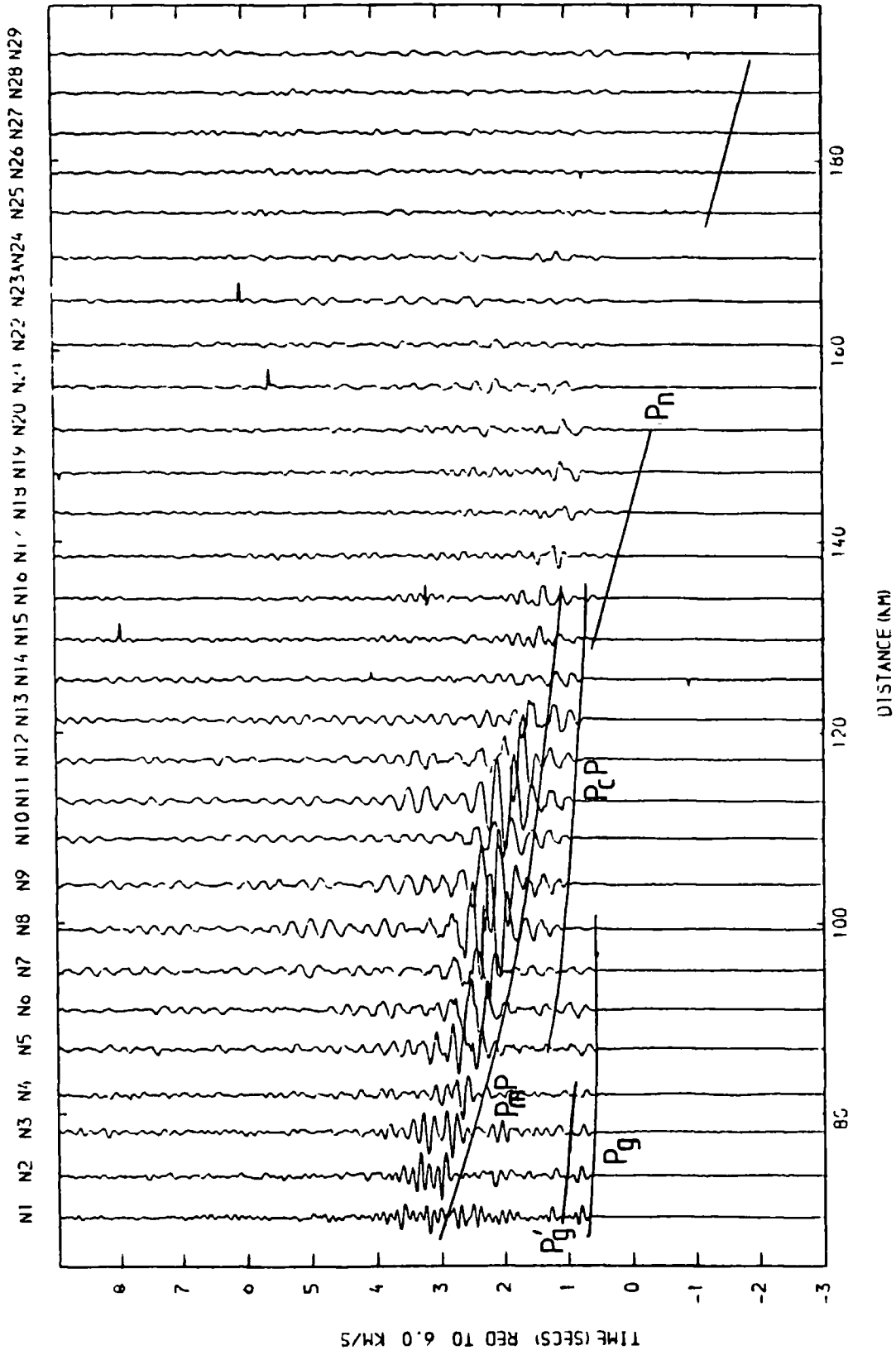


Fig 7.2 Reduced section of the North Sea shots recorded at S32.
 Unfiltered, amplitudes uncorrected

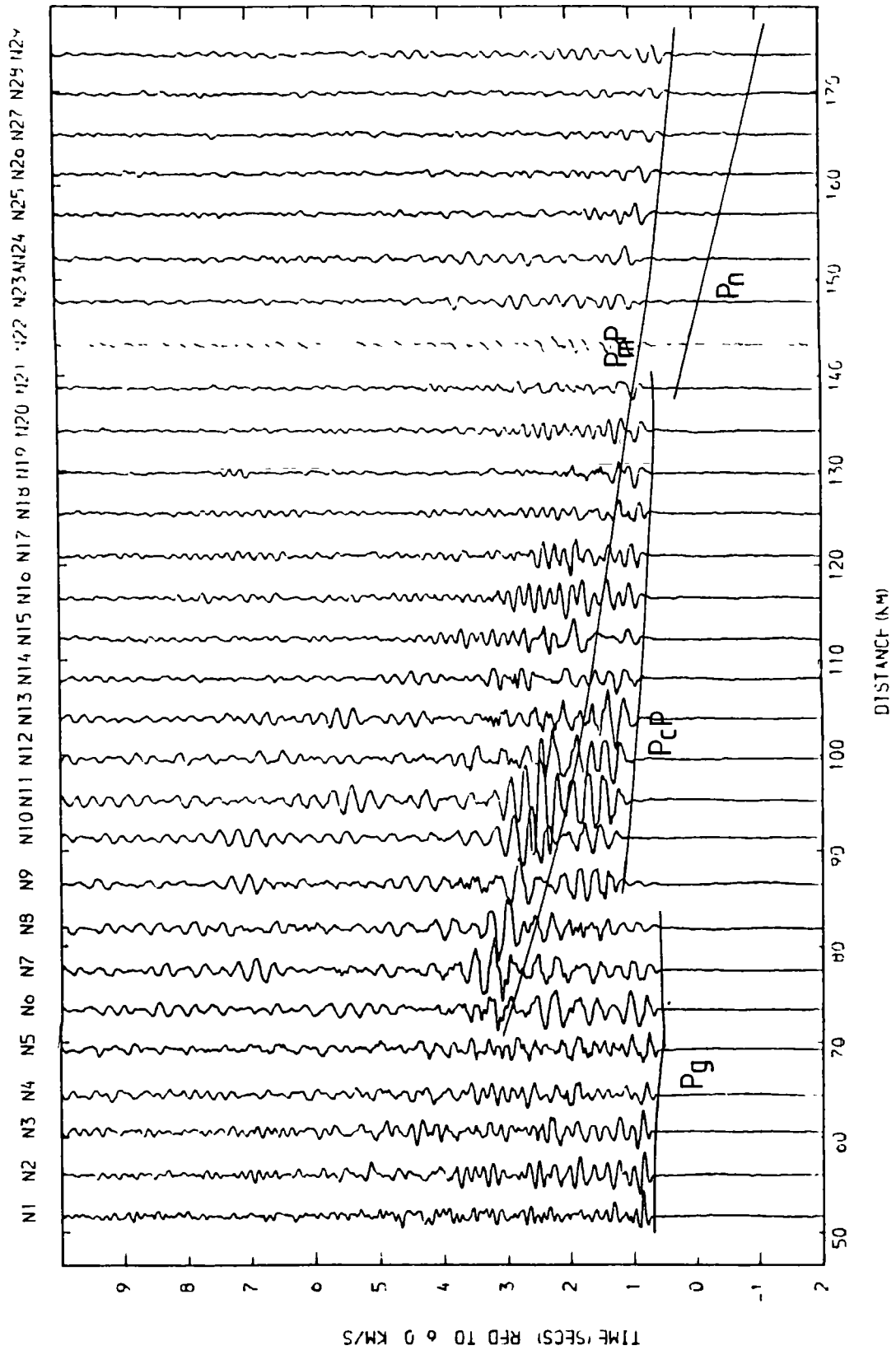


Fig 7.3 Reduced section of the North Sea shots recorded at S40. Unfiltered, amplitudes uncorrected

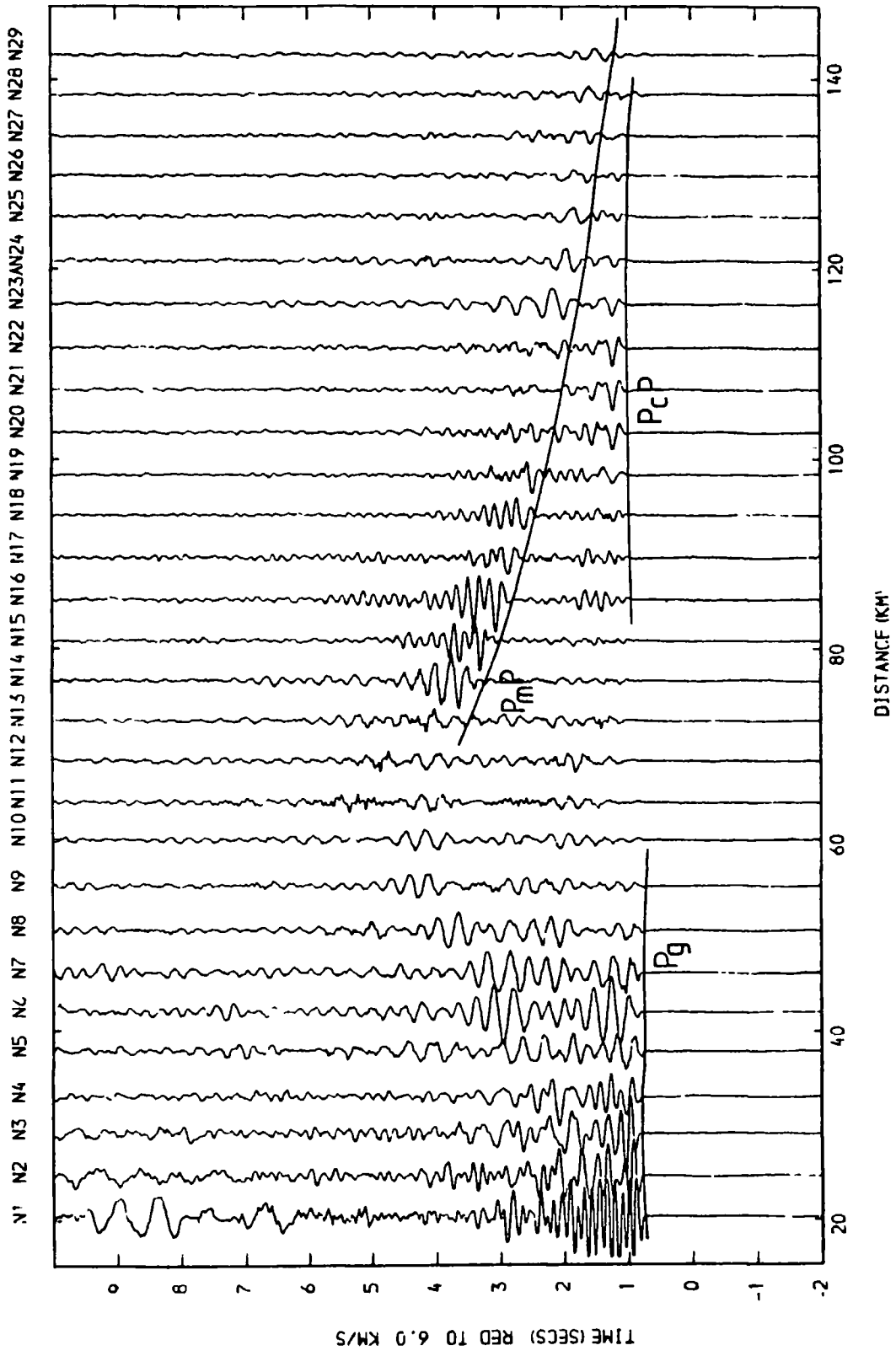


Fig 7.4 Reduced section of the North Sea shots recorded at S54. Unfiltered, amplitudes uncorrected

TABLE 7.1

Analysis of mid and lower crustal reflections of the North Sea.

A) Depth to Moho, Pn velocity and mean crustal velocity from PmP using the method of Holder and Bott (1971).

Station	Pn velocity km/s	Mean crustal vel. km/s	Depth to Moho km
S32	7.81	6.39	30.6
S34	7.72	6.34	29.6
S35	7.75	6.32	30.2
S38	7.63	6.34	29.8
S42	7.70	6.37	30.6

B) Depth to Moho and mean crustal velocity from X^2-T^2

Station	Mean crustal vel. km/s	Err. 95%	Depth to Moho km	Err. 95%
S32	6.27	0.07	29.6	0.8
S38	6.38	0.05	31.5	0.7

C) Depth to mid crustal layer and mean upper crustal velocity from PcP using X^2-T^2 method.

Station	Mean velocity km/s	Err. 95%	Depth km	Err. 95%
S32	6.11	0.08	20.8	2.1
S38	6.02	0.05	17.5	1.3

The lower velocity for Pg east of shot N11 and the greater thickness of Upper Palaeozoic and younger sediments east of N16 (see section 6.4) suggests that the apparent velocities determined from the wide-angle reflections and the apparent velocity of Pn have probably been underestimated.

A model based on the above results was tested using a synthetic seismogram program by Fuchs and Mueller (1971) based on the reflectivity method (see section 4.7.2). The model consists of two layers with a mid-crustal discontinuity at 19 km, where the velocity increases from 6.2-6.3 km/s to 6.6-6.7 km/s, and a Moho at 30 km, where the velocity increases from 6.7-6.8 km/s to about 7.9 km/s (Fig. 7.5). The amplitudes of Pg and Pn are controlled by the velocity gradient beneath the discontinuity, the low amplitude of Pn suggesting a sharp transition.

The synthetic seismogram shows a good fit with the travel times and amplitudes of common station section S32. PmP has a maximum amplitude at 100-105 km and PcP has a maximum amplitude at 110-120 km but the amplitude decays more rapidly with range on S32 than on the synthetic seismogram. The ratio between the amplitude of PmP at a range of 100 km and 180 km on the synthetic seismogram is about 5:1, but at least 20:1 at station S32. Comparison of the synthetic seismogram with other common station sections reveals a much less satisfactory fit between the amplitudes. PmP has a very small amplitude at a range of 100 km on common station section S19 (Fig. 7.1) and has a maximum

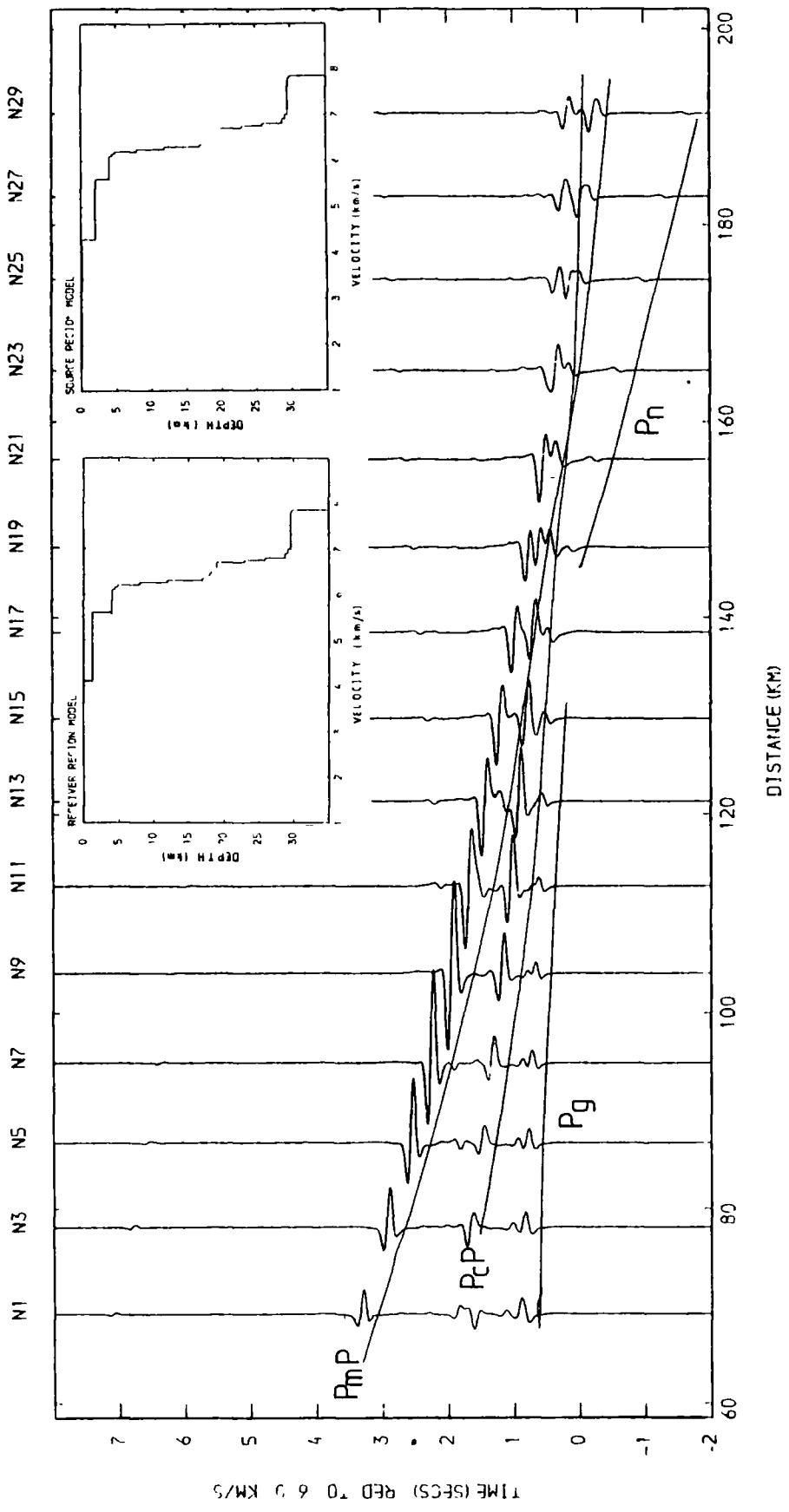


Fig 7.5 Synthetic seismogram of the North Sea shots recorded at S32

amplitude at a range of 80-90 km on common station section S54 (Fig. 7.4). The maximum amplitude for PcP varies between 100 km on common station section S40 (Fig. 7.3) and 140 km on common station section S19 (Fig. 7.1). It is difficult to account for these differences with lateral variations in the crustal structure alone. It is noticeable, however, that the change in character of PmP and PcP relates to the frequency of the trace, larger amplitude phases occurring where the frequency appears to be lower. This effect seems to be shot related and is investigated in more detail in section 7.4.

Despite difficulties modelling the amplitudes there is evidence of an increase in velocity from 6.2-6.3 km/s to 6.6-6.7 km/s at a depth of between 17 and 20 km, and a Moho at a depth of 30 km. There is little evidence, however, to indicate what the composition of the 6.6-6.7 km/s layer is and the position of the CSSP line to the south of the Caledonian Suture makes it difficult to extrapolate from Scotland where a few measurements are available. Smithson and Brown (1977) suggested that velocities of 6.6-7.0 km/s can be represented by intermediate granulites but without shear wave velocities or other evidence it is difficult to make any reliable estimates of the composition of the middle and lower crust.

7.3 Interpretation of the Irish Sea shots

Arrivals from the middle and lower crust are not as large and

clear in the Irish Sea as they are in the North Sea (Figs. 5.15, 5.16, 7.6 and 7.7) and because many of the stations in the Carlisle to Spadeadam region were not recording properly there are also fewer good quality common station sections. The only persistent arrivals apart from Pg are PmP and Pn, although PmP is not as prominent in relation to Pn as it is in the North Sea. There is no clear evidence for PcP. On common station sections S30, S31 and S32 (Fig. 5.12 and Appendix A) PmP is a large amplitude arrival in the range 90 to 120 km and appears to pass into a lower crustal channel wave of apparent velocity 6.8-7.0 km/s beyond 150 km. An x^2-t^2 plot for S32 gives an average crustal velocity of 6.51 +/- 0.04 km/s and a Moho depth of 33.5 +/- 0.8 km (Table 7.2). The increasing Pg time-terms from M25 to M7 (see section 6.2), however, suggest that the average crustal velocity and Moho depth calculated from the wide-angle reflections recorded at S32 are probably overestimates. Using the method of Holder and Bott (1971) on common stations S15 (Fig. 7.6) and S19 (Fig. 7.7) velocities of 6.30 km/s and 6.25 km/s and depths of 29.8 km and 29.4 km respectively were determined (Table 7.2). It is not possible to use this method for stations west of S25 because the critical distance does not appear on these sections, or for stations east of S10 because Pn is absent.

The synthetic seismogram model has no mid-crustal discontinuity but does have an increase in velocity to 6.8-7.0 km/s at a depth of about 25-26 km (Fig. 7.8). This is required to fit the observed velocity of PmP beyond 150 km and to obtain the correct

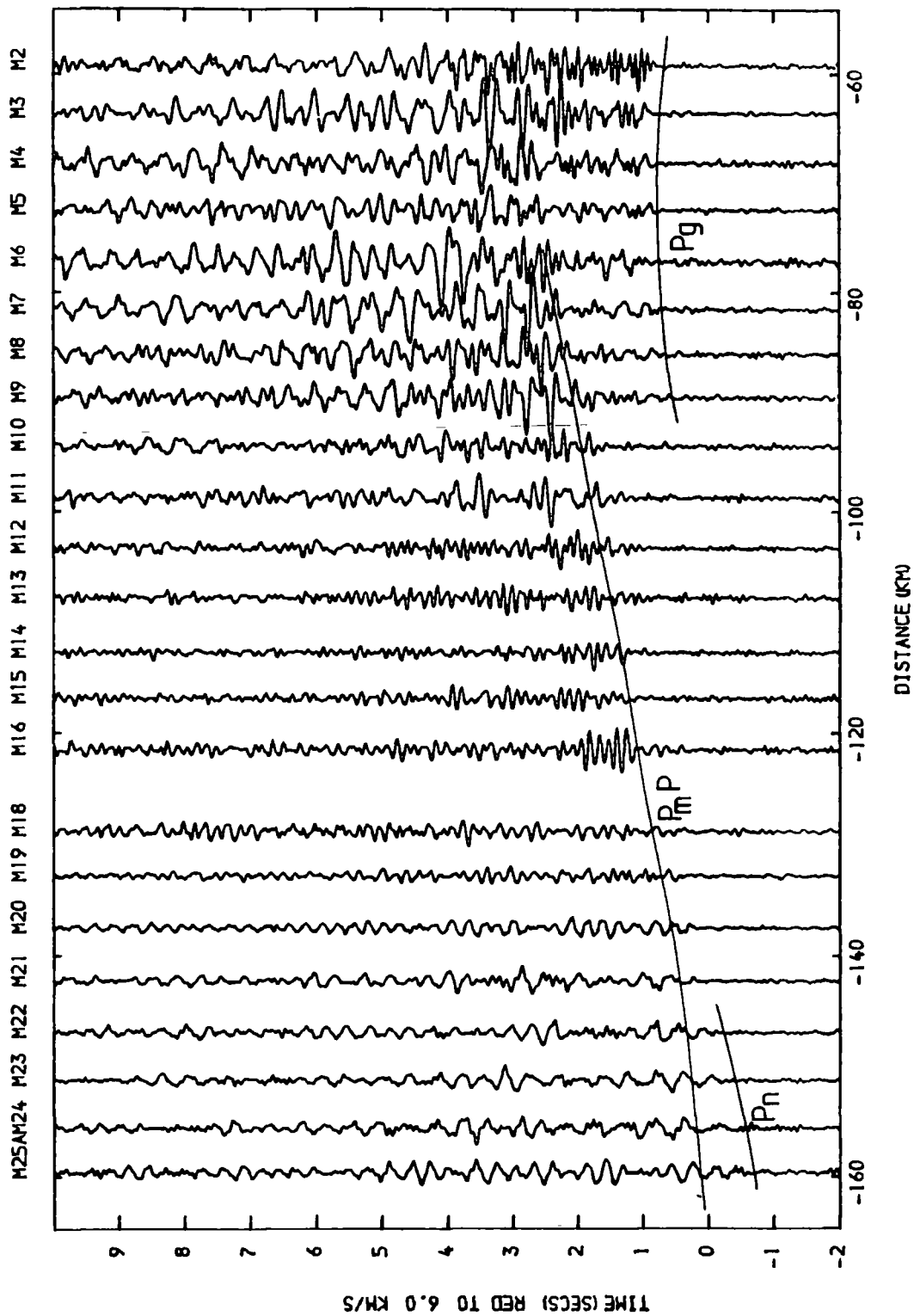


Fig 7.6 Reduced section of the Irish Sea shots recorded at S15. Filtered 2-12 Hz, amplitudes uncorrected.

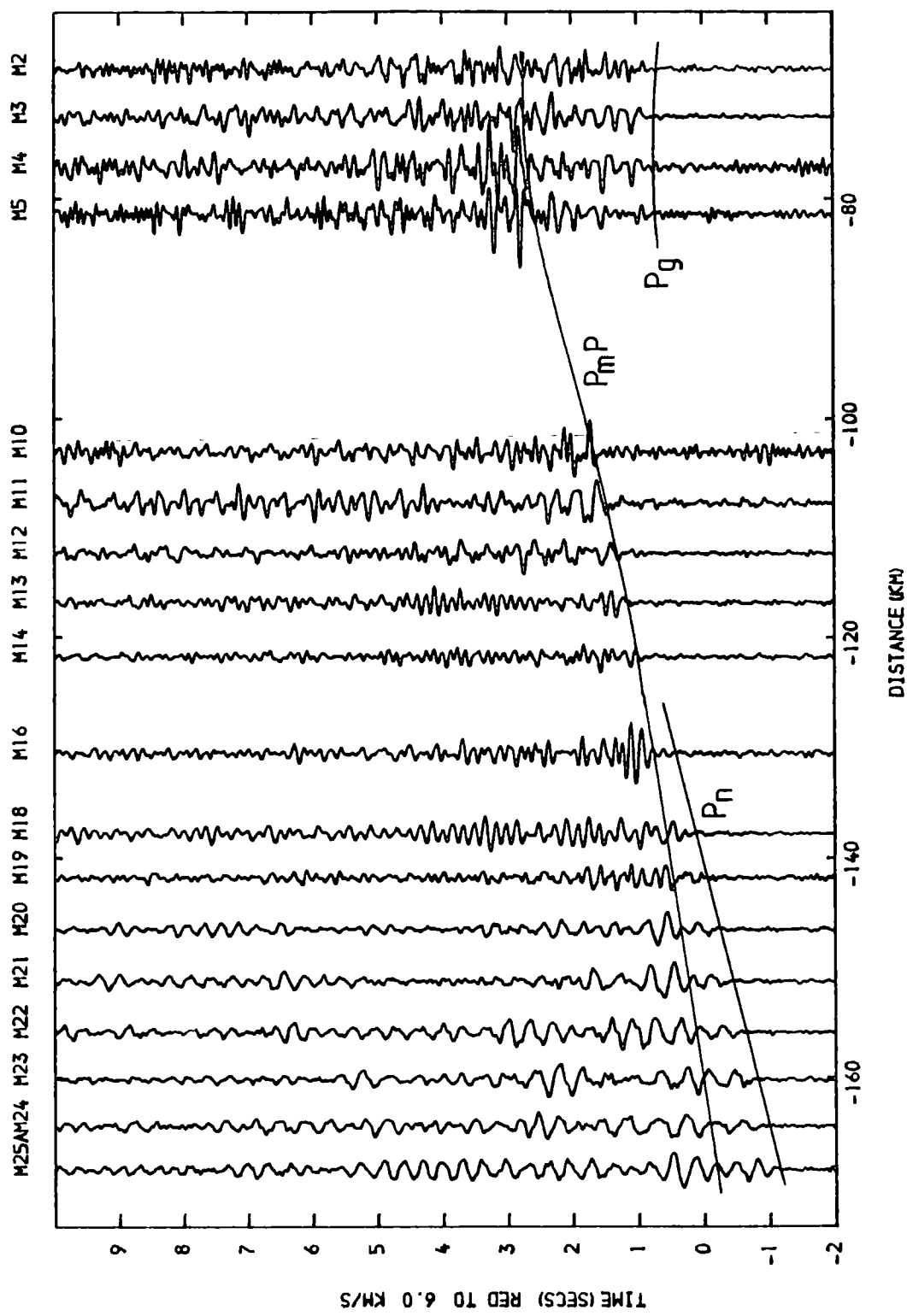


Fig 7.7 Reduced section of the Irish Sea shots recorded at S19.
 Filtered 2-12 Hz, amplitudes uncorrected

TABLE 7.2

Analysis of lower crustal reflections of the Irish Sea.

A) Depth to Moho, Pn velocity and mean crustal velocity from PmP using the method of Holder and Bott (1971).

Station	Pn velocity km/s	Mean crustal vel. km/s	Depth to Moho km
S15	7.85	6.30	29.8
S19	7.90	6.25	29.0

B) Depth to Moho and mean crustal velocity using X^2-T^2 method.

Station	Mean crustal vel. km/s	Err. 95%	Depth to Moho km	Err. 95%
S32	6.51	0.04	33.5	0.8

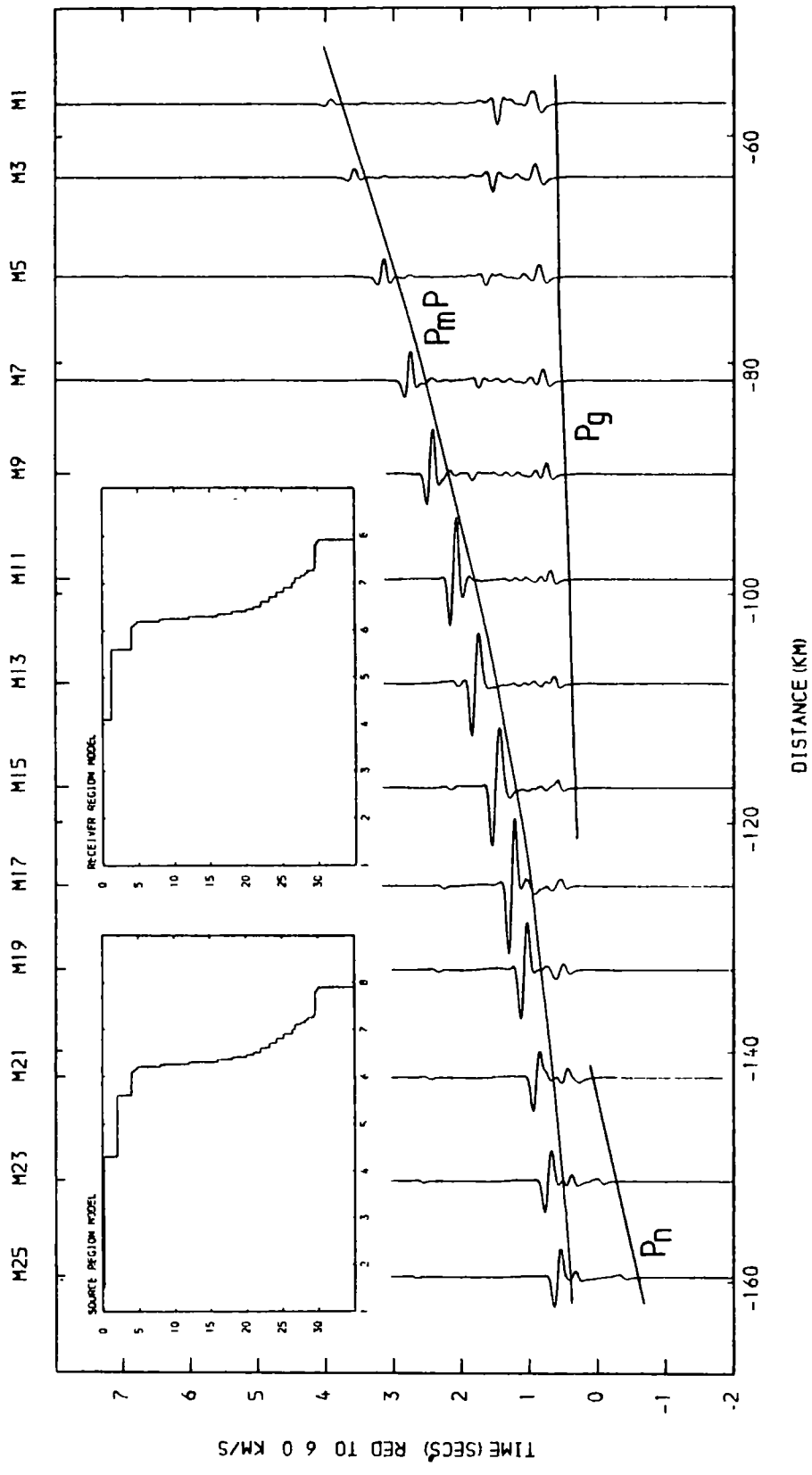


Fig 7.8 Synthetic seismogram of the Irish Sea shots recorded at S15

average crustal velocity. The model is designed to fit common station S15 (Fig. 7.7) and the fit with the travel times is good except in the range 60 to 80 km where delays caused by the Solway Basin are not taken into account. A comparison of the amplitudes, however, shows a rather poor agreement. Inspection of other common station sections reveals that the amplitude of PmP varies considerably from section to section. PmP is usually more prominent for shots M2 to M9 than for shots M11 to M16. These differences appear to relate to the frequency content of the shot in the same way as in the North Sea and will be discussed in the next section.

Despite difficulties modelling the amplitudes there appear to be different crustal structures beneath the Irish Sea and beneath the North Sea. The average crustal velocity beneath the Irish Sea is approximately 6.4 km/s and the depth to the Moho is about 29-30 km but there is no recognisable mid-crustal discontinuity and the velocity in the lower crust rises to around 7 km/s above the Moho. The higher velocity in the lower crust beneath the Irish Sea in comparison with the North Sea could indicate a more basic composition or higher metamorphic grade. Smithson and Brown (1977) suggested that velocities in excess of 7.0 km/s can represent pyroxene granulites while laboratory measurements by Hall and Simmons (1979) indicated that the lower crustal layer with a velocity of 7.0 km/s recorded by LISPB beneath Scotland can be interpreted as mafic garnet granulites gradational between gabbro and eclogite. Inclusions in volcanic rocks in the

Southern Uplands suggests rocks of predominantly gabbroic to dioritic character in the lower crust (Upton et al. 1983) but because of the Caledonian Suture it is difficult to extrapolate these measurements to the Irish Sea.

7.4 Shot characteristics

The frequency of an explosion at sea is determined largely by the gas bubble pulsation and the signal reverberation between the sea bottom and the sea surface (Burkhardt and Veas 1975, Jacob 1975). These two are dependent upon the water depth (h) and the charge weight (W). The charge weight applies to the weight of T.N.T. in kilogrammes. If a different explosive is used it is suggested by Jacob (1975) that the equivalent weight in T.N.T. should be determined. In the CSSP survey the explosive used was I.C.I. Geophex but it is not possible to relate this to T.N.T. in any simple way (D Kay I.C.I. pers. comm.). Despite this there is a broad similarity between the two, so for the purposes of this study they will be assumed to be equivalent.

The enhanced frequency F_a at the shot due to reverberation in the water column is given by

$$F_a = (2n-1)V_w/4h$$

where V_w is the velocity of sound in water, h is the depth of water and n is an integer.

Assuming that $V_w = 1490$ m/s, $n=1$ (higher orders of n relate to frequencies beyond the range of interest) and that h is measured in metres then

$$F_a = 372.5/h \text{ Hz}$$

If the weight of the explosives is given in kilogrammes then frequency F_b of the bubble pulsation is given by

$$F_b = (h+10)^{5/6}/CW^{1/3} \text{ Hz}$$

where $C=2.1 \text{ s m}^{5/6}\text{kg}^{-1/3}$ for T.N.T. (Burkhardt and Veis 1975). This formula assumes that the shot is suspended. All the CSSP shots were fired on the sea bottom and the formula is only a rough approximation in this situation.

The optimum depth for firing a shot occurs when the frequency of the bubble pulse and the reverberation are the same. This is given by

$$W = (h(h+10)^{5/6}/803)^3 \text{ kg}$$

where h is measured in metres. The optimum depths for the 150 kg and 450 kg shots are 90 m and 112 m respectively but most of the CSSP shots were fired at a depth shallower than this. A list of the bubble pulse and reverberation frequencies for all the shots is given in Tables 7.3 and 7.4.

In order to compare the theoretical frequency of the shots with the actual frequency, the amplitude spectra at a number of



TABLE 7.3

Reverberation frequency and bubble pulse frequency for the Irish Sea shots.

Shot	Depth(m)	Reverberation Frequency (Hz)	Bubble Pulse Frequency (Hz)
M1	33	11.3	2.1
M2	36	10.3	2.2
M3	42	8.8	2.4
M4	47	7.9	2.6
M5	55	6.8	2.9
M6	60	6.2	3.1
M7	64	5.8	3.2
M8	65	5.7	3.2
M9	63	5.9	3.2
M10	56	6.7	2.9
M11	67	5.6	3.3
M12	47	7.9	2.6
M13	55	6.8	2.9
M14	55	6.8	2.9
M15	63	5.9	3.2
M16	59	6.3	3.1
M17	53	7.0	2.8
M18	70	5.3	3.5
M19	61	6.1	3.1
M20	95	3.9	4.3
M21	139	2.7	5.8
M22	134	2.8	6.3
M23	134	2.8	6.3
M24	133	2.8	6.3
M25A	97	3.8	4.4
M25B	96	3.9	3.0
I1A	57	6.5	2.9
I2A	37	10.1	2.2
I3A	34	11.0	2.1
I4A	36	10.3	2.2
I5A	31	12.0	2.0
I1B	57	6.5	2.9
I2B	38	9.8	2.2
I3B	33	11.3	2.1
I4B	35	10.7	2.1
I5B	30	12.4	1.9

TABLE 7.4

Reverberation frequency and bubble pulse frequency for the North
Sea shots

Shot	Depth(m)	Reverberation Frequency (Hz)	Bubble Pulse Frequency (Hz)
N1	51	7.3	2.8
N2	61	6.1	3.1
N3	64	5.8	3.2
N4	74	5.0	3.6
N5	81	4.6	3.8
N6	97	3.8	4.4
N7	100	3.7	4.5
N8	100	3.7	4.5
N9	105	3.6	4.7
N10	105	3.6	4.7
N11	100	3.7	4.5
N12	100	3.7	4.5
N13	98	3.8	4.4
N14	93	4.0	4.3
N15	75	4.9	3.6
N16	73	5.1	3.6
N17	68	5.5	3.3
N18	69	5.4	3.3
N19	74	5.0	3.6
N20	76	4.9	3.6
N21	84	4.4	4.0
N22	82	4.5	3.9
N23A	82	4.5	3.9
N24	79	4.7	3.8
N25	72	5.2	3.5
N26	72	5.2	3.5
N27	74	5.0	3.6
N28	81	4.6	3.9
N29	85	4.4	4.0
N23B	85	4.4	2.8

stations were determined. Approximately 5 s of each trace was Fourier transformed starting in front of the first arrival. Because of the large amount of data involved it is convenient to present the results in the form of frequency contour plots (Figs. 7.9 to 7.14). The values of the contours are not important as it is the change in frequency from shot to shot that is significant. Superimposed upon the contour plots are the calculated bubble pulse and reverberation frequencies for each shot.

Contour plots for the Irish Sea shots at stations S1, S8, S30 and S32 are shown in Figs. 7.9, 7.10, 7.11, and 7.12. The similarity between the four plots shows that the variations in the observed frequencies are related to shot effects. Comparison with the reverberation frequency for each shot shows that this has the greatest effect on the shot frequency. M20 to M25 have a dominant frequency of between 2.5 and 4 Hz which increases to between 6 and 8 Hz for the remaining shots. For M2 to M9 there is also a good correlation with the bubble pulse frequency of 2 to 3 Hz, but there is no such match for the other shots. A survey of the sea floor sediments by Wright et al. (1971) shows that the sediments change from clay and sand under M1 to M9 to gravel for shots further west and it is possible that this affects the formation of the bubble pulse.

In the previous section it was seen that few coherent large amplitude arrivals appear to be visible on recordings of Irish Sea shots M10 to M15 (Fig 7.6 and 7.7). It is now seen that this

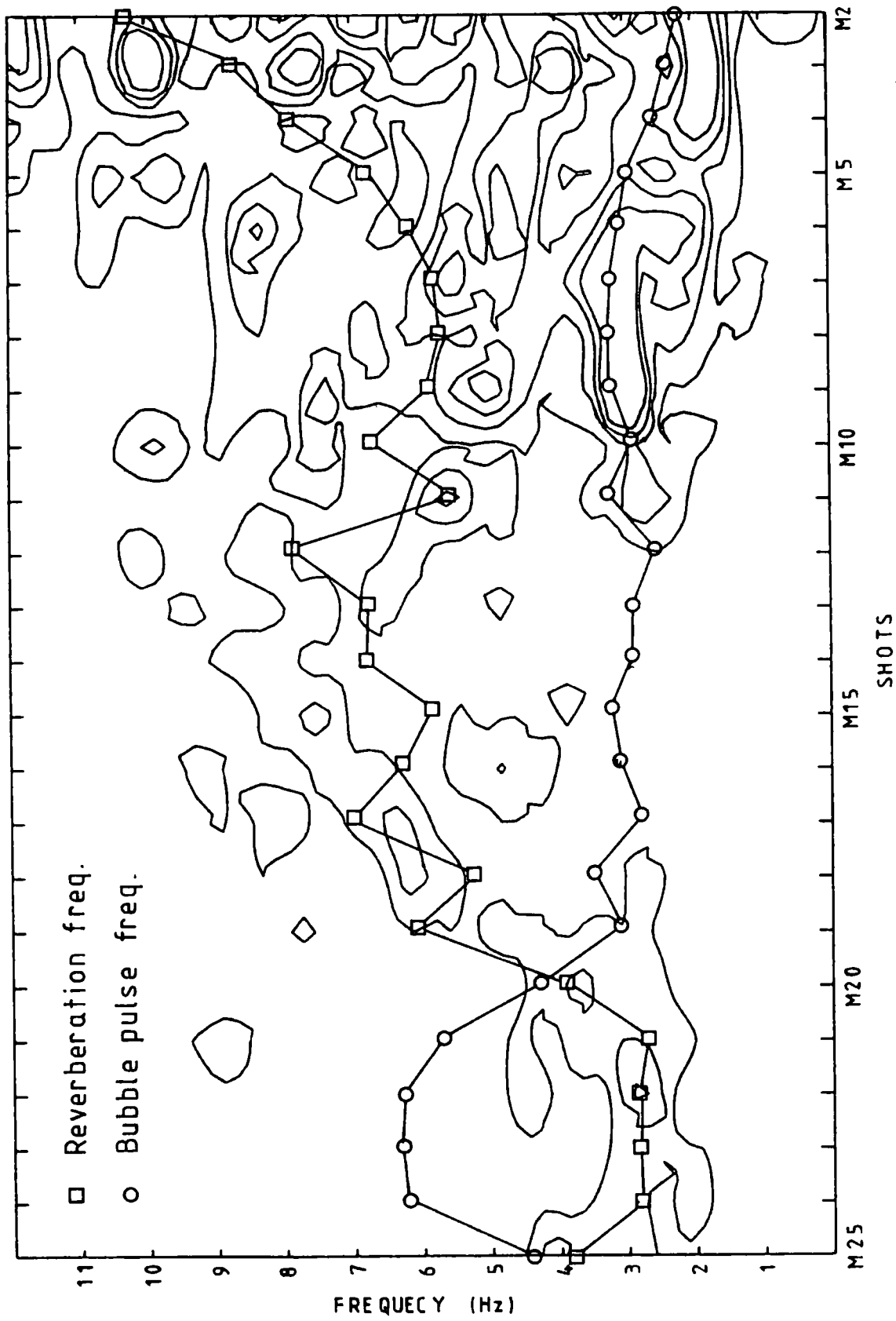


Fig 7.9 Frequency contour plot of Irish Sea shots at S1

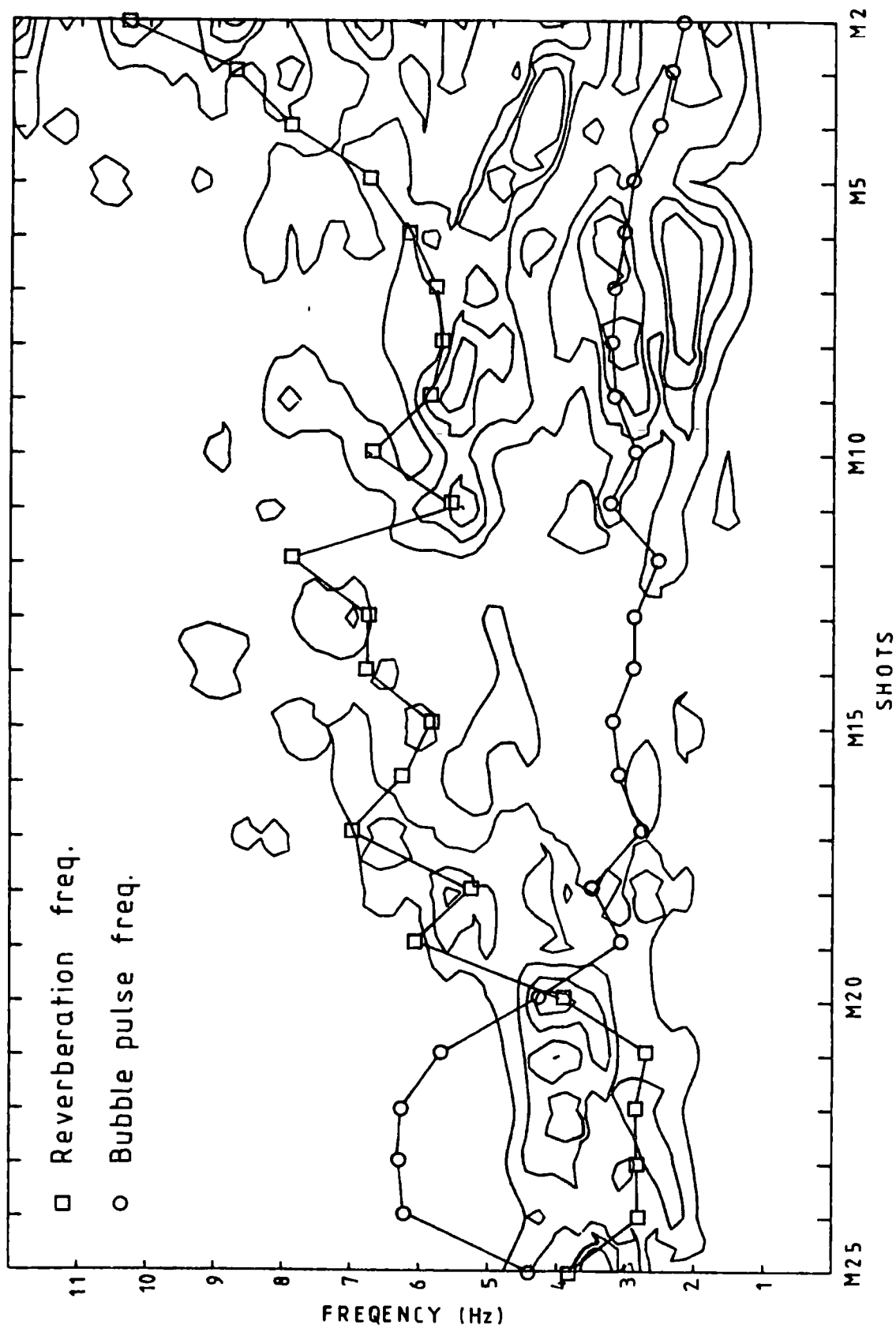


Fig 7.10 Frequency contour plot of Irish Sea shots at S8

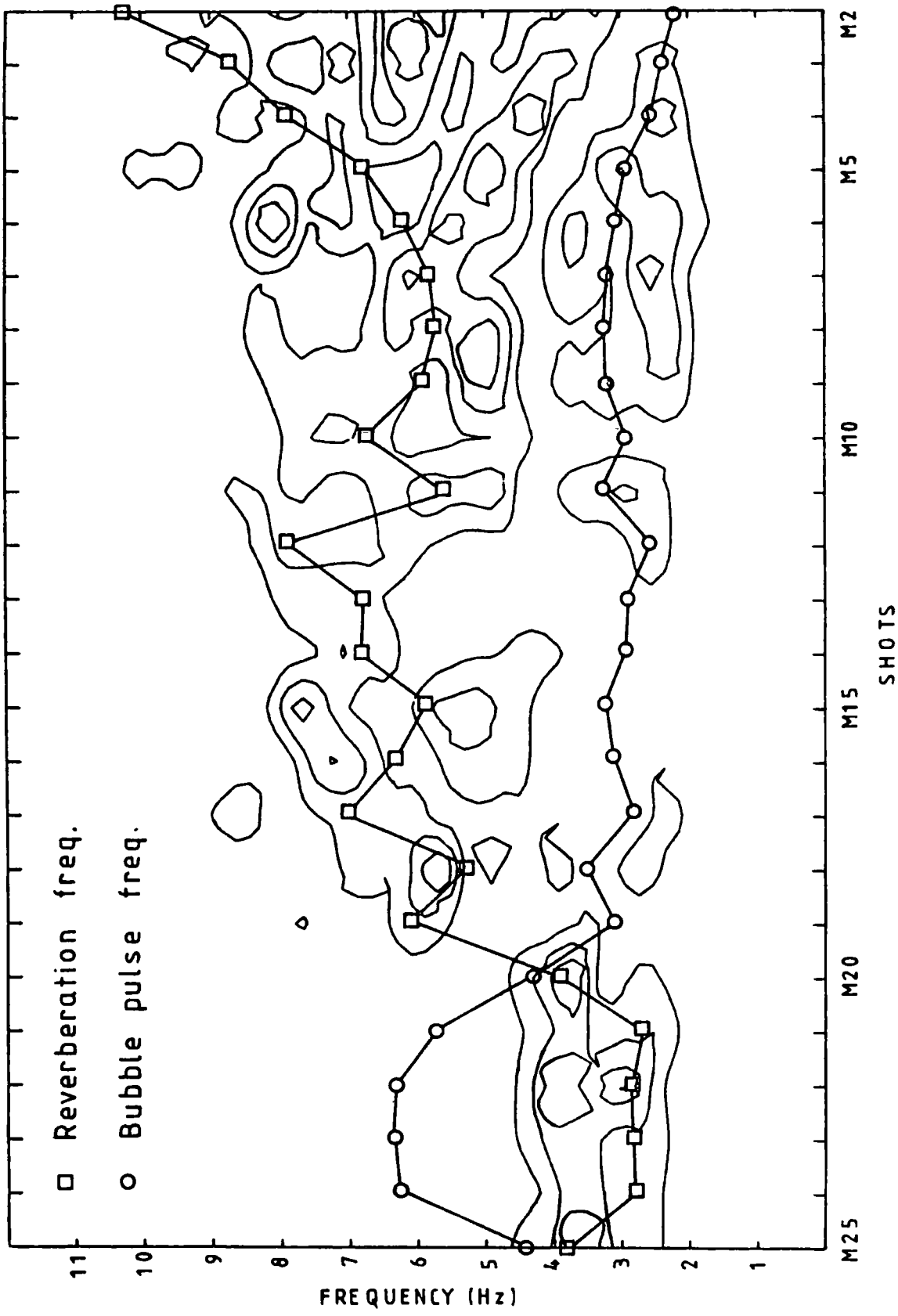


Fig 7.11 Frequency contour plot of Irish Sea shots at S30

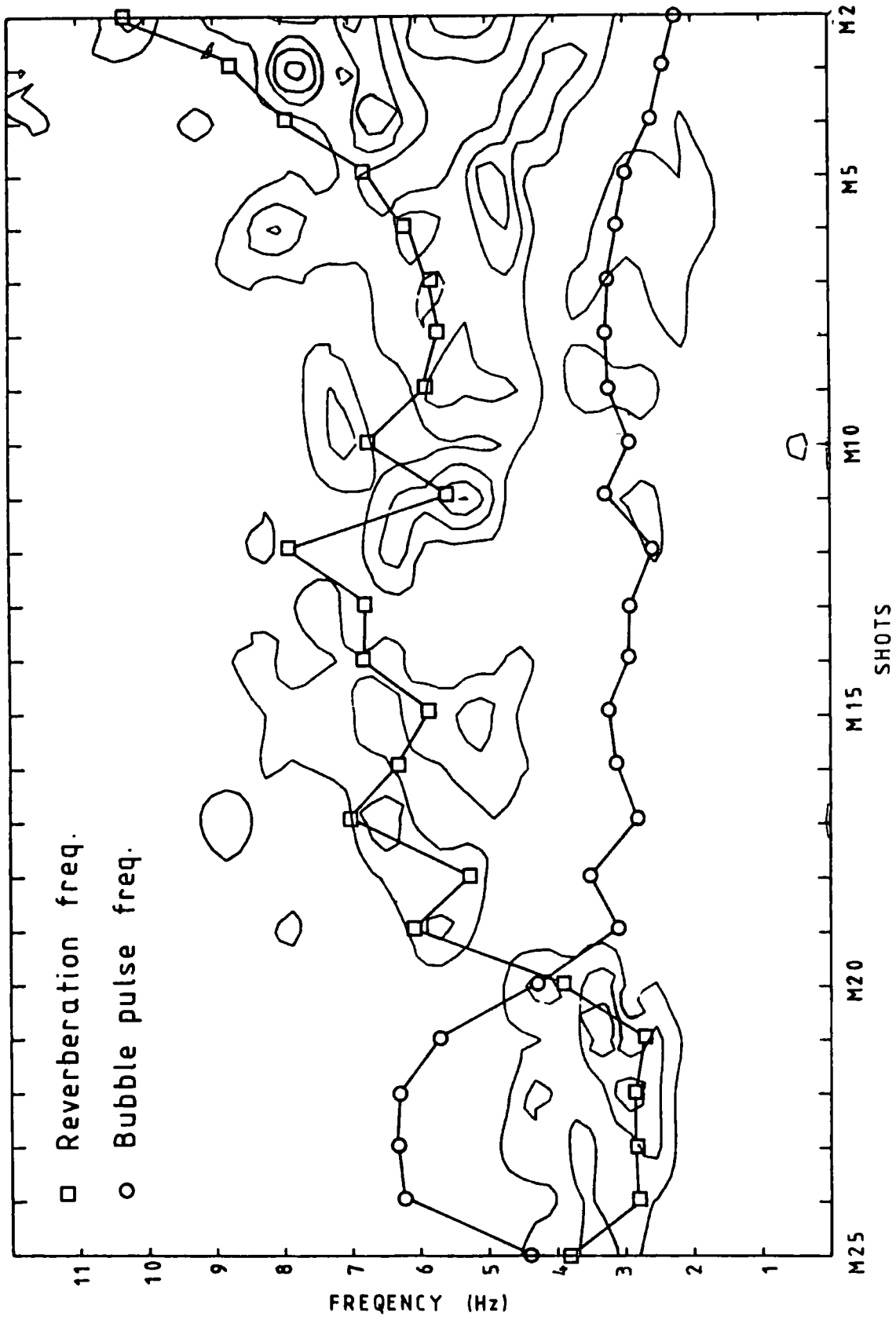


Fig 7.12 Frequency contour plot of Irish Sea shots at S32

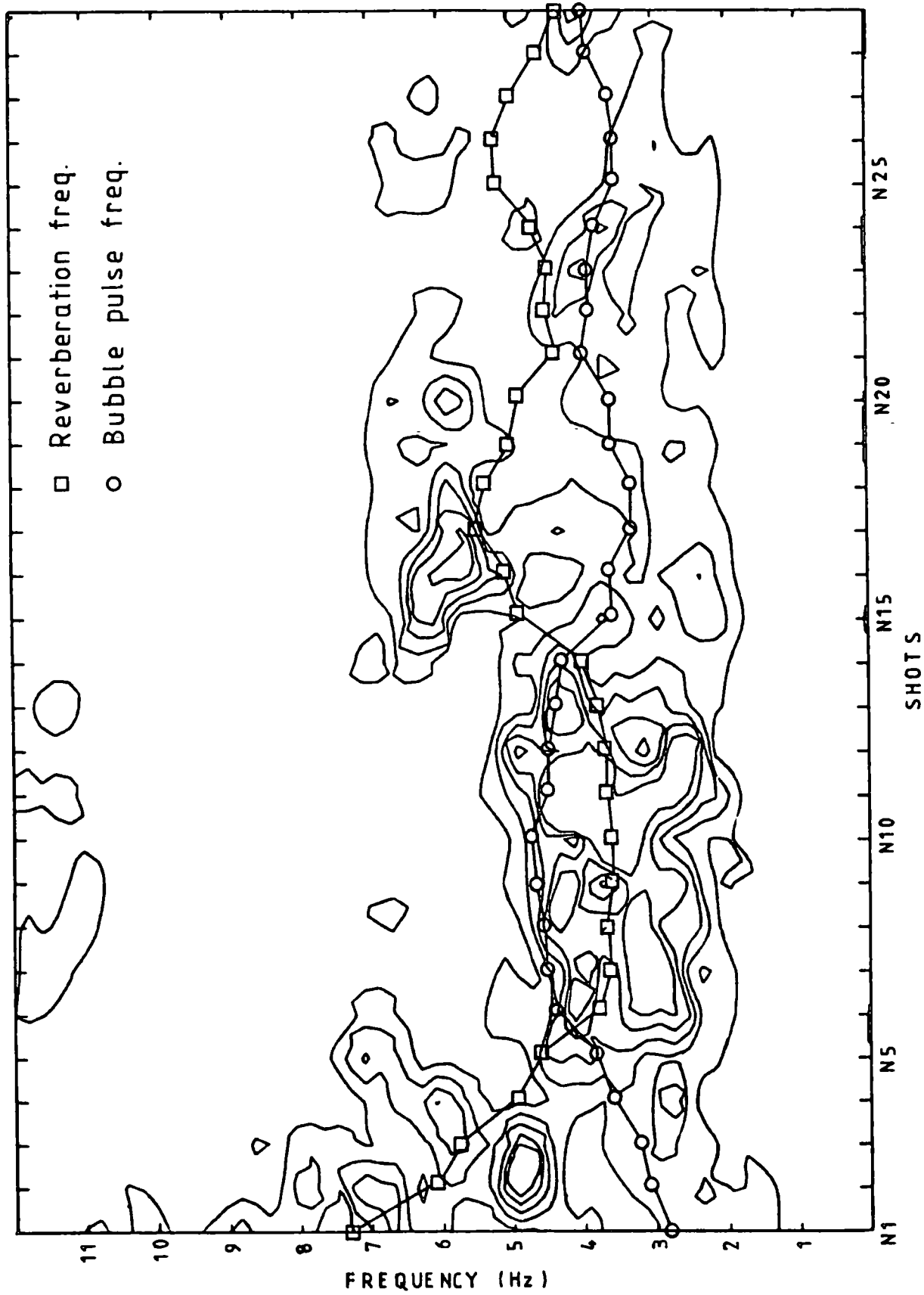


Fig 7.13 Frequency contour plot of North Sea shots recorded at S40

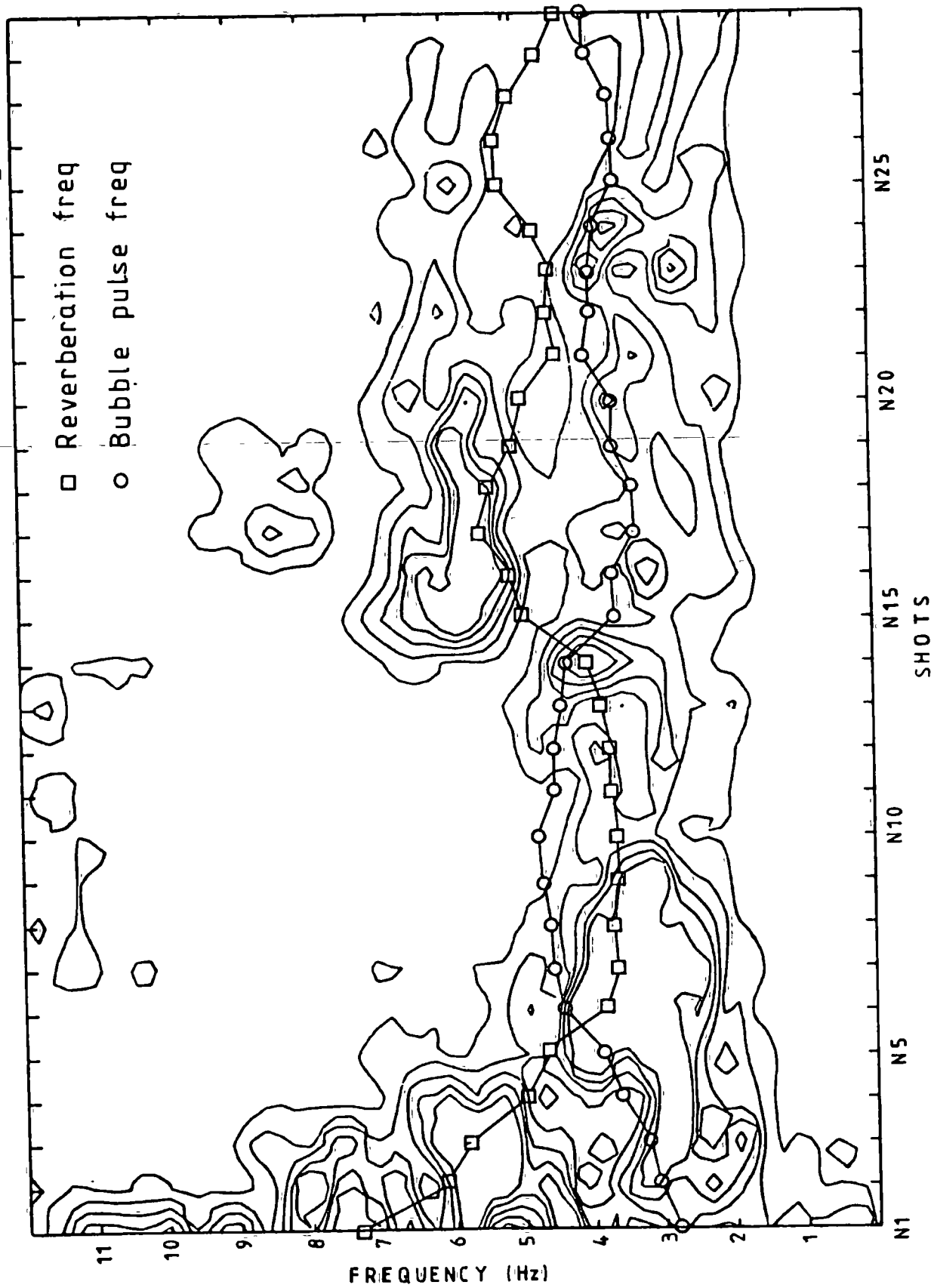


Fig 7.14 Frequency contour plot of North Sea shots recorded at S53

is the region in which the dominant shot frequency is above 6 Hz (Figs 7.9, 7.10, 7.11 and 7.12), the traces with larger amplitude and more coherent arrivals (M20 to M25) are characterised by lower frequencies of less than 4 Hz.

In the North Sea the shots generally show a narrower range of frequencies than in the Irish Sea (Figs 7.13 and 7.14) but the correlation between the reverberation frequency and the seismogram frequency is still good. Shots N6 to N14 are near their optimum depth and show a considerable amount of energy between 3 and 4 Hz. For shots N15 to N19 the frequency rises to between 5 and 6 Hz, although there is a small contribution at 2 to 3 Hz attributed to the bubble pulse. From N20 to N24 the shots are close to their optimum depth and the shot frequency is about 4 Hz.

These variations in the frequency of the North Sea shots relate closely to the character of the arrivals. At station S40 PmP is at a maximum at a range of 95 km at shot N11 (Fig. 7.3) and has a frequency of 4 Hz. At stations S19 and S56 (Figs. 7.1 and 7.5) PmP is almost unidentifiable at a range of 95 km, but the shots (N1 and N19) have higher dominant frequencies than N11 of 7 Hz and 6 Hz respectively. The range at which PcP has its maximum amplitude varies from 95 km at S40 (Fig. 7.3) to 140 km at S19 (Fig. 7.1), but whatever the range it invariably occurs between N6 and N14 or between N20 and N22, which are all shots with dominant frequencies of about 4 Hz.

There are two major implications of the above results. The first concerns the modelling of the amplitude characteristics of a common station seismogram. The amplitude characteristics of wide-angle reflections and head waves can be modelled by the introduction of velocity gradients above and below the interface. This is because they are usually neither true reflections nor head waves but diving rays turned within the velocity gradient. This suggests that because of the apparent variation in amplitude with shot frequency the modelling of the amplitudes of common station sections to determine the structure of velocity gradients at boundaries is unlikely to produce accurate results unless the explosions have been very carefully matched. The work of Burkhardt and Vees (1975) and Jacob (1975) has shown how the amplitude and frequency of a shot are determined by its size and depth of firing, but the significance of these variations in the interpretation of crustal seismic surveys appears not to be fully appreciated. Common station surveys with shots of different sizes are still often modelled for the amplitude characteristics, e.g. Wood and Barton 1983. This effect, however, is not a serious problem for common shot sections.

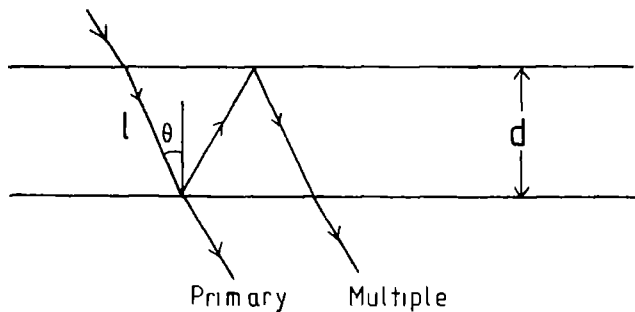
The second implication affects both common station and common shot sections. It appears that in certain circumstances the phases may be so reduced in amplitude as to be almost unidentifiable from the noise. This can be seen from the absence of PmP at a range of 90 km on common station record S8 for the

Irish Sea shots (Fig. 5.11) and its absence from 90 to 100 km on common station section S56 for the North Sea shots (Appendix A). It appears only to require a change from 4 Hz to 6 Hz to cause significant differences in amplitude.

This problem which makes it difficult to model the amplitudes of seismograms nevertheless provides important evidence on how the transmission characteristics of the crust depend upon frequency. There are three effects of possible significance and these are interference effects, anelastic losses and scattering.

7.5 Interference effects

Where the ground is layered it is possible to have multiple reflections within the layers which may constructively or destructively interfere with the primary wave. Consider a layer of uniform thickness



where d is the layer thickness, θ is the angle of incidence on the lower boundary and l is the path length of the primary wave through the layer.

Constructive interference between the primary and multiple

reflection occurs when

$$2l = n\lambda$$

and destructive interference occurs when

$$2l = (n+1/2)\lambda$$

where λ is the wavelength of the signal and n is an integer. It does not matter whether the velocities of the layers are increasing or decreasing or if high or low velocity layers are considered.

If an average velocity of 6.5 km/s is considered the equations for constructive and destructive interference become

$$2l = n6.5/f \text{ km} \quad \text{and} \quad 2l = 6.5(n+1/2)/f \text{ km}$$

respectively, where f is the frequency in Hz and l is the path length in kilometres.

The CSSP data shows high amplitude PmP and PcP phases for shot frequencies of about 4 Hz. If it is assumed that the high amplitude is caused by constructive interference in a layered crust then the path length through one of the layers would need to be 0.81 km. If it is also assumed that amplitude PmP has a maximum amplitude close to the critical distance then the angle of incidence would be approximately 50° to 60° suggesting a layer thickness of about 0.5 km. For the same layer thickness and angle of incidence constructive interference would also occur for frequencies of 8 Hz, 12 Hz, 16 Hz, etc, while destructive interference would occur for frequencies of 6 Hz, 10 Hz, 14Hz, etc.

Constructive interference, and hence large amplitudes, for signals with a dominant frequency of 4 Hz, and destructive interference, and hence small amplitudes, for signals with a dominant frequency of 6 Hz correlates well with the CSSP data. In order to test this result a lower crust composed of layers 0.5 km thick was modelled using the synthetic seismogram program described in section 4.7.2. The layers alternate in velocity between 6.0 and 6.5 km/s (Fig. 7.15). The program was run five times with the same model but using wavelets of frequencies 2 Hz, 4 Hz, 6 Hz, 8 Hz and 10 Hz. No anelastic losses were included in the model.

The results are shown in Fig. 7.16. There is a decrease in amplitude with frequency but there is no indication of an increase in amplitude for the 4 Hz and 8 Hz wavelets or a decrease in amplitude for the 6 Hz or 10 Hz wavelets. A possible explanation for the absence of any interference effects is that the reflection coefficients at the boundaries are too small for significant amounts of energy to be carried by the multiple reflection. The reflection coefficients calculated for the boundaries in the synthetic seismogram model indicate that less than 0.6% of the energy would pass into the first multiple.

7.6 Anelastic losses

Seismic energy can be lost in an anelastic medium because of

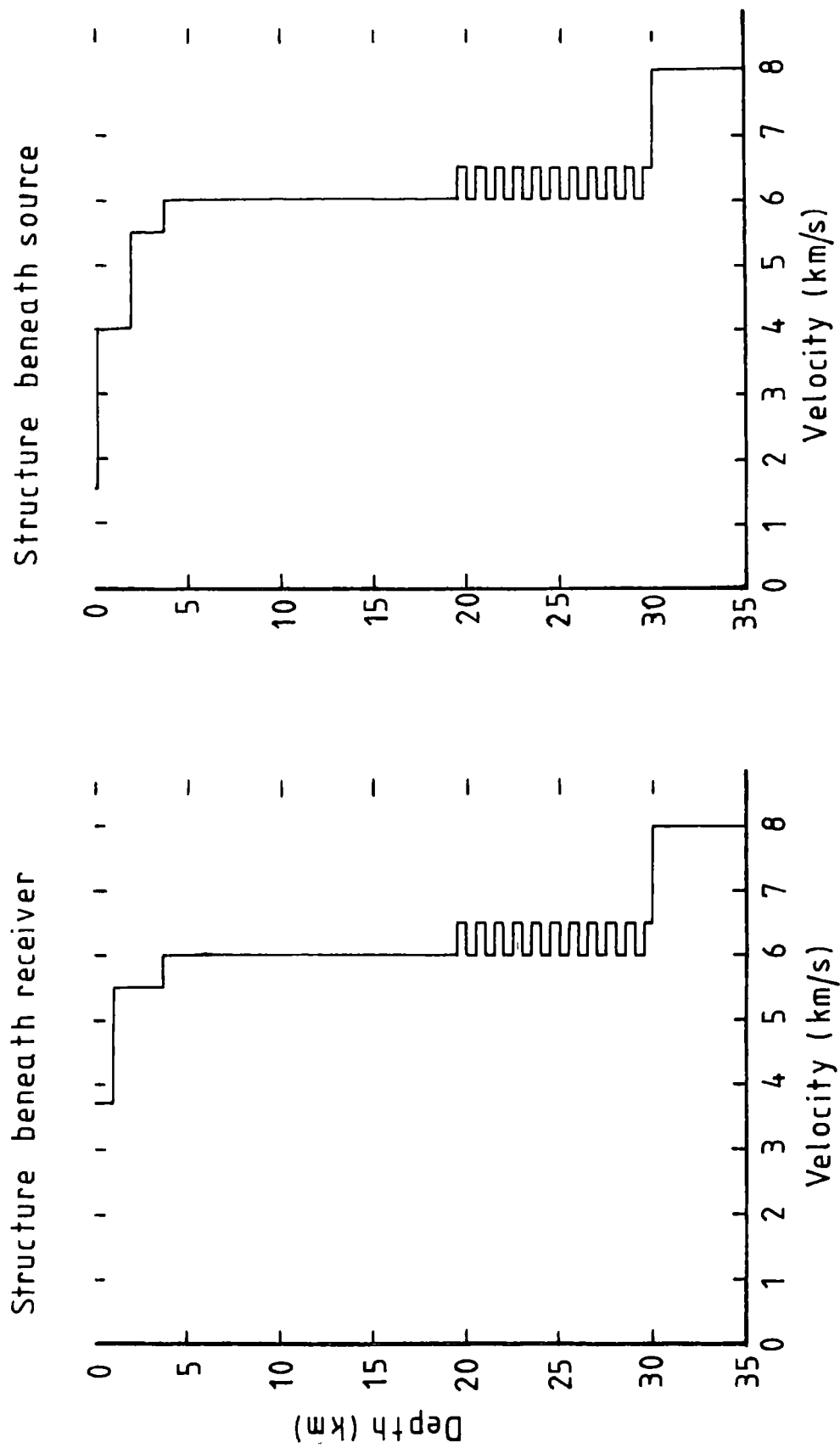


Fig 7.15 Seismic model used in the investigation of interference effects (see Fig 7.16)

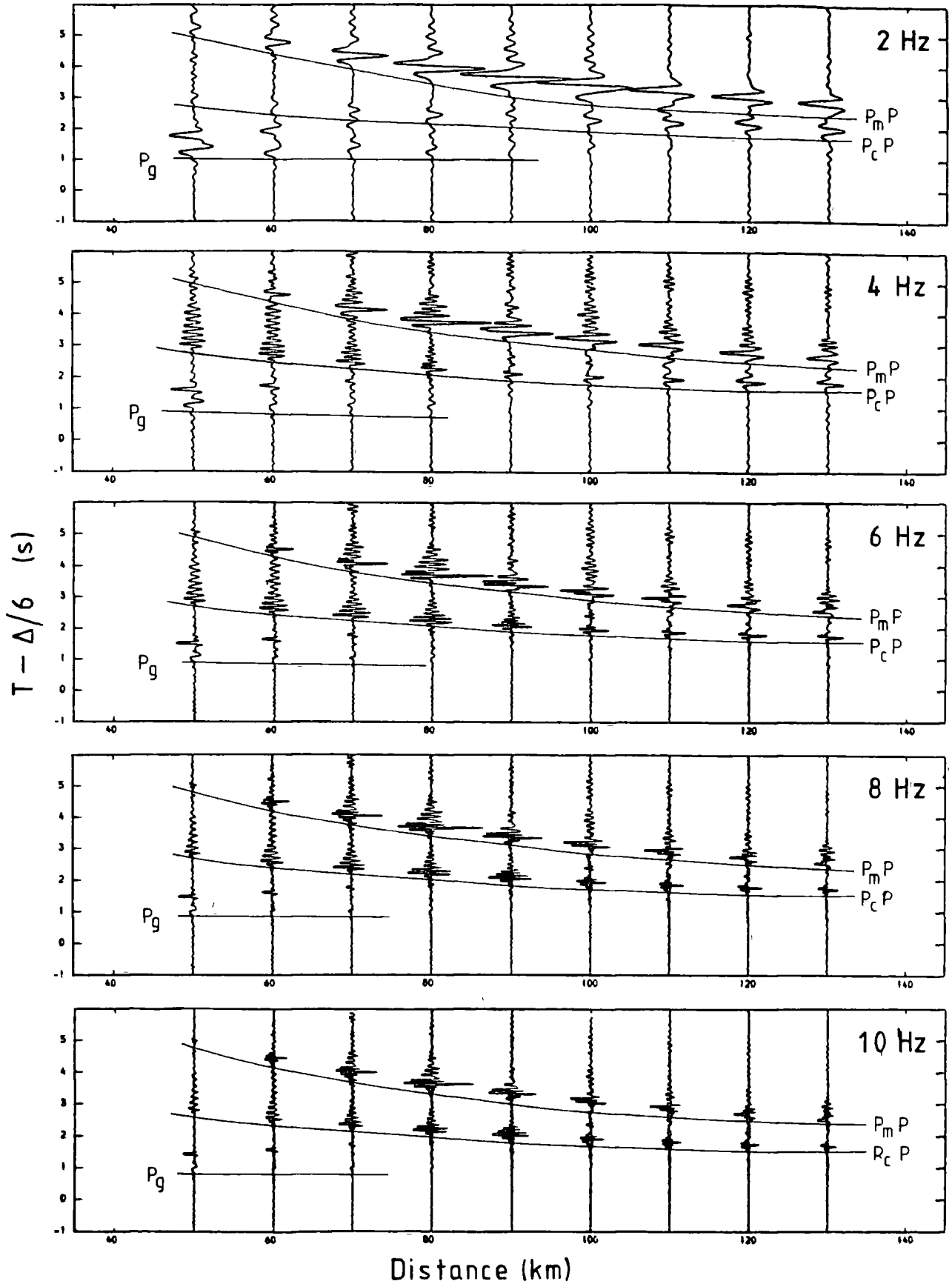


Fig 7.16 Synthetic seismograms of crustal model with a lower crust consisting of layers 0.5 km thick (see Fig 7.15) used to investigate interference effects. Source wavelets of 2Hz, 4Hz, 6Hz, 8Hz and 10Hz.

internal friction. For any medium these losses can be described by the frequency dependent attenuation coefficient, α . It is usual, however, to use the dimensionless quantity factor Q which is approximately independent of frequency and related to α by

$$Q = \pi f / c \alpha$$

where f = frequency and c = group velocity.

The reduction in amplitude of a seismic wave of wavelength λ , due to anelastic losses can be determined from Q by

$$A = A_0 \exp(-\pi x / \lambda Q)$$

where A_0 = initial amplitude and A = final amplitude.

and x = distance travelled by the wave

Q is well defined for the mantle but there are few reliable crustal values. Clowes and Kanasewich (1970) determined a value of Q of 1500 for the crystalline basement and suggested that it probably increases in the lower crust. Using a value of Q of 1500 it is possible to determine the relative decrease in amplitude likely for the CSSP shots. Comparing signals with frequencies of 3 Hz and 6 Hz (wavelengths of just over 2 km and 1 km respectively) travelling over a distance of 100 km suggests that the amplitude of the 6 Hz signal will be only 10% less than the 3 Hz signal. If a smaller Q of 1000 is assumed the difference between the two signals increases to 14%. Unless there are exceptionally low values of Q within the crust beneath the CSSP

profile, anelastic losses cannot explain its frequency dependent transmission characteristics.

7.7 Scattering

Scattering problems are best classified on a ka - kL diagram (Fig. 7.17) where ka is the wavenumber times the correlation distance, or inhomogeneity scale length, and kL is the wavenumber times the distance travelled through the medium (Aki and Richards 1980). It is important that the parameter a is understood.

Consider a three dimensional medium in which the velocity varies in all directions. The spatial fluctuations of slowness, $-\delta c/c_0$, can be described by its autocorrelation function, where the normalised autocorrelation function is defined by

$$N(r) = \langle u(r')u(r'+r) \rangle / \langle u^2 \rangle$$

and $u = -\delta c/c_0$. The velocity variations of the medium can be described statistically by $N(r)$. In the construction of Fig. 7.17 the cases $N(r) = \exp(-|r|/a)$ and $N(r) = \exp(-|r|^2/a^2)$ were used in the determination of the fractional energy loss, $\Delta I/I$, assuming a RMS velocity perturbation of 10% (Aki and Richards 1980). From this a becomes a measure of the inhomogeneity scale length, a sort of average wavelength for the velocity variations.

Scattering is negligible for both very small and very large values of ka (Fig. 7.17). Very small values of ka occur for

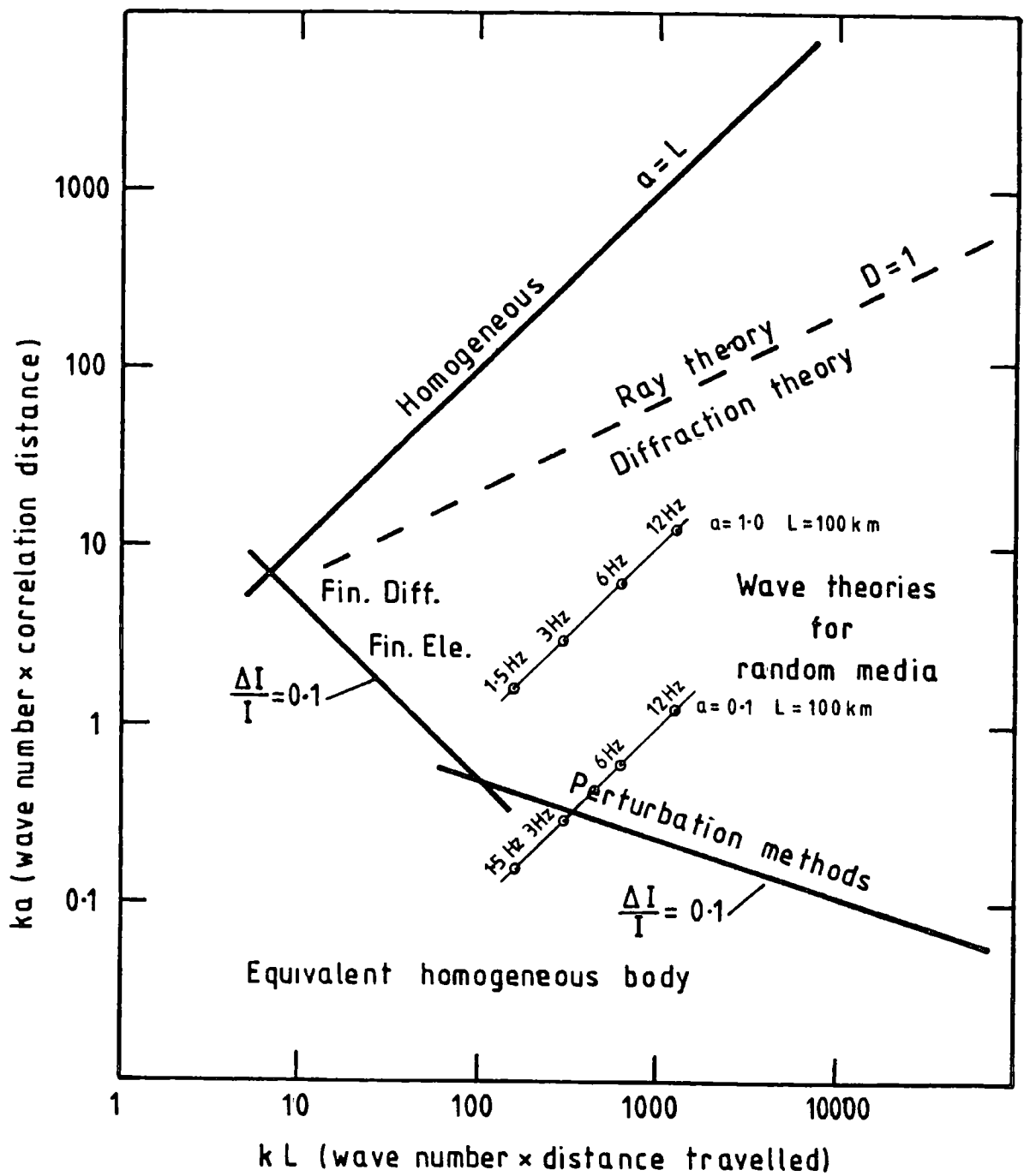


Fig 7.17 Classification of scattering problems and applicable methods (from Aki and Richards 1980)

scattering of seismic waves by individual crystals in a rock and large values of ka occur when seismic waves are scattered by bodies of continental size. In these situations the media are either effectively homogeneous or piecewise homogeneous. In between these two extremes scattering of energy can be a significant process. The various methods used to solve scattering problems (Fig. 7.17) are reviewed by Aki and Richards (1980).

It is of interest to discover where data from the CSSP project falls on the scattering diagram (Fig. 7.17). The points on Fig. 7.16 have been calculated for frequencies of 12 to 1.5 Hz (wavelengths of approximately 0.5 km to 4.0 km), a distance L of 100 km, corresponding to the range at which PmP and PcP are prominent, and inhomogeneity scale lengths of 0.1 km and 1.0 km. For $a = 1.0$ km all the points lie within the region where scattering is significant (Fig. 7.17), whereas when $a = 0.1$ km the frequencies below 3 to 4 Hz lie outside the area where scattering is important while higher frequencies lie inside. There is evidence to indicate that for layered half spaces containing random inhomogeneities scattering increases with the third power of the frequency (Malin 1980). This suggests that doubling the frequency from 3 Hz to 6 Hz would involve an 8 fold increase in the scattering. Scattering would appear to provide a more satisfactory explanation for the decrease in amplitude with increasing frequency than either anelastic losses or interference effects.

7.8 Summary

The middle and lower crust beneath the CSSP line shows the following characteristics.

(1) The crust beneath the Northumberland Trough and North Sea has an estimated mean crustal velocity of 6.35-6.4 km/s, a thickness of about 30 km and a sub-Moho velocity of about 7.9 km/s. There is also a mid-crustal discontinuity or velocity gradient where the velocity increases from about 6.3 to 6.6 km/s at a depth of approximately 19 km.

(2) The crust beneath the north Irish Sea and Carlisle region is less well defined than in the North Sea but appears to have an average velocity of about 6.4 km/s, a thickness of approximately 30 km and a sub-Moho velocity of about 7.9 km/s. No mid-crustal discontinuity or gradient has been recognised but the velocity increases to a velocity of 7 km/s at a depth of about 25 km.

(3) The crust under the whole CSSP line shows frequency dependent transmission characteristics. Crustal phases with frequencies of 4 Hz or less appear to have larger amplitudes than phases with a frequency of 5 Hz or more. This can be explained in part by scattering caused by inhomogeneities with a size of a few tens of metres to two hundred metres.

The points made in this summary are based on a preliminary interpretation. A full two-dimensional interpretation of the deep structure is being undertaken by A. H. J. Lewis.

CHAPTER 8 - SUMMARY AND CONCLUDING REMARKS

8.1 Summary

An outline of the current state of the understanding of the structure beneath northern England and adjacent marine areas has been given in Chapter 1. Results from the CSSP profile have been presented which improve upon this understanding. A summary of these results follows.

(1) Analysis of the first arrivals at short range define an Upper Palaeozoic and Mesozoic sequence (3.6-4.8 km/s) underlain by Lower Palaeozoic rocks (5.5-5.7 km/s) at a depth of 0.5 to 3.0 km. Beyond a range of 30 km the upper crustal phase Pg with a velocity of 6.15 km/s can be recognised along the whole profile except in the north-east where it dies out abruptly. This 6.15 km/s refractor is at a depth of approximately 4 km and identified as probably Precambrian crystalline basement possibly from south of the Iapetus Suture.

(2) Beneath the Northumberland Trough and Mid North Sea High prominent wide-angle reflections/diving waves were recorded from the Moho and a mid-crustal discontinuity or velocity gradient. The mid-crustal discontinuity or velocity gradient is at a depth of 17-20 km where the velocity increases from 6.2-6.3 km/s to 6.6-6.7 km/s. The Moho is at a depth of 30 km and the velocity beneath the Moho is about 7.9 km/s.

(3) Beneath the north Irish Sea and Carlisle Basin wide-angle reflections/diving waves from the Moho have been recognised. They indicate an average crustal velocity, including the sediments, of about 6.3-6.4 km/s and a Moho depth of 29-30 km. There is no evidence for a mid-crustal discontinuity or velocity gradient although the velocity increases at a depth of about 25-27 km to 6.8-7.0 km/s. The apparent velocity beneath the Moho is about 7.9 km/s.

(4) The crust beneath the CSSP profile appears to exhibit frequency dependent transmission characteristics. Crustal reflections and diving waves are most conspicuously developed for the shots in deeper water which have significant energy in the 2-5 Hz band. Energy above 6 Hz, from shots in shallower water, is believed to be scattered by inhomogeneities within the crust with of size of a few tens of metres to two hundred metres.

In section 1.10 several specific questions were put which it was hoped would be answered by the CSSP profile. Several of these questions have already been answered in the above summary, the remaining questions will be discussed below.

(1) There is no evidence for the presence of a low velocity zone in the upper crust under any part of the profile. The CSSP profile has demonstrated the importance of having closely spaced shots and stations and how they can be used to distinguish

between the effects of lateral and vertical variations in velocity.

(2) There is no evidence for the existence of oceanic crust from the Iapetus Ocean beneath the CSSP profile. Despite the variation in crustal structure between the North and Irish Seas both structures are of recognisable continental type (Belousov and Pavlenkova 1984).

8.2 Further work on the CSSP data

The Caledonian Suture Seismic Project collected a large amount of good quality seismic data. It has been possible to examine only a limited amount of the data in this study and it is suggested that the following work needs to be carried out on the remaining data.

(1) The airgun shots recorded at PUSS stations need to be digitised and analysed to provide better velocity control on the near surface sediments at sea.

(2) The airgun shots fired in the North Sea and recorded by the cassette recorders on the Northumberland coast need to be digitised and analysed. This will provide a better understanding of the shape of the Northumberland Trough.

(3) Shear waves recorded by three component seismometers need to be analysed to provide reliable estimates of Poisson's ratio.

This will lead to a better understanding of the composition of the crust.

(4) A more detailed investigation of the lateral variation in the mid and lower crust needs to be made using common offset and common mid-point sections. The transition between the lower crustal structure beneath the Northumberland Trough/North Sea and beneath the Carlisle Basin/north Irish Sea needs to be examined.

(5) Many of the CSSP shots were recorded by the UKAEA seismic array at Eskdalemuir. An investigation of this data will lead to a better understanding of how the structure changes to the north under the Southern Uplands.

8.3 Further work

It is clear from the previous section that there is still a considerable amount of information to be gained from the CSSP data. This study, however, has posed some questions that are best answered by further surveys. The most interesting question raised is whether the 6.15 km/s refractor extends northwards under the Southern Uplands. Two possible surveys are suggested to examine this problem.

(1) A north-south reversed wide-angle reflection/refraction profile between the Isle of Man and the Mull of Kintyre. Explosions and airguns could be used and stations deployed on the

Stranraer penninsular. This line has the advantage of crossing the CSSP profile and running parallel to the BIRPS deep reflection profile (Figs 1.5 and 6.4).

(2) A north-south reversed refraction line along the Northumberland coast passing close to stations S60, S61, S62 and S63 where the Pg refractor appears to dip northwards at about 8.6° (see section 6.4). This can be performed with less expense than (1) above if quarry blasts are used.

REFERENCES

- ADESANYA, O., 1982 Seismic velocities of the upper crust of the Southern Uplands. Unpublished PhD thesis, University of Glasgow.
- AGGER, H.E., & CARPENTER, E.W., 1964 A crustal study in the vicinity of the Eskdalemuir seismological array station. Geophys. J. R. astron. Soc. 9 69-83.
- AKI, K., & RICHARDS, P.G., 1980 Quantative seismology theory and methods, Vol II. W.H. Freeman & Co. San Francisco
- AL-CHALABI, M, 1970 The application of non-linear optimisation techniques in geophysics. Unpublished PhD thesis, University of Durham.
- ARCHER, S.H., 1971 Seismic investigations of the preDevonian basement of north-eastern England. Unpublished MSC thesis, University of Durham.
- ARMOUR, A, 1978 A seismic refraction study of the crustal structure of north-west Scotland and adjacent continental Margin. Unpublished PhD thesis, Durham University
- ASSUMPCAO, M., & BAMFORD, S.A.D., 1978 LISPB - V Studies of crustal shear waves. Geophys. J. R. astron. Soc. 54 61-73
- BACON, M., & McQUILLIN, R., 1972 Refraction seismic surveys in the north Irish Sea. J. geol. Soc. London. 128 613-621
- BAMFORD, S.A.D., 1971 An interpretation of first arrival data from the Continental Margin Refraction Experiment. Geophys. J. R. astron. Soc. 24 213-229
- 1972 Evidence for a low velocity zone in the crust beneath the Western British Isles. Geophys. J. R. astron. Soc. 30 101-105
- 1973 An example of the iterative approach of time-term analysis. Geophys. J. R. astron. Soc. 31 365-372
- 1976 MOZAIK time-term analysis. Geophys. J. R. astron. Soc. 44 433-446
- BAMFORD, S.A.D., & BLUNDEL, D.J., 1970 South-West Britain continental margin experiment. Rep. Inst. geol. Sci. London. 70/14

- BAMFORD, S.A.D., FABER, S., KAMINISKI, NUNN, K., PRODEHL, C., FUCHS, K., KING, R., & WILLMORE, P., 1976 A lithospheric seismic profile in Britain - I Preliminary results. Geophys. J. R. astron. Soc. 44 145-160
- BAMFORD, S.A.D., & CRAMPIN, S, 1977 Seismic anisotropy - the state of the art. Geophys. J. R. astron. Soc. 49 1-8
- BAMFORD, S.A.D., NUNN, K., PRODEHL, C., & JACOB, B., 1977 LISPB - III Upper crustal structure of Northern Britain J. geol. Soc. London. 133 481-488
- BAMFORD, S.A.D., NUNN, K., PRODEHL, C., & JACOB, B., 1978 LISPB - IV Crustal structure of northern Britain. Geophys. J. R. astron. Soc. 54 43-60
- BELOUSSOV, V.V., & PAVLENKOVA, N.I., 1984 The types of the Earth's crust. J. of Geodynamics. 1 167-183
- BERRY, M.J., & WEST, G.F., 1966 An interpretation of the first arrival data of the Lake Superior experiment by the time-term method. Bull. seismol. Soc. Am. 56 141-171
- BIRCH, F., 1960 The velocity of compressional waves in rocks to 10 Kilobars, Part 1. J. geophys. Res. 65 1083
- BLUNDELL, D.J., KING, R.F., & WILSON, C.D.V., 1964 Seismic investigations of the rocks beneath the northern part of Cardigan Bay, Wales. Q. J. geol. Soc. London. 120 35-50
- BLUNDELL, D.J., & PARKS, R., 1969 A study of the crustal structure beneath the Irish Sea. Geophys. J. R. astron. Soc. 17 45-62
- BOTT, M.H.P., 1961 A gravity survey off the NE coast of England. Proc. York. geol. Soc. 33 1-20
- 1968 The geological structure of the Irish Sea basin. In Geology of Shelf Seas Ed. D.T. Donovan, Oliver & Boyd, London
- 1974 The geological interpretation of a gravity survey of the English Lake District and the Vale of Eden. J. geol. Soc. London. 130 309-331
- BOTT, M.H.P., & MASSON-SMITH, D., 1957 The geological interpretation of a gravity survey of the Alston Block and Durham coalfield. Q. J. geol. Soc. London. 113 93-117

- 1960 A gravity survey of the
Criffell Granodiorite and the New Red Sandstone
deposits near Dumfries. Proc. Yorks. geol. Soc. 40
613-630
- BOTT, M.H.P., SUNDERLAND, J., SMITH, P.J., CASTEU, U., & SAXOV,
S., 1974 Evidence for continental crust beneath the Faeroe
Islands. Nature., London. 248 202-204
- BOTT, M.H.P., NIELSEN, P.H., & SUNDERLAND, J., 1976 Converted P-
waves at the continental margin between the Iceland-
Faeroe Ridge and the Faeroe Block. Geophys. J. R.
astron. Soc. 44 229-238
- BOTT, M.H.P., SWINBURN, P., & LONG, R.E., 1984 Deep structure and
origin of the Northumberland and Stainmore Troughs.
Proc. York. geol. Soc. 44 479-495
- BREWER, J.A., MATHEWS, D.H., WARNER, M.R., HALL, J., SMYTHE,
D.K., & WHITTINGTON, R.J., 1983 BIRPS deep seismic reflection
studies of the British Caledonides. Nature., London.
305 206-210
- BURKHARDT, H., & VEES, R., 1975 Explosions in shallow water for
deep seismic sounding experiments. J. Geophys. 41
463-474
- CERVENY, V., 1966 On dynamic properties of reflected and head
waves in the n-layered Earth's crust. Geophys. J. R.
astron. Soc. 11 139-147
- CERVENY, V., MOLOTKOV, I.A. PSENCIK, I. 1977 Ray method in
seismology. Univerzita Karlova, Prague
- CHRISTENSEN, N.I., 1980 Seismic velocities. In Handbook of
physical properties of rocks Vol. II Ed. R.S.
Carmichael, CRC Press.
- CHURCH, W.R., & GAYER, R.A., 1973 The Ballantrae Ophiolite.
Geol. Mag. 110 497-592
- CLAY, C.S., & MEDWIN, H., 1977 Acoustical oceanography:
principles and application. John Wiley and Sons
- CLOWES, R.M., & KANASEWICH, E.T., 1970 Seismic attenuation and
the nature of reflecting horizons within the crust.
J. geophys. Res. 75 6693-6705
- COCKS, L.R.M., & FORTEY, R.A., 1982 Faunal evidence for oceanic
separations in the Palaeozoic of Britain. J. geol.
Soc. London. 139 465-478

- COLLETTE, B.J., LAGAAY, R.A., RITSEMA, A.R., & SCHOUTEN, J.A.,
1967 Seismic investigations in the North Sea, 1 and
2. Geophys. J. R. astron. Soc. 12 363-373
-
- 1970 Seismic investigations in the North Sea, 3 to
7. Geophys. J. R. astron. Soc. 19 183-199
- CRAMPIN, S., CHESNOKOV, E.M., & HIPKIN, R., 1984 Seismic
anisotropy - the state of the art. First Break 2 9-
18
- DALEY, T., 1983 A magnetic study and evaluation of the Causey
Park Dyke, Northumberland Coalfield. Unpublished
MSc thesis, University of Durham
- DAVIES, C.R., 1983 A reversed seismic refraction profile across
the Solway Firth Basin in the north Irish Sea.
Unpublished BSc thesis, University of Durham
- DAY, G.A., COOPER, B.A., ANDERSON, C., BURGERS, W.F.J., RONNEVIK,
H.C., & SCHONEICH, H., 1981 Regional seismic structure maps of
the North Sea. Petroleum Geology of the Continental
Shelf of North-West Europe 76-84 Inst. of
Petroleum, London.
- DEWEY, J.F., 1971 A model for the Lower Palaeozoic of the
southern margin of the early Caledonides of Scotland
and Ireland. Scott. J. Geol. 7 219
- DOBRIN, M.B., 1976 Introduction to geophysical prospecting.
Third edition. McGraw-Hill
- DONATO, J.A., MARTINDALE, W., & TULLY, M.C., 1983 Buried
granites within the Mid North Sea High. J. geol.
Soc. London. 140 825-837
- FITCH, F.J., & MILLER, J.A., 1967 The age of the Whin Sill Geol.
Jour. 5 233-250
- FITTON, J.G., & HUGHES, D.J., 1970 Volcanism and plate
tectonics in the British Ordovician. Earth planet.
Sci. Lett. 8 223-228
- FUCHS, K., & MUELLER, S, 1971 Computations of synthetic
seismograms by the reflectivity method and
comparison with observations. Geophys. J. R. astron.
Soc. 23 417-433
- GREGORY, J.W., 1920 The red rocks of a deep bore at the north end
of the Isle of Man Trans. Instn. Min. Eng. 59 156-
160
- GREIG, D.C., 1971 British Regional Geology The South of Scotland,
Third edition, NERC, IGS

- GRIFFITH, D.J., 1974 Seismic basement of the Stainmore Trough. Unpublished MSc thesis, University of Durham.
- HAGEDOORN, J.G., 1959 The Plus-Minus method of interpreting seismic refraction sections. Geophys. Prosp. 7 158-182
- HALE, L.D., & THOMPSON, G.A., 1982 The seismic reflection character of the continental Mohorovic Discontinuity. J. geophys. Res. 87 4625-4635
- HALL, J., 1978 Crustal evolution in northwestern Britain and adjacent regions. In Crustal structure of the eastern North Atlantic seaboard. Eds D.R. Bowes & B.E. Leake
- HALL, J., & AL-HADDAD, F.M., 1976 Seismic velocities in the Lewisian metamorphic complex northwest Britain - 'in situ' measurements. Scott. J. Geol. 12 305-314
- HALL, J, POWELL, D.W., WARNER, M,R, EL-ISA, Z,H,M, ADESANYA, O, & BLUCK, B.J., 1983 Seismological evidence for shallow crystalline basement in the Southern Uplands of Scotland Nature 305 418-420
- ----- 1984 Reply to Seismological evidence for shallow crystalline basement in Southern Uplands, Scotland by Oliver & McKerrow 1984, Nature. London. 308 89-90
- HALL, J., & SIMMONDS, G., 1979 Seismic velocities of Lewisian metamorphic rocks at pressures to 8 kbar: relationship to crustal layering in northern Britain. Geophys. J. R. astron. Soc.
- HAWKINS, L.V., 1961 The reciprocal method of routine shallow seismic refraction investigations. Geophysics 26 806-819
- HEALY, J., 1971 A comment on the evidence for a worldwide zone of low seismic velocity at shallow depths in the Earths crust. Monogr. Am. geophys. Union. 14
- HOLDER, A.P., & BOTT, M.H.P., 1971 Crustal structure in the vicinity of the south-west England. Geophys. J. R. astron. Soc. 23 465-489
- HOUSE, M.R., RICHARDSON, J.B., CHALONER, W.G., ALLEN, J.R.L., HOLLAND, C.H., & WESTOLL, T.S., 1976 A correlation of Devonian rocks of the British Isles. Geol. Soc. London., Special Rep. No. 7

- JACOB, A.W.B., 1969 Crustal phase velocities observed at the Eskdalemuir seismic array. Geophys. J. R. astron. Soc. 18 189-
- 1975 Dispersed shots at optimum depth - an efficient seismic source for lithospheric studies. J. Geophys. 41 63-70
- JACOB, A.W.B., KAMINSKI, W., MURPHY, T., PHILLIPS, W.E.A., & PRODEHL, C., 1984 A crustal model for a NE/SW profile through Ireland. In press
- KIDD, R.G.W., 1972 Seismic investigation of the northern Pennine basement rocks. Unpublished MSc thesis, University of Durham.
- LANDISMAN, M., MUELLER, S., & MITCHELL, B., 1971 Review of evidence for velocity inversions in the continental crust. In The structure and physical properties of the Earth's crust. Ed. J. Heacock. Monogr. Am. geophys. Union. 14
- LAVING, G.J., 1971 Automatic methods for the interpretation of gravity and magnetic field anomalies and their application to marine geophysical surveys. Unpublished PhD thesis, University of Durham.
- LEDOUX, Y., 1957 Quelques exemples de diffractions en sismique refraction et leur application a la determination des vitesses verticales. Geophys. Prosp. 5 392-406
- LEEDER, M.R., 1971 Initiation of the Northumberland Basin. Geol. Mag. 108 511-516
- 1982 Upper Palaeozoic basins of the British Isles - Caledonide inheritance versus Hercynian plate margin processes. J. geol. Soc. London. 139 479-491
- LEGGETT, J.K., 1980 The sedimentological evolution of a Lower Palaeozoic accretionary fore-arc in the Southern Uplands of Scotland. Sedimentology 27 401-417
- LEGGETT, J.K., MCKERROW, W.S., & EALES, M.H., 1979 The Southern Uplands of Scotland: A Lower Palaeozoic accretionary prism. J. geol. Soc. London. 136 755-770
- LEGGETT, J.K., MCKERROW, W.S., & SOPER, N.J., 1983 A model for the crustal evolution of southern Scotland. Tectonics 2 187-210
- LINDSCALE, C.J., 1982 A refraction survey in County Durham. Unpublished MSc thesis, University of Durham.

- LONG, R.E., 1974 A compact portable seismic recorder. Geophys. J. R. astron. Soc. 37 91-98
- MALIN, P.E., 1980 A first order scattering solution for modelling elastic wave codas - I The acoustic case. Geophys. J. R. astron. Soc. 63 361-380
- MCKERROW, W.S., & COCKS, L.R.M. 1976 Progressive faunal migration across the Iapetus Ocean. Nature. London. 263 305-
- MCKERROW, W.S., LEGGETT, J.K., & EALES, 1977 Imbricate thrust model of the Southern Uplands of Scotland. Nature. London. 267 237-239
- MUELLER, S., 1977 A model of the continental crust. In The Earth's crust Ed. J. Heacock Monogr. Am. geophys. Union 20
- MUELLER, S., & LANDISMAN, M., 1966 Seismic studies of the Earths crust in continents. I Evidence for a low velocity zone in the upper part of the lithosphere. Geophys. J. R. astron. Soc. 10 525-538
- NUNNS, A., 1980 Marine geophysical investigations in the Norway - Greenland Sea between the latitudes of 62°N and 74°. Unpublished PhD thesis, University of Durham
- O'BRIEN, P.N.S., 1968 Lake Superior crustal structure - a reinterpretation of the 1963 seismic experiment. J. geophys. Res. 73 2669-2689
- OLIVER, G.J.H., & MCKERROW W.S., 1984 Seismological evidence for shallow crystalline basement in Southern Uplands, Scotland. Nature. London. 309 89
- PALMER, D., 1981 An introduction to the generalised reciprocal method of seismic refraction interpretation. Geophysics. 46 1508-1518
- PHILLIPS, W.E.A., STILLMAN, C.J., & MURPHY, T, 1976 A Caledonian plate tectonic model. J. geol Soc. London. 132 579-609
- POWELL, C.M.R., 1983 The Caledonian Suture Seismic Project: the near surface structure of the western Mid North Sea High. Unpublished BSc thesis, University of Durham
- POWELL, D.W., 1970 Magnetised rocks within the Lewisian of western Scotland and under the Southern Uplands. Scott. J. Geol. 6 353-369
- 1971 A model for the Lower Palaeozoic evolution of the southern margin of the early Caledonides of Scotland and Ireland. Scott. J. Geol. 7 369-372

- PRESS, F., 1966 Seismic velocities. In Handbook of physical constants Mem. geol. Soc. Am. 97 196
- PRODEHL, C., 1970 Seismic refraction study of crustal structure in the western United States. Bull. geol. Soc. Am. 81 2629-
- RAMSBOTTOM, W.H.C., 1973 Transgression and regression in the Dinantian: a new synthesis of British Dinantian stratigraphy. Proc. Yorks. geol. Soc. 39 567-607
- REITER, L., 1970 An investigation into the time-term method in refraction seismology. Bull. seismol. Soc. Am. 60 1-13
- ROBBINS, A.R., 1962 Long lines on the spheroid. Emp. Svy. Rev. 125
- SAVAGE, J., 1979 A seismic investigation of the lithosphere of the Gregory Rift. Unpublished PhD thesis, Durham University.
- SCHEIDEGGER, A.E., & WILLMORE, P., 1957 The use of least squares method for the interpretation of data from seismic surveys. Geophysics. 22 9-22
- SINHA, M.C., & URUSKI, C.I., 1982 Cruise report, R.R.S. Shackleton leg 6/82 Barry to Liverpool 30th June to 22nd July 1982. Dept. Geol. Sci., University of Durham
- SMITH, P.J., & BOTT, M.H.P., 1975 Structure of the crust beneath the Caledonian foreland and Caledonian belt of the north Scottish shelf region. Geophys. J. R. astron. Soc. 40 187-205
- SMITH, D.B., BRUNSTROM, R.G.W., MANNING, P.I., SIMPSON, S., & SHOTTON, F.W., 1974 A correlation of Permian rocks in the British Isles. J. geol. Soc. London. 130 1-45
- SMITHSON, S.B., & DECKER, E., 1974 A continental crustal model geothermal implications. Earth planet. Sci. Lett. 22 215-225
- SMITHSON, S.B., & BROWN, S.K., 1977 A model for the lower continental crust. Earth planet. Sci. Lett. 35 134-144
- SPJELDNAES, N., 1978 Faunal provinces and the Proto-Atlantic. In Crustal evolution in north-western Britain and adjacent regions Eds. D.R. Bowes & B.E. Leake, Steel House Press, Liverpool

- SUMMERS, T, 1982 A seismic study of crustal structure in the region of the Western Isles of Scotland. Unpublished PhD thesis, University of Durham
- SWINBURN, P.M., 1975 The crustal structure of Northern England. Unpublished Ph.D. thesis, University of Durham
- TAYLOR, B.J., BURGESS, I.C., LAND, D.H., MILLS, A.C., SMITH, D.B., & WARREN, P.T., 1971 British Regional Geology North England. Forth edition NERC IGS
- TELFORD, W.M., GELDART, L.P., SHERIFF, R.E., & KEYS, D.A., 1976 Applied Geophysics. Cambridge University Press
- THIRLWALL, M.F., 1981 Implications for the Caledonian Plate Tectonic models of chemical data from volcanic rocks of the British Old Red Sandstone. J. geol. Soc. London. 138 123-138
- THOMPSON, A.S., 1984 A geophysical model of the Solway Basin. Unpublished MSc thesis, University of Durham
- UPTON, B.J.G., ASPEN, P., & CHAPMAN, N.A., 1983 The upper mantle and deep crust beneath the British Isles evidence from inclusion in volcanic rocks. J. geol. Soc. London.
- WARNER, M.R., HIPKIN, R.G., & BROWITT, C.W., 1982 Southern Uplands seismic refraction profile - preliminary results. Geophys. J. R. astron. Soc. 69 279
- WHITCOMBE, D.N., & MAGUIRE, P.K.H., 1979 The response of the time-term method to simulated crustal structures. Bull. seismol. Soc. Am. 69 1455-1473
- WHITCOMBE, D.N., & RODGERS, 1981 The effects of refractor topography and anisotropy on time-term solutions of refractor anisotropy. Geophys. J. R. astron. Soc 67 449-464
- WILLIAMS, A., 1976 Plate tectonics and biofacies evolution as factors in Ordovician correlation. in The Ordovician System: proceedings of a Palae. Assoc. Symp. Birmingham, Sept.1974 Ed. M.G. Bassett
- WILLMORE, P.L., & BANCROFT, A.M., 1960 The time-term approach to refraction seismology. Geophys. J. R. astron. Soc. 3 419-432
- WOOD, R., & BARTON, P., 1983 Crustal thinning and subsidence in the North Sea Nature. London. 302 134-136

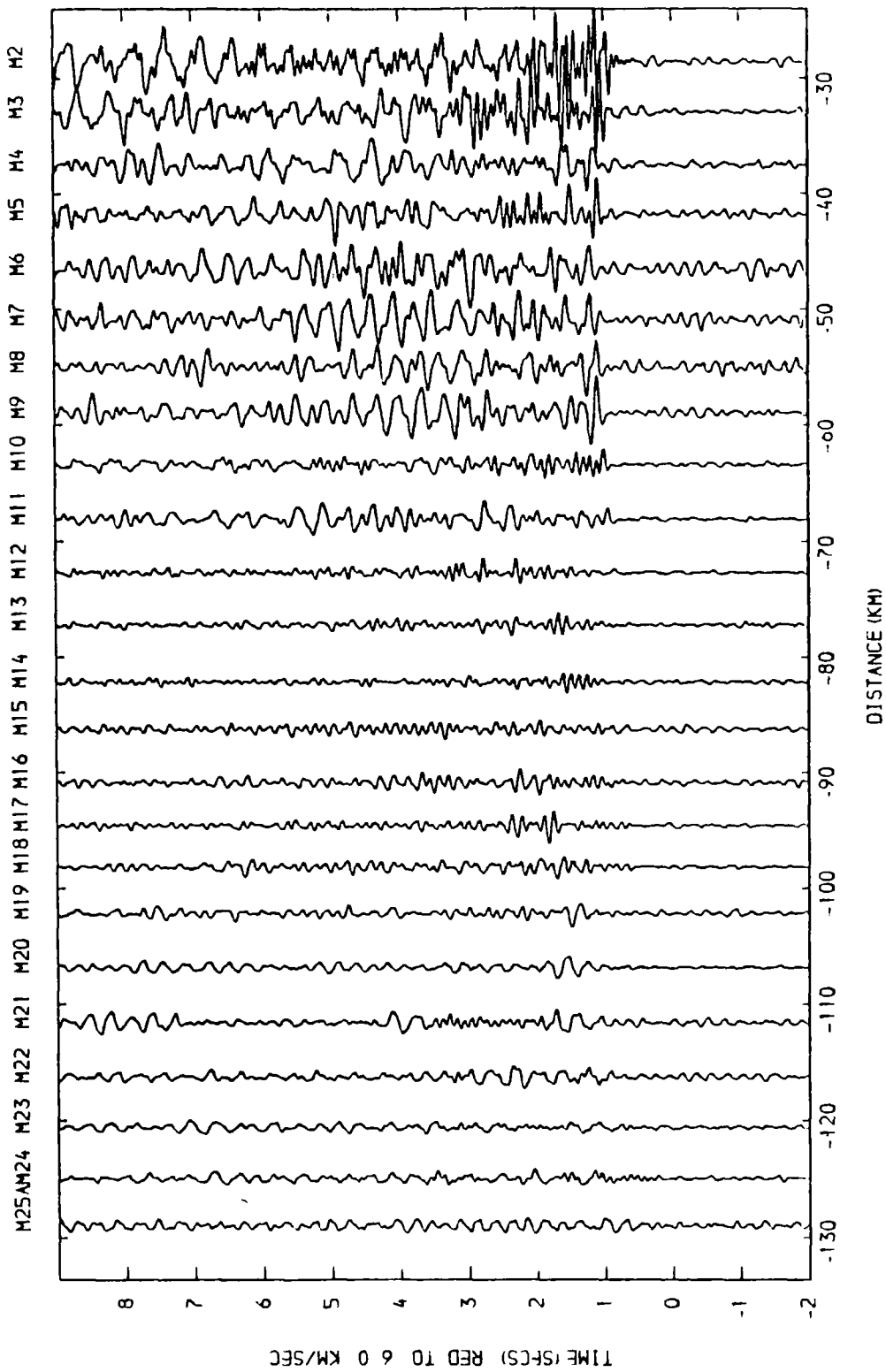
WRIGHT, J.E., HULL, J.H., McQUILLIN, R., & ARNOLD, S.E., 1971
Irish Sea investigations 1969-1970. Rep. Inst. geol.
Sci. London. 71/19

APPENDIX A

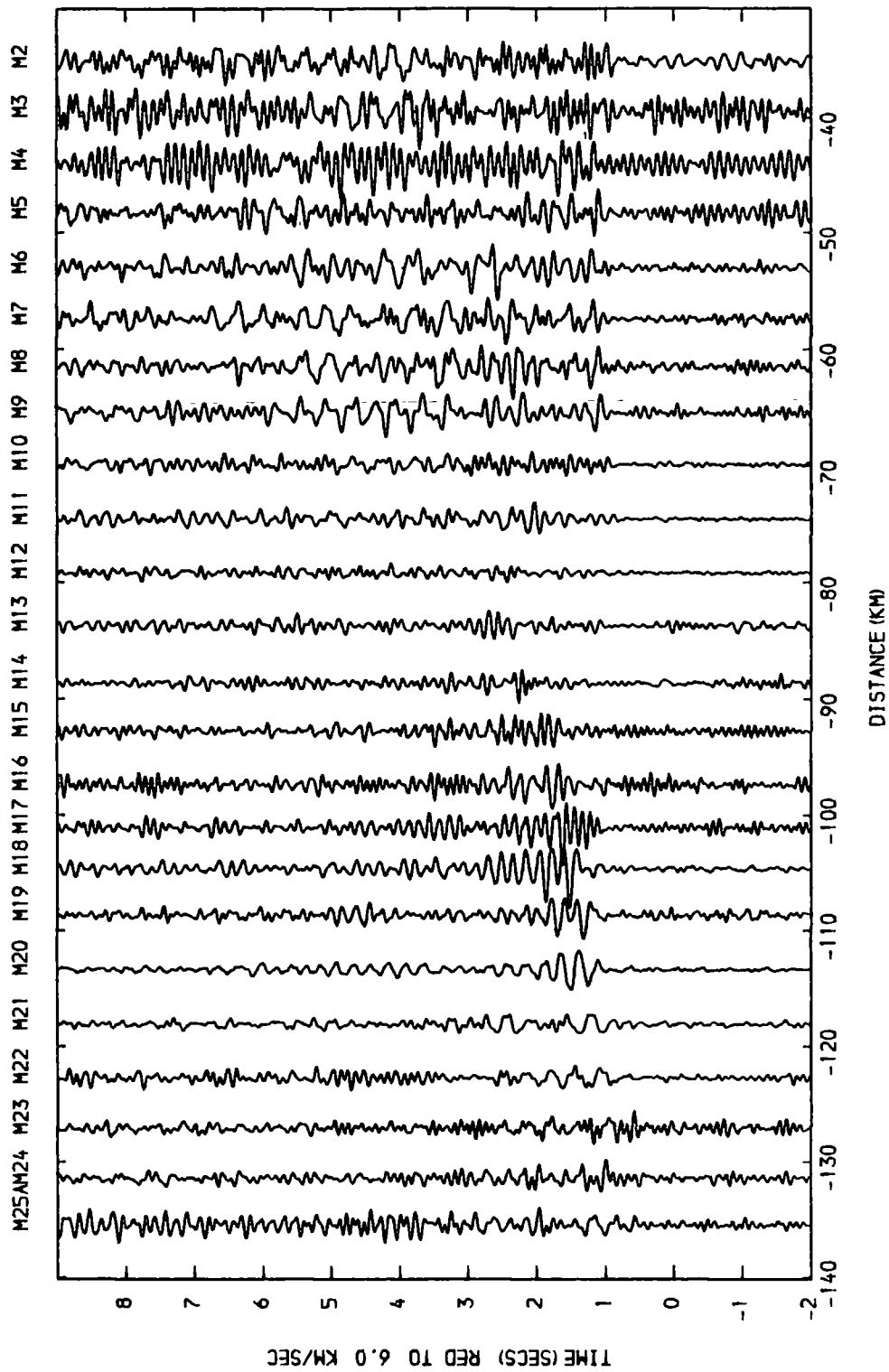
STACKED RECORD SECTIONS

The following Appendix contains record sections not included in the text. On all the sections south-west is to the left and north-east is to the right.

The travel-times for all the main phases are stored in data files on the University of Durham's computer (NUMAC). The filenames are GPT9:TMAT-PG, GPT9:TMAT-PN, GPT9:TMAT-PMP AND GPT9:PCP. The distances between all shots and stations are stored in GPT9:XMAT. Computer programs have been written by A.H.J. Lewis to access these data files.

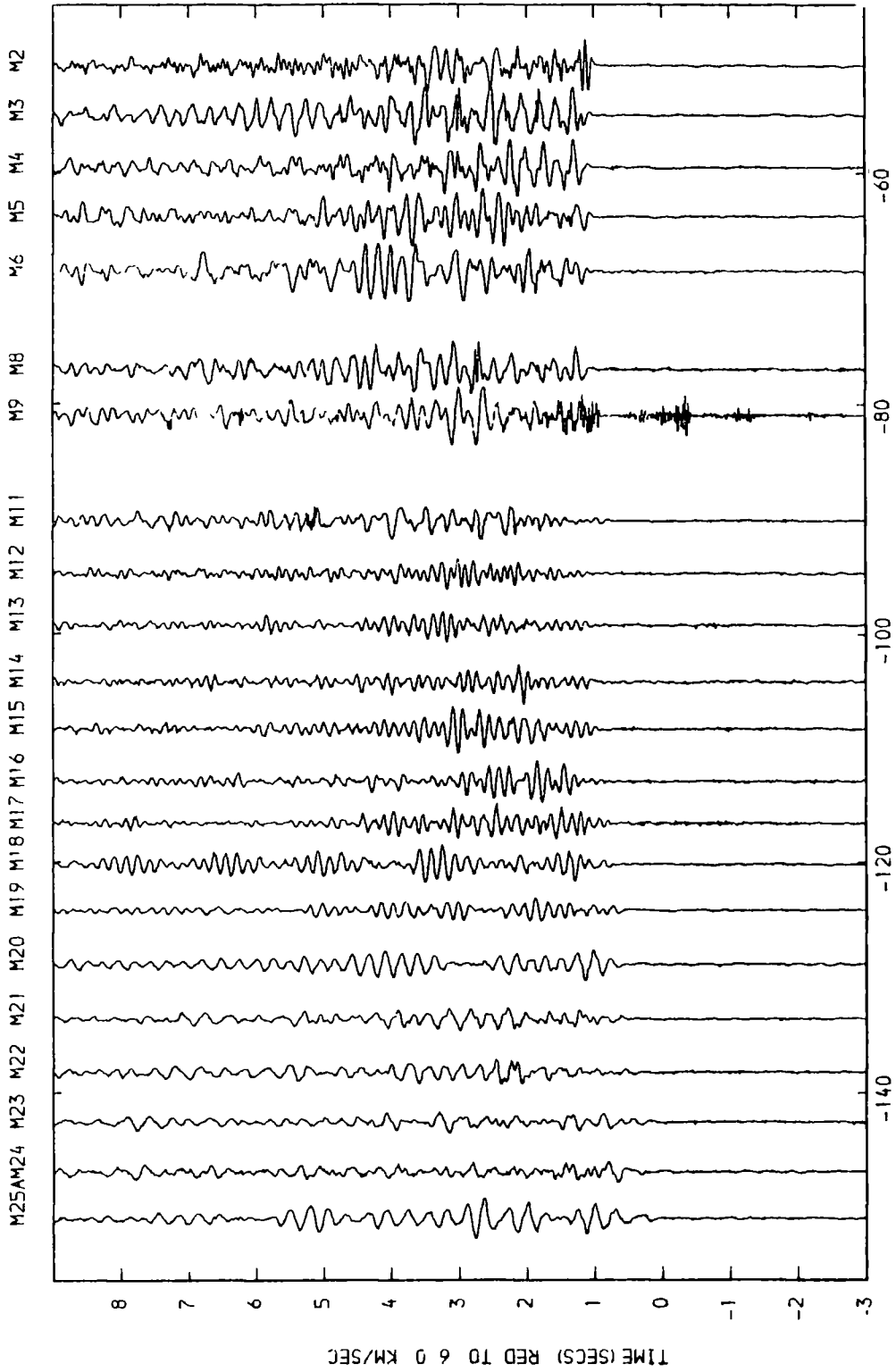


Reduced section of the Irish Sea shots recorded at S1.
 Filtered 2-12 Hz, amplitudes uncorrected.

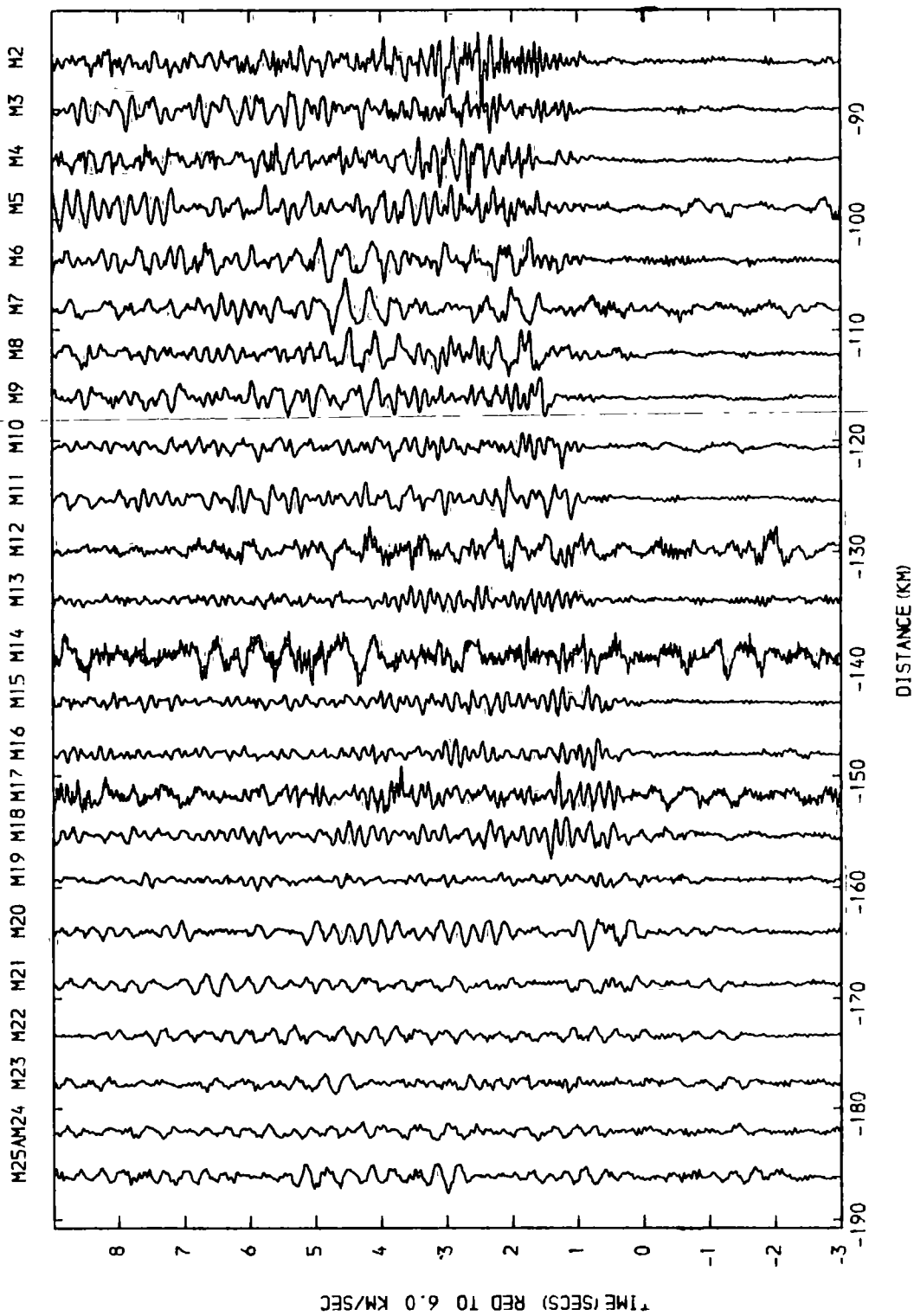


Reduced section of the Irish Sea shots recorded at S4.
 Filtered 2-12 Hz, amplitudes uncorrected.

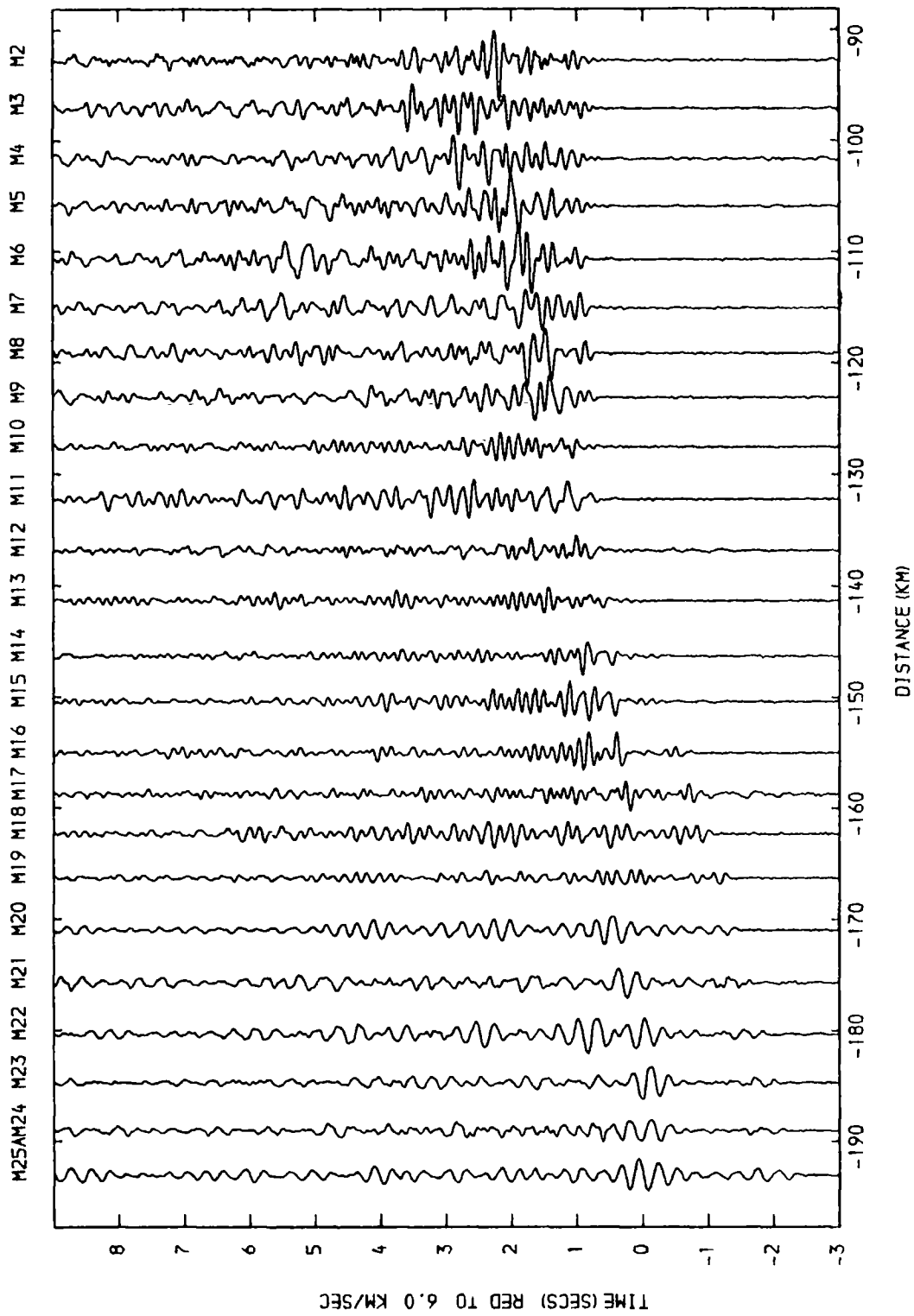
#



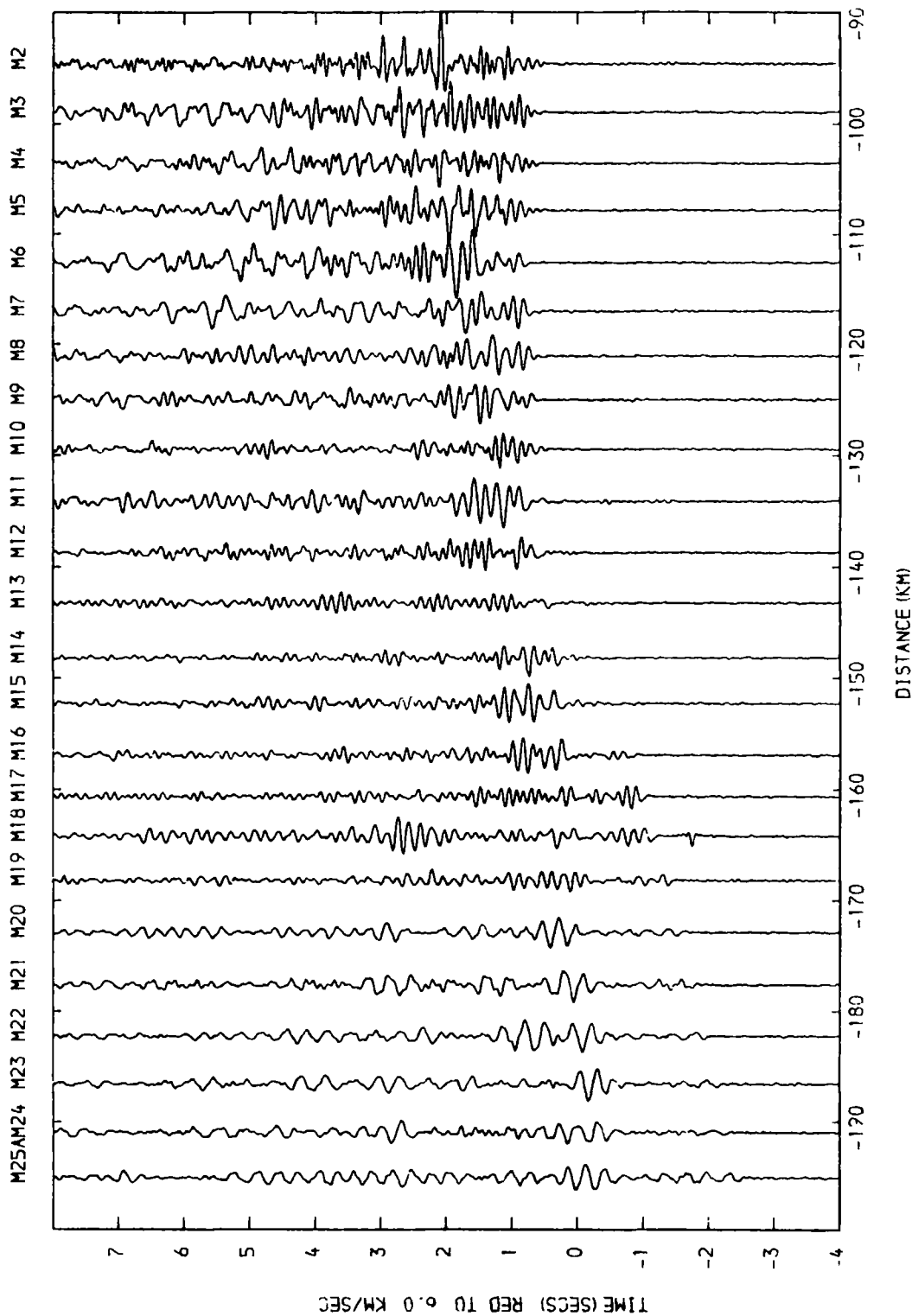
Reduced section of the Irish Sea shots recorded at S11.
Filtered 2-12 Hz, amplitudes uncorrected.



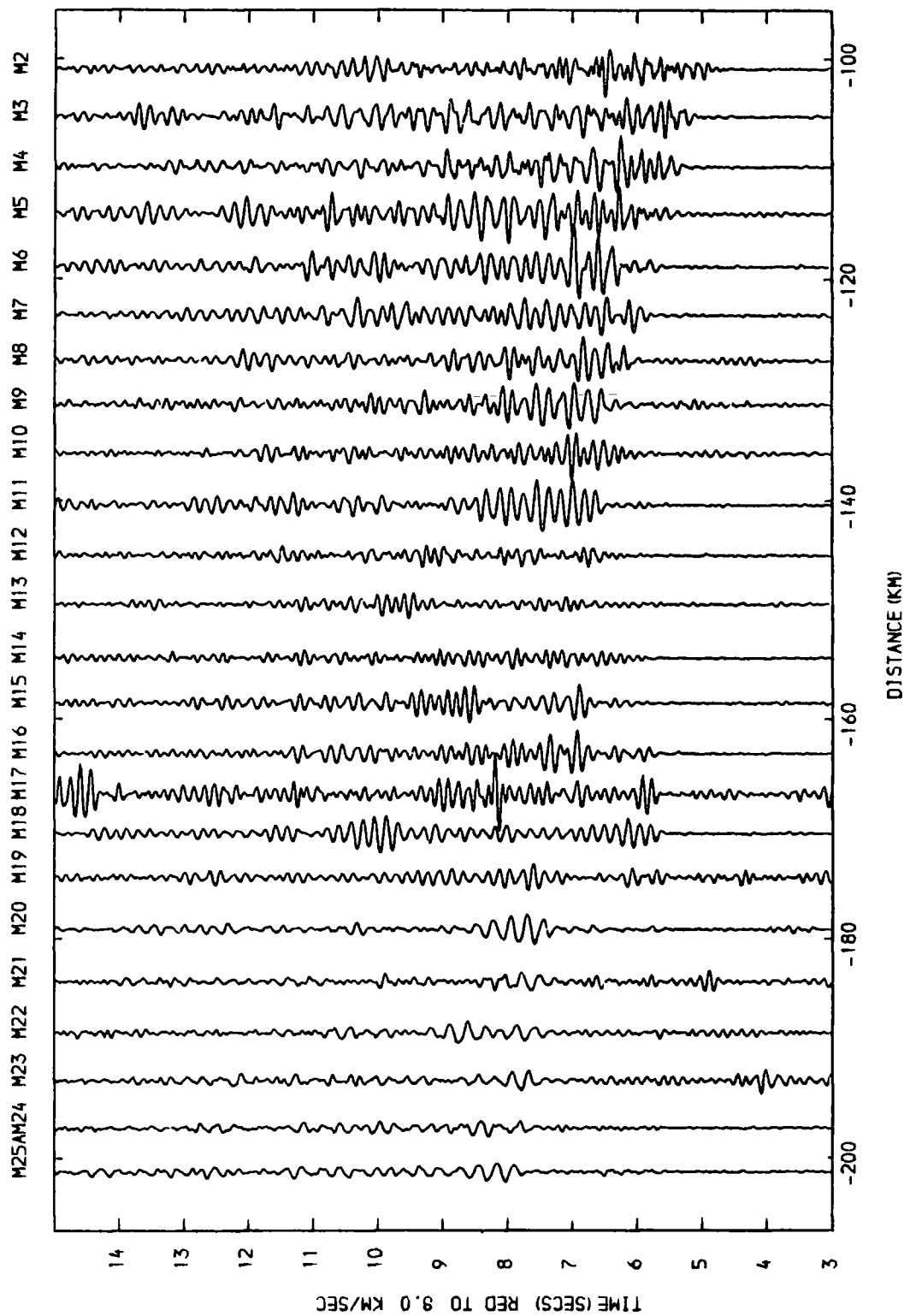
Reduced section of the Irish Sea shots recorded at S27.
 Unfiltered, amplitudes uncorrected.



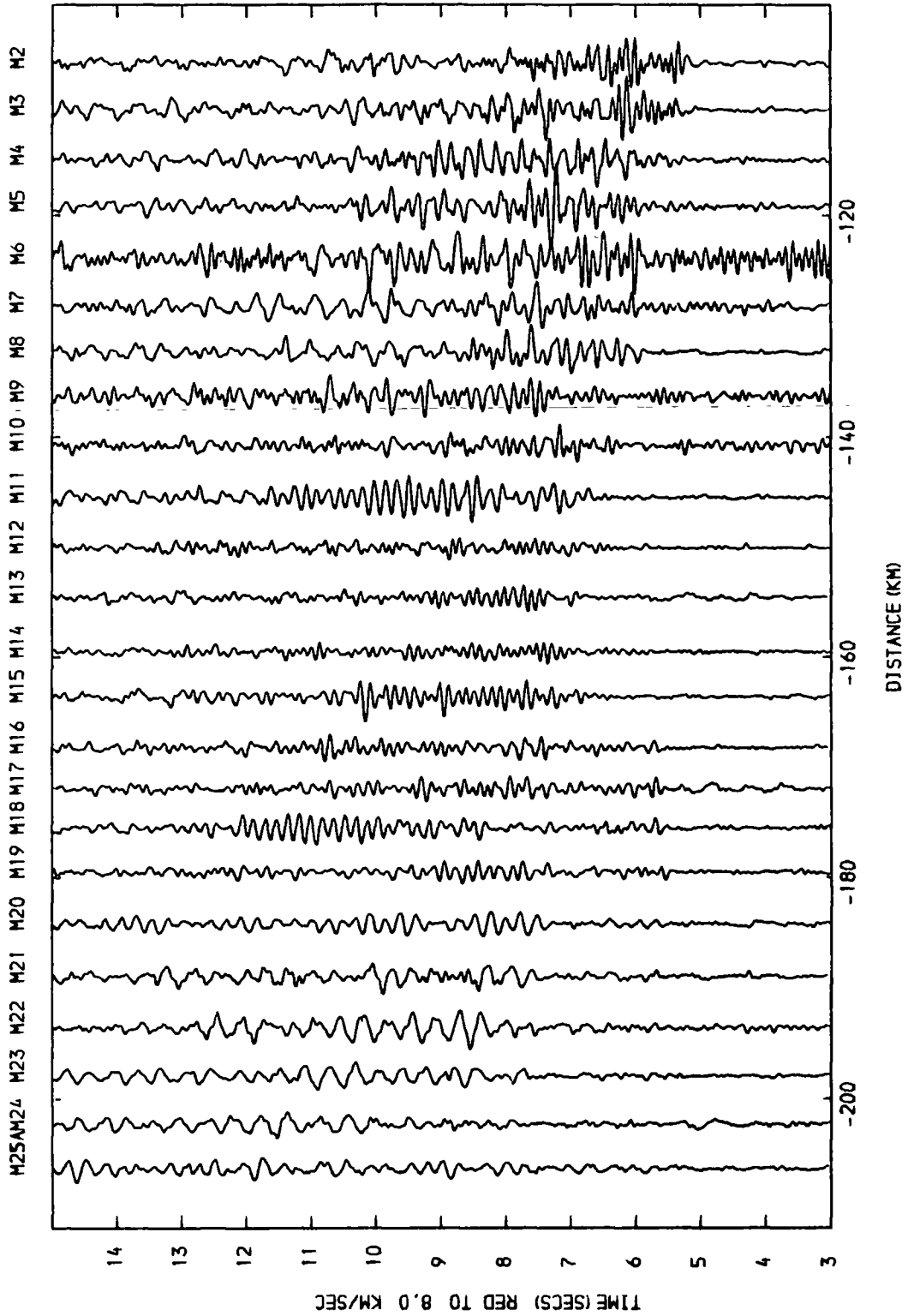
Reduced section of the Irish Sea shots recorded at S30.
 Filtered 2-12 Hz, amplitudes uncorrected.



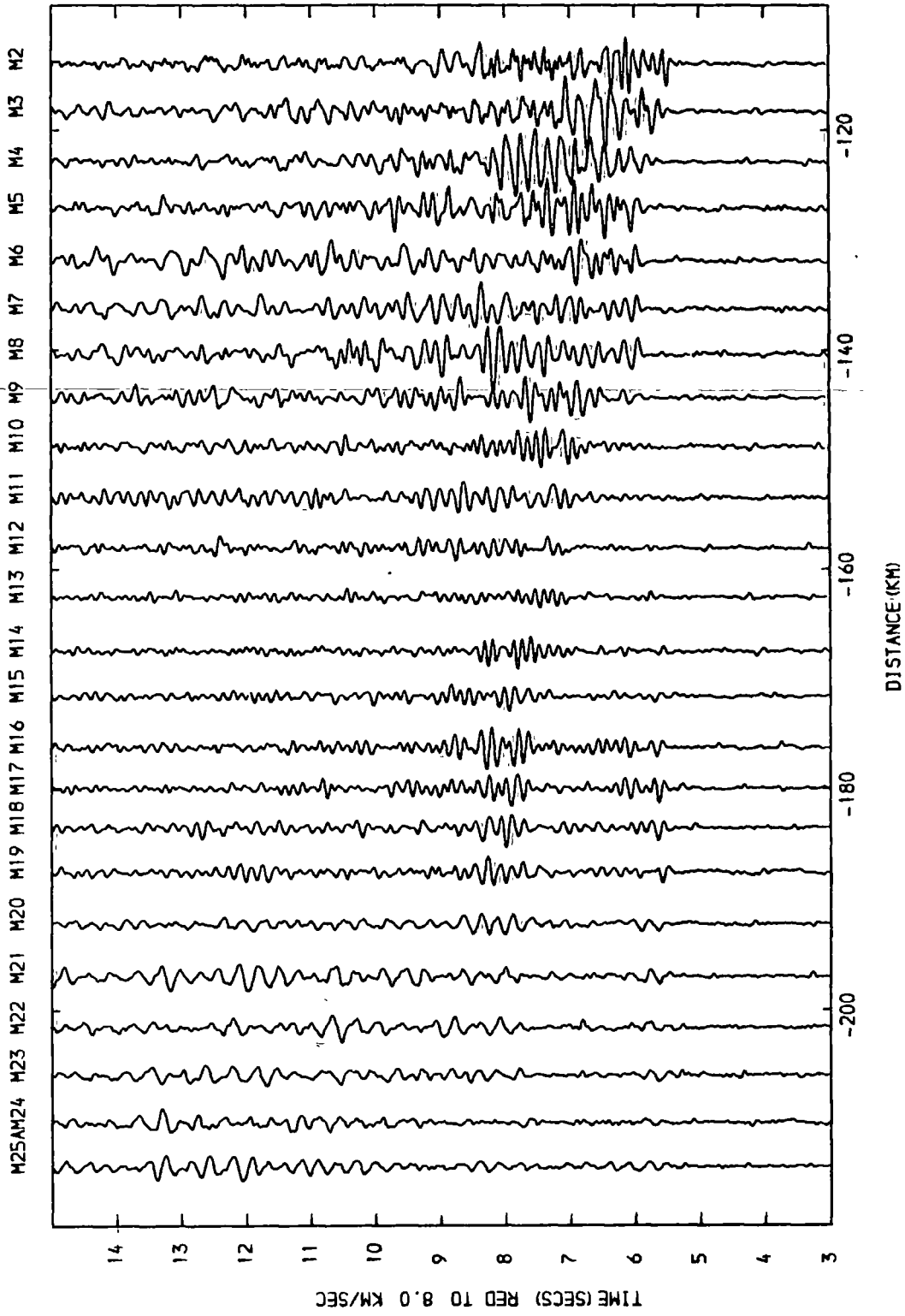
Reduced section of the Irish Sea shots recorded at S31.
 Filtered 2-12 Hz, amplitudes uncorrected.



Reduced section of the Irish Sea shots recorded at S34.
 Filtered 2-12 Hz, amplitudes uncorrected.

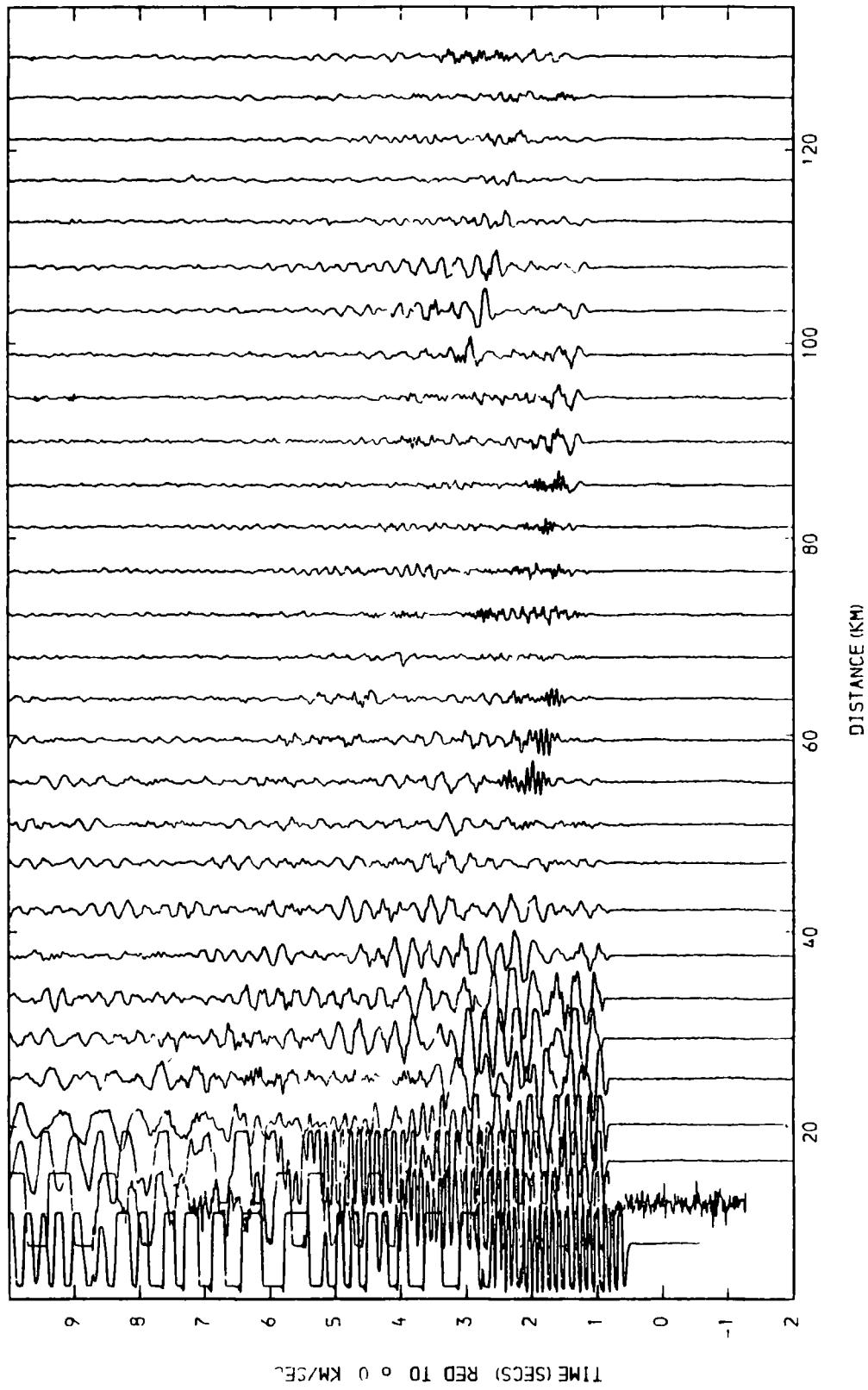


Reduced section of the Irish Sea shots recorded at S36.
 Filtered 2-12 Hz, amplitudes uncorrected.

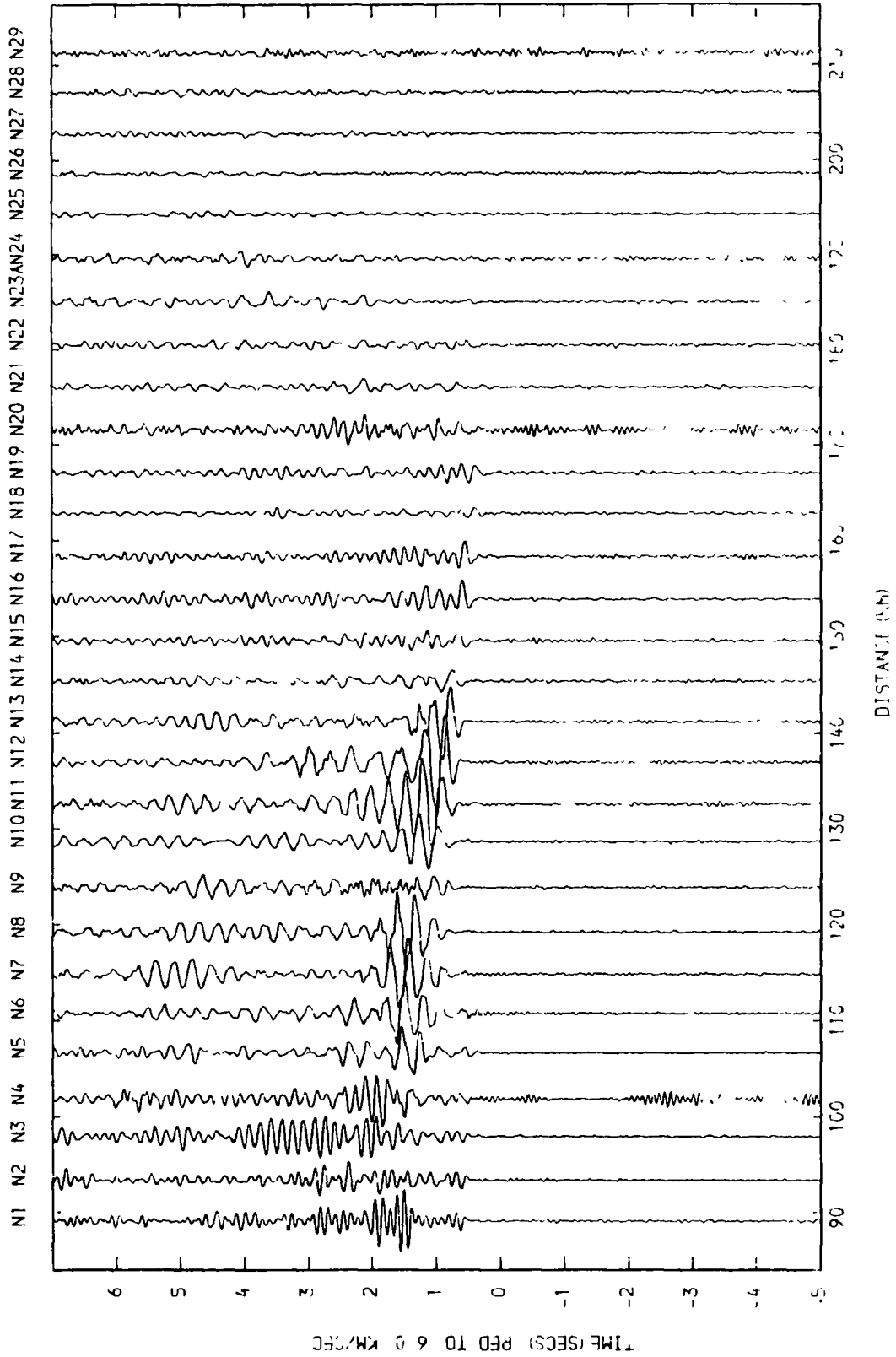


Reduced section of the Irish Sea shots recorded at S40.
 Filtered 2-12 Hz, amplitudes uncorrected.

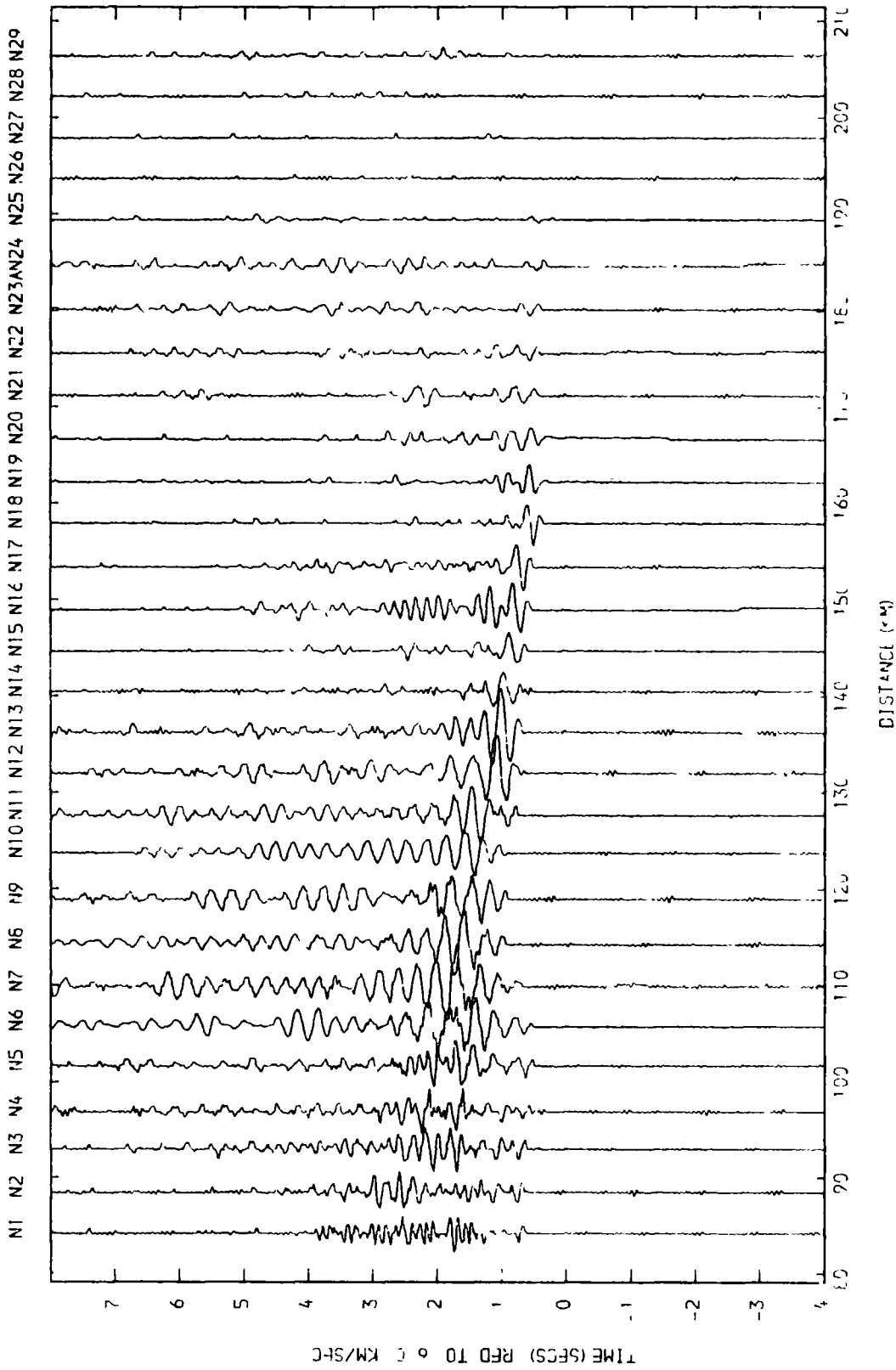
N1 N2 N3 N4 N5 N6 N7 N8 N9 N10 N11 N12 N13 N14 N15 N16 N17 N18 N19 N20 N21 N22 N23AN24 N25 N26 N27 N28 N29



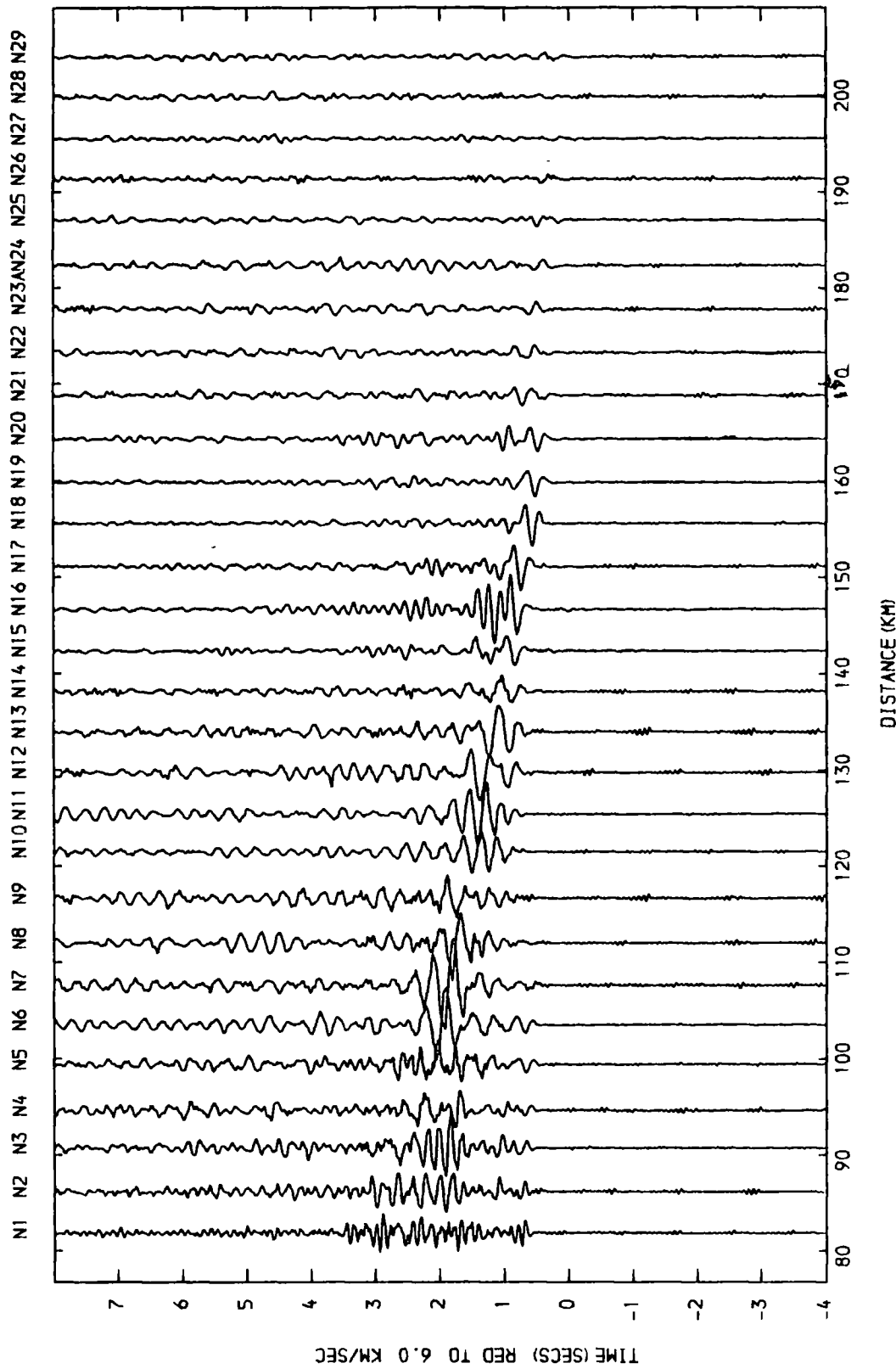
Reduced section of the North Sea shots recorded at S60.
Unfiltered, amplitudes uncorrected.



Reduced section of the North Sea shots recorded at S23
 Filtered 2-12 Hz, amplitudes uncorrected.

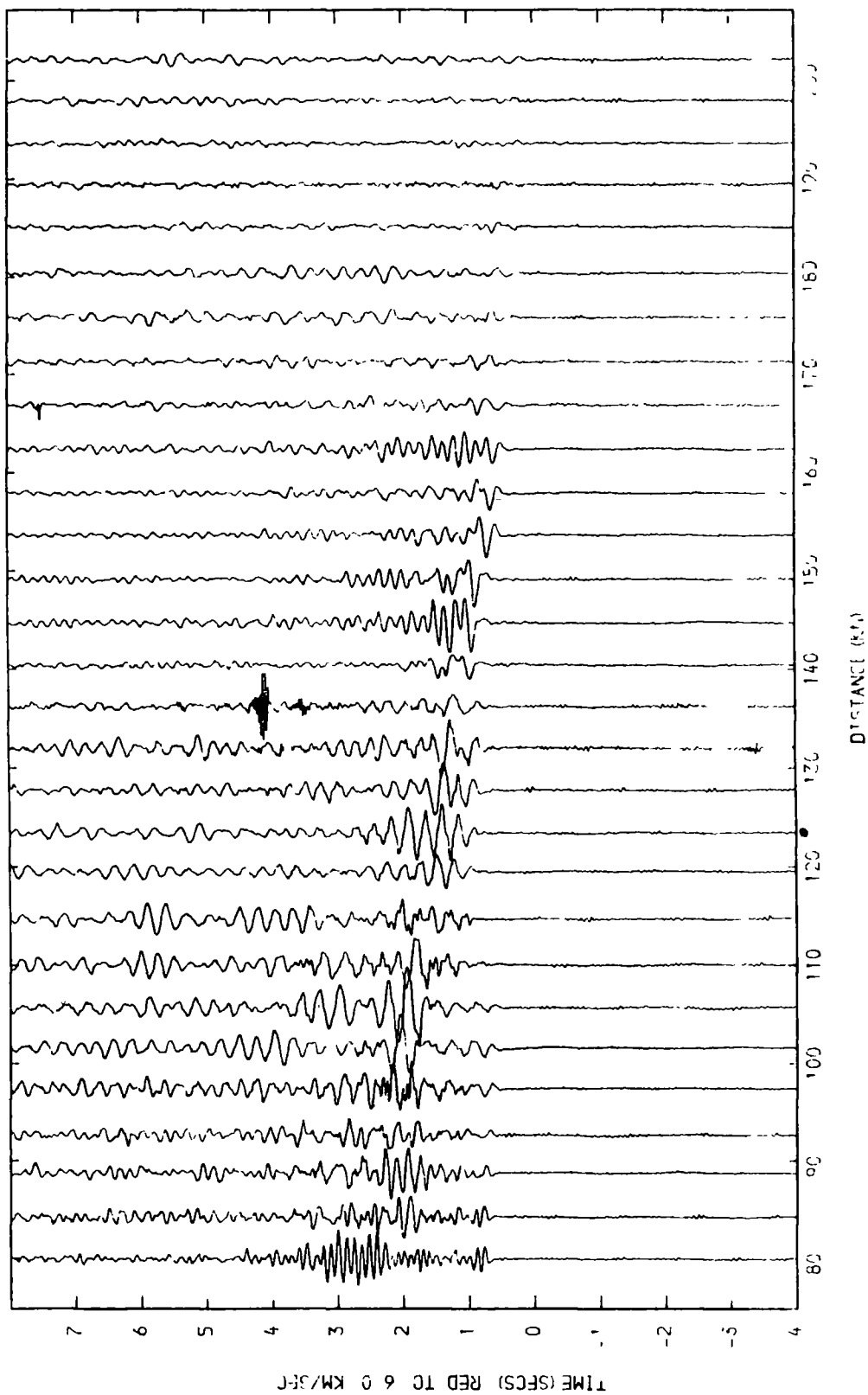


Reduced section of the North Sea shots recorded at S25.
 Unfiltered, amplitudes uncorrected.

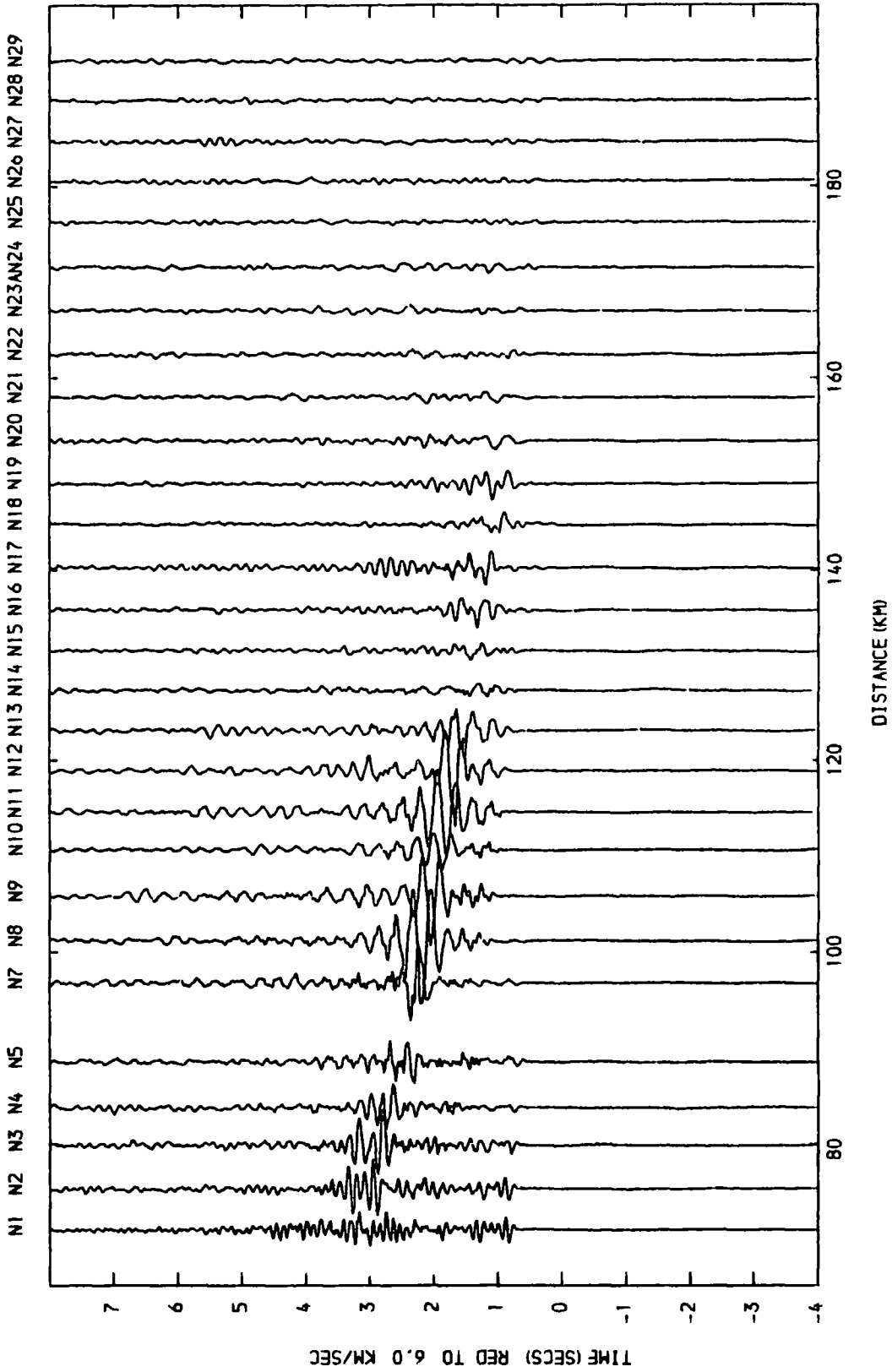


Reduced section of the North Sea shots recorded at S26.
 Unfiltered, amplitudes uncorrected.

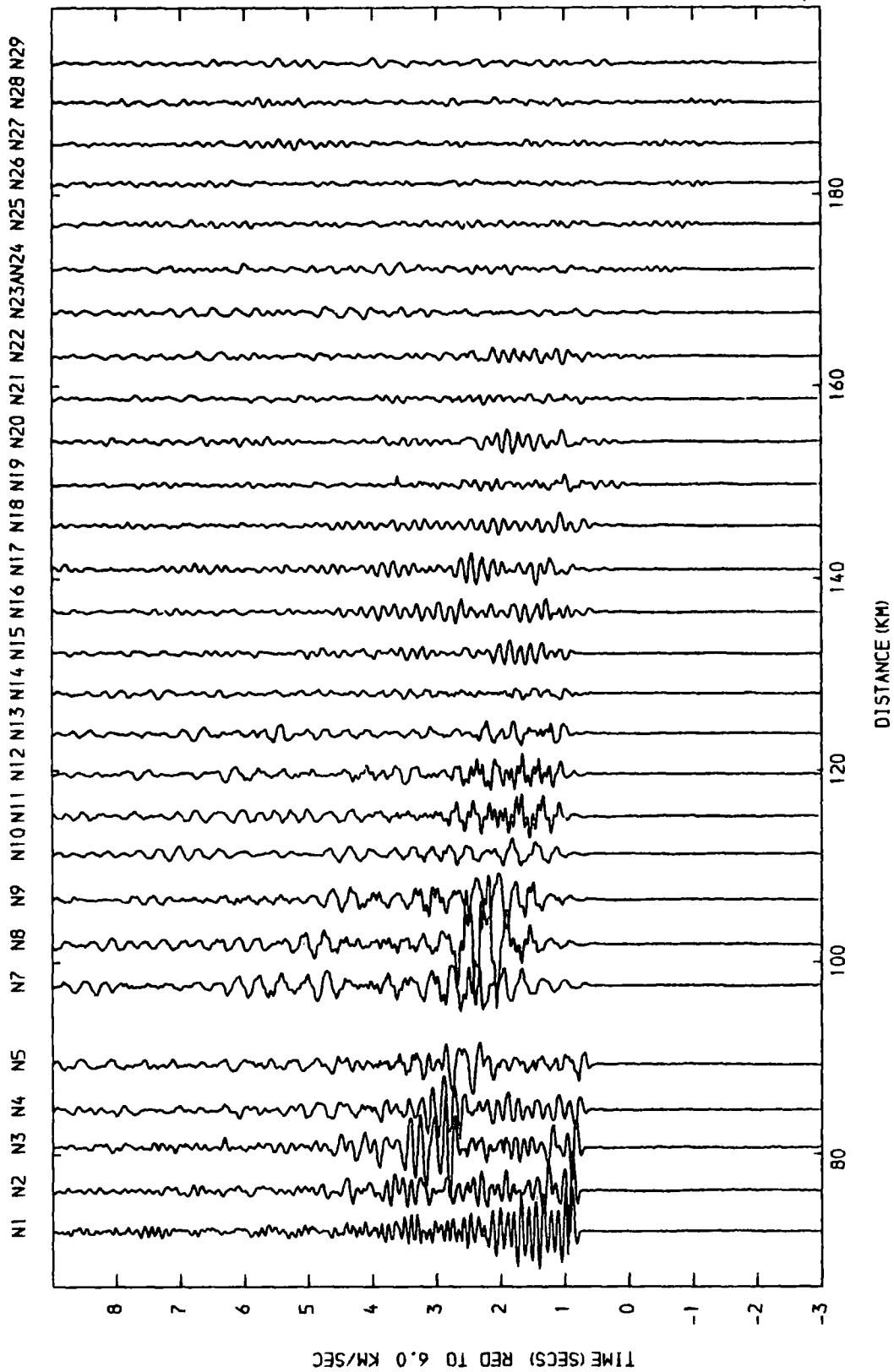
N1 N2 N3 N4 N5 N6 N7 N8 N9 N10 N11 N12 N13 N14 N15 N16 N17 N18 N19 N20 N21 N22 N23 AN24 N25 N26 N27 N28 N29



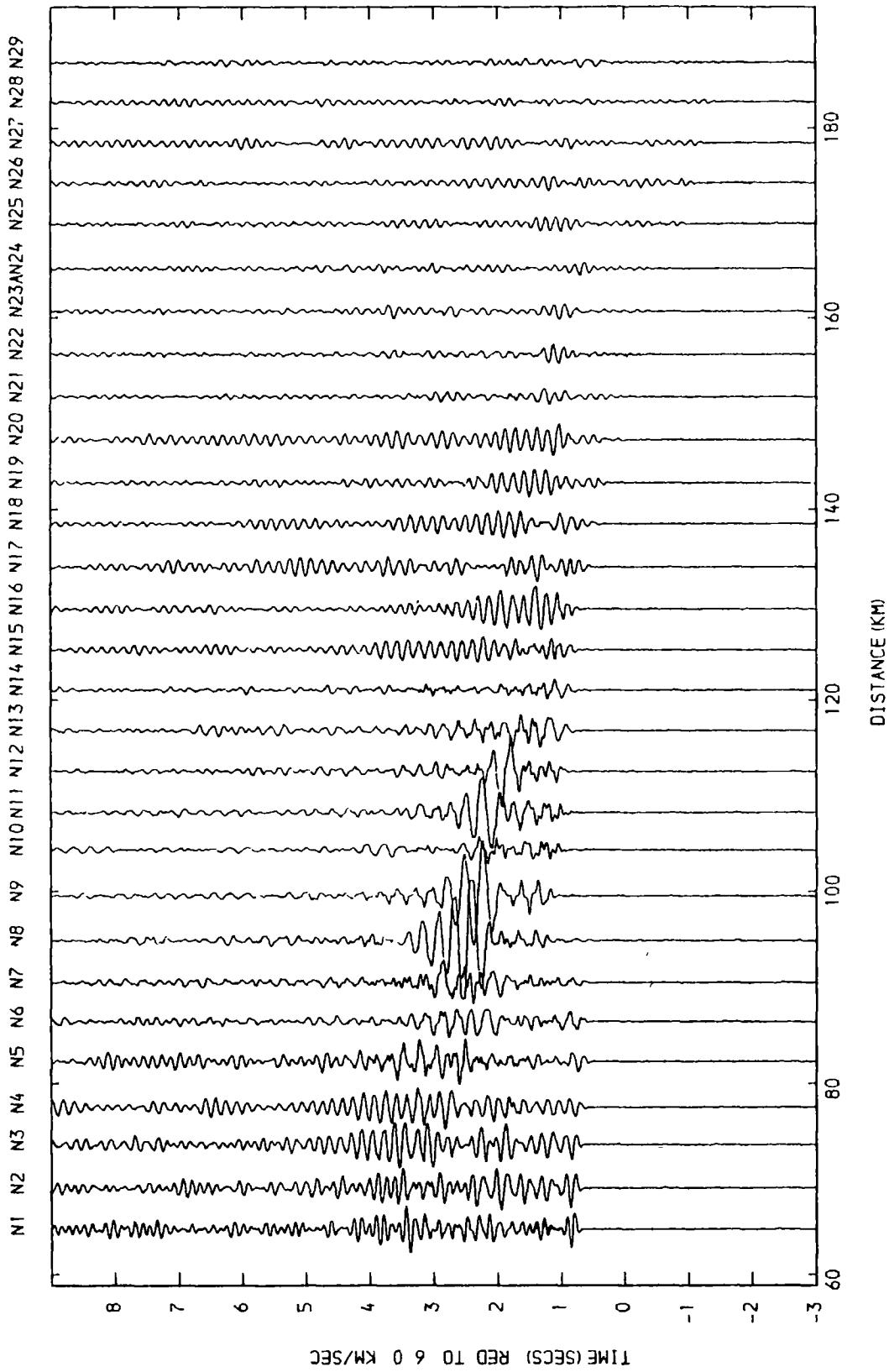
Reduced section of the North Sea shots recorded at S27.
Unfiltered, amplitudes uncorrected.



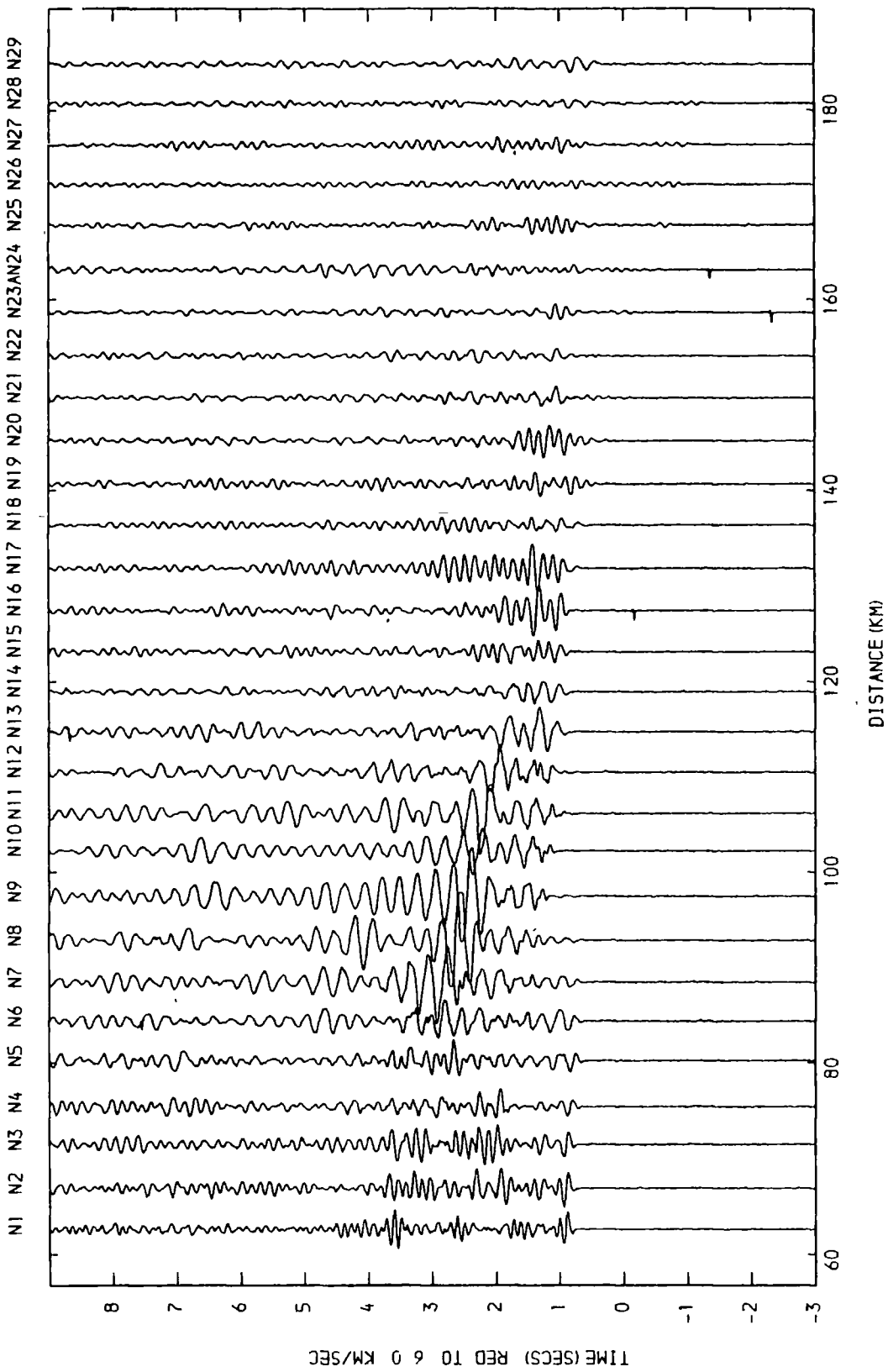
Reduced section of the North Sea shots recorded at S31.
 Unfiltered, amplitudes uncorrected.



Reduced section of the North Sea shots recorded at S31N
 Unfiltered, amplitudes uncorrected.

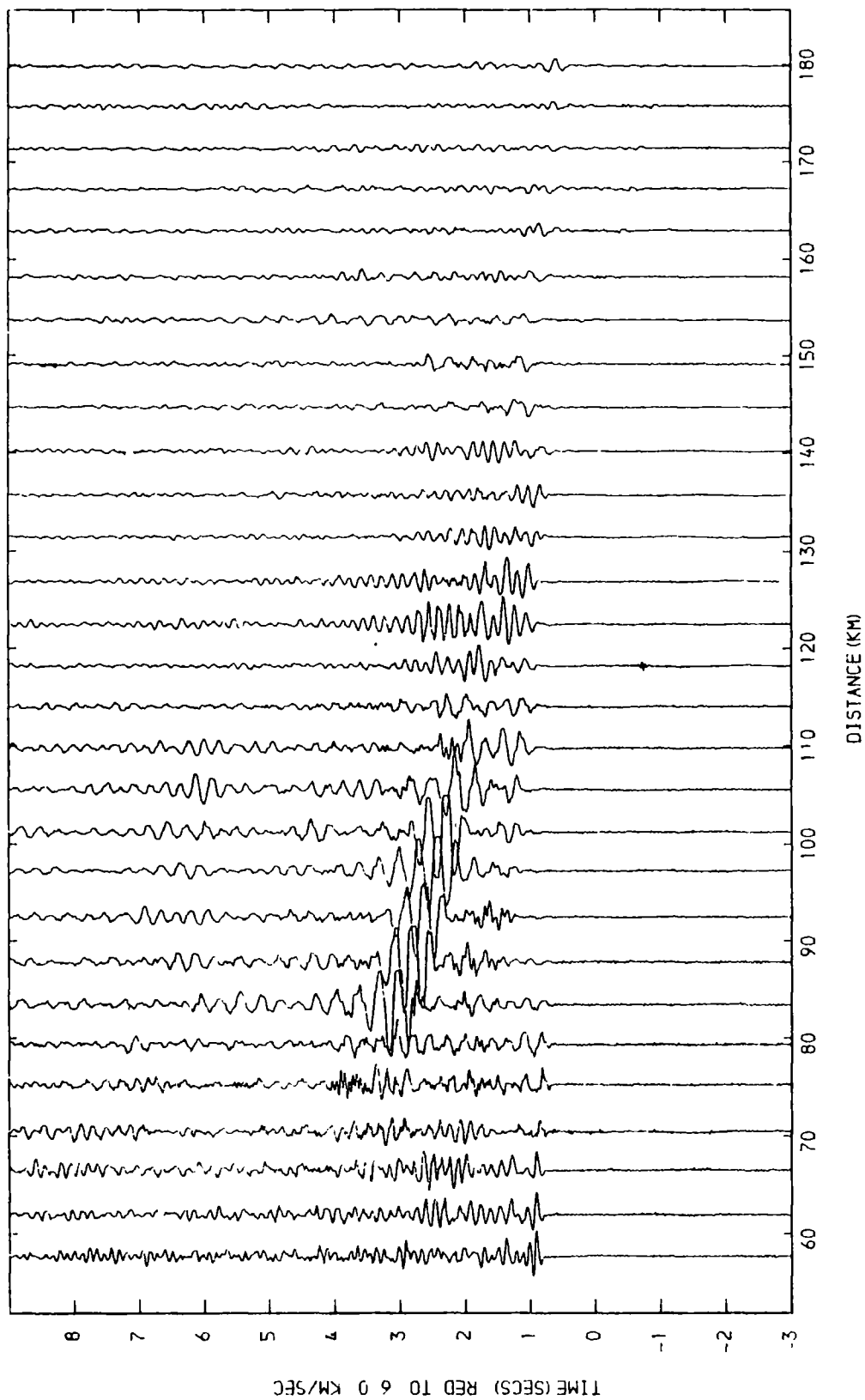


Reduced section of the North Sea shots recorded at S34.
 Unfiltered, amplitudes uncorrected.

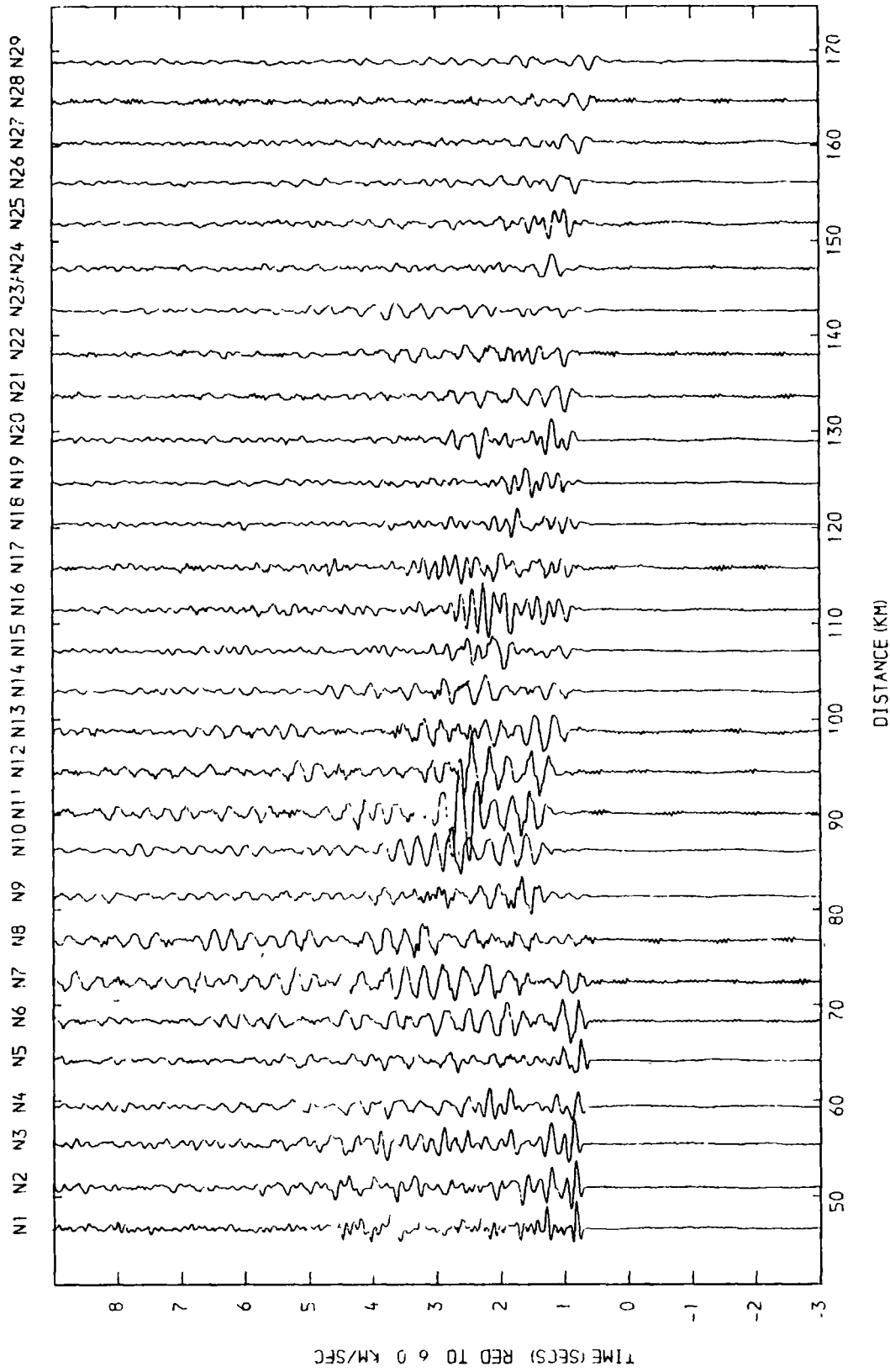


Reduced section of the North Sea shots recorded at S35.
 Unfiltered, amplitudes uncorrected.

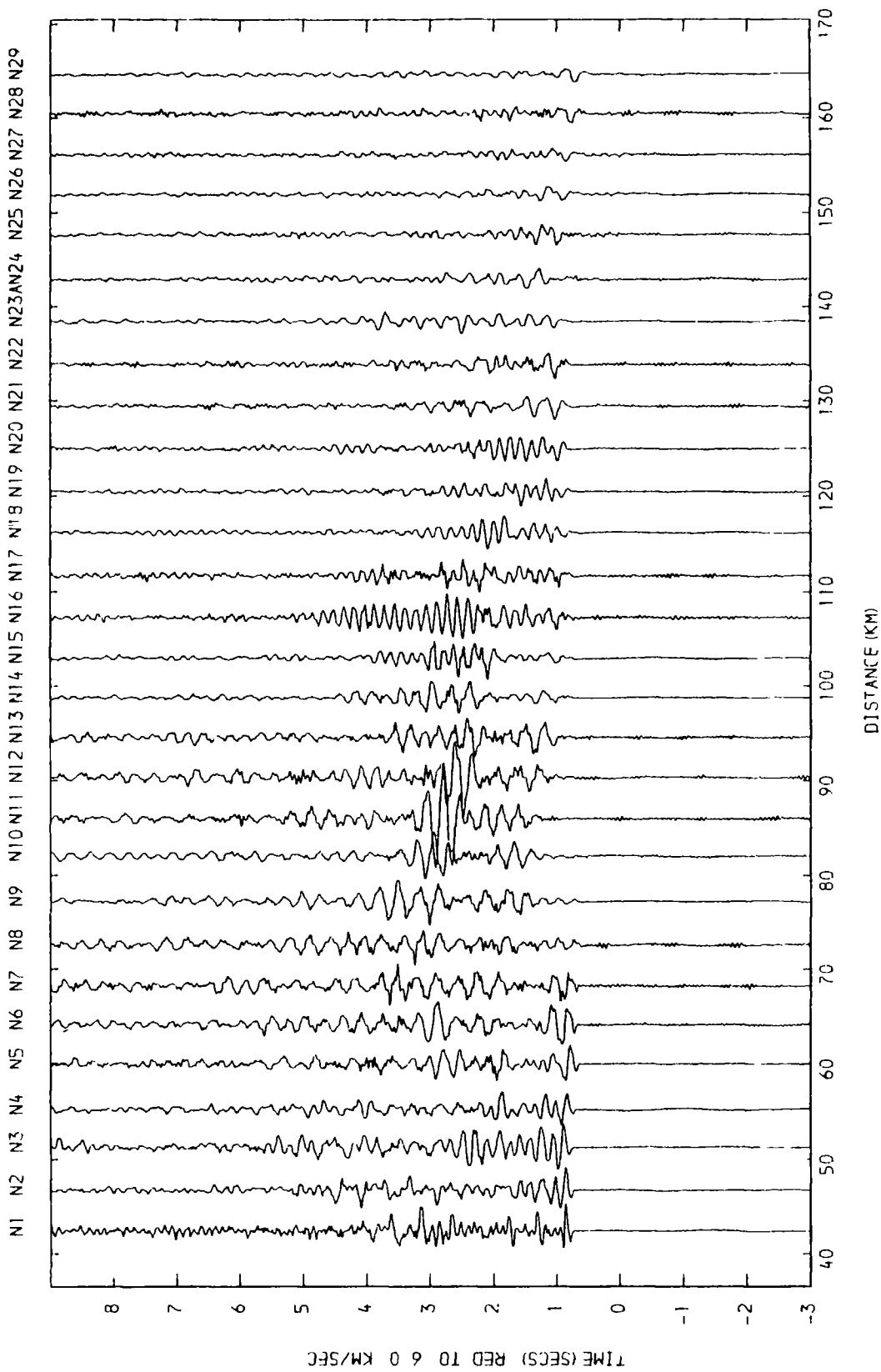
N1 N2 N3 N4 N5 N6 N7 N8 N9 N10 N11 N12 N13 N14 N15 N16 N17 N18 N19 N20 N21 N22 N23 N24 N25 N26 N27 N28 N29



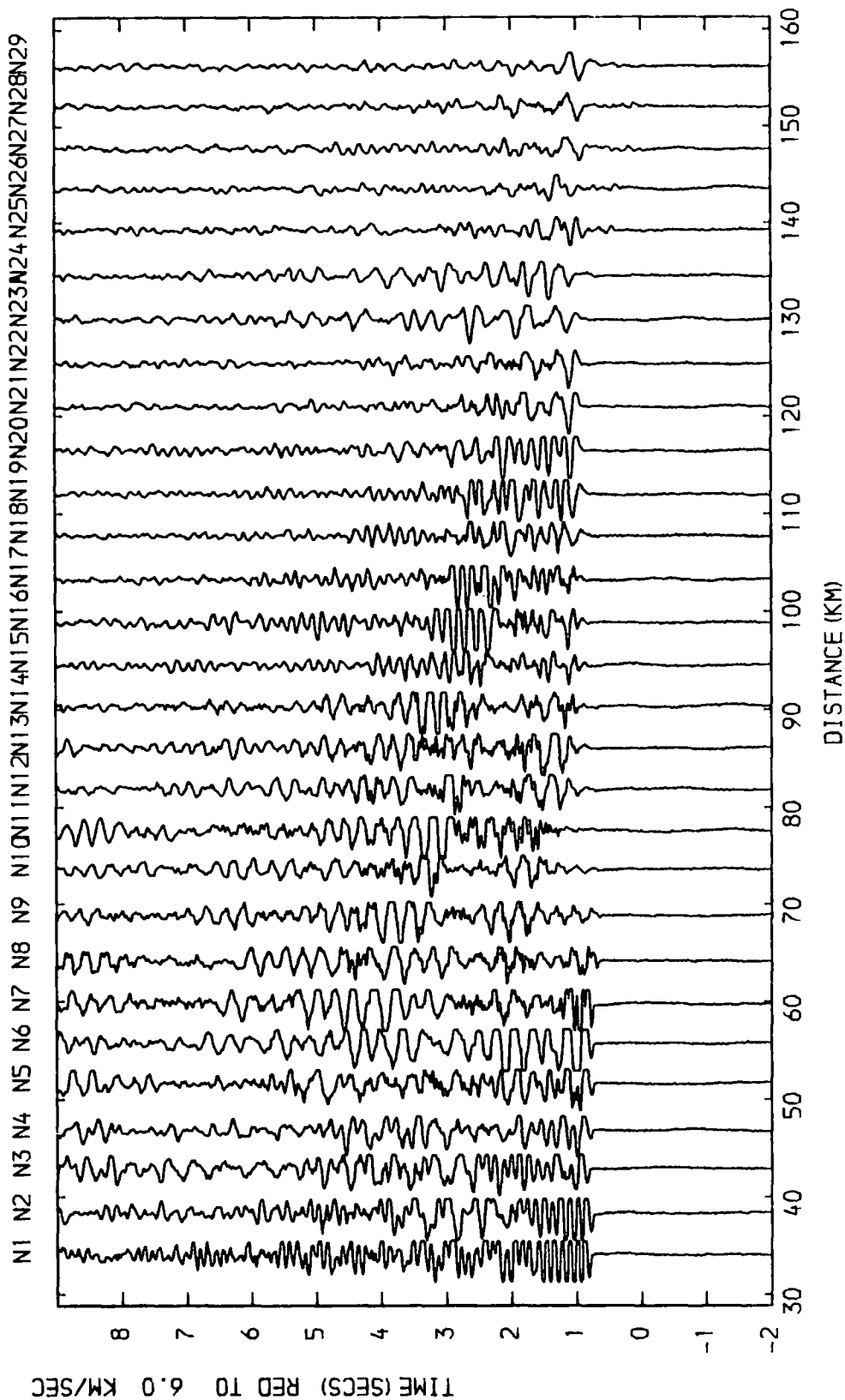
Reduced section of the North Sea shots recorded at S37.
Unfiltered, amplitudes uncorrected.



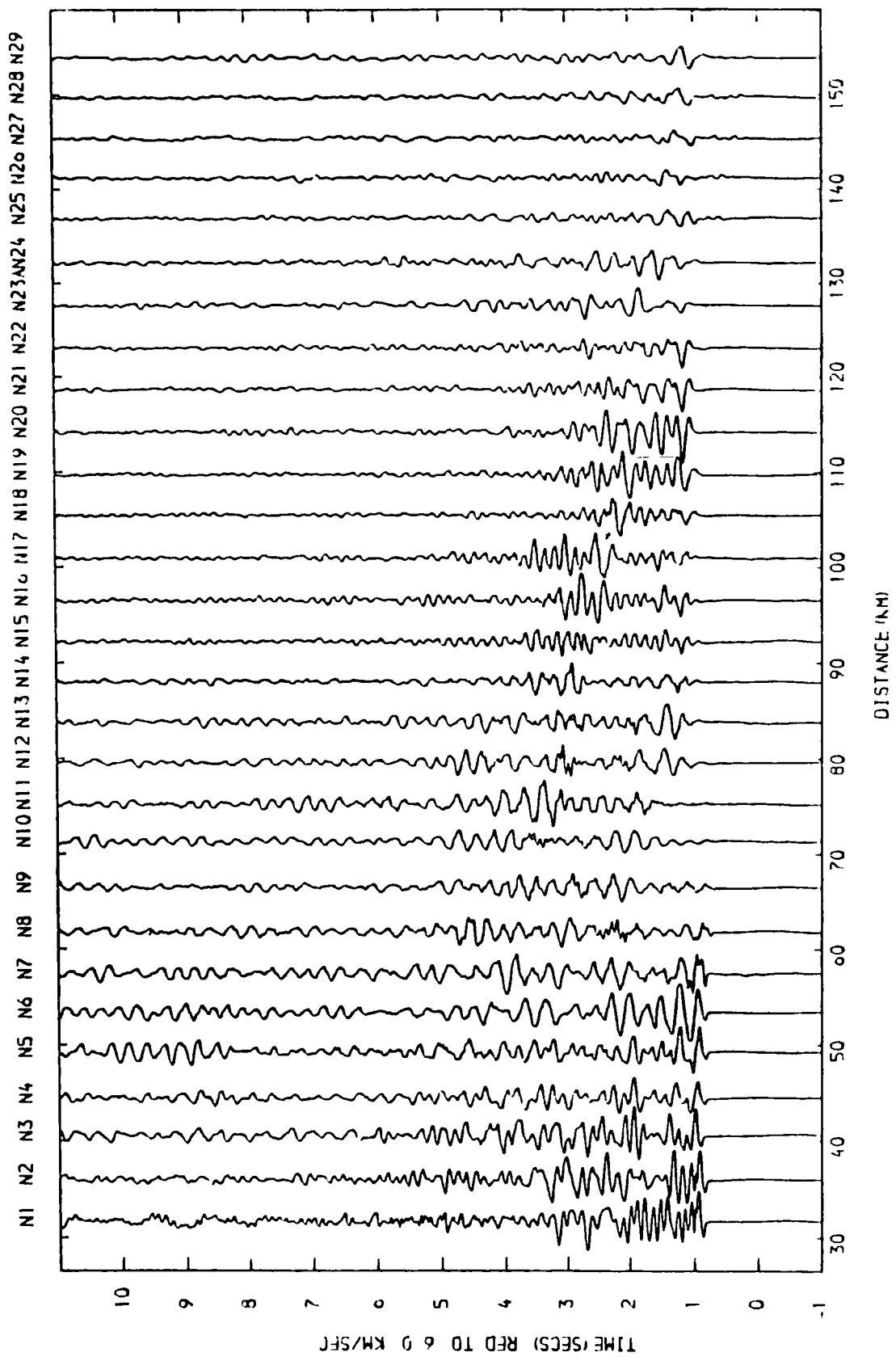
Reduced section of the North Sea shots recorded at S42.
 Unfiltered, amplitudes uncorrected.



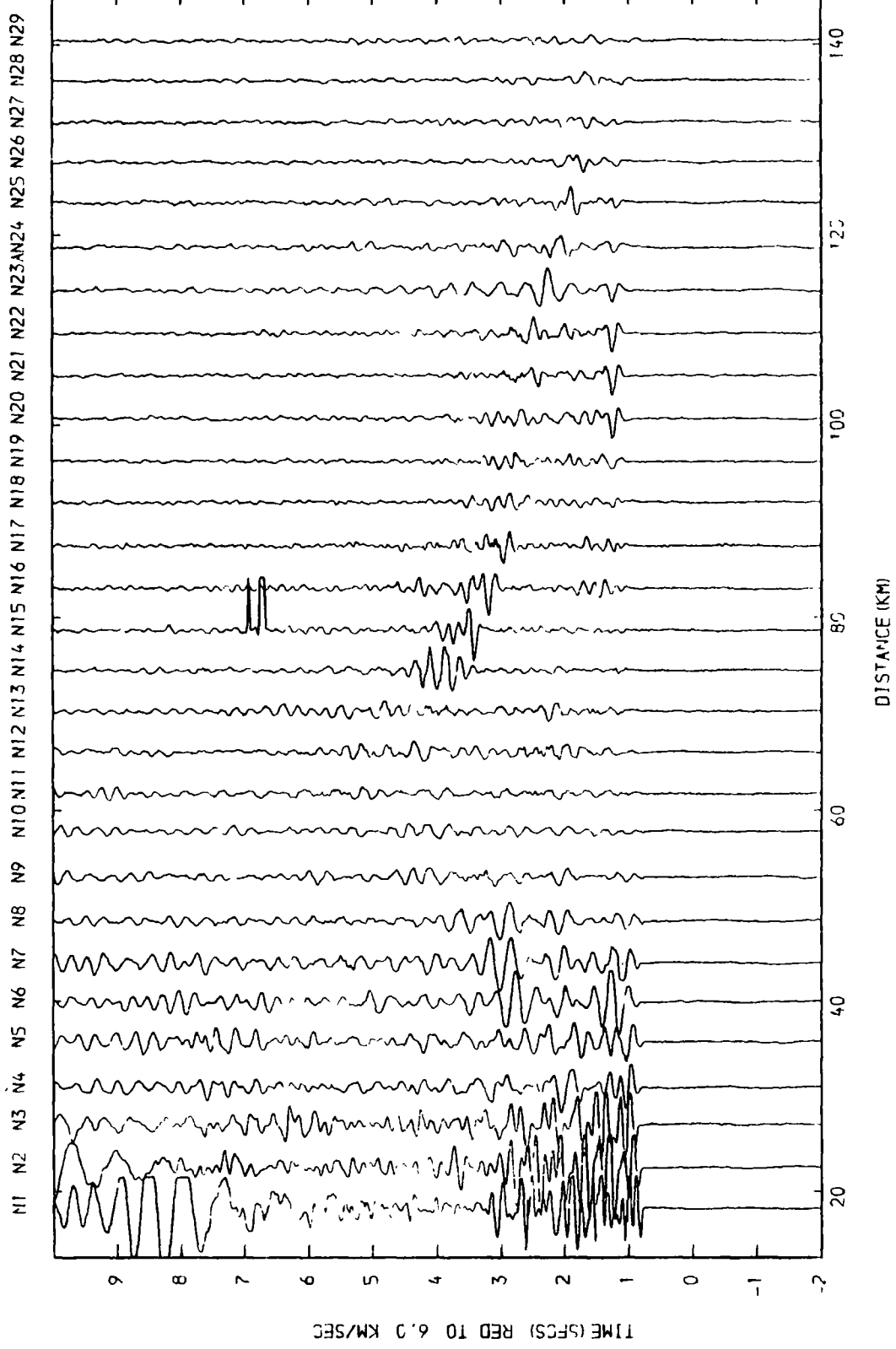
Reduced section of the North Sea shots recorded at S44.
 Unfiltered, amplitudes uncorrected.



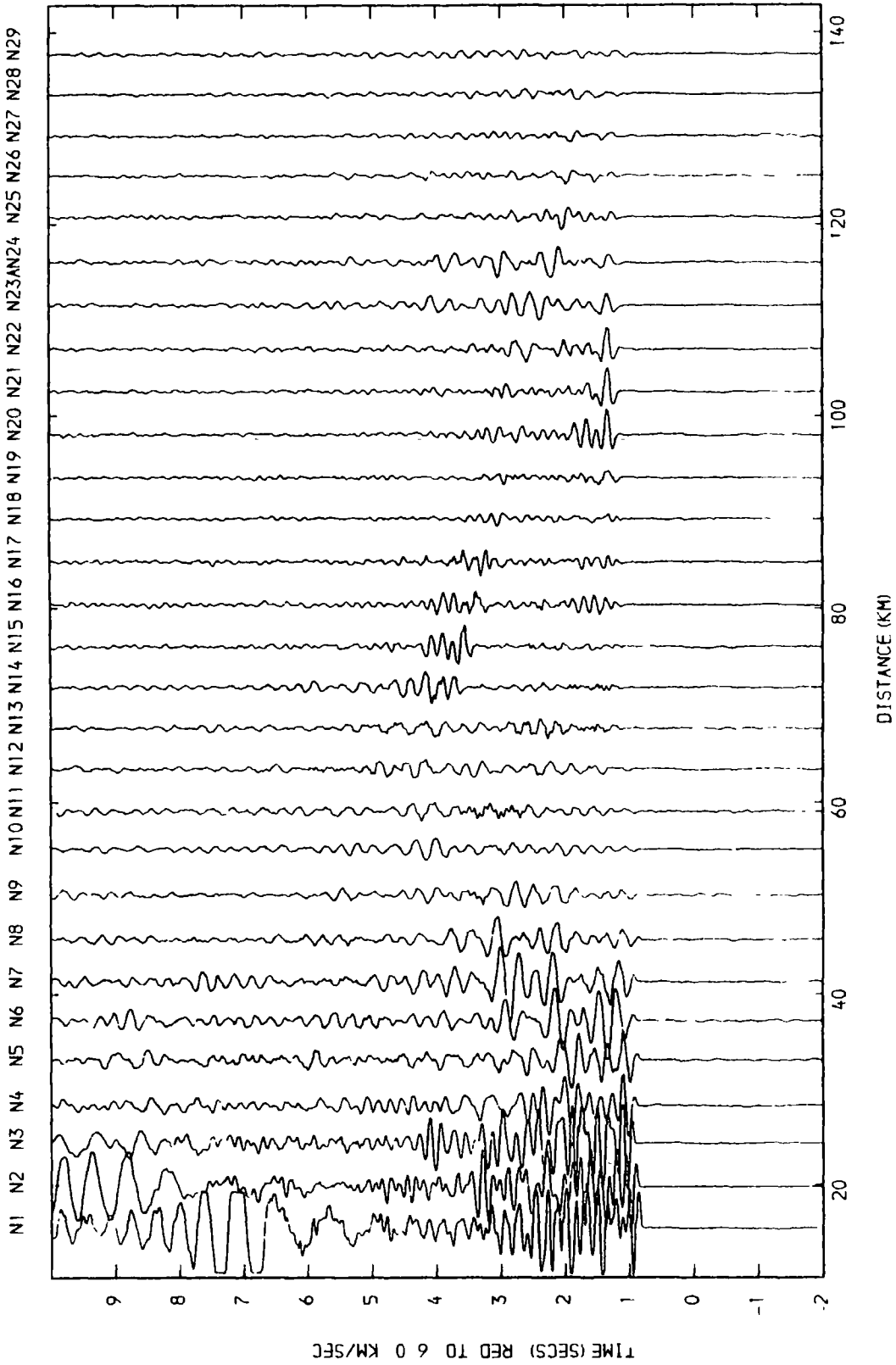
Reduced section of the North Sea shots recorded at S48.
 Unfiltered, amplitudes uncorrected.



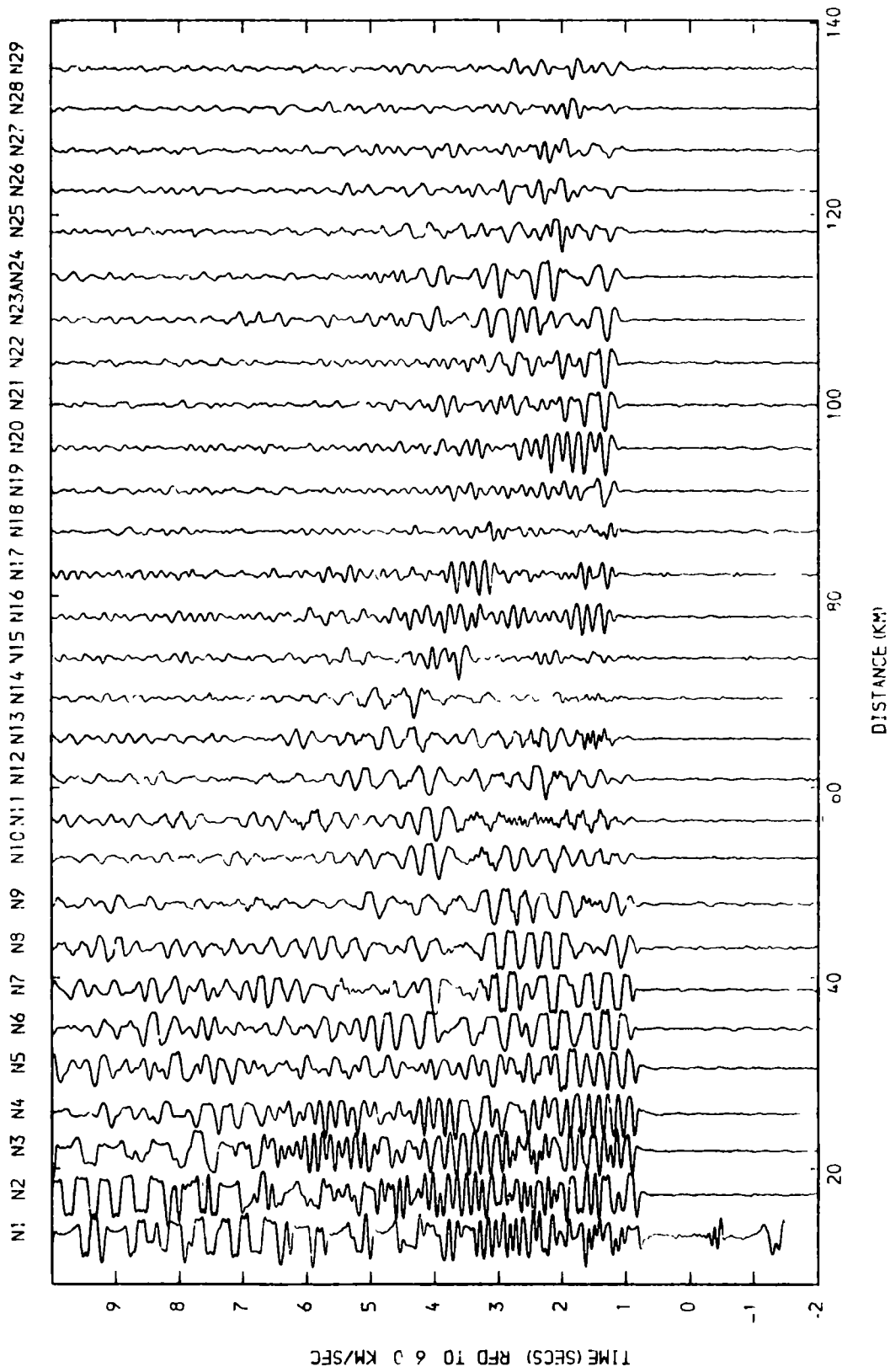
Reduced section of the North Sea shots recorded at S49.
 Unfiltered, amplitudes uncorrected.



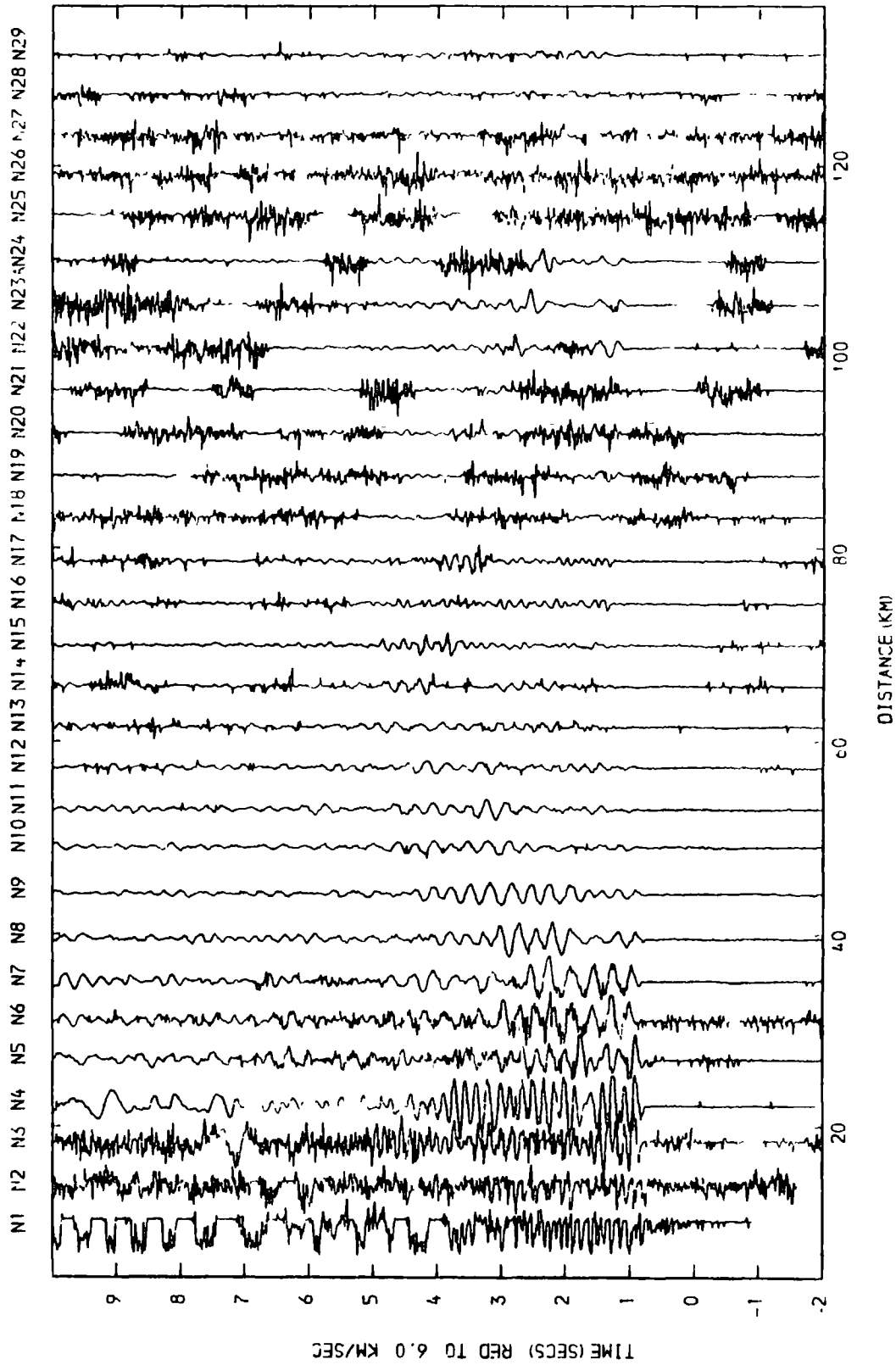
Reduced section of the North Sea shots recorded at S55.
 Unfiltered, amplitudes uncorrected.



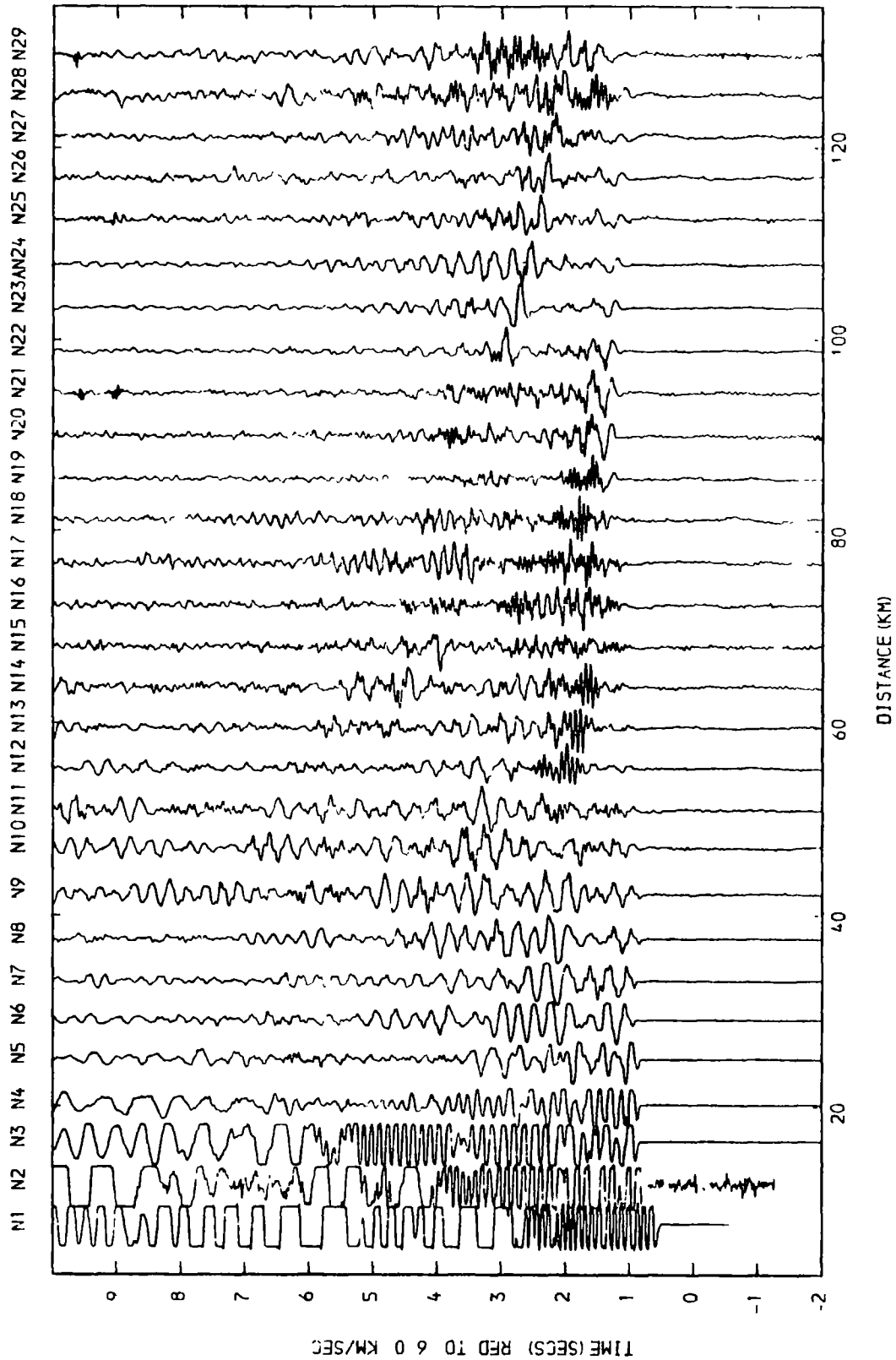
Reduced section of the North Sea shots recorded at S56.
 Unfiltered, amplitudes uncorrected.



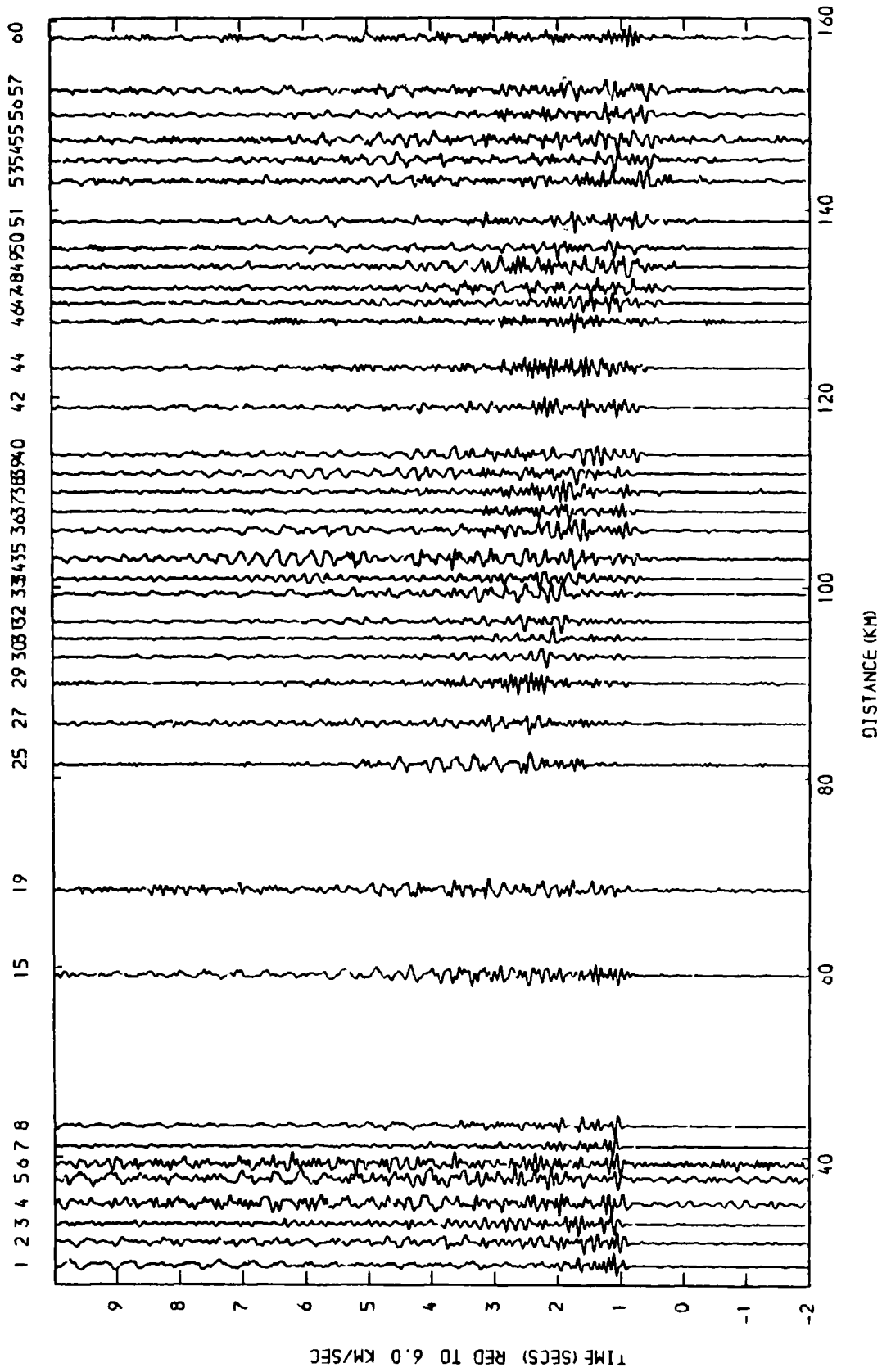
Reduced section of the North Sea shots recorded at S57.
 Unfiltered, amplitudes uncorrected.



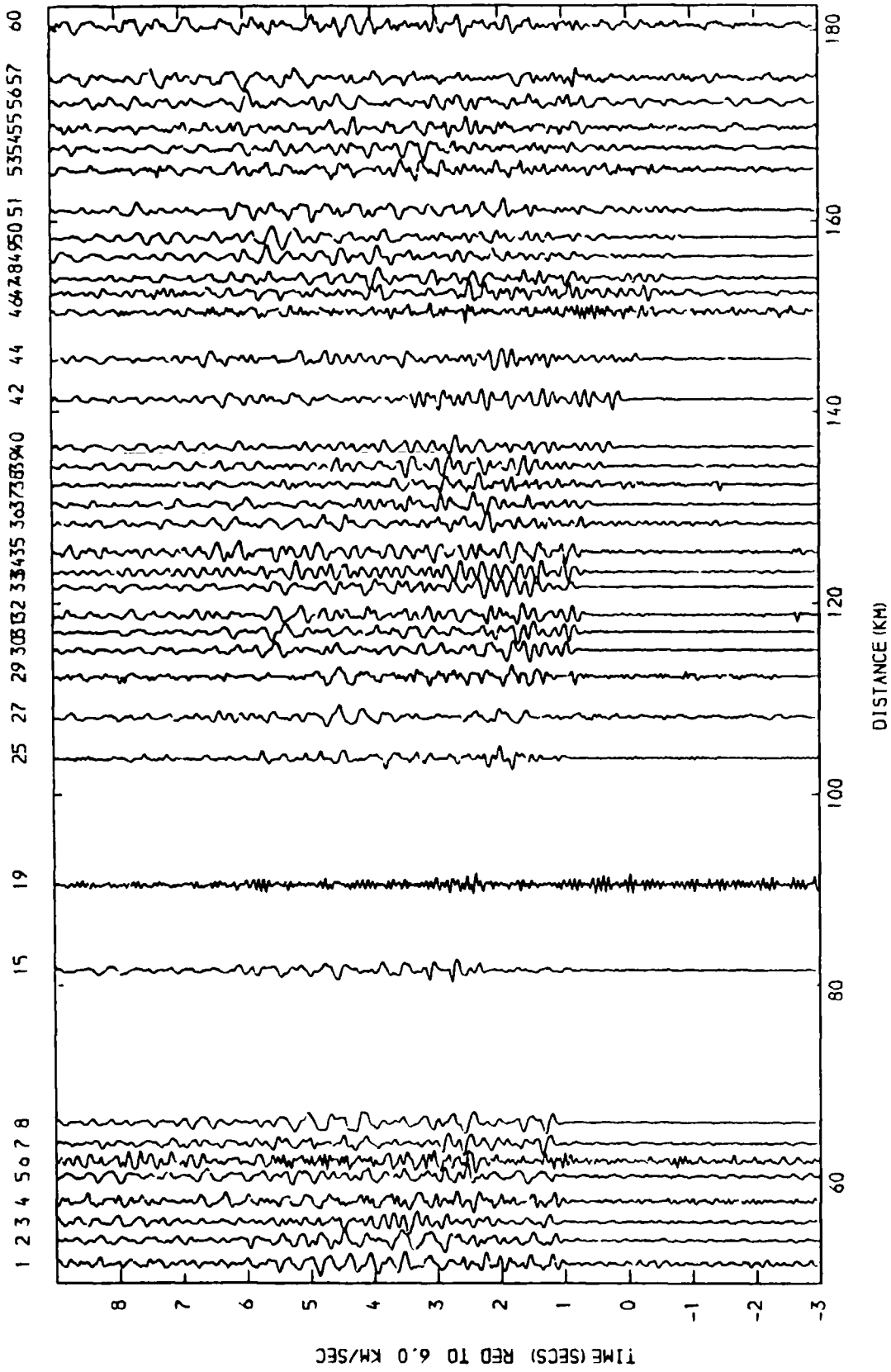
Reduced section of the North Sea shots recorded at S59.
 Unfiltered, amplitudes uncorrected.



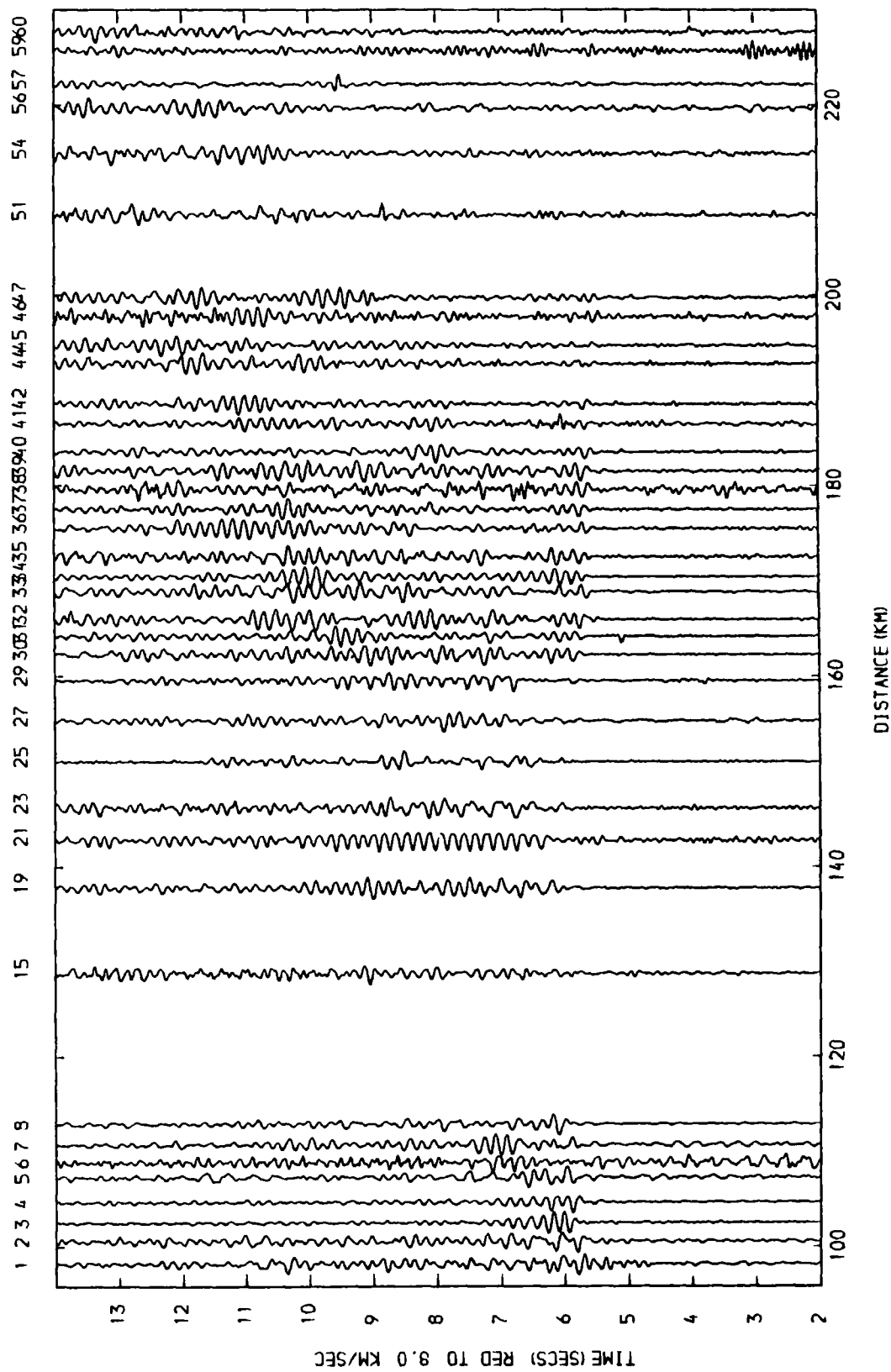
Reduced section of the North Sea shots recorded at S60.
 Unfiltered, amplitudes equalised.



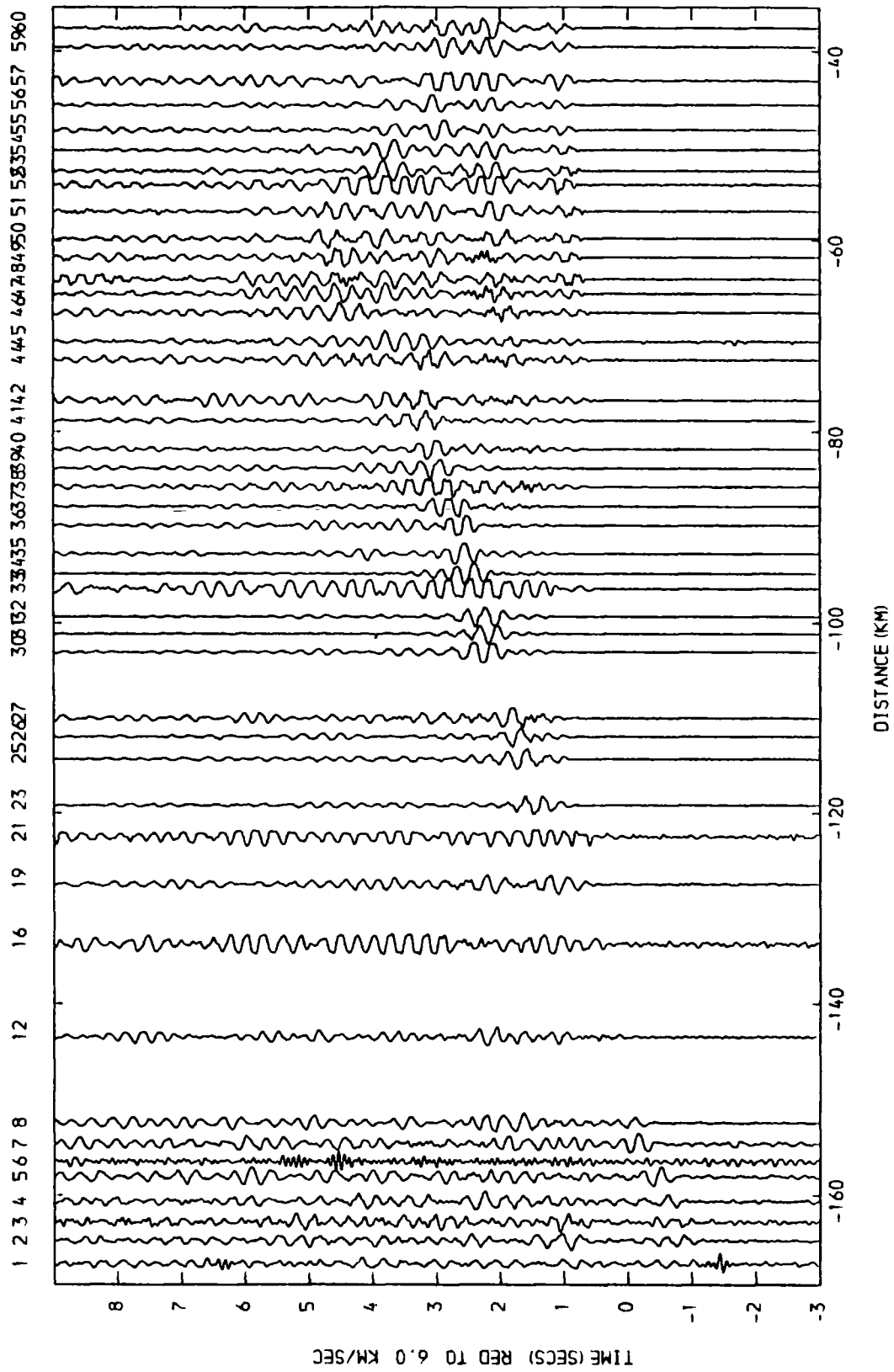
Reduced section for shot M2. Filtered 2-12 Hz, amplitudes equalised.



Reduced section for shot M7. Filtered 2-12 Hz, amplitudes equalised.



Reduced section for shot M18. Filtered 2-12 Hz, amplitudes equalised.



Reduced section for shot N8. Filtered 2-12 Hz, amplitudes equalised.

APPENDIX B

SHOT AND STATION INFORMATION

Analogue tapes are stored in the Department of Geological Sciences Seismic Processing Laboratory, room 233, with the cruise report and cruise logs. The cruise (Shack 6/82) merge-merge data tape is stored on the departmental NUMAC number, GPT9, and is called GPT9:SHK682.

The original digital tapes are stored in the Seismic Processing Laboratory, room 235, and duplicates are stored on the departmental NUMAC number GPT9.

RECORDING STATIONS

Sta. No.	Height (m)	Location		Seismometer Type	Recorder Type
		Lat.	Long.		
S1	20	54 47.711N	3 25.664W	Mk.III	Geostore radio link
S1a	21	54 47.679N	3 25.743W	HS 10	Reading cassette
S2	16	54 48.302N	3 23.658W	Mk.III	Geostore radio link
S2a	9	54 48.327N	3 23.731W	HS 10	Durham cassette
S3	41	54 49.064N	3 22.262W	Mk.III	Geostore base stat.
				HS 10	Durham cassette
S4	30	54 49.487N	3 20.389W	Mk.III	Geostore radio link
				HS 10	Reading cassette
S5	18	54 49.866N	3 18.008W	Mk.III	Geostore radio link
S5a	14	54 49.911N	3 17.959W	HS 10	Durham cassette
S6	7	54 50.138N	3 16.617W	Mk.III	Geostore radio link
S7	18	54 50.619N	3 15.085W	:	:
S8	17	54 51.694N	3 13.682W	:	:
S9	15	54 51.159N	3 11.184W	:	:
S10	18	54 52.103N	3 8.878W	:	:
S11	47	54 52.729N	3 7.077W	HS 10	Reading cassette
					Durham cassette
S12	41	54 53.360N	3 5.790W	Mk.III	Geostore radio link
				HS 10	Reading cassette
S13	34	54 53.758N	3 3.219W	Mk.III	Geostore radio link
S13a		54 53.65 N	3 3.35 W	HS10	Reading cassette
S14	38	54 54.315N	3 0.656W	Mk.III	Geostore radio link
S15	16	54 54.654N	2 59.700W	:	:
S16	16	54 55.543N	2 57.562W	Mk.II	Silver box (3 comp)
S17	30	54 55.895N	2 56.241W	HS 10	Reading cassette
S18	21	54 56.258N	2 53.461W	Mk.III	Geostore radio link
S19	21	54 56.532N	2 51.947W	:	:
S20	24	54 57.266N	2 50.464W	:	:
S21	62	54 57.566N	2 47.615W	:	:
S22	60	54 58.189N	2 46.560W	:	:
S23	85	54 58.215N	2 44.659W	:	:
S24	88	54 59.114N	2 42.204W	:	:
S25	104	54 59.615N	2 40.736W	:	:
S26	128	55 0.273N	2 38.841W	:	:
S27	190	55 0.558N	2 37.068W	:	Geostore base stat.
S28	210	55 0.978N	2 35.047W	HS 10	Durham cassette
S29	225	55 1.60 N	2 33.55 W	Mk.III	Geostore radio link
S30	212	55 1.902N	2 30.951W	:	:
S31	209	55 2.298N	2 29.293W	:	:
S32	226	55 2.878N	2 27.900W	:	:
S33	253	55 3.384N	2 25.296W	:	:
S33a	253	55 3.377N	2 25.306W	Mk.II	Silver box (3 comp)
S34	279	55 3.841N	2 24.035W	Mk.III	Geostore radio link
S35	258	55 4.255N	2 22.213W	:	:
S36	229	55 5.182N	2 19.884W	:	:
S37	206	55 5.447N	2 18.037W	:	:
S38	198	55 5.879N	2 16.248W	:	:
				HS 10	Reading cassette
S39	165	55 6.052N	2 14.403W	Mk.III	Geostore radio link

RECORDING STATIONS

Sta. No.	Height (m)	Location		Seismometer Type	Recorder Type
		Lat.	Long.		
S40	137	55 6.413N	2 12.634W	:	Geostore base stat.
S41	248	55 7.125N	2 10.132W	:	Geostore radio link
S42	298	55 7.717N	2 8.429W	:	:
S43	260	55 8.079N	2 6.308W	:	:
S44	256	55 8.609N	2 4.796W	:	:
S45	230	55 8.998N	2 3.131W	:	:
				HS 10	Reading cassette
S46	241	55 9.835N	2 0.648W	Mk.III	Geostore radio link
S47	219	55 10.028N	1 58.747W	:	:
S48	186	55 10.239N	1 57.340W	:	:
S49	171	55 10.892N	1 55.476W	:	Geostore base stat.
S50	156	55 11.159N	1 53.634W	:	Geostore radio link
S51	125	55 11.883N	1 51.236W	:	:
S52	100	55 12.570N	1 48.880W	Mk.II	Silver box (3 comp)
				HS 10	Reading cassette
S53	143	55 12.628N	1 47.440W	Mk.III	Geostore radio link
S54	181	55 13.170N	1 45.577W	:	Geostore base stat.
S55	114	55 13.523N	1 43.655W	:	:
S56	85	55 14.157N	1 41.386W	:	:
S57	51	55 14.533N	1 39.058W	:	:
				HS 10	Reading cassette
S58	49	55 14.753N	1 37.084W	Mk.III	Geostore radio link
				HS 10	Reading cassette
S59	35	55 15.237N	1 35.931W	Mk.III	Geostore radio link
				HS 10	Reading cassette
S60	5	55 15.450N	1 34.030W	Mk.III	Geostore radio link
S31N	272	55 6.50 N	2 32.94 W	Mk.III	Geostore radio link
S31S	420	54 59.843N	2 29.376W	:	:
				HS 10	Reading cassette
S61	43	55 27.772N	1 36.237W	Mk.II	Wooden box
S62	41	55 36.365N	1 48.579W	:	:
S63	70	55 23.345N	1 41.606W	:	:
S71	232	55 9.907N	2 0.430W	HS 10	Reading cassette
S72	201	55 4.680N	2 19.691W	:	:
S73	24	55 10.007N	2 2.830W	Mk.II	Silver box
S74	8	55 15.730N	1 34.885W	HS 10	Reading cassette
Scotland					
S81	56	54 41.674N	4 24.806W	Mk.II	Wooden box
S82	40	54 47.055N	4 5.768W	:	Durham cassette

RECORDING STATIONS

Sta. No.	Height (m)	Location		Seismometer Type		Recorder Type
		Lat.	Long.			
Isle of Man						
S91	149	54 18.769N	4 27.472W	Mk.II		Wooden box
S92	59	54 23.13 N	4 25.14 W	:		Durham cassette
Northumberland						
S100	43	55 12.902N	1 37.412W	HS 10		Reading cassette
S100a	43	55 12.899N	1 37.398W	:		:
S101	49	55 16.973N	1 40.270W	:		Durham cassette
S102	58	55 17.17 N	1 40.49 W	:		Reading cassette
S103	71	55 20.070N	1 41.155W	:		Durham cassette
S104	88	55 21.37 N	1 40.34 W	:		:
Weardale						
S111	283	54 36.519N	2 26.552W	HS 10		Durham cassette
S112				:		:
S113				:		:

Stations suffixed by an a are located within approximately 200 m of the station with the same number.

LAND SHOTS

Shot	Location		Time		Date
	Lat.	Long.			
Spadeadam	55 0.997N	2 35.064W	18 42 36.325	+/-0.005	2/7/82
Kirk`ton	55 9.938N	2 0.437W	15 09.43.746	+/-0.005	8/7/82

SHANNON SHOTS

Shot	Location		Time		Date
	Lat.	Long.			
K R 1	52 36.02N	9 29.11W	13 23 1.91		9/7/82
K R 2a	52 36.05N	9 28.57W	19 09 55.61		9/7/82
L H 1	52 37.48N	9 59.15W	13 40 29.7		8/7/82

SHOT LOCATION AND TIMES FOR THE IRISH SEA

Lat. and Long. taken from Decca fixes. Errors in shot location approx. +/- 100 m.

Error in shot time +/-0.03 s.

3 July 1982

<u>Shot</u>	<u>Lat.</u>	<u>Long.</u>	<u>Time(G.M.T)</u>	<u>Depth(m)</u>
M1	54 42.35N	3 48.56W	8 34 35.18	33
M2	54 41.68N	3 50.18W	9 3 36.03	36
M3	54 40.64N	3 53.80W	9 17 32.80	42
M4	54 39.64N	3 57.69W	9 32 17.06	47
M5	54 38.74N	4 1.35W	9 45 55.21	55
M6	54 37.74N	4 5.42W	10 1 14.86	60
M7	54 36.81N	4 9.16W	10 16 6.01	64
M8	54 35.83N	4 12.55W	10 32 8.57	65
M9	54 34.97N	4 15.90W	10 45 40.95	63
M10	54 34.02N	4 19.69W	11 1 8.95	56
M11	54 33.01N	4 23.68W	11 16 3.55	67
M12	54 32.01N	4 27.59W	11 31 13.61	47
M13	54 30.95N	4 31.35W	12 31 29.63	55
M14	54 29.70N	4 35.40W	12 46 24.20	55
M15	54 28.93N	4 38.97W	13 0 46.38	63
M16	54 27.84N	4 42.83W	13 17 14.92	59
M17	54 26.88N	4 45.86W	13 32 18.89	53
M18	54 26.06N	4 48.85W	13 47 7.69	70
M19	54 25.09N	4 52.15W	14 2 43.24	61
M20	54 23.89N	4 55.96W	14 17 0.98	95
M21	54 22.93N	5 0.02W	14 31 43.78	139
M22	54 21.95N	5 3.97W	14 46 1.19	134
M23	54 20.91N	5 7.57W	15 0 35.62	134
M24	54 19.77N	5 11.09W	15 15 32.78	133
M25a	54 18.83N	5 14.44W	15 30 39.63	97
M25b	54 18.78N	5 14.67W	16 1 15.26	96
I1a	54 14.59N	5 22.22W	16 51 17.39	57
I2a	54 10.25N	5 34.02W	17 41 53.72	37
I3a	54 5.84N	5 45.55W	18 31 28.24	34
I4a	54 0.80N	5 56.48W	19 32 21.10	36
I5a	53 54.51N	6 7.90W	20 32 3.35	31

4 July 1982

I1b	54 14.76N	5 22.43W	15 51 10.14	57
I2b	54 10.30N	5 33.83W	16 41 16.42	38
I3b	54 5.90N	5 45.51W	17 32 32.11	33
I4b	54 0.77N	5 56.31W	18 31 35.13	35
I5b	53 54.68N	6 7.68W	19 32 1.38	30

All shots fired on the sea bottom and 150 kg except for M25b which was 450 kg

SHOT LOCATIONS AND TIMES FOR THE NORTH SEA

Lat. and Long. taken from Decca fixes. Errors in shot location approx. +/- 100 m

Error in shot time +/-0.03 s.

11 July 1982

<u>Shot</u>	<u>Lat.</u>	<u>Long.</u>	<u>Time (G.M.T)</u>	<u>Depth (m)</u>
N1	55 17.39N	1 27.87W	8 32 25.32	51
N2	55 18.29N	1 24.13W	8 47 30.31	61
N3	55 19.26N	1 20.18W	9 2 7.87	64
N4	55 20.11N	1 16.80W	9 16 2.28	74
N5	55 21.11N	1 12.62W	9 30 59.35	81
N6	55 21.92N	1 8.99W	9 46 5.87	97
N7	55 22.84N	1 5.48W	10 0 53.58	100
N8	55 23.85N	1 1.72W	10 16 17.15	100
N9	55 24.92N	57.73W	10 30 54.57	105
N10	55 26.02N	53.60W	10 45 57.21	105
N11	55 26.78N	50.11W	11 0 54.88	100
N12	55 27.43N	46.12W	11 16 12.53	100
N13	55 28.01N	42.22W	11 31 6.42	98
N14	55 28.97N	38.60W	11 45 56.35	93
N15	55 29.64N	34.78W	12 46 41.39	75
N16	55 30.48N	30.96W	13 1 31.52	73
N17	55 31.29N	27.00W	13 17 7.06	68
N18	55 32.11N	22.96W	13 32 6.60	69
N19	55 33.03N	19.25W	13 46 4.74	74
N20	55 33.98N	15.33W	14 1 8.53	76
N21	55 34.92N	11.39W	14 16 9.56	84
N22	55 35.88N	7.54W	14 30 55.53	82
N23a	55 36.81N	3.52W	14 46 3.11	82
N24	55 37.71N	0.49E	15 1 6.14	79
N25	55 38.69N	4.66E	15 16 25.23	72
N26	55 39.57N	8.44E	15 31 4.17	72
N27	55 40.40N	12.15E	15 46 5.97	74
N28	55 41.27N	16.00E	16 1 5.86	81
N29	55 42.06N	19.71E	16 16 5.06	85
N23b	55 36.90N	3.35W	17 46 7.55	85

All shots fired on the sea bottom and 150 kg except for N23b which was 450 kg.

AMPLIFIER MODULATOR GAINS

The setting on the amp. mod. refers to the input voltage from the seismometer required to produce a 40% deviation of the carrier frequency. Two of the amp. mods. had fewer gain settings than rest, these settings are listed in the second column.

Setting	Setting	Input voltage (mV)
1		250
2		100
3		50
4		25
5	1	10
6	2	5
7	3	2.5
8	4	1.0
9	5	0.5
10	6	0.25

AMPLIFIER MODULATOR SETTINGS

The gains were set as follows for the Spadeadam shot on 2/7/82

Station	Gain	Station	Gain	Station	Gain
S1	6	S23	7	S43	7
S2	1*	S24	7	S44	7
S3	4	S25	7	S45	7
S4	1*	S26	7	S46	7
S5	4	S27	7	S47	7
S6	4	S29	7	S48	7
S7	5	S30	7	S49	8
S8	6	S31	7	S50	7
S9	6	S32	7	S51	7
S10	6	S33	7	S53	7
S12	7	S34	7	S54	7
S13	7	S35	7	S55	7
S14	7	S36	7	S56	7
S15	7	S37	7	S57	7
S18	7	S38	7	S58	7
S19	7	S39	7	S59	7
S20	7	S40	7	S60	7
S21	7	S41	7	S31N	7
S22	7	S42	7	S31S	7

* These amp mods had the different gain settings as mentioned in the previous table.

These gain settings were maintained for the duration of the survey except for the following changes.

Station	Time	Date	Gain change
S5	15:45	3/7/82	4 to 5
S1	8:28	7/7/82	6 to 7
S3	8:50	:	4 to 5
S5	9:23	:	5 to 6
S6	9:37	:	4 to 5
S7	9:46	:	5 to 6
S8	10:06	:	6 to 7
S9	10:29	:	6 to 7
S10	10:55	:	6 to 7
S2	8:21	9/7/82	1 to 2
S4	8:52	:	1 to 2

POLARITY OF GEOSTORE STATIONS

Normal polarity (N) is defined as the most common polarity exhibited. The stations exhibiting the opposite polarity are noted as being reversed (R). These polarities were determined from the first motion of first arrivals. Where no polarity is indicated no unambiguous direction of first motion has been seen for these stations.

Station	Polarity	Station	Polarity	Station	Polarity
S1	N	S23	R	S43	N
S2	N	S24	N	S44	N
S3	N	S25		S45	N
S4	N	S26	N	S46	N
S5	N	S27	N	S47	N
S6	N	S29	N	S48	N
S7	N	S30	N	S49	N
S8	N	S31	R	S50	N
S9	N	S32	N	S51	N
S10		S33		S53	R
S12	N	S34	N	S54	N
S13		S35	N	S55	N
S14	N	S36	R	S56	R
S15		S37	N	S57	N
S18	N	S38	N	S58	N
S19	N	S39	N	S59	N
S20		S40	N	S60	N
S21		S41	N	S31N	N
S22		S42	N	S31S	

GEOSTORE TAPES

Base Station S3

Geostore A

Stations recorded at this geostore were:- S1,S2,S3,S4,S5,S6,S7,S8
S9,S10

Internal clock set to G.M.T. and to day 1 on June 1 i.e. 3 July =
day 33

Tape No	Speed	Start		End	
		Time	Date	Time	Date
S3A/1	15/160	11:45	2/7/82	7:40	5/7/82
S3A/2	15/160	7:55	5/7/82	10:53	8/7/82
S3A/3	15/160	11:07	8/7/82	7:48	11/7/82
S3A/4	15/160	8:00	11/7/82	19:10	14/7/82

Geostore B

Stations recorded at this geostore were:- S1,S2,S3,S4,S5,S6,S7,S8
S9,S10

Internal clock set the same as Geostore B

Tape No	Speed	Start		End	
		Time	Date	Time	Date
S3B/1	15/160	11:45	2/7/82	22:55	5/7/82
S3B/2	15/160	9:49	6/7/82	8:10	9/7/82
S3B/3	15/160	8:35	9/7/82	9:20	12/7/82
S3B/4	15/160	9:35	12/7/82	20:45	15/7/82

Base Station S27

Geostore A

Stations recorded at this geostore were:- S13,S15,S19,S21,S23,S25
S27 & from 7/7/82 S18,S24,S26

The internal clock for A & B was set to the Julian day and G.M.T.

Tape No	Speed	Start		End	
		Time	Date	Time	Date
S27A/1	15/160	11:00	2/7/82	22:00	5/7/82
S27A/2	15/160	9:15	7/7/82	14:09	10/7/82
S27A/3	15/160	14:40	10/7/82	13:01	13/7/82
S27A/4	15/320	13:05	13/7/82	11:20	20/7/82

GEOSTORE TAPES

Base Station S27

Geostore B

Stations recorded at this geostore were:- S12,S14,S18,S20,S22,S24
S26 & from 7/7/82 S23,S25,S27

Tape No	Speed	Start		End	
		Time	Date	Time	Date
S27B/1	15/160	12:42	2/7/82		3/7/82
S27B/2	15/160	16:08	3/7/82	12:40	4/7/82
S27B/3	15/160	13:20	4/7/82	9:54	6/7/82
S27B/4	15/160	9:45	7/7/82	14:20	10/7/82
S27B/5	15/160	14:40	10/7/82	13:10	13/7/82
S27B/6	15/320	13:13	13/7/82	13:10	20/7/82

Base station S29

Stations recorded at this Geostore were:- S29,S30,S31,S32,S33
S31N,S31S

The internal clock was set to the Julian day and to B.S.T.

Tape No	Speed	Start		End	
		Time	Date	Time	Date
S29/1	15/160	11:41	2/7/82	22:15	3/7/82
S29/2	15/160	10:23	6/7/82	13:26	10/7/82
S29/3	15/160	13:42	10/7/82	12:15	13/7/82
S29/4	15/320	12:25	13/7/82	10:55	20/7/82

Base station S40

Geostore A

Stations recorded at this geostore were:- S34,S35,S36,S37,S38,S39
S40,S41

Internal clock set to G.M.T. and to day 1 on June 1 i.e. 7 July =
day 37

Tape No	Speed	Start		End	
		Time	Date	Time	Date
S40A/1	15/320	14:40	26/6/82	14:30	1/7/82
S40A/2	15/160	17:50	2/7/82	5:41	6/7/82
S40A/3	15/160	11:37	6/7/82	12:31	9/7/82
S40A/4	15/160	12:49	9/7/82	1:00	13/7/82

GEOSTORE TAPES

Base Station S40

Geostore B

Stations recorded at this geostore were:- S34,S35,S36,S37,S38,S39
S40,S41

Internal clock set as for geostore A

Tape No	Speed	Start		End	
		Time	Date	Time	Date
S40B/1	15/320	15:35	26/6/82	20:10	1/7/82
S40B/2	15/160	17:54	2/7/82	6:30	6/7/82
S40B/3	15/160	11:43	6/7/82	12:31	9/7/82
S40B/4	15/160	12:48	9/7/82	16:53	12/7/82
S40B/5	15/160	17:00	12/7/82	10:30	16/7/82

Base station S49

Geostore A

Stations recorded at this geostore were:- S42,S43,S44,S45,S46,S47
S48,S49 S50,S51

Internal clock set to G.M.T. but 1 day early i.e. 7 July = day 6

Tape No	Speed	Start		End	
		Time	Date	Time	Date
S49A/1	15/320	14:08	24/6/82	19:40	30/6/82
S49A/2	15/160	13:40	2/7/82	23:20	5/7/82
S49A/3	15/160	11:39	6/7/82	15:35	9/7/82
S49A/4	15/160	15:41	9/7/82	2:32	13/7/82

Geostore B

Stations recorded at this geostore were:- S42,S43,S44,S45,S46,S47
S48,S49,S50,S51

Internal clock set as for geostore A

Tape No	Speed	Start		End	
		Time	Date	Time	Date
S49B/1	15/320	14:28	24/6/82	19:40	30/6/82
S49B/2	15/160	13:15	2/7/82	0:19	6/7/82
S49B/3	15/160	15:15	6/7/82	15:43	9/7/82
S49B/4	15/160	15:57	9/7/82	19:38	12/7/82
49B/5	15/320	20:00	12/7/82	11:00	16/7/82

GHOSTORE TAPES

Base Station S54

Stations recorded at this geostore were:- S54,S55,S56,S57,S58,S59
S60

Internal clock set for G.M.T. and for the day in July i.e. 2 July
= day 2

Tape No	Speed	Start		End	
		Time	Date	Time	Date
S54/1	15/320	16:50	25/6/82	18:53	30/6/82
S54/2	15/160	11:40	2/7/82	22:50	5/7/82
S54/3	15/160	16:41	6/7/82	10:41	9/7/82
S54/4	15/160	11:12	9/7/82	20:58	12/7/82
S54/5	15/160	21:10	12/7/82		

GHOSTORE TAPES

Base Station S3

Base Station S27

Track No.	Stations A & B	Track No.	Stations	
			A	B
1	S1	1	S13	S12
2	Int.Clock	2	Int.Clock	
3	S2	3	S15	S14
4	S3	4	S19	S18
5	S4	5	S21	S20
6	S5	6	S23	S22
7		7		
8		8		
9	S6	9	S25	S24
10	S7	10	S27	S26
11	S8	11	S26*	S23*
12	S9	12	S24*	S25*
13	S10	13	S18*	S27*
14	MSF	14		MSF

*These stations were connected from 8:55 7/7/82

Geostore S27B was running fast for most of (all ?) the Irish Sea
shots.

GEOSTORE TAPES

Base Station S29

Track No.	Stations A & B
1	S33
2	Int.Clock
3	S32
4	S31N
5	S31S
6	S30
7	
8	
9	S29
10	S31
11	-
12	-
13	-
14	MSF

Base Station S40

Track No.	Stations A & B
1	S41
2	Int.Clock
3	S40
4	S39
5	S38
6	S37
7	
8	
9	S36
10	S35
11	S34
12	-
13	-
14	MSF

Base Station S49

Track No.	Stations A B
1	S53 S51
2	Int.Clock
3	S50 S50
4	S49 S49
5	S48 S48
6	S47 S47
7	
8	
9	S46 S46
10	S45 S45
11	S44 S44
12	S43 S43
13	S42 S42
14	MSF

Base Station S54

Track No.	Stations
1	-
2	Int.Clock
3	S55
4	S56
5	S57
6	S58
7	
8	
9	S59
10	S60
11	S54
12	-
13	-
14	MSF

SILVER BOX TAPES

Station S16

Silver box No. 4 used with 3 Mk.III seismometers

Ch. 5 In line horizontal seismometer
Ch. 7 Vertical seismometer
Ch. 9 Cross line horizontal seismometer

Tape No.	Gain	Start		End	
		Time	Date	Time	Date
S16/S/1	5	17:10	7/7/82	12:02	10/7/82
S16/S/2	7	12:14	10/7/82		

Station S33

Silver box No. 5 used with 3 Mk.III sesimometers

Ch. 5 In line horizontal seismometer
Ch. 7 Vertical seismometer
Ch. 9 Cross line horizontal seismometer

Tape No.	Gain	Start		End	
		Time	Date	Time	Date
S33/S/1		10:30	2/7/82	21:00	6/7/82
S33/S/2	7	14:00	9/7/82	2:00	14/7/82

Station S52

3 Mk.III seismometers used

Ch. 5 In line vertical seismometer
Ch. 7 Vertical seismometer
Ch. 9 Cross line horizontal seismometer

Tape No.	Gain	Start		End	
		Time	Date	Time	Date
S52/S/1		9:30	3/7/82	12:00	7/7/82
S52/S/2	6	15:27	9/7/82	18:00	13/7/82

SILVER BOX TAPES

Station S73

1 Mk.III seismometer used

Tape No.	Gain	Time	Start Date	Time	End Date
S73/S/1					

WOODEN BOX TAPES

Station S61

Ch. 7 Vertical Mk.III seismometer

Tape No.	Gain	Time	Start Date	Time	End Date
S61/W/1	6	18:50	9/7/82		
S61/W/2	6	6:20	11/7/82		
S61/W/3	7	16:40	12/7/82		

Station S62

Ch. 7 Vertical Mk.III seismometer

Tape No.	Gain	Time	Start Date	Time	End Date
S62/W/1	6	15:30	9/7/82		
S62/W/2	6	7:30	11/7/82		

Station S63

Ch. 7 Vertical Mk.III seismometer

Tape No.	Gain	Time	Start Date	Time	End Date
S63/W/1	6	15:46	12/7/82		

WOODEN BOX TAPES

Station S81

3 Mk.III seismometers used

Ch. 7 Vertical seismometer
Ch. 8 N-S horizontal seismometer
Ch. 9 E-W horizontal seismometer

Tape No.	Gain	Start		End	
		Time	Date	Time	Date
S81/W/1	6*	7:02	3/7/82	21:34	3/7/82
S81/W/2	6	14:13	4/7/82	21:11	4/7/82
S81/W/2	7**	6:47	5/7/82	18:01	5/7/82
S81/W/3	8	18:06	5/7/82	6:06	6/7/82

* Gain at 7 from 8:09 to 9:47

** Gain at 6 from 12:58 to 16:57

Station S91

3 Mk.III seismometers used

Ch. 7 N-S horizontal seismometer
Ch. 8 Vertical seismometer
Ch. 9 E-W horizontal seismometer

Tape No.	Gain	Start		End	
		Time	Date	Time	Date
S91/W/1	6	16:30	2/7/82	21:00	3/7/82
S91/W/2	6	15:06	4/7/82	18:35	5/7/82
S91/W/3	6	18:35	5/7/82	3:30	6/7/82

CASSETTE RECORDER TAPES

Shot	Station No.				
	S1	S5	S11	S12	S17
M1	1/2 R	5/3-4 D	11/3-4 D	-	-
M2	:	:	:	-	17/4 R
M3	1/3 R	:	:	-	:
M4	:	:	:	-	17/5 R
M5	:	:	:	-	:
M6	1/4 R	5/5-6 D	11/5-6 D	12/1 R	:
M7	:	:	:	:	:
M8	:	:	:	:	17/6 R
M9	1/5 R	:	:	12/2 R	:
M10	:	:	:	:	:
M11	:	:	:	:	17/7 R
M12	1/6 R	5/7-8 D	11/7-8 D	:	:
M13	1/7 R	:	:	12/3 R	17/8 R
M14	:	:	:	12/4 R	:
M15	1/8 R	5/9-10 D	11/9-10 D	:	17/9 R
M16	:	:	:	:	:
M17	:	:	:	12/5 R	:
M18	1/9 R	:	:	:	:
M19	:	:	:	:	17/10 R
M20	:	:	:	12/6 R	:
M21	1/10 R	5/11-12 D	11/11-12 D	:	:
M22	:	:	:	:	:
M23	:	:	:	:	17/11 R
M24	1/11 R	:	:	12/7 R	:
M25a	:	:	:	:	:
M25b	1/12 R	5/13-14 D	11/13-14 D	12/8 R	17/12 R
I1a	:	:	:	12/9 R	:
I2a	1/13 R	:	:	12/10 R	17/13 R
I3a	1/14 R	5/15-16 D	11/15-16 D	12/11 R	17/14 R
I4a	1/15 R	:	:	-	17/15 R
I5a	1/17 R	5/18-19 D	11/17 D	-	17/16 R
I1b	1/19 R ²	5/20-21 D	11/20-21 D	-	-
I2b	1/20 R	:	:	-	-
I3b	1/21 R	5/22-23 D	11/22-23 D	-	-
I4b	1/22 R	5/24-25 D	11/24-25 D	-	-
I5b	1/24 R	:	:	-	-

R Reading cassette

D Durham cassette

: Ditto

- No Tape

CASSETTE RECORDER TAPES

Shot	Station No.					
	S28	S38	S71	S72	S82	S92
M1	28/3-4 D	-	71/3 R	72/1 R	82/1-2 D	92/2 D
M2	:	-	:	:	:	:
M3	:	-	71/4 R	:	:	92/3-4 D
M4	:	-	:	72/2 R	:	:
M5	:	-	:	:	:	:
M6	:	-	71/5 R	:	:	:
M7	28/5-6 D	-	:	72/3 R	82/3-4 D	:
M8	:	-	:	:	:	:
M9	:	-	71/6 R	:	:	:
M10	:	-	:	72/4 R	:	92/5-6 D
M11	:	-	:	:	:	:
M12	:	-	:	:	:	:
M13	28/7-8 D	-	71/8 R	72/5 R	82/5-6 D	-
M14	:	-	:	72/6 R	:	-
M15	:	-	:	:	:	-
M16	28/9-10 D	-	71/9 R	:	:	-
M17	:	-	:	:	:	92/7-8 D
M18	:	-	:	72/7 R	82/7-8 D	:
M19	:	-	71/10 R	:	:	:
M20	:	-	:	:	:	:
M21	:	-	:	-	:	:
M22	28/11 D	-	:	-	:	:
M23	:	38/1 R	71/11 R	-	:	:
M24	:	:	:	-	:	92/9-10 D
M25a	:	:	:	-	82/9-10 D	:
M25b	28/12-13 D	38/2 R	:	-	:	:
I1a	:	:	71/12 R	-	:	92/11-12 D
I2a	28/14-15 D	38/3 R	71/13 R	-	82/11-12 D	:
I3a	:	38/4 R	71/14 R	-	:	:
I4a	28/16-17 D	38/5 R	71/16 R	-	:	92/13-14 D
I5a	:	38/6 R	71/18 R	-	82/13-14 D	92/15 D
I1b	28/20-21 D	-	-	-	-	92/16-17 D
I2b	:	-	-	72/8 R	-	:
I3b	28/22-23 D	-	-	72/9 R	-	92/18-19 D
I4b	:	-	-	72/10 R	-	:
I5b	28/24-25 D	-	-	72/11 R	-	92/20 D

CASSETTE RECORDER TAPES

Shot	Station No.					
	S11	S17	S28	S52	S57	S71
N1	-	17/25 R	28/45-46 D	52/1 R	-	71/21 R
N2	-	:	:	:	57/1 R	:
N3	-	:	:	:	:	:
N4	11/27-28 D	17/26 R	:	52/2 R	:	71/22 R
N5	:	:	:	:	57/2 R	:
N6	:	:	:	:	:	:
N7	:	17/27 R	:	52/3 R	:	71/23 R
N8	:	:	28/47-48 D	:	:	:
N9	:	:	:	:	57/3 R	:
N10	11/29-30 D	:	:	52/4 R	:	:
N11	:	17/28 R	:	:	:	71/24 R
N12	:	:	:	:	57/4 R	:
N13	:	:	:	:	:	:
N14	:	17/29 R	28/49-50 D	52/5 R	:	:
N15	11/31-32 D	17/30 R	:	52/6 R	57/6 R	71/26 R
N16	:	:	:	:	:	:
N17	:	:	:	52/7 R	:	:
N18	:	17/31 R	28/51-52 D	:	:	71/27 R
N19	11/33-34 D	:	:	:	57/7 R	:
N20	:	:	:	52/8 R	:	:
N21	:	17/32 R	:	:	:	:
N22	:	:	:	:	:	71/28 R
N23a	:	:	:	52/9 R	:	:
N24	:	17/33 R	28/53-54 D	:	57/8 R	:
N25	11/35-36 D	:	:	:	:	:
N26	:	:	:	52/10 R	:	71/29 R
N27	:	:	:	:	:	:
N28	:	17/34 R	:	:	57/9 R	:
N29	:	:	:	52/11 R	:	71/30 R
N23b	11/37-38 D	17/36 R	28/55-56 D	-	57/11 R	71/31 R

CASSETTE RECORDER TAPES

Station No.

Shot	S74	S111	S112	S113	S31S
N1	-	111/1-2 D	112/1-2 D	-	31S/1 R
N2	74/3 R	:	:	-	:
N3	:	:	:	-	:
N4	:	:	:	113/1-2 D	31S/2 R
N5	:	:	:	:	:
N6	74/4 R	:	:	:	:
N7	:	111/3-4 D	112/3-4 D	113/3-4 D	31S/3 R
N8	:	:	:	:	:
N9	:	:	:	:	:
N10	:	:	:	:	31S/4 R
N11	74/5 R	:	:	:	:
N12	:	:	:	:	:
N13	:	111/5-6 D	112/5-6 D	113/5-6 D	31S/5 R
N14	:	:	:	:	:
N15	74/6 R	:	:	:	31S/6 R
N16	74/7 R	111/7-8 D	:	113/7-8 D	31S/7 R
N17	:	:	112/7-8 D	:	:
N18	:	:	:	:	:
N19	:	:	:	:	:
N20	74/8 R	:	:	:	31S/8 R
N21	:	:	:	:	:
N22	:	111/9-10 D	:	113/9-10 D	:
N23a	:	:	112/9 D	:	31S/9 R
N24	74/9 R	:	:	:	:
N25	:	:	:	:	:
N26	:	:	:	:	31S/10 R
N27	74/10 R	:	:	:	:
N28	:	111/11-12 D	112/10-11 D	113/11-12 D	:
N29	:	:	:	:	31S/11 R
N23b	:	:	112/12 D	-	31S/12 R

Spadeadam shot

Shot time:- 18 42 36.325 2/7/82

Shot instant on cassette 28/1-2 D

Kirkwhelpington shot

Shot time:- 15 9 43.75 8/7/82

Shot instant on cassettes 71/19 R & 71/20 D

Shot also recorded at 17/23 R & 28/40-41 D

STORE 4 TAPES

The explosions and airgun shots were recorded on the Shackleton on 1/4" tape on a Racal Store 4DS recorder.

Shack 6/82 Explosive shots Irish Sea

Tape speed	3 3/4 ips
Channel 1	MSF
Channel 2	Hydrophone
Channel 3	Hull Geophone
Channel 4	Ship's Clock

Shack 6/82 Explosive shots North Sea

Tape speed	3 3/4 ips
Channel 1	MSF
Channel 2	Hydrophone
Channel 3	Hull Geophone
Channel 4	Ship's Clock

LOCATION OF PUSS'S

Irish Sea

North Sea

Explosion line 3/7/82

Explosion line 11/7/82

PUSS No.	Location		PUSS No.	Location	
	Lat.	Long.		Lat.	Long.
P1	54 18.77N	5 16.61W	P1	55 27.35N	0 47.92W
P2	54 18.36N	5 16.24W	P2	55 26.93N	0 47.74W
P3	54 17.98N	5 15.90W	P3	55 26.45N	0 47.31W
P4	54 27.14N	4 48.13W	P4	55 37.11N	0 5.19W
P5	54 26.52N	4 47.45W	P5	55 36.58N	0 4.97W
P6	54 26.07N	4 46.79W	P6	55 36.17N	0 4.72W

PUSS WINDOWS IRISH SEA EXPLOSIONS LINE

11 July 1982

PUSS No.	Window	Duration(min)	Shot No.
P1 & P4	1	5	M1
:	2	5	M4
:	3	5	M8
:	4	5	M12
:	5	10	M13
:	6	10	M17
:	7	10	M21
:	8	10	M25a
P2 & P5	1	10	M2
:	2	10	M6
:	3	10	M10
:	4	10	M15
:	5	10	M19
:	6	10	M23
P3 & P6	1	10	M3
:	2	10	M7
:	3	10	M11
:	4	10	M16
:	5	10	M20
:	6	10	M24

The following shots were not recorded:- M5,M9,M14,M18,M22,M25b
I1a to I5a and I1b to I5b

PUSS WINDOWS NORTH SEA EXPLOSIONS LINE

3 July 1982

PUSS No.	Window	Duration(min)	Shot No.
P1 & P4	1	5	N1
:	2	5	N5
:	3	10	N9
:	4	10	N13
:	5	10	N18
:	6	10	N22
:	7	10	N26
P2 & P5	1	5	N2
:	2	5	N6
:	3	5	N10
:	4	5	N14
:	5	10	N15
:	6	10	N19
:	7	10	N23a
:	8	10	N27
P3 & P6	1	5	N3
:	2	5	N7
:	3	10	N11
:	4	10	N16
:	5	10	N20
:	6	10	N24
:	7	10	N28

The following shots were not recorded:- N4, N8, N12, N17, N21, N25
N29, N23b

AIRGUN PROFILES

CASSETTE TAPES

Irish Sea airgun line

Shooting started:- 9:40 5/7/82
ended :- 3:00 6/7/82

<u>Station</u>	<u>Cassettes</u>	<u>Time</u>
S1	1/25 R - 1/37 R	7:55 - 17:18
S2	2/1-2 D - 2/11 D	7:58 - 16:40
S3	3/1-2 D - 3/11 D	7:51 - 15:45
S4	4/1 R - 4/9 R	8:09 - 15:46
S13	13/3 R - 13/10 R	8:30 - 15:01
S20	20/6 R - 20/14 R	8:22 - 16:00
S28	28/27-28 D - 28/39 D	7:59 - 18:00
S82	82/15-16 D - 82/31-32 D	7:57 - 23:30
S92	92/21-22 D - 92/41-42 D	7:55 - 3:01

North Sea airgun lines

Shooting started:- 18:00 9/7/82
ended :- 7:51 10/7/82

<u>Station</u>	<u>Cassettes</u>	<u>Time</u>
S28	28/44 D	5:58 -
S58	58/1 - 58/2	5:32 - 6:50
S59	59/2 R	5:22 - 5:35

Shooting started:- 20:00 12/7/82
ended :- 2:20 13/7/82

<u>Station</u>	<u>Cassettes</u>	<u>Time</u>
S59	59/3 R - 59/11 R	19:59 - 2:41
S74	74/13 R - 74/21 R	19:58 - 3:02
S100	100/1 R - 100/7 R	21:06 - 2:30
S100a	100a/1 R - 100a/9 R	21:24 - 4:00
S101	101/1-2 D - 101/9 D	21:02 - 3:58
S102	102/1 R - 102/7 R	20:46 - 2:00
S103	103/1-2 D - 103/9 D	20:26 - 3:31
S104	104/1-2 D - 20:15 D	20:15 - 3:05

STORE 4 TAPES

Some of the airgun shots were recorded on 1/4 inch tape on a Racal Store 4DS recorder

Shack 6/82 Airgun shots Irish Sea

Tape speed	3 3/4 ips
Channel 1	Ship's clock
Channel 2	Airgun
Channel 3	Airgun
Channel 4	MSF

Shack 6/82 Airgun shots North Sea

Tape speed	7 1/2 ips
Channel 1	Green hydrophone
Channel 2	Red hydrophone
Channel 3	Blue hydrophone
Channel 4	White hydrophone

The North Sea shots on the second airgun line were recorded from 20:00 every 2 minutes. For the key to the hydrophone colours see Figs. 2.5a and 2.5b.

LOCATION OF PUSS'S

<u>Irish Sea</u>			<u>North Sea</u>		
<u>PUSS No.</u>	<u>Location</u>		<u>PUSS No.</u>	<u>Location</u>	
	<u>Lat.</u>	<u>Long.</u>		<u>Lat.</u>	<u>Long.</u>
	Airgun line 4/7/82			Airgun line 8/7/82	
P7	54 19.09N	5 16.83W	P7	55 27.35N	0 47.90W
P8	54 18.46N	5 16.22W	P8	55 26.99N	0 47.46W
P9	54 17.98N	5 15.80W	P9	55 26.53N	0 47.23W
P10	54 26.97N	4 47.98W	P10	55 37.27N	0 5.14W
P11	54 26.47N	4 47.20W	P11	55 36.72N	0 5.01W
P12	54 26.13N	4 46.83W	P12	55 36.17N	0 4.81W
				Airgun line 12/7/82	
			P1	55 27.17N	0 46.41W
			P2	55 27.18N	0 46.57W
			P3	55 26.94N	0 47.41W
			P4	55 26.83N	0 47.97W
			P5	55 26.55N	0 48.80W
			P6	55 26.50N	0 49.23W

PUSS WINDOWS IRISH SEA AIRGUN LINE

Airgun shots :- started at 9:40 5 July 1982
finished at 3:00 6 July 1982

<u>PUSS No.</u>	<u>Window</u>	<u>Start time</u>	<u>Duration(m)</u>
P7 & P10	1	21:04	10
:	2	22:04	10
:	3	23:04	10
:	4	00:04	10
:	5	01:04	10
:	6	02:04	10
P8 & P11	1	21:24	10
:	2	22:24	10
:	3	23:24	10
:	4	00:24	10
:	5	01:24	10
:	6	02:24	10
P9 & P12	1	20:44	10
:	2	21:44	10
:	3	22:44	10
:	4	23:44	10
:	5	00:44	10
:	6	01:44	10

PUSS WINDOWS NORTH SEA AIRGUN LINE

Airgun shots :- started at 18:00 9 July 1982
finished at 7:51 10 July 1982

<u>PUSS No.</u>	<u>Window</u>	<u>Start time</u>	<u>Duration(m)</u>
P7 & P10	1	18:00	10
:	2	19:00	10
:	3	20:00	10
:	4	21:00	10
:	5	22:00	10
:	6	23:00	10
P8 & P11	1	18:20	10
:	2	19:20	10
:	3	20:20	10
:	4	21:20	10
:	5	22:20	10
:	6	23:20	10
P9 & P12	1	18:40	10
:	2	19:40	10
:	3	20:40	10
:	4	21:40	10
:	5	22:40	10
:	6	23:40	10

PUSS WINDOWS NORTH SEA AIRGUN LINE

Airgun shots :- started at 20:00 12 July 1982
finished at 2:20 13 July 1982

<u>PUSS No.</u>	<u>Window</u>	<u>Start time</u>	<u>Duration(m)</u>
P1	1	20:00	10
:	2	21:00	10
:	3	22:00	10
:	4	23:00	10
:	5	00:00	10
:	6	01:00	10
P2	1	20:09	10
:	2	21:09	10
:	3	22:09	10
:	4	23:09	10
:	5	00:09	10
:	6	01:09	10
P3	1	20:19	10
:	2	21:19	10
:	3	22:19	10
:	4	23:19	10
:	5	00:19	10
:	6	01:19	10
P4	1	20:29	10
:	2	21:29	10
:	3	22:29	10
:	4	23:29	10
:	5	00:29	10
:	6	01:29	10
P5	1	20:39	10
:	2	21:39	10
:	3	22:39	10
:	4	23:39	10
:	5	00:39	10
:	6	01:39	10
P6	1	20:49	10
:	2	21:49	10
:	3	22:49	10
:	4	23:49	10
:	5	00:49	10
:	6	01:49	10

AIRGUN SHOT TIMES

The recording number (Rec) for the Irish Sea shots refers to the number of the recording on the Store 4DS 1/4 inch FM tapes.

The codes IA, IB, IC and NB refer to the shot code on the digital tapes.

Where an airgun shot is close to an explosion, the explosion number is in the comment column.

AIRGUN SHOT TIMES AND LOCATIONS FOR THE IRISH SEA (5-6 JULY)

Maximum estimated error +/-10 ms

<u>Time(G.M.T)</u>	<u>Location</u>		<u>Comments</u>
	<u>Lat.</u>	<u>Long.</u>	
9 41 0.606			Test
9 47 0.606			Rec 2
9 54 0.604			
9 58 0.604	54 42.53N	3 47.94W	IA1
10 0 0.604	54 42.47N	3 48.11W	Rec 3
10 4 0.603	54 42.38N	3 48.49W	M1
10 8 0.603	54 42.28N	3 48.86W	
10 12 0.602	54 42.19N	3 49.24W	
10 16 0.602	54 42.10N	3 49.61W	
10 20 0.602	54 42.01N	3 49.98W	Rec 6
10 24 0.601	54 41.91N	3 50.37W	
10 28 0.601	54 41.81N	3 50.76W	
10 32 0.600	54 41.71N	3 51.14W	
10 36 0.600	54 41.60N	3 51.52W	
10 40 0.600	54 41.50N	3 51.90W	Rec 7
10 44 0.600	54 41.39N	3 52.29W	
10 48 0.599	54 41.27N	3 52.70W	
10 52 0.599	54 41.15N	3 53.12W	
10 56 0.598	54 41.03N	3 53.55W	
11 0 0.598	54 40.90N	3 53.98W	Rec 8
11 4 0.598	54 40.76N	3 54.42W	
11 8 0.597	54 40.64N	3 54.88W	
11 12 0.597	54 40.51N	3 55.33W	IA20
11 16 0.597	54 40.38N	3 55.77W	
11 20 0.596	54 40.26N	3 56.22W	Rec 9
11 24 0.596	54 40.12N	3 56.68W	
11 28 0.596	54 39.98N	3 57.14W	
11 32 0.595	54 39.84N	3 57.61W	
11 36 0.595	54 39.71N	3 58.06W	
11 40 0.595	54 39.57N	3 58.52W	Rec 10
11 44 0.595	54 39.43N	3 59.01W	
11 48 0.594	54 39.29N	3 59.51W	
11 52 0.594	54 39.15N	3 59.98W	
11 56 0.594	54 39.03N	4 0.43W	
12 0 0.593	54 38.90N	4 0.88W	Rec 11
12 4 0.593	54 38.78N	4 1.33W	M5
12 8 0.593	54 38.68N	4 1.80W	
12 12 0.592	54 38.58N	4 2.26W	
12 16 0.592	54 38.48N	4 2.72W	
12 20 0.592	54 38.37N	4 3.18W	Rec 12
12 24 0.592	54 38.27N	4 3.67W	
12 28 0.592	54 38.16N	4 4.15W	
12 32 0.591	54 38.05N	4 4.63W	
12 36 0.591	54 37.94N	4 5.10W	
12 40 0.591	54 37.82N	4 5.57W	Rec 13
12 44 0.591	54 37.70N	4 6.07W	
12 48 0.591	54 37.58N	4 6.57W	

<u>Time (G.M.T)</u>	<u>Location</u>		<u>Comments</u>
	<u>Lat.</u>	<u>Long.</u>	
12 52 0.591	54 37.46N	4 7.09W	
12 56 0.591	54 37.34N	4 7.59W	
12 58 0.591	54 37.28N	4 7.84W	Spurious shot
13 0 0.590	54 37.22N	4 8.09W	Rec 14
13 2 0.590			
13 4 0.590			
13 6 0.590			
13 8 0.590			
13 10 0.590			Rec 15
13 12 0.590			
13 14 0.590			
13 16 0.590			
13 18 0.590			
13 20 0.589	54 36.92N	4 10.42W	Rec 16
13 22 0.589	54 36.97N	4 10.65W	
13 24 0.589	54 37.03N	4 10.87W	
13 26 0.589	54 37.08N	4 11.10W	
13 28 0.589	54 37.14N	4 11.33W	
13 30 0.589	54 37.20N	4 11.56W	Rec 17
13 34 0.589	54 37.32N	4 12.00W	
13 38 0.588	54 37.46N	4 12.44W	
13 42 0.588	54 37.60N	4 12.87W	
13 46 0.588	54 37.75N	4 13.30W	
13 50 0.588	54 37.89N	4 13.73W	Rec 18
13 54 0.587	54 38.03N	4 14.16W	
13 58 0.587	54 38.17N	4 14.60W	
14 2 0.587	54 38.30N	4 15.06W	
14 6 0.586	54 38.41N	4 15.54W	
14 10 0.586	54 38.52N	4 16.03W	Rec 19
14 14 0.586	54 38.63N	4 16.51W	
14 18 0.585	54 38.73N	4 17.01W	
14 22 0.585	54 38.81N	4 17.52W	
14 26 0.585	54 38.88N	4 18.04W	
14 30 0.584	54 38.95N	4 18.56W	Rec 20
14 34 0.584	54 39.01N	4 19.04W	
14 38 0.583	54 39.07N	4 19.51W	
14 42 0.583	54 39.12N	4 19.97W	
14 46 0.582	54 39.17N	4 20.44W	
14 50 0.582	54 39.22N	4 20.93W	Rec 21
14 52 0.582	54 39.24N	4 21.17W	
14 54 0.581	54 39.27N	4 21.42W	
14 56 0.581	54 39.29N	4 21.66W	
14 58 0.580	54 39.32N	4 21.91W	
15 0 0.580	54 39.35N	4 22.15W	Rec 22
15 2 0.580	54 39.36N	4 22.40W	
15 4 0.579	54 39.33N	4 22.63W	MSF suspect
15 6 0.579	54 39.25N	4 22.82W	
15 8 0.578	54 39.11N	4 22.94W	
15 10 0.578	54 38.97N	4 23.01W	Rec 23
15 12 0.578	54 38.82N	4 23.08W	
15 14 0.577	54 38.68N	4 23.15W	

<u>Time (G.M.T)</u>	<u>Location</u>		<u>Comments</u>
	<u>Lat.</u>	<u>Long.</u>	
15 16 0.577	54 38.54N	4 23.21W	
15 18 0.577	54 38.41N	4 23.28W	
15 20 0.576	54 38.28N	4 23.33W	Rec 24
15 22 0.576	54 38.15N	4 23.34W	IB2
15 24 0.575	54 38.03N	4 23.36W	
15 26 0.575	54 37.91N	4 23.38W	
15 28 0.574	54 37.78N	4 23.40W	
15 30 0.574	54 37.63N	4 23.41W	Rec 25
15 32 0.573	54 37.50N	4 23.42W	
15 34 0.573	54 37.36N	4 23.40W	
15 36 0.572	54 37.25N	4 23.37W	
15 38 0.572	54 37.15N	4 23.34W	
15 40 0.571	54 37.04N	4 23.31W	Rec 26
15 42 0.570	54 36.92N	4 23.24W	
15 44 0.570	54 36.81N	4 23.16W	
15 46 0.569	54 36.70N	4 23.08W	
15 48 0.569	54 36.58N	4 23.00W	
15 50 0.568	54 36.47N	4 22.91W	Rec 27
15 52 0.568	54 36.36N	4 22.83W	
15 54 0.567	54 36.24N	4 22.75W	
15 56 0.567	54 36.12N	4 22.66W	
15 58 0.566	54 36.00N	4 22.58W	
16 0 0.566	54 35.88N	4 22.50W	Rec 28
16 2 0.565	54 35.76N	4 22.40W	
16 4 0.564	54 35.64N	4 22.30W	
16 6 0.564	54 35.51N	4 22.20W	
16 8 0.563	54 35.39N	4 22.10W	
16 10 0.562	54 35.26N	4 22.01W	Rec 29
16 12 0.562	54 35.14N	4 21.91W	
16 14 0.561	54 35.02N	4 21.82W	
16 16 0.560	54 34.89N	4 21.71W	
16 18 0.560	54 34.77N	4 21.62W	
16 20 0.559	54 34.63N	4 21.55W	Rec 30
16 22 0.559	54 34.50N	4 21.49W	
16 24 0.558	54 34.37N	4 21.44W	
16 26 0.558	54 34.24N	4 21.40W	
16 28 0.557	54 34.10N	4 21.37W	
16 30 0.557	54 33.96N	4 21.36W	Rec 31
16 32 0.556	54 33.83N	4 21.37W	
16 34 0.556	54 33.68N	4 21.38W	
16 36 0.555	54 33.54N	4 21.42W	
16 38 0.555	54 33.40N	4 21.47W	
16 40 0.554	54 33.25N	4 21.53W	Rec 32
16 42 0.554	54 33.11N	4 21.58W	
16 44 0.553	54 32.96N	4 21.63W	
16 46 0.553	54 32.82N	4 21.68W	
16 48 0.552	54 32.67N	4 21.72W	
16 50 0.552	54 32.53N	4 21.77W	Rec 33
16 52 0.551	54 32.39N	4 21.82W	
16 54 0.551	54 32.25N	4 21.86W	
16 56 0.550	54 32.10N	4 21.91W	

<u>Time (G.M.T)</u>	<u>Location</u>		<u>Comments</u>
	<u>Lat.</u>	<u>Long.</u>	
16 58 0.550	54 31.96N	4 21.96W	
17 0 0.549	54 31.81N	4 22.01W	Rec 34
17 2 0.549	54 31.67N	4 22.04W	
17 4 0.548	54 31.52N	4 22.08W	
17 6 0.548	54 31.38N	4 22.11W	
17 8 0.547	54 31.23N	4 22.14W	
17 10 0.547	54 31.08N	4 22.17W	Rec 35
17 12 0.546	54 30.93N	4 22.21W	
17 14 0.546	54 30.78N	4 22.24W	
17 16 0.546	54 30.64N	4 22.25W	
17 18 0.545	54 30.49N	4 22.24W	
17 20 0.545	54 30.34N	4 22.22W	Rec 36
17 22 0.545	54 30.20N	4 22.17W	
17 24 0.544	54 30.06N	4 22.13W	
17 26 0.544	54 29.92N	4 22.12W	
17 28 0.544	54 29.79N	4 22.13W	
17 30 0.543	54 29.65N	4 22.13W	Rec 37
17 32 0.543	54 29.51N	4 22.15W	
17 34 0.543	54 29.37N	4 22.16W	
17 36 0.542	54 29.23N	4 22.17W	
17 38 0.542	54 29.09N	4 22.19W	
17 40 0.542	54 28.95N	4 22.22W	Rec 38
17 42 0.542	54 28.80N	4 22.21W	
17 44 0.541	54 28.65N	4 22.18W	
17 46 0.541	54 28.50N	4 22.14W	
17 48 0.541	54 28.35N	4 22.11W	
17 50 0.541	54 28.21N	4 22.07W	Rec 39
17 52 0.541	54 28.07N	4 22.03W	
17 54 0.540	54 27.93N	4 21.99W	
17 56 0.540	54 27.79N	4 21.95W	
17 58 0.540	54 27.64N	4 21.92W	
18 0 0.540	54 27.49N	4 21.90W	Rec 40
18 2 0.540	54 27.34N	4 21.84W	
18 4 0.539	54 27.18N	4 21.80W	
18 6 0.539	54 27.03N	4 21.75W	
18 8 0.539	54 26.86N	4 21.70W	
18 10 0.539	54 26.71N	4 21.72W	Rec 41
18 12 0.538	54 26.66N	4 21.86W	
18 14 0.538	54 26.69N	4 22.04W	
18 16 0.538	54 26.74N	4 22.20W	
18 18 0.538	54 26.77N	4 22.35W	
18 20 0.538	54 26.80N	4 22.49W	Rec 42
18 22 0.537	54 26.87N	4 22.60W	
18 24 0.537	54 26.94N	4 22.72W	Not readable
18 26 0.537	54 27.02N	4 22.84W	
18 28 0.537	54 27.09N	4 22.96W	
18 30 0.537	54 27.17N	4 23.07W	Rec 43
18 32 0.536	54 27.24N	4 23.18W	
18 34 0.536	54 27.30N	4 23.31W	
18 36 0.536	54 27.34N	4 23.44W	
18 38 0.536	54 27.40N	4 23.57W	IB100

<u>Time(G.M.T)</u>	<u>Location</u>		<u>Comments</u>
	<u>Lat.</u>	<u>Long.</u>	
18 40 0.536	54 27.45N	4 23.69W	Rec 44
18 42 0.535	54 27.51N	4 23.81W	
18 44 0.535	54 27.58N	4 23.94W	
18 46 0.535	54 27.64N	4 24.06W	
18 48 0.535	54 27.68N	4 24.19W	
18 50 0.535	54 27.70N	4 24.31W	Rec 45
18 52 0.534	54 27.71N	4 24.45W	
18 54 0.534	54 27.72N	4 24.58W	
18 56 0.534	54 27.73N	4 24.71W	
18 58 0.534	54 27.75N	4 24.84W	
19 0 0.534	54 27.76N	4 24.97W	Rec 46
19 2 0.533	54 27.78N	4 25.09W	
19 4 0.533	54 27.80N	4 25.21W	
19 6 0.533	54 27.84N	4 25.33W	
19 8 0.533	54 27.88N	4 25.45W	
19 10 0.533	54 27.92N	4 25.57W	Rec 47
19 12 0.533	54 27.96N	4 25.69W	
19 14 0.532	54 28.01N	4 25.81W	
19 16 0.532	54 28.05N	4 25.92W	
19 18 0.532	54 28.10N	4 26.04W	
19 20 0.532	54 28.13N	4 26.15W	Rec 48
19 22 0.532	54 28.14N	4 26.27W	
19 24 0.532	54 28.14N	4 26.39W	
19 26 0.531	54 28.14N	4 26.51W	
19 28 0.531	54 28.15N	4 26.62W	
19 30 0.531	54 28.15N	4 26.74W	Rec 49
19 32 0.531	54 28.16N	4 26.87W	
19 34 0.531	54 28.16N	4 26.99W	
19 36 0.530	54 28.17N	4 27.11W	
19 38 0.530	54 28.18N	4 27.23W	
19 40 0.530	54 28.18N	4 27.35W	Rec 50
19 42 0.530	54 28.18N	4 27.47W	
19 44 0.530	54 28.19N	4 27.59W	
19 46 0.529	54 28.19N	4 27.71W	
19 48 0.529	54 28.22N	4 27.83W	
19 50 0.529	54 28.28N	4 27.95W	Rec 51
19 52 0.529	54 28.34N	4 28.06W	
19 54 0.529	54 28.41N	4 28.17W	
19 56 0.528	54 28.48N	4 28.29W	
19 58 0.528	54 28.54N	4 28.40W	
20 0 0.528	54 28.60N	4 28.49W	Rec 52
20 2 0.528	54 28.66N	4 28.60W	
20 4 0.528	54 28.72N	4 28.71W	
20 6 0.527	54 28.79N	4 28.83W	
20 8 0.527	54 28.86N	4 28.94W	
20 10 0.527	54 28.92N	4 29.06W	Rec 53
20 12 0.527	54 28.98N	4 29.17W	
20 14 0.527	54 29.05N	4 29.30W	
20 16 0.526	54 29.11N	4 29.40W	
20 18 0.526	54 29.17N	4 29.50W	
20 20 0.526	54 29.23N	4 29.60W	Rec 54

<u>Time(G.M.T)</u>	<u>Location</u>		<u>Comments</u>
	<u>Lat.</u>	<u>Long.</u>	
20 22 0.526	54 29.29N	4 29.71W	
20 24 0.526	54 29.35N	4 29.82W	
20 26 0.525	54 29.41N	4 29.93W	
20 28 0.525	54 29.47N	4 30.04W	
20 30 0.525	54 29.52N	4 30.15W	Rec 55
20 32 0.525	54 29.58N	4 30.27W	
20 34 0.525	54 29.61N	4 30.39W	
20 36 0.525	54 29.63N	4 30.51W	
20 38 0.524	54 29.66N	4 30.63W	
20 40 0.524	54 29.68N	4 30.75W	Rec 56
20 42 0.524	54 29.70N	4 30.87W	
20 44 0.524	54 29.73N	4 30.98W	
20 46 0.524	54 29.75N	4 31.10W	
20 48 0.524	54 29.74N	4 31.20W	
20 50 0.523	54 29.73N	4 31.30W	Rec 57
20 52 0.523	54 29.70N	4 31.39W	
20 54 0.523	54 29.68N	4 31.47W	
20 56 0.523	54 29.66N	4 31.57W	
20 58 0.523	54 29.64N	4 31.66W	
21 0 0.522	54 29.62N	4 31.75W	Rec 58
21 2 0.522	54 29.60N	4 31.87W	
21 4 0.522	54 29.59N	4 32.00W	
21 6 0.522	54 29.58N	4 32.13W	
21 8 0.522	54 29.59N	4 32.26W	
21 10 0.521	54 29.61N	4 32.40W	Rec 59
21 12 0.521	54 29.63N	4 32.53W	
21 14 0.521	54 29.65N	4 32.67W	
21 16 0.521	54 29.67N	4 32.81W	
21 18 0.521	54 29.70N	4 32.95W	
21 20 0.520	54 29.72N	4 33.08W	Rec 60
21 22 0.520	54 29.74N	4 33.24W	
21 24 0.520	54 29.77N	4 33.40W	
21 26 0.520	54 29.79N	4 33.56W	
21 28 0.520	54 29.82N	4 33.72W	
21 30 0.519	54 29.84N	4 33.88W	Rec 61
21 32 0.519	54 29.86N	4 34.04W	
21 34 0.519	54 29.88N	4 34.20W	
21 36 0.519	54 29.91N	4 34.37W	
21 38 0.519	54 29.93N	4 34.53W	
21 40 0.518	54 29.94N	4 34.67W	Rec 62
21 42 0.518	54 29.90N	4 34.84W	
21 44 0.518	54 29.85N	4 35.01W	
21 46 0.518	54 29.81N	4 35.19W	
21 48 0.517	54 29.77N	4 35.36W	
21 50 0.517	54 29.73N	4 35.52W	Rec 63
21 52 0.517	54 29.69N	4 35.70W	
21 54 0.517	54 29.65N	4 35.88W	
21 56 0.517	54 29.61N	4 36.06W	
21 58 0.516	54 29.57N	4 36.25W	
22 0 0.516	54 29.52N	4 36.44W	Rec 64
22 2 0.516	54 29.47N	4 36.66W	

<u>Time (G.M.T)</u>	<u>Location</u>		<u>Comments</u>
	<u>Lat.</u>	<u>Long.</u>	
22 4 0.516	54 29.42N	4 36.88W	
22 6 0.515	54 29.37N	4 37.10W	
22 8 0.515	54 29.33N	4 37.32W	
22 10 0.515	54 29.28N	4 37.53W	Rec 65
22 12 0.515	54 29.24N	4 37.75W	
22 14 0.514	54 29.19N	4 38.97W	
22 16 0.514	54 29.14N	4 38.19W	
22 18 0.514	54 29.10N	4 38.40W	
22 20 0.514	54 29.05N	4 38.63W	Rec 66
22 22 0.513	54 28.99N	4 38.87W	
22 24 0.513	54 28.94N	4 39.12W	M15
22 26 0.513	54 28.88N	4 39.37W	
22 28 0.513	54 28.82N	4 39.62W	
22 30 0.512	54 28.76N	4 39.87W	Rec 67
22 32 0.512	54 28.70N	4 40.12W	
22 34 0.512	54 28.65N	4 40.37W	
22 36 0.512	54 28.59N	4 40.61W	
22 38 0.511	54 28.54N	4 40.86W	
22 40 0.511	54 28.48N	4 41.11W	Rec 68
22 42 0.511	54 28.42N	4 41.38W	
22 44 0.511	54 28.36N	4 41.65W	
22 46 0.510	54 28.30N	4 41.92W	
22 48 0.510	54 28.24N	4 42.18W	
22 50 0.510	54 28.17N	4 42.44W	Rec 69
22 52 0.509	54 28.10N	4 42.70W	
22 54 0.509	54 28.03N	4 42.96W	
22 56 0.509	54 27.96N	4 43.22W	
22 58 0.508	54 27.89N	4 43.48W	
23 0 0.508	54 27.82N	4 43.74W	Rec 70
23 2 0.508	54 27.74N	4 44.01W	
23 4 0.507	54 27.66N	4 44.29W	
23 6 0.507	54 27.59N	4 44.57W	
23 8 0.507	54 27.51N	4 44.85W	
23 10 0.506	54 27.43N	4 45.12W	Rec 71
23 12 0.506	54 27.35N	4 45.40W	
23 14 0.506	54 27.27N	4 45.68W	
23 16 0.505	54 27.20N	4 45.95W	
23 18 0.505	54 27.12N	4 46.23W	
23 20 0.505	54 27.04N	4 46.51W	Rec 72
23 22 0.504	54 26.96N	4 46.80W	
23 24 0.504	54 26.89N	4 47.09W	
23 26 0.504	54 26.81N	4 47.39W	
23 28 0.503	54 26.74N	4 47.68W	
23 30 0.503	54 26.66N	4 47.98W	Rec 73
23 32 0.503	54 26.58N	4 48.27W	
23 34 0.502	54 26.50N	4 48.56W	
23 36 0.502	54 26.43N	4 48.84W	
23 38 0.502	54 26.36N	4 49.12W	
23 40 0.501	54 26.28N	4 49.41W	Rec 74
23 42 0.501	54 26.21N	4 49.71W	
23 44 0.501	54 26.14N	4 50.01W	

<u>Time (G.M.T)</u>	<u>Location</u>		<u>Comments</u>
	<u>Lat.</u>	<u>Long.</u>	
23 46 0.500	54 26.06N	4 50.30W	
23 48 0.500	54 25.99N	4 50.60W	
23 50 0.500	54 25.92N	4 50.89W	Rec 75
23 52 0.499	54 25.85N	4 51.18W	
23 54 0.499	54 25.78N	4 51.48W	
23 56 0.499	54 25.70N	4 51.78W	
23 58 0.498	54 25.63N	4 52.07W	
0 0 0.498	54 25.56N	4 52.37W	Rec 76
0 2 0.498	54 25.50N	4 52.65W	
0 4 0.497	54 25.44N	4 52.93W	
0 6 0.497	54 25.37N	4 53.22W	
0 8 0.497	54 25.31N	4 53.50W	
0 10 0.496	54 25.24N	4 53.78W	Rec 77
0 12 0.496	54 25.18N	4 54.06W	
0 14 0.496	54 25.12N	4 54.35W	
0 16 0.495	54 25.06N	4 54.62W	
0 18 0.495	54 24.99N	4 54.90W	
0 20 0.494	54 24.93N	4 55.18W	Rec 78
0 22 0.494	54 24.87N	4 55.43W	
0 24 0.494	54 24.81N	4 55.69W	
0 26 0.493	54 24.75N	4 55.94W	
0 28 0.493	54 24.68N	4 56.20W	
0 30 0.493	54 24.63N	4 56.45W	Rec 79
0 32 0.492	54 24.57N	4 56.69W	
0 34 0.492	54 24.50N	4 56.92W	
0 36 0.492	54 24.43N	4 57.15W	
0 38 0.491	54 24.36N	4 57.38W	
0 40 0.491	54 24.29N	4 57.61W	Rec 80
0 42 0.491	54 24.23N	4 57.84W	
0 44 0.490	54 24.16N	4 58.07W	
0 46 0.490	54 24.09N	4 58.30W	
0 48 0.490	54 24.03N	4 58.53W	
0 50 0.489	54 23.96N	4 58.77W	Rec 81
0 52 0.489	54 23.89N	4 59.00W	
0 54 0.489	54 23.83N	4 59.24W	
0 56 0.488	54 23.76N	4 59.47W	
0 58 0.488	54 23.69N	4 59.71W	
1 0 0.488	54 23.62N	4 59.95W	Rec 82
1 2 0.487	54 23.56N	5 0.19W	
1 4 0.487	54 23.50N	5 0.42W	
1 6 0.487	54 23.43N	5 0.65W	
1 8 0.486	54 23.37N	5 0.89W	
1 10 0.486	54 23.31N	5 1.13W	Rec 83
1 12 0.486	54 23.24N	5 1.36W	
1 14 0.485	54 23.18N	5 1.59W	
1 16 0.485	54 23.12N	5 1.82W	
1 18 0.485	54 23.05N	5 2.05W	
1 20 0.484	54 22.99N	5 2.29W	Rec 84
1 22 0.484	54 22.91N	5 2.53W	
1 24 0.484	54 22.84N	5 2.77W	
1 26 0.483	54 22.76N	5 3.01W	

<u>Time (G.M.T)</u>	<u>Location</u>		<u>Comments</u>
	<u>Lat.</u>	<u>Long.</u>	
1 28 0.483	54 22.69N	5 3.25W	
1 30 0.483	54 22.62N	5 3.48W	Rec 85
1 32 0.482	54 22.55N	5 3.71W	
1 34 0.482	54 22.47N	5 3.94W	
1 36 0.482	54 22.39N	5 4.17W	
1 38 0.481	54 22.31N	5 4.40W	
1 40 0.481	54 22.23N	5 4.62W	Rec 86
1 42 0.481	54 22.14N	5 4.85W	
1 44 0.480	54 22.05N	5 5.08W	
1 46 0.480	54 21.96N	5 5.33W	
1 48 0.480	54 21.87N	5 5.56W	
1 50 0.479	54 21.78N	5 5.80W	Rec 87
1 52 0.479	54 21.69N	5 6.03W	
1 54 0.479	54 21.60N	5 6.27W	
1 56 0.478	54 21.50N	5 6.52W	
1 58 0.478	54 21.41N	5 6.76W	
2 0 0.477	54 21.31N	5 7.00W	Rec 88
2 -2 0.477	54 21.22N	5 7.22W	
2 4 0.477	54 21.13N	5 7.45W	
2 6 0.476	54 21.03N	5 7.68W	
2 8 0.476	54 20.95N	5 7.93W	M23
2 10 0.476	54 20.86N	5 8.17W	Rec 89
2 12 0.475	54 20.78N	5 8.41W	
2 14 0.475	54 20.69N	5 8.66W	
2 16 0.475	54 20.61N	5 8.90W	
2 18 0.474	54 20.52N	5 9.14W	
2 20 0.474	54 20.43N	5 9.38W	Rec 90
2 22 0.473	54 20.35N	5 9.62W	
2 24 0.473	54 20.26N	5 9.86W	
2 26 0.473	54 20.18N	5 10.11W	
2 28 0.472	54 20.11N	5 10.35W	
2 30 0.472	54 20.04N	5 10.59W	Rec 91
2 32 0.472	54 19.97N	5 10.81W	
2 34 0.471	54 19.91N	5 11.05W	
2 36 0.471	54 19.86N	5 11.31W	
2 38 0.471	54 19.82N	5 11.57W	
2 40 0.470	54 19.77N	5 11.83W	Rec 92
2 42 0.470	54 19.73N	5 12.10W	
2 44 0.470	54 19.69N	5 12.37W	
2 46 0.469	54 19.65N	5 12.64W	
2 48 0.469	54 19.60N	5 12.91W	
2 50 0.469	54 19.56N	5 13.18W	Rec 93
2 52 0.468	54 19.51N	5 13.45W	
2 54 0.468	54 19.47N	5 13.72W	
2 56 0.467	54 19.42N	5 14.00W	
2 58 0.467	54 19.38N	5 14.27W	
3 0 0.467	54 19.33N	5 14.54W	Rec 94

AIRGUN SHOT TIMES AND LOCATIONS FOR THE 1st NORTH SEA LINE (12/7/82)

Maximum estimated error +/-16 ms

<u>Time(G.M.T)</u>	<u>Location</u>		<u>Comments</u>
	<u>Lat.</u>	<u>Long.</u>	
20 0 0.032	55 16.76N	1 30.92W	Gun 1 test
20 2 0.032	55 16.82N	1 30.72W	Gun 2 test
20 4 0.032	55 16.87N	1 30.51W	Gun 1&2 test
20 6 0.032	55 16.93N	1 30.27W	NB3
20 8 0.032	55 17.00N	1 30.02W	
20 10 0.033	55 17.06N	1 29.77W	
20 12 0.033	55 17.11N	1 29.55W	
20 14 0.033	55 17.16N	1 29.36W	
20 16 0.033	55 17.21N	1 29.16W	
20 18 0.033	55 17.26N	1 28.96W	
20 20 0.033	55 17.31N	1 28.77W	
20 22 0.034	55 17.37N	1 28.54W	
20 24 0.034	55 17.44N	1 28.30W	
20 26 0.034	55 17.50N	1 28.05W	
20 28 0.034	55 17.57N	1 27.80W	
20 30 0.034	55 17.64N	1 27.55W	
20 32 0.034	55 17.71N	1 27.30W	
20 34 0.034	55 17.77N	1 27.05W	
20 36 0.034	55 17.84N	1 26.81W	
20 38 0.035	55 17.90N	1 26.57W	
20 40 0.035	55 17.97N	1 26.34W	
20 42 0.035	55 18.04N	1 26.09W	
20 44 0.035	55 18.12N	1 25.83W	
20 46 0.035	55 18.19N	1 25.56W	
20 48 0.035	55 18.26N	1 25.28W	
20 50 0.035	55 18.33N	1 25.00W	
20 52 0.036	55 18.40N	1 24.72W	
20 54 0.036	55 18.47N	1 24.45W	
20 56 0.036	55 18.53N	1 24.20W	
20 58 0.036	55 18.59N	1 23.94W	
21 0 0.036	55 18.66N	1 23.68W	
21 2 0.036	55 18.73N	1 23.41W	
21 4 0.036	55 18.80N	1 23.15W	
21 6 0.036	55 18.87N	1 22.90W	
21 8 0.037	55 18.93N	1 22.65W	
21 10 0.037	55 18.99N	1 22.40W	
21 12 0.037	55 19.05N	1 22.15W	
21 14 0.037	55 19.11N	1 21.89W	
21 16 0.037	55 19.17N	1 21.63W	
21 18 0.037	55 19.23N	1 21.38W	
21 20 0.037	55 19.28N	1 21.11W	
21 22 0.037	55 19.33N	1 20.83W	
21 24 0.038	55 19.38N	1 20.56W	
21 26 0.038	55 19.43N	1 20.28W	
21 28 0.038	55 19.48N	1 20.01W	
21 30 0.038	55 19.53N	1 19.73W	
21 32 0.038	55 19.58N	1 19.45W	

<u>Time (G.M.T)</u>	<u>Location</u>		<u>Comments</u>
	<u>Lat.</u>	<u>Long.</u>	
21 34 0.038	55 19.63N	1 19.17W	
21 36 0.038	55 19.68N	1 18.90W	
21 38 0.038	55 19.74N	1 18.62W	
21 40 0.039	55 19.79N	1 18.34W	
21 42 0.039	55 19.84N	1 18.07W	
21 44 0.039	55 19.89N	1 17.81W	
21 46 0.039	55 19.94N	1 17.55W	
21 48 0.039	55 19.99N	1 17.28W	
21 50 0.039	55 20.04N	1 17.01W	
21 52 0.039	55 20.08N	1 16.73W	N4
21 54 0.040	55 20.14N	1 16.45W	
21 56 0.040	55 20.19N	1 16.17W	
21 58 0.040	55 20.24N	1 15.90W	
22 0 0.040	55 20.29N	1 15.63W	
22 2 0.040	55 20.35N	1 15.38W	
22 4 0.040	55 20.41N	1 15.12W	
22 6 0.040	55 20.47N	1 14.86W	
22 8 0.040	55 20.53N	1 14.60W	
22 10 0.041	55 20.58N	1 14.34W	
22 12 0.041	55 20.64N	1 14.08W	
22 14 0.041	55 20.71N	1 13.81W	
22 16 0.041	55 20.77N	1 13.54W	
22 18 0.041	55 20.83N	1 13.27W	
22 20 0.041	55 20.90N	1 13.02W	
22 22 0.041	55 20.96N	1 12.79W	
22 24 0.042	55 21.03N	1 12.54W	
22 26 0.042	55 21.10N	1 12.30W	N5
22 28 0.042	55 21.16N	1 12.05W	
22 30 0.042	55 21.23N	1 11.79W	
22 32 0.042	55 21.30N	1 11.53W	
22 34 0.042	55 21.37N	1 11.25W	
22 36 0.042	55 21.43N	1 10.98W	
22 38 0.042	55 21.49N	1 10.73W	
22 40 0.043	55 21.56N	1 10.47W	
22 42 0.043	55 21.63N	1 10.23W	
22 44 0.043	55 21.69N	1 9.99W	
22 46 0.043	55 21.76N	1 9.76W	
22 48 0.043	55 21.82N	1 9.53W	
22 50 0.043	55 21.87N	1 9.30W	
22 52 0.043	55 21.93N	1 9.07W	N6
22 54 0.044	55 22.00N	1 8.83W	
22 56 0.044	55 22.06N	1 8.59W	
22 58 0.044	55 22.12N	1 8.35W	
23 0 0.044	55 22.18N	1 8.11W	
23 2 0.044	55 22.24N	1 7.88W	
23 4 0.044	55 22.30N	1 7.64W	
23 6 0.044	55 22.37N	1 7.41W	
23 8 0.044	55 22.43N	1 7.18W	
23 10 0.045	55 22.49N	1 6.96W	
23 12 0.045	55 22.55N	1 6.73W	
23 14 0.045	55 22.62N	1 6.50W	

<u>Time (G.M.T)</u>	<u>Location</u>		<u>Comments</u>
	<u>Lat.</u>	<u>Long.</u>	
23 16 0.045	55 22.68N	1 6.27W	
23 18 0.045	55 22.75N	1 6.05W	
23 20 0.045	55 22.81N	1 5.82W	
23 22 0.045	55 22.87N	1 5.57W	N7
23 24 0.046	55 22.93N	1 5.32W	
23 26 0.046	55 23.00N	1 5.07W	
23 28 0.046	55 23.06N	1 4.81W	
23 30 0.046	55 23.13N	1 4.56W	
23 32 0.046	55 23.19N	1 4.31W	
23 34 0.046	55 23.26N	1 4.07W	
23 36 0.046	55 23.32N	1 3.83W	
23 38 0.046	55 23.37N	1 3.59W	
23 40 0.047	55 23.43N	1 3.34W	
23 42 0.047	55 23.49N	1 3.09W	
23 44 0.047	55 23.56N	1 2.85W	
23 46 0.047	55 23.63N	1 2.60W	
23 48 0.047	55 23.70N	1 2.35W	
23 50 0.047	55 23.77N	1 2.09W	
23 52 0.047	55 23.84N	1 1.83W	N8
23 54 0.047	55 23.90N	1 1.59W	
23 56 0.048	55 23.97N	1 1.34W	
23 58 0.048	55 24.04N	1 1.09W	
0 0 0.048	55 24.11N	1 0.84W	
0 2 0.048	55 24.17N	1 0.61W	
0 4 0.048	55 24.23N	1 0.39W	
0 6 0.048	55 24.29N	1 0.17W	
0 8 0.048	55 24.35N	59.93W	
0 10 0.049	55 24.41N	59.70W	
0 12 0.049	55 24.47N	59.46W	
0 14 0.049	55 24.53N	59.22W	
0 16 0.049	55 24.60N	58.98W	
0 18 0.049	55 24.66N	58.73W	
0 20 0.049	55 24.72N	58.49W	
0 22 0.049	55 24.80N	58.24W	
0 24 0.049	55 24.88N	57.99W	
0 26 0.050	55 24.97N	57.73W	N9
0 28 0.050	55 25.05N	57.48W	
0 30 0.050	55 25.13N	57.23W	
0 32 0.050	55 25.22N	56.97W	
0 34 0.050	55 25.30N	56.73W	
0 36 0.050	55 25.38N	56.49W	
0 38 0.050	55 25.47N	56.24W	
0 40 0.051	55 25.55N	55.99W	
0 42 0.051	55 25.60N	55.79W	
0 44 0.051	55 25.65N	55.58W	
0 46 0.051	55 25.70N	55.36W	
0 48 0.051	55 25.75N	55.14W	
0 50 0.051	55 25.80N	54.92W	
0 52 0.051	55 25.85N	54.70W	
0 54 0.051	55 25.90N	54.48W	
0 56 0.052	55 25.95N	54.26W	

<u>Time (G.M.T)</u>	<u>Location</u>		<u>Comments</u>
	<u>Lat.</u>	<u>Long.</u>	
0 58 0.052	55 26.00N	54.06W	
1 0 0.052	55 26.05N	53.85W	
1 2 0.052	55 26.12N	53.60W	
1 4 0.052	55 26.19N	53.36W	
1 6 0.052	55 26.26N	53.12W	
1 8 0.052	55 26.33N	52.88W	
1 10 0.053	55 26.40N	52.63W	
1 12 0.053	55 26.46N	52.39W	
1 14 0.053	55 26.53N	52.15W	
1 16 0.053	55 26.60N	51.89W	
1 18 0.053	55 26.66N	51.64W	
1 20 0.053	55 26.73N	51.39W	
1 22 0.053	55 26.80N	51.17W	
1 24 0.053	55 26.86N	50.96W	
1 26 0.054	55 26.92N	50.76W	
1 28 0.054	55 26.99N	50.55W	
1 30 0.054	55 27.05N	50.34W	
1 32 0.054	55 27.11N	50.12W	
1 34 0.054	55 27.17N	49.92W	
1 36 0.054	55 27.23N	49.72W	
1 38 0.054	55 27.29N	49.52W	
1 40 0.054	55 27.35N	49.30W	
1 42 0.054	55 27.40N	49.09W	
1 44 0.054	55 27.45N	48.88W	
1 46 0.054	55 27.49N	48.67W	
1 48 0.054	55 27.54N	48.45W	
1 50 0.055	55 27.59N	48.24W	
1 52 0.055	55 27.64N	48.04W	
1 54 0.055	55 27.69N	47.83W	
1 56 0.056	55 27.74N	47.62W	
1 58 0.056	55 27.80N	47.40W	
2 0 0.056	55 27.84N	47.20W	NB181
2 2 0.056			
2 4 0.056			
2 6 0.056			
2 8 0.056			
2 10 0.056			
2 12 0.056			
2 14 0.056			
2 16 0.056			
2 18 0.056			
2 20 0.057			

To take account of the distance of the airguns behind the ship 0.02 min has been added to the longitude of the original Decca fixes. No change in the latitude was necessary.

TABLE OF JULIAN DAY NUMBERS FOR 1982

23 June	174		
24 June	175	9 July	190
25 June	176	10 July	191
26 June	177	11 July	192
27 June	178	12 July	193
28 June	179	13 July	194
29 June	180	14 July	195
30 June	181	15 July	196
		16 July	197
1 July	182	17 July	198
2 July	183	18 July	199
3 July	184	19 July	200
4 July	185	20 July	201
5 July	186	21 July	202
6 July	187	22 July	203
7 July	188	23 July	204
8 July	189	24 July	205

DIGITAL TAPES

There are two sets of digital tapes, one set is stored in the Department of Geological Sciences Seismic Processing Laboratory, room 235, the other set is kept by NUMAC, the university mainframe computer, stored on the Departmental number GPT9. The digital tapes stored in the SPL are called CSSPNN where NN is the tape number and the tapes kept by NUMAC are called GPT9:CSPNNB. The digital tape name and file number of every tape is store in the data file GPT9:CSSP-TAPES.

Irish Sea shots

Tape name	Stations
CSSP05	S31N, S31S, S32, S33, S34, S35, S36, S37, S38, S39, S40, S41
CSSP06	S1, S2, S3, S4, S5, S6, S7, S8, S9, S10
CSSP09	S54, S55, S56, S57, S58, S59, S60
CSSP10	S42, S43, S44, S45, S46, S47, S51
CSSP11	S13, S15, S19, S21, S48, S49, S50, S53
CSSP13	S23, S25, S27, S29, S30, S31
CSSP19	S91EW, S91, S91NS, S81EW, S81, S81NS
CSSP21	S33T, S33, S33R, S52T, S52, S52R
CSSP22	S11

Irish Sea airgun shots

Tape name	Shots	Stations
CSSP14	IA	S1
CSSP17	IB, IC	S91EW, S91, S91NS, S81EW, S81, S81NS

North Sea explosions

Tape name	Stations
CSSP01	S38, S39, S40, S41, S48, S49, S50, S53
CSSP02	S34, S35, S36, S37, S42, S43, S44, S45, S46, S47, S51
CSSP03	S12, S14, S20, S22, S54, S55, S56, S57, S58, S59, S60
CSSP04	S29, S30, S31, S31N, S31S, S32, S33
CSSP07	S13, S15, S19, S21, S23, S25, S27, S26, S24, S18
CSSP12	S1, S2, S3, S4, S5, S6, S7, S8, S9, S10
CSSP16	S16T, S16, S16R, S52T, S52, S52R, S33T, S33, S33R
CSSP20	S61, S63
CSSP22	S11

North Sea airgun shots

Tape name	Shots	Stations
CSSP14	NB	S54, S56, S57, S58, S59, S60
CSSP18	NB	S61, S63

All stations recording the Spadeadam, Kirkwhelpington and Shannon shots are stored on CSSP15.

The location of every trace in terms of digital tape name and file number is stored in GPT9:CSSP-TAPES.

APPENDIX C

COMPUTER PROGRAMS

PLOT Plots stacked seismic sections.

FREQPLOT Plots amplitude spectra.

CORRNAV Determines the position of a ship given DECCA fixes
 and the ships heading and speed.

```

> 1 C*****
> 2 C
> 3 C
> 4 C
> 5 C
> 6 C
> 7 C
> 8 C
> 9 C
> 10 C
> 11 C
> 12 C
> 13 C
> 14 C
> 15 C
> 16 C
> 17 C
> 18 C
> 19 C
> 20 C
> 21 C
> 22 C
> 23 C
> 24 C
> 25 C
> 26 C
> 27 C
> 28 C
> 29 C
> 30 C
> 31 C
> 32 C
> 33 C
> 34 C
> 35 C
> 36 C
> 37 C
> 38 C
> 39 C
> 40 C
> 41 C
> 42 C
> 43 C
> 44 C
> 45 C
> 46 C
> 47 C
> 48 C
> 49 C
> 50 C
> 51 C
> 52 C
> 53 C
> 54 C
> 55 C
> 56 C
> 57 C
> 58 C*****
> 59 C
> 60 C
> 61 C
> 62 C
> 63 C
> 64 C
> 65 C
> 66 C
> 67 C
> 68 C
> 69 C
> 70 C
> 71 C
> 72 C
> 73 C
> 74 C
> 75 C
> 76 C
> 77 C
> 78 C
> 79 C
> 80 C
> 81 C
> 82 C
> 83 C
> 84 C
> 85 C
> 86 C
> 87 C
> 88 C

```

PLOT

```

PROGRAM FOR PLOTTING REDUCED SECTIONS OF
SEISMIC REFRACTION DATA FROM DIGITAL TAPES WRITTEN
IN THE DURHAM SELF-DEFINING TAPE FORMAT (DSDTF)
AND COPIED FROM TAPE TO DISK USING PROGRAM
GPT9:TR-CSP.COM

$R PLOT.COM+*GHOST
UNIT 1  OUTPUT FROM GPT9:TR-CSP.COM
UNIT 8  OUTPUT OF HEADER BLOCK READ IN FROM UNIT 1
UNIT 7  OUTPUT CONTAINING SAMPLE NUMBERS AND TIMES
        OF THE SECTION IF TRACE PLOTTED
UNIT 9  PLOTFILE

UNITS 5 & 6 ARE USED FOR INTERACTIVE INPUT OF DATA
IF THE SECTION IS REQUIRED UNREDUCED A REDUCTION
VELOCITY OF 0.0 SHOULD BE USED

THERE IS AN UPPER LIMIT OF 32768 BYTES(16384SAMPLES)
OF DATA TO EACH TRACE ON UNIT 1
THE MAXIMUM NO. OF TRACES(N) IS 90
ADDITIONAL RESTRICTIONS ARE:-
    MAX. NO. OF SAMPLES PER TRACE = 126000/N
    UPPER LIMIT OF 10000 SAMPLES

FILTERING OF TRACES GREATER THAN 4096 SAMPLES
IS NOT POSSIBLE

IT HELPS THE AUTOMATIC AMPLITUDE ROUTINE IF
AT LEAST SOME OF THE TRACES ARE IN DISTANCE
ORDER. IT ONLY BREAKS DOWN IF TWO TRACES HAVE
THE SAME OR VERY NEARLY THE SAME RANGE

X(A,B)  - ARRAY WITH THE AMPLITUDE OF SAMPLES
TSAM(A,B) - ARRAY WITH THE TIME OF SAMPLES
        A - TRACE NUMBER
        B - SAMPLE NUMBER

N        - NUMBER OF TRACES
VRED    - REDUCTION VELOCITY (KM/S)
TLEN    - LENGTH OF PLOT (SECONDS)
TSRED   - REDUCED START TIME OF PLOT (SECONDS)

THE PLOT DISTANCES ARE CALCULATED BY GPT9:TR-CSP.COM
FROM THE SHOT AND STATION LAT/LONG ON THE DSDTF TAPE
USING A SUBROUTINE BASED ON THE PROGRAM DISTAZ BY
G. K. WESTBROOK.
THIS PROGRAM USES THE SIGN OF THE AZIMUTH TO PLOT
WEST TO THE RIGHT AND EAST TO THE LEFT. IF ALL PLOTS
ARE REQUIRED WITH INCREASING RANGE TO THE RIGHT THE
AZIMUTH MUST BE POSITIVE.

```

```

THE MAIN ROUTINE EXISTS ONLY TO MAKE THE TRACE
ARRAY, X, INTO A 2-D ARRAY WHOSE DIMENSIONS ARE
DETERMINED BY THE NUMBER OF TRACES

REAL*4 X(126000), TSAM(126000)
WRITE (6,10)
10 FORMAT ('NO. OF TRACES'/'..... 15')
READ (5,20) N
20 FORMAT (15)
30 NARG = 126000 / N
CALL MAINP(N, NARG, X, TSAM)
STOP
END

SUBROUTINE MAINP(N, NARG, X, TSAM)

DIMENSION PROJ(20), TITLE(20), STAR(20), IEVENT(90,5),
1 ISTAT(90,5), DUMP(20), IEVEN(5), ISTAT(5)
REAL*4 ESEC(90), DIST(90), SAMRAT(90), XTEMP(10000), KSSEC(90),
1 GAIN(90), TSAM1(10000), TSAM(N,NARG), X(N,NARG)
REAL*8 DTEVE(90), DTST(90)
INTEGER*4 IEHOUR(90), IEMIN(90), NST(90), NEND(90), KSHOUR(90),
1 KSMIN(90), LX(90), IPOL(90), JSAMP(90), KSDAY(90),
2 IEDAY(90)
INTEGER*2 LEN, ISAM(16500)

```

```

> 89 C
> 90 C READ TITLE
> 91 C
> 92 WRITE (6,10)
> 93 10 FORMAT ('PROJECT TITLE')
> 94 READ (5,60) PROJ
> 95 WRITE (6,20)
> 96 20 FORMAT ('SECTION TITLE')
> 97 READ (5,60) TITLE
> 98 C
> 99 C READ IN PLOTTING PARAMETERS
> 100 C
> 101 WRITE (6,30)
> 102 30 FORMAT ('TRACE LENGTH(SECS) RED.VEL(KM/SEC) AND START TIME'/
> 103 1'(UNREDUCED SECTION RED.VEL=0.0)'/.....-----..... 3F5.2')
> 104 READ (5,40) TLEN, VELR, TSRED
> 105 40 FORMAT (3F5.2)
> 106 WRITE (6,50)
> 107 50 FORMAT ('SECTION TYPE, COM. EVENT=1, COM. STAT.=2, OTHER=0')
> 108 READ (5,210) ITYPE
> 109 C
> 110 C READ HEADING
> 111 C
> 112 READ (1,60) STAR
> 113 READ (1,60) DUMP
> 114 READ (1,60) STAR
> 115 READ (1,60) DUMP
> 116 60 FORMAT (20A4)
> 117 C
> 118 WRITE (7,70)
> 119 70 FORMAT ('FILE START EVENT START 1ST SAMPLE LAST SAMPLE PLO
> 120 1T START RED. PLOT START RED. PLOT END')
> 121 WRITE (7,80)
> 122 80 FORMAT ('TIME (SECS) TIME (SECS) PLOTTED PLOTTED TIM
> 123 1E (SECS) TIME (SECS) TIME (SECS)')
> 124 C
> 125 C READ IN TRACE DATA
> 126 C
> 127 DO 120 I = 1, N
> 128 READ (1,90) (IEVENT(I,J),J=1,2), ELAT, ELONG, EELEV, IEDAY(I),
> 129 1 IEHOUR(I), IEMIN(I), ESEC(I), (ISTAT(I,J),J=1,2), SLAT, SLONG,
> 130 2 SELEV, KSDAY(I), KSHOUR(I), KSMIN(I), KSSEC(I), JSAMP(I),
> 131 3 SAMRAT(I), GAIN(I), IPOL(I), DIST(I), DAZ
> 132 WRITE (8,90) (IEVENT(I,J),J=1,2), ELAT, ELONG, EELEV, IEDAY(I),
> 133 1 IEHOUR(I), IEMIN(I), ESEC(I), (ISTAT(I,J),J=1,2), SLAT, SLONG,
> 134 2 SELEV, KSDAY(I), KSHOUR(I), KSMIN(I), KSSEC(I), JSAMP(I),
> 135 3 SAMRAT(I), GAIN(I), IPOL(I), DIST(I), DAZ
> 136 90 FORMAT (2A4, 2X, 3F12.6, I4, I4, I2, 2X, I2, F8.4, 2X, 2A4, 2X,
> 137 1 3F12.6, I4, I4, I2, 2X, I2, F8.4, 2X, I6, F10.4, 10X,
> 138 2 E10.4, 2X, A4, 2F10.3)
> 139 IF (ITYPE .EQ. 1 .AND. DAZ .LT. 0.0) DIST(I) = -DIST(I)
> 140 IF (ITYPE .EQ. 2 .AND. DAZ .GT. 0.0) DIST(I) = -DIST(I)
> 141 CALL READ(ISAM, LEN, 0, LNUM, 1, &460)
> 142 LENG = LEN / 2
> 143 C
> 144 C CONVERT FILE START TIME AND SHOT TIME TO SECONDS
> 145 C
> 146 CALL SECOND(KSHOUR, KSMIN, KSSEC, DTST, I)
> 147 CALL SECOND(IEHOUR, IEMIN, ESEC, DTEVE, I)
> 148 C
> 149 C DETERMINE WHICH PART OF THE DATA TO PLOT
> 150 C
> 151 CALL SAMPLE(DTST, DTEVE, TSRED, DIST, NST, SAMRAT, NEND, TLEN,
> 152 1 I, VELR, TSAM, NARG, N)
> 153 LX(I) = NEND(I) - NST(I) + 1
> 154 IF (LX(I) .LE. NARG) GO TO 100
> 155 NEND(I) = NST(I) + NARG - 1
> 156 LX(I) = NARG
> 157 100 K = 1
> 158 NS = NST(I)
> 159 NE = NEND(I)
> 160 DO 110 J = NS, NE
> 161 X(I,K) = ISAM(J)
> 162 K = K + 1
> 163 110 CONTINUE
> 164 120 CONTINUE
> 165 C
> 166 C MEAN CORRECT
> 167 C
> 168 CALL MEAN(X, N, LX, NARG)
> 169 C
> 170 C BANDPASS FILTER
> 171 C
> 172 WRITE (6,130)
> 173 130 FORMAT ('FILTERING YES = 1 NO = 0')
> 174 READ (5,210) NI
> 175 IF (NI .NE. 1) GO TO 190
> 176 WRITE (6,140)
> 177 140 FORMAT ('ENTER F1,F2,F3,F4'/.....-----..... 5F5.2')
> 178 READ (5,150) F1, F2, F3, F4
> 179 150 FORMAT (5F5.2)

```

```

> 180      DO 190 J = 1, N
> 181          LXN = LX(J)
> 182          WRITE (7,160) LXN
> 183      160  FORMAT (I5)
> 184          SAMRT = SAMRAT(J)
> 185          DO 170 I = 1, LXN
> 186              XTEMP(I) = X(J,I)
> 187      170  CONTINUE
> 188          CALL BPASS(LXN, F1, F2, F3, F4, XTEMP, SAMRT)
> 189          DO 180 I = 1, LXN
> 190              X(J,I) = XTEMP(I)
> 191      180  CONTINUE
> 192      190  CONTINUE
> 193      C
> 194      C  ADJUST AMPLITUDE
> 195      C
> 196          WRITE (6,200)
> 197      200  FORMAT ('UNC. AMP. PLOT = 0 CORR.AMP. PLOT = 1 OR EQUAL.PLOT = 2')
> 198          READ (5,210) NOR
> 199      210  FORMAT (I1)
> 200          IF (NOR .EQ. 0) GO TO 230
> 201          IF (NOR .EQ. 1) GO TO 220
> 202          CALL NORM(X, N, LX, NARG)
> 203          GO TO 230
> 204      220  CONTINUE
> 205          DO 230 I = 1, N
> 206              IF (GAIN(I) .NE. 0.001221) CALL AMP(X, I, N, LX, GAIN, NARG)
> 207      230  CONTINUE
> 208      C
> 209      C  CHECK AND CHANGE POLARITY
> 210      C
> 211          DO 240 I = 1, N
> 212              IF (IPOL(I) .EQ. 2) CALL POLAR(X, I, N, LX, NARG)
> 213      240  CONTINUE
> 214      C
> 215      C  READ IN PLOT SCALE
> 216      C
> 217          KP = 0
> 218      250  WRITE (6,260)
> 219      260  FORMAT ('TIMESCALE(CM/SEC),DISTANCE(CM/KM),RETURN FOR DEFAULT
> 220          1  "/.....----- 2F5.2')
> 221          READ (5,270) TSCALE, DSCALE
> 222      270  FORMAT (2F5.2)
> 223          IF (TSCALE .EQ. 0.0) TSCALE = 2.0
> 224          IF (DSCALE .EQ. 0.0) DSCALE = 0.4
> 225      C
> 226          IF (KP .EQ. 1) GO TO 280
> 227      C
> 228      C
> 229          CALL AMPFAC(X, N, LX, DIST, NOR, NARG, TSCALE, AMARG)
> 230          AMARG = AMARG * 1.5
> 231      C
> 232      C  PLOT AXES
> 233      C
> 234      280  DMIN = 999.0
> 235          DMAX = -999.0
> 236          DO 290 I = 1, N
> 237              IF (DMAX .LT. DIST(I)) DMAX = DIST(I)
> 238              IF (DMIN .GT. DIST(I)) DMIN = DIST(I)
> 239      290  CONTINUE
> 240          TMIN = TSRED
> 241          TMAX = TSRED + TLEN
> 242          CALL PAPER(1)
> 243          T = (TMAX - TMIN) * TSCALE
> 244      300  D = (DMAX - DMIN + (2*AMARG)) * DSCALE
> 245          CALL PSPACE(0.1, D/25.4 + 0.1, 0.1, T/25.4 + 0.1)
> 246          CALL CSPACE(0.0, D/25.4 + 0.1 + 0.45, 0.0, T/25.4 + TMAX/10.0)
> 247          CALL MAP(DMIN - AMARG, DMAX + AMARG, TMIN, TMAX)
> 248          CALL CTRMAG(8)
> 249          SY = 1.0
> 250          SX = 5.0
> 251          IF (DSCALE .GT. 2.0) SX = 0.5
> 252          IF (TSCALE .GT. 8.0) SY = 0.5
> 253          CALL SCALSI(SX, SY)
> 254      C
> 255      C  LABEL AXES
> 256      C
> 257          CALL PLOTCS(DMIN + (DMAX - DMIN)/2.3, TMIN - 1/TSCALE,
> 258          1  'DISTANCE(KM)', 13)
> 259          CALL CTRORI(1.0)
> 260          CALL PLOTCS(DMIN - AMARG - 1.1/DSCALE, TMIN + 3.0/TSCALE,
> 261          1  'TIME(SECS) RED TO      KM/SEC', 29)
> 262          CALL PLOTNF(DMIN - AMARG - 1.1/DSCALE, TMIN + 6.4/TSCALE, VELR, 1)
> 263          CALL CTRORI(0.0)

```

```

> 264 C
> 265 C PLOT TRACES
> 266 C
> 267 DO 350 I = 1, N
> 268 CALL MAP(DMIN - AMARG - DIST(I), DMAX + AMARG - DIST(I), TMIN,
> 269 1 TMAX)
> 270 NUM = LX(I)
> 271 DO 310 K = 1, NUM
> 272 XTEMP(K) = X(I,K)
> 273 TSAM1(K) = TSAM(I,K)
> 274 310 CONTINUE
> 275 CALL PTPLOT(XTEMP, TSAM1, 1, NUM, -2)
> 276 DO 320 K = 1, 5
> 277 IEVEN(K) = IEVENT(I,K)
> 278 ISTA(K) = ISTAT(I,K)
> 279 320 CONTINUE
> 280 IF (ITYPE .EQ. 2) GO TO 330
> 281 IF (ITYPE .EQ. 1) GO TO 340
> 282 CALL PLOTCS(0, TMAX + 1.3/TSCALE, ISTA, 4)
> 283 330 CALL PLOTCS(0, TMAX + 0.5/TSCALE, IEVEN, 4)
> 284 GO TO 350
> 285 340 CALL PLOTCS(0, TMAX + 0.5/TSCALE, ISTA, 4)
> 286 350 CONTINUE
> 287 CALL BORDER
> 288 C
> 289 C WRITE PLOT PARAMETERS
> 290 C
> 291 CALL PSPACE(D/25.4 + 0.1 + 0.02, D/25.4 + 0.1 + 0.36, 0.1, T/25.4
> 292 1 + 0.1)
> 293 CALL MAP(0.0, 10.0, 0.0, 10.0)
> 294 CALL BORDER
> 295 CALL CTRMAG(15)
> 296 CALL PLOTCS(1.0, 9.0, PROJ, 30)
> 297 CALL PLOTCS(1.0, 8.0, TITLE, 30)
> 298 CALL CTRMAG(12)
> 299 IF (ITYPE .EQ. 0) GO TO 370
> 300 IF (ITYPE .EQ. 1) GO TO 360
> 301 CALL PLOTCS(1.0, 6.5, 'COMMON STATION SECTION', 22)
> 302 CALL PLOTCS(1.5, 6.0, 'STATION', 7)
> 303 CALL PLOTCS(4.0, 6.0, ISTAT, 4)
> 304 GO TO 370
> 305 360 CALL PLOTCS(1.0, 6.5, 'COMMON EVENT SECTION', 20)
> 306 CALL PLOTCS(1.5, 6.0, 'SHOT', 4)
> 307 CALL PLOTCS(4.0, 6.0, IEVENT, 4)
> 308 370 CALL CTRMAG(10)
> 309 IF (NI .EQ. 0) GO TO 380
> 310 CALL PLOTCS(1.0, 4.5, 'FILTER(HZ)', 10)
> 311 CALL PLOTNF(4.0, 4.5, F2, 1)
> 312 CALL PLOTNF(5.5, 4.5, F3, 1)
> 313 GO TO 390
> 314 380 CALL PLOTCS(1.0, 4.5, 'FILTER - NONE', 15)
> 315 390 CALL PLOTCS(1.0, 3.5, 'AMPLITUDE', 9)
> 316 IF (NOR .EQ. 2) GO TO 400
> 317 IF (NOR .EQ. 0) GO TO 410
> 318 CALL PLOTCS(1.5, 3.0, 'CORRECTED TO COMMON GAIN', 24)
> 319 GO TO 420
> 320 400 CALL PLOTCS(1.5, 3.0, 'EQUALISED', 9)
> 321 GO TO 420
> 322 410 CALL PLOTCS(1.5, 3.0, 'UNADJUSTED', 10)
> 323 420 CONTINUE
> 324 C
> 325 C ASK IF PLOT WANTED AT ANOTHER SCALE
> 326 C
> 327 WRITE (6,430)
> 328 430 FORMAT ('DO YOU WANT THE SAME PLOT AT ANOTHER SCALE Y=1 N=0')
> 329 READ (5,440) KP
> 330 440 FORMAT (I1)
> 331 IF (KP .EQ. 0) GO TO 450
> 332 CALL FRAME
> 333 GO TO 250
> 334 450 CALL GREND
> 335 460 RETURN
> 336 END

```

```

> 337 C
> 338 C*****
> 339 C
> 340 C          SUBROUTINE SECOND
> 341 C          -----
> 342 C
> 343 C          CONVERTS THE TIME IN HOURS MINS AND SECONDS
> 344 C          TO SECONDS
> 345 C
> 346 C*****
> 347 C
> 348 C          SUBROUTINE SECOND(IHOUR, IMIN, DSECS, DTIME, I)
> 349 C          REAL*4 DSECS(90)
> 350 C          REAL*8 DTIME(90), DATIME
> 351 C          INVTGER*4 IHOUR(90), IMIN(90)
> 352 C
> 353 C          ITIME = (IHOUR(I)*3600) + (IMIN(I)*60)
> 354 C          DATIME = ITIME
> 355 C          DTIME(I) = DATIME + DSECS(I)
> 356 C          RETURN
> 357 C          END
> 358 C
> 359 C*****
> 360 C
> 361 C          SUBROUTINE MEAN
> 362 C          -----
> 363 C
> 364 C          MEAN CORRECTS THE DATA
> 365 C
> 366 C*****
> 367 C
> 368 C          SUBROUTINE MEAN(X, N, LX, NARG)
> 369 C          REAL*4 X(N,NARG)
> 370 C          INVTGER*4 LX(N)
> 371 C
> 372 C          DO 30 J = 1, N
> 373 C             XTOT = X(J,1)
> 374 C             LEN = LX(J)
> 375 C             DO 10 I = 2, LEN
> 376 C                XTOT = XTOT + X(J,I)
> 377 C          10 CONTINUE
> 378 C             XAV = XTOT / LEN
> 379 C             DO 20 I = 1, LEN
> 380 C                X(J,I) = X(J,I) - XAV
> 381 C          20 CONTINUE
> 382 C          30 CONTINUE
> 383 C          RETURN
> 384 C          END
> 385 C
> 386 C*****
> 387 C
> 388 C          SUBROUTINE NORM
> 389 C          -----
> 390 C
> 391 C          NORMALISES THE SEISMIC TRACES TO 1.0
> 392 C
> 393 C*****
> 394 C
> 395 C          SUBROUTINE NORM(X, N, LX, NARG)
> 396 C          REAL*4 X(N,NARG)
> 397 C          INVTGER*4 LX(N)
> 398 C
> 399 C          DO 50 I = 1, N
> 400 C             XMAX = -1000.0
> 401 C             LEN = LX(I)
> 402 C             DO 10 J = 1, LEN
> 403 C                Y = ABS(X(I,J))
> 404 C                IF (Y .GT. XMAX) XMAX = Y
> 405 C          10 CONTINUE
> 406 C             IF (XMAX .EQ. 0.0) GO TO 30
> 407 C             DO 20 J = 1, LEN
> 408 C                X(I,J) = X(I,J) / XMAX
> 409 C          20 CONTINUE
> 410 C             GO TO 50
> 411 C          30 WRITE (6,40) I
> 412 C          40 FORMAT (1X, 'MAXAMP=0-NORMALIZATION NOT POSSIBLE,TRACE NO-', I6)
> 413 C          50 CONTINUE
> 414 C          RETURN
> 415 C          END

```

```

> 416 C
> 417 C*****
> 418 C
> 419 C      SUBROUTINE SAMPLE
> 420 C      -----
> 421 C
> 422 C      CALCULATES THE FIRST AND LAST SAMPLES REQUIRED
> 423 C      FROM THE TRACE ARRAYS FOR PLOTTING
> 424 C      VELR      -      RED. VEL.
> 425 C      DTEVE    -      SHOT TIME
> 426 C      DTST     -      FILE START TIME
> 427 C      TSRED    -      START TIME(RED) OF PLOT WANTED
> 428 C      TSAM     -      TIME(RED) OF SAMPLES TO BE PLOTTED
> 429 C      TLEN     -      LENGTH(RED.TIME) OF PLOT
> 430 C      NST      -      1st SAMPLE TO BE PLOTTED
> 431 C      NEND     -      LAST SAMPLE TO BE PLOTTED
> 432 C
> 433 C*****
> 434 C
> 435 C      SUBROUTINE SAMPLE(DTST, DTEVE, TSRED, DIST, NST, SAMPR, NEND,
> 436 C      1 TLEN, I, VELR, TSAM, NARG, N)
> 437 C      REAL*4 DIST(90), SAMPR(90), TSAM(N,NARG), VELR
> 438 C      REAL*8 DTPLT(90), DSAMNO, DSAM, DTST(90), DTEVE(90)
> 439 C      INTEGER*4 NST(90), NEND(90)
> 440 C
> 441 C      T CORR = 0.0
> 442 C      IF (VELR .EQ. 0.0) GO TO 10
> 443 C      DTPLT(I) = ABS(DIST(I)) / VELR + DTEVE(I) + TSRED
> 444 C      GO TO 20
> 445 C      10 DTPLT(I) = DTEVE(I) + TSRED
> 446 C      20 IF (DTPLT(I) .GE. DTST(I)) GO TO 30
> 447 C      T CORR = DTST(I) - DTPLT(I)
> 448 C      DTPLT(I) = DTST(I)
> 449 C      30 DSAMNO = (DTPLT(I) - DTST(I)) * SAMPR(I) + 1.0
> 450 C      NST(I) = IDINT(DSAMNO) + 1
> 451 C      TSAM(I,1) = TSRED + T CORR + (NST(I) - DSAMNO) / SAMPR(I)
> 452 C      DSAM = 1.0 / SAMPR(I)
> 453 C      DO 50 J = 2, 10000
> 454 C      K = J - 1
> 455 C      TSAM(I,J) = TSAM(I,K) + DSAM
> 456 C      40 IF (TSAM(I,J) .GT. (TSRED + TLEN)) GO TO 60
> 457 C      50 CONTINUE
> 458 C      60 NEND(I) = NST(I) + K
> 459 C      WRITE (7,70) DTST(I), DTEVE(I), NST(I), NEND(I), DTPLT(I),
> 460 C      1 TSAM(I,1), TSAM(I,K)
> 461 C      70 FORMAT (F10.3, 4X, F10.3, 5X, I5, 8X, I5, 7X, F10.3, 4X, F9.3, 8X,
> 462 C      1 F9.3)
> 463 C      NDIFF = NEND(I) - NST(I)
> 464 C      IF (NDIFF .GT. NARG) NEND(I) = NARG + NST(I)
> 465 C      80 RETURN
> 466 C      END
> 467 C
> 468 C*****
> 469 C
> 470 C      SUBROUTINE POLAR
> 471 C      -----
> 472 C
> 473 C      MULTIPLIES THE SIGNAL BY -1.0
> 474 C
> 475 C*****
> 476 C
> 477 C      SUBROUTINE POLAR(X, I, N, LX, NARG)
> 478 C      REAL*4 X(N,NARG)
> 479 C      INTEGER*4 LX(N)
> 480 C
> 481 C      LXN = LX(I)
> 482 C      DO 10 J = 1, LXN
> 483 C      X(I,J) = -X(I,J)
> 484 C      10 CONTINUE
> 485 C      RETURN
> 486 C      END

```

```

> 487 C
> 488 C*****
> 489 C
> 490 C SUBROUTINE AMP
> 491 C
> 492 C
> 493 C CONVERTS SIGNALS TO SAME GAIN
> 494 C BASED ON GAIN 7 FOR THE AMPLIFIER MODULATOR UNITS
> 495 C FROM THE NERC SEISMIC EQUIPMENT POOL
> 496 C TO CHANGE TO ANOTHER BASE CHANGE THE VALUE
> 497 C 0.001221. IT ONLY OCCURS TWICE, IN THIS SUBROUTINE
> 498 C AND ONCE IN THE SUBROUTINE CALL
> 499 C
> 500 C*****
> 501 C
> 502 C SUBROUTINE AMP(X, J, N, LX, GAIN, NARG)
> 503 C REAL*4 X(N,NARG), GAIN(N)
> 504 C INTEGER*4 LX(N)
> 505 C
> 506 C FAC = GAIN(J) / 0.001221
> 507 C LENG = LX(J)
> 508 C DO 10 I = 1, LENG
> 509 C X(J,I) = X(J,I) * FAC
> 510 C 10 CONTINUE
> 511 C RETURN
> 512 C END
> 513 C
> 514 C*****
> 515 C
> 516 C SUBROUTINE AMPFAC
> 517 C
> 518 C
> 519 C ADJUSTS THE AMPLITUDES FOR PLOTTING
> 520 C
> 521 C*****
> 522 C
> 523 C SUBROUTINE AMPFAC(X, N, LX, DIST, NOR, NARG, TSCALE, DMIN)
> 524 C
> 525 C REAL*4 X(N,NARG), DIST(N), XMAX(90), XMIN(90)
> 526 C INTEGER*4 LX(N)
> 527 C
> 528 C IF (NOR .EQ. 2) GO TO 40
> 529 C
> 530 C DO 20 I = 1, N
> 531 C NUM = LX(I)
> 532 C XMAX(I) = -1000.0
> 533 C XMIN(I) = 1000.0
> 534 C DO 10 K = 1, NUM
> 535 C IF (XMAX(I) .LT. X(I,K)) XMAX(I) = X(I,K)
> 536 C IF (XMIN(I) .GT. X(I,K)) XMIN(I) = X(I,K)
> 537 C 10 CONTINUE
> 538 C 20 CONTINUE
> 539 C
> 540 C MAX = 0.0
> 541 C MIN = 0.0
> 542 C DO 30 I = 1, N
> 543 C MAX = MAX + XMAX(I)
> 544 C MIN = MIN + XMIN(I)
> 545 C 30 CONTINUE
> 546 C
> 547 C AVMAX = MAX / N
> 548 C AVMIN = MIN / N
> 549 C AVER = ABS(AVMAX) + ABS(AVMIN)
> 550 C GO TO 50
> 551 C 40 AVER = 1.5
> 552 C IF (TSCALE .GT. 8.0) AVER = 0.5
> 553 C
> 554 C 50 WRITE (6,60) AVER
> 555 C 60 FORMAT ('AMPFAC = ', F15.3)
> 556 C WRITE (6,70)
> 557 C 70 FORMAT ('ENTER ALTERNATIVE AMPFAC (FOR DEFAULT VALUE ABOVE, RETURN)
> 558 C 1/'A SMALLER VALUE GIVES A PROPORTIONALLY BIGGER AMPLITUDE'/
> 559 C 2 '..... F8.3')
> 560 C READ (5,80) AV
> 561 C 80 FORMAT (F8.3)
> 562 C IF (AV .NE. 0.0) AVER = AV
> 563 C DMIN = 100.0
> 564 C IF (N .EQ. 1) GO TO 100
> 565 C DO 90 I = 2, N
> 566 C IF (ABS(DIST(I) - DIST(I - 1)) .LT. DMIN) DMIN = ABS(DIST(I) -
> 567 C 1 DIST(I - 1))
> 568 C 90 CONTINUE
> 569 C GO TO 110
> 570 C 100 DMIN = 5.0

```

```

> 571 C
> 572 110 DO 130 I = 1, N
> 573     NUM = LX(I)
> 574     DO 120 K = 1, NUM
> 575     X(I,K) = (X(I,K)*DMIN) / AVER
> 576 120 CONTINUE
> 577 130 CONTINUE
> 578     RETURN
> 579     END
> 580 C
> 581 C*****
> 582 C   SUBROUTINE BPASS1
> 583 C   -----
> 584 C
> 585 C   AN EDITED VERSION OF BRIAN RUSSELL'S SUBROUTINE TO
> 586 C   PERFORM BANDPASS FILTERING ON EACH SEISMIC TRACE.
> 587 C   SUBROUTINES FFTA SINTAB & HANN ARE CALLED.
> 588 C
> 589 C   X = INPUT ARRAY
> 590 C   LX = LENGTH OF X
> 591 C   SAMPR = SAMPLING RATE
> 592 C   F1,F2,F3,F4 = DEFINES FREQUENCY RANGE FOR HANNING WINDOW
> 593 C
> 594 C   F1 MUST BE GREATER THAN THE FUNDAMENTAL FREQUENCY
> 595 C   F4 MUST BE LESS THAN THE NYQUIST FREQUENCY
> 596 C
> 597 C*****
> 598 C
> 599 C   SUBROUTINE BPASS(LX, F1, F2, F3, F4, X, SAMPR)
> 600 C   DIMENSION X(4096), Y(4096), S(4096), F(4096)
> 601 C
> 602 C   LEN = LX
> 603 C   CALL PAD(LEN, X)
> 604 C   L1 = LEN / 2 + 1
> 605 C   L2 = L1 + 1
> 606 C   DO 10 I = 1, LEN
> 607 C     S(I) = 0.0
> 608 C     Y(I) = 0.0
> 609 C 10 CONTINUE
> 610 C
> 611 C   TRANSFORM THE TIME SERIES
> 612 C
> 613 C   CALL SINTAB(LEN, S)
> 614 C   SIGNI = -1.0
> 615 C   CALL FFTA(LEN, X, Y, SIGNI, S)
> 616 C   DF = SAMPR / DFLOAT(LEN)
> 617 C   DO 20 I = 1, L1
> 618 C     F(I) = DF * DFLOAT(I)
> 619 C 20 CONTINUE
> 620 C
> 621 C   SET UP SAMPLE NUMBERS FOR HANNING WINDOW LIMITS
> 622 C
> 623 C   DO 30 I = 2, L1
> 624 C     IF (F1 .GE. F(I - 1) .AND. F1 .LE. F(I)) JJ = I - 1
> 625 C     IF (F2 .GE. F(I - 1) .AND. F2 .LE. F(I)) J = I - 1
> 626 C     IF (F3 .GE. F(I - 1) .AND. F3 .LE. F(I)) K = I - 1
> 627 C     IF (F4 .GE. F(I - 1) .AND. F4 .LE. F(I)) KK = I - 1
> 628 C 30 CONTINUE
> 629 C   CALL HANN(X, L1, JJ, KK, J, K)
> 630 C   CALL HANN(Y, L1, JJ, KK, J, K)
> 631 C   DO 40 I = L2, LEN
> 632 C     X(I) = X(LEN - I + 2)
> 633 C     Y(I) = -Y(LEN - I + 2)
> 634 C 40 CONTINUE
> 635 C   SIGNI = 1.0
> 636 C   CALL FFTA(LEN, X, Y, SIGNI, S)
> 637 C   RETURN
> 638 C   END
> 639 C
> 640 C*****
> 641 C
> 642 C   SUBROUTINE FFTA
> 643 C   -----
> 644 C
> 645 C   DESCRIPTION - THIS SUBROUTINE COMPUTES THE FAST FOURIER
> 646 C   TRANSFORM BY THE COOLEY-TUKEY ALGORITHM.
> 647 C   PARAMETERS - LX=NUMBER OF DATA POINTS
> 648 C   X=ARRAY CONTAINING REAL PART OF TRANSFORM
> 649 C   Y=ARRAY CONTAINING IMAGINARY PART OF TRANSFORM
> 650 C   SIGNI=+1. FOR FORWARD TRANSFORM
> 651 C   =-1. FOR REVERSE TRANSFORM
> 652 C   S=ARRAY OF SINE VALUES GENERATED BY SUBROUTINE
> 653 C   SINTAB CALLED BY FFTA
> 654 C
> 655 C   SOURCE - CLAERBOUT, MODIFIED BY ALAN NUNNS
> 656 C*****
> 657 C
> 658 C   SUBROUTINE FFTA(LX, X, Y, SIGNI, S)
> 659 C   DIMENSION X(LX), Y(LX), S(LX)
> 660 C   SC = 1.0
> 661 C   IF (SIGNI .LT. 0.0) SC = 1.0 / LX

```

```

> 662      NN = LX / 2
> 663      N = LX / 4
> 664      J = 1
> 665      DO 30 I = 1, LX
> 666          IF (I .GT. J) GO TO 10
> 667          TEMPX = X(J) * SC
> 668          TEMPY = Y(J) * SC
> 669          X(J) = X(I) * SC
> 670          Y(J) = Y(I) * SC
> 671          X(I) = TEMPX
> 672          Y(I) = TEMPY
> 673      10  M = NN
> 674      20  IF (J .LE. M) GO TO 30
> 675          J = J - M
> 676          M = M / 2
> 677          IF (M .GE. 1) GO TO 20
> 678      30  J = J + M
> 679          L = 1
> 680          NL = NN
> 681      40  ISTEP = 2 * L
> 682          IND = 1
> 683          DO 100 M = 1, L
> 684              INDN = IND - N - 1
> 685              IF (INDN) 50, 60, 70
> 686      50  WX = S(1 - INDN)
> 687              WY = S(IND) * SIGNI
> 688              GO TO 80
> 689      60  WX = 0.
> 690              WY = SIGNI
> 691              GO TO 80
> 692      70  WX = -S(INDN + 1)
> 693              WY = S(N + 1 - INDN) * SIGNI
> 694      80  DO 90 I = M, LX, ISTEP
> 695              TEMPX = WX * X(I + L) - WY * Y(I + L)
> 696              TEMPY = WX * Y(I + L) + WY * X(I + L)
> 697              X(I + L) = X(I) - TEMPX
> 698              Y(I + L) = Y(I) - TEMPY
> 699              X(I) = X(I) + TEMPX
> 700      90  Y(I) = Y(I) + TEMPY
> 701      100 IND = IND + NL
> 702          L = ISTEP
> 703          NL = NL / 2
> 704          IF (L .LT. LX) GO TO 40
> 705          RETURN
> 706          END
> 707      C
> 708      C*****
> 709      C
> 710      C   SUBROUTINE SINTAB
> 711      C   -----
> 712      C
> 713      C DESCRIPTION - THIS SUBROUTINE RETURNS VALUES
> 714      C S(I)=SIN(2*PI*(I-1)/LX)  I=1,2,...,LX/4+1
> 715      C WHERE LX=2**INTEGER IS THE NUMBER OF POINTS IN THE
> 716      C TIME SERIES IN MAIN
> 717      C
> 718      C WRITTEN BY ALAN NUNNS
> 719      C*****
> 720      C
> 721      C   SUBROUTINE SINTAB(LX, S)
> 722      C   DIMENSION S(LX)
> 723      C   DOUBLE PRECISION ARG, DELARG
> 724      C   NI = LX / 4 + 1
> 725      C   ARG = 0.0
> 726      C   DELARG = 0.6283185307179586D01 / LX
> 727      C   DO 10 I = 1, NI
> 728      C       S(I) = DSIN(ARG)
> 729      C       ARG = ARG + DELARG
> 730      C 10 CONTINUE
> 731      C RETURN
> 732      C END

```

```

> 733 C
> 734 C*****
> 735 C
> 736 C SUBROUTINE HANN
> 737 C
> 738 C AN EDITED VERSION OF A SUBROUTINE BY BRIAN RUSSELL
> 739 C IT APPLIES A HANNING WINDOW TO THE TRANSFORMED DATA
> 740 C BETWEEN THE FREQUENCIES SET UP IN BPASS
> 741 C
> 742 C X = SPECTRUM OF DATA
> 743 C N = SIZE OF ARRAY
> 744 C JJ = ELEMENT OF ARRAY STARTING WINDOW
> 745 C KK = ELEMENT OF ARRAY ENDING THE WINDOW
> 746 C J = ELEMENT OF ARRAY ENDING RISING TAPER
> 747 C K = ELEMENT OF ARRAY STARTING DECREASING TAPER
> 748 C
> 749 C VALUE OF WINDOW BETWEEN J & K = 1
> 750 C WINDOW = 0 AT JJ & KK
> 751 C
> 752 C*****
> 753 C
> 754 C SUBROUTINE HANN(X, N, JJ, KK, J, K)
> 755 C DIMENSION X(N)
> 756 C NN = N - 1
> 757 C PI2 = 0.62831853071796D+01
> 758 C IF (JJ .EQ. 1) GO TO 20
> 759 C DO 10 I = 2, JJ
> 760 C 10 X(I - 1) = X(I - 1) * 0.0D0
> 761 C 20 IF (J .EQ. JJ) GO TO 40
> 762 C CON1 = PI2 / DFLOAT(2*(J - JJ))
> 763 C DO 30 I = JJ, J
> 764 C ARG = DFLOAT(I - JJ) * CON1
> 765 C 30 X(I) = X(I) * 0.5D0 * (.1D+01 - COS(ARG))
> 766 C 40 IF (K .EQ. KK) GO TO 60
> 767 C CON2 = PI2 / DFLOAT(2*(KK - K))
> 768 C DO 50 I = K, KK
> 769 C ARG = DFLOAT(KK - I) * CON2
> 770 C 50 X(I) = X(I) * 0.5D0 * (.1D+01 - COS(ARG))
> 771 C 60 IF (KK .EQ. N) GO TO 80
> 772 C DO 70 I = KK, NN
> 773 C 70 X(I + 1) = X(I + 1) * 0.0D0
> 774 C 80 RETURN
> 775 C END
> 776 C
> 777 C*****
> 778 C
> 779 C SUBROUTINE PAD
> 780 C
> 781 C
> 782 C CHECKS TO SEE IF THE DATA LENGTH IS 2**N AND IF
> 783 C NOT PADS THE ARRAY WITH ZEROS
> 784 C
> 785 C X = DATA ARRAY
> 786 C LX = LENGTH OF ARRAY
> 787 C
> 788 C*****
> 789 C
> 790 C SUBROUTINE PAD(LX, X)
> 791 C REAL*4 X(4096)
> 792 C DO 10 I = 1, 12
> 793 C IF (LX .EQ. 2**I) GO TO 50
> 794 C IF (LX .LT. 2**I) GO TO 20
> 795 C 10 CONTINUE
> 796 C 20 IDAT = 2 ** I
> 797 C WRITE (6,30) IDAT
> 798 C 30 FORMAT ('TRACE PADDED WITH ZEROS TO ', I4, ' POINTS')
> 799 C LXN = IDAT
> 800 C LXT = LX + 1
> 801 C DO 40 I = LXT, LXN
> 802 C X(I) = 0.0
> 803 C 40 CONTINUE
> 804 C LX = LXN
> 805 C 50 RETURN
> 806 C END

```

```

> 1 C*****
> 2 C
> 3 C PROGRAM FREQPLOT
> 4 C -----
> 5 C
> 6 C THIS PROGRAM TRANSFORMS A TIME SERIES INTO
> 7 C THE FREQUENCY DOMAIN USING A FAST FOURIER TRANSFORM
> 8 C ROUTINE AND PLOTS THE AMPLITUDE SPECTRUM.
> 9 C AN OPTION EXISTS TO SMOOTH THE SPECTRUM.
> 10 C THE FFT WORKS ON DATA OF LENGTH 2**N, IF INPUT IS
> 11 C LESS THAN THIS THE DATA WILL BE AUTOMATICALLY PADDED
> 12 C
> 13 C THIS PROGRAM OPERATES ON SEISMIC DATA WRITTEN IN
> 14 C DURHAM SELF DEFINING TAPE FORMAT (DSDTF) AND
> 15 C TRANSFERED TO DISC FILE USING GPT9:TR-CSP.COM
> 16 C
> 17 C UNIT 1 - INPUT
> 18 C CARD 1 - HEADER INFORMATION FROM DSDTF DIGITAL TAPES
> 19 C CARD 2 - I*2 UNFORMATTED BINARY DATA
> 20 C
> 21 C UNITS 5 & 6 USED FOR INTERACTIVE USE
> 22 C
> 23 C UNIT 8 - OUTPUT
> 24 C
> 25 C UNIT 9 - PLOTFILE
> 26 C
> 27 C *GHOST ROUTINES ARE USED
> 28 C*****
> 29 C
> 30 C
> 31 C DIMENSION IST(1)
> 32 C INTEGER*2 ISAM(20000), LEN
> 33 C REAL*8 X(8200), Y(8200), S(8200), XS(8200), DTEVE, DTST, SIGNI
> 34 C REAL*4 ISTAT(5), IEVENT(5), A(8200), XCOORD(8200), XCO(8200),
> 35 C 1_____KSSEC, TSAM(8200)
> 36 C DATA IST(1) /1/
> 37 C COMMON /B/ LSAMP
> 38 C COMMON /D/ NRANGE
> 39 C
> 40 C
> 41 C
> 42 C WRITE (6,10)
> 43 C 10 FORMAT ('TRACE LENGTH(SECS),RED VEL(KM/S), AND START TIME(SECS)'/
> 44 C 1'(UNREDUCED RED VEL =0.0)'/'.-----..... 3F5.2')
> 45 C READ (5,20) TLEN, VELR, TSRED
> 46 C 20 FORMAT (3F5.2)
> 47 C
> 48 C
> 49 C
> 50 C READ (1,30) (IEVENT(J),J=1,2), IEDAY, IEHOUR, IEMIN, ESEC,
> 51 C 1(ISTAT(J),J=1,2), KSDAY, KSHOUR, KSMIN, KSSEC, SAMPR, GAIN, IPOL,
> 52 C 2DIST
> 53 C 30 FORMAT (2A4, 38X, I4, 1X, I2, 2X, I2, F8.4, 2X, 2A4, 38X, I4, 1X,
> 54 C 1 I2, 2X, I2, F8.4, 8X, F10.4, 10X, E10.4, 2X, A4, F10.3)
> 55 C CALL READ(ISAM, LEN, 0, LNUM, 1, &240)
> 56 C LENG = LEN / 2
> 57 C DO 40 J = 1, LENG
> 58 C X(J) = ISAM(J)
> 59 C 40 CONTINUE
> 60 C
> 61 C CONVERT TIME TO SECS
> 62 C
> 63 C CALL SECOND(KSHOUR, KSMIN, KSSEC, DTST)
> 64 C CALL SECOND(IEHOUR, IEMIN, ESEC, DTEVE)
> 65 C
> 66 C DETERMINE WHICH PART OF DATA IS WANTED
> 67 C
> 68 C CALL SAMPLE(DTST, DTEVE, TSRED, DIST, NST, SAMPR, NEND, TLEN,
> 69 C 1 VELR, XCO, LENG)
> 70 C LX = NEND - NST + 1
> 71 C NS = NST
> 72 C NE = NEND
> 73 C K = 1
> 74 C DO 50 I = NS, NE
> 75 C X(K) = -X(I)
> 76 C K = K + 1
> 77 C 50 CONTINUE
> 78 C
> 79 C APPLY COS TAPER,MEAN CORRECT DATA,
> 80 C CHECK DATA LENGTH AND PAD IF NECESSARY
> 81 C
> 82 C 60 FORMAT (F10.2)
> 83 C NRANGE = 1
> 84 C LSAMP = LX
> 85 C CALL MEAN1(IST, X)
> 86 C WRITE (6,70)
> 87 C 70 FORMAT ('NO OF POINTS IN COSINE TAPER'/'.....')
> 88 C READ (5,80) J
> 89 C 80 FORMAT (I5)
> 90 C IF (J .LT. 1) GO TO 90

```

```

> 91      ISIGN = +1
> 92      CALL COSTAP(LX, X, 1, J, ISIGN)
> 93      ISIGN = -1
> 94      K = LX - J + 1
> 95      CALL COSTAP(LX, X, K, LX, ISIGN)
> 96      90 CALL PAD(LX, X)
> 97      CALL MEAN1(IST, X)
> 98      C
> 99      C PLOT TRACE
> 100     C
> 101     XMAXI = 0.0
> 102     XMINI = 0.0
> 103     DO 100 I = 1, LX
> 104     A(I) = X(I)
> 105     IF (X(I) .GT. XMAXI) XMAXI = X(I)
> 106     IF (X(I) .LT. XMINI) XMINI = X(I)
> 107     K = I + 1
> 108     XCO(K) = XCO(I) + 1 / SAMPR
> 109     S(I) = 0.0
> 110     Y(I) = 0.0
> 111     100 CONTINUE
> 112     ALX = LX
> 113     CALL PAPER(1)
> 114     CALL PSPACE(0.10, 0.55, 0.58, 0.8)
> 115     CALL MAP(XCO(1), XCO(LX), XMINI + XMINI/4.0, XMAXI + XMAXI/4.0)
> 116     CALL CTRMAG(8)
> 117     CALL SCALES
> 118     CALL PTPLOT(XCO, A, 1, LX, -2)
> 119     CALL PLOTCS(XCO(1) + (XCO(LX) - XCO(1))*0.25, XMINI - (XMAXI -
> 120     1 XMINI)*0.35, 'TIME(SECS) RED TO KM/SEC', 30)
> 121     CALL PLOTNP(XCO(1) + (XCO(LX) - XCO(1))*0.55, XMINI - (XMAXI -
> 122     1 XMINI)*0.35, VELR, 1)
> 123     CALL BORDER
> 124     C
> 125     C TRANSFORM DATA, CALC AMP. SPECTRUM
> 126     C NORMALISE TO MAX. AMPLITUDE AND
> 127     C SMOOTH IF REQUIRED
> 128     C
> 129     CALL SINTAB(LX, S)
> 130     SIGNI = -1.0
> 131     CALL FFTA(LX, X, Y, SIGNI, S)
> 132     LSAMP = LX / 2 + 1
> 133     FFREQ = SAMPR / LX
> 134     XMAX = 0.0
> 135     DO 110 I = 1, LX
> 136     XS(I) = DSQRT(X(I)**2 + Y(I)**2)
> 137     IF (I .EQ. 1) XCOORD(I) = 0.0
> 138     K = I - 1
> 139     XCOORD(I) = FFREQ * FLOAT(K)
> 140     IF (XS(I) .GT. XMAX) XMAX = XS(I)
> 141     110 CONTINUE
> 142     WRITE (6,120)
> 143     120 FORMAT ('SPECTRUM SMOOTHING REQUIRED ENTER 1')
> 144     READ (5,130) MOV
> 145     130 FORMAT (I1)
> 146     IF (MOV .NE. 1) GO TO 140
> 147     CALL MOVAV(LSAMP, XS)
> 148     140 CONTINUE
> 149     C
> 150     C LIST RESULTS
> 151     C
> 152     C WRITE (8,262) ISTAT, IEVENT
> 153     150 FORMAT (2A4, 2X, 2A4)
> 154     C WRITE (8,265) LX, SAMPR
> 155     160 FORMAT (I5, F10.3)
> 156     C WRITE (8,270)
> 157     170 FORMAT ('/ REAL IMAG. AMP')
> 158     180 FORMAT (F10.3, 3X, F10.3, 3X, F10.3)
> 159     DO 190 I = 1, LX
> 160     WRITE (8,180) X(I), Y(I), XS(I)
> 161     A(I) = XS(I)
> 162     190 CONTINUE
> 163     C
> 164     C PLOTTING POWER SPECTRUM
> 165     C
> 166     CALL PSPACE(0.10, 0.55, 0.05, 0.45)
> 167     WRITE (6,200)
> 168     200 FORMAT ('MAXIMUM FREQUENCY TO PLOT IN HZ (F5.2)')
> 169     READ (5,210) FREQ
> 170     210 FORMAT (F5.2)
> 171     IF (FREQ .GT. SAMPR/2.0 .OR. FREQ .EQ. 0.0) FREQ = SAMPR / 2.0
> 172     CALL MAP(0.0, FREQ, 0.0, XMAX)
> 173     CALL AXES
> 174     CALL PLOTCS(FREQ/3.0, 1.05*XMAX, IEVENT, 10)
> 175     CALL PLOTCS(FREQ/2.0, 1.05*XMAX, ISTAT, 10)
> 176     CALL PTPLOT(XCOORD, A, 1, LSAMP, -2)
> 177     CALL PLOTCS(FREQ/3.0, -0.10*XMAX, 'FREQUENCY (HZ)', 15)
> 178     CALL CTRMAG(6)
> 179     CALL PLOTCS(FREQ*3.0/4.0, 0.95*XMAX, 'SAMP.RATE', 9)
> 180     CALL PLOTNP(FREQ*15.0/16.0, 0.95*XMAX, SAMPR, 2)

```

```

> 181      CALL PLOTCS(FREQ*3.0/4.0, 0.9*XMAX, "LEN(SECS)", 9)
> 182      YX = LX
> 183      EN = (YX - 1.0) / SAMPR
> 184      CALL PLOTNF(FREQ*15.0/16.0, 0.9*XMAX, EN, 2)
> 185      IF (MOV .NE. 1) GO TO 220
> 186      CALL PLOTCS(FREQ*3.0/4.0, 0.85*XMAX, "SMOOTHED SPECTRUM", 18)
> 187      GO TO 230
> 188      220 CALL PLOTCS(FREQ*3.0/4.0, 0.85*XMAX, "SPECTRUM NOT SMOOTHED", 22)
> 189      C 310 CALL PLOTCS(FREQ*3.0/4.0, 0.80*XMAX, "TRUE MAX. AMP.", 14)
> 190      C      CALL PLOTNF(FREQ*15.0/16.0, 0.80*XMAX, XMAX, 2)
> 191      230 CALL GRENDD
> 192      240 STOP
> 193      END
> 194      C
> 195      C*****
> 196      C      SUBROUTINE MEAN1
> 197      C      -----
> 198      C
> 199      C      THIS SECTION FINDS THE MEAN VALUE OF THE
> 200      C      SAMPLES IN ASAM AND SUBTRACTS THIS FROM
> 201      C      EACH VALUE TO REMOVE ANY D.C. LEVEL.
> 202      C      THE ROUTINE IS USED WITH PROGRAMS GEOSXCT AND DURHSECT
> 203      C
> 204      C      ASAM = DATA ARRAY (SEISMIC TRACES)
> 205      C      JSTRT = STARTING ELEMENT OF EACH TRACE
> 206      C
> 207      C*****
> 208      C
> 209      SUBROUTINE MEAN1(JSTRT, ASAM)
> 210      DIMENSION JSTRT(25)
> 211      REAL*8 ASAM(75000)
> 212      COMMON /B/ LSAMP
> 213      COMMON /D/ NRANGE
> 214      AAV = 0.0
> 215      JBEG = JSTRT(NRANGE)
> 216      DO 10 I = 1, LSAMP
> 217          AAV = AAV + ASAM(JBEG + I - 1)
> 218      10 CONTINUE
> 219      AAV = AAV / LSAMP
> 220      DO 20 I = 1, LSAMP
> 221          ASAM(JBEG + I - 1) = ASAM(JBEG + I - 1) - AAV
> 222      20 CONTINUE
> 223      RETURN
> 224      END
> 225      C
> 226      C*****
> 227      C
> 228      C      SUBROUTINE FFTA
> 229      C      -----
> 230      C
> 231      C      DESCRIPTION - THIS SUBROUTINE COMPUTES THE FAST FOURIER
> 232      C      TRANSFORM BY THE COOLEY-TUKEY ALGORITHM.
> 233      C      PARAMETERS - LX=NUMBER OF DATA POINTS
> 234      C      X=ARRAY CONTAINING REAL PART OF TRANSFORM
> 235      C      Y=ARRAY CONTAINING IMAGINARY PART OF TRANSFORM
> 236      C      SIGNI=+1. FOR FORWARD TRANSFORM
> 237      C      =-1. FOR REVERSE TRANSFORM
> 238      C      S=ARRAY OF SINE VALUES GENERATED BY SUBROUTINE
> 239      C      SINTAB CALLED BY FFTA
> 240      C
> 241      C      SOURCE - CLAEBOU, MODIFIED BY ALAN NUNNS
> 242      C*****
> 243      C
> 244      SUBROUTINE FFTA(LX, X, Y, SIGNI, S)
> 245      IMPLICIT REAL*8(A - H, O - Z)
> 246      DIMENSION X(LX), Y(LX), S(LX)
> 247      SC = 1.0
> 248      IF (SIGNI .LT. 0.0) SC = 1.0 / LX
> 249      NN = LX / 2
> 250      N = LX / 4
> 251      J = 1
> 252      DO 30 I = 1, LX
> 253          IF (I .GT. J) GO TO 10
> 254              TEMPX = X(J) * SC
> 255              TEMPY = Y(J) * SC
> 256              X(J) = X(I) * SC
> 257              Y(J) = Y(I) * SC
> 258              X(I) = TEMPX
> 259              Y(I) = TEMPY
> 260      10 M = NN
> 261      20 IF (J .LE. M) GO TO 30
> 262          J = J - M
> 263          M = M / 2
> 264          IF (M .GE. 1) GO TO 20
> 265      30 J = J + M
> 266          L = 1
> 267          NL = NN
> 268      40 ISTEP = 2 * L
> 269          IND = 1
> 270          DO 100 M = 1, L

```

```

> 271         INDN = IND - N - 1
> 272         IF (INDN) 50, 60, 70
> 273     50    WX = S(1 - INDN)
> 274         WY = S(IND) * SIGNI
> 275         GO TO 80
> 276     60    WX = 0.
> 277         WY = SIGNI
> 278         GO TO 80
> 279     70    WX = -S(INDN + 1)
> 280         WY = S(N + 1 - INDN) * SIGNI
> 281     80    DO 90 I = M, LX, ISTEP
> 282         TEMPX = WX * X(I + L) - WY * Y(I + L)
> 283         TEMPY = WX * Y(I + L) + WY * X(I + L)
> 284         X(I + L) = X(I) - TEMPX
> 285         Y(I + L) = Y(I) - TEMPY
> 286         X(I) = X(I) + TEMPX
> 287     90    Y(I) = Y(I) + TEMPY
> 288     100  IND = IND + NL
> 289         L = ISTEP
> 290         NL = NL / 2
> 291         IF (L .LT. LX) GO TO 40
> 292         RETURN
> 293         END
> 294     C
> 295     C*****
> 296     C
> 297     C   SUBROUTINE SINTAB
> 298     C   -----
> 299     C
> 300     C DESCRIPTION - THIS SUBROUTINE RETURNS VALUES
> 301     C S(I)=SIN(2*PI*(I-1)/LX) I=1,2,...,LX/4+1
> 302     C WHERE LX=2**INTEGER IS THE NUMBER OF POINTS IN THE
> 303     C TIME SERIES IN MAIN
> 304     C
> 305     C WRITTEN BY ALAN NUNNS
> 306     C*****
> 307     C
> 308     C   SUBROUTINE SINTAB(LX, S)
> 309     C   IMPLICIT REAL*8(A - H,O - Z)
> 310     C   DIMENSION S(LX)
> 311     C   DOUBLE PRECISION ARG, DELARG
> 312     C   N1 = LX / 4 + 1
> 313     C   ARG = 0.0
> 314     C   DELARG = 0.6283185307179586D01 / LX
> 315     C   DO 10 I = 1, N1
> 316     C     S(I) = DSIN(ARG)
> 317     C     ARG = ARG + DELARG
> 318     C 10 CONTINUE
> 319     C   RETURN
> 320     C   END
> 321     C
> 322     C*****
> 323     C
> 324     C   SUBROUTINE MOVAV
> 325     C   -----
> 326     C   THIS SMOOTHS THE POWER SPECTRUM USING A QUADRATIC
> 327     C   FIVE-POINT FORMULA
> 328     C
> 329     C   X = SPECTRUM OF DATA
> 330     C   LSAMP = SIZE OF ARRAY
> 331     C
> 332     C*****
> 333     C
> 334     C   SUBROUTINE MOVAV(LSAMP, X)
> 335     C   REAL*8 X(LSAMP)
> 336     C   LSAM = LSAMP - 2
> 337     C   DO 10 I = 3, LSAM
> 338     C     X(I) = X(I) - 3 * (X(I - 2) - 4*X(I - 1) + 6*X(I) - 4*X(I + 1) +
> 339     C     1 X(I + 2)) / 35
> 340     C 10 CONTINUE
> 341     C   X(1) = X(1) - (X(1) - 4*X(2) + 6*X(3) - 4*X(4) + X(5)) / 70
> 342     C   X(2) = X(2) + (X(1) - 4*X(2) + 6*X(3) - 4*X(4) + X(5)) * 2 / 35
> 343     C   L = LSAMP
> 344     C   X(L - 1) = X(L - 1) + (X(L - 4) - 4*X(L - 3) + 6*X(L - 2) - 4*X(L
> 345     C   1 - 1) + X(L)) * 2 / 35
> 346     C   X(L) = X(L) - (X(L - 4) - 4*X(L - 3) + 6*X(L - 2) - 4*X(L - 1) +
> 347     C   1X(L)) / 70
> 348     C   RETURN
> 349     C   END

```

```

> 350 C
> 351 C*****
> 352 C
> 353 C SUBROUTINE PAD
> 354 C -----
> 355 C
> 356 C CHECKS TO SEE IF THE DATA LENGTH IS 2**N AND IF
> 357 C NOT PADS THE ARRAY WITH ZEROS
> 358 C
> 359 C X = DATA ARRAY
> 360 C LX = LENGTH OF ARRAY
> 361 C
> 362 C*****
> 363 C
> 364 C SUBROUTINE PAD(LX, X)
> 365 C REAL*8 X(LX)
> 366 C DO 10 I = 1, 11
> 367 C IF (LX .EQ. 2**I) GO TO 70
> 368 C IF (LX .LT. 2**I) GO TO 20
> 369 C 10 CONTINUE
> 370 C 20 WRITE (6,30)
> 371 C 30 FORMAT ('ENTER NO. OF POINTS TO BE PADDED TO(2**N),FOR DEFAULT
> 372 C 1 '/'ENTER 0'/'..... 15')
> 373 C READ (5,40) IDAT
> 374 C 40 FORMAT (I5)
> 375 C IF (IDAT .EQ. 0) IDAT = 2 ** I
> 376 C WRITE (6,50) IDAT
> 377 C 50 FORMAT ('DATA ARRAY BEING PADDED WITH ZEROS TO ', I4, ' POINTS')
> 378 C LXN = IDAT
> 379 C LXT = LX + 1
> 380 C DO 60 I = LXT, LXN
> 381 C X(I) = 0.0
> 382 C 60 CONTINUE
> 383 C LX = LXN
> 384 C 70 RETURN
> 385 C END
> 386 C
> 387 C*****
> 388 C
> 389 C SUBROUTINE COSTAP
> 390 C -----
> 391 C
> 392 C APPLIES A COSINE TAPPER TO THE TWO ENDS
> 393 C OR THE TIME SERIES
> 394 C
> 395 C F = DATA ARRAY
> 396 C LX = LENGTH OF DATA
> 397 C L1 = FIRST POINT OF TAPPER
> 398 C L2 = LAST POINT OF TAPER
> 399 C
> 400 C*****
> 401 C
> 402 C SUBROUTINE COSTAP(LX, F, L1, L2, ISIGN)
> 403 C REAL*8 F(LX)
> 404 C DELARG = 3.14159265 / FLOAT(L2 - L1 + 1)
> 405 C ARG = 0.0
> 406 C DO 10 I = L1, L2
> 407 C F(I) = F(I) * 0.5 * (1 - ISIGN*COS(ARG))
> 408 C ARG = ARG + DELARG
> 409 C 10 CONTINUE
> 410 C RETURN
> 411 C END
> 412 C
> 413 C*****
> 414 C
> 415 C SUBROUTINE SECOND
> 416 C -----
> 417 C
> 418 C CONVERTS THE TIME IN HOURS MINS AND SECONDS
> 419 C TO SECONDS
> 420 C
> 421 C*****
> 422 C
> 423 C SUBROUTINE SECOND(IHOUR, IMIN, DSECS, DTIME)
> 424 C REAL*8 DTIME, DATIME
> 425 C
> 426 C ITIME = (IHOUR*3600) + (IMIN*60)
> 427 C DATIME = ITIME
> 428 C DTIME = DATIME + DSECS
> 429 C WRITE (7,10) DTIME
> 430 C 10 FORMAT (F10.2)
> 431 C RETURN
> 432 C END

```

```

> 433 C
> 434 C*****
> 435 C
> 436 C          SUBROUTINE SAMPLE
> 437 C          -----
> 438 C
> 439 C          CALCULATES THE FIRST AND LAST SAMPLES REQUIRED
> 440 C          FROM THE TRACE ARRAYS FOR PLOTTING
> 441 C          VELR      -      RED. VEL.
> 442 C          TEVE     -      SHOT TIME
> 443 C          TST      -      FILE START TIME
> 444 C          TSRED    -      START TIME(RED) OF PLOT WANTED
> 445 C          TSAM     -      TIME(RED) OF SAMPLES TO BE PLOTTED
> 446 C          TLEN     -      LENGTH(RED.TIME) OF PLOT
> 447 C          NST      -      1st SAMPLE TO BE PLOTTED
> 448 C          NEND     -      LAST SAMPLE TO BE PLOTTED
> 449 C
> 450 C*****
> 451 C
> 452 C          SUBROUTINE SAMPLE(DTST, DTEVE, TSRED, DIST, NST, SAMPR, NEND,
> 453 C          1      TLEN, VELR, TSAM, LENG)
> 454 C          REAL*4 DIST, SAMPR, TSAM(2048), VELR
> 455 C          REAL*8 DTST, DSAMNO, DSAM, DTST, DTEVE
> 456 C          INTEGER*4 NST, NEND
> 457 C
> 458 C          IF (VELR .EQ. 0.0) GO TO 10
> 459 C          DTST = DIST / VELR + DTEVE + TSRED
> 460 C          GO TO 20
> 461 C          10 DTST = DTEVE + TSRED
> 462 C          20 DSAMNO = (DTST - DIST) * SAMPR + 1.0
> 463 C          NST = IDINT(DSAMNO) + 1
> 464 C          TSAM(1) = TSRED + (NST - DSAMNO) / SAMPR
> 465 C          DSAM = 1.0 / SAMPR
> 466 C          WRITE (7,30) SAMPR, DSAM
> 467 C          30 FORMAT (F7.3, 2X, F9.7)
> 468 C          DO 50 J = 2, 10000
> 469 C             K = J - 1
> 470 C             TSAM(J) = TSAM(K) + DSAM
> 471 C          40 IF (TSAM(J) .GT. (TSRED + TLEN)) GO TO 60
> 472 C          50 CONTINUE
> 473 C          60 NEND = NST + K
> 474 C          WRITE (7,70) DTST, DTEVE, NST, NEND, TSAM(1), TSAM(K), DTST
> 475 C          70 FORMAT (2(2X,F9.3), 2(2X,I5), 3(2X,F9.3))
> 476 C          IF (NEND .GT. LENG) GO TO 110
> 477 C          IF (NST .LE. 0) GO TO 90
> 478 C          80 CONTINUE
> 479 C          GO TO 140
> 480 C          90 WRITE (6,100)
> 481 C          100 FORMAT ('YOU ARE TRYING TO PLOT BEFORE THE FIRST SAMPLE')
> 482 C          GO TO 130
> 483 C          110 WRITE (6,120)
> 484 C          120 FORMAT ('YOU ARE TRYING TO PLOT AFTER THE LAST SAMPLE')
> 485 C          130 STOP
> 486 C          140 RETURN
> 487 C          END

```

```

> 1 C*****
> 2 C
> 3 C
> 4 C          CORRNAV
> 5 C
> 6 C
> 7 C          THIS PROGRAMME CALCULATES THE POSITION OF A SHIP USING
> 8 C          DECCA FIXES AND THE SHIPS SPEED AND HEADING BY VECTOR
> 9 C          ADDITION AND SUBTRACTION. IT INCORPORATES THE PROGRAMME
> 10 C         DISTAZ WRITTEN BY G. K. WESTBROOK WHICH CALCULATES THE
> 11 C         DISTANCE BETWEEN TWO POINTS GIVEN THEIR POSITION
> 12 C         IN DEGREES OF LATITUDE AND LONGITUDE.
> 13 C
> 14 C         IT CAN BE USED WHEN THE SHIPS POSITION IS KNOWN FROM DECCA
> 15 C         FIXES, SAY, EVERY 20 MINS AND THE SHIPS WATER SPEED AND
> 16 C         HEADING IS KNOWN MORE FREQUENTLY, SAY, EVERY 2 MINS. THIS
> 17 C         PROGRAM WILL CALCULATE THE SHIPS DRIFT AND DETERMINE THE
> 18 C         SHIPS POSITION AT 2 MINUTE INTERVALS CORRECTED FOR DRIFT
> 19 C
> 20 C         INPUT
> 21 C         -----
> 22 C
> 23 C         UNIT - 3
> 24 C         CARD 1 - TITLE (HE) (20A4)
> 25 C         NBLOC SETS OF CARDS
> 26 C         CARD 1 - NUMBER OF TIMES SHIPS SPEED AND HEADING IS KNOWN BETWEEN
> 27 C         SUCCESSIVE DECCA FIXES (NT) (I2)
> 28 C         NEXT NT CARDS - TIME, SHIPS SPEED, SHIPS HEADING (TIMS,VSEA,AZSEA)
> 29 C         (F5.2,3X,F5.2,2X,F6.1)
> 30 C
> 31 C         UNIT - 5
> 32 C         CARD 1 - NUMBER OF DECCA FIXES (NBLOC) (I3)
> 33 C         CARD 2 - TITLE (HEA) (20A4)
> 34 C         CARD 3 - DEG. LONG. PER KM, DEG LAT. PER KM (CLA,CLO)
> 35 C         (2(F10.8),3X)
> 36 C         NEXT NBLOC CARDS - ID,TIME,LAT(DEG),LAT(MIN),LONG(DEG),LONG(MIN)
> 37 C         OF DECCA FIXES
> 38 C         (NS,TIMD,DL(BL),DM(BM),PL(CL),PM(CM))
> 39 C         (I3,4X,F5.2,4X,2(F4.0,1X,F6.2,3X))
> 40 C
> 41 C         OUTPUT
> 42 C         -----
> 43 C
> 44 C         UNIT - 6  CONTAINS DISTANCE AND AZIMUTH BETWEEN SUCCESSIVE DECCA
> 45 C         DECCA FIXES FOLLOWED BY DISTANCE AND AZIMUTH
> 46 C         FROM THE DECCA FIX CALCULATED FROM THE SHIPS SPEED
> 47 C         AND HEADING
> 48 C
> 49 C         UNIT - 7  DISTANCE AND AZIMUTH OF POSITION CALCULATED FROM THE
> 50 C         SHIPS SPEED AND HEADING FROM THE DECCA FIX FOLLOWED
> 51 C         BY THE CORRECTION FOR THE INTERMEDIATE POSITIONS
> 52 C
> 53 C         UNIT - 8  CORRECTED POSITIONS
> 54 C
> 55 C*****
> 56 C
> 57 C         DOUBLE PRECISION AL, OL, ERQ, PRQ, A, B, SS, VS, SI, V, CO, S,
> 58 C         1   SDL, CDL, DIF, S1, C1, G, GA, EC, EL, TA, GS, VRR, ORR,
> 59 C         2   VELRR, ORRR, VELR, OR, VSEAR, AZSEAR, VDR, ODR, VCORR,
> 60 C         3   OCOORR, V, KTK, VSEA, AZSEA, ORT, ORRT, ARG, ARG1, ODRT,
> 61 C         4   ARG2, DLA, DLO, CLA, CLO, ALT, OLT
> 62 C         INTEGER P
> 63 C         DIMENSION NL(150), A(2,300), NS(300), B(2,300), SI(150), CO(150),
> 64 C         1   V(150), VS(300), SS(300), GA(150), TA(300), GS(300),
> 65 C         2   TIMD(150), TIMS(1300), VRR(300), ORR(300), VSEA(1300),
> 66 C         3   AZSEA(1300), VELR(1300), OR(1300), VSEAR(300),
> 67 C         4   AZSEAR(300), VDR(300), ODR(300), VCOORR(1300),
> 68 C         5   OCOORR(1300), VEL(1300), ALT(20), OLT(20), HE(20),
> 69 C         6   HEA(20)
> 70 C
> 71 C
> 72 C         SET UP OUTPUT AND READ HEADINGS OF INPUT FILES
> 73 C
> 74 C
> 75 C         WRITE (6,10)
> 76 C         10 FORMAT (/'          FILENAME IS "DISTAZ.DECCA"')
> 77 C         20 FORMAT (/' NUMBER LATITUDE LONGITUDE TIME OF FIXES    DISTAN
> 78 C         ICE AND AZIMUTH')
> 79 C         WRITE (7,30)
> 80 C         30 FORMAT (/'          FILENAME IS "CORR-VECT"')
> 81 C         WRITE (8,40)
> 82 C         40 FORMAT (/' FINAL CORRECTED LATS. AND LONGS.' )
> 83 C         READ (5,50) NBLOC
> 84 C         50 FORMAT (I3)
> 85 C         READ (3,60) HE
> 86 C         WRITE (7,70) HE
> 87 C         READ (5,60) HEA
> 88 C         WRITE (6,70) HEA
> 89 C         WRITE (8,70) HE
> 90 C         60 FORMAT (20A4)

```

```

> 91      WRITE (6,20)
> 92      70 FORMAT (/20A4)
> 93      DTR = 0.017453292
> 94      READ (5,80) CLA, CLO
> 95      80 FORMAT (2(F10.8,3X))
> 96      CLA = CLA * DTR
> 97      CLO = CLO * DTR
> 98      KTK = 1.852
> 99      ER = 6378.16
> 100     PR = 6356.775
> 101     ERQ = ER ** 2
> 102     PRQ = PR ** 2
> 103     EC = (ERQ - PRQ) / ERQ
> 104     EL = (ERQ - PRQ) / PRQ
> 105     READ (5,120) NS(1), TIMD(1), DL, DM, PL, PM
> 106     DO 280 M = 1, NBLOC
> 107     90 READ (3,100) NT
> 108     100 FORMAT (I2)
> 109     C
> 110     C
> 111     C      STEP 1 - CALCULATE RESULTANT DISTANCE + AZIMUTH FROM DECCA FIXES
> 112     C
> 113     C
> 114     IF (M .EQ. 1) GO TO 110
> 115     TIMD(1) = TIMD(K)
> 116     DL = BL
> 117     DM = BM
> 118     PL = CL
> 119     PM = CM
> 120     110 AL = (DL + DM/60.0) * DTR
> 121     CL = (PL + PM/60.0) * DTR
> 122     B(1,1) = AL
> 123     B(2,1) = CL
> 124     SS(1) = DSIN(AL)
> 125     TA(1) = SS(1) / DCOS(AL)
> 126     VS(1) = ER / DSQRT(1 - EC*SS(1)**2)
> 127     GS(1) = DSQRT(EL*SS(1)**2)
> 128     I = 1
> 129     K = 22
> 130     READ (5,120) NS(K), TIMD(K), BL, BM, CL, CM
> 131     120 FORMAT (I3, 4X, F5.2, 4X, 2(F4.0,1X,F6.2,3X))
> 132     AL = (BL + BM/60.0) * DTR
> 133     CL = (CL + CM/60.0) * DTR
> 134     B(1,K) = AL
> 135     B(2,K) = CL
> 136     S1 = DSIN(AL)
> 137     C1 = DCOS(AL)
> 138     V1 = ER / DSQRT(1 - EC*S1**2)
> 139     DIF = B(2,I) - CL
> 140     CDL = DCOS(DIF)
> 141     SDL = DSIN(DIF)
> 142     SS(K) = S1
> 143     VS(K) = V1
> 144     TA(K) = S1 / C1
> 145     GS(K) = DSQRT(EL*S1**2)
> 146     G = GS(K)
> 147     T = (1.0 - EC + EC*V1*S1/(VS(I)*SS(I))) * TA(I)
> 148     AT = ATAN(T)
> 149     PAZ = C1 * T - S1 * CDL
> 150     SL = SDL
> 151     AZ = ATAN2(SL,PAZ)
> 152     HQ = EL * C1 ** 2 * COS(AZ) ** 2
> 153     H = SQRT(HQ)
> 154     BAZ = ABS(AZ) - 3.1415926
> 155     IF (BAZ .GT. - 1.0 .OR. BAZ .LT. - 2.14159) GO TO 130
> 156     FD = SDL * COS(AT) / SIN(AZ)
> 157     D = ARSIN(FD)
> 158     GO TO 140
> 159     130 D = ARSIN(COS(AT)*PAZ/COS(AZ))
> 160     140 DIST = V1 * D * (1.0 - D**2*HQ*(1.0 - HQ)/6.0 + D**3*G*H*(1.0 -
> 161     1 2.0*HQ)/8.0 + D**4*(HQ*(4.0 - 7.0*HQ) - 3.0*G**2*(1.0 - 7.0*HQ))
> 162     2 /120.0 - D**5*G*H/48.0)
> 163     AZ = AZ + 3.1415926
> 164     DAZ = AZ / DTR
> 165     WRITE (6,150) NS(K), BL, BM, CL, CM, TIMD(I), TIMD(K), DIST, DAZ
> 166     150 FORMAT (/I3, 5X, 2(F3.0,1X,F6.2,2X), F5.2, ' TO ', F5.2, ' = ',
> 167     1 F7.3, 6X, F8.3)
> 168     VRR(I) = DIST
> 169     ORR(I) = AZ

```

```

> 170 C
> 171 C
> 172 C STEP 2 - CALCULATES RESULTANT DISTANCE + HEADING USING SHIPS
> 173 C SPEED + HEADING
> 174 C
> 175 C
> 176 READ (3,160) TMS(1), VSEA(1), AZSEA(1)
> 177 READ (3,160) TMS(2), VSEA(2), AZSEA(2)
> 178 160 FORMAT (F5.2, 3X, F5.2, 2X, F6.1)
> 179 VSEA(1) = VSEA(1) * KTK / 30
> 180 VSEA(2) = VSEA(2) * KTK / 30
> 181 AZSEA(1) = AZSEA(1) * DTR
> 182 AZSEA(2) = AZSEA(2) * DTR
> 183 CALL VELADD(VSEA(1), VSEA(2), AZSEA(1), AZSEA(2), VELRR, ORT)
> 184 VELR(2) = VELRR
> 185 OR(2) = ORT
> 186 SUB = OR(2) / DTR
> 187 WRITE (6,180) VELR(2), SUB
> 188 MET = NT - 1
> 189 DO 170 J = 2, MET
> 190 L = J + 1
> 191 READ (3,160) TMS(L), VSEA(L), AZSEA(L)
> 192 VSEA(L) = VSEA(L) * KTK / 30
> 193 AZSEA(L) = AZSEA(L) * DTR
> 194 CALL VELADD(VELR(J), VSEA(L), OR(J), AZSEA(L), VELRR, ORT)
> 195 VELR(L) = VELRR
> 196 OR(L) = ORT
> 197 SUB = OR(L) / DTR
> 198 WRITE (6,180) VELR(L), SUB
> 199 170 CONTINUE
> 200 SUB = OR(L) / DTR
> 201 VSEAR(I) = VELR(NT)
> 202 AZSEAR(I) = OR(NT)
> 203 180 FORMAT (2(3X,F8.3))
> 204 C
> 205 C
> 206 C STEP 3 - CALCULATES RESULTANT DRIFT DISTANCE + AZ USING VALUES
> 207 C FROM STEPS 1 & 2
> 208 C
> 209 C
> 210 ARG1 = ORR(I) - AZSEAR(I)
> 211 VDR(I) = DSQRT(VSEAR(I)**2 + VRR(I)**2 - 2.0*VSEAR(I)*VRR(I)*
> 212 1 DCOS(ARG1))
> 213 ARG2 = (VDR(I)**2 + VSEAR(I)**2 - VRR(I)**2) / (?*VDR(I)*VSEAR(
> 214 1 I))
> 215 ORRT = DARCOB(ARG2)
> 216 IF (VRR(I) .GT. VSEAR(I) .AND. ARG1 .LT. 0.0) ODR(I) = ORRT - 3.
> 217 1 1415926 + AZSEAR(I)
> 218 IF (VRR(I) .LT. VSEAR(I) .AND. ARG1 .LT. 0.0) ODR(I) = ORRT +
> 219 1 AZSEAR(I) + 3.1415926
> 220 IF (ARG1 .GT. 0.0) ODR(I) = 3.1415926 + AZSEAR(I) - ORRT
> 221 190 ODRT = ODR(I) / DTR
> 222 WRITE (7,200) VDR(I), ODRT
> 223 200 FORMAT (/^DRIFT DISTANCE(KM) + AZIMUTH=^, F8.3, 2X, F8.3)
> 224 RNT = FLOAT(NT)
> 225 VDR(I) = VDR(I) / RNT
> 226 C
> 227 C
> 228 C STEP 4 - CALCULATE SHIPS DISTANCE + AZ CORRECTED FOR DRIFT
> 229 C
> 230 C
> 231 WRITE (7,210)
> 232 210 FORMAT (/^ TIME DIST(KM) AZIMUTH^)
> 233 DO 230 J = 1, NT
> 234 CALL VELADD(VSEA(J), VDR(I), AZSEA(J), ODR(I), VELRR, ORT)
> 235 VCORR(J) = VELRR
> 236 OCORR(J) = ORT / DTR
> 237 WRITE (7,220) TMS(J), VCORR(J), OCORR(J)
> 238 220 FORMAT (1X, F5.2, 3X, F6.3, 2X, F7.3)
> 239 230 CONTINUE

```

```

> 240 C
> 241 C
> 242 C
> 243 STEP 5 - CALCULATE CORRECTED LATS. AND LONGS.
> 244 C
> 245 C
> 246 C
> 247 WRITE (8,240)
> 248 240 FORMAT (' TIME LAT. LONG.')
> 249 ALT(1) = B(1,1)
> 250 OLT(1) = B(2,1)
> 251 WRITE (8,250) TIMD(1), DL, DM, PL, PM
> 252 250 FORMAT (/1X, F5.2, 2(3X,F4.0,1X,F6.2), 3X, 'DECCA FIX')
> 253 C
> 254 DO 270 I = 1, NT
> 255 J = I + 1
> 256 OCORR(I) = OCORR(I) * DTR
> 257 DLA = VCORR(I) * DCOS(OCORR(I))
> 258 DLO = VCORR(I) * DSIN(OCORR(I))
> 259 ALT(J) = ALT(I) + DLA * CLA
> 260 OLT(J) = OLT(I) + DLO * CLO
> 261 ALI = ALT(J) / DTR
> 262 OLI = OLT(J) / DTR
> 263 ALR = AINT(ALI)
> 264 AMR = (ALI - ALR) * 60.0
> 265 OLR = AINT(OLI)
> 266 OLM = (OLI - OLR) * 60.0
> 267 WRITE (8,260) TIMS(I), ALR, AMR, OLR, OLM
> 268 260 FORMAT (1X, F5.2, 2(3X,F4.0,1X,F6.2))
> 269 270 CONTINUE
> 270 CONTINUE
> 271 WRITE (8,250) TIMD(K), BL, BM, CL, CM
> 272 STOP
> 273 END
> 274 C
> 275 C
> 276 C
> 277 C VECTOR ADDITION SUBROUTINE
> 278 C
> 279 C
> 280 C
> 281 SUBROUTINE VELADD(V1, V2, O1, O2, VELRR, ORT)
> 282 DOUBLE PRECISION V1, V2, O1, O2, VELRR, ORT, ORRR
> 283 VELRR = DSQRT(V1**2 + V2**2 + 2.0*V1*V2*DCOS(O2 - O1))
> 284 ORRR = DARSIN(V2*DSIN(O2 - O1)/VELRR)
> 285 ORT = O1 + ORRR
> 286 RETURN
> 287 END

```

